

**INTERACTION OF SURFACTANT-SURFACTANT,
SURFACTANT-SALT AND SURFACTANT-
POLYELECTROLYTES IN AQUEOUS MEDIA**

**THESIS SUBMITTED IN FULFILLMENT OF
REQUIRMENTS FOR THE DEGREE OF
DOCTOR OF PHILOSOPHY (SCIENCE)
OF
JADAVPUR UNIVERSITY, INDIA**



**By
SOURAV DAS, M.Sc.**

2022

Prof. Soumen Ghosh, M. Sc., Ph. D.
Professor of Chemistry & Co-ordinator,
Centre for Surface Science
Department of Chemistry, **Jadavpur University**
Kolkata – 700 032, West Bengal, India



Awards of Prof. B. N. Ghosh from ICS, Dr. B. C. Deb from ISCA, Bronze Medal from
CRSI, Visiting Chair Professor of St. F. X. University, Canada &

Selected as Top 2% World Ranking Scientist in Chemical Physics by Scientists of Stanford University, USA.

Phone : +91-33-2457 2503

Fax : 91-33-2414 4266

Mob - 9432 075 363

E-Mail – gsoumen17@yahoo.co.in/
soumen.ghosh@jadavpuruniversity.in

CERTIFICATE FROM THE SUPERVISOR

This is to certify that the thesis entitled “**INTERACTION OF SURFACTANT-SURFACTANT, SURFACTANT-SALT AND SURFACTANT-POLYELECTROLYTES IN AQUEOUS MEDIA**” submitted by **Sri. Sourav Das**, who got his name registered on 09.05.2016 for the award of **Ph.D. (Science) degree** of **Jadavpur University**, is absolutely based upon his own work under the supervision of **Prof. Soumen Ghosh** and that neither this thesis nor any part of it has been submitted for any degree/diploma or any other academic award anywhere before.

Soumen Ghosh
17.06.2022

Soumen Ghosh

Centre for Surface Science

Department of Chemistry

Jadavpur University

Kolkata- 700032

Prof. Soumen Ghosh
Department of Chemistry
Jadavpur University
Kolkata-700 032, W.B., India

“Nothing in life is to be feared, it is only to be understood. Now is the time to understand more, so that we may fear less.”

Marie Curie (1867-1934)

Dedicated To
My Beloved Parents

DECLARATION

I hereby declare that the work incorporated in the present dissertation was carried out by me at the centre for surface science, Department of Chemistry, Jadavpur University, Kolkata-700032, India. The entire work or any part of it has never been submitted before for any prize or degree anywhere.

Sourav Das 17.06.2022
(SOURAV DAS)

ACKNOWLEDGEMENT

The research findings embodied in the dissertation “*Interaction of Surfactant - Surfactant, Surfactant - Salt and Surfactant - Polyelectrolytes in Aqueous Media*” were realized by me at the Centre for Surface Science, Department of Chemistry, Jadavpur University, Kolkata, India.

At the outset, I would like to take the privilege of expressing my sincere thanks and deep sense of gratitude to Prof. Soumen Ghosh, Department of Chemistry, Jadavpur University not only for his unreserved inspiration, affectionate guidance, suggestions and advice, he gave me maintaining patience and understanding throughout the tenure of the work, but also for the great human being and the nice, warm person he is.

I acknowledge with pleasure the inspiration received from Prof. Satya Priya Moulik, Prof. Bijan Das and Prof. Chittaranjan Sinha during the execution of the work.

I would like to extend my sincere thanks to Prof. Swapan Kumar Bhattacharya, HOD, Department of Chemistry, Jadavpur University for getting me the central instrumental facilities throughout my research work. Author also expresses his heartiest thanks to all the faculty members, Department of Chemistry, Jadavpur University, and also university administration for smooth running his research work.

I warmly remember the all-out unconditional cooperation received from my colleagues, Dr. Nitai Patra, Dr. Arpan Mal, Dr. Jayabrata Maity, Mr. Rajesh Banik, Mr. Bipin Bihari Mandal, Ms. Ankita Saha, Ms. Tanaya Saha, Mr. Raju Sardar and Mrs. Sudipta Chakraborty for both technical and emotional support.

The author is highly indebted to Dr. Pinki Saha Sardar, Dr. Totan Ghosh, Dr. Anjoy Majhi, Dr. Arnab Halder, Mr. Sandip Paul, Dr. Dhiman Ray, Dr. Pritam Roy, Mr. Arnab Banerjee and Dr. Manas Barai.

I am also thankful to Central Instrumentation Facility, IICB and IACS; DBT-IPLS and CRNN, University of Calcutta for getting me some instrumentation facility.

The financial assistance received from Council of Scientific and Industrial Research (CSIR), Govt. of India during the tenure of the work is acknowledged with thanks.

The author will remain ever grateful to his parents and other members of his family for their unreserved endurance, encouragement and loving support.

Centre for Surface Science
Department of Chemistry
Jadavpur University
Kolkata – 700032
India


(SOURAV DAS) 17.06.2022

PREFACE

Surfactant-salt mixtures find wide spread uses in biological, technological, medical formulations, pharmaceuticals, and enhanced oil recovery for the purpose of improved solubilisation, suspension and dispersion. Various organic and inorganic salts are used for this purpose.

Mixed surfactants are extensively used in recent times in the various combinations of conventional cationic, anionic, gemini, zwitterionic and non-ionic forms. Studies of mixed surfactants are recently gained importance owing to the 'mixed micelle' formation in aqueous solution which helps the understanding of the various biological supra-molecular assemblies, ions transfer, drug delivery and the formation of mimic biological systems. In technology, mixed surfactants are used in pharmaceuticals, detergency, foods, cosmetics, solubilization of drugs and enhanced oil recovery.

Interaction of bio polyelectrolyte (carbohydrate polymers, proteins, polypeptides, DNA etc.) with surfactant of different kinds has been focused much for their applications in biology, foods, drug delivery and biotechnology. Binding of proteins with surfactants either stabilises or denatures (unfolding form) them. The excellent example of protein-surfactant system for functionalization of enzymes, sodium-potassium and various metabolites in our body is PLP (protein-lipid-protein) membrane. The interaction of various biopolyelectrolyte - surfactant systems invitro could help us to explore several biological processes in human body.

Ionic liquids with long hydrocarbon tails constitute a special class of surfactants. Room Temperature Ionic liquids (RTILs) are the salts whose melting points are below 100⁰C. There are many kinds of ionic liquids. As mentioned, long chain ionic liquids (**Surface Active Ionic Liquid, SAIL**) behave as surfactants. Now-a-days, the ionic liquids are emerging in the present scenario due to their low vapour pressure, low volatility, significant conductivity, high thermal stability and non-flammability. Owing to their several physicochemical properties SAILS can be used in drug delivery, microbial activity, catalyst and alternative solvent to the traditional organic solvents for synthesis of materials.

For this reason, the interaction of SAILS with salts, conventional surfactants and bio polyelectrolytes are very important in the recent times.

CONTENTS

	Page No.
Introduction	1-80
Chapter-I	81-117
Formation of Mixed Micelle in an Aqueous Mixture of a Surface Active Ionic Liquid and a Conventional Surfactant: Experiment and Modeling. (<i>J. Chem. Eng. Data</i> 63 (2018) 3784-3800, published)	
Chapter-II	118-159
Studies on the self-aggregation, interfacial and thermodynamic properties of a surface active imidazolium-based ionic liquid in aqueous solution: Effects of salt and temperature. (<i>J. Mol. Liq.</i> , 320 (2020) 114497, published)	
Chapter - III	160-220
A detailed assessment on the interaction of sodium alginate with a surface-active ionic liquid and a conventional surfactant: a multitechnique approach. (<i>Phys. Chem. Chem. Phys.</i> , 2022 , 24 , 13738-13762, published)	
Chapter – IV	221-251
Physicochemical and Spectroscopic Study on the Interaction of a Novel Aza benzo crown Dye with Different Surfactants. (Communicated)	
Chapter – V	252-290
Addressing the Interaction of Stem Bromelain with different anionic Surfactants, below, at and above CMC in Phosphate Buffer at pH 7: Physicochemical, Spectroscopic, Molecular docking Study. (Communicated)	
Summary and Conclusions	291-296
Appendix (Basic Data)	i –clxv
List of Publications and Reprints	A-C

Introduction

Introduction

The word ‘SURFACTANTS’ come from SURFace ACTive ageNTS.¹ These are the major components of soaps and detergents for the purpose of cleaning at laundry and households. Detergent has been used for commercial purpose as a ‘self-activated’ cleaning agent since its first preparation² in 1907 by a German company, which is termed as ‘PERSIL’ in form of laundry detergent. Historically, ‘PERSIL’ had been prepared by sodium PERborate (acting as bleaching agent) and sodium SILicate (base washing agent), but none of these components are conventional surfactants which we have used in our daily lives as versatile washing agents. In this connection, it is worth mentioning the word ‘SURFACTANS’ which activate the interfaces (either interfaces of air-liquid, solid-liquid or interface of two immiscible liquids; Fig.1) by reducing surface tension of a liquid, an important parameter in surface chemistry, formed by molecules with dual solubility towards both in water and oil media. Surfactant molecules reside on the interface by approaching their polar heads to the interface and consequently, lowering the free energy of interface. In addition of lowering surface or interfacial tension, apart from its rich detergency properties (soluble or insoluble substances), surfactants are used in many every day products (toothpaste, shampoo, conditioner, shaving foam, facewash, toilet cleaner, adhesive, hair gel, ink, etc.) as emulsifier, dispersants, wetting, foaming and stabilizing agents.

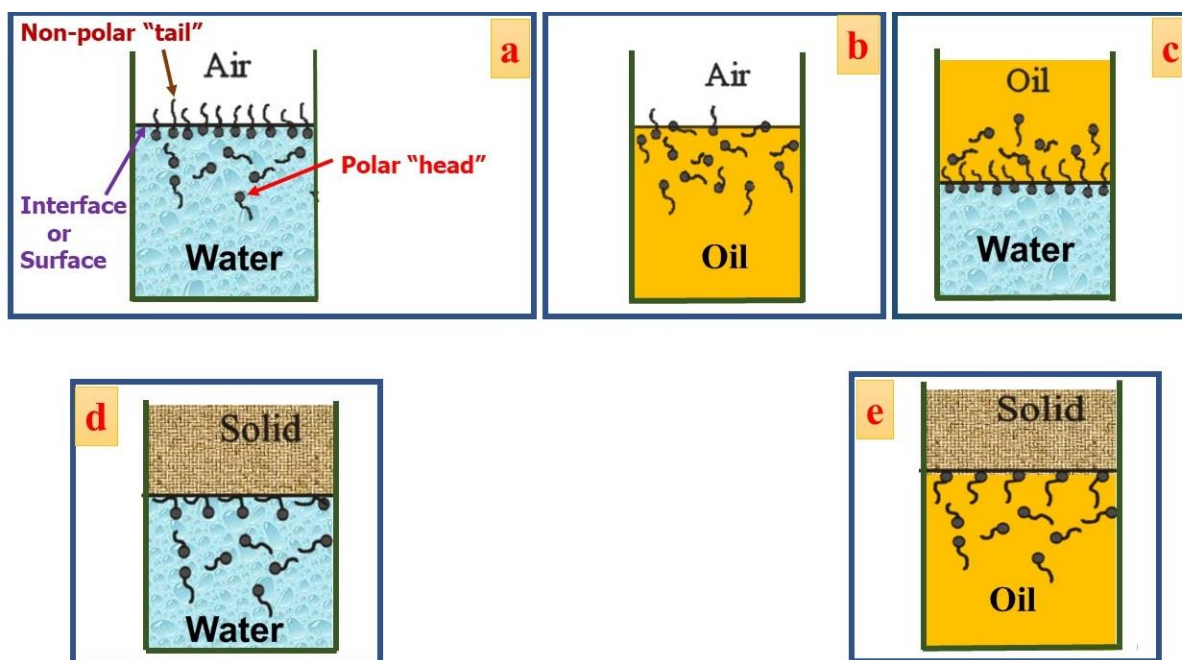


Fig. 1. Adsorption pattern of surfactants at different interfaces: (a) air-water interface, (b) air-oil interface, (c) oil-water interface, (d) solid-water interface and (e) solid-oil interface.

Due to the dual solubility nature, surfactants are often called amphiphiles. Typically, surfactants are formulated by a long alkyl hydrocarbon chain (8-22 carbon atoms)³ known as hydrophobic tail and a hydrophilic head group which may be cationic,⁴⁻¹³ anionic,¹⁴⁻²⁰ nonionic²¹⁻²⁴ and zwitterionic^{25, 26} in nature. While normal soaps are prepared by the saponification of naturally occurring fatty acids (triglycerides) from vegetable and animal sources, surfactants are prepared from petroleum products and their structure can be modulated in various forms⁴⁻²⁶; such fabrication is not possible in common soaps. A modern detergent at least contains 10-20 components, in which surfactants and fatty acid-based salts (sodium and potassium salts of C₁₂₋₁₈ long alkyl chain,^{3, 27, 28} which are extracted from palm kernel oil, coconut oil, soy bean oil and animal fats by the process of saponification) are the major one. The use of surfactants is more fascinating over soaps as surfactants are more effective to clean a surface in presence of hard water and even at low temperature.

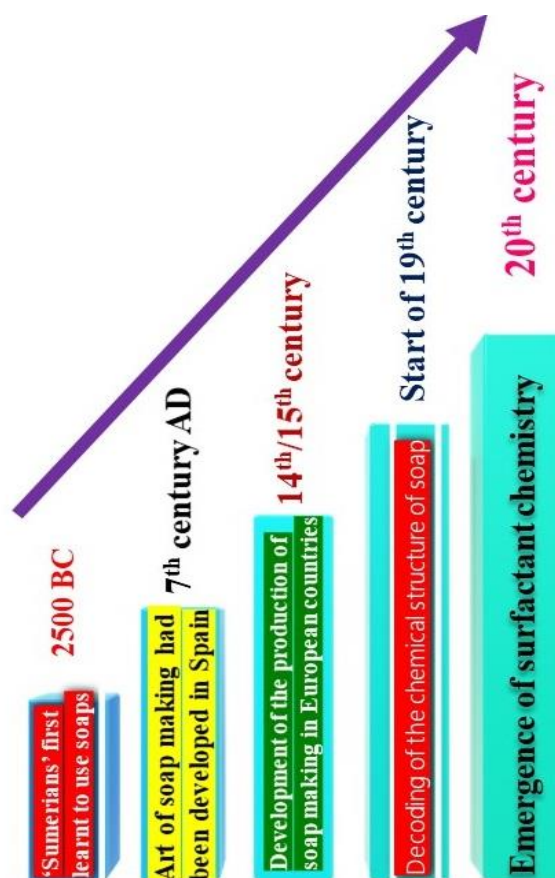


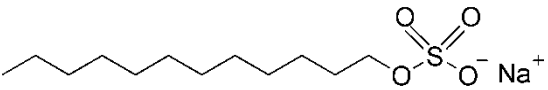
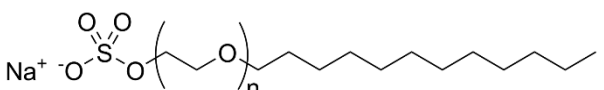
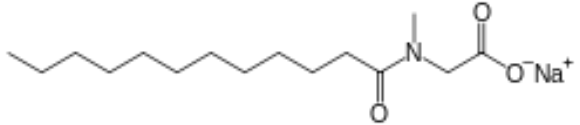
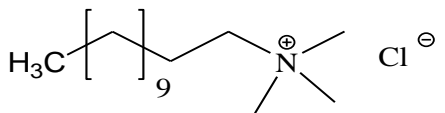
Fig. 2. Evolution of surfactants from Sumerians to modern century.

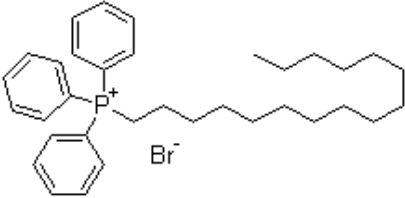
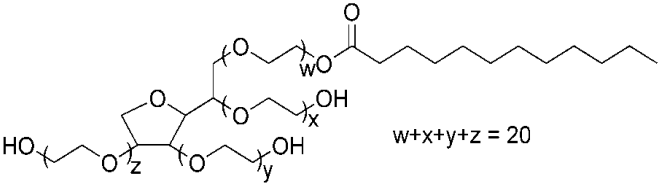
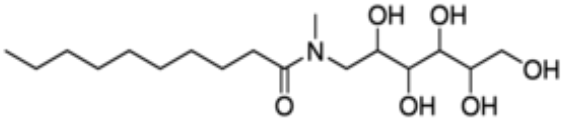
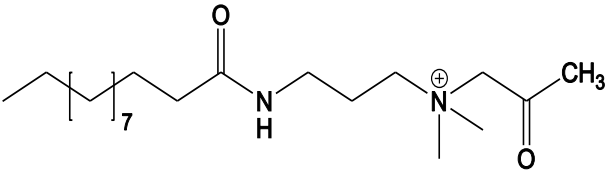
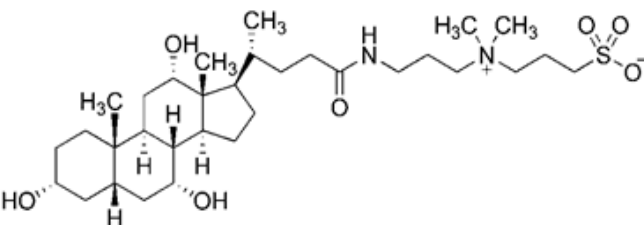
Even surfactants play a significant role in our biological system too. Biological cell membranes (lipid bilayer) contain amphiphile like molecules (phospholipids)²⁹ which conduct selective transportation of ions, proteins and other molecules inside and outside of cell. Bile salt (steroidal anionic surfactants) is present as a major organic solute in bile juice facilitating dietary fats adsorption in intestinal.³⁰ Human lungs produce pulmonary surfactant which is known as pulmonary epithelial lining fluid (ELF) helping in increase lung compliance and total lung capacity. ELF contains lipoprotein type surfactant which is secreted from lung epithelial type II cells and has been transported to alveolar space to decrease surface tension at air-liquid interface in the lung.³¹

1. Cataloguing of surfactants:

Surfactants are generally classified according to the charge of head groups in aqueous solution. Some surfactants which have been commonly used are given in the Table below:

Table 1. General classification of surfactants

Types of Surfactants	Examples
<p>Anionic Surfactant:</p> <p>This type of surfactants has negatively charged head groups and positively charged counterions. Head groups may be alkyl-sulfates, sulfonates, sulfosuccinates, carboxylates, N-acyl amino acids etc. Counterions may be positively charged alkali metal ions (Na^+/K^+) or quaternary ammonium cations. Anionic surfactants have been used mostly in daily products. Anionic surfactants are almost used in every household product.</p>	<p>Sodium lauryl sulphate (SLS/SDS)</p>  <p>Sodium laureth sulfate (SLES)</p>  <p>Sodium lauryl sarcosinate (SDDS)</p> 
<p>Cationic Surfactant:</p> <p>These surfactants have positive charged head groups (alkyl quaternary ammonium salts, phosphonium salts, amine salts, amine oxides etc.) along with negatively charged counterions (mainly Cl^- and Br^-). Preparations</p>	<p>Dodecyltrimethylammonium chloride (DTAC)</p>  <p>1-hexadecyltriphenylphosphonium bromide (C16TPB)</p>

<p>of these type of surfactants are expensive, so their use is limited.</p>	
<p>Nonionic Surfactant:</p> <p>These types of surfactants have no electrical charges. These are miscible in water due to the presence of polar functionality present in their structures. Polyoxyethylenes, alkylpolyglucosides, polyglycidols, N-based glucamine surfactants belong to this class. They are hugely produced industrially after anionic surfactants.</p>	<p>Polyoxyethylene (20) sorbitan monolaurate (Tween-20)</p>  <p>$w+x+y+z = 20$</p> <p>N-decanoyl-N-methylglucamine (MEGA-10)</p> 
<p>Zwitterionic Surfactants:</p> <p>These surfactants contain both negative and positive charged centres and can be used either as anionic or cationic surfactants with variation of pH. Imidazole derivatives, phosphatides, betaines etc. belong to this class. The source of positive charge is contributed by generally ammonium ions and negative charge by sulfates, carboxylates or sulfonate ions. These surfactants have excellent dermatological properties. Zwitterionic surfactants are frequently used in cosmetic products, shampoos, hand and dishwashing liquids because of their high frothing properties and less sensitive to skin.</p>	<p>Lauramidopropyl betaine</p>  <p>3-[(3-cholamidopropyl) dimethylammonio]-1-propanesulfonate (CHAPS)</p> 

Beyond broad classification, surfactants are again subdivided into some special classes. Significant attention has been paid in past two decades about these kinds of surfactants

Ionic Liquids

Ionic Liquids (ILs) have been designated as the molten salts (purely ionic semi organic molecules) whose melting points are below 100 °C (212 °F).³² Melting point of common table salt (NaCl) is around 801 °C, this obviously indicates that there is a significant difference between ionic liquids with typical inorganic salts. This difference is due to the components (ions) by which these are formed; typical inorganic salts are formed by small symmetrical ions, while ionic liquids are formed by large unsymmetrical cations with large anions (Fig. 3.) and charges are distributed over large volume through resonance.

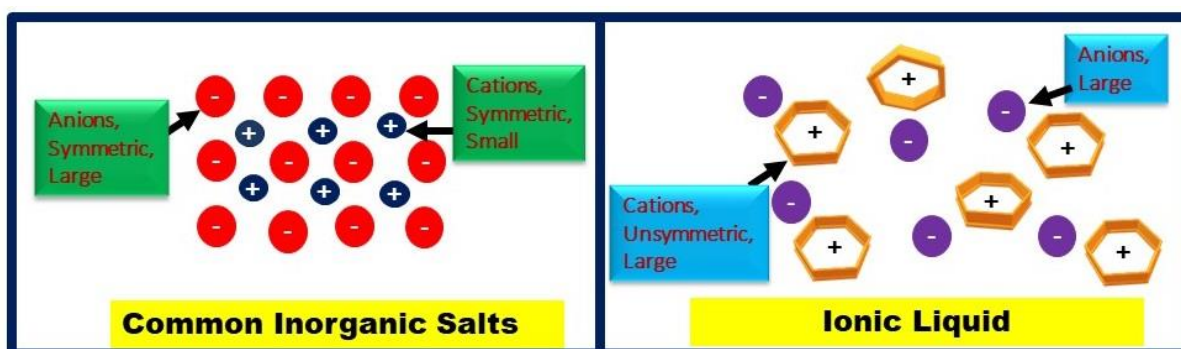


Fig. 3. Comparative diagrams of anions and cations with possible orientation between conventional inorganic salts with ionic liquids.

Ethyl ammonium nitrate (m.p. 52–55 °C) was the first synthesized ionic liquid reported by Gabriel and Weiner in 1888.³³ Room Temperature Ionic Liquid (RTIL) was first synthesized (ethylammonium nitrate, $(\text{C}_2\text{H}_5)\text{NH}_3^+\cdot\text{NO}_3^-$ (m.p. 12 °C)) by Paul Walden, a Russian, Latvian and German chemist in 1914.³⁴ Ionic liquids have wide range of melting temperatures below 100°C. Some ionic liquids with long alkyl chains attached to imidazolium N-atom in combination with halide anions (one such example is 1-hexadecyl-3-methyl imidazolium chloride, (m.p. 64-65°C)) are solid in room temperature, some containing large organic /inorganic anions are generally liquids in room temperature and their melting points are even below 0°C (e.g., 1-ethyl-3-methylimidazolium ethylsulfate (m.p.<-20 °C), EMIM dicyanamide (m.p. -21°C) etc.). Ionic liquids are formed (Fig. 4) by typical organic cations, e.g., alkyl-imidazolium, -pyridinium, -ammonium, -phosphonium and -pyrrolidinium types in combination with anions, e.g., organic triflate, dicyanamide, acetate, trifluoroacetate, trifluoromethylsulfate, or inorganic halides (bromide or chloride), hexafluorophosphate, nitrate, perchlorate, chloroaluminate, tetrafluoroborate.³⁵ Presently the use of ionic liquids is found as an upsurge of interest due to their low vapour pressure, significant conductivity, low volatility, high thermal stability and non-flammability. Owing to their several physicochemical

properties, ILs can be used in drug delivery,³⁶ antimicrobial activity,³⁷ micellar catalysis³⁸ and alternative solvent by replacing the traditional organic solvents³⁹.

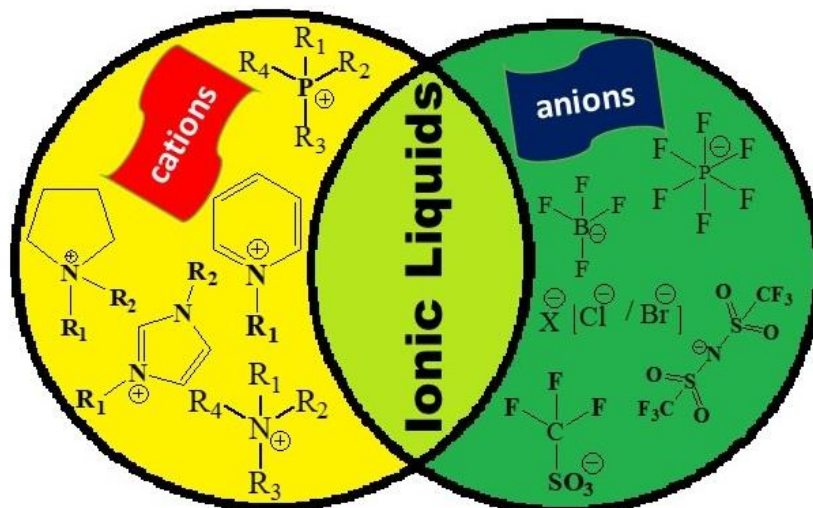


Fig.4. Some commonly used cations (within yellow segment) and anions (within green segment) forming ionic liquids.

Ionic liquids (IL) with di-alkyl imidazolium, di-alkyl pyridinium and alkylammonium type fragments have been considered a special type of surfactants, called Surface Active Ionic Liquids (SAILs), since the last two decades. Among the different cations which form SAILs, di-alkyl imidazolium ionic liquids have gained a special attention as varieties of imidazolium compounds have been formed by tuning N-substituents the with different alkyl groups along with counter anions by simple one-pot synthesis.⁴⁰⁻⁴² Surface activity of many ionic liquids have been reported in past and preceding literatures⁴³⁻⁶⁰ and most of the investigations have been done in aqueous solution.

Gemini Surfactant

Gemini surfactants are the special class of surfactants (Fig. 5) comprising with a extended hydrocarbon chain attached to a polar head group, a rigid or non-rigid spacer, and another hydrocarbon chain with another polar head group in sequential arrangement having rich surface activity than the traditional surfactants. This polar head groups may be positive (ammonium),⁶¹ negative (sulphates, carboxylate, etc.)⁶² and also nonionic (carbohydrate based)⁶³ in nature. Spacer length may contain 2 to 12 methylene groups; may be flexible (saturated hydrocarbon chain) or rigid (stilbene). Gemini surfactants were first synthesized by Button *et al.* in 1971⁶⁴.

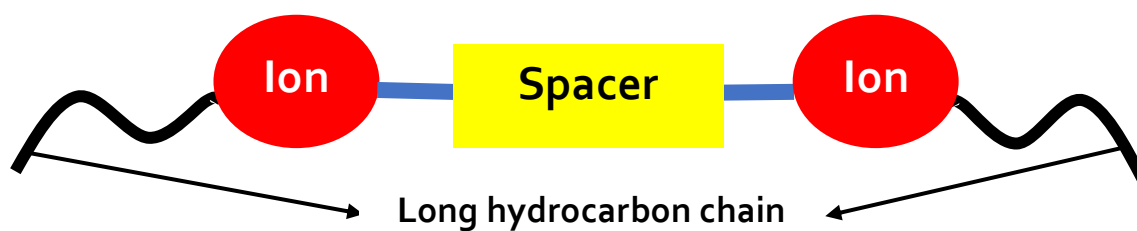


Fig. 5. Schematic representation of gemini surfactants

The term ‘Gemini’ was first coined by Menger *et al.* in 1991.⁶⁵ Spacers may be connected to the two identical head groups or alternatively it may be connected to the midway of long hydrocarbon tails.

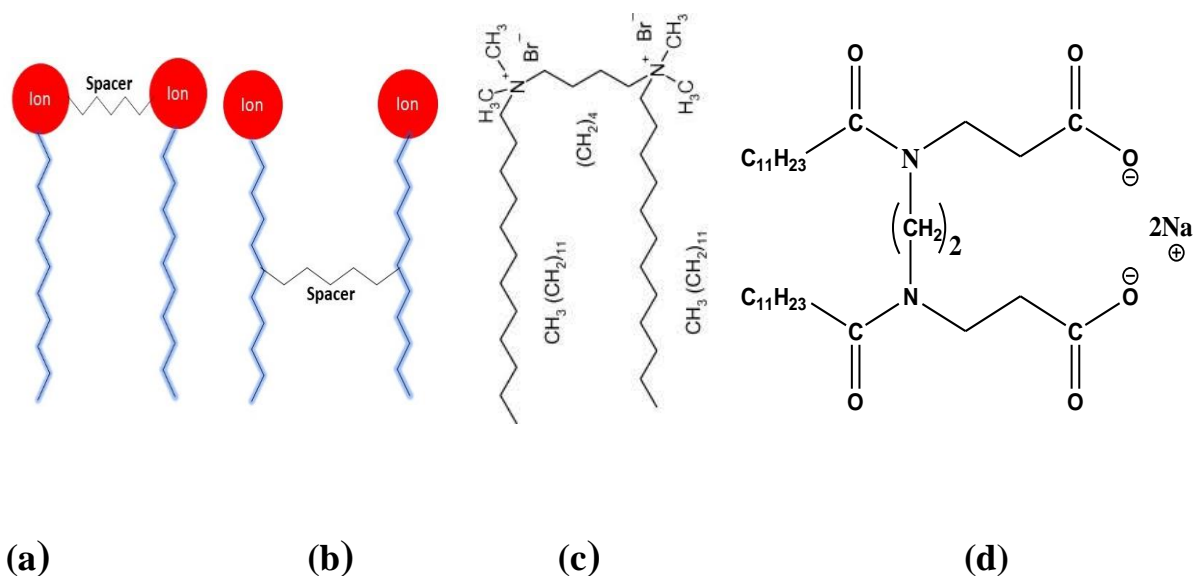


Fig. 6. Different types of gemini surfactants (a and b), cationic gemini surfactant [(c): 1,3-butan-bis-(dimethyl dodecyl ammonium bromide); 12-4-12] and anionic gemini surfactant [(d):N, N'-ethylene (bis(sodium N-dodecanoyl-β-alaninate)); 212]

Fluorosurfactants

These are the distant class of surfactants where at least one hydrogen of alkane chain is replaced by F-atom. Fluorosurfactants are used in versatile applications, such as, firefighting application, biomedicines, cosmetics, adhesives etc.⁶⁶⁻⁶⁸ The surface activity of these surfactants has been detected by the number of fluorine atoms which replace the alkane hydrogens. Fluorosurfactants have greater surface activity than the traditional organic surfactants.

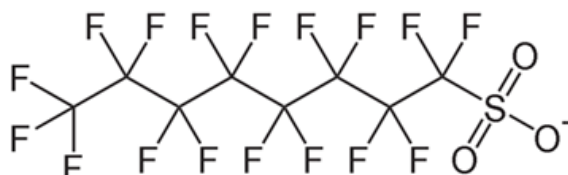


Fig. 7. Perfluorooctane sulfonate (PFOS) generally used in firefighting foam.

SILICONE surfactants

Silicone surfactants (siloxane-polyoxyalkylene copolymers) are the special class of surfactants containing permethylated siloxane hydrophobic groups in addition with one or more hydrophilic polar groups which can be anionic, cationic, nonionic or zwitterionic in nature. Nonionic groups comprising either polyoxyethylene (PEO) and polyoxypropylene (PPO) in nature are the most common. Silicon surfactants reduce surface tension effectively to 15-20 mN.m⁻¹ than the typical hydrocarbon surfactants both in aqueous and non-aqueous solvents.⁶⁹ These surfactants show unique spreading properties, thereby they have been used commonly as stabilizers in polyurethane foams, conditioner in textile, additive in ink and emulsifier in cosmetic industries.⁷⁰

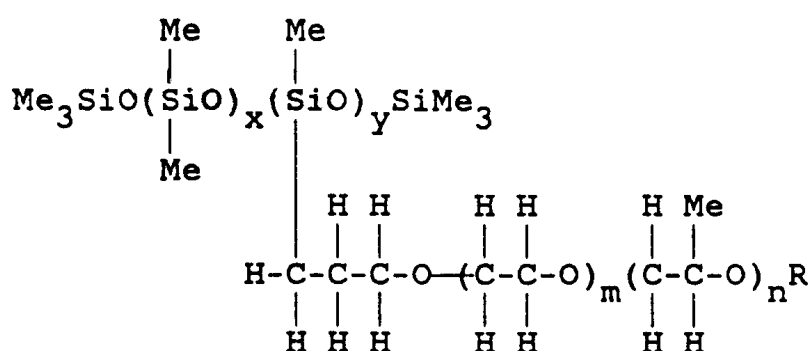


Fig. 8. General structure of silicone surfactants; x = 7 to 10, y = 2 to 5, m = 5 to 15, n = 0 to 5 and R is the alkyl group which have been selected for the compatibility of surfactants in special purpose.

There exists a balance between hydrophilicity and lipophilicity for different amphiphilic molecules depending on their structure. This is termed as hydrophilic lipophilic balance (HLB), which is essential for classification of surfactants as oil soluble or water soluble according to its relative solubility.

2. Aggregation of Surfactants

Most significant property of surfactant is to form self-aggregates in solution. Hydrophobic parts of surfactants can make favourable contact to each other at bulk to avoid unfavourable interaction of them with polar solvents, resulting in the formation of arrangements at bulk where the hydrophobic tails (Fig. 9A) attract each other into an oil-like core and at the same time hydrophilic heads are exposed to the polar environment. Such self-assembly of surfactants (either small or large sized) is called micelle (Fig. 9B) and that threshold concentration of surfactants above which micelles are formed called Critical Micelle Concentration (CMC). Micellization is a dynamic process in which free surfactant molecules are in equilibrium with micelles. Micelles are colloidal dimensions. Self-assembly of surfactants in solution was first anticipated by McBain in 1913.⁷¹ Although that time he was harshly criticized by a group of scientists in a meeting of Royal Society in London, later it was scientifically established that surfactant can practically aggregate in solution which was proved by its superior detergency properties by which they easily remove dirt and dissolve it to its hydrophobic core. The driving force of micelle formation is mostly hydrophobic in nature generated between the hydrophobic tails; apart from that, electrostatic and van der Waals forces have played major role for ionic surfactants by binding the counterions to the oppositely charged micellar heads to neutralize the charge and concomitant the repulsion between head groups. Positive entropy contribution plays a significant role in the micellization process as the loss of entropy due to aggregate of the surfactant monomers is overshadowed by the gain in entropy by the free water molecules that were "trapped" in the solvation cage around the surfactant monomers through H-bonding interaction among them.⁷² Basically, CMC which is addressing 'inexact' but 'convenient' is not a particular surfactant concentration, rather than a narrow range of surfactant concentrations.⁷³ Depending on microenvironments and nature of surfactants, micelles can be obtained in different shapes discussed elsewhere.

Reverse micelles are formed in a solution in which the content of a non-polar solvent (e.g., alkanes, haloalkanes, aromatic solvents etc.) is maximum than the polar one (just like water droplets in oil system) and surfactants are used to stabilize the components in solution as the

amphiphiles form aggregates. This method was used for the formation of one type microemulsion.⁷⁴ In reverse micelle (Fig. 9C), polar head groups are oriented to inner micellar core (which have been termed as Water pool, designated 'W' in Fig. 9C) around the water molecules, while the hydrophobic parts are exposed outside the non-polar solvents. Reverse micelles are in nanometre dimensions and their size can be increased by increasing water content in solution. These water pools of reverse micelles are used for synthesis of nano materials⁷⁵ and solubilization of proteins⁷⁶.

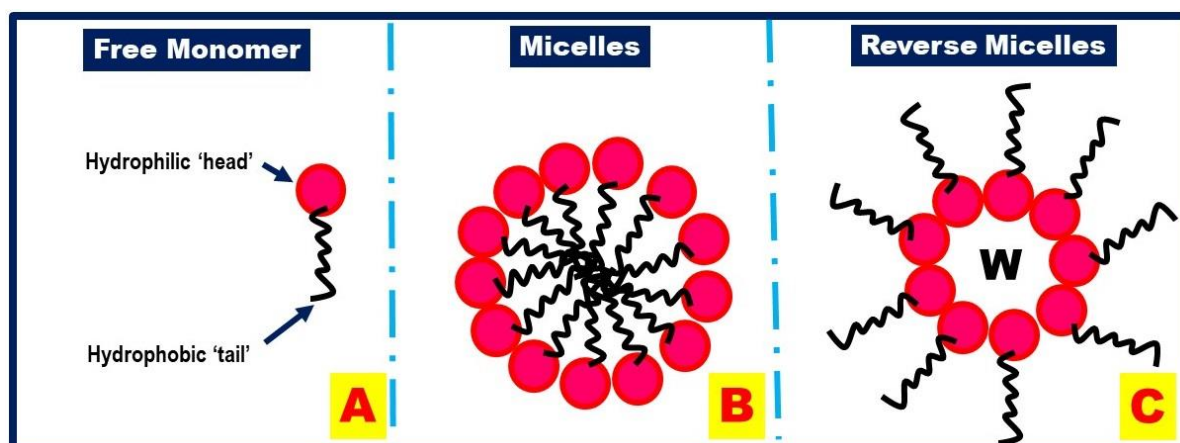


Fig. 9. Aggregates of surfactants in solution: (A) free monomer, (B) normal micelle (spherical structure), (C) reverse micelle.

3. Determination of CMC

CMC is the most fundamental property of surfactants. There are numerous methods existing in literatures for the determination of CMC. For instance, in accordance with Mukerjee and Mysels,⁷⁷ there are 71 possible methods which they have been taken from literatures and have critically discussed each method. The appropriate choice of methods however, depends on the availability of instruments, personal preference of investigator and the relationship between the technique and the ultimate application. A virtuous number of methods can be used for the determination of CMC, viz., conductometry, tensiometry, viscometry, vapour pressure osmometry, turbidimetry, light scattering, fluorimetry (steady state fluorimetry, steady state anisotropy and time resolved fluorimetry), calorimetry, spectrophotometry, magnetic resonance etc. Among them, the methods used most frequently are tensiometry, conductometry

and fluorimetry. Conductometry methods are only applicable for ionic surfactants. Physical properties of surfactants in solution are measured using different techniques with variation of surfactant concentration showing a distinct feature in appearance of different plots in different methods (Fig. 10).

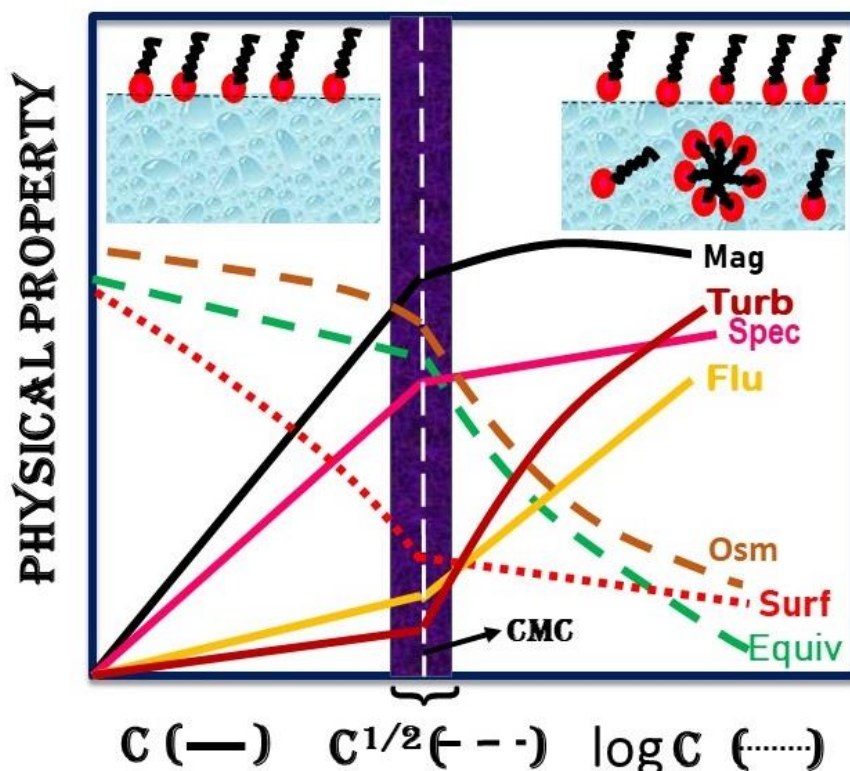


Fig. 10.

Evaluation of CMC of a surfactant with variation of surfactant concentration (C) by different methods: viz., Mag: magnetic resonance; Turb: turbidimetry; Flu: Fluorimetry; Spec: spectrophotometry (plotted against C); Surf: surface tension (against log C); Equiv: equivalent conductance; Osm: osmotic coefficient (against $C^{1/2}$).

All physical properties show the distinct breaks which are considered as CMC denoted by the dotted white line. It is to be noted that CMC is not just a point but rather a narrow range (shown by a narrow bar denoted by a second bracket), as CMC is method dependent. Significant increase of scattering radiation above CMC using light scattering method⁷⁸ manifests the direct evidence of large assemblies after CMC, as this scattering phenomenon depends on the size of scattering units in solution. Another important proof for compactness of surfactant monomers in micelle has been made after focusing the self-diffusion of monomers after CMC by nuclear

magnetic resonance (NMR) study.⁷⁹ Both light scattering and magnetic resonance study correct the approach of self-assembly of micellar structure which was first proposed by McBain. Isothermal titration calorimetry (ITC) study not only gives the information about CMC, but also gives the direct information about standard enthalpy of micellization (ΔH^0_{obs} , cf. Fig. 11a) and standard Gibbs free energy of micellization (ΔG^0). Pyrene (a fluorescent probe) has been widely used as a solvetochromic probe as the ratio of first (I_1) and third (I_3) vibronic peaks of pyrene strongly depend on solvent polarity. The ratio of (I_1/I_3) vs. $\log C$ has been plotted with sigmoidal fitting to determine CMC from the midpoint of sigmoid or taking intercept at the post micellar region (cf. Fig. 11b)⁸⁰ to maintain CMC values to keep close proximity with other techniques (specially conductometry). 1,6-Diphenyl-1,3,5-hexatriene (DPH) has been used as a fluorescence probe to determine CMC^{81,82} by steady state anisotropy method considering its linear structure, which helps to detect its rotation when free in solution being its dimer formation or in micellar environment. Initial decrease in anisotropy of DPH is observed with increasing surfactant concentration; then after further addition of surfactant, anisotropy remains constant [cf. Fig. 11c]. CMC has been measured from the intercept of two consecutive slopes [Fig. 11c]. It has also been mentioned that, acceptable limit for the determination of CMC (method to method variation) is within $\pm 10\%$.

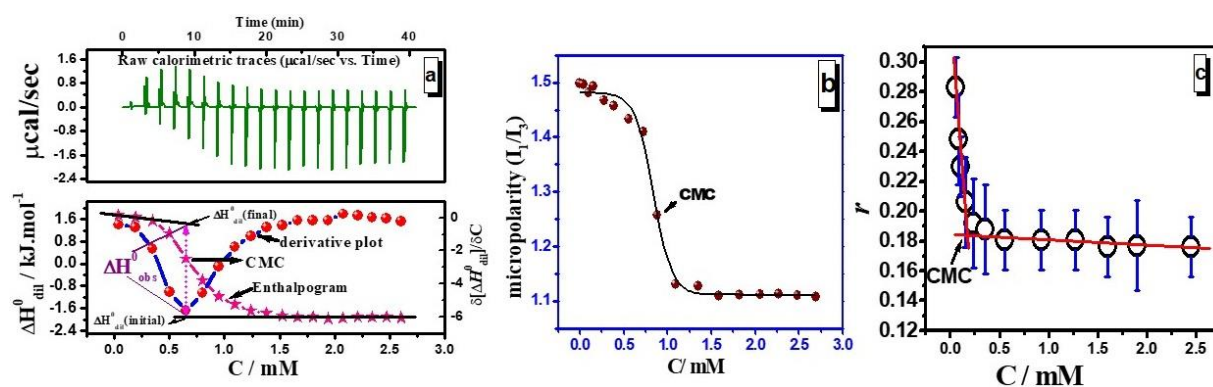


Fig. 11. Determination of CMC: (a) upper region: raw calorimetric data, lower region: enthalpy of dilution (ΔH^0_{dil}) vs. concentration (C) of surfactant. Here enthalpy of micellization (ΔH^0_{obs}) is also determined; (b) ratio of I_1/I_3 vs. C ; (c) steady state anisotropy (r) of DPH vs. C .

4. Micellar characteristics

Structures, Shapes, Microenvironment and properties of micelles: In the year 1936, Hartley⁸³ has proposed that the micelles are essentially spherical. This proposal also supports McBain's⁸⁴ idea which published in 1920. Hartley's spherical micelle model describes the micelles should contain 50-100 monomers which are associated in a relatively narrow concentration range and the diameter of this associate structure is approximately twice the length of hydrocarbon chain. Interior of micelles is essentially hydrophobic as described here, while head groups bind with a fraction of counterions to avoid the close proximity due to repulsive interaction between them. Classical Hartley model described successfully many characteristics of one surfactant system having ionic properties. Ionic micelles form electrical double layer structure⁸⁵ which exhibits electrophoresis under an electric field by virtue of its surface charge and zeta potential. 'Stern layer' is formed by the ionic micelles to the immediate environment in which head groups and oppositely charged counter ions are in close proximity through electrostatic interaction. On the other hand, 'Gouy Chapman layer' is formed around the outside of 'Stern layer' contents, both can unbind free monomers, counterions and free water molecules which solvate micelle through ion-dipole interaction. Both 'Stern layer' and 'Gouy Chapman layer' have been jointly called electrical double layer (Fig. 12). Inside 'Stern layer', there exists hydrophobic core of micelles. Both Stern layer and core jointly form the micellar kinetic part. Gouy Chapman layer is also called diffuse layer. The boundary of the diffuse layer is also described as shear or slipping plane, which can move with the micelle in solution. The slipping plane potential (Fig.12) is called zeta potential (ζ) which is often used to designate the stability of colloidal dispersions. Micellar solution in which zeta potential values are beyond ± 30 mV in magnitude is called stable solution. In case of nonionic micelles, some water molecules arrest inside the core just in the close proximity of head groups (palisade layer) through the H- bonding interaction with polyethylene oxide groups.

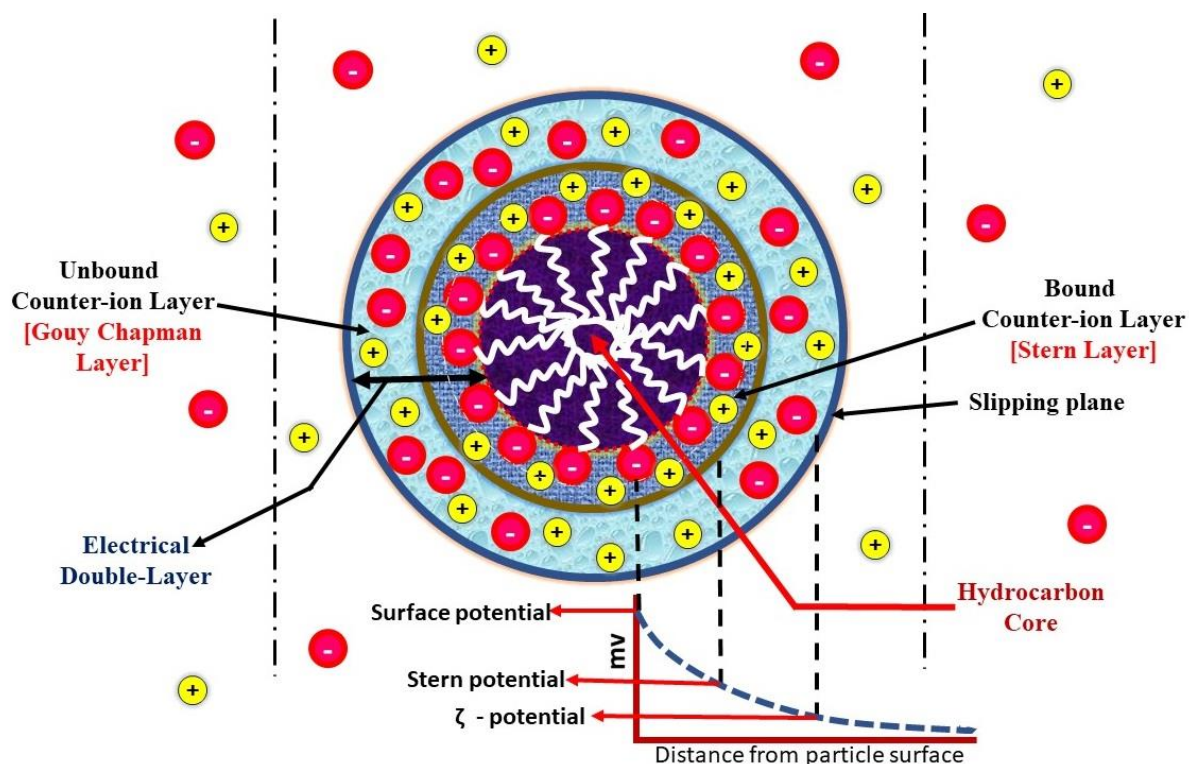


Fig. 12. Schematic representation of ionic micelles demonstrating counter ion binding, charge neutralization, micellar core and electrical double layer assuming spherical symmetry of micelle.

Using Hartley's concept as a starting point, modern science has developed more convenient microscopic picture of micelles, outcome is that of course micelles are not static. Rapid interchange of molecules between micelles and solution phase is possible. If we design a high-resolution camera or freeze the motion of molecules, then we can find micelles as irregular molecular cluster rather than smooth, perfectly uniform. Hartley's simple 'two-states' spherical micellar model has opened a criticism as several experimental facts cannot be explained by this model. Menger⁸⁶ have proposed a molecular model that differs substantially from Hartley⁸³ in point of view of solubilization of non-polar substances to micelles. Menger's 'porous cluster' model⁸⁶ states that water molecules penetrate inside a micelle upto a certain distance (3-4 methylene carbon atoms after the head group); i.e., greater ease of penetration inside the micelle and a relatively smaller interior or core supported by NMR and fluorescence measurements.

Apart from classical spherical micelle, other proposed geometry is rodlike micelle of Debye,⁸⁷ lamellar type of Philippoff,⁸⁸ disk or cylindrical structure of Harkins,⁸⁹ worm-like structure,⁹⁰ ellipsoid shape,⁹¹ and spherical bilayer (vesicle)⁹² structure. Israelachvili *et al.*⁹³,⁹⁴ proposed the concept of packing parameter to distinguish the different supramolecular assemblies form in solution. The amphiphile packing parameter (P) of micelle can be evaluated from the following equation:

$$P = \frac{\vartheta}{Al_c} \quad (1)$$

ϑ is the volume of hydrophobic chain (nm^3) assuming it as incompressible and l_c is the maximum effective length of hydrophobic chain of an amphiphile (nm). A is the surface area of headgroup at micellar-solution interface ($\text{nm}^2/\text{molecule}$). n_c is the number of carbon atoms in the hydrophobic chain. For pure amphiphiles, the effective length and volume of hydrophobic chain are calculated using Tanford's formula.^{95, 96}

$$l_c \leq l_{max} \approx (0.154 + 0.126 n_c) \text{ and } \vartheta = (0.0274 + 0.0269n_c) \quad (2)$$

where, l_{max} is the maximum length of the monomer chain.

Packing parameter values for different aggregates are tabulated as follows:

Aggregates	P
Micelles	< 0.333
Non-spherical aggregates	$0.333 < P < 0.50$
Bilayers and vsicles	$0.5 < P < 1$
Inverted aggregates	> 1

Some aggregated molecular geometries have been seen in Fig. 13.

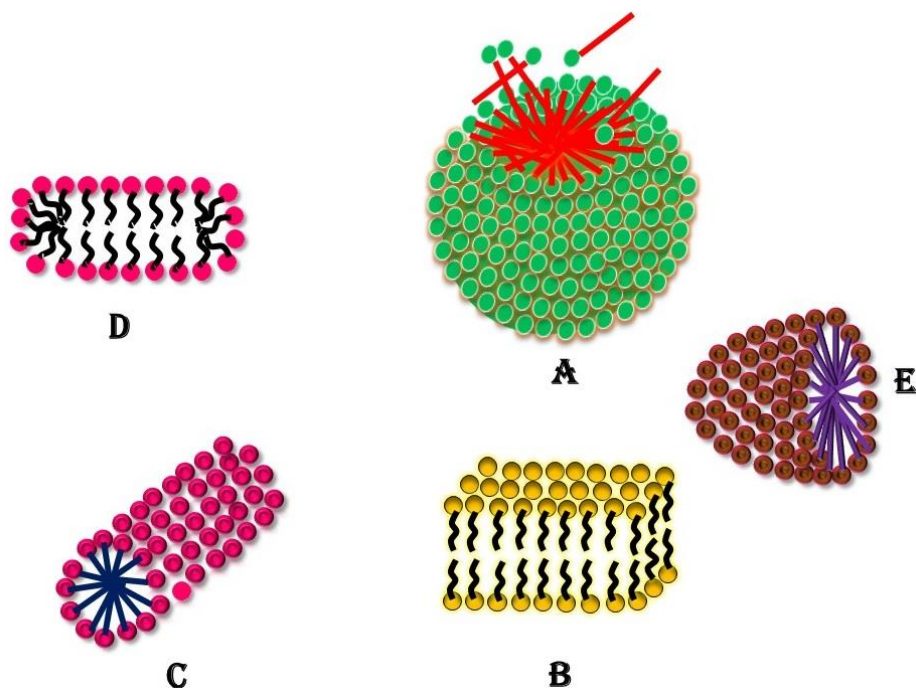


Fig. 13. Schematic representation of geometrical forms of aggregates. A: spherical micelle; B. lamellar or bilayer arrangement; C: rodlike micelle, D: wormlike or cylindrical micelle and E: oblate ellipsoid (bisected) micelle.

Modern technological developments lead us to obtain the images and experimental proof of different types of micelles. DLS (dynamic light scattering) method gives us first-hand experience of micellar size (average hydrodynamic diameter) and diffusivity by considering the size distribution assuming spherical micelles⁹⁷ without distinguishing the micellar real shape. Micellar shape and also size can be determined using static light scattering (SLS), small angle neutron scattering (SANS), small angle X-ray scattering (SAXS), Cryo-transmission electron microscopy (cryo-TEM) and atomic force microscopy (AFM) techniques.⁹⁸⁻¹⁰¹ Cryo-TEM is the only technique that can distinguish between linear and branched micelles. Shapes of micelles undergo transition in presence of various inorganic and organic salts. Few examples have been listed here in support of spherical to cylindrical and spherical to wormlike or rod like transitions: transformation of sodium dodecyl sulfate micelles from spherical to cylindrical conformation in presence of concentrated NaCl solution;¹⁰² Na₂SO₄ induced transformation of sodium alkylbenzenesulfonate from spherical to cylindrical micelles and finally multilamellar vesicle at high salt concentration;¹⁰³ cetyl trimethyl ammonium bromide, cetyl pyridinium chloride micelles transform to wormlike micelle in presence salicylate salts^{104, 105} etc.

Aggregation number: Number of molecules which aggregate in micellar assembly is called aggregation number (n). Classical method for the determination of aggregation number had been introduced by Debye¹⁰⁶ using elastic light scattering technique. Intensity of scattered radiation at different angles below and above CMC has been measured for the determination of average aggregation number as well as average molecular weight (M_w) of the aggregates. Other technique which has been employed for the determination of aggregation number as well as hydrodynamic diameter, is namely, laser light scattering.¹⁰⁷⁻¹⁰⁹ Another important technique which is much popular even for the present time is the fluorescence quenching of a luminescent probe by a hydrophobic quencher.^{110, 111} Distribution of probe and also quencher amongst micelles follow Poisson statistics, describe one probe which resides in a micelle predominately quenched by a quencher. Surfactant solutions were prepared well above their CMC and probe concentration has been fixed both in quencher and micellar solution. The ratio of [probe] to [micelles] and [quencher] to [micelles] values kept lower enough to ensure Poisson distributions. Both probe and quencher should be chosen in such a way that both resides on micellar interiors or at least at the surface. In the fluorescence technique, the probes not only interact with micellar system giving information about aggregation number, but also it determines the polarity of micellar core, its immediate environments and the equilibrium of substrate-micelle interaction. Probes frequently chosen for the determination of mean aggregation number are pyrene, anthracene sulphonate, safranin-T, fluorescein etc.; on the other hand, quenchers have been used like, cetylpyridinium chloride, dodecyl pyridinium chloride, thiourea, inorganic complex of Ru^{2+} , Cu^{2+} , Ni^{2+} etc. Mean aggregation number can be estimated by both steady state and time resolved fluorescence methods on depending the nature of quenching either static or dynamic. Static quenching method is used extensively (in which method it is assumed that increasing quencher concentration may decrease the emission of probe located on micelle, but does not change its life time) using the following relation,

$$\ln \frac{F}{F_0} = \frac{n[Q]}{[Surf]-CMC} \quad [3]$$

where F and F_0 are the fluorescence intensities in presence and absence of quencher, [Surf] is the total concentration of surfactant, [Q] is the quencher concentration, n is the average aggregation number at CMC. Plot of $\ln (F/F_0)$ vs. [Q] readily yields the value of n from the slope.

In case of dynamic quenching in which the increasing quencher concentration changes the lifetime of a probe along with the decrease in fluorescence intensity, the above equation gives the erroneous result in aggregation number values. It is seen that mean aggregation number determined by steady state measurement is found lower than those calculated in time resolved method specially for the system of relatively large micro viscosity and lower aggregation number.¹¹² Fluorescence decay curve of micelle solubilized probe in presence of ‘immobile’ quencher shows the different nature than the free probe located on the same micelle. Under such situation, fluorescence decay curve in presence of quencher can be fitted by the following equation:^{111, 113, 114}

$$I_t = I_0 \exp \left\{ -\frac{t}{\tau_0} - R[1 - \exp(-k_Q t)] \right\} \quad [4]$$

I_t and I_0 are the fluorescence intensities at time t and zero respectively. k_Q is the first order quenching rate constant. τ_0 is the lifetime of a probe in absence of quencher. R can be written as, $R = \frac{[Q]}{[Micelle]}$; $[Micelle]$ is the concentration of micelle. R values are adjusted close to 1 and not exceeded to 2 for theoretical consideration.¹¹⁵ Taking the value of R , average no of aggregation number (n) can be calculated at a particular quencher concentration $[Q]$ using the following relation:

$$n = R \frac{([Surf] - CMC)}{[Q]} \quad [5]$$

Light scattering experiment prove overestimate to mass and hence the volume of micelles as this experiment includes solvation and also counter ion binding to the micelles. Comparing both fluorescence and light scattering study, it is possible to estimate solvation and counterion binding. Size and dispersity of micelles can be governed by several internal and external factors:

- (I) *Internal factor*: Greater the length of hydrocarbon chain length of a homologous series of surfactants, larger the number of aggregation number. Recent study¹¹⁶ evaluates that micelle aggregation number increases linearly by nearly 16 monomers per micelle with single increase of each carbon atom to alkyl group. On the other hand, decrease in hydrophilicity of head group, e.g., greater the degree of ion binding, shorter polyoxyethylene group etc causes the increase in aggregation number (n). Tanford⁹¹ predicted to increase micellar aggregation number to

maximum for a given alkyne chain length for spherical and ellipsoid structures over a given ellipticity ranges. It is seen that ¹¹⁷ increase of spacer length of gemini surfactants from 2 to 12, decreases aggregation number from approximately 48 to 11 in aqueous solution at 298.15K. So, it is obvious that, increase in effective head group size (relatively bulky head groups) decreases the aggregation number. The aggregation number of bile salt micelles can have lower ^{118, 119} of 4-10. Aggregation numbers of cationic surfactants vary within 20-100 in aqueous solution.

- (II) *External factors:* With increasing salinity of the medium, aggregation number decreases, as increase in salt concentration or higher pH screens the head group charges of surfactant monomers residing at the Stern layer and consequently increases micellar aggregation number than those measured in pure aqueous solution.^{112, 120} Although, increase in temperature slightly decreases aggregation number of ionic surfactants, but the significant increase in aggregation number of nonionic surfactants is due to ‘cloud point’ phenomenon.¹²¹ Addition of slight amounts of non-amphiphilic organic compound of little solubility will often produces an apparent increase in micellar size although that may be more an effect of solubilization than an increase in number of surfactant molecules present in the micelle.

Degree of counterion binding: Counterions are the integral part of the micelles,^{122, 123} to the stern layer of micelle. Degree of counterion binding is essential parameter to know the electrical double layer and also for the calculation of thermodynamic parameters for the micellization process. Extent of degree of counterion binding (g) varies from 20–80% depending on amphiphiles, solution media, additives etc. Counterion binding can be determined by various methods, of which, the most popular method is conductometry measurement.

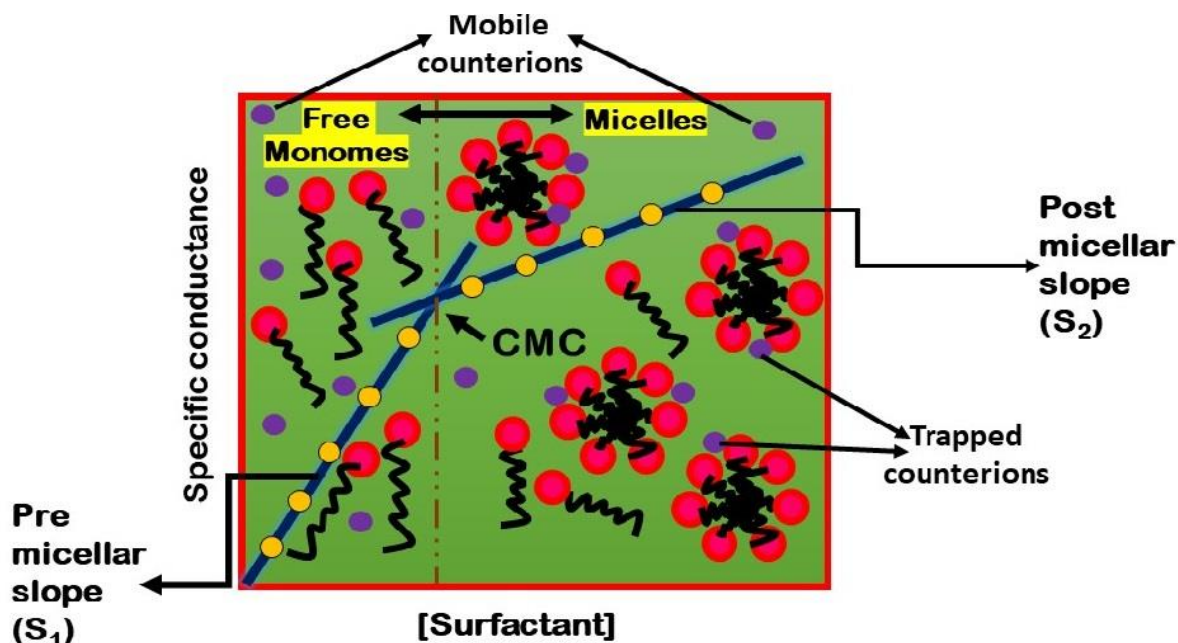


Fig. 14. Specific conductance vs. [Surfactant] profile for determination of CMC and degree of counterion binding using pre (S_1) and post micellar (S_2) slope.

Initially, at low surfactant concentration, free surfactant monomers with counterions both contribute to specific conductance value. With increasing surfactant concentrations, the increasing proportion of both monomer and counterions increase specific conductance value monotonously (shown in Fig 14). However, after micellization, some counterions bind to the micelles and formed micelles become less mobile due to larger size. The only contribution to specific conductance values is a smaller number of free monomers and unbound counterions (Fig.14), leading to offset of specific conductance values. Due to this conductometric phenomenon two distinct slopes of separate magnitude (S_1 and S_2) are found and these are used in a simple relation to determine degree of counterion binding (g), as follows,

$$g = 1 - \frac{S_2}{S_1} \quad (6)$$

Although this method is based on some assumptions, it is quite good indeed and uncertainty of the degree of counterion binding is within the acceptable error range (approximately 2-3%).

Another important technique is to determine degree of counterion binding (g) by measuring CMCs of surfactants at various salt concentrations of different salts (different added counterions). The plots of $\log(\text{CMC})$ vs. $\log C_i$ yield g by using the following equation,¹²⁴ where C_i is the total counterion concentration in molarity unit:

$$\log(CMC) = -g \log C_i + \text{constant} \quad (7)$$

Apart from above two methods, electrochemical method¹²⁵⁻¹²⁷ has been used for measuring degree of counterion binding. In this process, activities of counterion ($a_{ion\pm}$) have been measured by an ion selective membrane electrode coupled with a standard electrode (Ag/AgCl or calomel) forming a cell. The following equation can be used:

$$a_{ion\pm} = g a_{ion\pm}^{BP} + (1 - g) a_{ion\pm}^{DH} \quad (8)$$

where $a_{ion\pm}$, $a_{ion\pm}^{BP}$, and $a_{ion\pm}^{DH}$ are the activities of the surfactant from membrane electrode potential (E_M), break point of activity-concentration curve and Debye-Hückel equation respectively. Membrane electrode potential is given by the following equation,

$$E_M = K_M^0 \pm \frac{RT}{F} \ln a_{ion\pm} \quad (9)$$

K_M^0 being constant, depends on electrode system. But again, it has been ascertained that, conductance method is the simplest and quite popular than the other two.

5. Factors affecting micelle formation and CMC

The hydrophobic group: Micelle formation becomes easier in solution with greater hydrophobicity of nonpolar tail part, and has been evidence in case of increased alkyne chain length in a homologous series;¹²⁸ thus hydrocarbon chain length shows major influence on CMC.¹²⁹ In fact, CMC decreases in a logarithmic pattern as the number of carbon atoms increases in hydrophobic part in a homologous series of carbon number, n_c . With the addition of each methylene group, for straight chain hydrocarbon surfactants, CMC usually reduced to approximately one half of its previous value of about 16 carbon atoms or less bound to a single terminal head group. However, this is more pronounced for nonionic surfactants in which CMC value decreases by a factor of 3 upon addition of one more methylene group to the chain¹³⁰ without any additives. Different effects on CMC have been observed by the insertion of phenyl or other linking groups, polar substituent groups on the hydrocarbon chain, branching on hydrophobic tail etc. Klevens¹³¹ had given a mathematical relation between the hydrocarbon chain length and CMC, as,

$$\log_{10} CMC = A - B n_c \quad (10)$$

where, A and B are constants to homologous series under constant condition of temperature and pressure, etc. Although B is fairly constant with a magnitude approximate to $\log 2$ for all the paraffin salts belonging single ionic head group, A is different for each type of head group. However, B has the different value for the system of two different head group and for the nonionic surfactants.

Polarity of the medium: Polarity of the medium favour surfactant association. When polarity of the solvent decreases, CMC value will decrease. It has been seen that CMC increases in general for all types of surfactants in different volume fractions of polar organic solvent (acting as cosolvent which has dielectric constant values either greater or less than water) in comparison with purely aqueous medium.^{132, 133} Polarity of the medium also influences the formation of the different aggregates. Normal micelles have been formed in sufficiently polar medium, while reverse micelles are formed in nonpolar medium with a trace amount of water contents.

Temperature: The CMC values of the most ionic surfactant go through a minimum as variation of temperature from 0 to 60-70°C.¹³⁴⁻¹³⁶ Although nonionic and zwitterionic surfactants have not so predictable minimum CMC with variation of temperature, some nonionic have been shown CMC minimum.¹³⁷ The possible minimum value of CMC with increase in temperature may be addressed in terms of degree of hydration of head groups and hydrophobic tails. There are two factors contributing with increase of temperature, at lower range, desolvation of water structure around surfactant hydrophilic groups before CMC-minimum leading to earlier micellization and in the higher temperature range (after CMC-minimum), the breakdown of water structures from the surfactant hydrophobic tails, which is unfavourable in the process of micellization, leading to CMC at high surfactant concentration. The desolvated head groups also promote repulsive type interaction among them as the mobility of the counterions increases at higher temperature. In this connection, it is said that surfactants have characteristic temperature, known as 'Krafft temperature', which is essential to understand the phase behaviour of surfactant solutions at different temperatures. Fig. 15, displays such phase diagram. In this diagram, there exists three distinct zones, A, B and C, which have been designated as free surfactant monomers in solution, monomers in equilibrium with micelle and coexistence of monomers and precipitate (crystals) in solution respectively. At point P, all the three phases remain coexist, the temperature corresponds to this point P called Krafft temperature (T_k). To avoid precipitation of crystal formation, working solution temperature should be above T_k .

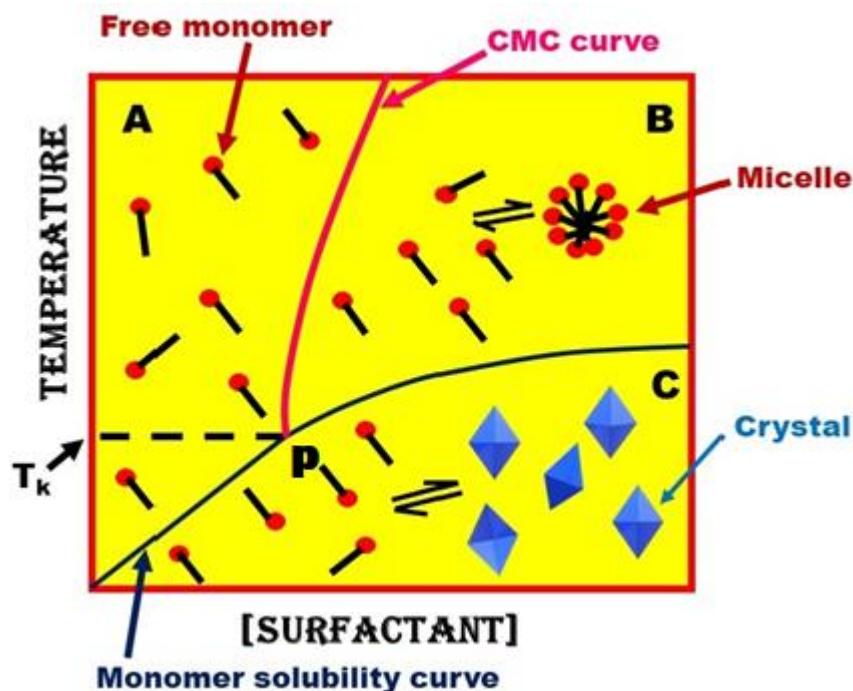


Fig. 15. Temperature vs. [surfactant] profile showing different state of aggregations of surfactant monomers in solution and the Krafft temperature (T_k)

Pressure: The consequence of pressure^{138, 139} on self-aggregation of surfactants has been discussed. CMC increases initially with increase of pressure and finally decreases at high pressure region. The turnover of CMC at high pressure region has been observed for all kinds of surfactants. It is seen that the threshold pressure in which CMC is maximum, varies from surfactant to surfactant, lied between 75-150 MPa range. In the low-pressure region, the applied thrust destructs water structure to support wider distribution of surfactant monomers in solution to oppose their tendency to aggregate, while at high pressure, the monomers associate to micelle to the change of dielectric constant of the medium. This has been supported by the measurement of aggregation number, which shows a minimum for ionic surfactants and a rapid initial decrease for nonionic surfactants with respect to pressure.

Electrolyte effect: Electrolytes effectively reduced CMC for ionic surfactants mainly. Less effect has been observed for zwitterionic and nonionic surfactants. The effect of added electrolytes with the same charge as the native counterion of surfactants on studying the micellization of ionic surfactant¹²⁴ has been empirically quantified by the following relation;

$$\log_{10} CMC = -a \log_{10} C_{salt} + b \quad (11)$$

where a and b are constants for a given head group for a particular temperature and C_{salt} is total concentration of monovalent counterion in molarity unit. The decrease of CMC has been shown more pronounced in presence of bivalent or trivalent counterions than the monovalent counterion of same salt type for ionic surfactants. Enhanced counterions in presence of added electrolytes effectively screen the head group charge of monomers at the micellar interface and consequently, less electrostatic repulsion between the surfactant monomers at the same time reduces CMC. Sometimes, relative reduction of CMC of an ionic surfactant by different electrolytes of different valencies may be explained by the effective nuclear charge (change to radius ratio of hydrated counterions), valency or hydration ability of counterions in solution and sometimes may not. It has been said that, counterions have specific effect for individual surfactants, yet not properly understandable.

In case of nonionic and zwitterionic surfactants, the impact of electrolytes on micellization process is significantly less. In this connection, Shinoda¹⁴⁰ has proposed an empirical relation between CMC of nonionic/zwitterionic surfactants with added electrolyte concentration (C_s) in molarity unit:

$$\log_{10} CMC = -\alpha C_s + \text{constant} \quad (\text{for, } C_s < 1) \quad (12)$$

where, α is a constant for a specific surfactant, nature of salts and temperature.

Electrolyte effect on the micellization of nonionic and zwitterionic surfactants and the observed change in CMC cannot be explained by the same perception of electrostatic screening model those appearing in fully ionic surfactants (discussed above). Solubility of many materials in water can be effectively altered by addition of electrolytes. Addition of such electrolytes can reduce (salting out) or increase (salting in) solubility for a material in solution depending on nature of electrolytes. For zwitterionic and nonionic surfactants, added salt will decrease solubility (salting out) if salt acts as a water structure breaker and CMC will decrease; on the other hand, if added salts make the water structure (salting in), solubility of surfactants increase and as well as CMC. Organic materials (non electrolytes) also increase or decrease CMC in the micellization process of surfactants.¹⁴¹⁻¹⁴³ So, to sum up, it has been said that interaction phenomenon of different inorganic/organic salts with various surfactants may influence on solvent structure, polarity of the medium and also on electrostatic interaction, still remaining a matter of further investigation.

Counterion of surfactants: It is not surprising that CMC decreases with the increase of degree of counterion binding (g), as the ionic head groups face repulsive interaction at the micellar interface. From the outcome of regular solution theory, it is said that the extent of pairing of counterion increases with the increase of polarizability and valency, although a larger radius of hydration will result in ion separation. It is seen that the extent of decrease of CMC of a surfactant depends on the hydrated radius of its counterions; the more the hydrated radius, less efficient its tendency to decrease CMC. In general, it is found that for a given hydrophobic tail and a polar head, CMC decreases in the order, $\text{Li}^+ > \text{Na}^+ > \text{K}^+ > \text{Cs}^+ > \text{N}(\text{CH}_3)_4^+ > \text{N}(\text{CH}_2\text{CH}_3)_4^+ > \text{N}(\text{CH}_3\text{CH}_2\text{CH}_3)_4 > \text{Ca}^{2+} \approx \text{Mg}^{2+}$ for anionic surfactants (like, surfactant of dodecyl sulfate salts,^{144, 145} while for a cationic surfactant (e.g., cetyltrimethylammonium bromide¹⁴⁶) CMC decreases by the anionic counterions shown in the order (formers are more efficient than latters): $\text{PO}_4^{3-} \approx \text{Citrate}^{3-} > \text{SO}_4^{2-} \approx \text{Oxalate}^{2-} > \text{I}^- > \text{Br}^- > \text{Cl}^- > \text{F}^-$.

Effect of pH: Solution pH has relatively less effect on the industrially important surfactants having long alkyl chain length of strong acid. Unlike the salt of strong acid, significant pH effect has been observed on carboxylate acid surfactants as the carboxylate groups are not fully ionized near or below pK_a . Since head group repulsion rendered surfactants to aggregate and it is controlled by the variation of pH, CMC is changed. When pH of the solution remains near or above pK_a of alkyl ammonium salts, CMC decreases. pH has no effect on the CMC of nonionic surfactant. However, at very low pH, there is a possibility of protonation of ether oxygen of polyoxyethylene surfactants and eventually, the characteristics of the system is changed.¹⁴⁷

6. Cloud Point:

Nonionic surfactant shows temperature instability. At relatively higher temperature, nonionic surfactants lead to formation of aggregate in solution (not like micellar aggregate) due to dehydration of polar moieties. As a result, the conformational change of polyoxyethylene moieties is possible and turbidity appears. The average threshold temperature at which turbidity (phase separation) appears on heating and disappears on cooling is called Critical Solution Temperature (CST) of cloud point (CP) of surfactant.¹⁴⁸⁻¹⁵¹ Clouding phenomenon of some uncharged polymers having appreciable hydrophobicity is also found in literature.¹⁵²⁻¹⁵⁴ Although clouding phenomena of individual nonionic surfactants, viz., triton X-100, brij 56, alkyl (linear, branched and cyclic) phenyl ethoxylates, igepal etc., block copolymers, methyl cellulose in water have been amply investigated in past, present time witnesses the investigation of CP originating from the combination of surfactants, polymers or both polymer

with surfactant in presence of other additives¹⁵⁵⁻¹⁶¹ and also variation of solvents. Both increase and decrease of cloud point have been observed for particular nonionic surfactant or uncharged polymers in comparison to their native states in aqueous solution with the influence of additives. Normally, water structure breaking species increase CP and water structure forming species decrease CP.¹ The presence of both CP (one is upper critical solution temperature (UCST) and another is lower critical solution temperature (LCST) has been reported for triblock copolymer (pluronics).¹⁶² The effect of nonionic surfactants on the clouding phenomena of neutral polymers has been described by Flory-Huggins theory^{163,164} relating to the structure of surfactants during phase separation and temperature effect on aggregation number. Cloud point temperature for nonionic surfactants, as well as ionic surfactants combined with nonionic surfactant or combination of uncharged polymers (including proteins) with various surfactants (including lipids, amphiphilic drugs etc.) is very much essential in clinical preparations especially for drug immobilization, biomedical formulations, industrial extractions, enhanced oil recovery process,¹⁶⁵⁻¹⁶⁸ where certain temperature is need to be adjusted for formulation of materials.

7. Thermodynamics of micellization:

Micellization process is energetically controlled by thermodynamic principles. During micellization of surfactant, the so called ‘iceberg’ structure around the surfactant monomer disrupts with a resultant increase in entropy.^{169,170}

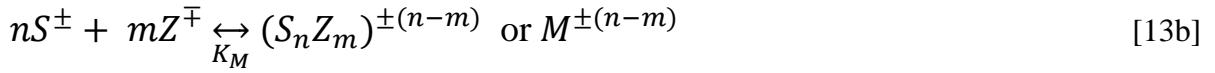
Two approaches have been used extensively in classical literature and these are accepted as useful models of micellization: (i) the mass action model, and (ii) the phase separation model or pseudo phase model.^{149,171}

❖ According to the mass action model, after CMC, monomer and micelles are interdependent to each other as with the increase of monomer concentration, micelle concentration also increases and vice versa according to the following equilibrium:



for a nonionic surfactant, S, S_n, n and K_M denote surfactant monomers, micelles, aggregation number and equilibrium micellization constant respectively.

In case of ionic surfactants, while studying micellization, the above equilibrium takes the new equilibrium incorporating the charges and counterions:



for a ionic surfactant, where Z^{\pm} and m denote counterions and no of counterions are attached to the micelle in the above equilibrium process.

Hence, it is written as, for nonionics, neglecting activity effect,

$$K_M = \frac{a_M}{a_S^n} \approx \frac{C_M}{C_S^n} \quad [13c]$$

where, a is the activity coefficient and C is the concentration.

For ionic surfactants,

$$K_M = \frac{a_M^{\pm(n-m)}}{a_{S^{\pm}}^n a_{Z^{\mp}}^m} \approx \frac{C_M^{\pm(n-m)}}{C_{S^{\pm}}^n C_{Z^{\mp}}^m} \quad [13d]$$

For nonionic surfactants, standard Gibbs free energy of micellization can be given by the following relation:

$$\Delta G_M^0 = -RT \ln K_M = -RT \ln C_M + nRT \ln C_S \quad [14]$$

Change of standard Gibbs free energy of micellization per monomeric unit (n) can be presented as:

$$\frac{\Delta G_M^0}{n} = \Delta G_{mic}^0 = -\frac{RT}{n} \ln C_M + RT \ln C_S \quad [15]$$

At CMC, percentage of monomers forms micelles which are very small. Hence, the eq. 15 can be approximated as:

$$\Delta G_M^0 = RT \ln C_S = RT \ln CMC \quad [16]$$

For ionic surfactants,

$$\Delta G_M^0 = -RT \ln K_M = -RT \ln C_M^{\pm(n-m)} + nRT \ln C_S^{\pm} + mRT \ln C_Z^{\mp} \quad [17]$$

Therefore, it can be written as standard Gibbs free energy change per monomeric unit in the following form:

$$\frac{\Delta G_M^0}{n} = \Delta G_{mic}^0 = -\frac{RT}{n} \ln C_M^{\pm(n-m)} + RT \ln C_S^{\pm} + \frac{m}{n} RT \ln C_Z^{\mp} \quad [18]$$

Again, as the percentage of monomers is very small and usually n is large, the eq. 18 is transformed as

$$\Delta G_{mic}^0 = RT \ln C_S^\pm + \frac{m}{n} RT \ln C_Z^\mp \quad [19]$$

For normal ionizable surfactants, it can be written as

$$C_S^\pm = C_Z^\mp \quad [20]$$

$$\text{Hence, at CMC, it is obviously, } C_S^\pm = C_Z^\mp = CMC \quad [21]$$

$$\text{so that, } \Delta G_{mic}^0 = \left(1 + \frac{m}{n}\right) RT \ln CMC = (1 + g) RT \ln CMC \quad [22]$$

where, g is the fraction or degree of counterion binding.

If $g = 0$, there is no counterion binding in case of nonionic surfactant,

$$\Delta G_{mic}^0 = RT \ln CMC \quad [23]$$

On the other hand, if 100% counterions are bound, $g = 1$ and the Eq. 22 takes the form:

$$\Delta G_{mic}^0 = 2RT \ln CMC \quad [24]$$

The above relation is based on constant condition of aggregation number (n) and several valid approximations.

- ❖ Pseudophase model is based on the assumption that, micelles are considered to constitute a new phase at or above CMC and concentration of monomers remains invariant at or above CMC.

According to Pseudophase model, the following equilibrium can be conferred based on phase equilibrium: **monomer** \leftrightarrow **micelle (Pseudophase)** [25]

At a constant temperature, chemical potential of free surfactant monomers (μ_S) in solution is equal to chemical potential of surfactant monomers in pseudo micellar phase ($\mu_S^{micelle}$).

Thus, for nonionic surfactant,

$$\mu_S = \mu_S^{micelle} \text{ or } \mu_M \quad [26]$$

The eq. 26 can be written for nonionic surfactant,

$$\mu_S^0 + RT \ln a_S = \mu_M^0 + RT \ln a_M \quad [27]$$

$$\text{or, } \Delta G_m^0 = \mu_M^0 - \mu_S^0 = RT \ln a_S \approx RT \ln CMC \quad [28]$$

Since, a_M (activity of micelle considering it as a separate pure phase or pseudo phase) = 1,
in case of ionic surfactant,

$$\mu_S^\pm + \frac{m}{n} \mu_Z^\mp = \mu_M^\pm \quad [29] \quad \text{as, } \mu_S = \mu_M$$

Therefore, the eq. 29 is transform to

$$\mu_{S^\pm}^0 + RT \ln a_{S^\pm} + \frac{m}{n} \mu_{Z^\mp}^0 + \frac{m}{n} RT \ln a_{Z^\mp} = \mu_{M^\pm}^0 + RT \ln a_{M^\pm} \quad [30]$$

$$\text{Or, } \left[\mu_{M^\pm}^0 - \left(\mu_{S^\pm}^0 + \frac{m}{n} \mu_{Z^\mp}^0 \right) \right] = RT \ln a_{S^\pm} + \frac{m}{n} RT \ln a_{Z^\mp} - RT \ln a_{M^\pm} \quad [31]$$

$$\text{hence, } \Delta G_m^0 = RT \ln a_{S^\pm} + \frac{m}{n} RT \ln a_{Z^\mp} - RT \ln a_{M^\pm} \quad [32]$$

$$\text{Since, } a_{M^\pm} = 1, \Delta G_m^0 = RT \ln a_{S^\pm} + \frac{m}{n} RT \ln a_{Z^\mp} = \left(1 + \frac{m}{n} \right) RT \ln CMC \quad [33]$$

$$\text{Or, } \Delta G_m^0 = (1 + g) RT \ln CMC \quad [34]$$

In the equations [29] to [33], μ_M^\pm is actually $\mu_M^{\pm(n-m)}$; the factor (n-m) has been neglected for simplicity.

We get the same equation for ΔG_m^0 from pseudophase model that we get from mass action model. μ_S^0 and μ_M^0 are the standard chemical potentials of monomer and micelle respectively, and, a_S and a_M are the activities for the same respectively. Here, it is noted that, for the above two methods, equilibrium concentration of free monomer (C_S) is considered to be equivalent to CMC.

In case of mass action model, including the contribution of aggregation number (n)¹⁷², standard Gibbs free energy of micellization (ΔG_{mic}^0) and standard enthalpy of micellization (ΔH_{mic}^0) can be expressed by,

$$\Delta G_{mic}^0 = (1 + g) RT \ln X_{CMC} + \frac{RT}{n} \ln[2n(n + m)] \quad [35]$$

$$\text{and, } \Delta H_{mic}^0 = -RT^2 \left[(1 + g) \frac{d \ln X_{CMC}}{dT} + \ln X_{CMC} \frac{dg}{dT} + \frac{d \left[\left(\frac{1}{n} \right) \ln \{ 2n(n+m) \}}{dT} \right] \right] \quad [36]$$

CMC has been expressed in mole fraction (X_{CMC}) unit in the above two equations. Here, g is the number of counterion binding and n is the aggregation number. Usually, the second and third terms of equations [35] and [36] are small. In the pseudophase model, the terms can be conceptually avoided.

Thus, for ionic micelles,

$$\Delta H_{mic}^0 = -RT^2 \left[(1 + g) \frac{d \ln X_{CMC}}{dT} + \ln X_{CMC} \frac{dg}{dT} \right] \quad [37]$$

and for nonionic micelles,

$$\Delta H_{mic}^0 = -RT^2 \frac{d \ln X_{CMC}}{dT} \quad [38]$$

Entropy of micellization (ΔS_{mic}^0) can be calculated from Gibbs- Helmholtz equation,

$$\Delta S_{mic}^0 = \frac{\Delta H_{mic}^0 - \Delta G_{mic}^0}{T} \quad [39]$$

CMC should be measured at different temperature in order to evaluate ΔH_{mic}^0 and ΔS_{mic}^0 using equations 35 to 39, whichever is applicable for different systems. ΔS_{mic}^0 values are normally positive. Negative entropy contribution due to amphiphilic association in micelle or the solvation of monomers are overshadowed by the disruption of iceberg structure around the monomers to take them into micelle, this process in terms increase the overall entropy.

It may be mentioned that for calculation of thermodynamic parameters, CMC should be converted in mole fraction unit (stated earlier). The van't Hoff method is used to calculate standard enthalpy of micellization (ΔH_{mic}^0) by measuring the CMC values at different temperatures using the equation 38. By using ITC (isothermal titration calorimetry), both CMC and ΔH_{mic}^0 can be measured directly. Determination of ΔH_{mic}^0 using calorimetry method gives the exact value with high precision of accuracy.¹⁷³⁻¹⁷⁶ The enthalpies determined by van't Hoff method (by determining CMC at different temperatures) are generally found dissimilar with those calculated by direct method, especially for ionic surfactants.¹⁷⁷⁻¹⁸⁰

Neither the mass action model nor the pseudophase model for micellization of surfactant is precisely correct. In both approaches, it is considered that equilibrium free monomer concentration during micellization process is equivalent to CMC. It is also conveniently considered that, both the aggregation number and degree of counterion binding are independent on temperature or at least independent within the investigated temperature range. Despite these limitations, these two models are the simplified version to determine thermodynamic parameters.

Besides these two above models, there are also some other approaches. A thermodynamic model is developed by Hill¹⁸¹ for small system and applied by Hall and Pethica to nonionized and noninteracting systems.¹⁴⁹ Hall¹⁸²⁻¹⁸⁴ has developed detailed treatment of multicomponent system of interacting aggregates. Corkill and coworkers¹⁸⁵⁻¹⁸⁷ has been proposed another thermodynamic approach for nonionic surfactant systems. Tanford¹⁸⁸ has proposed an interesting model for micelle formation based on micelle shape. This geometrical approach is extended by Israelachvili *et al.*⁹³ and is further developed by Ruckenstein and Nagarajan.¹⁸⁹

Several variables such as, change in aggregation number, micellar shape and size, counter ion condensation and micellar solvation with variation of temperatures and other environmental changes provide challenges to determine thermodynamic parameters with absolute precision making this topic worthy of further investigation.

8. Theory of mixed micelles:

In aqueous solution, two or more surfactants exhibit rich interfacial properties, such as, decrease of CMC, higher surface activity, increase of intensity of scattered radiation, etc., compared to their individual components. Mixed micelles are formed in solution by active participation of both surfactants (Fig. 16) and formed micelles after CMC; are in equilibrium with individual monomeric species.⁹ Low concentration of mixed surfactants mixture has been allowed to the treatment of potential skin irritation.¹⁹⁰ As the smaller number of surfactants can be required to form mixed micelle, it is also beneficiary for the environment as the amount of surfactant release.¹⁹¹ Mixed micelle has enhanced the substantial absorption of hydrophobic drugs in human body.^{192, 193} It is interesting to observe that equimolar mixture of cationic and anionic surfactants may form insoluble ion pair, they get solubilized if the proportion of one component is appreciably higher than other in solution. Vesicle like structure has also been reported in literatures by the conjugation of catanionic surfactants.¹⁹⁴⁻¹⁹⁶ Mixture of cationic

and anionic surfactants can be used for the use of cleansing product to reduce water hardness.¹⁹⁷ Mixed micelles of ionic-ionic,¹⁹⁸⁻²⁰⁷ ionic-nonionic,²⁰⁸⁻²¹⁴ and nonionic-nonionic²¹⁵⁻²¹⁷ combinations have been reported in literature; among them, nonionic-nonionic and cationic-cationic combinations are rare. Mixed micelle formation of surface active ionic liquid (SAIL) in combination with anionic,²¹⁸⁻²²⁴ amphiphilic drugs,²²⁵⁻²²⁹ cationic^{9, 230-237} and nonionic surfactants^{21, 238-243} have also been studied significantly.

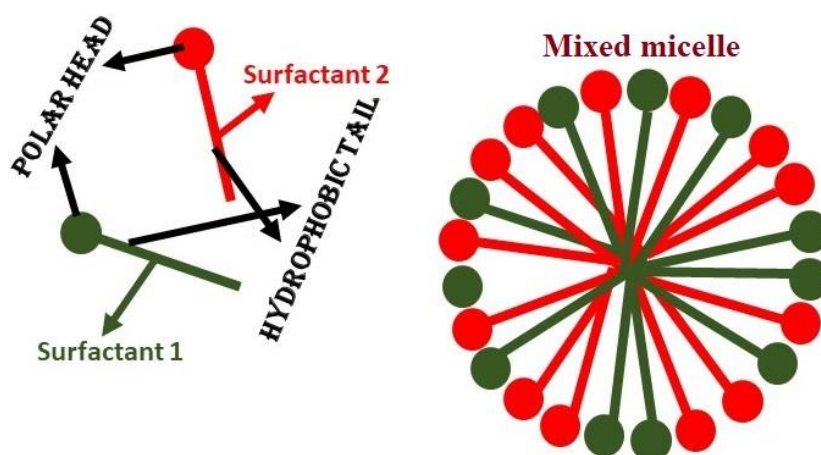


Fig. 16. Schematic representation of a mixed micelle formed by two ionic surfactants (Surfactant 1 (olive green) and Surfactant 2 (red)).

A simple theory is proposed by Clint²⁴⁴ to determine CMC assuming the ideal mixing by the monomeric amphiphiles during mixed micelle formation. The proposed relation made by Clint's²⁴⁴ assumption is given here:

$$\frac{1}{(CMC)_{max}} = \sum_i \frac{\alpha_i}{(CMC)_i} \quad [40]$$

where, α_i and $(CMC)_i$ are the stoichiometric mole fraction and CMC of i^{th} component respectively. If the mixing of surfactant components forming mixed micelle is not ideal, eq. [40] takes the form:

$$\frac{1}{(CMC)_i} = \sum_i \frac{\alpha_i}{f_i (CMC)_i} \quad [41]$$

where, f_i is the activity coefficient of the i^{th} species.

Clint's²⁴⁴ theory provides an adequate description where nearly ideal mixing might be expected, i.e., homologous series of surfactants with similar head groups; but on the other hand, fails to predict either $(CMC)_{max}$ or the monomeric compositions in the mixed micelle formed

by different head group of surfactants. In this connection it has been noted that a theory which is based on Regular Solution Theory (RST) provides a way to deal with both enthalpic as well as entropic factors in the mixed micelle formation. Prediction of this theory gives the satisfactory result with the experimental CMCs ($(CMC)_{max}$) on the compositions of ionic-nonionic or nonionic-nonionic mixed micelle.

Lange²⁴⁵ developed an equation for binary mixtures of nonionics which accurately described CMC-dependence upon bulk composition assuming ideal mixing, *i.e.*, the only contribution to the free energy of mixing came from the entropy change upon mixing of two surfactant species within the micelle. A similar treatment was also developed independently by Lange²⁴⁶ and Shinoda²⁴⁷ assuming ideal mixing for homologous pair of ionic surfactants. Later, Moroi and coworkers²⁴⁸ have extended Lange-Shinoda approach of ionic and nonionic surfactants. Theories were developed in mid to late seventies^{248, 249} to account for micellar mole fraction, activity coefficient, extent of interaction among the surfactants in mixed micelles. Rubingh²⁴⁹ formulated a theoretical approach to relate monomer concentration to micellar molefraction of surfactants. Although satisfactory result found to explain a micellar system,^{250, 251} Rubingh²⁴⁹ theory was criticized on thermodynamic grounds. Motomura *et al.*²⁵⁰ proposed a mixed micellar theory claiming to be a better description of mixed surfactant solution. In the early nineties, Sarmoria *et al.*²⁵² and Puvvada *et al.*²⁵³ have developed a molecular thermodynamic model (SPB model) for mixed surfactant systems. Majority of the studies which describe mixed micellar system till now have been based on Rubingh²⁴⁹ theory as it includes a specific interaction parameter (β) measuring the interaction between surfactants either synergistic or antagonistic. Rubingh treatment is itself simpler than SPB model.

Rubingh's treatment on binary mixtures:

If two surfactants 1 and 2 form mixed micelle, the mole fraction of surfactant 1 can be estimated from the known values of CMC of individual surfactants, C_1 and C_2 and the CMC of mixed micelle, C^* and stoichiometric mole fraction of surfactant 1 (α) in the total mixed solute.

List of symbols:

μ_1 = chemical potential of monomeric surfactant 1

μ_1^0 = standard chemical potential of monomeric surfactant 1

μ_{1M} = chemical potential of 1 in micelle

μ_{1M^0} = chemical potential of 1 in pure micelle

C_1^m and C_2^m = concentration of monomeric surfactants 1 and 2

f_1 and f_2 = activity coefficient of surfactants 1 and 2 in mixed micelle

x = mole fraction of surfactant 1 in mixed micelle.

The chemical potential of monomeric component 1 in mixed micelle solution can be written as:

$$\mu_1 = \mu_1^0 + RT \ln C_1^m \quad [42]$$

and chemical potential of component 1 in mixed micelle is

$$\mu_{1M} = \mu_{1M^0} + RT \ln f_1 x \quad [43]$$

By using a phase separation model of micellization, we can write for component 1 in the pure micelle,

$$\mu_{1M^0} = \mu_1^0 + RT \ln C_1 \quad [44]$$

As, at equilibrium since $\mu_1 = \mu_{1M}$, we obtain from Eq. [42], [43] and [44] that for component 1,

$$C_1^m = x f_1 C_1 \quad [45]$$

Similarly, for component 2, we may write,

$$C_2^m = (1 - x) f_2 C_2 \quad [46]$$

Below C^* , the concentration of component 1 is given by,

$$C_1^m = \alpha C \quad [47]$$

here, C is total surfactant concentration of surfactants 1 and 2 in solution.

Similarly, for component 2, we can write,

$$C_2^m = (1 - \alpha) C \quad [48]$$

At the mixed CMC (C^*), by considering the Eqs. [45], [46], [47] and [48], it can be written

$$\alpha C^* = x f_1 C_1 \quad [49]$$

$$(1 - \alpha) C^* = (1 - x) f_2 C_2 \quad [50]$$

Eliminating x from equation [49] and [50], we can write,

$$\frac{1}{C^*} = \frac{\alpha}{f_1 C_1} + \frac{1 - \alpha}{f_2 C_2} \quad [51]$$

Since, $f_1 = f_2$ (ideal approximation), then Eq. [51] reduces to,

$$\frac{1}{C^*} = \frac{\alpha}{C_1} + \frac{1 - \alpha}{C_2} \quad [52]$$

Equation [52] is derived by Lange, Beck and Clint.

On the other hand, we can eliminate C^* between the two equations ([49] and [50]) to get the mole fraction of component 1 at CMC (Eq. [53]),

$$x = \frac{\alpha f_2 C_2}{\alpha f_2 C_2 + (1 - \alpha) f_1 C_1} \quad [53]$$

Relationships of monomer concentrations valid above CMC can be developed from the following relation:

$$x = \frac{\alpha C - C_1^m}{C - C_1^m - C_2^m} \quad [54]$$

Substituting C_1^m and C_2^m from Eqs. [45] and [46] to Eq. [54], one can get a quadratic expression of x ; upon solving yields the following value of x .

$$x = \frac{-(C - \Delta) + \sqrt{(C - \Delta)^2 + 4\alpha C \Delta}}{2\Delta} \quad [55] \quad \text{where, } \Delta = f_2 C_2 - f_1 C_1$$

Finally, using [45] again, the monomer concentration of component 1 can be written explicitly,

$$C_1^m = \frac{-(C - \Delta) + \sqrt{(C - \Delta)^2 + 4\alpha C \Delta}}{\left(\frac{f_2 C_2}{f_1 C_1}\right) - 1} \quad [56] \quad \text{and, } C_2^m = \left(1 - \frac{C_1^m}{f_1 C_1}\right) f_2 C_2 \quad [57]$$

Although, Eqs. [56] and [57] correct the expression for micellar composition and monomer concentrations, remain incomplete without some relation between activity coefficients in micelle and micellar composition. Regular solution approximation can be used to determine activity coefficient of monomers in mixed micellar state.

$$f_1 = \exp \beta (1 - x)^2 \quad [58] \quad \text{and, } f_2 = \exp \beta x^2 \quad [59]$$

This parameter β (stated earlier) is also molecular interaction in mixed micelle,

$$\beta = \frac{N (W_{11} + W_{22} - 2W_{12})}{RT} \quad [60]$$

where, W_{11} and W_{22} are the energies of interaction between surfactant molecules in pure micelles and W_{12} is the interaction between two species in mixed aggregate. N is Avogadro number. It can be demonstrated within regular solution context, the excess enthalpy (H_E) is given by,

$$H_E = \beta RT x (1 - x) \quad [61]$$

Since, β cannot be 0, this model considers both enthalpy and entropy (for ideal mixing) contribution in mixed micelle formation. If β is negative, then it can be said that the interaction between surfactants is synergistic in mixed micelle and reverse is true for antagonistic type interaction. β can be calculated using the following relationships in terms of C_1 , C_2 , α and C^* ,

$$\frac{x^2 \ln\left(\frac{C^* \alpha}{C_1 \alpha}\right)}{(1-x)^2 \ln\left(\frac{C^* (1-\alpha)}{(1-x)}\right)} = 1 \quad [62]$$

Eq. [62] is solved iteratively for x , and substitution of x into equation [63] yields the immediate solution of β .

$$\beta = \ln \left[\frac{\left(\frac{C^* \alpha}{C_1 \alpha}\right)}{(1-x)^2} \right] \quad [63]$$

Mixed micellization studies have been attempted in details by several workers.^{246, 253-257} CMC values for the mixtures of alkyl sulphate anions^{246, 258} and also quaternary ammonium cations²⁵⁹ have been studied. Moroi *et al.*²⁴⁸ and others²⁶⁰⁻²⁶² have been studied the mixtures of ionic and nonionic surfactants to evaluate CMC. Although it has been seen that CMCs for mixed surfactant systems lies in between the CMC of pure surfactants, several studies show that CMC of mixed surfactant system are even higher than pure parent components.²⁶³⁻²⁶⁵

9. Interaction of macrocycle with surfactants:

An enormous attention has been focused in the synthesis of aza-crown compounds in the past and preceding years. The aza-crowns have intermediate complexation properties between those of the all-oxygen bound crowns which have strong intake affinity towards alkali and alkaline

earth metal ions, and those of the all-nitrogen bound cyclams, which are strongly bound with heavy-metal cations inside its cavity due to less electronegativity and strong complexing ability of N over O atom. These have important uses as artificial receptors in molecular recognition processes²⁶⁶ and in some cases, complexation of anions which have close similarity with the ions found in definite biological systems.²⁶⁷⁻²⁶⁹ Thus, the introduction of biological entities into the crown ether macromolecules has provided researcher with an even greater insight into biological ionophores, such as, macrolide antibiotics, cyclic peptides etc.^{270, 271} These crown-based macrocycles have also an enhanced complexing ability for ammonium salts,^{272, 273} through H-bonding²⁷⁴⁻²⁷⁷ and for transition-metal ions^{273, 278} over the crowns containing only oxygen atoms. An extensive number of aza-crowns have been synthesized; among them, benzo aza-crowns have been studied broadly on its complexation affinity towards main group and also transition metal ions since its discovery in the mid-1970s.²⁷⁹⁻²⁸² Surfactant mediated assemblies in solution have great potential applications in routine life. The simplest assembly is termed as micelle and the corresponding surfactant concentration abbreviated as critical micelle concentration (CMC).²⁸³ These micellar properties are affected by influence of several additives, i.e., non-polar and polar organic compounds, small number of electrolytes, etc.²⁸³. Recently, increasing effort is being emphasized to the study of the assimilation or solubilization of neutral molecules into micelle in aqueous solution. Although, a lot of studies have already been reported on the complexation properties of crowns with various cations, anions and neutral organic molecules, less attention has been devoted on the interaction of crowns with surface active agents²⁸⁴⁻²⁸⁸ in both pre and post micellar regime and majority of them (surfactants) are anionic in nature. The inclusion of crown macromolecules to the surfactant solutions during micellization results to the formation of inclusion complexes mediated by crown with oppositely charged counterions of surfactants or simply association with monomeric and aggregated form of surfactants, and as a result, these crowns alter the adsorption of surfactants at interfaces and also influence in bulk micellization process.

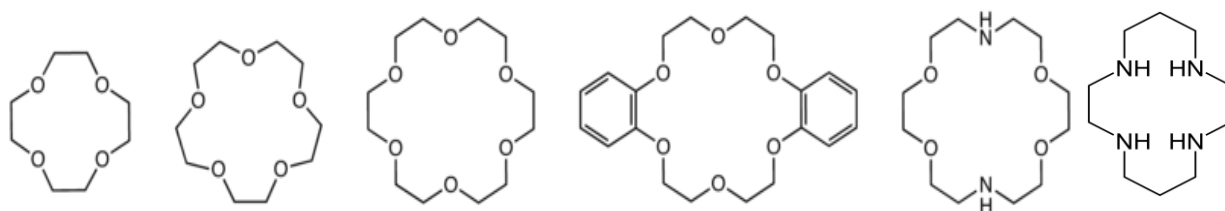


Fig. 17. Structures of common crown ethers (from left to the right): 12-crown-4, 15-crown-5, 18-crown-6, dibenzo-18-crown-6, diaza-18-crown-4, and, Cyclam (1,4,8,11-tetraazacyclotetradecane)

10. Uncharged and Charged (Polyelectrolyte) Polymers and Proteins & their interaction with surfactants:

The word '*polymer*' came from a Greek words; *poly*,- 'many' and *mer*,- 'part', suggesting a large molecule or a macromolecule formed by many repeating subunits joined together normally by covalent bonds. This combination process of repeating subunits is called polymerization. These repeating subunits are called monomers. But the monomers sometimes are not at all intact in the polymer chain. This often creates confusion or misconception with the term 'polymer' due to inconsistency of monomers. For example, polyvinyl alcohol is a highly versatile polymer but there is, in fact, no such monomer as vinyl alcohol. To address this inconsistency of monomers in polymer chain, Hermann Staudinger in 1920 introduced the term 'macromolecules'²⁸⁹ meaning 'large molecules' (macro in Greek means large) for such polymeric compounds and it is now used almost interchangeably with the word polymer. If -A- is the structural unit, then a macromolecule or polymer molecule is represented by:



where n is an integer, defined as the degree of polymerization of the macromolecule. Polymer molecules were generally considered as physical assemblies of uncharged monomers, so these are called associated colloids before 1930. The variety of their molecular compositions and also altered physicochemical properties make them useful in many pharmaceutical, industrial, technical and medical purposes. Improvement in formulations have been obtained, much need in industry, by the use of current synthetic methodologies and through the understanding of the molecular interactions in conjugation with polymers and the other components of a care product. The macromolecules generally found in nature including proteins, carbohydrates, nucleic acids are known as bio-macromolecules or biopolymers²⁹⁰ whereas, widely used plastics, rubbers and adhesives are the synthetic polymers.

Proteins are the functional form of polypeptides. Proteins are biopolymers built from amino acids. Proteins contain more than 50 amino acid residues. There are 20 amino acids that are common to all living organisms on Earth. These are all α -amino acids having the amine group attached to the (alpha-) carbon atom next to the carboxyl group in conjugation with unique side chains (aliphatic, acyclic, aromatic, containing hydroxyl or sulphur, etc.). All the naturally occurring amino acids are L-amino acids (chiral), with the exception of glycine (achiral). Many of the constituent amino acids can act as either weak acids or bases depending

on pH, or contain polar groups (hydrophilic character) that may be partly dissociated if the side chain is polar or hydrophobic, if it is nonpolar in nature. So, the protein charge can be easily tuned by varying the solution pH. It is seen that above the isoelectric point (pI), the net charge of protein is negative and below it is positive. At their isoelectric point pI, which is the pH at which proteins have zero net charge, proteins adopt their most compact conformations and also less water soluble. The specific function and structure of each protein depends on its amino acid sequence, which is called the primary structure. A polypeptide chain, therefore, has a N-terminal (amine group of first amino acid) and a C-terminal (carboxyl group of last amino acid) section.^{29 291-293} A polypeptide chain when assembles into two dimensions, the structure is called secondary structure. Typical secondary structure motives can be classified into α -helices and β -sheets. Folding of these motives into the three-dimensional space results in the fully functional form of protein, called native structure, and the structure is called tertiary structure. The quaternary structure is the assembly of folded proteins into larger functional complexes. Proteins are generally surface active. Proteins can be stabilized by the hydrogen bond, disulphide bridges, electrostatic interaction, complex formation with metal ions, and by the hydrophobic effects among the amino acid residues that favours a folded conformation overcoming the entropy disadvantage. The proteins can undergo both specific and non-specific interactions with different kind of substance, and minor to major structural or configurational changes of protein may arise by such interactions under various environmental constraints, viz., pH, temperature, pressure, additives, etc.

Polymer classification:

Polymers are categorised according to their source of availability and structure of monomer chain. According to the source of availability, there are three types of polymers as natural, synthetic and semi-synthetic polymers. Carbohydrates (inulin, cellulose, alginate, starch, glycogen), proteins (collagen, silk, keratin), natural rubber and DNA are in the class of natural polymers. Polyethylene, polyvinyl chloride, polystyrene etc., are in the group of synthetic polymers whereas cellulose nitrate, acetate (rayon) are semi-synthetic polymers.

The polymers can be classified on the basis of their chemical structures as shown in Fig 18. Homopolymers comprise of identical bonding linkages to each similar monomer unit. Copolymers are usually indicating two or more different types of monomer units. Furthermore, depending on the arrangement of the types of monomers in the copolymer chain, the following classifications can be shown (Fig.18): (i) In random copolymers, two or more different repeating units are distributed randomly, (ii) Alternating copolymers are comprises of

alternating sequences of the different monomers, (iii) In block copolymers, the sequences of monomer are afterwards sequences of another monomer, (iv) Graft copolymers consist of a chain which are formed by one kind of monomers with branches of another type.

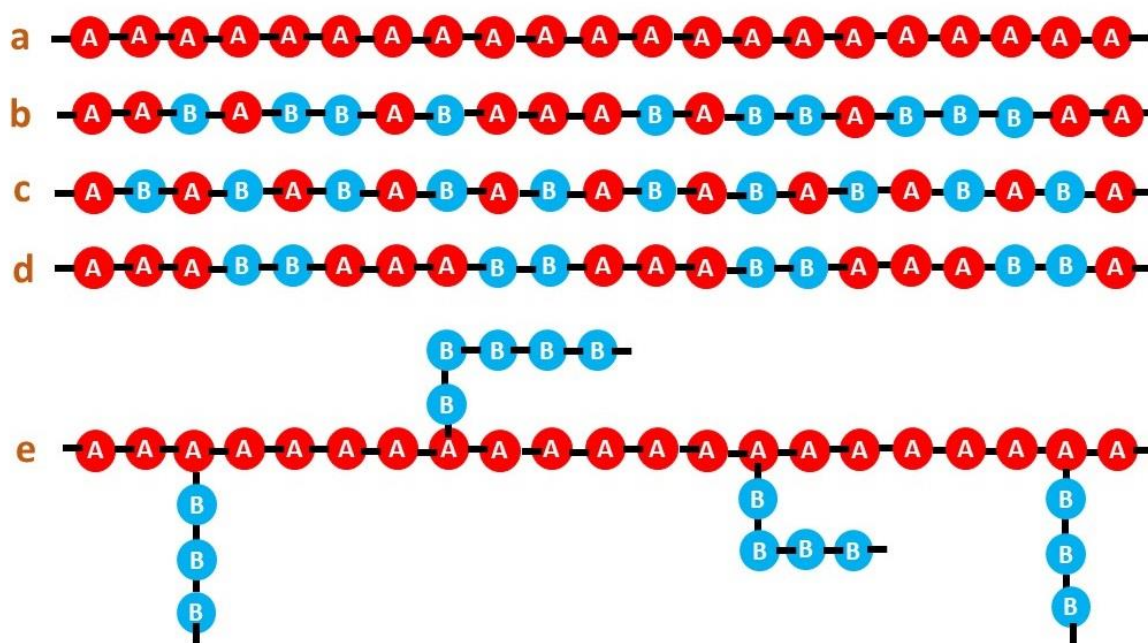


Fig. 18. Types of polymers (a) homopolymer (b) random copolymer (c) alternating copolymer (d) block copolymer, and (e) graft copolymer.

On the basis of the ionic charge of the monomeric groups, the polymers can be further classified as: nonionic (polyethylene oxide, polyethylene glycol), anionic (sodium carboxymethylcellulose, polyacrylic acid, sodium alginate, sodium polystyrene sulfonate) and cationic (polyDADMAC) polymers. Charged polymers are called polyelectrolytes. These have both conductive properties in aqueous solution like salts and viscous properties like polymers. Biological molecules such as polypeptides, DNA can be classified as polyelectrolytes. Recently, polyelectrolytes have gained significant interest as thickeners, conditioners, dispersant agents, ion-exchanger, emulsifiers, and clarifying agents. Significant attention has been paid for elucidating the properties of natural polyelectrolytes (e.g, alginate, carboxymethyl cellulose, starch etc.) in the pharmaceutical and food processing industries as their biodegradable and biocompatible properties.

Polymers can also be classified according to their structure. Normally, the constitutional units initially form a linear chain. Cyclic polymer molecules result if the two

ends of a linear polymer molecule are connected. Small amounts of cyclic molecules are often formed during the synthesis of linear chains as by-products. Combinations of linear molecules, with cyclic molecules, and of cyclic macromolecules themselves lead to a great variety of molecular designs. It can be further categorized according to their applications as rubber or elastomer (e.g., natural rubber, BUNA-S), thermosetting polymer (e.g., bakelite), thermoplastic polymer (e.g., polyvinyl chloride), plastic (e.g., nonionic), fiber (e.g., nylon) and resin (e.g., polysulphides).

Rheological and physicochemical properties of polymeric solution are obtained by the configuration of polymer chain depends on the interaction of the monomer blocks with each other and the solvent. Upon dissolution in solvent, the polymer chains implement different forms, such as, an extended configuration, a random coil, or a helical form. The polymeric chains expand in good solvents leading to significant increase in viscosity of the solution. This change in viscosity in solution depends on type of polymer, and charge density of the polymer (in case of ionic polymer or polyelectrolytes), polymer concentration and molecular weight of the polymer. The polymer molecules are mostly stringing of atoms connected to each other by covalent bonds. One can form a polymer that exhibits more than one kind of affinity or interaction by combining different kinds of monomer in the same polymeric species.²⁹⁴ The study of polymeric solutions can be essential in understanding various physicochemical properties, such as: molecular weight distribution, the charge density of ionizable polymer, polymeric chain configuration, radius of gyration, the degree of association of polymer molecule with the solvent molecules as well as the effect of other solutes present in the solution on the configuration and characterization of the macromolecule.

The electrostatic interactions between the charges on the polyion chain and those between the polyion and the surrounding counterions play very important roles in determining the behaviour of polyelectrolytes in solution, which are quite distinct from that of the non-polyelectrolytes (uncharged polymers). The conformations of polyelectrolytes in dilute solutions depend on the fraction of charged groups present on the polymers and the ionic strength of the solution. Weakly charged polyelectrolytes (or macromolecules carrying a small percentage of ionizable groups) in solution can mainly show the interplay between the non-coulombic interactions, viz., van der Waals interaction, hydrogen bonding and other molecular interactions which play an important role in governing their conformations.

Polymers are mixtures of the species of various molecular weights. The knowledge of distribution of molecular weights determines the mechanical strength of polymer and also has

been shown to be essential in many applications, including the flow of melts, adhesion, flocculation, or in aging behaviour. Owing to the difficulties in measuring a distribution of molecular weights in detail, several mathematical forms are frequently used. The individual polymer chains do not all have the same size or mass in any polymer sample. Thus, they have various average molecular weights like number average molecular weight (\overline{M}_n), mass average molecular weight (\overline{M}_w), and viscosity average molecular weight (\overline{M}_v).

They are defined as

$$\overline{M}_n = \frac{\sum_i n_i M_i}{\sum_i n_i} \quad (64)$$

where n_i is the number of molecules of molecular weight M_i .

$$\overline{M}_w = \frac{\sum_i n_i M_i^2}{\sum_i n_i} \quad (65)$$

\overline{M}_w is always greater than \overline{M}_n , the ratio of $\overline{M}_w/\overline{M}_n$ known as polydispersity index, gives an idea of molecular weight distribution. Larger values of $(\overline{M}_w/\overline{M}_n) > 2$ specify a very widespread distribution with substantial amounts of material at both extremes. A monodisperse polymer sample having a unique molecular mass, $M = \overline{M}_n = \overline{M}_w$ can be measured by osmometry where as \overline{M}_w can be measured by light scattering experiment. Another useful technique for the determination of molecular mass is the viscosity average molecular mass (\overline{M}_v). \overline{M}_v can be defined as:

$$\overline{M}_v = \left(\frac{\sum_i n_i M_i^{1+\alpha}}{\sum_i n_i M_i} \right)^{\frac{1}{\alpha}} \quad (66)$$

where ‘ α ’ is constant lying between 0.5 and 2.0. Normally, $\overline{M}_w > \overline{M}_v > \overline{M}_n$. For ‘ α ’ = 1, theoretically $\overline{M}_w = \overline{M}_v$. For a monodisperse polymer, molecular mass, $M = \overline{M}_n = \overline{M}_w = \overline{M}_v$.

Solution Properties of Polymer

Viscosity is a convenient method to characterize a polymer solution. This can be attained by measuring the clearance time “t” of a dilute polymer solution with a laminar flow through a capillary in an Ubbelohde viscometer and comparing with the time of flow for the solvent, t_0 . The relative viscosity is obtained from the flow time multiplying with the density of the solution and the solvent. The common nomenclatures in relation to the solution viscosity are given below.

$$\text{Relative viscosity: } \eta_{rel} = \frac{\eta}{\eta_0} \approx \frac{t\rho}{t\rho_0} \quad (67)$$

where, ρ and ρ_0 are the solution and solvent density, respectively. For fairly dilute solution, its density is considered equivalent to the pure solvent, therefore the relative viscosity definitions are often used in practice.

$$\text{Specific viscosity: } \eta_{sp} = \frac{\eta - \eta_0}{\eta_0} = \eta_{rel} - 1 \quad (68)$$

$$\text{Reduced viscosity: } \eta_{red} = \frac{\eta_{sp}}{C} \quad (69)$$

$$\text{Intrinsic viscosity: } [\eta] = \left(\frac{\eta_{sp}}{C} \right)_{C=0} = \left(\ln \frac{\eta_{rel}}{C} \right)_{C=0} \quad (70)$$

where η_0 and η denote the measured viscosity coefficients of the pure solvent and the solution, respectively. C is the concentration of dilute polymer solution expressed in gm dL^{-1} . The specific viscosity is a measure of the thickening effect of the polymer solution as compared to the solvent. This quantity depends on polymer concentration and hence, the reduced viscosity (η_{red}) is informative to specify a polymer system. The intrinsic viscosity is expressed in terms of the Huggins equation.²⁹⁵ Thus,

$$\frac{\eta_{sp}}{C} = [\eta] + k_H [\eta]^2 C \quad (71)$$

The plot of $\frac{\eta_{sp}}{C}$ vs C normally gives a straight line, whose extrapolation to zero polymer concentration gives the intrinsic viscosity, $[\eta]$ and from the slope we can determine k_H which is a constant known as Huggins constant. k_H is approximately 2.0 for solid uncharged spheres, both in theory²⁹⁶ and practice²⁹⁷. For flexible polymer molecules in good solvents, k_H is often near to 0.35. Somewhat higher values appear in poor solvents. The intrinsic viscosity gives an idea about the polymer configuration; its lower value suggests globular feature while for higher value, it represents open or non-globular configuration of the polymer.

However, in presence of a polyelectrolyte, we cannot determine $[\eta]$ in purely aqueous solution using Huggins equation as it is shown that at high polyelectrolyte concentration region, reduced viscosity (η_{red}) decreases with decreasing concentration of polyelectrolyte (which is similar with the uncharged polymers), while at low polyelectrolyte concentration region, η_{red} levels into a plateau and increases again with decreasing polyelectrolyte concentration. In order to address this problem for determination of $[\eta]$, it is recommended to prepare polyelectrolyte in low concentration of salt solution. Under this situation, polyelectrolytes behave like uncharged polymers.

It is observed that all the plots of $\frac{\eta_{sp}}{C}$ vs. C at different solvent media are nicely linear to yield $[\eta]$ and k_H from the intercept and slope, respectively. The intrinsic viscosity is independent on polymer concentration but depends on the nature of molecular weight of the polymer and solvent. It can be utilised to calculate the viscosity average molecular weight, \overline{M}_v from the Mark-Houwink equation: ²⁹⁸

$$[\eta] = K(\overline{M}_v)^\alpha \quad (72)$$

where K and α are constants, whose values depend on the nature of polymer-solvent system as well as on the temperature. These constants can conveniently be found for common polymer/solvent combinations in the literature. ²⁹⁹

In mixed aquo-organic solvent media, the value of $[\eta]$ is in between aqueous and organic solvent. There, structure is also varied with different mixed solvents and salt medium. ³⁰⁰ Banerjee *et al.* ³⁰¹ and Dan *et al.* ³⁰² have reported $[\eta]$ values of different gums and inulin in salt water media, respectively. Magnitude of $[\eta]$ in salt solution is lower than aqueous solution. It was proposed that in salt solution, polymer has a compact structure and it has elongated structure in mixed solvent medium. Nandi *et al.* ³⁰³ have investigated $[\eta]$ of sodium carboxymethylcellulose in aqueous solution as well as acetonitrile-water medium in presence of different ionic strength of NaCl by 'isoionic dilution' method at different temperatures. It is seen that, $[\eta]$ value is found larger in aqueous solution in comparison with mixed solvent medium and with increase in temperature.

Hydration

The outer layer of the polymer is protected through hydration; their stability, local viscosity, solubilisation, interaction, etc. are functions of hydration and the vicinal water structure. Water soluble polymers solubilize in water through hydration using their available hydrophilic centres. Different methods such as viscosity, diffusion, infrared spectroscopy, calorimetry, acoustic, light scattering, etc. can be utilized to characterize their hydration behaviour. ³⁰⁴⁻³⁰⁷ Nuclear magnetic resonance studies have also been suitable. ³⁰⁸ If the hydrated entities are constant shearing stress (as in viscosity) or are under constant influence of compression and rarefaction (as in ultrasound), the method would essentially monitor the strongly attached water molecules. The estimation of hydration by the simple non-equilibrium method of conductometry is based on the concept of obstruction ³⁰⁹ to the ionic transport offered by the hydrated polymers. When obstructed, the ions take a detour, resulting in an increase in the

overall resistance of the solution. They may, however, penetrate the loosely solvated portion of the polymer. This may lead to lowering of hydration that corresponds to the primary hydration envisaged by Frank and Evans.³¹⁰

Based on the above obstruction principle, the hydration of the polymer (or dispersion) of any shape can be quantitatively estimated by the method of conductance on the basis of the following relation:³¹¹

$$\frac{k'}{k} = 1 - 1.93 V_h \left(\frac{k'}{k}\right) c \quad (73)$$

where k' and k are the values of specific conductance in the presence and absence of obstructants, V_h is the hydrated specific volume, and c is the concentration of the obstructant, expressed in g/ mL. Therefore, a direct estimate of V_h is thus possible without assuming any shape. From the known specific volume of the water free or dry material, the extent of hydration can be estimated.

Polymer–Solvent interaction

The characteristics of polymers in solution are extremely dependent upon the quality of solvent. A dissolved polymer will encounter attractive forces between certain segments of polymer that induce cohesion. Energy must be given to the system to keep away the molecular species from their nearest neighbours. This is entitled as cohesive energy, and is associated with ΔH_{mix} the volume fractions, the volume of mixing, and the cohesive energy densities of the components:

$$\Delta H_{\text{mix}} = V_{\text{mix}}(\delta_1 - \delta_2)^2 \varphi_1 \varphi_2 \quad (74)$$

V_{mix} is termed as the volume of mixing, δ_1 and φ_1 are defined as the solubility parameter and volume fraction of the solvent respectively. δ_2 and φ_2 are the solubility parameter and volume fraction of the polymer respectively. Since ΔH_{mix} should be small for spontaneous dissolution to happen, the solubility parameters of the solvent and polymer must be as close in value as possible. In an ideal solvent, the solvent molecules have identical properties to those of the polymer and such the polymer would have analogous preference for a solvent molecule as for another polymer molecule. This results in formation of random configuration of the chains. The opposite is true a poor solvent, and the polymer chains will contract. This will influence the viscosity of solution. When the concentration of polymer in a solvent is suitably low, the polymer-polymer interactions can be ignored. As a result, a single flexible linear polymer chain having many internal degrees of freedom, may fold in various ways to curtail polymer solvent contact. This folding can produce a range of structures, such as, unperturbed or perturbed coils, wormlike coils and also structures which resembling Euclidian bodies like spheres.

Self-Assembling of Polymer

Apart from well-established ionic and nonionic surfactants, some polymers are also capable of undergoing self-assembling process when dissolved in selective solvents. Associative polymer has attracted rigorous interest from both industrial and academic viewpoints due to their wide applications in pharmaceuticals and biomedicine.³¹² The polymer usually comprises of a hydrophilic group with hydrophobic domains distributed along its backbone. Hence, when the polymer dissolves in water, clusters of hydrophobic domains are formed yielding a network structure. For the end-capped water-soluble polymer, the hydrophobic group is located at both ends of the polymer, with the hydrophilic segments separating them. Such polymer associated with strong hydrophobic segments forms flower-like micelles.^{313,314} An associative polymer represents a class of polymers that possess surfactant-like properties. They are used as thickening agents in environment friendly coating applications. Studies of the self-association of water-soluble block^{315,316} and graft^{317,318} copolymers have been found extensive interest.

The laser light scattering is an efficient technique to investigate the association behaviours of the polymer in dilute solution. Two common approaches can be used, i.e., static light scattering (SLS)³¹⁹ and dynamic light scattering (DLS)³²⁰. Through the study of SLS, the weight average molar mass (\overline{M}_w), average second-virial coefficient (\overline{A}_2), the overall geometry (shape) of the scattering species and the average radius of gyration (\overline{R}_g) can be obtained. From DLS, the translational diffusion coefficient (\overline{D}_0), average hydrodynamic radius (\overline{R}_h) and the polymer chain conformation can be determined. For example, DLS has been used to study the random association of hydrophobically modified water-soluble polymers, statistical copolymers, block copolymers composed of elastin-like and poly (ethylene glycol) (PEG) blocks, and multiblock copolymers. Marieta *et al.*³²¹ has investigated self-aggregation of a polyelectrolyte having N-alkyl-N, N-dimethyl-N-(2-hydroxypropyl) ammonium chloride based on polysaccharides by using of steady state fluorescence and viscometry techniques. Recently, Yao *et al.*³¹⁸ studied the self-aggregation behaviour and morphology of graft copolymers, oligo (9, 9-dihexyl)-fluorene-graft-poly (ethylene oxide) (OHF-g-PEO) in aqueous solutions by light scattering, steady-state fluorescence spectroscopy, time-resolved fluorescence, and transmission electron microscopy (TEM).

Interaction of Surfactant with Polymer or Protein

The interaction of polymer or protein with surfactant in aqueous solution has become a very fascinating topic due to the wide range of domestic, pharmaceutical and industrial applications,

such as, detergency, food formulations, paints, drug formulation and delivery, formulation for crop disease control, high-power solid-state batteries, cosmetics, coatings, water purification, enhanced oil recovery, etc.³²² Polymer or protein-surfactant mixtures are fundamental units of almost all biological cells. Frequently, they are used together, in particular, in complex colloidal systems to attain colloidal stability, emulsification or flocculation, structuring and suspending properties as well as rheology. In industrial applications, the surfactants act as detergents or dispersing and wetting agents, and the polymers play the unique role as thickeners in water-based formulations. The solution behaviour of polymer itself, the formation of polymer-surfactant complexes in aqueous solution and the manipulation of surfactant adsorption by polymers are active fields of interest in colloid science. Polymers are generally used as viscosity modifiers. Such a growing demand compels more investigations of polymer-surfactant interaction to enrich the practical as well as fundamental knowledge of colloid chemistry.

Three types of interactions are prevalent in polymer-surfactant systems, viz, (i) self-interaction among surfactant molecules, (ii) self-interaction among polymer molecules, and (iii) interaction between polymer and surfactant. The first two kinds can be either intermolecular or intramolecular. Depending upon the relative magnitude of the above three interactions, there may arise a number of physicochemical phenomena in polymer-surfactant system, which is a unique property of a particular polymer-surfactant complex. Surfactant-polymer interactions involve a complex balance of factors assisting and retarding association. The dominating forces can be categorized into either dispersion (van der Waals) forces, dipolar interactions (including hydrogen bonding or acid-base), coulombic (electrostatic) attractions as well as repulsions and the hydrophobic effect.³²³ While the electrical processes are fairly straightforward involving the interaction of surfactant molecule with the charged species present upon the polymer, the remaining interactions are not easily quantified and can be quite complex. Polymers in particular add their own new twist since they may possess in solution as secondary and tertiary structures that must be altered during the surfactant binding process in order to afford the bound surfactant molecules.³²⁴ Any and all of these changes of the polymers in assistance with surfactants result in major alterations in the macroscopic and microscopic properties of the system. Forces which opposing the association of molecules usually include thermal energy, entropic consideration, and repulsive interactions among the similar electrical charges.³²⁵

The polymer-surfactant interaction is complex and conspicuous in nature; constant configurational changes can occur. Quantitative understanding of the interaction process can

be thermodynamically achieved as every physical and chemical process is guided by the rules of thermodynamics. Initially, the surfactant monomers get attached to the polymer chain and undergo hydrophobic interaction. Normally, by the interaction of a polymer with an amphiphile, a state of critical aggregation concentration (CAC) appears after that induced small micelles start to form in the system, and get bound to the polymer at specific sites that complete at a concentration called the saturation concentration, C_s . From that state, amphiphile monomers populate at the interface and start forming normal micelles in solution at the saturation point, C_e^* (called the extended critical micelle concentration).³²⁶⁻³²⁸ A complete course of oppositely charged polymer-surfactant interaction is schematically presented in Fig. 19. It has been stated that uncharged polymer containing polarizable groups show more or less same interaction pattern with ionic surfactants.^{329, 330} The interaction between oppositely charged polymer with surfactants is governed mainly by electrostatic interaction, while for uncharged polymer with charged surfactants mainly hydrophobic interaction play significant role.³²⁶⁻³²⁸ The lower value of CAC than CMC is ascribed to site specific surfactant-polymer interaction by way of elimination of water from the segmental domains of the polymer to induce formation of small micelle aggregates. Determination of NMR chemical shift³³¹ and polarity at different regions of micellar microphase using fluorescence measurements³³² can provide useful information on the interaction process. Using neutron scattering technique, Cabane³³³ has shown the thermodynamics of binding of polyethylene oxide (PEO) with small aggregates of SDS before formation of its free micelles and also predicted the allowed stoichiometry of smaller aggregates of SDS bound to PEO macromolecule.

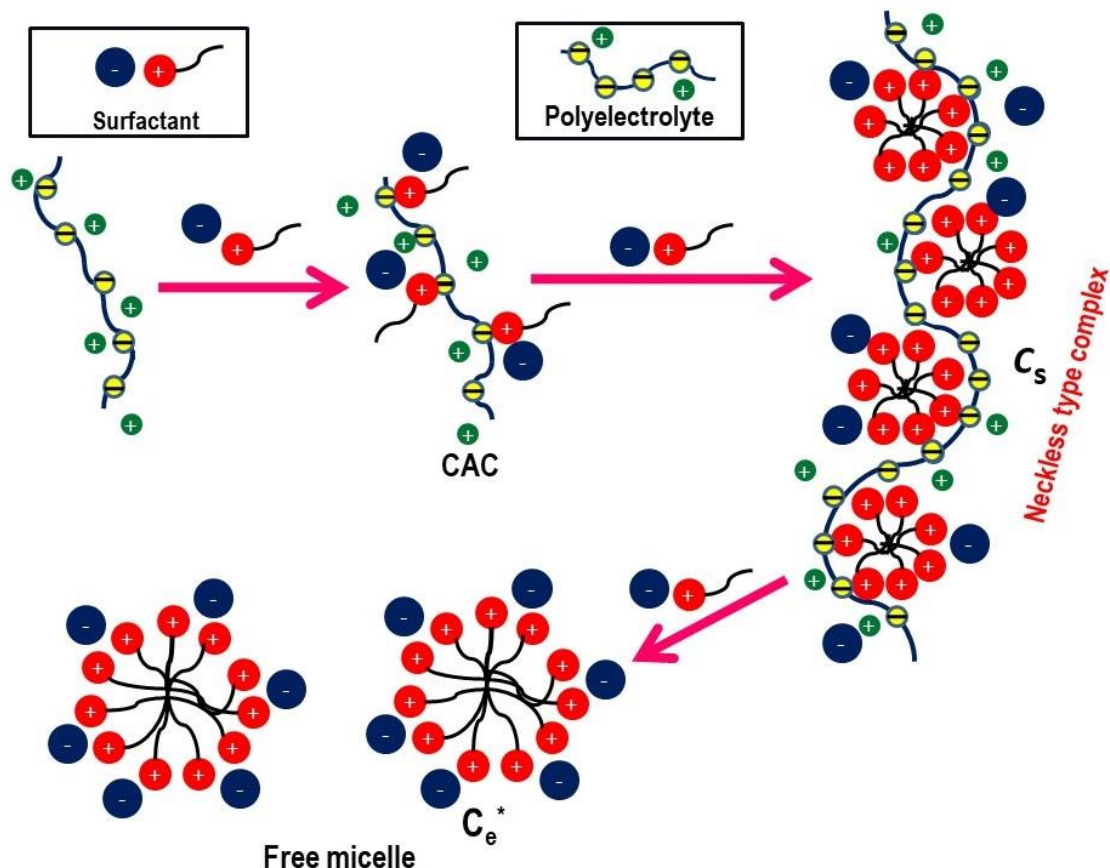


Fig. 19. Schematic representation for the interaction between a cationic polyelectrolyte with an anionic surfactant in aqueous solution

The exact characteristics of the polymer - surfactant or protein–surfactant complex is variable because they depend on the nature of the macromolecules and the surfactants. If the surfactant has bulky head group, the polymer has rigid backbone or if the polarity of both the surfactant head group and the polymer are identical, then the polymer–surfactant complex formation is less favoured. Neutral polymers interact with both anionic and cationic surfactants, but their mode of interaction is different. Generally, cationic surfactants weakly interact with neutral polymers than anionic surfactants of similar chain length. Due to strong electrostatic attraction polyelectrolytes interact with oppositely charged surfactants, but similarly charged polymer and surfactant interact only when polymer is markedly hydrophobic. Some model systems in this category include aqueous solutions of polyethylene oxide (PEO)-sodium dodecyl sulfate (SDS),^{334, 335} polyvinylpyrrolidone (PVP)–SDS,³³⁶ PEO-cetyltrimethylammonium bromide (CTAB)³³⁷ and polyethylene glycol (PEG)-CPC³³⁸.

In the interaction process between polymer and oppositely charged surfactant, hydrophobicity of the complex further increases leading to their self-aggregation to form coacervates. The coacervates may induce turbidity to the solution, precipitation of the complex, etc. This initial interaction is electrostatic in nature, which is reinforced by hydrophobic interaction between the hydrophobic domains of the polymer and the surfactant tail. Such interaction decreases the degree of residual charge on the polymer, resulting in hydrophobicity of the complex. If the electrostatic interaction is dominant in the polymer–surfactant complex (PS-complex), the peripheral binding of the surfactant monomers onto the oppositely charged peripheral polymer sites leads to coacervation. At a certain surfactant concentration, maximum precipitation of the coacervate takes place. Beyond saturation of the polymer adsorption sites, the surfactant forms free aggregates in the bulk solution. The resolubilization process is assumed to be solubilization of the coacervates, that form in solution before the free aggregates, in the hydrophobic micellar domain. Sometimes, adsorption of surfactant onto the polymer binding sites causes unfolding of the polymer (mostly observed in case of proteins). This unfolding process is driven by increasing surfactant concentration. The unfolding exposes the charged sites, that increase the solubility of the amphiphile adsorbed on the polymer backbone through the increasing degree of solvation, as well as undergoes a second mode of amphiphile adsorption onto the polymer. During this mode of adsorption, the local [surfactant] in the vicinity of the polymer increases below the CMC of free surfactants resulting in smaller aggregates of surfactant wrapping onto the polymer backbone.³³⁹ The second mode of oppositely charged polymer–surfactant interaction, however, comprises the adsorption of both monomeric and aggregated surfactant structures wrapping around the polymer.³²⁶⁻³²⁸

The interplay between proteins and surfactants has a say on the protein denaturation and received much attention^{340,341} but the process is in general not well understood. Interaction of proteins with the anionic surfactant SDS are mostly found in literature. Proteins studied are lysozyme^{342, 343} bovine serum albumin (BSA),^{344, 345} trypsin,^{346, 347} papain,³⁴⁸ and bromelain³⁴⁹ etc. Apart from SDS, different other surfactants (including conventional cationic surfactants, SAILS, gemini surfactants, nonionic surfactants) have been used in past and preceding years³⁵⁰⁻³⁵⁹ to elucidate protein-surfactant interactions. Surfactants denature proteins differently than classical denaturants such as guanidine hydrochloride (GdnHCl) and urea. Surfactants interact strongly with protein as compared with other denaturants such as urea and GdnHCl which weakly interact with the protein backbone. Depending on the method of denaturation, the end state may be different; it is typically a completely feature-less random coil with considerable conformational freedom in presence of chemical denaturants, while the

thermally denatured state and the acid-denatured state of protein tend to be compact and contain residual secondary structure.³⁶⁰ Numerous factors influence the interactions between surfactants and proteins. The mode of the interactions with proteins has been found to be both electrostatic and hydrophobic³⁶¹ depending on the nature of both proteins and surfactants. Thus, proteins are denatured by surfactants at millimolar concentrations, while urea and GdnHCl denature proteins at molar concentrations. Proteins act as polyelectrolyte depending on the pH of the solution. At isoelectric pH, the overall charge of a protein is 'zero'. Above isoelectric pH, it carries negative charge, and below isoelectric pH, it carries positive charge which facilitates the interaction between oppositely charged species. Interactions between SDS and proteins carrying a positive net charge leading to precipitation of the complex, because of charge neutralization. Often, it is possible to redissolve the precipitated complex by adding excess amount of SDS; however, some protein-surfactant complexes are not readily redissolved.³⁴²

Factors influencing the polymer surfactant interaction

Several factors trigger the association of surfactant in presence of polymer in the same way as they do with micellization of the surfactant in the absence of polymer, confirming the similarity of the two processes. Contributing terms for the surfactant in the presence of polymer are:

Specific binding: electrostatic attraction between the polar moieties of the surfactant and the polymer.

Nonspecific binding: hydrophobic part of the polymer protects the micellar core from the aqueous environment and vice versa.

Other factors that play an important role in the interaction are the following:

Surfactant alkyl chain length: It is possible to tune the hydrophobicity of a polymer chain by modifying the surfactant's chain length. In a homologous series, the initial binding concentration, CAC decreases with increasing number of alkyl chain carbons (n) of the surfactant binding to the polymer.³⁶² This same observation has also been found for sodium alginate- ILs (1-alkyl-3-methylimidazolium bromide, C_nMIMBr, where n = 12, 14 and 16) increasing the alkyl carbon length of IL from 12 to 16.³⁶³ The morphology, size and charge of the polymer-surfactant complex is drastically modified on varying chain length as evidenced when studying hydroxyethyl cellulose with tetradecyltrimethylammonium bromide (TTAB) and cetyltrimethylammonium bromide (CTAB).³⁶⁴ Neutron reflection illustrates that in the lower concentration regime of sodium polystyrene sulfonate (NaPSS) - alkyl

trimethylammonium bromide (ATAB) interaction, a 20-22 Å ‘thin’ adsorbed film occupies the interface, but this changes into a ‘thick sandwich’ layer at higher concentration. However, for ATAB (C₁₆), only ‘thin’ monolayer adsorption occurs at all concentration.³⁶⁵

Types of surfactants: The interaction between uncharged water – soluble polymers are much more facile with anionic surfactants than with cationic.^{366, 367} Dodecylammonium thiocyanate (DA⁺SCN⁻) interacts quite strongly with polyvinylacetate (PVAc), as found from specific viscosity data at low DASCN concentration, whereas the corresponding halides show comparatively weak interaction.³⁶⁷ Petcova *et al.*³⁶⁸ have compared the foam formation and its stability for the investigation of cationic polymer polyvinylamine (PVAm) with anionic surfactant sodium dodecyl sulphate (SDS) and another anionic surfactant sodium dodecyl oxyethylene sulphate (SDP1S) individually. They showed that the ethoxy group in SDP1S enhances the surfactant association with the polyelectrolyte molecules (PVAm) than SDS and consequently, the formation and stabilization of foam decreases from the solution containing PVAm with SDP1S. Interaction between polymer and surfactant having opposite charges is much more complex from a physicochemical point of view as compared to interaction between nonionic polymer with ionic surfactants. The contribution of both electrostatic and hydrophobic interactions interplay in the former, whereas the hydrophobic effect is the deciding factor in the latter. Nonionic polymers and nonionic surfactants show only very weak interactions. One exception is the strong interaction between polyoxyethylated nonionic surfactants and polyacrylic acid.³⁶⁹

Temperature: Temperature plays a significant role in maintaining system equilibrium. Surface activity of PS-complex may be invariant with temperature, but CAC increases with increase in temperature. Increasing temperature generally induces a high degree of ionization and lower aggregation number.³⁷⁰

Medium: With addition of alcohol, the dielectric constant of the medium decreases which enhanced stability of the aggregates formed and a close proximity of the head groups over the micelle surface. It also influences the various charge effects involved including counterion dissociation which in turn depends on the size and shape of micelles. Interaction mainly occurs through the penetration of alcohol molecules into micelles formed around the protein. Protein-surfactant interaction studied by potentiometry has been found to increase in presence of alcohol.³⁷¹

Additives: Addition of salt can enhance oppositely charged polyelectrolyte-surfactant complex (lower CAC) up to certain increasing concentration, then above a threshold salt concentration, it suppresses the complex formation and finally at higher salt concentration, complexation

between oppositely charged polyelectrolyte-surfactant is completely hampered.^{372, 373} Such observation has been found when studying the complex formation between NaCMC- DTAB in presence of NaBr. Addition of salt or nonionic surfactant may either induce or screen the polymer-surfactant interaction, will produce either a constant or an accelerated CAC due to reduced monomer concentration with polymer, as manifested in NaCMC-cationic gemini / TX-100 combination.³⁷⁴ Addition of salt also increases the binding ratio of surfactant to polymer. For PVP/SDS system, addition of 0.1 M NaCl increased the ratio to 0.9 SDS per base mol of PVP from 0.3/1 ratio which is observed in water.²⁹⁴ The counterions of surfactants modified the water structure differently which influenced the interaction between nonionic polymer with charged hydrophobic surfactants, and it has been reported by Saito and Kitamura³⁷⁵ that chaotropic (structure - breaking) anions (counterions) tend to increase the tendency of cationic surfactant (mostly for the surfactants containing long chain alkyl group) to associate with uncharged polymer, whereas, kosmotropic (structure-making) anions do the reverse. The organic anions with small hydrophobic groups are quite similar to kosmotropes like chloride ion in the interaction of the polymers and the long- chain cations.

Molecular Weight of Polymer: A minimum molecular weight of polymer must be required to ensure complete interaction with surfactant. Molecular weight of polymer depends significantly on polymer architecture.³⁷⁶ In case of polystyrene sulfonate (PSS), due to rigidity of the chain, they cannot effectively bend around surfactant micelles. SDS interacts differently with polyethylene glycol (PEG) if the PEG molecular weight is greater than equal to 1500: an exothermic interaction at low [SDS]; on the other hand, interaction between PEG-SDS is endothermic at higher [SDS].³⁷⁷ Francois *et al.*³⁷⁸ found that the polyethylene oxide (PEO) - SDS interaction is independent of the PEO molecular weight ranging from 6,000-900,000. It is seen that phase separation is more pronounced in presence of larger alkyl chain length and also in presence of higher molecular weight of polymer; specially for oppositely charged polyelectrolyte and surfactant. Increase of molecular weight of polyelectrolyte has the same impact on the polyelectrolyte-surfactant complex as increasing polyelectrolyte concentration and for the both cases, extended critical micelle concentration (C_e^*) increases and CAC hardly changes for the same polyelectrolyte-surfactant system. Tseng *et al.*³⁷⁹ have observed that in presence of oppositely charged polyacrylic acid (PAA) with tetradecyltrimethyl ammonium bromide (C_{14} TAB), when PAA molecular weight was less than 5,000, no precipitation is formed due to the aggregation of polyelectrolyte-surfactant complex; while for $\geq 130,000$, stable aggregates were formed and they are precipitated.

Amount of polymer: CAC and C_e^* values depend on polymer concentration; CAC decreases slightly with increasing polymer concentration; C_e^* on the other hand increases linearly with it. The number of available binding sites increases with increasing polymer concentration, leading to enlarge the interaction region, i.e., the binding of induced small micelles to the polymer completes at higher surfactant concentration. Both the critical concentrations corresponding to the polymer saturation by surfactant micelles (p_{sc} or C_s) and free micelle formation (C_e^*) increases with increasing polymer concentration as expected from the mass balance consideration.

Polymer Structure and Hydrophobicity: The polymer flexibility influences the activity to interact with the surfactant molecules. The lack of interaction activity of the polymer, such as, hydroxyethyl cellulose (HEC) may be due to a lower level of macromolecular flexibility,³⁸⁰ but even the more flexible polysaccharide dextran shows little tendency to interact with SDS and dodecylbenzenesulfonate sodium (DDBS). The influence of macromolecular flexibility is shown by the relatively strong interaction of SDS with amylose (which can undergo a helix-coil transition) and the relatively weak interaction of SDS with amylopectin (which cannot).³⁸¹ Fishman and Miller³⁸² reported that interaction of polymers (derived from starch) towards a cationic surfactant (CTAB) could be induced in highly alkaline solution ($pH \geq 12$). The same phenomenon is observed with insulin, dextran and starch; this demonstrated the role of the negative charge of the polymers at high pH by way of ionization of their hydroxyl groups.

The Role of Organic Solvent to Polymer-Surfactant Interaction and Micelle formation

Polymer-surfactant interactions are mostly studied in aqueous medium. The interaction process is highly affected in the presence of organic solvent. In practice (especially in cosmetics and pharmaceuticals), alcohol like additives is frequently used for better solubility, dispersity and durability. Isopropanol is non-toxic and bio-friendly and has safe uses in the formation of emulsion, microemulsion, and other cosmetic formulations.

Polar solvents like methanol, polyols, and acetone increase the CMC. In presence of organic solvent, the solubility of a surfactant increases that is, the solution becomes more hydrophobic. Concomitantly, the dielectric constant of the solvent decreases. Both these factors help to increase the CMC, a process known as the cosolvent effect.³⁸³ However, an opposing effect can occur for middle chain alcohols (e.g. C5–C9), a decrease in the CMC is due to solubilization of these hydrophobic counterparts of large chain alcohols in the micellar palisade

leading to reduce surface charge density on micelle surface and increase in hydrophobic interaction between the surfactants and the added alkanols. This is known as the “cosurfactant effect”.³⁸⁴ Ethanol, propanol and isopropanol bring about both effects: CMC-decrease at low alkanol concentration and CMC-increase at higher concentration. In general, short chain alcohols act as cosolvents; they are localized in the continuous phase and affect the solvent structure around the headgroup.³⁸⁵ Medium chain alcohols partition between the palisade region and the aqueous solution, whereas long chain alcohols are solubilized into the micellar core. For SDS, a decrease in the CMC with increasing ethanol content is observed at low ethanol concentrations (cosurfactant effect), which is subsequently converted to the cosolvency effect at higher ethanol concentration, that is, with increasing CMC by the increasing amount of ethanol. Hence, the CMC goes through a minimum at some ethanol concentration.³⁸⁴ Therefore, it will be informative to see what happens if such organic compounds are added to polymer-surfactant systems. The driving force for polymer/surfactant complexation is due to the adsorption of polymer segments into the micelle palisade layer³⁸⁶ shielding part of the hydrophobic core of the micelle from the aqueous phase. This is a more favourable arrangement, as the polymer is inherently more hydrophobic than water, and thus, a decrease in the micellization concentration of the surfactant results. If the solvent polarity is altered, this will cause a change in the effective dielectric constant of the medium, which in turn will have a profound effect on the electrostatic interactions present between the bound micelles. Shirahama *et al.*³⁸⁷ observed that the binding affinity of dodecyl pyridinium chloride to poly(styrene sulfonate) decreased with an increase in ethanol content. Griffiths *et al.*³⁸⁸ investigated the effect of increasing ethanol concentration on the interaction between the nonionic PVP and the SDS. Recently, Sultana *et al.*³⁸⁹ has recently studied the influence of different aqua-organic mixed solvents (9% w/w of acetonitrile, DMF and dioxane) for the interaction of nonionic PVP with tetradecyltrimethylammonium bromide (TTAB) at different temperatures. They showed that CMC_e of TTAB increases in presence of aqua-organic mixed solvent comparing with pure water medium.

Structure of polymer-surfactant complex

The structure of polymer surfactant complex is still not convincing. Different models have been proposed such as (A) “Necklace-bead” model in which clusters of micelles are stabilized by the polymer³⁹⁰ Fig. 20 (a and b), (B) “Rod like” prolate ellipsoidal surfactants aggregate with a semi minor axis (the surfactant chain length)³⁹¹ (Fig. 20 c), and (C) Flexible capped helical cylindrical micelle with polymer wrapping round the micelle (Fig. 20d). Among these, the

necklace model is best supported by SANS,³⁹² SAXS,³⁹³ viscometry,³⁹⁴ and NMR³⁹⁵. It has been reported that NMR can distinguish the two possible “necklace and bead” models; in one the surfactant aggregates with polymer wrapping by hydrophobic interaction (Fig. 20a) and in the other the polymer backbone is used with the hydrophobic moiety of micelles (Fig. 20 b).³⁹⁵

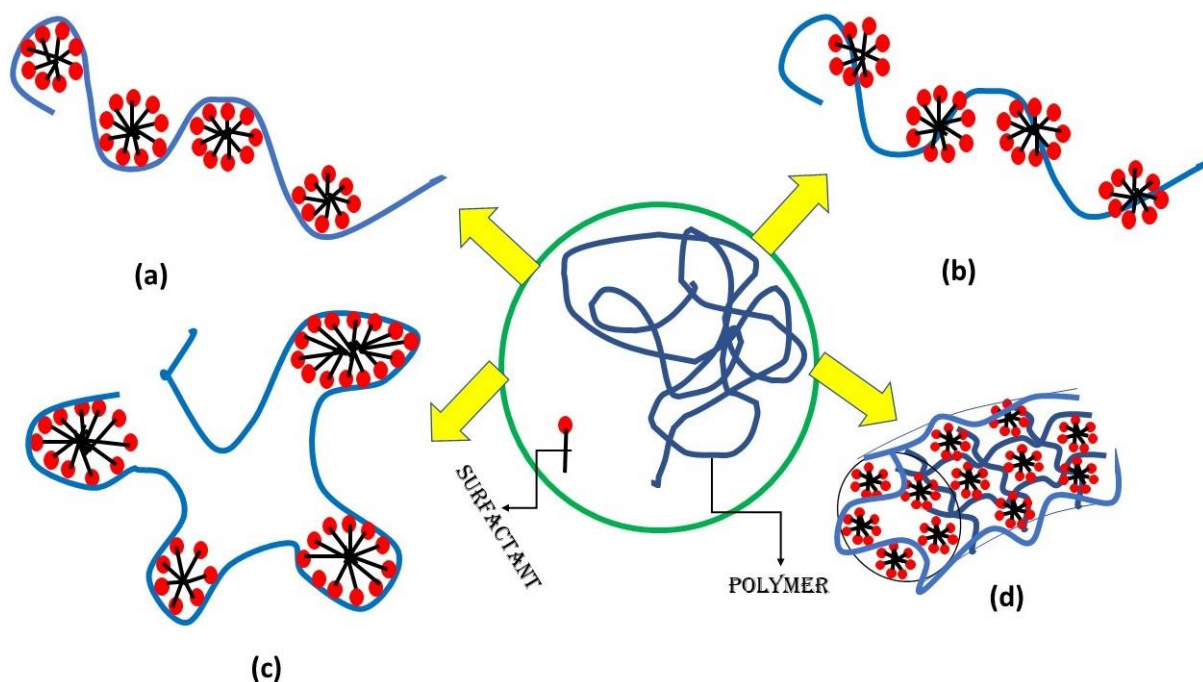


Fig. 20. Structure of polymer-surfactant complexes (a) and (b) two possible necklace bead structures (c) rod like prolate ellipsoidal and (d) flexible capped helical cylindrical micelle.

Techniques for evaluating the Interaction Process between polymer and surfactant:

Surfactants bind strongly with proteins and polymers, inducing a conformational change. Many experimental methods can be applied to understand the topology and other characteristics of polymer or protein - surfactant interaction, such as ITC for the determination of binding enthalpy,³⁹⁶ DSC for thermal denaturation of protein,³⁹⁷ turbidimetry for protein aggregation, fluorimetry for polarity,³⁹⁸ NMR for the structure of the complex,^{395,399} circular dichroism and cyclic voltammetry,⁴⁰⁰ SANS⁴⁰¹ and viscometry to examine conformational changes upon protein (or polymer) unfolding and denaturation, electrophoretic mobility to determine the number of binding sites in protein etc.⁴⁰² Several frequently used techniques to study polymer-surfactant interaction process are presented below in relation to the information derived on the interacting systems.

Tensiometry: Commonly used method for quick determination of surface tension (γ) with significant accuracy is the du Noüy ring detachment method. It is based on the measurement of the force P , required to detach a horizontal platinum ring (of radius R) from the surface of the experimental liquid. The force required to overcome the pull is due to surface tension. So, $P = 4\pi R\gamma$, or, $\gamma = P/4\pi R$. The precise relation is expressed as, $\gamma = (P/4\pi R) \phi$, where ϕ is the Harkins and Jordan correction factor depending on the size of the ring, thickness of the wire, and, density of the liquid etc.⁴⁰³ The measured γ at different [surfactant] or C when plotted as γ vs. $\log C$ produces a decline ending a plateau whose junction is the CMC. For polymer–surfactant interaction, tensiometry can reveal the nature of interaction of the surfactant with polymer both at the interface, and in the bulk. Jones³³⁴ reported two new transitions (denoted by CAC and C_e^*) in PEO/ SDS interaction in tensiometric isotherm comparing with the tensiometric profile of pure SDS in aqueous solution. A more or less general tensiometric profile for neutral polymer -ionic surfactant and surfactant interaction with ionic polymer are shown in Fig. 21.

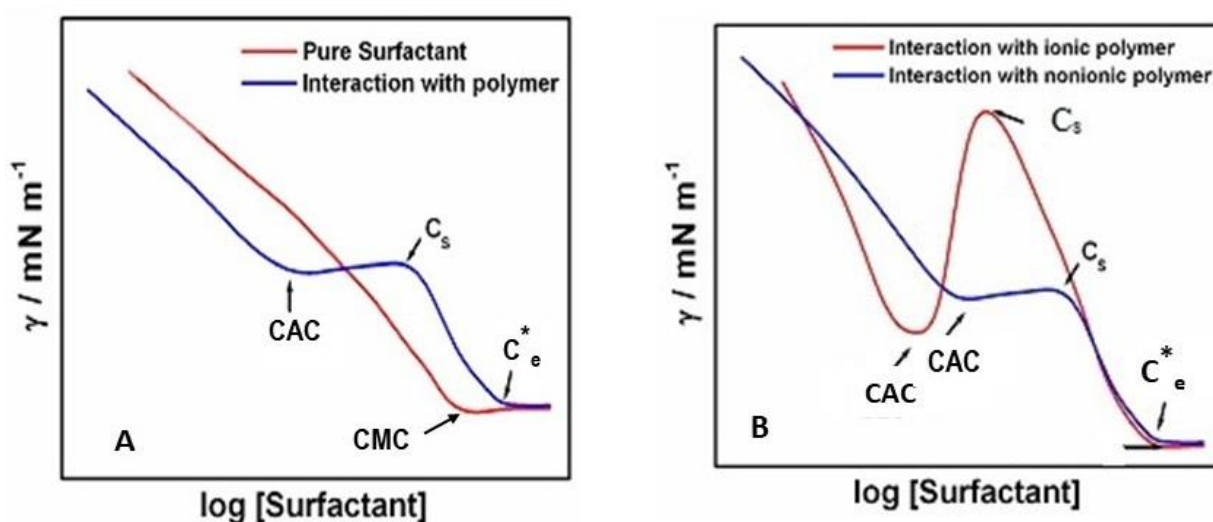


Fig. 21. Schematic presentation of tensiometric profile of (A) polymer/surfactant interaction (B) Comparison between neutral polymer-surfactant and charged polymer-surfactant interaction.

An additional transition, C_s , intermediate between CAC and C_e^* was also observed. It was reported that $CAC < CMC < C_e^*$, with CAC pointing the onset of polymer – surfactant interaction, CAC representing the saturation of PEO chain with SDS aggregates and C_e^* being the extended CMC of SDS in presence of the polymer or protein. Tensiometrically, it was shown that feebly surface-active hydroxyethyl cellulose (HEC) showed a small interaction with SDS, whereas much more surface-active methyl cellulose (MeC) showed pronounced interaction. Lower CAC

compared with CMC implies that the adsorbed or aggregated state of the SDS with the polymer represents a more favourable energy state for the surfactant molecules than the regular micelles. It has been observed that CAC is only weakly dependent on polymer concentration in solution, i.e., the concentration of the onset of polymer – surfactant interaction is solely a function of the surfactant concentration for a particular polymer.³³⁴ On the other hand, the value of C_e^* is directly proportional to the polymer concentration. In case of oppositely charged polyelectrolyte-surfactant system, CAC is lowered by one order of magnitude or more leading to a strong electrostatic driving force. However, the values of CMC and CAC are comparable for systems like PEO–SDS.⁴⁰⁴ A point to worth noting is that the polymers containing charge centres essentially along the backbone lead to much lower surface tension in the precipitation zone with surfactant, also, that in some instances, it is not possible to solubilize the stoichiometric precipitation aggregates by addition of excess surfactant, especially if the charge density of the polyelectrolyte is high.⁴⁰⁵

Conductometry: Conductometry is a potential method for probing the bulk property of interaction between neutral polymer and an ionic surfactant. The specific conductance (κ) of a solution depends on several factors, such as, the concentration of the ions in solution, the mobility of the ions, etc. Now, addition of the surfactants in the aqueous phase makes the amphiphilic molecules to dissociate to furnish the amphiphile ions and the counter-ions. On successive additions, the concentration of ions increases and thereby the conductance (κ) goes on increasing till the CMC is reached. At CMC, a number of monomer ions aggregate to form micelles with adhered counter-ions. Thus, the number of free ions in solution decreases and also the mobility of the aggregates decreases; thereby the rate of increase of κ decreases. Thus, we obtain two straight lines with different slopes before and after CMC. From the cross-section of these two lines, we get the CMC (Fig. 14).⁴⁰⁶ Generally, two break points are obtained in case of polymer-surfactant interaction. The break point in the lower concentration range (CAC) can be explained by the loss of free ions of the surfactant from the solution due to addition it upon polymer backbone. The second break (C_e^*) corresponds to the formation of free micelles in solution that depends on polymer concentration.

Microcalorimetry: ITC (isothermal titration calorimetry) is a versatile, sensitive technique to determine the enthalpy change in polymer surfactant binding process. The heat produced by different physical and chemical processes in the bulk of a solution can provide valuable insights into the origin and nature of polymer – surfactant interactions and the factors that influence them. The processes which give rise to measurable enthalpy changes are (a) demicellization

(b) dilution effect of surfactants (c) conformational changes of polymer and (d) binding interaction (mostly electrostatic and hydrophobic) which gives the most significant and measurable enthalpy change. Bloor *et al.*⁴⁰⁶ have studied the SDS–PVP system using ITC and EMF measurements. Olofsson and Wang⁴⁰⁷ have also investigated the interaction between uncharged polymers and ionic surfactants using this technique. Majhi *et al.*¹⁷⁴ have used the methods of microcalorimetry, conductometry, fluorimetry and dynamic light scattering (DLS) for the understanding of the interaction of both anionic and cationic surfactants with PVP and other natural and hydrophobically modified polymers and proteins in aqueous medium. Recently, Mal *et al.*³²⁸ have been investigated on the interaction of cetyltrimethylammonium p-toluenesulfonate (CTAT) with NaCMC and hydroxy ethyl cellulose (HEC) by using different physicochemical techniques including ITC.

Turbidity: The aggregation of surfactant bound polymer produces turbidity in solution. According to Dubin *et al.*⁴⁰⁸ the electrophoretic mobility of such complexes approaches zero in the vicinity of the turbidity maximum. According to their observation, the progressive binding of the micelles to the polymer (which enhances most for oppositely charged polyelectrolytes) eventually leads to charge neutralization; the higher order aggregation of these electrically neutral complexes produces multi-polymer complexes that scattered light strongly. After saturation, the complexes again acquire a net charge, and then dissociation of the complex takes place due to repulsion. Hence, turbidity decreases. Salt effect on the interaction of anionic polyelectrolyte, NaCMC (sodium salt of carboxymethyl cellulose) with cationic Gemini surfactant has been investigated using turbidimetric titration by Wang *et al.*³⁷⁴ Turbidimetric experiments on the polymer/surfactant interaction were also cited elsewhere.^{328, 409, 410}

Viscometry: Solution viscosity is also an important indication to the bulk complexation process because of changes in the conformation of the polymer–surfactant complex in solution. Jones³³⁴ reported a steady increase in the relative viscosity of PEO on adding increasing amount of SDS. A clear change in viscosity is occurred at a concentration about C^*_e , but no prominent slope change near cac . These results obviously imply a change in polymer conformation, viz. an enlargement of the polymer coils, on association with the charged surfactant, as reported by Takagi *et al.*⁴¹¹ and by Nagarajan and Kalpakci³⁸⁰ for PEO/SDS systems. From rheological analysis, Prud'homme and Uhl⁴¹² demonstrated that coiling of polymer chain is collapsed and viscosity decreases with increasing concentration of SDS, followed by gel formation (network structure formation) and higher viscosity due to coiling follows at higher SDS concentration. Viscosity changes of the carbohydrate polymer inulin on

interaction with alkyl trimethyl ammonium halides has been reported by Dan et al.⁴¹³ Similar studies are also found in literature. However, it is seen that, viscosity decreases rapidly with increase in concentration of surfactants in presence of oppositely charged polyelectrolyte-surfactant complex.⁴¹⁴

Light Scattering: Static light scattering can be used in polymer–surfactant systems to obtain information on aggregate size, shape and mass. Dubin and co-worker⁴¹⁵ have made extensive use of static and dynamic light scattering techniques to study aggregate size and the role of micellar surface charge in polymer–surfactant systems. Micellar surface charge density can be varied by using ionic–nonionic mixed surfactant systems. Wang and co-workers⁴¹⁶ used light scattering technique to study the interaction between Fullerene containing polyacryl and Triton-X-100. For DLS study, particle dimension (hydrodynamic diameter) diffusion coefficient and Zeta-potential can be determined. Literature is fairly rich with such information.

Microscopy: Visible microscopy is generally not suitable to observe the nm-scale structure of polymer-surfactant complex in bulk solution. Scanning electron microscopy (SEM), transmission electron microscopy (TEM), and atomic force microscopy (AFM) are powerful techniques allowing visual observation of aggregate structures with adequate image enlargement. Spectacular examples include the thread-like structures sometimes observed in micellar and polymer-surfactant system by TEM.^{414,417} The morphological transformations of fullerene containing amphiphilic copolymers (PPA-b-C60) by the addition of nonionic aromatic surfactant (TX-100) were observed by Wang et al.⁴¹⁶

Fluorimetry: A variety of static and dynamic fluorescence techniques have been applied to polymer-surfactant systems. Steady state techniques, including depolarization measurements, give information on such quantities as probe environments, microviscosity, and aggregation number of the aggregates. Time-resolved techniques have become particularly powerful yielding surfactant aggregation number, and polydispersity measurements as well as kinetic information. Both small probe molecules and polymer-anchored probe may be used. For pyrene, the most widely used probe for such studies, the measurement is provided by the ratio of the first to third vibronic fluorescence peaks. Turro and co-workers⁴¹⁸ investigated both PVP/SDS and PEO/SDS systems using pyrene. They actually speculate that an interaction is involved between pyrene and the polymer at the micellar surface. Recently Mal *et al.*³²⁸ have been investigated life time of pyrene when studying the interaction of 0.01g% NaCMC and HEC individually with the increasing concentration of CTAT. They found that average life time vs. [CTAT] shows several break points which one similar with CAC, C_s and C*_e.

Fluorescence spectroscopy is a powerful technique for the investigation of protein structure, dynamics, and conformations. The intrinsic fluorescence emission from tryptophan residue within proteins is an inherent probe and is sensitive to the microenvironment surrounding the fluorophore residue.⁴¹⁹ Fluorescence spectra are usually used to detect the effect of molecules on proteins, as it is supposed that fluorescence techniques are relatively more sensitive in interpreting small changes at the molecular level.

UV-visible Spectroscopy: The main use of UV-vis spectroscopy in polymer–surfactant interactions involve the interpretation of absorbance wavelength shifts of dye which is solubilized in hydrophobic domains of the aggregates. Many such studies are performed in connection with fluorescence measurements. UV–vis spectroscopy is an important tool to explore conformational changes in protein molecules.⁴²⁰ Proteins generally show absorption maxima between 275 and 280 nm, due to absorbance of the two aromatic amino acids tyrosine (Tyr) and tryptophan (Trp). The absorbance intensity of Trp and Tyr around 280 nm depends on the microenvironment. The exposed residues to solvent and those that are buried have different contributions to the absorption.

Circular Dichroism: Circular dichroism (CD) is an authentic method in structural biology that has been used to study proteins and biomolecules since 1960s.⁴²¹ This spectroscopic method depends upon the differential absorption of left and right-circularly polarized light by optically active molecules.⁴²¹ A molecule shows optical activity (or chirality) if it can rotate the plane of polarized light. In proteins, different optical activity generates due to the presence of L-amino acids and different folding of the polypeptide chain. Far-UV CD spectra, typically in the range 250-190 nm gives the informations of peptide backbone conformation, particularly secondary structure.⁴²² α -helix, β -sheet, and random coil structures each gives characteristic shape and magnitude in CD spectrum. From Far-UV CD spectra, it is thus possible to estimate the fraction of secondary structure elements. The information deducted from CD spectra does not provide information about where in the sequence the secondary structures are located, but gives an average of the total content of secondary elements. In the far-UV CD spectral region α -helical proteins can be characterized by three peaks; two negatives at \sim 222 and \sim 208 nm and a stronger positive at \sim 192 nm. Spectra arising from β -sheets can be characterized by a small negative peak near 217 nm and a positive peak near 195 nm that has approximately half the intensity of the α -helix peak in this region.⁴²³ β -sheets give rise to considerably less intense signals than helices and show far more variation in spectral characteristics; the latter is partly attributable to the fact that β -sheets are much more structurally diverse than α -helices with

strands which may run parallel or anti-parallel to each other, and with sheets displaying differing degrees of twisting. While far UV CD spectroscopy gives information of secondary structure of protein, near UV CD (250-300 nm) can be used to indicate changes in tertiary structure. Aromatic side chains in asymmetric environments have optical activity in folded proteins. Signals in the region from 250-270 nm are attributable to phenylalanine (Phe) residues, signals from 270-290 nm are attributable to Tyr residues, and those from 280-300 nm are attributable to Trp. Disulphide bonds give rise to broad weak signals throughout the near-UV spectrum. A protein can hold a large degree of secondary structure without having a well-defined three-dimensional structure (e.g., molten globule state). In this condition, the signal in the near UV region will be almost zero. Another important class of protein called proteolytic cysteinyl protease class has lesser amount of α -helix (or $\alpha+\beta$ class proteins, e.g., papain, bromelain, etc.) structure. Bromelain shows negative ellipticities at 208, 215, and 222 nm in CD spectrum and it is seen that the peak at 208 nm is more intense than that at 222 nm.⁴²⁴ A significant signal in the near UV CD region is a good sign of a folded protein. In general, the signal in the near-UV region is much weaker than the signal in the far-UV region. Near UV CD thus requires substantial amounts of protein compared to near UV CD.

Other methods which are used to investigate the bulk complexation of proteins with surfactants are DSC for thermal change due to the interaction; fluorimetry for polarity; NMR for structure of complex; SANS for conformational change, and rheology, electrophoresis to understand the internal dynamics and the number of binding sites, etc.

11. Scope and Objectives of the present work

Self-aggregation of amphiphiles with different types of polymers including biopolymers (proteins) comes well under ‘soft colloid’ or in general ‘soft systems’ under differential environmental conditions and in presence of additives. Such investigations have potential implications and applications in pharmaceutical preparations, chemical synthesis, enzymatic reactions, oil recovery, painting, coating, drug encapsulation and delivery, synthesis of nanomaterials, synthetic membrane formation and their pharmaceutical and biological uses, etc. Although amphiphilic aggregation and their interaction with polymer/protein, salts or with other surfactants/ILs (mixed micelle formation) have a long tradition of exploration, their profound uses and applications add upsurge interest to this field, but the exploration is yet challenging because of vast coverage of this field, and scope of availability of numerous amphiphile and polymeric compounds by virtue of isolation, synthesis and chemical modification.

In recent years, ionic liquids (ILs) have generated intense scientific and industrial interests due to their special physicochemical properties. ILs bearing long alkyl chains are emerging as novel surfactants because of their inherent amphiphilic character and are named as surface-active ionic liquids (SAILs). Imidazolium-based SAILs have been most studied in the field of colloid and interface chemistry. It is reported that both cationic and anionic SAILs have more superior surface activity than the corresponding traditional ionic surfactants, which have comparable structures with the same hydrophobic chain. For SAILs, one of the great advantages is that their physicochemical properties which can be designed by reasonable selection of cations, anions, and substituents. Unique physicochemical properties and superior surface activity of SAILs can be exploited as a potential substitute for traditional surfactants in some applications. Recently, the application of ILs in the life sciences is becoming one of the hotspots in the research arena. By considering several utilities of ionic liquids in both industrial and medicinal purpose, investigations have been performed to elucidate the property of micelles made by ILs in combination with various additives (e.g., salts, macrocycles, conventional surfactants, and biopolymers, etc.).

Proteins are abundant and vital in living systems and participate in nearly all biological processes. The function of a protein directly depends on its structure. Since surfactants can change the conformation of the water-soluble proteins, protein– surfactant interactions are being widely studied. The protein – surfactant interaction not only provides the denaturing and renaturing capacity of surfactants on proteins, but also has importance in biological, industrial, cosmetic, and pharmaceutical fields.

Macrocyclic crown ether related compounds are well known and widely synthesized for their applications in biological chemistry for their selective binding with cations, drug delivery, mimic to biological molecules, etc. Surfactants form micelles and solubilize the macrocyclic compounds in its hydrophobic core and form inclusion complex, though the macrocyclic compounds are not soluble in water. Interaction of such types of macrocyclic compound with surfactants has not been studied widely.

In this dissertation, the micellization of surface-active ionic liquid (SAIL), 1-hexadecyl-3-methyl imidazolium chloride in conjugation with dodecyltrimethylammonium bromide (DTAB) forming mixed micelles in various stoichiometry has been investigated thoroughly by conductometry, tensiometry, spectrofluorimetry methods. Interaction parameters, micellar composition of two surfactants in binary mixture of surfactants, activity coefficient of two components in micellar medium have also been calculated using established theoretical models discussed elsewhere. CMC of pure and mixed surfactants in different stoichiometry, counterion

binding of the micelles and thermodynamics of mixed micellization using regular solution theory (RST) have been studied. Micellization of the same surface-active ionic liquid (1-hexadecyl-3-methyl imidazolium chloride) has been investigated in presence of different salts having different valences with variation of temperature and salt concentrations by conductometry, tensiometry, fluorimetry, microcalorimetry and dynamic light scattering methods. One of the motives of this work was to compare the van't Hoff enthalpy (by determining CMC at different temperatures) and the enthalpy by direct calorimetric measurements and found the dissimilarity between the two values. The dissimilarity has also been observed in the CMC order assisted by different anions (counterion of salts) when comparing CMC trend with the Hofmeister series of anions. Micellization of same ionic liquid and a conventional surfactant, 1-hexadecyltriphenylphosphonium bromide individually has been investigated in presence of an oppositely charged bio polyelectrolyte, sodium alginate. Alginate is a biodegradable polymer with less toxic agent. Alginate has several applications in biomedical and food industry due to its enrich gelling property. Change of conformation of polyelectrolyte and point of appearance of turbidity due to charge neutralization on the polyelectrolyte backbone, critical aggregation points (CAC, C_s , C_e^*), morphology of polyelectrolyte-surfactant complex, and thermodynamics of micellization in absence and presence of sodium alginate have been predicted by tensiometry, conductometry, fluorimetry, dynamic light scattering, infrared and transmission electron microscopy, etc. in this present study also.

Stem bromelain (BM), a proteolytic enzyme isolated from pineapple (*ananas cosmosus*) stem belongs to cysteine proteinase family. This protein belongs to $\alpha + \beta$ protein class with 23% helical structure, containing five (5) tryptophan (Trp.) units, whose characteristic absorbance (~280 nm) and emission (~354nm) varies with solvent polarities, determine the exposure of Trps in different environments, mediated by the interaction with surfactants. In this present study, we have used two bile salt surfactants sodium cholate (NaC) and sodium deoxycholate (NaDC) along with two conventional anionic surfactants sodium lauroylsarcosinate (SDDS) and sodium dodecylbenzene sulfonate (SDBS), which interact with BM (0.005%) at phosphate buffer medium of pH 7. Bromelain has various health benefits including sinus problems, reducing inflammation, and improving digestion. Bromelain also improves the condition of osteoarthritis and sometimes also impede the growth of a tumour. Due to this several potential effect, bromelain shows the enormous possibility of research in present times. However, only

a limited amount of research work about interaction of bromelain with surfactants have been found in literature so far.

Aza-crown ethers containing nitrogen atoms have been used commonly for the chelation of heavy metal ions and also has potential applications in magnetic resonance imaging (MRI) and positron emission tomography (PET). Benzo aza-crowns have superior host-guest activity comparing with the traditional crowns. In this connection, a comprehensive investigation has been executed on the interaction of a synthesized chromophoric dihydroxy dibenzoaza-crown (1,16-dihydroxy-tetraaza-30-crown-8) with arbitrarily chosen surfactants, conventional cationic DTAB, anionic SDS, cationic gemini (butanediyl-1,4-bis (dimethylcetylammmonium bromide),16-4-16), surface active ionic liquid (1-hexadecyl-3-methylimidazolium chloride) and nonionic surfactant (polyoxyethylene sorbitan monostearate, Tween-60] covering all the classes in 15% EtOH-water medium at 298.15 K. Conductometry, tensiometry, UV-Vis spectroscopy, isothermal titration calorimetry, spectrofluorimetry were employed to elucidate the interaction of crown-surfactants both in surface and in bulk. Such type of comprehensive study is seldom found in literature.

This dissertation (thesis) comprises the following sections: Introduction, Five chapters entailing research findings, Summary and Conclusion section and an Appendix containing all the basic data. Photocopies of the published papers are also attached.

References:

1. M. J. Rosen and J. T. Kunjappu, *Surfactants and interfacial phenomena*, John Wiley & Sons, 2012.
2. K. Morwind, J. P. Koppenhöfer and P. Nüßler, in *Markenmanagement: Grundfragen der identitätsorientierten Markenführung*, eds. H. Meffert, C. Burmann and M. Koers, Gabler Verlag, Wiesbaden, 2002, DOI: 10.1007/978-3-322-92976-1_20, pp. 477-505.
3. K. Sakamoto, R. Lochhead, H. Maibach and Y. Yamashita, *Cosmetic science and technology: theoretical principles and applications*, Elsevier, 2017.
4. O. Kaczerewska, R. Martins, J. Figueiredo, S. Loureiro and J. Tedim, *Journal of Hazardous Materials*, 2020, **392**, 122299.
5. A. A. Ivanova, A. N. Cheremisin, A. Barifcani, S. Iglauer and C. Phan, *Journal of Molecular Liquids*, 2020, **299**, 112104.
6. K. M. Z. Hossain, V. Calabrese, M. A. da Silva, S. J. Bryant, J. Schmitt, J. L. Scott and K. J. Edler, *Carbohydrate Polymers*, 2020, **233**, 115816.
7. V. Kumar, N. Pal, A. K. Jangir, D. L. Manyala, D. Varade, A. Mandal and K. Kuperkar, *Colloids and Surfaces A: Physicochemical and Engineering Aspects*, 2020, **588**, 124362.
8. S. Mondal, A. Pan, A. Patra, R. K. Mitra and S. Ghosh, *Soft matter*, 2018, **14**, 4185-4193.
9. S. Das, S. Ghosh and B. Das, *Journal of Chemical & Engineering Data*, 2018, **63**, 3784-3800.
10. A. Saha, A. Mal and S. Ghosh, *Journal of Molecular Liquids*, 2020, **309**, 113084.

11. N. Pal, N. Saxena and A. Mandal, *Colloid and Polymer Science*, 2017, **295**, 2261-2277.
12. B. Vyas, S. A. Pillai, D. Ray, V. K. Aswal, M.-R. Wang, L.-J. Chen and P. Bahadur, *Journal of Molecular Liquids*, 2020, **300**, 112341.
13. A. Ali, U. Farooq, S. Uzair and R. Patel, *Journal of Molecular Liquids*, 2016, **223**, 589-602.
14. P. Saha, D. K. Pyne, S. Ghosh, S. Banerjee, S. Das, S. Ghosh, P. Dutta and A. Halder, *RSC advances*, 2018, **8**, 584-595.
15. N. Patra, D. Ray, V. K. Aswal and S. Ghosh, *ACS omega* 2018, **3**, 9256-9266.
16. V. Singh and R. Tyagi, *Colloid Polymer Science* 2017, **295**, 601-611.
17. R. Hu, S. Tang, M. Mpelwa, L. Jin, Z. Jiang, S. Feng and Y. Zheng, *Journal of Dispersion Science and Technology*, 2020, DOI: 10.1080/01932691.2020.1843478, 1-11.
18. S. Mondal and S. Ghosh, *Chemical Physics Letters*, 2021, **762**, 138144.
19. R. Bordes and K. Holmberg, *Advances in Colloid and Interface Science*, 2015, **222**, 79-91.
20. K. Kumar, B. S. Patial and S. Chauhan, *The Journal of Chemical Thermodynamics*, 2015, **82**, 25-33.
21. T. Inoue and H. Yamakawa, *Journal of Colloid and Interface Science*, 2011, **356**, 798-802.
22. M. Abe, H. Uchiyama, T. Yamaguchi, T. Suzuki, K. Ogino, J. F. Scamehorn and S. D. Christian, *Langmuir*, 1992, **8**, 2147-2151.
23. A. Pan, S. S. Mati, B. Naskar, S. C. Bhattacharya and S. P. Moulik, *The Journal of Physical Chemistry B*, 2013, **117**, 7578-7592.
24. A. Patist, S. S. Bhagwat, K. W. Penfield, P. Aikens and D. O. Shah, *Journal of Surfactants and Detergents*, 2000, **3**, 53-58.
25. A. Kroflič, B. Šarac and M. Bešter-Rogač, *Langmuir*, 2012, **28**, 10363-10371.
26. T. Yoshimura, T. Ichinokawa, M. Kaji and K. Esumi, *Colloids and Surfaces A: Physicochemical and Engineering Aspects*, 2006, **273**, 208-212.
27. J. A. Kent, in *Riegel's Handbook of Industrial Chemistry*, ed. J. A. Kent, Springer US, Boston, MA, 2003, DOI: 10.1007/0-387-23816-6_27, pp. 1098-1140.
28. M. Howell, (Ed.). *Handbook of Detergents, Part D: Formulation (1st ed.)*. CRC Press. 2005, <https://doi.org/10.1201/9781420028713>.
29. B. Alberts, A. Johnson, J. Lewis, M. Raff, K. Roberts, P. Walter, D. Bray and J. Watson, *Mol Biol.*, 2002.
30. J. Maldonado-Valderrama, P. Wilde, A. Macierzanka and A. Mackie, *Advances in Colloid and Interface Science*, 2011, **165**, 36-46.
31. E. J. A. Veldhuizen and H. P. Haagsman, *Biochimica et Biophysica Acta (BBA) - Biomembranes*, 2000, **1467**, 255-270.
32. R. Hayes, G. G. Warr and R. Atkin, *Chemical reviews*, 2015, **115**, 6357-6426.
33. S. Gabriel and Weiner, *deutschen chemischen Gesellschaft*, 1888, **21**, 2669-2679.
34. P. Walden, *Bull. Acad. Imper. Sci.*, 1914, **1800**.
35. P. Stepnowski, *International Journal of Molecular Sciences* 2006, **7**, 497-509.
36. J. L. Shamshina, P. S. Barber and R. D. Rogers, *Expert Opinion on Drug Delivery*, 2013, **10**, 1367-1381.
37. K. M. Docherty and C. F. Kulpa Jr, *Green Chemistry*, 2005, **7**, 185-189.
38. K. Bica, P. Gärtner, P. J. Gritsch, A. K. Ressimann, C. Schröder and R. Zirbs, *Chemical Communications*, 2012, **48**, 5013-5015.
39. R. D. Rogers and K. R. Seddon, *Science*, 2003, **302**, 792-793.
40. H. Srour, H. Rouault, C. C. Santini and Y. Chauvin, *Green Chemistry* 2013, **15**, 1341-1347.

41. D. J. Kim, K. H. Oh and J. K. Park, *Green Chemistry* 2014, **16**, 4098-4101.
42. G. Damilano, D. Kalebić, K. Binnemans and W. Dehaen, *Rsc Advances*, 2020, **10**, 21071-21081.
43. J. Sirieix-Plénet, L. Gaillon and P. Letellier, *Talanta*, 2004, **63**, 979-986.
44. Q. Q. Baltazar, J. Chandawalla, K. Sawyer and J. L. Anderson, *Colloids and Surfaces A: Physicochemical and Engineering Aspects*, 2007, **302**, 150-156.
45. M. Blesic, A. Lopes, E. Melo, Z. Petrovski, N. V. Plechkova, J. N. Canongia Lopes, K. R. Seddon and L. P. N. Rebelo, *The Journal of Physical Chemistry B*, 2008, **112**, 8645-8650.
46. B. Dong, X. Zhao, L. Zheng, J. Zhang, N. Li and T. Inoue, *Colloids and Surfaces A: Physicochemical and Engineering Aspects*, 2008, **317**, 666-672.
47. O. A. El Seoud, P. A. R. Pires, T. Abdel-Moghny and E. L. Bastos, *Journal of Colloid and Interface Science*, 2007, **313**, 296-304.
48. T. Inoue, H. Ebina, B. Dong and L. Zheng, *Journal of colloid and interface science*, 2007, **314**, 236-241.
49. J. Łuczak, J. Hupka, J. Thöming and C. Jungnickel, *Colloids and Surfaces A: Physicochemical and Engineering Aspects*, 2008, **329**, 125-133.
50. T. Singh and A. Kumar, *The Journal of Physical Chemistry B*, 2007, **111**, 7843-7851.
51. S. L. I. Toh, J. McFarlane, C. Tsuris, D. W. DePaoli, H. Luo and S. Dai, *Solvent Extraction and Ion Exchange*, 2006, **24**, 33-56.
52. J. Wang, H. Wang, S. Zhang, H. Zhang and Y. Zhao, *The Journal of Physical Chemistry B*, 2007, **111**, 6181-6188.
53. J. Łuczak, C. Jungnickel, M. Joskowska, J. Thöming and J. Hupka, *Journal of Colloid and Interface Science*, 2009, **336**, 111-116.
54. S. Dorbritz, W. Ruth and U. Kragl, *Advanced Synthesis & Catalysis*, 2005, **347**, 1273-1279.
55. B. Dong, Y. a. Gao, Y. Su, L. Zheng, J. Xu and T. Inoue, *The Journal of Physical Chemistry B*, 2010, **114**, 340-348.
56. H. Wang, L. Zhang, J. Wang, Z. Li and S. Zhang, *Chemical Communications*, 2013, **49**, 5222-5224.
57. K. Thakkar, B. Bharatiya, V. K. Aswal and P. Bahadur, *RSC advances*, 2016, **6**, 80585-80594.
58. P. D. Galgano and O. A. El Seoud, *Journal of Colloid and Interface Science*, 2011, **361**, 186-194.
59. A. Pal and M. Saini, *Journal of Surfactants and Detergents*, 2019, **22**, 491-499.
60. M. T. Garcia, I. Ribosa, J. J. Gonzalez and F. Comelles, *Journal of Molecular Liquids*, 2020, **318**, 114040.
61. F. M. Menger, J. S. Keiper and V. Azov, *Langmuir*, 2000, **16**, 2062-2067.
62. T. Yoshimura and K. Esumi, *Journal of Colloid and Interface Science*, 2004, **276**, 231-238.
63. L.-H. Lin and Y.-C. Lai, *Colloids and Surfaces A: Physicochemical and Engineering Aspects*, 2011, **386**, 65-70.
64. C. A. Bunton, L. B. Robinson, J. Schaak and M. Stam, *The Journal of Organic Chemistry*, 1971, **36**, 2346-2350.
65. F. M. Menger and C. J. J. o. t. A. c. s. Littau, 1991, **113**, 1451-1452.
66. R. Renner, "The long and the short of perfluorinated replacements", *Environmental Science & Technology* / january 1, 2006, 12-13.
67. M. R. Porter, *Handbook of surfactants*, Springer, 2013.
68. A. R. Sontake and S. M. Wagh, *J Chem. Eng. Sci*, 2014, **2**, 11-14.
69. X. Li, R. M. Washenberger, L. E. Scriven, H. T. Davis and R. M. Hill, *Langmuir*, 1999, **15**, 2278-2289.

70. R. M. Hill, *Silicone surfactants*, CRC Press, 1999.
71. J. McBain, *Trans. Faraday Soc*, 1913, **9**, 99-112.
72. R. Schmid, *Monatshefte für Chemie / Chemical Monthly*, 2001, **132**, 1295-1326.
73. J. J. Sheng, in *Modern Chemical Enhanced Oil Recovery*, ed. J. J. Sheng, Gulf Professional Publishing, Boston, 2011, DOI: <https://doi.org/10.1016/B978-1-85617-745-0.00007-3>, pp. 239-335.
74. S. Ray and S. Moulik, *Langmuir*, 1994, **10**, 2511-2515.
75. R. S. Chaurasiya and H. U. Hebbar, in *Nanoscience in Food and Agriculture 4*, eds. S. Ranjan, N. Dasgupta and E. Lichtfouse, Springer International Publishing, Cham, 2017, DOI: 10.1007/978-3-319-53112-0_5, pp. 181-211.
76. E. P. Melo, M. R. Aires-Barros and J. M. Cabral, *Biotechnology annual review*, 2001, **7**, 87-129.
77. P. Mukerjee and K. J. Mysels, *Critical micelle concentrations of aqueous surfactant systems*, National Standard reference data system, 1971.
78. E. W. Anacker and H. M. Ghose, *Journal of the American Chemical Society*, 1968, **90**, 3161-3166.
79. B. Lindman, M. C. Puyal, N. Kamenka, B. Brun and G. J. T. J. o. P. C. Gunnarsson, 1982, **86**, 1702-1711.
80. J. Aguiar, P. Carpena, J. A. Molina-Bolívar and C. Carnero Ruiz, *Journal of Colloid and Interface Science*, 2003, **258**, 116-122.
81. X. Zhang, J. K. Jackson and H. M. Burt, *Journal of biochemical biophysical methods* 1996, **31**, 145-150.
82. S. Das, N. Patra, A. Banerjee, B. Das and S. Ghosh, *Journal of Molecular Liquids*, 2020, **320**, 114497.
83. G. S. Hartley, *The colloidal state. 2. Aqueous Solutions of paraffin-chain salts: a study in micelle formation*, Hermann, 1936.
84. J. W. McBain and C. Salmon, *Journal of the American Chemical Society*, 1920, **42**, 426-460.
85. D. J. Shaw, *Introduction to colloid and surface chemistry*, Butterworths, 1980.
86. F. M. Menger, *Accounts of Chemical Research*, 1979, **12**, 111-117.
87. P. Debye and E. Anacker, *The Journal of Physical Chemistry*, 1951, **55**, 644-655.
88. W. J. J. o. C. S. Philippoff, 1950, **5**, 169-191.
89. W. D. Harkins and R. Mittelman, *Journal of Colloid Science*, 1949, **4**, 367-381.
90. S. Liu, Y. I. Gonzalez, D. Danino and E. W. J. M. Kaler, 2005, **38**, 2482-2491.
91. C. Tanford, *The Journal of Physical Chemistry*, 1972, **76**, 3020-3024.
92. R. Salkar, D. Mukesh, S. Samant and C. J. L. Manohar, 1998, **14**, 3778-3782.
93. J. N. Israelachvili, D. J. Mitchell and B. W. Ninham, *Journal of the Chemical Society, Faraday Transactions 2: Molecular Chemical Physics* 1976, **72**, 1525-1568.
94. J. N. Israelachvili, *Intermolecular and surface forces*, Academic press, 2011.
95. S. Ghosh, G. B. Ray and S. Mondal, *Fluid Phase Equilibria*, 2015, **405**, 46-54.
96. C. Tanford, *The hydrophobic effect: formation of micelles and biological membranes 2d ed*, J. Wiley., 1980.
97. E. Sutherland, S. M. Mercer, M. Everist and D. G. Leaist, *Journal of Chemical & Engineering Data*, 2009, **54**, 272-278.
98. L. Pérez, A. Pinazo, M. R. Infante and R. Pons, *The Journal of Physical Chemistry B*, 2007, **111**, 11379-11387.

99. S. M. F. Tavernier, C. G. Vonk and R. Gijbels, *Journal of Colloid and Interface Science*, 1981, **81**, 341-353.
100. N. Berclaz, M. Müller, P. Walde and P. L. Luisi, *The Journal of Physical Chemistry B*, 2001, **105**, 1056-1064.
101. J. Gustafsson, T. Nylander, M. Almgren and H. Ljusberg-Wahren, *Journal of Colloid and Interface Science*, 1999, **211**, 326-335.
102. S. Hayashi and S. Ikeda, *The Journal of Physical Chemistry*, 1980, **84**, 744-751.
103. A. S. Rafique, S. Khodaparast, A. S. Poulos, W. N. Sharratt, E. S. Robles and J. T. Cabral, *Soft Matter*, 2020, **16**, 7835-7844.
104. H. Hoffmann, G. Platz, H. Rehage and W. Schorr, *Advances in Colloid and Interface Science*, 1982, **17**, 275-298.
105. D. Varade, T. Joshi, V. K. Aswal, P. S. Goyal, P. A. Hassan and P. Bahadur, *Colloids and Surfaces A: Physicochemical and Engineering Aspects*, 2005, **259**, 95-101.
106. K. S. Schmitz, *Introduction to dynamic light scattering by macromolecules*, Elsevier, 2012.
107. B. Chu, *Laser light scattering*, 1974, **75**, 12150.
108. E. Pike, in *Photon Correlation Spectroscopy and Velocimetry*, Springer, 1977, pp. 3-21.
109. J. Stetefeld, S. A. McKenna and T. R. Patel, *Biophysical Reviews*, 2016, **8**, 409-427.
110. N. J. Turro and A. Yekta, *Journal of the American Chemical Society*, 1978, **100**, 5951-5952.
111. P. P. Infelta, *Chemical Physics Letters*, 1979, **61**, 88-91.
112. R. G. Alargova, I. I. Kochijashky, M. L. Sierra and R. Zana, *Langmuir*, 1998, **14**, 5412-5418.
113. A. Yekta, M. Aikawa and N. J. Turro, *Chemical Physics Letters*, 1979, **63**, 543-548.
114. M. Almgren, *Advances in colloid and interface science*, 1992, **41**, 9-32.
115. M. Almgren, J. E. Leofroth and J. Van Stam, *The Journal of Physical Chemistry* 1986, **90**, 4431-4437.
116. R. C. Oliver, J. Lipfert, D. A. Fox, R. H. Lo, S. Doniach and L. Columbus, *PLOS ONE*, 2013, **8**, e62488.
117. H. Nakahara, A. Nishino, A. Tanaka, Y. Fujita and O. Shibata, *Colloid Polymer Science* 2019, **297**, 183-189.
118. D. M. Small, in *The Bile Acids Chemistry, Physiology, and Metabolism*, Springer, 1971, pp. 249-356.
119. D. Madenci and S. U. Egelhaaf, *Current Opinion in Colloid & Interface Science*, 2010, **15**, 109-115.
120. P. Lianos and R. Zana, *Journal of Colloid and Interface Science*, 1981, **84**, 100-107.
121. R. Zana and C. Weill, *Journal de Physique Lettres*, 1985, **46**, 953-960.
122. J. F. Scamehorn, *Phenomena in mixed surfactant systems*. United States: N. p., 1986.
123. H. Evans, *Journal of the Chemical Society, Faraday Transactions 1: Physical Chemistry in Condensed Phases*, 1956, 579-586.
124. M. Corrin and W. D. Harkins, *Journal of the American Chemical Society*, 1947, **69**, 683-688.
125. L. Shedlovsky, C. W. Jakob and M. B. Epstein, *The Journal of Physical Chemistry*, 1963, **67**, 2075-2078.
126. R. Zana, *Journal of Colloid and Interface Science*, 1980, **78**, 330-337.
127. P. K. Das Gupta and S. P. Moulik, *Colloid and Polymer Science*, 1989, **267**, 246-254.
128. M. R. Rahman and N. Islam, *Int. J. Sci. Eng. Res*, 2015, **6(1)**, 1508-1516..
129. C. Tanford, *Proceedings of the National Academy of Sciences of the United States of America*, 1974, **71**, 1811-1815.

130. T. Tadros, in *Encyclopedia of Colloid and Interface Science*, ed. T. Tadros, Springer Berlin Heidelberg, Berlin, Heidelberg, 2013, DOI: 10.1007/978-3-642-20665-8_60, pp. 209-210.
131. H. B. Klevens, *Journal of the American Oil Chemists Society*, 1953, **30**, 74-80.
132. A. Rodríguez, M. d. M. Graciani and M. L. Moyá, *Langmuir*, 2008, **24**, 12785-12792.
133. S. Das, B. Naskar and S. Ghosh, *Soft Matter*, 2014, **10**, 2863-2875.
134. B. D. Flockhart, *Journal of Colloid Science*, 1961, **16**, 484-492.
135. L. Tennouga, A. Mansri, K. Medjahed, A. Chetouani and I. Warad, *Mater Environ Sci*, 2015, **6**, 2711-2716.
136. N. Muller, *Langmuir*, 1993, **9**, 96-100.
137. E. Mohajeri and G. D. Noudeh, *E-Journal of Chemistry*, 2012, **9**, 961739.
138. S. Kaneshina, O. Shibata, M. Nakamura and M. Tanaka, *Colloids and Surfaces*, 1983, **6**, 73-82.
139. K. Hara, H. Kuwabara, O. Kajimoto and K. Bhattacharyya, *Journal of Photochemistry and Photobiology A: Chemistry*, 1999, **124**, 159-162.
140. K. Shinoda, T. Yamaguchi and R. J. B. o. t. C. S. o. J. Hori, 1961, **34**, 237-241.
141. T. Mukhim, J. Dey, S. Das and K. Ismail, *Journal of Colloid and Interface Science*, 2010, **350**, 511-515.
142. S. Pal, A. R. Das and S. P. Moulik, *Indian journal of biochemistry & biophysics*, 1982, **19**, 295-300.
143. B. K. Roy and S. P. Moulik, *Colloids and Surfaces A: Physicochemical and Engineering Aspects*, 2002, **203**, 155-166.
144. M. Benrraou, B. L. Bales and R. Zana, *The Journal of Physical Chemistry B*, 2003, **107**, 13432-13440.
145. P. Mukerjee, *Advances in Colloid and Interface Science*, 1967, **1**, 242-275.
146. B. Naskar, A. Dan, S. Ghosh, V. K. Aswal and S. P. Moulik, *Journal of Molecular Liquids*, 2012, **170**, 1-10.
147. J. Bloor, J. Morrison and C. Rhodes, *Journal of pharmaceutical sciences*, 1970, **59**, 387-391.
148. J. H. Clint, *Surfactant aggregation*, Springer Science & Business Media, 2012.
149. M. J. Schick, *Nonionic surfactants: physical chemistry*, CRC Press, 1987.
150. J. L. Williams and N. J. Stein, *Journal of the American Oil Chemists Society*, 1965, **42**, 1054-1056.
151. Z. Wang, J.-H. Xu, W. Zhang, B. Zhuang and H. Qi, *Colloids and Surfaces B: Biointerfaces*, 2008, **61**, 118-122.
152. G. Campese, E. Rodrigues, E. Tambourgi and A. Pessoa Jr, *Brazilian Journal of Chemical Engineering*, 2003, **20**, 335-337.
153. G. Mannella, V. La Carrubba and V. J. R. o. S. I. Brucato, 2013, **84**, 075118.
154. K. Solec, *Macromolecules*, 1970, **3**, 665-673.
155. M. Osa, H. Shiraki, U. Morinaga and T. Yoshizaki, *Polymer Journal*, 2013, **45**, 681-684.
156. M. M. Alam, S. Mahbub, M. M. Hosen, D. Kumar and M. A. Hoque, *Chemical Papers*, 2021, **75**, 3457-3468.
157. J. Gurung and A. K. Pulikkal, *Chemical Engineering Communications*, 2020, **207**, 1462-1473.
158. M. J. Hossain, N. H. Al-Shaalan, M. R. Amin, S. Aktar, S. Rana, S. M. Wabaidur, M. A. Rub, M. A. Hoque, S. E. Kabir and A. M. Asiri, *Journal of Chemical & Engineering Data*, 2020, **65**, 841-847.
159. P. Patidar and A. Bahadur, *Journal of Molecular Liquids*, 2018, **249**, 219-226.
160. N. Dave and T. Joshi, *Journal of Dispersion Science Technology* 2018, **39**, 548-551.

161. S. Murugesan and R. Iyyasamy, *Separation Science Technology* 2017, **52**, 1929-1937.
162. D. Patel, S. Agarwal, D. Ray, K. Kuperkar, V. K. Aswal and P. Bahadur, *Colloids and Surfaces A: Physicochemical and Engineering Aspects*, 2021, **617**, 126330.
163. P. J. Flory, *The Journal of chemical physics*, 1941, **9**, 660-660.
164. P. J. Flory, *The Journal of chemical physics*, 1942, **10**, 51-61.
165. Å. Norström, *European Journal of Clinical Pharmacology*, 2005, **60**, 915-915.
166. G. J. Hirasaki, C. A. Miller and M. Puerto, *SPE journal*, 2011, **16**, 889-907.
167. P. Samaddar and K. Sen, *Journal of Industrial and Engineering Chemistry*, 2014, **20**, 1209-1219.
168. S. Gunnam, *Asian Journal of Pharmaceutics : Free full text articles from Asian J Pharm* 2018, **12**.
169. G. Némethy and H. A. Scheraga, *The Journal of Chemical Physics*, 1962, **36**, 3401-3417.
170. J. L. Kavanau, *Nature*, 1963, **198**, 525-530.
171. D. Hall and B. Pethica, *Journal*, 1967, **1**, 516-557.
172. Y. Moroi, *Micelles: theoretical and applied aspects*, Springer Science & Business Media, 1992.
173. G. Olofsson and W. J. J. o. t. B. C. S. Loh, 2009, **20**, 577-593.
174. P. R. Majhi and S. P. J. T. J. o. P. C. B. Moulik, 1999, **103**, 5977-5983.
175. J. Lah, C. Pohar and G. Vesnaver, *The Journal of Physical Chemistry B*, 2000, **104**, 2522-2526.
176. G. C. Kresheck, *The Journal of Physical Chemistry B*, 1998, **102**, 6596-6600.
177. A. Chatterjee, S. P. Moulik, S. K. Sanyal, B. K. Mishra and P. M. Puri, *The Journal of Physical Chemistry B*, 2001, **105**, 12823-12831.
178. S. K. Hait, P. R. Majhi, A. Blume and S. P. Moulik, *The Journal of Physical Chemistry B*, 2003, **107**, 3650-3658.
179. J. Enderby and G. Neilson, *F. Franks, Plenum Press, New York* 1979, **6**, 1.
180. S. P. Moulik and D. Mitra, in *Recent Trends In Surface And Colloid Science*, World Scientific, 2012, pp. 51-68.
181. T. L. Hill, *Thermodynamics of Small Systems: Two Volumes Bound as One. 1-2*, Dover, 1994.
182. D. Hall, *Transactions of the Faraday Society*, 1970, **66**, 1351-1358.
183. D. G. Hall, *Journal of the Chemical Society, Faraday Transactions 2: Molecular and Chemical Physics*, 1972, **68**, 1439-1447.
184. D. G. Hall, *Journal of the Chemical Society, Faraday Transactions 2: Molecular Chemical Physics* 1977, **73**, 897-910.
185. J. M. Corkill, J. F. Goodman, T. Walker, J. Wyer and D. Tabor, *Proceedings of the Royal Society of London. A. Mathematical and Physical Sciences*, 1969, **312**, 243-255.
186. J. Corkill and K. Herrmann, *The Journal of Physical Chemistry*, 1963, **67**, 934-937.
187. J. M. Corkhill and J. F. Goodman, *Advances in Colloid and Interface Science*, 1969, **2**, 298-330.
188. C. Tanford, *The Journal of Physical Chemistry*, 1974, **78**, 2469-2479.
189. R. Nagarajan and E. Ruckenstein, *Journal of Colloid and Interface Science*, 1977, **60**, 221-231.
190. M. T. García, I. Ribosa, J. Sanchez Leal and F. Comelles, *Journal of the American Oil Chemists Society*, 1992, **69**, 25-29.
191. T. C. G. Kibbey and K. F. Hayes, *Environmental Science & Technology*, 1997, **31**, 1171-1177.
192. B. J. Aungst and S. Phang, *International Journal of Pharmaceutics*, 1995, **117**, 95-100.
193. M. Noriyuki, N. Yasuko, K. Mariko, M. Shozo and S. Hitoshi, *International Journal of Pharmaceutics*, 1980, **4**, 281-290.
194. M. Bergström, *Langmuir*, 1996, **12**, 2454-2463.

195. A. Mal, S. Bag, S. Ghosh and S. P. Moulik, *Colloids and Surfaces A: Physicochemical and Engineering Aspects*, 2018, **553**, 633-644.
196. R. Dutta, S. Ghosh, P. Banerjee, S. Kundu and N. Sarkar, *Journal of Colloid and Interface Science*, 2017, **490**, 762-773.
197. R. M. Hill, K. Ogino and M. Abe, *Surfactant science series*, 1993, **46**, 317.
198. M. J. Blandamer, B. Briggs, P. M. Cullis and J. B. Engberts, *Physical Chemistry Chemical Physics* 2000, **2**, 5146-5153.
199. S. P. Moulik, M. E. Haque, P. K. Jana and A. R. Das, *The Journal of Physical Chemistry*, 1996, **100**, 701-708.
200. N. Azum, A. Z. Naqvi, M. Akram and D. Kabir ud, *Journal of Colloid and Interface Science*, 2008, **328**, 429-435.
201. P. Parekh, D. Varade, J. Parikh and P. Bahadur, *Colloids and Surfaces A: Physicochemical and Engineering Aspects*, 2011, **385**, 111-120.
202. H. Gandhi, D. Varade and P. Bahadur, *Tenside, surfactants, detergents*, 2002, **39**, 16-19.
203. S. Mahbub, S. Rana, M. Abdul Rub, M. A. Hoque, S. E. Kabir and A. M. Asiri, *Journal of Chemical & Engineering Data*, 2019, **64**, 4376-4389.
204. C. Das, T. Chakraborty, S. Ghosh and B. Das, *Colloid Journal*, 2010, **72**, 788-798.
205. A. George, S. Vora, A. Dogra, H. Desai and P. Bahadur, *Journal of Surfactants and Detergents*, 1998, **1**, 507-514.
206. N. Azum, M. Abdul Rub, A. M. Asiri, H. M. Marwani and M. Akram, *Journal of Saudi Chemical Society*, 2020, **24**, 683-692.
207. N. Azum, M. A. Rub and A. M. Asiri, *The Journal of Chemical Thermodynamics*, 2019, **128**, 406-414.
208. D. M. Ćirin, M. M. Poša and V. S. Krstonošić, *Chemistry Central Journal*, 2011, **5**, 89.
209. A. Mandal, S. Ray and S. Moulik, 1980, **84**, 856-859.
210. R. K. Mahajan, N. Kaur and M. S. Bakshi, *Colloids and Surfaces A: Physicochemical and Engineering Aspects*, 2005, **255**, 33-39.
211. A. Sahu, S. Choudhury, A. Bera, S. Kar, S. Kumar and A. Mandal, *Journal of Dispersion Science and Technology*, 2015, **36**, 1156-1169.
212. K. Ogino, N. Tsubaki and M. Abe, *Journal of Colloid and Interface Science*, 1984, **98**, 78-83.
213. T. Joshi, J. Mata and P. Bahadur, *Colloids and Surfaces A: Physicochemical and Engineering Aspects*, 2005, **260**, 209-215.
214. K. S. Sharma, C. Rodgers, R. M. Palepu and A. K. Rakshit, *Journal of Colloid and Interface Science*, 2003, **268**, 482-488.
215. S. Ghosh and T. Chakraborty, *The Journal of Physical Chemistry B*, 2007, **111**, 8080-8088.
216. L. Guo, R. H. Colby, M. Y. Lin and G. P. Dado, *Journal of Rheology*, 2001, **45**, 1223-1243.
217. H. G. Thomas, A. Lomakin, D. Blankschtein and G. B. Benedek, *Langmuir*, 1997, **13**, 209-218.
218. P. Jafari-Chashmi and A. Bagheri, *Journal of Molecular Liquids*, 2018, **269**, 816-823.
219. X.-f. Gu, J. Huo, R.-t. Wang, D.-c. Wu and Y.-l. Yan, *Journal of Dispersion Science and Technology*, 2015, **36**, 334-342.
220. N. A. Smirnova, A. A. Vanin, E. A. Safonova, I. B. Pukinsky, Y. A. Anufrikov and A. L. Makarov, *Journal of colloid and interface science*, 2009, **336**, 793-802.
221. H. Kumar and G. Kaur, *Journal of Dispersion Science and Technology*, 2021, **42**, 970-983.
222. X. Wang, R. Wang, Y. Zheng, L. Sun, L. Yu, J. Jiao and R. Wang, *The Journal of Physical Chemistry B*, 2013, **117**, 1886-1895.

223. F. Comelles, I. Ribosa, J. J. González and M. T. Garcia, *Journal of Colloid and Interface Science*, 2014, **425**, 44-51.
224. R. Vashishat, R. Sanan and R. K. Mahajan, *RSC Advances*, 2015, **5**, 72132-72141.
225. R. Patel, A. B. Khan, N. Dohare, M. Maroof Ali and H. K. Rajor, *Journal of Surfactants and Detergents*, 2015, **18**, 719-728.
226. A. Pal and A. Yadav, *Journal of Molecular Liquids*, 2019, **279**, 43-50.
227. U. Farooq, R. Patel and A. Ali, *Journal of Solution Chemistry*, 2018, **47**, 568-585.
228. A. B. Khan, M. Ali, N. A. Malik, A. Ali and R. Patel, *Colloids and Surfaces B: Biointerfaces*, 2013, **112**, 460-465.
229. U. Saha, A. Banerjee and B. Das, *Journal of Molecular Liquids*, 2020, **309**, 113164.
230. U. Farooq, A. Ali, R. Patel and N. A. Malik, *Journal of Molecular Liquids*, 2017, **234**, 452-462.
231. R. Sharma, S. Mahajan and R. K. Mahajan, *Colloids and Surfaces A: Physicochemical and Engineering Aspects*, 2013, **427**, 62-75.
232. G. Luo, X. Qi, C. Han, C. Liu and J. Gui, *Journal of Surfactants and Detergents*, 2013, **16**, 531-538.
233. A. Pal and R. Punia, *Journal of Molecular Liquids*, 2019, **296**, 111831.
234. X. Qi, X. Zhang, G. Luo, C. Han, C. Liu and S. Zhang, *Journal of Dispersion Science and Technology*, 2013, **34**, 125-133.
235. A. Pal and R. Punia, *Colloid and Polymer Science*, 2019, **297**, 1541-1557.
236. A. K. Tiwari, Sonu and S. K. Saha, *The Journal of Chemical Thermodynamics*, 2013, **60**, 29-40.
237. L. Qin and X.-H. J. R. a. Wang, 2017, **7**, 51426-51435.
238. D. Bhatt, K. Maheria and J. Parikh, *The Journal of Chemical Thermodynamics*, 2014, **74**, 184-192.
239. H. Pathan, R. Patil, D. Ray, V. K. Aswal, P. Bahadur and S. Tiwari, *Journal of Molecular Liquids*, 2019, **290**, 111235.
240. F. Comelles, I. Ribosa, J. J. González and M. T. Garcia, *Langmuir*, 2012, **28**, 14522-14530.
241. T. Misono, H. Sakai, K. Sakai, M. Abe and T. Inoue, *Journal of Colloid and Interface Science*, 2011, **358**, 527-533.
242. T. Misono, K. Okada, K. Sakai, M. Abe and H. J. J. o. o. s. Sakai, 2016, **65**, 499-506.
243. N. Li, S. Zhang, H. Ma and L. Zheng, *Langmuir*, 2010, **26**, 9315-9320.
244. J. H. Clint, *Journal of the Chemical Society, Faraday Transactions 1: Physical Chemistry in Condensed Phases*, 1975, **71**, 1327-1334.
245. H. Lange and K. Beck, *Kolloid-Zeitschrift Zeitschrift Fur Polymere* 1973, **251**, 424-431.
246. H. Lange, *Kolloid-Zeitschrift* 1953, **131**, 96-103.
247. K. Shinoda, *The Journal of Physical Chemistry*, 1954, **58**, 541-544.
248. Y. Moroi, N. Nishikido, M. Saito and R. Matuura, *Journal of Colloid and Interface Science*, 1975, **52**, 356-363.
249. D. Rubingh and K. J. v. Mittal, 1979, **1**, 337-354.
250. N. Turro, P. Kuo, P. Somasundaran and K. Wong, *The Journal of Physical Chemistry* 1986, **90**, 288-291.
251. M. J. Rosen and F. Zhao, *Journal of Colloid and Interface Science*, 1983, **95**, 443-452.
252. C. Sarmoria, S. Puvvada and D. Blankschtein, *Langmuir*, 1992, **8**, 2690-2697.
253. K. Shinoda, *The Journal of Physical Chemistry*, 1954, **58**, 1136-1141.
254. F. Tokiwa, *Journal of Colloid and Interface Science*, 1968, **28**, 145-148.

255. T. Kato, H. Takeuchi and T. Seimiya, *Journal of Colloid and Interface Science*, 1990, **140**, 253-257.
256. A. Makayssi, R. Bury and C. Treiner, *Langmuir*, 1994, **10**, 1359-1365.
257. T. R. Desai and S. G. Dixit, *Journal of Colloid and Interface Science*, 1996, **177**, 471-477.
258. F. Tokiwa, K. Ohki and I. Kokubo, *Bulletin of the Chemical Society of Japan*, 1968, **41**, 2845-2848.
259. B. W. Barry, J. C. Morrison and G. F. J. Russell, *Journal of Colloid and Interface Science*, 1970, **33**, 554-561.
260. K. Kuriyama, *Kolloid-Zeitschrift und Zeitschrift für Polymere*, 1962, **180**, 55-64.
261. J. Corkill, J. Goodman and J. Tate, *Transactions of the Faraday Society*, 1964, **60**, 986-995.
262. M. J. Schick and D. J. Manning, *Journal of the American Oil Chemists Society*, 1966, **43**, 133-136.
263. N. J. Turro and P. C. C. Lee, *The Journal of Physical Chemistry*, 1982, **86**, 3367-3371.
264. N. Muller and H. Simsohn, *The Journal of Physical Chemistry*, 1971, **75**, 942-945.
265. G. Sugihara and P. Mukerjee, *The Journal of Physical Chemistry*, 1981, **85**, 1612-1616.
266. I. O. Sutherland, *Chemical Society Reviews*, 1986, **15**, 63-91.
267. M. W. Hosseini, J. M. Lehn, S. R. Duff, K. Gu and M. P. Mertes, *The Journal of Organic Chemistry*, 1987, **52**, 1662-1666.
268. J.-M. Lehn, *Science*, 1985, **227**, 849-856.
269. P. Yohannes, M. P. Mertes and K. B. Mertes, *Journal of the American Chemical Society*, 1985, **107**, 8288-8289.
270. E. Bayer, Rapp, W., New polymer supports for solid-liquid-phase peptide synthesis, De Gruyter 2019.
271. S. Omura, *Macrolide antibiotics: chemistry, biology, and practice*, Academic press, 2002.
272. J. M. Lehn and P. Vierling, *Tetrahedron Letters*, 1980, **21**, 1323-1326.
273. R. M. Izatt, J. S. Bradshaw, S. A. Nielsen, J. D. Lamb, J. J. Christensen and D. Sen, *Chemical Reviews*, 1985, **85**, 271-339.
274. S. Kado and K. Kimura, *Journal of the American Chemical Society*, 2003, **125**, 4560-4564.
275. R. C. Helgeson, J. M. Timko and D. J. Cram, *Journal of the American Chemical Society* 1973, **95**, 3023-3025.
276. G. W. Gokel and B. J. Garcia, *Tetrahedron Letters*, 1977, **18**, 317-320.
277. R. M. Izatt, J. S. Bradshaw, M. L. Colter, Y. Nakatsuji, N. O. Spencer, M. F. Brown, G. Arena, P. K. Tse and B. E. Wilson, *The Journal of Organic Chemistry*, 1985, **50**, 4865-4872.
278. J. H. Nelson, *Synthesis and Reactivity in Inorganic and Metal-Organic Chemistry*, 1980, **10**, 325-326.
279. J. Lockhart, A. Robson, M. Thompson, S. D. Furtado, C. Kaura and A. J. J. o. t. C. S. Allan, *Perkin Transactions 1*, 1973, 577-581.
280. J. C. Lockhart and M. E. Thompson, *Journal of the Chemical Society, Perkin Transactions 1*, 1977, DOI: 10.1039/P19770000202, 202-204.
281. C. J. Pedersen, *Angewandte Chemie International Edition in English*, 1988, **27**, 1021-1027.
282. S. A. Hogberg and D. J. Cram, *The Journal of Organic Chemistry*, 1975, **40**, 151-152.
283. S. Das, S. Mondal and S. Ghosh, *Journal of Chemical Engineering Data* 2013, **58**, 2586-2595.
284. R. Singh and R. Garg, *E-Journal of Chemistry*, 2010, **7**, 578-582.
285. R. Garg, R. Singh and S. Mehta, *Asian Journal of Research in Chemistry*, 2010, **3**, 71-77.

286. E. Caponetti, D. Chillura-Martino and L. Pedone, *Langmuir*, 2004, **20**, 3854-3862.
287. E. Vikingstad and J. Bakken, *Journal of Colloid and Interface Science*, 1980, **74**, 8-15.
288. N. Gol'dshleger, I. Kalashnikova, V. Baulin and A. Y. Tsvadze, *Protection of Metals, Physical Chemistry of Surfaces* 2011, **47**, 471-477.
289. H. Staudinger, *Schweiz. Cherniker Ztg*, 1919, 1-5; 28-33; 60-64.
290. S. F. Sun, *Physical chemistry of macromolecules: basic principles and issues*, John Wiley & Sons, 2004.
291. M. A. Gauthier and H.-A. Klok, *Chemical Communications*, 2008, issue 23 ,2591-2611.
292. M. M. Gromiha, *Protein bioinformatics: from sequence to function*, academic press, 2010.
293. K. D. Schwenke, in *Studies in Interface Science*, eds. D. Möbius and R. Miller, Elsevier, 1998, vol. 7, pp. 1-50.
294. K. P. Ananthapadmanabhan, *Interactions of surfactants with polymers and proteins*, CRC Press, 2018.
295. M. L. Huggins, *Journal of the American Chemical Society*, 1942, **64**, 2716-2718.
296. R. Simha, *Journal of Applied physics*, 1952, **23**, 1020-1024.
297. P. Y. Cheng and H. K. Schachman, *Journal of Polymer Science*, 1955, **16**, 19-30.
298. R. A. Alberty and F. Daniels, *Physical Chemistry, 5th edition*. John Wiley and Sons: New York,, 1979.
299. *Polymer Handbook*, J. Brandrup and E. Immergut, Wiley-Interscience, Chichester, 1989. pp. ix + parts I to VIII.
300. I. Yilgor, T. C. Ward, E. Yilgor and G. E. Atilla, *Polymer*, 2006, **47**, 1179-1186.
301. P. Banerjee, I. Mukherjee, S. Bhattacharya, S. Datta, S. P. Moulik and D. Sarkar, *Langmuir*, 2009, **25**, 11647-11656.
302. A. Dan, S. Ghosh and S. P. Moulik, *Biopolymers: Original Research on Biomolecules*, 2009, **91**, 687-699.
303. P. Nandi, A. Bhattarai and B. J. J. o. P. S. P. B. P. P. Das, 2007, **45**, 1765-1770.
304. A. Silberberg, J. Eliassaf and A. Katchalsky, *Journal of Polymer Science*, 1957, **23**, 259-284.
305. H. Kitano, K. Ichikawa, M. Ide, M. Fukuda and W. J. L. Mizuno, 2001, **17**, 1889-1895.
306. R. J. Robson and E. A. J. T. J. o. P. C. Dennis, 1977, **81**, 1075-1078.
307. C. Branca, S. Magazu, G. Maisano, F. Migliardo, P. Migliardo and G. Romeo, *The Journal of Physical Chemistry B*, 2002, **106**, 10272-10276.
308. Y. Miwa, H. Ishida, M. Tanaka and A. J. J. o. B. S. Mochizuki, *Polymer Edition*, 2010, **21**, 1911-1924.
309. P. Elworthy, A. Florence and A. Rahman, *The Journal of Physical Chemistry*, 1972, **76**, 1763-1767.
310. H. S. Frank and M. W. Evans, *The Journal of chemical physics*, 1945, **13**, 507-532.
311. B. Geetha and A. B. Mandal, *The Journal of chemical physics*, 1996, **105**, 9649-9656.
312. M. Hans, K. Shimoni, D. Danino, S. J. Siegel and A. Lowman, *Biomacromolecules*, 2005, **6**, 2708-2717.
313. K. Tam, R. Jenkins, M. Winnik and D. Bassett, *Macromolecules*, 1998, **31**, 4149-4159.
314. G.-E. Yu, Y.-W. Yang, Z. Yang, D. Attwood, C. Booth and V. M. Nace, *Langmuir*, 1996, **12**, 3404-3412.
315. E. Alami, M. Almgren, W. Brown and J. Francois, *Macromolecules*, 1996, **29**, 2229-2243.
316. S. Dai, K. Tam and R. Jenkins, *European polymer journal*, 2000, **36**, 2671-2677.

317. M. Pitsikalis, J. Woodward, J. W. Mays and N. J. M. Hadjichristidis, 1997, **30**, 5384-5389.
318. J. H. Yao, K. Y. Mya, X. Li, M. Parameswaran, Q.-H. Xu, K. P. Loh and Z.-K. Chen, *The Journal of Physical Chemistry B*, 2008, **112**, 749-755.
319. P. J. Flory, *Principles of polymer chemistry*, Cornell University Press, 1953.
320. W. Brown, *Dynamic light scattering: the method and some applications*, Clarendon Press, 1993.
321. M. Nichifor, S. Lopes, M. Bastos and A. J. T. J. o. P. C. B. Lopes, 2004, **108**, 16463-16472.
322. B. Kronberg, K. Holmberg and B. Lindman, *Surface chemistry of surfactants and polymers*, John Wiley & Sons, 2014.
323. J. Xia, P. L. Dubin and Y. Kim, *The Journal of Physical Chemistry*, 1992, **96**, 6805-6811.
324. Q. Qiu, P. Somasundaran and B. A. Pethica, *Langmuir*, 2002, **18**, 3482-3486.
325. P. Hansson, *The Journal of Physical Chemistry B*, 2009, **113**, 12903-12915.
326. D. Ray, S. Das, R. De and B. Das, *Carbohydrate Polymers*, 2015, **125**, 255-264.
327. S. Ghosh, A. Mal, T. Chakraborty, G. C. De and D. G. Marangoni, *Journal of Surface Science and Technology*, 2017, **32**, 107-114.
328. A. Mal, A. Saha, G. Dinda and S. Ghosh, *Journal of Molecular Liquids*, 2020, **299**, 112153.
329. M. Prasad, R. Palepu and S. P. Moulik, *Colloid and Polymer Science*, 2006, **284**, 871-878.
330. N. Sardar, M. Kamil and D. Kabir ud, *Industrial & Engineering Chemistry Research*, 2012, **51**, 1227-1235.
331. P. Roscigno, F. Asaro, G. Pellizer, O. Ortona and L. Paduano, *Langmuir*, 2003, **19**, 9638-9644.
332. P. Chandar, P. Somasundaran and N. J. Turro, *Macromolecules*, 1988, **21**, 950-953.
333. B. Cabane and R. Duplessix, *Colloids and Surfaces*, 1985, **13**, 19-33.
334. M. N. Jones, *Journal of Colloid and Interface Science*, 1967, **23**, 36-42.
335. N. Péron, R. Mészáros, I. Varga and T. Gilányi, *Journal of Colloid and Interface Science*, 2007, **313**, 389-397.
336. B. Mandal, S. P. Moulik and S. Ghosh, *Colloid and Polymer Science*, 2014, **292**, 2485-2495.
337. B. M. Folmer and B. Kronberg, *Langmuir*, 2000, **16**, 5987-5992.
338. I. García-Mateos, S. Pérez and M. M. Velázquez, *Journal of Colloid and Interface Science*, 1997, **194**, 356-363.
339. C. Honda, H. Kamizono, K.-i. Matsumoto and K. Endo, *Journal of Colloid and Interface Science*, 2004, **278**, 310-317.
340. D. E. Otzen, *Biophysical Journal*, 2002, **83**, 2219-2230.
341. P. Sehgal and D. E. Otzen, 2006, **15**, 890-899.
342. M. D. Lad, V. M. Ledger, B. Briggs, R. J. Green and R. A. Frazier, *Langmuir*, 2003, **19**, 5098-5103.
343. J. Narayanan, A. A. Rasheed, J. R. J. J. o. c. Bellare and i. science, 2008, **328**, 67-72.
344. N. J. Turro, X.-G. Lei, K. Ananthapadmanabhan and M. Aronson, *Langmuir*, 1995, **11**, 2525-2533.
345. S. F. Santos, D. Zanette, H. Fischer and R. Itri, *Journal of Colloid and Interface Science*, 2003, **262**, 400-408.
346. S. Ghosh and A. Banerjee, *Biomacromolecules*, 2002, **3**, 9-16.
347. S. Ghosh, *Colloids and Surfaces B: Biointerfaces*, 2008, **66**, 178-186.
348. S. Ghosh, *Colloids and Surfaces A: Physicochemical and Engineering Aspects*, 2005, **264**, 6-16.
349. R. Bhattacharya and D. Bhattacharyya, *Biochimica et Biophysica Acta (BBA) - Proteins and Proteomics*, 2009, **1794**, 698-708.

350. R. Vashishat, S. Chabba and R. K. Mahajan, *RSC Advances*, 2017, **7**, 13041-13052.
351. X. Wang, J. Liu, L. Sun, L. Yu, J. Jiao and R. Wang, *The Journal of Physical Chemistry B*, 2012, **116**, 12479-12488.
352. B. Mandal, S. Mondal, A. Pan, S. P. Moulik and S. Ghosh, *Colloids and Surfaces A: Physicochemical and Engineering Aspects*, 2015, **484**, 345-353.
353. I. Jha, M. Bisht, N. K. Mogha and P. Venkatesu, *The Journal of Physical Chemistry B*, 2018, **122**, 7522-7529.
354. D. Wu, G. Xu, Y. Sun, H. Zhang, H. Mao and Y. Feng, *Biomacromolecules*, 2007, **8**, 708-712.
355. M. Subramanian, B. S. Sheshadri and M. P. Venkatappa, *The Journal of Biochemistry*, 1984, **95**, 413-421.
356. M. Tian, J. Zhu, J. Guo and X. Guo, *Journal of Surfactants and Detergents*, 2021, **24**, 111-119.
357. Y. Nozaki, J. A. Reynolds and C. Tanford, *Journal of Biological Chemistry*, 1974, **249**, 4452-4459.
358. S. Mondal, M. L. Raposo, G. Prieto and S. Ghosh, *Journal of Chemical & Engineering Data*, 2016, **61**, 1221-1228.
359. A. Ray and G. J. J. o. t. A. C. S. Nemethy, 1971, **93**, 6787-6793.
360. A. R. Fersht and V. Daggett, *Cell*, 2002, **108**, 573-582.
361. D. E. Otzen, L. Christiansen and M. SchÜlein, *Protein Science*, 1999, **8**, 1878-1887.
362. D. Mitra, S. C. Bhattacharya and S. P. Moulik, *The Journal of Physical Chemistry B*, 2008, **112**, 6609-6619.
363. D. V. de Freitas, B. L. Kuhn, C. R. Bender, A. M. Furuyama Lima, M. de Freitas Lima, M. J. Tiera, C. L. Kloster, C. P. Frizzo and M. A. Villetti, *Journal of Molecular Liquids*, 2020, **297**, 111734.
364. S. Panmai, R. K. Prud'homme, D. G. Peiffer, S. Jockusch and N. J. Turro, *Langmuir*, 2002, **18**, 3860-3864.
365. D. Taylor, R. Thomas, P. Li and J. Penfold, *Langmuir*, 2003, **19**, 3712-3719.
366. B. Jan, *Chemical Society Reviews*, 1993, **22**, 85-92.
367. S. Saito and M. Yukawa, *Journal of Colloid and Interface Science*, 1969, **30**, 211-218.
368. R. Petkova, S. Tcholakova and N. D. Denkov, *Colloids and Surfaces A: Physicochemical and Engineering Aspects*, 2013, **438**, 174-185.
369. S. Saito, *Colloid and Polymer Science*, 1979, **257**, 266-272.
370. K. Hayakawa, JCT Kwak in *Cationic Surfactants: Physical Chemistry* (D. N. Rubingh and PM Holland, eds.) *Surfactant Sci. Ser. No 37*, *Journal*, 1991.
371. N. Alizadeh, B. Ranjbar and M. Mahmodian, *Colloids and Surfaces A: Physicochemical and Engineering Aspects*, 2003, **212**, 211-218.
372. B. Lindman, K. Thalberg, E. Goddard and K. J. C. P. Ananthapadmanabhan (eds.), CRC Press, Boca Raton, FL, 1993, pp. 1-427.
373. P. P. Mishra, J. Bhatnagar and A. Datta, *The Journal of Physical Chemistry B*, 2005, **109**, 24225-24230.
374. X. Wang, J. Wang, Y. Wang and H. Yan, *Langmuir*, 2004, **20**, 9014-9018.
375. B. Cabane and R. Duplessix, *J. Phys. France*, 1982, **43**, 1529-1542.
376. R. Mészáros, I. Varga and T. Gilányi, *The Journal of Physical Chemistry B*, 2005, **109**, 13538-13544.
377. L. Bernazzani, S. Borsacchi, D. Catalano, P. Gianni, V. Mollica, M. Vitelli, F. Asaro and L. Feruglio, *The Journal of Physical Chemistry B*, 2004, **108**, 8960-8969.
378. J. Francois, J. Dayantis and J. Sabbadin, *European Polymer Journal*, 1985, **21**, 165-174.

379. H.-W. Tseng, P.-C. Chen, H.-W. Tsui, C.-H. Wang, T.-Y. Hu and L.-J. Chen, *Journal of the Taiwan Institute of Chemical Engineers*, 2018, **92**, 50-57.
380. R. Nagarajan and B. Kalpakci, in *Microdomains in Polymer Solutions*, Springer, 1985, pp. 369-381.
381. T. Takagi and T. J. B. o. t. C. S. o. J. Isemura, 1960, **33**, 437-441.
382. M. M. Fishman and R. S. Miller, *Journal of Colloid Science*, 1960, **15**, 232-235.
383. J. B. Huang, M. Mao and B. Y. Zhu, *Colloids and Surfaces A: Physicochemical and Engineering Aspects*, 1999, **155**, 339-348.
384. S. Cinelli, G. Onori and A. Santucci, *Colloids and Surfaces A: Physicochemical and Engineering Aspects*, 1999, **160**, 3-8.
385. R. Zana, *Advances in Colloid and Interface Science*, 1995, **57**, 1-64.
386. P. C. Griffith, P. Stilbs, A. M. Howe and T. Cosgrove, *Langmuir*, 1996, **12**, 2884-2893.
387. K. Shirahama, J. Liu, I. Aoyama and N. Takisawa, *Colloids and Surfaces A: Physicochemical and Engineering Aspects*, 1999, **147**, 133-138.
388. P. C. Griffiths, N. Hirst, A. Paul, S. M. King, R. K. Heenan and R. Farley, *Langmuir*, 2004, **20**, 6904-6913.
389. S. Sultana, M. M. Rahman, M. R. Amin, S. Rana, M. A. Hoque, D. Kumar and M. Alfakeer, *Molecular Physics*, 2021, **119**, e1892848.
390. K. Holmberg, B. Jönsson, B. Kronberg and B. Lindman, *Polymers in Aqueous Solution*, Wiley-Blackwell, 2002.
391. J. A. Reynolds and C. Tanford, *Journal of Biological Chemistry*, 1970, **245**, 5161-5165.
392. E. Seth and V. K. Aswal, *Journal of Macromolecular Science, Part B*, 2003, **42**, 85-94.
393. C. Sun, J. Yang, X. Wu, X. Huang, F. Wang and S. Liu, *Biophysical journal*, 2005, **88**, 3518-3524.
394. S. Shinagawa, K. Kameyama and T. Takagi, *Biochimica et Biophysica Acta (BBA) - Protein Structure and Molecular Enzymology*, 1993, **1161**, 79-84.
395. L. A. Bastardo, J. Iruthayaraj, M. Lundin, A. Dedinaite, A. Vareikis, R. Makuška, A. van der Wal, I. Furó, V. M. Garamus and P. M. Claesson, *Journal of Colloid and Interface Science*, 2007, **312**, 21-33.
396. J. Kevelam, J. F. L. van Breemen, W. Blokzijl and J. B. F. N. Engberts, *Langmuir*, 1996, **12**, 4709-4717.
397. I. Portnaya, U. Cogan, Y. D. Livney, O. Ramon, K. Shimoni, M. Rosenberg and D. Danino, *Journal of Agricultural and Food Chemistry*, 2006, **54**, 5555-5561.
398. N. J. Turro, X.-G. Lei, K. P. Ananthapadmanabhan and M. Aronson, *Langmuir*, 1995, **11**, 2525-2533.
399. J. Oakes, *Journal of the Chemical Society, Faraday Transactions 1: Physical Chemistry in Condensed Phases*, 1974, **70**, 2200-2209.
400. Y. Ding, Y. Shu, L. Ge and R. Guo, *Colloids and Surfaces A: Physicochemical and Engineering Aspects*, 2007, **298**, 163-169.
401. C. H. Spink and J. B. Chaires, *Journal of the American Chemical Society*, 1997, **119**, 10920-10928.
402. E. Blanco, J. M. Ruso, G. Prieto and F. Sarmiento, *Journal of Colloid and Interface Science*, 2007, **316**, 37-42.
403. W. D. Harkins and H. F. Jordan, *Journal of the American Chemical Society*, 1930, **52**, 1751-1772.
404. C. D. V. M. Narváez, T. Mazur and V. Sharma, *Soft Matter*, 2021, **17**, 6116-6126.
405. E. D. Goddard and R. B. Hannan, *Journal of the American Oil Chemists' Society*, 1977, **54**, 561-566.

406. D. M. Bloor, J. F. Holzwarth and E. Wyn-Jones, *Langmuir*, 1995, **11**, 2312-2313.
407. G. Wang and G. Olofsson, *The Journal of Physical Chemistry B*, 1998, **102**, 9276-9283.
408. D. R. Rigsbee and P. L. Dubin, *Langmuir*, 1996, **12**, 1928-1929.
409. T. Chakraborty, I. Chakraborty and S. Ghosh, *Langmuir*, 2006, **22**, 9905-9913.
410. P. L. Dubin and R. Oteri, *Journal of colloid and interface science*, 1983, **95**, 453-461.
411. T. Takagi, K. Tsujii and K. Shirahama, *The Journal of Biochemistry*, 1975, **77**, 939-947.
412. R. K. Prud'homme and J. T. Uhl, *Society of Petroleum Engineers Journal*, 1984, **24**, 431-434.
413. A. Dan, S. Ghosh and S. P. Moulik, *The Journal of Physical Chemistry B*, 2009, **113**, 8505-8513.
414. N. Plucktaveesak, A. J. Konop and R. H. Colby, *The Journal of Physical Chemistry B*, 2003, **107**, 8166-8171.
415. Y. Li, P. L. Dubin, H. A. Havel, S. L. Edwards and H. Dautzenberg, *Macromolecules*, 1995, **28**, 3098-3102.
416. C. Wang, P. Ravi and K. C. Tam, *Langmuir*, 2006, **22**, 2927-2930.
417. B. Naskar, A. Dan, S. Ghosh and S. P. Moulik, *Carbohydrate Polymers*, 2010, **81**, 700-706.
418. N. J. Turro, B. H. Baretz and P. L. Kuo, *Macromolecules*, 1984, **17**, 1321-1324.
419. J. R. Lakowicz, *Principles of fluorescence spectroscopy*, Springer science & business media, 2013.
420. P. Pirzadeh, A. A. Moosavi-Movahedi, B. Hemmateenejad, F. Ahmad, M. Shamsipur and A. A. Saboury, *Colloids and Surfaces B: Biointerfaces*, 2006, **52**, 31-38.
421. L. Whitmore and B. A. Wallace, *Biopolymers: Original Research on Biomolecules*, 2008, **89**, 392-400.
422. T. E. Creighton, *Proteins: structures and molecular properties*, Macmillan, 1993.
423. R. W. Woody and A. K. Dunker, *Circular dichroism and the conformational analysis of biomolecules*, 1996, 109-157.
424. Y. Jiang, M. Tian, Y. Wang, W. Xu and X. Guo, *Journal of Molecular Liquids*, 2021, **328**, 115439.

Chapter I

Formation of Mixed Micelle
in an Aqueous Mixture of a
Surface-Active Ionic Liquid
and a Conventional
Surfactant: Experiment and
Modeling

Formation of Mixed Micelle in an Aqueous Mixture of a Surface-Active Ionic Liquid and a Conventional Surfactant: Experiment and Modeling ‡

ABSTRACT: The aggregation behavior in binary mixtures of two surfactants, 1-hexadecyl-3-methylimidazolium chloride and dodecyltrimethylammonium bromide has been investigated in aqueous solutions using conductometric, tensiometric, spectrofluorimetric and Zeta potential measurements. The counterion-binding, aggregation number, and anisotropy of the micellar environment have been ascertained. The results have been analysed on the basis of the theories of Clint, Rubingh, and Motomura. The thermodynamic parameters of the micellization process have been evaluated and discussed. The interfacial adsorptions of the mixed surfactants including their surface excesses and head-group areas have also been evaluated. Existence of an attractive interaction among the constituents of the mixed surfactant systems investigated has been inferred.

(‡ Published in *J. Chem. Eng. Data* 63 (2018) 3784-3800)

1. INTRODUCTION

Surfactants find widespread applications in both industry and everyday life.¹⁻³ Because of the amphiphilic chemical structure, surfactant in an aqueous solution has a preference towards interfacial adsorption at low concentration; whereas beyond a critical concentration, it self-aggregates to form assembled structure whose size, shape and average number of amphiphile per aggregated structure depend on the amphiphile concentration and other physicochemical parameters like temperature, presence of salt, etc. The critical amphiphile concentration required for the onset of the formation of an aggregated structure, referred to as a micelle, is called critical micellar concentration (*cmc*).⁴⁻⁶

Mixed surfactant systems almost invariably manifest enhanced interfacial properties (*e. g.*, decreased critical micellar concentration, higher surface activity, etc.) compared to those of their individual components.⁷⁻¹⁵ This behavior of mixed surfactants allows their use in low concentrations in cosmetic industries to avoid potential skin irritation.^{16,17} It can also be beneficial for the environment as the amount of surfactants released and hence their impact could be substantially reduced.¹⁸ In the pharmaceutical field, the absorption of various drugs in the human body is found to be enhanced by mixed micelles.¹⁹⁻²¹ Mixtures of cationic and

anionic surfactants find use in cleansing products to facilitate their dissolution and improved tolerance of water hardness.²² In view of the remarkable application potential and economic viability of mixed surfactant systems, a significant amount of research work has been devoted for searching and elucidating the physicochemical properties of these systems.

Recent years have witnessed²³⁻³¹ an upsurge of interest in the self-aggregation aptitude of a new class of ionic liquids, known as the surface active ionic liquids (ILs). This is because of the possibility of fine-tuning of the hydrophobicity of ionic liquid molecules by varying the length of the alkyl chains, the type of the head-group or the nature and size of the counterions which might permit the modulation of the structure and the delicate dynamics of their micellar aggregates for specific purposes.

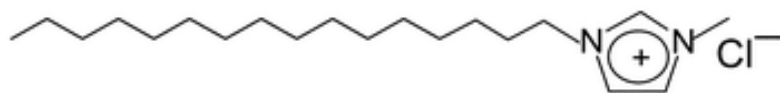
The micellar and thermodynamic properties of the imidazolium-based surface active ionic liquids^{32,33} and their mixtures with anionic, nonionic, zwitterionic and gemini surfactants have been investigated in detail.^{34,35} However, studies involving ILs and cationic surfactants are scarce with the exception of a very few reports.^{36,37} In general, mixtures of cationic surfactants have, so far, been paid relatively less attention.^{11,33,38}

In this work, the micellar and thermodynamic behavior of the mixed micelles formed in the aqueous mixtures of two cationic surfactants - 1-hexadecyl-3-methylimidazoliumchloride (HDMimCl), and dodecyltrimethylammonium bromide (DTAB) have been investigated in order to shed light on various interactions prevailing in this system. The two surfactants with different lengths of the alkyl groups have been selected such that they differ in their *cmc*s by one order of magnitude capable of producing discernible effects in their mixtures.

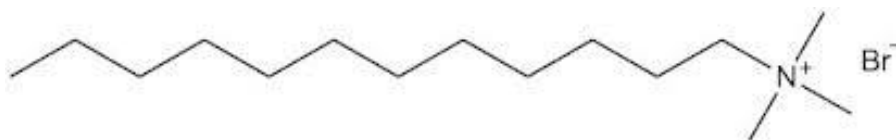
2. EXPERIMENTAL SECTION

2.1 Materials

HDMimCl was purchased from Acros Organics and reagent grade DTAB was procured from Sigma Aldrich. These were used as received without any further purification. Their structures are shown in Figure 1. Pyrene was purchased from Sigma Aldrich. Cetylpyridinium chloride (CPC) purchased from Acros Organics was used as a quencher. 1,6-diphenyl-1,3,5-hexatriene (DPH) from Sigma Aldrich was prepared in THF and used without purification. The specifications of the chemicals used in this study are listed in Table 1.



(A)



(B)

Figure 1. Structure of (A) HDMimCl, (B) DTAB**Table 1. Properties of the Materials Used in the Study**

Material	Chemical formula	CAS	Supplier	Purity (mass fraction)
1-Hexadecyl-3-methylimidazolium chloride monohydrate	$C_{20}H_{39}ClN_2 \cdot H_2O$	404001-62-3	Acros Organics (USA)	0.98
Pyrene	$C_{16}H_{10}$	129-00-0	Sigma-Aldrich	0.99
Cetylpyridinium chloride monohydrate	$C_{21}H_{38}ClN \cdot H_2O$	6004-24-6	Acros Organics	≥ 0.98
1,6-Diphenyl-1,3,5-hexatriene	$C_6H_5(CH=CH)_3C_6H_5$	1720-32-7	Sigma-Aldrich	0.98
Dodecyltrimethylammonium bromide	$CH_3(CH_2)_{11}N(CH_3)_3Br$	1119-94-4	Sigma-Aldrich	0.98

2.2 Methods

2.2.1 Conductometry. The specific conductivity measurements of the pure surfactants as well as their mixtures were performed on a Thermo scientific conductivity meter, USA (working frequency of 2 kHz as checked against a Pye Unicam PW 9509 conductivity meter). A dip-type conductivity cell with a cell constant of 1 cm^{-1} was used. The specific conductivity at each mole fraction of the surfactants was measured by successive additions of the stock solutions in

triply distilled water (uncertainty = $1 \mu\text{S}\cdot\text{cm}^{-1}$). The temperatures (303.15, 313.15 and 323.15) K with an uncertainty of ± 0.1 K were maintained by a thermostatic water bath.

2.2.2. Tensiometry. Surface tension was measured at air/solution interface using a calibrated Krüss (Germany) tensiometer (Model-K8) by duNoüy ring detachment method within an accuracy of $\pm 0.1 \text{ mN}\cdot\text{m}^{-1}$ at 313.15 ± 0.1 K.

The tensiometer was connected to a water flow thermostat to maintain the desired temperature equilibration. Prior to each measurement, the ring was heated briefly by holding it above a Bunsen burner until glowing. Duplicate measurements were performed in each case to check the reproducibility. The calibration of the instrument was performed daily prior to the measurement with triply-distilled water-at the experimental temperature available in the literature.³⁹

2.2.3. Zeta potential. Zeta potential measurements were performed on a Nano ZS Zetasizer (Malvern, UK) at 90° scattering angle with a He-Ne laser ($\lambda = 632.8 \text{ nm}$) at (298.15 ± 0.1) K. For measurements, at (298.15 ± 0.1) K with 90° scattering angle using a gold coated copper electrode in the cell. All experimental solutions were filtered 3 - 4 times through membrane filters (porosity $0.25 \mu\text{m}$) to remove dust particles. Zeta Potential of all experimental solutions was measured 3 times and average values are taken.

2.2.4. Spectrofluorimetry. Steady state fluorescence experiments were carried out in order to evaluate the aggregation number of the micelles with a Hitachi F-7000 spectrofluorimeter with a 150W xenon lamp at (298.15 ± 0.005) K. Pyrene was used as the probe and its concentration was approximately equal to 0.07 mM in all experiments so as to avoid the interference of pyrene in the micellization processes. Cetylpyridinium chloride (CPC) was used as the quencher. Pyrene fluorescence was measured at 335 nm excitation and 10 nm band pass and emission was monitored between 350-450 nm at 1nm band pass. The quencher solution was added successively into the mixed surfactant solutions with different compositions. Intensity of pyrene without (I_0) and with quencher (I) was measured at first vibronic peak of pyrene at 375 nm for the determination of aggregation number of mixed surfactants.

2.2.5. Fluorescence Anisotropy. Steady-state fluorescence anisotropy was measured using the probe DPH in a Perkin-Elmer LS 55 (USA) fluorescence spectrophotometer with a Peltier attachment using quartz cell of 1 cm path length at (313.15 ± 0.005) K. The concentration of DPH remains constant at 0.001 mM throughout the experiment. Anisotropy measurements were performed with a polarization filter having “L-format” configuration. The anisotropy values were averaged over an integration time of 20s and a maximum number of three measurements were taken for each sample.

3. RESULTS AND DISCUSSION

3.1. Critical Micellar Concentrations

The values of the specific conductances (κ) as a function of surfactant molality (m) for the pure as well as the mixed surfactant solutions having different mole fractions of HDMimCl obtained from conductometry at three desired temperatures are recored in Table 2. A representative plot (Figure 2) shows the concentration dependence of the specific conductance of the aqueous mixtures of HDMimCl and DTAB with varying mole fractions at 303.15 K.

The critical micellar concentrations (cmc) were determined from the inflections in the specific conductance vs. surfactant concentration profiles. The characteristic features of the specific conductance-concentration profiles (Figure 2) are the existence of distinct breaks. Below the cmc , the addition of surfactant to an aqueous solution causes an increase in the number of charge carriers (the surfactant ions and counterions) and consequently, an increase in the specific conductivity of the solution. Above the cmc , further addition of surfactant increases the micelle concentration while the monomer concentration remains invariant. Since a micelle is much larger than the surfactant monomer, it is transported more slowly through the solution and hence is a less efficient charge carrier. Thus, the rate of increase in the specific conductivity with surfactant concentration above cmc is smaller than that below it thus manifesting a break point. The experimental data points below and above the inflection were fitted to two linear equations, and the intersection provided a measure of the cmc of the surfactant system. This procedure is found to be reliable and convenient for the systems under investigation as the slopes of the two linear segments in the pre- and post-micellar regimes of the specific conductance vs. surfactant concentration profiles vary appreciably, thus enabling unambiguous determination of the $cmcs$. The cmc values of the mixed surfactant solutions in conjunction with those of the pure components at different temperatures thus obtained are collected in Table 3. The $cmcs$ of aqueous HDMimCl and DTAB are found to be in good agreement with those reported in the literature.^{40,41} The micellization process depends, in general, on two factors, namely, the electrostatic interactions between the charged head groups of the mixing surfactant components, and the hydrophobic interactions owing to their hydrocarbon tails.⁴²⁻⁴⁶ In the present study, both HDMimCl and DTAB surfactant ions bear positive charges which would try to hinder the formation of mixed micelles. So, in the mixtures studied the first factor opposes mixed micelle formation. The cmc values of the surfactant mixtures are found to fall in between the $cmcs$ of the pure components. The hydrophobic

interactions predominate over the electrostatic interactions thus favoring the micellization process in the mixed systems.

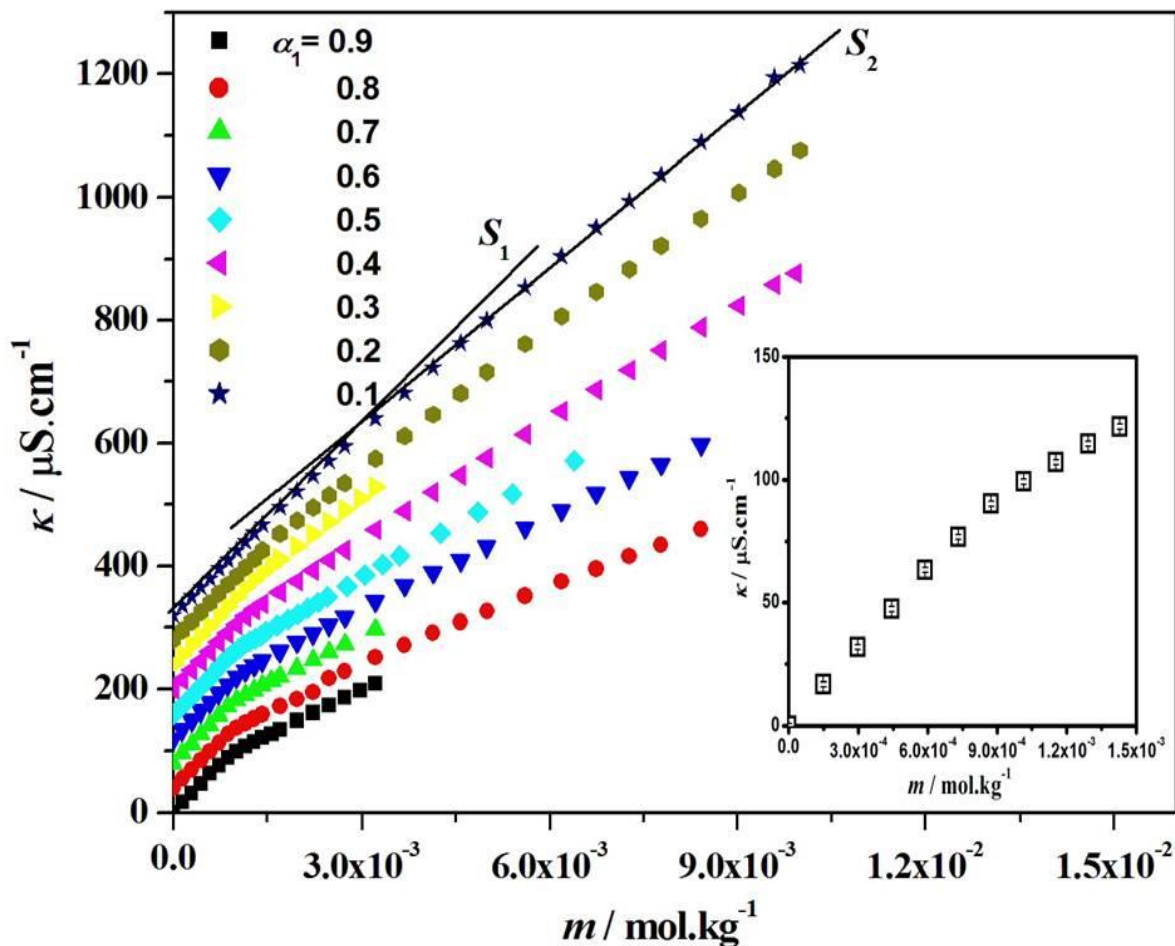


Figure 2. Specific conductance (κ) vs. molality (m) plot of different mole fractions (α_1) of surfactants at 303.15 K at 0.1 MPa. The plots have been shifted vertically by $40 \mu\text{S cm}^{-1}$ for clarity of presentation. Error bar is introduced for $\alpha_1 = 0.9$ in the inset. The error bars for all the mole fractions are same.

3.2. Counterion Binding

Ionic micelles often bind a considerable fraction of counterions, which can be conveniently quantified from electrochemical measurements. Following the procedure of Evans,^{14,15} the degrees of counterion binding (g) have been evaluated (Table 4) from the specific conductance vs. concentration profiles using the following equation:

$$g = 1 - \frac{S_2}{S_1} \quad (1)$$

where S_1 and S_2 are respectively the pre- and post-micellar slopes obtained from the plots of specific conductance of the surfactant solution as a function of concentration.

3.3. Interactions of Surfactants in Micelles

In order to check whether the mixed surfactant systems studied here behave ideally, the critical micellar concentrations were calculated (cmc_C) using the Clint model⁴⁷ for the prediction of the cmc of a mixed surfactant system with a known stoichiometric composition from a knowledge of the individual $cmcs$ of the components by employing the following equation assuming ideal mixing:

$$\frac{1}{cmc_C} = \frac{\alpha_1}{cmc_1} + \frac{\alpha_2}{cmc_2} \quad (2)$$

where cmc_1 and cmc_2 are the $cmcs$ of components, respectively and α -values are their stoichiometric mole fractions. The cmc_C values thus computed are recorded in Table 3. Eq. 2 reveals the difference between ideal and non-ideal mixtures of surfactants. A lower observed cmc value for the mixture, *i.e.*, a negative deviation from Eq. 2 indicates synergistic interactions (attractive interactions) among the mixing components, whereas a positive deviation signifies antagonistic interactions (repulsive interactions).

From the cmc_C values listed in Table 3, it is at once evident that the mixed HDMimCl + DTAB system always yielded an enhanced interfacial property over the entire range of composition within the temperature range (303.15 - 323.15) K, *i.e.*, synergism prevails in this system. This phenomenon may be ascribed to a resultant attractive interaction between the amphiphiles due to non-ideal mixing.

The observed non-ideality can, however, be taken into account by considering the activity coefficients (f) of the surfactants into the Clint model,⁴⁷ and the cmc of the mixture (cmc_{mix}) under this situation can be conveniently expressed through the following equation

$$\frac{1}{cmc_{\text{mix}}} = \frac{\alpha_1}{f_1 cmc_1} + \frac{\alpha_2}{f_2 cmc_2} \quad (3)$$

where f_1 and f_2 are the activity coefficients of components 1 and 2, respectively. For ideal cases, $f_1 = f_2 = 1$, and Eq. 3 reduces to the ideal form, Eq. 2.

The micellar mole fraction of component 1 (X_1), that of component 2 (X_2) and molecular interaction parameter of the mixed micelle (β^R) can be calculated by solving the following coupled equations put forwarded by Rubingh⁴⁸ based on regular solution theory (RST)

$$\frac{X_1^2 \ln\left(\frac{\alpha_1 cmc}{X_1 cmc_1}\right)}{X_2^2 \ln\left(\frac{\alpha_2 cmc}{X_2 cmc_2}\right)} = 1 \quad (4)$$

$$\beta^R = \frac{\ln\left(\frac{\alpha_1 cmc}{X_1 cmc_1}\right)}{X_2^2} \quad (5)$$

The values of X_1 , X_2 , β^R , and cmc_{mix} have been evaluated by an iterative solution of Eqs. 4 and 5. The parameter β^R is an indicator not only of the degree of interaction between the two surfactants, but also accounts for the deviation from ideality. For ideal mixing of two surfactants, β^R assumes a value of zero. A positive β^R value indicates repulsive (antagonistic) interactions among the mixing components, whereas a negative value of β^R implies an attractive (synergistic) interaction.⁷⁻¹¹

The calculated values of X_1 , β^R , and cmc_{mix} are summarized in Table 3. As expected from the analysis of Table 3, the β^R values are negative over the whole range of composition at the investigated temperatures, which indicates that formation of micelle is favored. The present surfactant mixtures, thus, manifest synergism during formation of the mixed micelles. The magnitude of the β^R values increase with the increase in the mole fraction of DTAB for the three investigated temperatures. The extent of inclusion of DTAB monomer into the mixed micelle is low (Table 3) and it is negligible in HDMimCl-rich mixtures. With the increase in the amount of DTAB (α_2), the micellar mole fractions of HDMimCl (X_1) have not been reduced enough thus resulting in an enhanced synergism in the mixed micelle. According to the RST, the values of the activity coefficients of surfactants 1 and 2 within the mixed micelle (f_1 and f_2) can be evaluated from the equations:

$$f_1 = \exp(\beta^R X_2^2) \quad (6)$$

$$f_2 = \exp(\beta^R X_1^2) \quad (7)$$

The values of f_1 , and f_2 as a function of the stoichiometric mole fraction of HDMimCl thus obtained are listed in Table 3. The values of f_1 and f_2 are found to be less than unity over the entire composition range of the present system indicating non-ideal behavior and attractive interactions between the components.

For the present HDMimCl + DTAB system, the population of HDMimCl in the micellar phase (X_1) is higher at all its stoichiometric proportions (α_1). The lower *cmc* value of HDMimCl as compared to DTAB reflects relatively higher affinity of the former towards self-aggregation, which is amply manifested in the above computation. The interaction parameters are found to be negative over the entire composition range at all the temperatures investigated. This implies a strong synergistic interaction in the present surfactant system as also inferred from the Clint model.⁴⁷

The surfactant mole fractions in micelle obtained from the Rubingh's model⁴⁸ have been compared with the micellar mole fractions in the ideal state as computed by applying Motomura's approximation⁴⁹

$$X_1(\text{ideal}) = \frac{\alpha_1 cmc_2}{\alpha_1 cmc_2 + \alpha_2 cmc_1} \quad (8)$$

It is clear from Table 3 that X_1 values are lower than the $X_1(\text{ideal})$ values for the present mixed surfactant system. This suggests that higher amount of DTAB is present in the micellar phase than that in the ideal mixed state.

A negative value of the interaction parameter (β^R) indicates the existence of attractive interactions between the constituent surfactants in the mixed micelles. Positive values of β^R arise when repulsive interactions prevail, while β^R values close or equal to zero indicate ideal mixing. In the present study, the β^R values are always found to be negative thus demonstrating attractive interactions between the constituents in the mixed micelles. In accordance with the RST, for any given mixed system β^R should remain independent of mixture composition which is often not realized in practice. In the present study, the parameter β^R was found to be composition dependent at the three temperatures investigated. The non-constancy of β^R with mixture composition has also been reported earlier for a variety of surfactant mixtures, manifesting the shortcomings of the Rubingh's approach for binary mixtures.^{45, 50-52}

Table 3. Experimental Critical Micellar Concentrations (cmc_{mix}), Calculated Critical Micellar Concentrations (cmc_{mix}) according to Rubingh, Calculated Critical Micellar Concentrations (cmc_{mix}) according to Clint, Micellar Mole Fractions of HDMimCl (X_1) according to the Regular Solution Theory (RST) and Motomura Model, the Interaction Parameters of the Mixed Micelle (β^R), and the Activity Coefficients of HDMimCl (f_1) and DTAB (f_2) within the Mixed Micelle according to RST at Different Stoichiometric Mole Fractions of HDMimCl (α_1) for Aqueous HDMimCl + DTAB systems at (303.15, 313.15, and 323.15 K) at 0.1 MPa^a

T/K	α_1	$10^4 cmc_{mix} / \text{mol.kg}^{-1}$			X_1 (RST)	X_1 (Motomura)	β^R / kT	f_1	f_2
		Exptl.	Rubingh	Clint					
303.15	0.0	149.7							
	0.1	25.56	26.59	57.64	0.558	0.654	-3.35	0.51	0.35
	0.2	18.16	17.93	35.69	0.635	0.809	-3.25	0.64	0.27
	0.3	13.16	13.17	25.85	0.669	0.879	-3.66	0.66	0.19
	0.4	12.74	11.96	20.26	0.728	0.919	-3.12	0.79	0.19
	0.5	11.70	10.77	16.65	0.772	0.944	-2.92	0.86	0.17
	0.6	11.21	10.20	14.14	0.825	0.962	-2.56	0.92	0.17
	0.7	10.43	9.55	12.29	0.865	0.975	-2.41	0.95	0.15
	0.8	9.56	8.87	10.86	0.893	0.986	-2.56	0.97	0.12
	0.9	9.37	9.03	9.73	0.959	0.994	-1.78	0.99	0.15
1.0	8.82								
313.15	0.0	157.5							
	0.1	27.03	28.03	60.56	0.558	0.654	-3.32	0.52	0.35
	0.2	19.46	19.04	37.48	0.637	0.810	-3.15	0.65	0.27
	0.3	14.05	13.98	27.14	0.672	0.879	-3.62	0.67	0.19
	0.4	13.91	12.88	21.27	0.736	0.919	-2.91	0.81	0.20
	0.5	12.77	11.62	17.49	0.783	0.945	-2.69	0.88	0.19
	0.6	11.38	10.40	14.85	0.813	0.963	-2.79	0.91	0.15
	0.7	11.10	10.17	12.40	0.872	0.975	-2.35	0.96	0.16
	0.8	10.52	9.87	11.40	0.921	0.986	-2.12	0.99	0.17
	0.9	9.99	10.39	10.22	0.972	0.994	-1.38	0.99	0.27
1.0	9.26								
323.15	0.0	166.5							
	0.1	28.00	27.58	67.26	0.548	0.637	-3.56	0.47	0.33
	0.2	19.8	19.51	42.15	0.62	0.798	-3.48	0.59	0.25

	0.3	16.43	16.39	30.68	0.673	0.871	-3.43	0.69	0.21
	0.4	15.99	15.95	24.12	0.735	0.913	-2.77	0.82	0.22
323.15	0.5	14.34	14.30	19.87	0.776	0.941	-2.68	0.87	0.19
	0.6	14.20	14.17	16.90	0.846	0.959	-2.04	0.95	0.22
	0.7	12.58	12.57	14.70	0.867	0.974	-2.25	0.96	0.17
	0.8	12.11	12.11	13.00	0.926	0.984	-1.87	0.99	0.19
	0.9	11.18	27.58	11.66					
	1.0	10.57							

^a Relative standard uncertainties: $u_r(\text{cmc}_{\text{mix}}) = 0.03$, $u_r(X_1) = 0.03$, $u_r(\beta^R) = 0.04$, $u_r(f_1) = 0.05$, and $u_r(f_2) = 0.05$.

3.4. Thermodynamics of Micellization

The regular solution theory (RST)⁴⁸ has been used to compute the thermodynamic functions of mixing which assumes that the excess entropy of mixing is zero. This theory has been amply used to describe the behavior of a variety of mixed surfactants in aqueous solutions by the researchers.⁵³⁻⁶⁶

According to this theory, the excess free energy (G^E), excess enthalpy (H^E), and enthalpy of micellization (ΔH_M) are given by^{55,56}

$$G^E = H^E = \Delta H_M = RT[X_1 \ln(f_1) + X_2 \ln(f_2)] \quad (9)$$

The excess free energy of micellization represents the deviation from the ideal behavior ($G^E = \Delta G_M - \Delta G_M^{\text{ideal}}$). For an ideal mixing, the free energy of micellization, can be given by

$$\Delta G_M^{\text{ideal}} = RT[X_1 \ln(X_1) + X_2 \ln(X_2)] \quad (10)$$

The nonideal free energy of micellization is given by

$$\Delta G_M = RT[X_1 \ln(X_1 f_1) + X_2 \ln(X_2 f_2)] \quad (11)$$

Using the values of the enthalpy of micellization and free energy of micellization, the entropy of micellization can be obtained from

$$\Delta S_M = \frac{\Delta H_M - \Delta G_M}{T} \quad (12)$$

where T is the temperature in absolute scale.

Table 4 demonstrates that the free energy of micellization on a real state (ΔG_M) has a negative deviation from the free energy of micellization on an ideal state ($\Delta G_M^{\text{ideal}}$), favoring the formation of mixed micelle. The negative value of excess free energy of micellization indicates the energetic stabilization accompanied by the mixed micelle formation.^{57,58} The

negative values of enthalpy of micellization (ΔH_M) shown in Table 4 imply that micellization of HDMimCl + DTAB is an exothermic process in aqueous solutions over the entire temperature range investigated here. This indicates that the total energy change including translational energy loss by the individual surfactants and the heat released by the interaction among the hydrocarbon bonds is less than the energy absorbed due to the destruction of the iceberg structure of water during micellization. Further, the degree of disorderliness increases due to micellization and the entropy change is favourable to the formation of mixed micelle as demonstrated by the positive values of the entropy of micellization (ΔS_M), *cf.* Table 4. The contribution of $T\Delta S_M$ towards ΔG_M is always found to be more than 50% for $\alpha_1 \geq 0.5$ indicating that micellization is an entropically-driven process for $\alpha_1 \geq 0.5$ while it becomes an enthalpy-driven process for $\alpha_1 < 0.5$. The leading role played by the entropy in the process of mixed micellization has also been reported earlier for other mixed surfactant systems.⁵⁹⁻⁶⁶ It is also seen that the ratio of $T\Delta S_M$ to ΔG_M varies with the mixture composition α_1 . This may be ascribed to the variation of the contributions from the electrostatic attraction between the surfactant molecules, the steric effect and molecular repulsion with α_1 .

Table 4. Degrees of Counterion-binding (g), Free Energy of Micellization for Ideal Mixing ($\Delta G_M^{\text{ideal}}$), Non-ideal Free Energy of Micellization (ΔG_M), Excess Free Energy (G_M^E), Non-ideal Enthalpy of Micellization (ΔH_M), Non-ideal Entropy of Micellization ($T\Delta S_M$), and $|T\Delta S_M / \Delta G_M|$ at Various Stoichiometric Mole Fractions of HDMimCl (α_1) for HDMimCl + DTAB Mixed Systems at (303.15, 313.15 and 323.15) K at 0.1 MPa Evaluated from Conductivity Measurement ^a

T	α_1	G	$\Delta G_M^{\text{ideal}}$	ΔG_M	G_M^E	ΔH_M	$T\Delta S_M$	$ T\Delta S_M / \Delta G_M $
K			(kJ.mol ⁻¹)	(kJ.mol ⁻¹)	(kJ.mol ⁻¹)	(kJ.mol ⁻¹)	(kJ.mol ⁻¹)	
303.15	0.0	0.74						
	0.1	0.16	-1.73	-3.84	-2.11	-2.11	1.73	0.45
	0.2	0.24	-1.65	-3.57	-1.92	-1.92	1.65	0.46
	0.3	0.29	-1.60	-3.69	-2.09	-2.09	1.60	0.43
	0.4	0.37	-1.47	-3.05	-1.58	-1.58	1.47	0.48
	0.5	0.45	-1.35	-2.67	-1.31	-1.31	1.36	0.51
	0.6	0.46	-1.17	-2.11	-0.94	-0.94	1.17	0.55
	0.7	0.49	-0.99	-1.73	-0.73	-0.73	1.00	0.58
	0.8	0.50	-0.86	-1.50	-0.64	-0.64	0.86	0.57
	0.9	0.54	-0.43	-0.63	-0.20	-0.20	0.43	0.68
1.0	0.55							
313.15	0.0	0.70						
	0.1	0.18	-1.79	-3.96	-2.16	-2.16	1.80	0.45
	0.2	0.24	-1.70	-3.64	-1.93	-1.93	1.71	0.47
	0.3	0.28	-1.64	-3.76	-2.11	-2.11	1.65	0.44
	0.4	0.40	-1.50	-3.00	-1.50	-1.50	1.50	0.50
	0.5	0.41	-1.36	-2.57	-1.21	-1.21	1.36	0.53
	0.6	0.45	-1.25	-2.37	-1.12	-1.12	1.25	0.53
	0.7	0.47	-0.99	-1.68	-0.69	-0.68	1.00	0.59
	0.8	0.48	-0.72	-1.12	-0.39	-0.39	0.73	0.65
	0.9	0.52	-	-	-	-	-	-
1.0	0.54							
0	0	0.68						
	0.1	0.19	-1.85	-4.27	-2.42	-2.42	1.85	0.45
	0.2	0.23	-1.78	-4.06	-2.28	-2.28	1.78	0.46

	0.3	0.28	-1.69	-3.73	-2.03	-2.03	1.70	0.43
	0.4	0.42	-1.55	-3.03	-1.48	-1.48	1.55	0.48
323.15	0.5	0.44	-1.43	-2.71	-1.28	-1.28	1.43	0.51
	0.6	0.47	-1.15	-1.89	-0.74	-0.74	1.15	0.55
	0.7	0.47	-1.05	-1.78	-0.73	-0.73	1.05	0.58
	0.8	0.56	-0.71	-1.06	-0.35	-0.35	0.71	0.57
	0.9	0.53	-	-	-	-	-	-
	1.0	0.46						

^aRelative standard uncertainty of g : $u_r(g) = 0.04$.

3.5. Interfacial properties at air water interface

The cmc values can also be calculated from tensiometric data at 313.15 K from the intersection of the two lines before and after the cmc as depicted in Figure 3. From Table 5, it is evident that the experimental cmc values obtained from surface tension are found to be lower than those computed theoretically (cmc_c); this may be attributed to the synergism in the process of mixed micelle formation. For all the compositions of binary surfactants of HDMimCl and DTAB, several interfacial parameters can be calculated using the Eqs. 13-16 and these have been listed in Table 5. The surface excess (Γ_{max}) at the air/water interface can be calculated by the Gibbs adsorption equation⁶⁷ as given below:

$$\Gamma_{max} = -\frac{1}{2.303iRT} \lim_{C \rightarrow cmc} \left(\frac{\partial \gamma}{\partial \log C} \right) \text{mol.m}^{-2} \quad (13)$$

The Γ_{max} appeared in the above equation can be defined as how much the air/water interface can be covered by surfactants reducing the surface tension of water at cmc while γ is the surface tension expressed in mN.m^{-1} and i , R and T are the number of species per surfactant molecule at air/water interface, universal gas constant and temperature at Kelvin scale respectively.

The number of species (i) participating at the air/water interface for various binary combinations of HDMimCl and DTAB can be calculated using the equation,⁶⁶ $i = \sum n_i X_i$, where n_i is the number of species of HDMimCl and DTAB individually. For both pure and mixed components, the value of i is 2.

The addition of even a very small amount of HDMimCl to DTAB increases the Γ_{\max} values of the mixtures. There are two opposing contributing factors that determine the Γ_{\max} for binary combinations of surfactants:⁴⁶ (a) the hydrophobic interactions between the tails of surfactants, (b) the repulsive interactions between the surfactant bulky head groups of same charge. Long chain HDMimCl has the greater surface activity than DTAB, so the Γ_{\max} value of the former is larger than later. The interesting fact is that with the increase in the mole fraction of DTAB, there is an overall increase of Γ_{\max} values and even the value is higher at high mole fractions of DTAB than the individual two components. Probably, with the increasing DTAB content, the bulky head group of HDMimCl decreases at the air/water interface and also synergistic interaction increases as compared to bulk.

The minimum area per surfactant monomer (A_{\min}) can be calculated using the following equation:

$$A_{\min} = \frac{10^{18}}{N_A \Gamma_{\max}} \text{ nm}^2 \text{ molecule}^{-1} \quad (14)$$

A_{\min} values has the reverse trend than that of Γ_{\max} as expected. 16-carbon chain IL has the greater hydrophobic interaction at pure state than pure DTAB attributed to the closely packed structure of HDMimCl ($A_{\min}= 0.80$) at air/water interface. With the increase of DTAB content, the repulsion between larger imidazolium group decreases, A_{\min} decreases resulting the formation of closely packed structure.

The efficiency of interfacial adsorption can be predicted using pC_{20} values. The more efficiency the adsorption, more is the decrease of surface tension by the amphiphiles. C_{20} values are empirically defined as the reduction of surface tension by the amphiphiles to 20 mN.m⁻¹. pC_{20} value can be calculated using the Eq. 15,

$$pC_{20} = -\log C_{20} \quad (15)$$

From Table 5, it is evident that pC_{20} values increase with the increase of mole fraction of HDMimCl due to greater surface activity of HDMimCl.

The surface pressure at cmc (π_{cmc}) can be obtained using Eq. 16.

$$\pi_{cmc} = \gamma_0 - \gamma_{cmc} \quad (16)$$

where γ_0 and γ_{cmc} are the surface tension of pure solvent and surface tension at *cmc* of the solution of individual and mixed surfactants respectively. The value of π_{cmc} of DTAB is greater than HDMimCl. π_{cmc} values are more or less same for the different mole fractions of surfactants.

The packing parameter (P) deals with the micellar geometry predicted by Israelachvili³⁴ by the following equation:

$$P = \frac{v}{l_c A} \quad (17)$$

where l_c is the maximum effective length of hydrophobic tail of a monomer, A is surface area of head group of surfactant monomer and v is the hydrophobic chain volume assuming to be fluid and incompressible. Both l_c and v of a saturated hydrocarbon chain of carbon number C_n , can be evaluated using Tanford⁶⁹ formulae:

$$l_c = (0.154 + 0.1265 C_n) \text{ nm} \quad (18)$$

$$v = (0.0274 + 0.0269 C_n) \text{ nm}^3 \quad (19)$$

As the exact determination of the head group area (A) of micellar surface is quite difficult,⁷⁰ A_{\min} values obtained from tensiometry were used instead of A as stated earlier.^{68,70,71} For the binary mixed surfactant system, the modified form of Israelachvili (Eq. 20)^{37,68,70-72} was used

$$P_{\text{eff}} = \left(\frac{v}{l_c A_{\min}} \right)_{\text{eff}} = \frac{\sum v_i X_i}{(\sum A_i X_i) l_c} \quad (20)$$

For all stoichiometric mole fractions (X_i) of binary mixture of HDMimCl and DTAB, l_c is equal to value of longer component HDMimCl. It is well documented that for the mixed micellization of ternary alkyl (C_{12} -, C_{14} - and C_{16} -) triphenylphosphonium bromides the value of l_c to be taken the larger component C_{16} -triphenylphosphonium bromide⁵⁷. A_i is equal to the A_{\min} value of individual components of HDMimCl and DTAB. Calculated P_{eff} values are displayed in Table 5. For spherical micelles, $P \leq 0.333$; for nonspherical shape, $0.333 < P < 0.5$; for vesicles and bilayers, $0.5 < P < 1$; and for inverted structures, $P > 1$. From Table 5, it is evident that for HDMimCl and DTAB and all the mole fractions of their binary combinations, $P < 0.333$. So, all the individual and mixed micelle investigated here are spherical in shape.

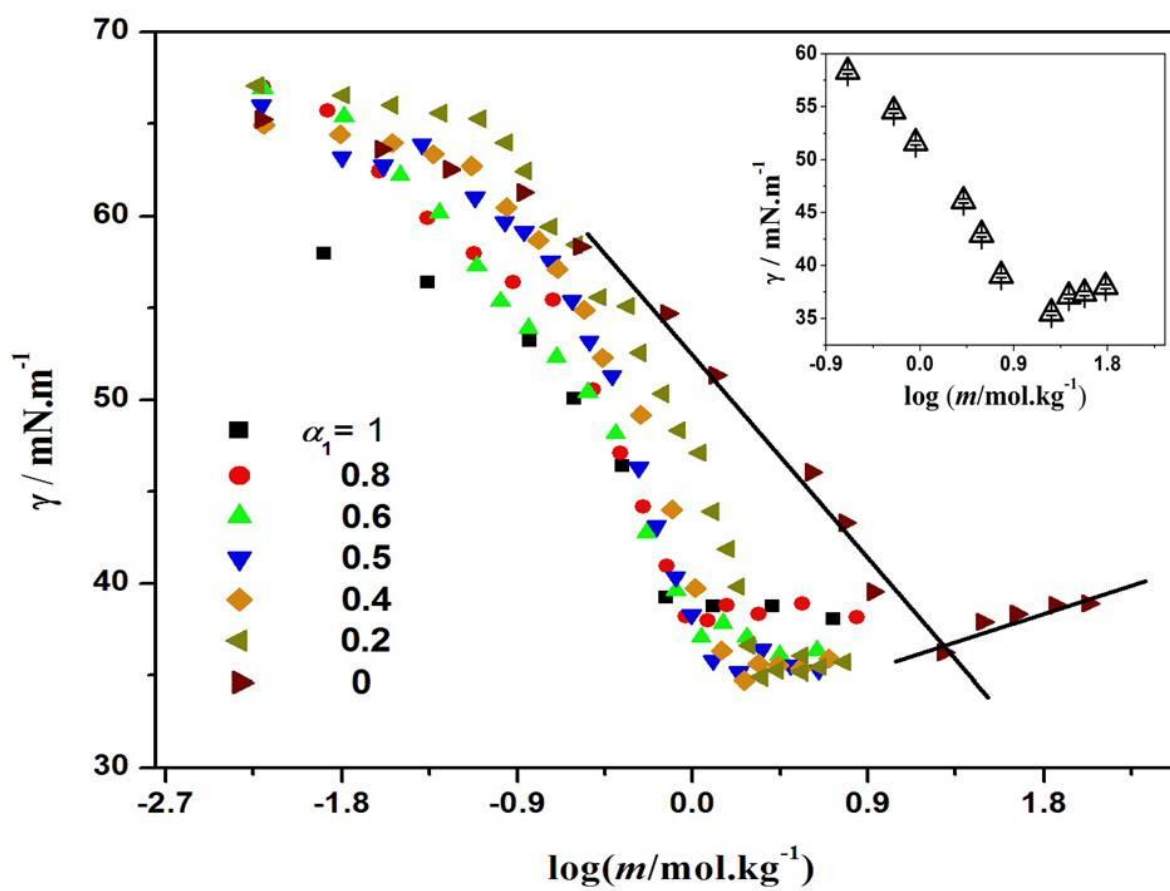


Figure 3. Tensiometric isotherms at various mole fractions of IL and DTAB at 313.15 K at 0.1MPa. Error bar is introduced for $\alpha_1 = 0$, separately in the insert. The error bar for all the mole fractions is same.

Table 5. Experimental Critical Micellization Concentration (cmc), Calculated Critical Micellization Concentration according to Clint (cmc_c), Surface Pressure at cmc (π_{cmc}), Surface Excess at the Air-water Interface (Γ_{max}), Minimum Area Per Surfactant Monomer (A_{min}), Efficiency of Interfacial Adsorption (pC_{20}), and Packing Parameter (P) for Various Mole fraction of HDMimCl (α_1) in HDMimCl + DTAB Mixtures at 313.15 K^a

α_1	1	0.9	0.8	0.7	0.6	0.5	0.4	0.3	0.2	0.1	0
cmc (mmol.kg ⁻¹)	0.89	0.97	1.06	1.11	1.21	1.46	1.78	2.24	2.48	3.15	12.9
cmc_c (mmol.kg ⁻¹)	-	0.98	1.09	1.23	1.42	1.67	2.02	2.55	3.49	5.49	-
$10^3\pi_{cmc}$ (J.m ⁻²)	28.8	31.3	29.7	30.0	30.3	31.4	29.9	31.7	32.0	32.1	32.5
$10^6\Gamma_{cmc}$ (mol.m ⁻²)	2.06	1.88	1.84	2.05	2.12	2.63	2.65	2.63	2.67	2.66	1.52
A_{min} (nm ² .molecule ⁻¹)	0.80	0.88	0.90	0.81	0.80	0.63	0.63	0.63	0.62	0.62	1.09
pC_{20}	3.4	3.9	3.4	3.5	3.4	3.3	3.1	3.2	3.0	2.9	2.5
P	0.26	0.25	0.23	0.22	0.21	0.20	0.18	0.17	0.17	0.16	0.15

^aThe uncertainty limit of cmc (mM), π_{cmc} (J.m⁻²), Γ_{cmc} (mol.m⁻²), A_{min} (nm².molecule⁻¹), and pC_{20} are ± 4 , ± 3 , ± 5 , ± 5 , and ± 3 % respectively.

3.6. Mixture of HDMimCl and DTAB in different mole fractions and effect of temperature

Due to the 16-carbon chain, HDMimCl has the greater surface activity than the DTAB. So in aqueous solution, micellization starts earlier in HDMimCl than the DTAB. cmc_c of HDMimCl is ~ 1 mmol.kg⁻¹ and for DTAB is ~ 14 mmol.kg⁻¹ at room temperature. When they are mixed together in definite mole fraction (α), the cmc of mixed surfactant system decreases dramatically even at a low HDMimCl content ($\alpha_1 = 0.1$). So a strong synergistic interaction is observed in the mixed micellization of DTAB and HDMimCl. The experimental values of $cmcs$ for different mole fractions of HDMimCl are listed in Table 3. It is seen that at 303.15K, cmc of HDMimCl is 0.882 mmol.kg⁻¹ and DTAB is 14.97 mmol.kg⁻¹, but when mixed together at very low content of HDMimCl ($\alpha_1 = 0.1$), the cmc is 2.556 mmol.kg⁻¹. The specific conductance (κ) vs. molality (m) plot at 0.5 mole fraction of HDMimCl for three desired temperatures is displayed in Figure 4. It is observed that cmc increases with the increase of [DTAB] as well as with temperatures. For all compositions, it is obvious that with increasing temperatures, cmc increases which is listed in Table 3.

3.7. Comparison of Experimental and Theoretical $cmcs$

The experimental values of $cmcs$ are listed for individual and mixed surfactants of different mole fractions in Table 3. Considering Rubingh's RST,⁴⁸ the X_1 values were calculated by an iterative method, which were then used to calculate the values of f_1 and f_2 using Eqs. 6 and 7, and hence the values of $cmcs$ using Eq. 3. The cmc values thus calculated agreed very well with the experimental values. The conclusion is that RST is fairly valid for the mixed micellization of HDMimCl and DTAB. Experimental $cmcs$, along with the $cmcs$ calculated by Rubingh and Clint equations are listed in Table 3 and are displayed graphically in Figure 5.

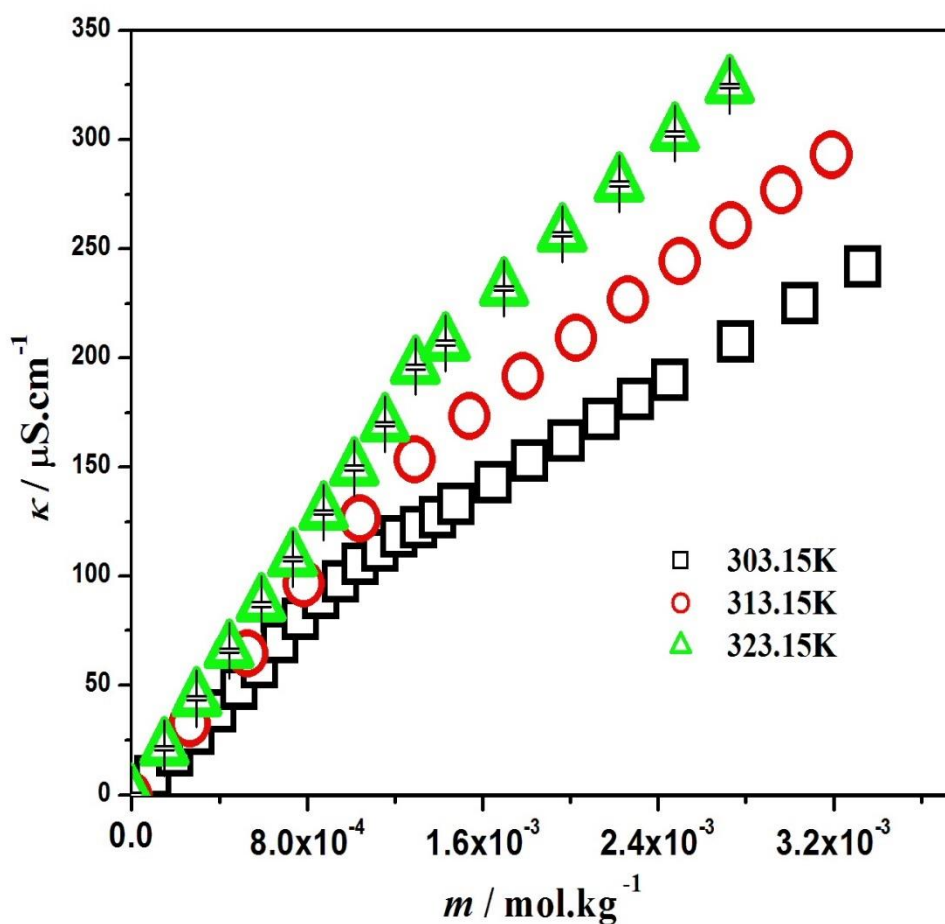


Figure 4. Plot of specific conductance vs. concentration for mixtures of DTAB and HDMimCl at 0.5 mole fraction of each at three different temperatures at 0.1 MPa. Error bar is introduced for 323.15 K. The error bar for all the temperatures is same.

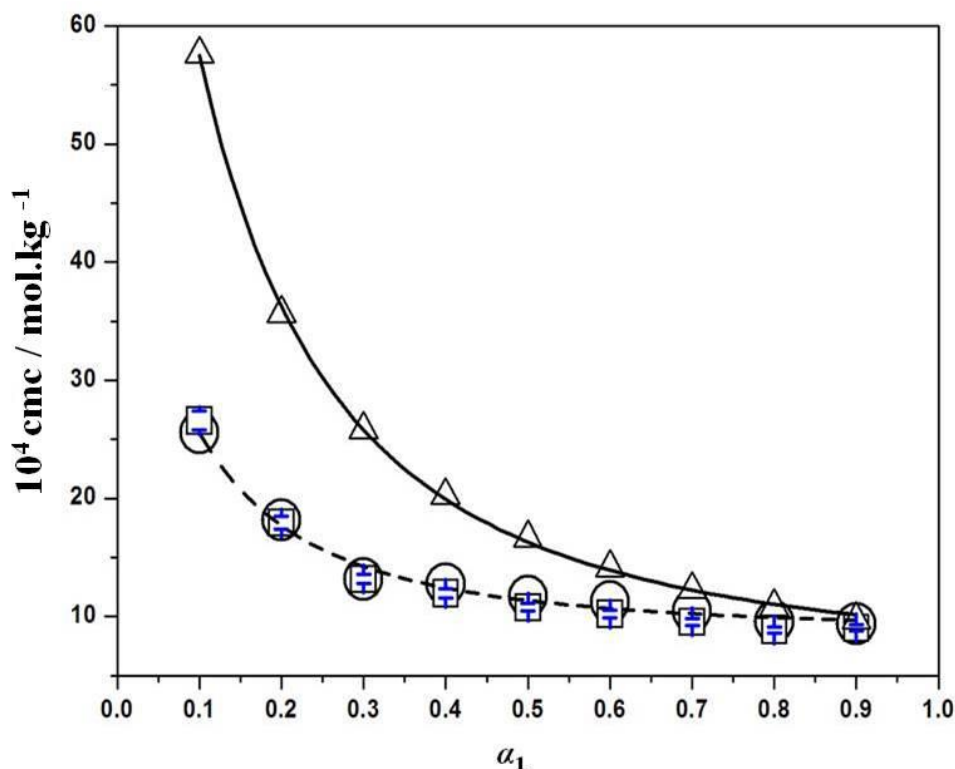


Figure 5. Plot of cmc vs. mole fraction for the mixed micellization of DTAB and HDMimCl: experimental $cmcs$ (\square), and calculated from RST (\circ) at 303.15 K at 0.1 MPa. Solid line represents $cmcs$ calculated from Clint model. Error bar is introduced for experimental $cmc(\square)$ values.

3.8. Determination of various interaction and thermodynamic parameters experimentally

HDMimCl is a long chain ionic liquid which forms micelle more easily than does DTAB (Table 3). The extent of incorporation of DTAB monomer into the mixed micelle is low in all the surfactant mixtures investigated (Table 3) and it is found to be negligible when the DTAB-content of the mixtures is low. With the increase in the amount of DTAB, the micellar mole fractions of HDMimCl (X_1) would not get reduced enough. So HDMimCl also plays a leading role in DTAB-rich mixtures in the process of micellization. Table 3 and Figure 6 demonstrate that there is a negligible effect of temperature on β^R . Degree of counter ion binding (g) is found to increase significantly with the increase in the mole fraction of the HDMimCl at a particular temperature (Table 4) manifesting the formation of micelles at lower surfactant concentration when HDMimCl-content is high. That Cl^- is more hydrated than Br^- ³⁸ is reflected in the higher g value of DTAB compared to HDMimCl in pure state (Table 4). For the case of mixed

micelles, both Cl^- and Br^- ions are present as counterions. But here, the solvation of the counterions is overshadowed by the compactness and charge density of the micelle with the increase in the HDMimCl-content. The nonideal character of micelle formation is further supported by the difference of X_1 and X_1^{ideal} (Motomura) values (Table 3). The activity coefficients are found to increase which approach unity for low mole fractions of DTAB at a particular temperature; this is reflected in the lower difference of cmc_{mix} and cmc_C (Clint) for the high mole fraction of HDMimCl leading to ideality. The g value, in general, decreases from 303.15 K to 313.15 K, but increases slightly at 323.15 K. It is probably due to the fact that at high temperature, the effect of mobility of counterions predominates over the effect of desolvation of counterions.

From Table 4, it is evident that the free energy of micellization (ΔG_M) is negative and becomes more negative as the concentration of DTAB in the surfactant mixtures increases over the entire range of the investigated temperatures. The ΔG_M values are also found to increase as the temperature increases in any given mixture. The negative values of ΔG_M suggest that the process of micellization in the investigated surfactant mixtures is, in general, spontaneous, and that the process becomes more spontaneous as the DTAB-content increases or as the temperature is elevated. The difference in ΔG_M and $\Delta G_M^{\text{ideal}}$ values is also significant indicating deviation of ideality for the mixed micellar system. We have also obtained a similar trend for the values of ΔH_M indicating that translational energy loss by monomers and heat generation due to hydrophobic interaction is lesser than the energy absorbed by breaking the iceberg structure of water during micellization. Olasani *et al.*⁴³ investigated the interactions of CTAB + DTAB in aqueous medium. The values of ΔG_M and β^R are more negative for CTAB + DTAB system than our system indicating that micellization of HDMimCl + DTAB is less energetically feasible than CTAB+ DTAB system.⁴³ The values of ΔS_M for all the HDMimCl + DTAB mixtures are found to be positive, indicating that the degree of disorderliness increases due to micellization and that the entropy change is favourable. The From Table 4 it is apparent that the process of micellization gradually becomes more entropy-driven as the mixtures gets richer in the HDMimCl while enthalpy factor somewhat overrides the entropy-contribution in DTAB-rich region.

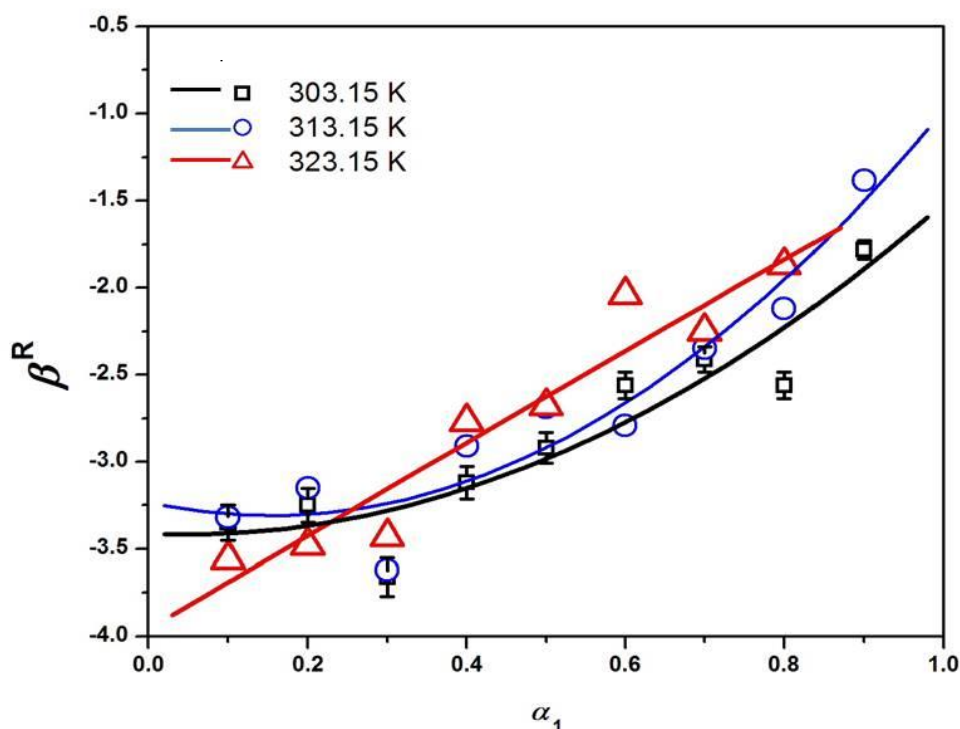


Figure 6. Dependence of the interaction parameter (β^R) on the temperature and mole fraction of HDMimCl. Points are fitted with second order polynomial. Error bar is introduced for 303.15 K and error bar of β^R for all other temperatures are same.

3.9. Aggregation number (N), Zeta potential (ζ) and anisotropy (r) for different mole fractions of HDMimCl and DTAB in surfactant mixtures

The aggregation number of a micelle can be conveniently determined by measuring the steady-state fluorescence quenching using hydrophobic quencher using the equation⁷⁻¹¹

$$\ln \frac{I_0}{I} = \frac{[Q]N}{[Surf] - [CMC]} \quad (21)$$

$[Surf]$ is the initial concentration of the surfactant solution (here, 0.05 mol.kg⁻¹), $[Q]$ is the concentration of the quencher which is added to the surfactant solution and the plot is presented

in Figure 7. Following Eq. 21, if $\ln \frac{I_0}{I}$ values are plotted as a function of $[Q]$,

(Figure 8), the aggregation numbers (N) of individual components and different mixtures of HDMimCl and DTAB can be determined from the slopes. From Table 6, it is evident that the aggregation number of mixed system increase initially with the increase in the mole fraction of HDMimCl (α_1), but further increase of the mole fraction of HDMimCl causes an overall

decrease of aggregation number. When the mole fraction of HDMimCl is low, HDMimCl causes a reduction in the head group repulsions between surfactant monomers of two components. Thus, a large number of surfactant molecules are required to form the micellar aggregates; hence, aggregation number would increase initially. At high mole fractions of HDMimCl, however, it acts as a cosolvent. A cosolvent generally enhances the electrostatic interactions in solution. So, the head groups of HDMimCl prevent large number of surfactant monomers to assemble to form the micellar aggregates. So, the aggregation number decrease afterwards.³⁶

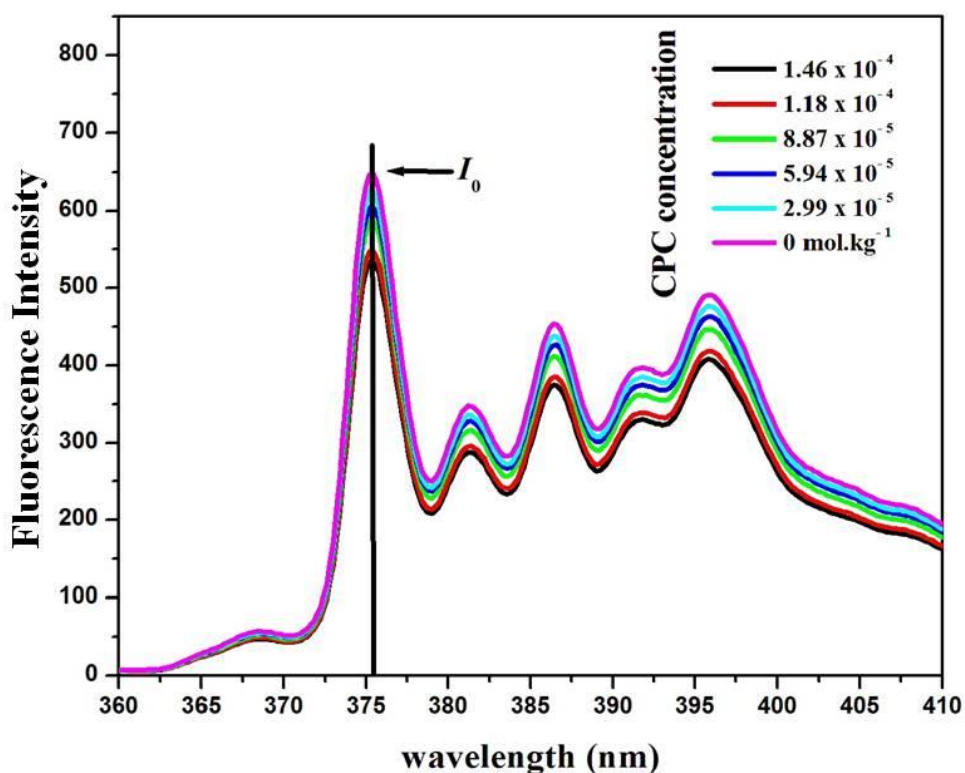


Figure 7. Quenching of pyrene by CPC at $\alpha_1 = 0.1$. Total CPC concentration decreases from 1.46×10^{-4} M from top to bottom.

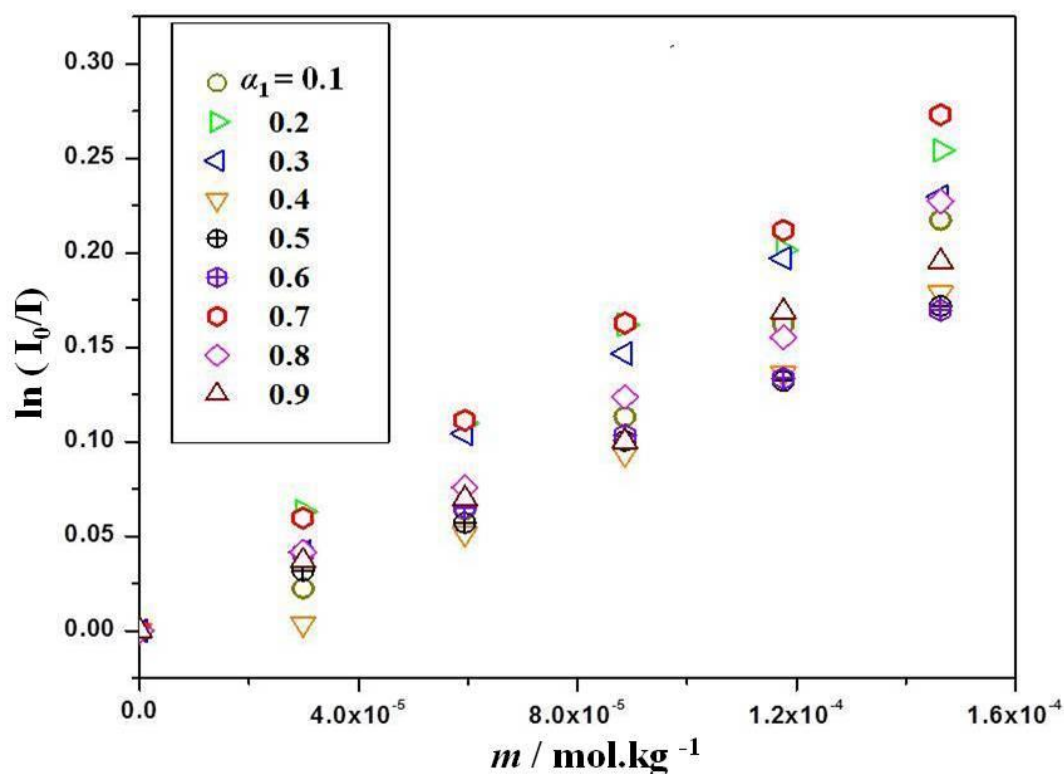


Figure 8. Plot of $\ln(I_0/I)$ vs. $[Q]$ for the determination of aggregation number.

Table 6. Aggregation Number (N), Zeta Potential (ξ) and Anisotropy (r) of Mixed Surfactant System HDMimCl + DTAB as a Function of the Stoichiometric Mole Fractions (α_1) of HDMimCl at 298.15K^a

Mole fraction (α_1)	1	0.9	0.8	0.7	0.6	0.5	0.4	0.3	0.2	0.1	0
Aggregation number(N) (0.05mol.kg ⁻¹)	54	56	59	61	56	57	62	79	70	62	49
Zeta Potential (ξ)/ mV (0.05mol.kg ⁻¹)	32.5	34.6	46.2	47.3	35.5	36.8	29.6	24.7	19.9	5.9	28.9
Anisotropy (r)	0.045	0.041	0.039	0.038	0.032	0.03	0.029	0.025	0.028	0.026	0.025

^aRelative standard uncertainties: $u_r(N) = 0.04$, $u_r(\xi) = 0.03$, $u_r(r) = 0.05$

Zeta potential (ζ) values are displayed in Table 6. The values of Zeta potential are positive for all the individual and mixed surfactant systems of different mole fractions of HDMimCl and DTAB. From Table 4, it is evident that number of counterion binding of HDMimCl is lower than DTAB. So the adsorption of Br^- in DTAB micelle is greater than that of Cl^- in HDMimCl in Stern layer and also the ζ potential value of DTAB is less than HDMimCl. It is also reported that at higher concentration of DTAB, the counterion binding increases resulting the minimization of ζ potential.⁷³ But in the mixture of HDMimCl and DTAB, the situation is quite different. With increase of the mole fraction of DTAB, the degree of counter-ion binding decreases (*cf.* Table 4), so the counterions behave like free salts which decrease the thickness of Gouy-Chapman layer and decrease the ζ potential with the increase of DTAB. The effect of counter-ion binding for the pure surfactant is overshadowed by the increasing salt concentrations with the increase of the mole fraction of DTAB. It is reported that in presence of increasing concentration of electrolytes, the ζ potential decreases.^{73,74} At $\alpha_1 = 0.9$, the micelles are mostly formed by HDMimCl and its ζ potential is comparable with pure HDMimCl. The increasing of ζ potential with increasing mole fraction of HDMimCl makes the micelles more stable.

The steady state fluorescence anisotropy (r) can be defined by Eq. 22,

$$r = \frac{(I_v - GI_h)}{(I_v + 2GI_h)} \quad (22)$$

and the G factor expressed as Eq. 23,

$$G = \frac{I_v}{I_h} \quad (23)$$

where, I_v and I_h are vertically and horizontally polarized emission intensity respectively when the vertically polarized light is used to excite the pure and mixed micelle solutions containing DPH as fluorescent probe. G factor relates the sensitivity of the instrument for vertically and horizontally polarized light ratio. The values of r mainly detects the restriction of the probe in the micellar environment. With increase of the mole fraction of HDMimCl, the anisotropy and also microviscosity of the micellar environment increase. As HDMimCl increases, the hydrophobicity of the micellar medium increases which restrict the hydrophobic DPH more (Figure 9).

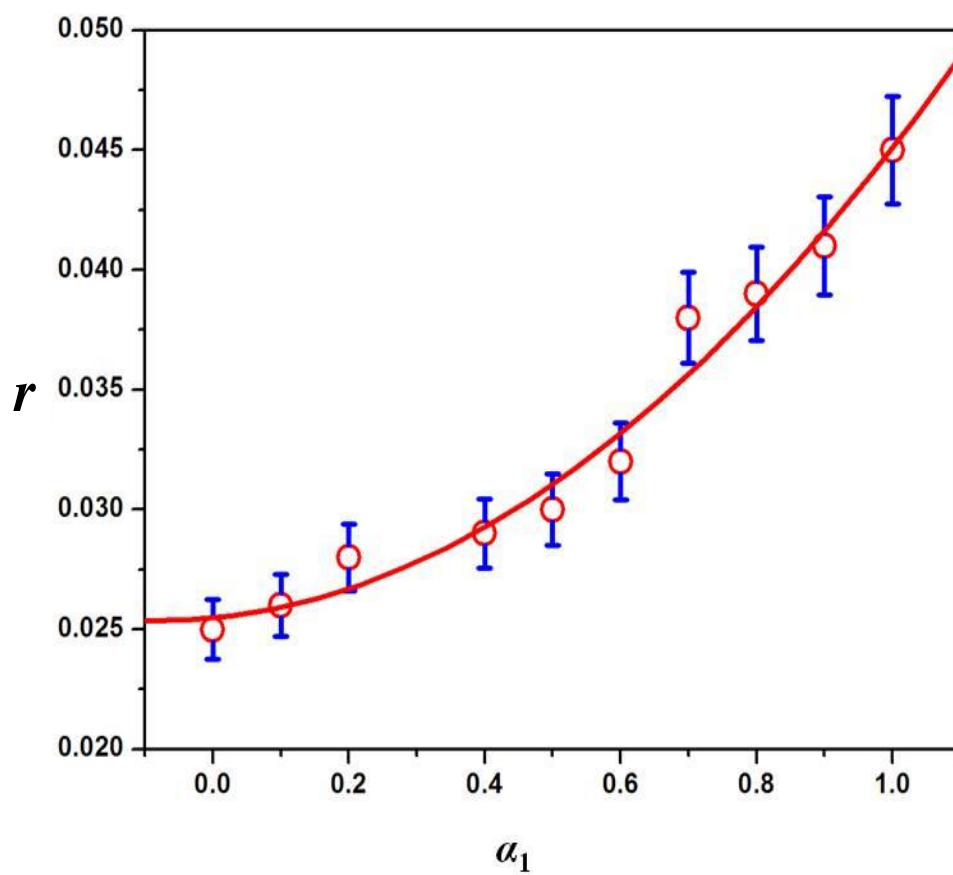


Figure 9. Steady state fluorescence anisotropy at different mole fractions of DTAB and HDMimCl at 313.15 K at 0.1 MPa. Error bar is introduced.

4. Conclusions:

Micellization behavior of binary mixtures of 1-hexadecyl-3-methylimidazolium chloride (HDMimCl) and dodecyltrimethylammonium bromide (DTAB) was investigated in aqueous solutions using conductometry, tensiometry, spectrofluorimetry along with Zeta potential and fluorescence anisotropy measurements. The regular solution theory (RST) and other thermodynamic models of micellar solutions e.g., Clint's model, Rubingh's model and Motomomura's model were employed to estimate the compositions of the mixed micelle, the parameters characterizing the interactions between the surfactants, the activity coefficients in the mixed micelle, and other parameter relating to micellization. The critical micellar concentrations (*cmc*) of HDMimCl-DTAB mixtures demonstrate some negative deviation from the ideal behavior, implying a nonideal mixing. Mixed micelles of HDMimCl-DTAB are also characterized by negative interaction parameter values, *i.e.*, the actual mixed micelles are thermodynamically more stable compared to hypothetical ideal state. Thermodynamic parameters indicate that the spontaneous process of micellization is entropically favorable for HDMimCl-rich mixtures while it is enthalpy-driven for DTAB-rich mixtures. The contributions from the electrostatic attraction between the surfactant molecules, the steric effect, and the repulsive molecular interaction vary with the mixture composition. Evaluation of the packing parameter values indicate spherical shape of the micelles formed individual and mixed surfactant solutions. Aggregation number of the mixed micelles initially increase with the increase in the HDMimCl-content followed by a decrease in the HDMimCl-rich region. Hydrophobicity of the mixed micellar solutions increases with the increase in the amount of the HDMimCl in the binary surfactant mixtures.

References

1. J. F. Scamehorn, *In Phenomena in Mixed Surfactant Systems*, Washington D.C., 1989.
2. P. M. Holland, *In Mixed Surfactants Systems*, Holland, P. M., Rubingh, D. N., Eds.; ACS Symposium Series 501; American Chemical Society: Washington D.C., 1992.
3. S. Qi, S. Roser, K. J. Edler, C. Pigliacelli, M. Rogerson, I. Weuts, F. V. Dycke, S. Stokbroekx, *Pharm. Res.*, 2013, **30**, 290-302.
4. M. R. Molla, M. A. Rub, A. Ahmed, M. A. Hoque, *J. Mol. Liq.*, 2017, **238**, 62-70.
5. D. Kumar, M. A. Rub, *J. Mol. Liq.*, 2017, **238**, 389-396.
6. M. Rahman, M. A. Khan, M. A. Rub, M. A. Hoque, A. M. Asiri, *J. Chem. Eng. Data*, 2017, **62**, 1464-1474.
7. S. Ghosh, *J. Colloid Interface Sci.*, 2001, **244**, 128-138.
8. S. P. Moulik, S. Ghosh, *J. Mol. Liq.*, 1997, **72**, 145-161.
9. C. Das, T. Chakraborty, S. Ghosh, B. Das, *Colloids Polym. Sci.*, 2008, **286**, 1143-1155.
10. D. Tikarika, B. Kumar, S. Ghosh, A. K. Tiwari; S. K. Saha, N. Barbero, P. Quagliotto, K. K. Ghosh, *J. Nanofluids*, 2013, **2**, 316-324.
11. C. Das, T. Chakraborty, S. Ghosh, B. Das, *Colloid J.*, 2010, **72**, 788-798.
12. I. M Umlong, K. Ismail, *J. Surface Sci. Technol.*, 2006, **22**, 101-117.
13. M. Colic, N. Kallay, *J. Surface Sci. Technol.*, 1988, **4**, 53-66.
14. S. K. Suri, H. S. Randhawa, *J. Surface Sci. Technol.* 1989, **5**, 355-363.
15. S. K. Sultana, S. G. T. Bhat, A. K. Rakshit, *J. Surface Sci. Technol.* 1997, **13**, 20-31
16. M. T. Garcia, I. Ribosa, L. J. Sanchez, F. Comelles, *J. Am Oil Chem. Soc.* 1992, **69**, 25-29.
17. L. D. Rhein, F. A. Simion, R. L. Hall, R. H. Cagan, J. Mattai, H. I. Maibach, *Dermatologica* , 1990, **180**, 18-23.
18. T. C. G. Kibbey, K. F. Hayes, *Environ. Sci. Technol.*, 1997, **3**, 1171-1177.
19. B. J. Aungst, S. Phang, *Int. J. Pharma.*, 1995, **117**, 95-100.
20. N. Muranushi, M. Kinugawa, Y. Nakajima, S. Muranushi, H. Sekaji, (I) *Int. J. Pharma.* 1980 ,**4**, 271-279.
21. N. Muranushi, M. Kinugawa, Y. Nakajima, S. Muranushi, H. Sekaji, (II) *Int. J. Pharma.* 1980, **4**, 281-290.
22. K. Ogino, M. Abe, *Mixed surfactant systems*. Dekker, New York, 1993.
23. J. L. Anderson, V. Pino, E. C. Hagberg, V. V. Sheares, D. W. Armstrong, *Chem. Comm.* 2003, **47**, 2444-2445.
24. M. Ao, P. Huang, G. Xu, X. Yang, Y. Wang, *Colloid Polymer Sci.* 2009, **287**, 395-402.
25. M. Blesic, M. Marques, N. V. Plechkova, K. R. Seddon, L. P. N. Rebelo, A. Lopes, *Green Chem.* 2007, **9**, 481-490.

26. A. Cornellias, L. Perez, F. Comelles, I. Robosa, A. Manresa, M. T. Garcia, *J. Colloid Interf. Sci.* 2011, **355**,164-171.
27. P. D. Galgano, O. A. El Seoud, *J. Colloid Interf. Sci.* 2010, **345**, 1-11.
28. T. Inoue, H. Ebina, B. Dong, L. Zheng, *J. Colloid Interf. Sci.*, 2007, **314**, 236-241.
29. J. Łuczak, J. Hupka, J. Thoming, C. Jungnickel, *Colloids Surf. A: Physicochem. Eng. Aspects*, 2008, **329**, 125-133.
30. T. Singh, A. Kumar, *J. Phys. Chem. B*, 2007, **111**, 7843-7851.
31. R. Vanyúr, L. Biczók, Z. Miskolczy, *Colloids Surf. A: Physicochem. Eng. Aspects*, 2007, **299**, 256-261.
32. A. Pal, A. Pillania, *J. Mol. Liquids* 2015 ,**212**, 818-824.
33. B. Dong, N. Li, L. Zheng, L. Yu, T. Inoue, *Langmuir* 2007, **23**, 4178-4182.
34. F. Comelles, I. Ribosa, J. J. Gozalez, M. T. Garcia, *J. colloid Interface Sci.* 2017, **490**, 119 - 128.
35. N. A. Smirnova, E. A. Safonova, *Colloid J.*, 2012, **74**, 254-265.
36. A. Pal, A. Pillania, *Fluid Phase Equilib.* 2015, **389**, 67-73.
37. C. Chadha, G. Singh, G. Singh, H. Kumar, T. S. Kang, *RSC Adv.* 2016, **6**, 38238- 38251.
38. T. Chakraborty, S. Ghosh, S. P. Moulik, *J. Phys. Chem. B*, 2005, **109**, 14813-14823.
39. N. B. Vargaftik, B. N. Volkov, L. D. Voljak, *J. Phys. Chem. Ref. Data*, 1983, **12**, 817-820.
40. E. Junquera, E. Aicart, *Langmuir* 2002, **18**, 9250-9258.
41. D. Ray, R. De, B. Das, *Carbohydr. Polym.*, 2014, **113**, 208–216.
42. A. Kumar, G. Kaur, G. R. Chaudhary, S. K. Mehta, *J. Mol. Liq.*, 2014, **198**, 37-43.
43. O. S. Esan, M. O. Osundiya, C. O. Aboluwoye, O. Olanrewaju, J. Ige, *ISRN Thermodynamics*, 2013, 1-7.
44. Q. Zhou, M. J. Rosen, *Langmuir*, 2003, **19**, 4555-4562.
45. M. A. Rub, N. Azum, F. Khan, A. M. Asiri, *J. Chem. Thermodyn.*, 2018, **121**, 199-210.
46. R. Sharma, S. Mahajan, R. L. Mahajan, *Colloids and Surfaces A: Physicochem. Eng. Aspects*, 2013, **427**, 62– 75.
47. J. H. Clint, *J. Chem. Soc., Faraday Trans. 1*, 1975, **71**, 1327-1334.
48. D. N. Rubingh, *Surface concentrations and molecular interactions in binary mixtures of surfactants. In: Mittal KL (ed) Solution chemistry of surfactants, Vol 1. Plenum Press, New York*, 1979, 337–359.
49. K. Motomura, M. Yamanaka, M. Aratono, *Colloid. Polym. Sci.*, 1984, **262**, 948-955.
50. M. A. Rub, N. Azum, A. M. Asiri, *J. Chem. Eng. Data* 2017, **62**, 3216-3228.
51. A. Rodríguez, M. Mar Graciani, A. J. Moreno-Vargas, M. L. Moyá, *J. Phys. Chem. B*, 2008, **112**, 11942-11949.
52. G. B. Ray, I. Chakraborty, S. Ghosh, S. P. Moulik, *J. Colloid Interf. Sci.*, 2007, **307**, 543-553.

53. E. P. Schulz, J. L. M. Rodriguez, R. M. Minardi, D. B. Miraglia, P. C. Schulz, *J Surfact Deterg* 2013, **16**, 795-803.
54. J. M. Hierrezuelo, J. Aguiar, C. C. Ruiz, *Colloids and Surfaces A: Physicochem. Eng. Aspects*, 2005, **264**, 29-36.
55. Z. H. Ren, J. Huang, Y. C. Zheng, L. Lai, L. L. Hu, *J. Chem. Eng. Data*, 2017, **62**, 1782-1787.
56. U. Patel, P. Parekh, N. V. Sastry, V. K. Aswal, P. Bahadur, *J. Mol. Liq.*, 2017, **225**, 888-896.
57. A. Z. Naqvi, S. Noori, Kabir-ud-Din, *Colloids and Surfaces A: Physicochem. Eng. Aspects* 2015, **477**, 9-18.
58. P. Zheng, X. Zhang, J. Fang, W. Shen, *J. Chem. Eng. Data*, 2016, **61**, 979- 986.
59. M. J. Rosen, J. T. Junkappu, *Surfactants and interfacial phenomena, 4th ed.*; Wiley-Interscience: Hoboken, NL, 2012.
60. S. Chauhan, K. Sharma, *J. Chem. Thermodyn.*, 2014, **71**, 205-211.
61. Z. H. Ren, Y. Luo, Y. C. Zheng, C. J. Wang, D. P. Shi, F. X. Li, *J. Mater. Sci.*, 2015, **50**, 1965-1972.
62. Z. H. Ren, J. Huang, Y. Luo, Y. C. Zheng, P. Mei, L. Lai, Y. L. Chang, *J. Ind. Eng. Chem.*, 2016, **36**, 263-270.
63. Z. H. Ren, Y. Luo, Y. C. Zheng, D. P. Shi, P. Mei, F. S. Li, *J. Solution Chem.*, 2014, **43**, 853-869.
64. S. Shimizu, P. A. R. Pires, W. Loh, O. A. E. Seoud, *Colloid Polym. Sci.*, 2004, **282**, 1026-1032.
65. E. Sikorska, D. Wyrzykowski, K. Szutkowski, K. Greber, E. A. Lubecka, I. Zhukov, *J. Therm. Anal. Calorim.*, 2016, **123**, 511-523.
66. Z. H. Ren, J. Huang, Y. C. Zheng, L. L. Hu, *J. Chem. Eng. Data*, 2017, **62**, 1782-1787.]
67. S. Das, S. Maiti, S. Ghosh, *RSC Adv.*, 2014, **4**, 12275-12286.
68. G. B. Ray, S. Ghosh, S. P. Moulik, *J. Chem. Sci.* 2010, **122**, 109-117.
69. C. Tanford, *The Hydrophobic Effect*, 2nd ed.; Wiley-Interscience: New York, 1980.
70. G. B. Ray, I. Chakraborty, S. Ghosh, S. P. Moulik, C. Holgate, K. Glenn, R. M. Palepu, *J. Phys. Chem. B*, 2007, **111**, 9828-9837.
71. S. Ghosh, T. Chakraborty, *J. Phys. Chem. B*, 2007, **111**, 8080-8088.
72. J. N. Israelachvili, *In Intermolecular and surface forces (London: Academic Press)*, 2nd ed.; chap. 17, 1991, 370.
73. R. Sabate, M. Gallardo, J. Estelrich, *Electrophoresis*, 2000, **21**, 481-485.
74. B. Naskar, A. Dey, S. P. Moulik, *J Surfact. Deterg.* 2013, **16**,785-794.

Table 2. Specific Conductance (κ) vs. Molality (m) Data in Aqueous HDMimCl + DTAB Solutions for Different Mole fractions of HDMimCl (α_1) at (303.15, 313.15, and 323.15) K at 0.1 MPa

$\alpha_1 = 1.0$						$\alpha_1 = 0.9$					
T = 303.15 K		T = 313.15 K		T = 323.15 K		T = 303.15 K		T = 313.15 K		T = 323.15 K	
m (mol.kg ⁻¹)	κ (μ S.cm ⁻¹)	m (mol.kg ⁻¹)	κ (μ S.cm ⁻¹)	m (mol.kg ⁻¹)	κ (μ S.cm ⁻¹)	m (mol.kg ⁻¹)	κ (μ S.cm ⁻¹)	m (mol.kg ⁻¹)	κ (μ S.cm ⁻¹)	m (mol.kg ⁻¹)	κ (μ S.cm ⁻¹)
0	0	0	0	0	0	0	0	0	0	0	0
0.00011	12.06	0.00011	15.22	0.00011	17.15	0.00015	16.88	0.00015	20.40	0.00015	21.58
0.00022	23.39	0.00022	29.50	0.00022	33.40	0.00029	31.88	0.00029	39.78	0.00029	45.66
0.00033	34.10	0.00033	43.20	0.00033	49.10	0.00044	47.38	0.00044	58.98	0.00044	68.96
0.00043	44.40	0.00043	56.00	0.00043	64.00	0.00059	63.38	0.00059	78.08	0.00059	91.06
0.00052	54.10	0.00052	68.60	0.00052	79.10	0.00073	76.78	0.00073	96.18	0.00073	114.06
0.00062	63.60	0.00062	80.30	0.00062	92.90	0.00087	90.28	0.00087	113.18	0.00087	135.36
0.00071	72.60	0.00071	91.80	0.00071	106.1	0.00101	99.28	0.00101	125.88	0.00101	155.26
0.00079	80.90	0.00079	102.4	0.00079	118.8	0.00115	107.28	0.00115	136.18	0.00115	170.46
0.00088	88.00	0.00088	111.8	0.00088	133.3	0.00129	114.78	0.00129	145.48	0.00129	183.76
0.00096	93.30	0.00096	119.2	0.00096	142.9	0.00143	121.68	0.00143	154.18	0.00143	195.06
0.00104	97.70	0.00104	125.4	0.00104	152.8	0.00156	128.18	0.00156	162.78	0.00156	205.76
0.00112	101.7	0.00112	130.7	0.00112	161.1	0.00169	135.48	0.00169	171.18	0.00169	216.46
0.00119	105.5	0.00119	135.8	0.00119	168.2	0.00196	148.58	0.00196	187.28	0.00196	236.96
0.00126	108.8	0.00126	140.6	0.00126	175.0	0.00222	161.38	0.00222	202.58	0.00222	255.96
0.00133	111.9	0.00133	145.1	0.00133	180.8	0.00248	173.78	0.00248	217.18	0.00248	274.86
0.00139	115.0	0.00139	149.1	0.00139	186.2	0.00273	186.08	0.00273	231.78	0.00273	293.66
0.00146	118.3	0.00146	153.5	0.00146	191.7	0.00297	197.08	0.00297	246.28	0.00297	311.66
0.00153	121.1	0.00153	157.3	0.00153	197.0	0.00321	208.08	0.00321	259.68	0.00321	327.66

$\alpha_1 = 0.8$						$\alpha_1 = 0.7$					
0	0	0	0	0	0	0	0	0	0	0	0
0.00015	15.77	0.00015	17.05	0.00015	20.87	0.00015	15.96	0.00015	19.18	0.00015	22.93
0.00029	30.12	0.00029	35.16	0.00029	43.29	0.00029	31.39	0.00029	37.90	0.00029	44.93
0.00044	45.32	0.00044	52.16	0.00044	64.59	0.00044	46.89	0.00044	56.20	0.00044	66.63
0.00059	60.02	0.00059	69.56	0.00059	85.99	0.00059	61.79	0.00059	74.20	0.00059	88.63
0.00073	74.02	0.00073	85.56	0.00073	106.49	0.00073	76.89	0.00073	90.60	0.00073	109.43
0.00087	87.62	0.00087	101.26	0.00087	127.39	0.00087	90.99	0.00087	109.2	0.00087	129.73
0.00101	97.82	0.00101	116.36	0.00101	146.59	0.00101	101.69	0.00101	126.1	0.00101	149.23
0.00115	105.52	0.00115	128.56	0.00115	163.09	0.00115	109.79	0.00115	138.1	0.00115	168.23
0.00129	112.22	0.00129	137.76	0.00129	175.99	0.00129	117.59	0.00129	148.4	0.00129	183.23
0.00143	119.32	0.00143	146.96	0.00143	187.29	0.00143	124.99	0.00143	157.7	0.00143	196.03
0.00169	131.92	0.00169	162.96	0.00169	204.49	0.00156	132.29	0.00156	166.6	0.00156	207.83
0.00196	143.52	0.00196	179.06	0.00196	222.19	0.00169	139.39	0.00169	175.1	0.00169	218.93
0.00222	154.82	0.00222	194.26	0.00222	238.79	0.00196	153.09	0.00222	208.1	0.00222	260.53
0.00248	177.32	0.00248	208.96	0.00248	253.79	0.00222	166.59	0.00248	224.5	0.00248	279.83
0.00273	188.92	0.00273	223.06	0.00273	270.09	0.00248	179.09	0.00273	240.2	0.00273	299.03
0.00321	210.92	0.00297	236.96	0.00321	300.89	0.00273	191.69	0.00321	271.3	0.00321	336.03
0.00368	231.32	0.00321	250.26	0.00368	340.89	0.00321	216.09				
0.00412	250.52	0.00345	262.96	0.00412	362.89						
0.00458	268.92	0.00368	276.06	0.00458	389.89						
0.00500	286.52	0.00391	287.96	0.00500	414.89						
0.00561	311.52	0.00458	323.26	0.00561	449.89						
0.00619	334.52	0.00521	354.26	0.00619	487.89						
0.00674	355.52	0.00581	384.26	0.00674	523.89						
0.00727	376.52	0.00638	423.26	0.00727	554.89						

$\alpha_1 = 0.6$						$\alpha_1 = 0.5$					
0	0	0	0	0	0	0	0	0	0	0	0
0.00015	15.11	0.00015	17.93	0.00015	21.09	0.00009	8.34	0.00027	32.95	0.00015	21.41
0.00029	29.60	0.00029	35.71	0.00029	41.96	0.00019	17.98	0.00053	64.45	0.00029	43.96
0.00044	44.40	0.00044	53.91	0.00044	62.56	0.00029	27.69	0.00078	96.75	0.00044	65.76
0.00059	58.40	0.00059	72.91	0.00059	83.86	0.00039	38.10	0.00104	126.35	0.00059	87.06
0.00073	73.20	0.00073	89.81	0.00073	104.06	0.00049	48.30	0.00129	153.45	0.00073	107.76
0.00087	86.70	0.00087	106.71	0.00087	124.06	0.00058	57.80	0.00154	173.45	0.00087	129.26
0.00101	99.40	0.00101	124.11	0.00101	144.36	0.00068	69.50	0.00178	191.55	0.00101	149.66
0.00115	109.3	0.00115	138.21	0.00115	162.96	0.00077	80.30	0.00203	209.45	0.00115	169.86
0.00129	117.7	0.00129	149.41	0.00129	181.06	0.00086	89.70	0.00226	226.75	0.00129	195.96
0.00143	125.6	0.00143	159.71	0.00143	195.36	0.00095	97.50	0.0025	244.35	0.00143	206.96
0.00169	141.3	0.00169	178.51	0.00169	213.76	0.00104	105.4	0.00273	260.95	0.00169	232.16
0.00196	155.7	0.00196	196.91	0.00196	234.46	0.00113	111.3	0.00296	276.85	0.00196	256.76
0.00222	169.7	0.00222	214.21	0.00222	256.26	0.00122	117.9	0.00319	293.15	0.00222	279.96
0.00248	183.6	0.00248	229.01	0.00248	274.66	0.00131	122.2	0.00342	309.05	0.00248	302.56
0.00273	197.3	0.00273	243.71	0.00273	299.56	0.00139	126.7	0.00386	340.05	0.00273	324.56
0.00321	222.6	0.00321	272.41	0.00321	346.96	0.00148	132.9	0.00429	369.05	0.00345	381.56
0.00368	248.1	0.00368	303.81	0.00368	380.96	0.00165	142.7	0.00471	399.05	0.00414	443.56
0.00414	269.4	0.00414	333.81	0.00414	408.96	0.00182	152.6	0.00512	427.05	0.00479	501.56
0.00458	288.8	0.00458	357.81	0.00458	431.96	0.00198	161.9	0.00552	454.05	0.00541	557.56
0.00500	311.4	0.00500	388.81	0.00500	456.96	0.00214	171.9	0.00629	507.05	0.00600	606.56
0.00561	341.4	0.00561	426.81	0.00561	502.96	0.00230	181.0	0.00703	554.05	0.00674	669.56
0.00619	370.4	0.00619	453.81	0.00619	544.96	0.00246	189.9	0.00774	602.05	0.00744	720.56
0.00674	398.4	0.00674	495.81	0.00674	582.96	0.00276	207.3	0.00875	652.00	0.00810	778.00
0.00727	423.4	0.00727	528.81	0.00727	623.96	0.00305	224.8	0.00939	695.00	0.00872	830.00
0.00778	445.4	0.00778	557.81	0.00778	659.96	0.00333	241.8	0.01059	772.00	0.00931	881.00
0.00843	477.4	0.00843	598.81	0.00843	698.96	0.00361	257.4	0.01169	841.00	0.00987	924.00
0.00902	507.4	0.00902	636.81	0.00902	746.96	0.00425	293.7	0.01273	905.00		
0.00959	535.4	0.00959	665.81	0.00959	783.96	0.00485	328.2	0.01368	962.00		
0.01000	557.4	0.01000	703.81	0.01000	814.96	0.00540	358.2	0.01458	1013.0		
						0.00639	411.2	0.01500	1089.0		
						0.00726	445.2	0.01521	1102.0		
						0.00802	498.0				
						0.00931	560.0				
						0.01034	610.0				
						0.01118	653.0				
						0.01138	662.0				

$\alpha_1 = 0.4$						$\alpha_1 = 0.3$					
0	0	0	0	0	0	0	0	0	0	0	0
0.00015	15.09	0.00015	17.68	0.00015	21.43	0.00015	16.74	0.00015	20.83	0.00015	23.16
0.00029	30.54	0.00029	35.39	0.00029	43.14	0.00029	32.46	0.00029	39.77	0.00029	45.86
0.00044	45.44	0.00044	53.39	0.00044	63.64	0.00044	47.46	0.00044	58.97	0.00044	68.56
0.00059	61.04	0.00059	71.09	0.00059	106.64	0.00059	63.26	0.00059	77.87	0.00059	90.86
0.00073	76.54	0.00073	87.79	0.00073	127.24	0.00073	79.46	0.00073	97.27	0.00073	113.06
0.00087	90.94	0.00087	105.19	0.00087	148.34	0.00087	94.86	0.00087	114.77	0.00087	135.26
0.00101	104.94	0.00101	122.59	0.00101	189.14	0.00101	109.96	0.00101	132.87	0.00101	156.76
0.00115	118.14	0.00115	138.39	0.00115	208.24	0.00115	124.96	0.00115	149.97	0.00115	178.26
0.00129	129.34	0.00129	153.39	0.00129	225.24	0.00129	137.96	0.00129	166.77	0.00129	199.16
0.00143	138.64	0.00143	167.69	0.00143	239.94	0.00143	149.76	0.00143	183.47	0.00143	219.96
0.00169	157.34	0.00169	190.99	0.00169	260.44	0.00156	160.76	0.00156	198.17	0.00156	240.06
0.00196	175.34	0.00196	209.09	0.00196	284.24	0.00169	171.46	0.00169	211.97	0.00169	258.46
0.00222	192.94	0.00222	228.49	0.00222	305.34	0.00196	192.26	0.00196	237.07	0.00196	290.36
0.00248	209.64	0.00248	247.29	0.00248	329.34	0.00222	212.16	0.00222	262.47	0.00222	319.26
0.00273	226.14	0.00273	266.99	0.00273	352.34	0.00248	231.56	0.00248	285.97	0.00248	347.26
0.00321	258.74	0.00321	305.89	0.00321	398.34	0.00273	251.16	0.00273	310.67	0.00273	375.26
0.00368	289.74	0.00368	340.89	0.00368	441.34	0.00297	269.86	0.00321	354.67	0.00297	401.26
0.00414	320.14	0.00414	374.89	0.00414	482.34						
0.00458	348.14	0.00458	409.89	0.00458	519.34						
0.00500	376.14	0.00500	442.89	0.00500	553.34						
0.00561	414.14	0.00561	488.89	0.00561	610.34						
0.00619	452.14	0.00619	531.89	0.00619	661.34						
0.00674	487.14	0.00674	571.89	0.00674	711.34						
0.00727	519.14	0.00727	608.89	0.00727	759.34						
0.00778	551.14	0.00778	646.89	0.00778	803.34						
0.00842	589.14	0.00842	686.89	0.00842	859.34						
0.00902	624.14	0.00902	730.89	0.00902	910.34						
0.00959	658.14	0.00959	766.89	0.00959	959.34						
0.00993	676.14	0.00993	800.89	0.00993	988.34						

$\alpha_1 = 0.2$						$\alpha_1 = 0.1$					
0	0	0	0	0	0	0	0	0	0	0	0
0.00015	15.07	0.00015	18.35	0.00015	20.01	0.00015	15.46	0.00015	17.57	0.00015	21.16
0.00029	29.94	0.00029	36.38	0.00029	41.72	0.00029	30.42	0.00029	36.10	0.00029	43.26
0.00044	45.54	0.00044	53.58	0.00044	63.42	0.00044	45.42	0.00044	54.30	0.00044	65.06
0.00059	59.94	0.00059	72.08	0.00059	85.02	0.00059	59.82	0.00059	73.00	0.00059	87.06
0.00073	75.14	0.00073	89.78	0.00073	105.22	0.00073	76.02	0.00073	89.30	0.00073	107.36
0.00087	89.74	0.00087	107.18	0.00087	125.82	0.00087	90.32	0.00087	107.9	0.00087	128.96
0.00101	103.64	0.00101	124.38	0.00101	145.72	0.00101	105.12	0.00101	125.0	0.00101	149.06
0.00115	117.84	0.00115	141.08	0.00115	165.82	0.00115	119.92	0.00115	141.9	0.00115	170.76
0.00129	131.84	0.00129	157.48	0.00129	186.42	0.00129	134.02	0.00129	158.6	0.00129	191.06
0.00143	145.64	0.00143	174.28	0.00143	207.02	0.00143	148.02	0.00143	174.9	0.00143	210.76
0.00169	172.34	0.00169	201.48	0.00169	238.32	0.00169	175.92	0.00169	206.4	0.00169	238.86
0.00196	194.04	0.00196	228.18	0.00196	272.32	0.00196	201.82	0.00196	236.3	0.00196	271.96
0.00222	214.94	0.00222	252.58	0.00222	306.02	0.00222	227.22	0.00222	263.5	0.00222	306.66
0.00248	234.84	0.00248	275.18	0.00248	332.02	0.00248	251.32	0.00248	291.9	0.00248	340.66
0.00273	255.04	0.00273	298.18	0.00273	365.02	0.00273	275.02	0.00273	321.4	0.00273	374.66
0.00321	294.44	0.00321	347.18	0.00321	415.02	0.00321	320.02	0.00321	374.4	0.00321	441.66
0.00368	331.44	0.00368	394.18	0.00368	468.02	0.00368	362.02	0.00368	425.4	0.00368	501.66
0.00414	366.44	0.00414	436.18	0.00414	525.02	0.00414	403.02	0.00414	473.4	0.00414	559.66
				0.00458	577.02	0.00458	443.02	0.00458	519.4	0.00458	613.66
				0.00500	627.02	0.00500	480.02	0.00500	563.4	0.00500	667.66
				0.00561	697.02	0.00561	534.02	0.00561	626.4	0.00561	748.66
				0.00619	761.02	0.00619	584.02	0.00619	684.4	0.00619	818.66
				0.00674	822.02	0.00674	631.02	0.00674	743.4	0.00674	887.66
				0.00727	881.02	0.00727	674.02	0.00727	795.4	0.00727	952.66
				0.00778	937.02	0.00778	716.02	0.00778	846.4	0.00778	1010.7
				0.00842	1008.0	0.00843	769.02	0.00843	910.4	0.00843	1093.7
				0.00902	1073.0	0.00902	817.02	0.00902	969.4	0.00902	1169.66
				0.00959	1124.0	0.00959	874.02	0.00959	1021.4	0.00959	1241.66
				0.01000	1168.0	0.01000	894.02	0.01000	1062.4	0.01000	1262.66

 $\alpha_1 = 0.0$

0	0	0	0	0	0
0.00178	193.71	0.00178	234.15	0.00178	281.54
0.00353	374.11	0.00353	467.05	0.00353	546.64
0.00524	553.11	0.00524	668.05	0.00524	801.64
0.00692	727.11	0.00692	871.05	0.00692	1048.6
0.00857	893.11	0.00857	1070.0	0.00857	1284.6
0.01019	1055.1	0.01019	1263.1	0.01019	1515.6
0.01178	1210.1	0.01178	1453.1	0.01178	1741.6
0.01333	1361.1	0.01333	1633.1	0.01333	1955.6
0.01486	1491.1	0.01486	1802.1	0.01486	2162.6
0.01636	1568.1	0.01636	1932.1	0.01636	2343.6
0.01784	1618.1	0.01784	2009.1	0.01789	2472.6
0.01929	1661.1	0.01929	2075.1	0.01929	2577.6
0.02071	1701.1	0.02071	2131.1	0.02071	2652.6
0.02211	1739.1	0.02211	2186.1	0.02211	2722.6
0.02348	1776.1	0.02348	2239.1	0.02348	2789.6
0.02483	1813.1	0.02483	2286.1	0.02483	2851.6
0.02615	1850.1	0.02615	2336.1	0.02615	2918.6
0.02746	1885.1	0.02746	2381.1	0.02746	2973.6
0.02874	1919.1	0.02874	2426.1	0.02874	3036.6
0.03000	1953.1	0.03000	2467.1	0.03000	3096.6

Chapter II

Studies on the self-aggregation, interfacial and thermodynamic properties of a surface-active imidazolium-based ionic liquid in aqueous solution: Effects of salt and temperature

Studies on the self-aggregation, interfacial and thermodynamic properties of a surface-active imidazolium-based ionic liquid in aqueous solution: Effects of salt and temperature‡

ABSTRACT

The influence of four sodium salts (NaCl, NaBr, Na₂SO₄, and Na₃PO₄) on the self-aggregation, interfacial, and thermodynamic properties of a surface-active ionic liquid (1-hexadecyl-3-methylimidazolium chloride, C₁₆MImCl) has been explored in aqueous solutions by conductometry, tensiometry, spectrofluorimetry, isothermal titration calorimetry and dynamic light scattering (DLS). Analyses of the critical micellar concentration (*cmc*) values indicate that the anions of the added salts promote the self-aggregation of C₁₆MImCl in the order: Cl⁻ < Br⁻ < PO₄³⁻ < SO₄²⁻. Melting of iceberg, in general, governs the process of micellization of aqueous C₁₆MImCl in presence of the investigated salts within the investigated temperature range (298.15-318.15 K), while the dehydration of imidazolium head groups takes the leading role below 303.15 K for the C₁₆MImCl-Na₃PO₄ system. The results indicate that addition of salt leads to a greater spontaneity of micellization, and that exothermicity prevails in these systems. Differential effect of the salts on the interfacial properties of C₁₆MImCl has been interpreted on the basis of the coupled influence of the electrostatic charge neutralization of surfactants at the interface, and the van der Waals repulsion of surfactant tails and electrostatic repulsion of surfactant head groups. C₁₆MImCl has been shown to form spherical micelles in presence of varying amounts of NaCl, Na₂SO₄ and Na₃PO₄, while there occurs probably a transition in the micellar geometry from spherical to non-spherical shape when added NaBr concentration exceeds 0.01 mol.kg⁻¹. Fluorescence studies demonstrate that a combined quenching mechanism is operative for the quenching of pyrene fluorescence in the investigated C₁₆MImCl-salt systems. Micellar aggregation numbers obtained from Steady State Fluorescence Quenching method have always been found be somewhat smaller than those estimated from Time Resolved Fluorescence Quenching method. The order of instability of the C₁₆MImCl-micelles ascertained from Zeta potential measurements conforms to what has been inferred from the *cmc* values. The hydrodynamic diameters of C₁₆MImCl-micelles, obtained from DLS studies, have been found to increase with increasing salinity of the solutions.

(‡ Published in *J. Mol. Liq.*, 320 (2020) 114497)

1. Introduction

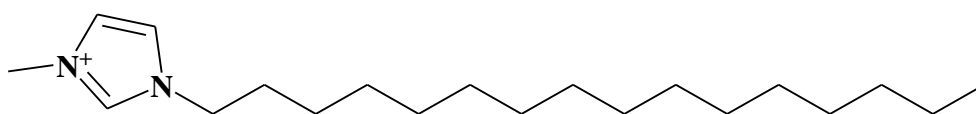
In recent years, considerable attention is being paid to the studies on ionic liquids with surface activity (commonly referred to as surface active ionic liquids) in colloid and interface science.¹⁻⁹ Surface active ionic liquids, like conventional surfactants, form self-aggregates¹⁰⁻¹⁸ owing to the balance of hydrophilic and hydrophobic interactions above a particular concentration known as the critical micellar concentration (*cmc*).¹⁹⁻²² Current interest in the area of surface active ionic liquids stems from the ease of fine-tuning of the hydrophobicity of ionic liquid molecules by varying the length of the hydrocarbon chains, the type of the head-group or the

nature and size of the counterions which might permit the modulation of the structure and the delicate dynamics of their self-aggregates for specific purposes. Additives could also result in the modification of the interaction and self-aggregation behavior of surfactants appreciably.²³⁻³⁵ Studies on surfactant solutions in presence of a salt have been shown to provide important insight into various interactions prevailing in these solutions.³²⁻³⁶ Surfactant-salt mixtures find widespread use in biological, technological, medical formulations, pharmaceuticals, enhanced oil recovery for the purpose of improved solubilization, suspension and dispersion.² Various organic and inorganic salts in combination with various surfactants are also used for this purpose.^{3-9,14-47} However, there had been, so far, a very few attempts which explored the effect of salts on the self-aggregation properties of surface active ionic liquid solutions.⁴⁸⁻⁵² Keeping this in view, we have taken up a comprehensive program to investigate the self-aggregation, interfacial, and thermodynamic properties of a surface active ionic liquid (1-hexadecyl-3-methylimidazolium chloride) in presence of each of sodium chloride (NaCl), sodium bromide (NaBr), sodium sulfate (Na₂SO₄), and sodium phosphate (Na₃PO₄) in aqueous solutions. Different experimental techniques *e. g.*, conductometry, tensiometry, spectrofluorimetry, isothermal titration calorimetry and dynamic light scattering methods have been employed to explore the very many facets of micellization behavior of the selected surface active ionic liquid-salt solutions in aqueous media.

2. Experimental

2.1. Materials

1-Hexadecyl-3-methylimidazolium chloride (C₁₆MImCl) (structure shown in Fig.1), and 1-hexadecylpyridinium chloride (CPC) have been purchased from Acros Organics. These were used as received. Reagent grade sodium chloride (NaCl), sodium bromide (NaBr), sodium sulfate (Na₂SO₄) and sodium phosphate (Na₃PO₄, 12H₂O) were purchased from Sigma Aldrich. Pyrene solutions prepared in ethanol and 1,6-diphenyl-1,3,5-hexatriene (DPH) solutions prepared in tetrahydrofuran (THF), were purchased from Sigma Aldrich, and were used as fluorophore. Triply distilled water with a specific conductance around 0.98 μs.cm⁻¹ at 298.15 K was used to prepare the different solutions throughout the experiments at different temperatures.



Cl⁻

Fig. 1. Structure of 1-hexadecyl-3-methylimidazolium chloride.

2.2. Methods

2.2.1. Conductometry

Measurements on specific conductivities (κ) have been carried out using an Orion (Thermo Fisher, USA) conductivity meter with a conductivity cell of cell constant 1 cm^{-1} , dipped in the experimental solution maintained within 0.05 K of the desired temperature in a thermostatic water bath.

The specific conductances of aqueous $\text{C}_{16}\text{MImCl}$ solutions in absence as well as in the presence of the salts (NaCl , NaBr , Na_2SO_4 , and Na_3PO_4) have been plotted against the concentration of $\text{C}_{16}\text{MImCl}$ (please see the representative Fig. 2). The specific conductance *vs.* surfactant concentration profiles have always been found to reveal inflections. For any given system, the values of the specific conductances above and below the inflection point have been fitted to two separate linear equations, squared correlation coefficient (r^2) being always greater than or equal to 0.99, and the intersection of these straight lines provided an estimate of the *cmc* (*cf.* Table 1). As the inflection points for $\text{C}_{16}\text{MImCl}$ solutions in presence of salts having higher concentrations obtained by conductometry have been found to be incompatible with those obtained from other experimental techniques employed here to represent the *cmc* values, conductometric determination of *cmc* has been restricted to low-salt solutions.

2.2.2. Tensiometry

Surface tensions at air/water interface have been measured using a calibrated Krüss (Germany) tensiometer by du Noüy ring detachment method with an accuracy of $\pm 0.1 \text{ mN.m}^{-1}$. The platinum ring has been thoroughly cleaned by water and acetone successively and has been dried in ethanol oxidizing flame before and after each experiment. The tensiometer was connected to a water-flow cryostat in order to maintain the temperature equilibration. The surface tension *vs.* surfactant concentration for aqueous $\text{C}_{16}\text{MImCl-NaCl}$, $\text{C}_{16}\text{MImCl-NaBr}$, $\text{C}_{16}\text{MImCl-Na}_2\text{SO}_4$, and $\text{C}_{16}\text{MImCl-Na}_3\text{PO}_4$ solutions in presence of varying concentration of the added salts at 298.15 K have been shown in Figs. 3(a) through 3(d). Tensiometry records the threshold surfactant concentration required to saturate the air/solution interface as the *cmc* which has been obtained (listed in Table 1) from a sharp break in these surface tension *vs.* surfactant concentration profiles; a representative plot showing such a break has been shown in Fig. 3(a).

2.2.3. Isothermal titration calorimetry (ITC)

ITC measurements were carried out with GE Microcal ITC 200(Northampton, USA) microcalorimeter. Distilled water was taken as reference in the whole experiments. Surfactant solutions in water and different salt solutions having initial concentrations approximately ten times their *cmc* values measured by conductometry were prepared, taken in syringe and added to the respective solutions initially 0.5 μl , then 2 μl (total 20 additions) with an interval of 120s. The temperature was kept constant at 298.15 K throughout the experiments. ITC experiments directly measure the enthalpy of micellization (ΔH_m^0) (shown in Table 2.) as well as the *cmcs* (cf. Table 1) accurately.^{10,17,52,58-62}

2.2.4. Fluorimetry

Steady-state fluorescence measurements have been made on a Perkin-Elmer LS 55 (USA) fluorescence spectrophotometer with a Peltier attachment using quartz cell of 1 cm path length at 298.15 K. Pyrene has been used as the probe. The excitation of pyrene has been performed at 335 nm with a band pass of 14 nm and emission has been monitored at 371nm (I_1) and 384 nm (I_3) using a band pass of 4 nm. To determine the micropolarity (I_1/I_3), a set of aqueous $\text{C}_{16}\text{MImCl}$ solution in absence and in presence of different salts having varying concentrations have been prepared, where both the surfactant concentration ($10 \times 10^{-3} \text{ mol.kg}^{-1}$ for micropolarity study, and $12 \times 10^{-3} \text{ mol.kg}^{-1}$ for steady-state quenching study) and the pyrene concentration ($1 \times 10^{-6} \text{ mol.kg}^{-1}$) were kept fixed for each of the solution for the measurement. All solutions have been well sonicated and kept for 4-5 hours for equilibrium before irradiation. Experimental (I_1/I_3) values have been listed in Table 4.

Steady-state fluorescence anisotropy measurements were performed on the same instrument [Perkin-Elmer LS 55 (USA)] fitted with a polarizer using DPH as probe in a quartz cell of 1 cm path length at 298.15 K. Excitation wavelength has been fixed at 353 nm and emission of DPH has been measured at 437 nm. Initially a measured amount of DPH is added to water or to salt solution taken in a quartz cell and then the stock surfactant solution (having concentration approximately 15 times the *cmc* measured with the above-mentioned techniques) with the same amount of DPH is added to the cuvette. The concentration of the probe has been fixed at $2 \times 10^{-6} \text{ mol.kg}^{-1}$ both in cuvette and in the stock solution. DPH, because of its rod like shape, is used as a fluorescent anisotropic probe as it retains the polarization in the restricted medium. The steady state anisotropy (r) can be defined by the following equation^{18, 53, 54}:

$$r = \frac{I_v - GI_h}{I_v + 2GI_h} \quad (1)$$

where I_v and I_h are respectively the fluorescence intensities when the emission polarizer parallel and perpendicular to the exiting electromagnetic radiation, and the factor G , defined as the ratio of I_v to I_h , rectifies the unequal transmission generated by the diffraction gratings of the instrument for the horizontally and vertically polarized lights.

Time-resolved fluorescence decay has been measured in Horiba-Jobin-Yvon Fluoro Cube fluorescence lifetime system by the time-correlated single photon counting (TCSPC) technique. A Nano LED (IBH, UK) at 330 nm has been used as the excitation source for pyrene and the decay emission has been recorded at 374 nm. A TBX photon detection module has been used as the detector. The decay data have been fitted with the help of IBH DAS-6 decay analysis software by nonlinear least square procedure so that the values of residuals (χ^2) do not exceed 1.5. The lamp profile was collected using a dilute aqueous micellar solution of sodium dodecyl sulfate as a scatterer in place of the experimental solution. Pyrene has been used as probe, and its concentration has been fixed at 10^{-4} mol. L⁻¹ so that it cannot form excimer in the micellar region. CPC has been used as the quencher, and final CPC concentration has been kept fixed within 0.3×10^{-3} mol.kg⁻¹ to avoid micelle formation of CPC itself in the experimental solutions for both steady state and time resolved experiments. The ratio of ([quencher]/[micelle]) in pyrene-solubilized micellar solution has been kept near unity to ensure the residence of one quencher molecule per micelle, as stated in the earlier literatures.⁵⁵⁻⁵⁷ The initial concentrations of C₁₆MImCl prepared in water and in different salt solutions have been kept fixed at 12×10^{-3} mol.kg⁻¹. Mean (average) fluorescence lifetimes (τ_{av}) for bi-exponential iterative fittings have been calculated from the pre-exponential factors (a_1 and a_2) and the decay times (τ_1 and τ_2) by using the following equation:

$$\tau_{av} = a_1\tau_1 + a_2\tau_2 \quad (2)$$

2.2.5. Dynamic light scattering (DLS) and Zeta potential

DLS measurements have been carried out using a Nano ZS Zetasizer (Malvern, UK) at 90° scattering angle with a He-Ne laser having wavelength (λ) of 632.8 nm at 298.15 K.

Zeta potential measurements have been performed at 298.15 K with 90° scattering angle using a gold coated copper electrode in the cell. All experimental solutions (concentration fixed at 10×10^{-3} mol.kg⁻¹) were filtered 3-4 times through membrane filters (porosity 0.25 μ m) to remove dust particles. The values of Zeta potential have been measured 3 times for all experimental solutions and average values are taken. The values of the hydrodynamic diameter (D_h) and the Zeta potential (ζ) are recorded in Table 4.

3. Results and discussions

3.1. Critical micellar concentration (cmc)

The values of *cmc* of aqueous C₁₆MImCl solutions in absence of any added salt obtained from conductometry, tensiometry, fluorimetry and isothermal titration calorimetry at 298.15 K in the present study (Table 1) are found to be in good agreement with each other and also with the literature reports.^{17,18,63} At the other four temperatures namely, 303.15, 308.15, 313.15 and 318.15 K, the literature *cmc* values obtained from conductometry and tensiometry have been listed in Table 1(a).

3.2. Degree of counter-ion Binding (β)

Conductivity measurements can be conveniently used to quantify the fraction of counterions that binds with the ionic micelles. Indeed, the degree of counterion binding (β) can be calculated from the specific conductivity vs. concentration profiles of the surfactant solutions by using the following equation:

$$\beta = 1 - \frac{S_2}{S_1} \quad (3)$$

where S_1 and S_2 represent respectively the pre- and postmicellar slopes shown in the conductometric profiles in Fig. 2(b). The β values for the systems C₁₆MImCl-NaCl thus obtained are listed in Table 2. It has been observed that these values are found to be strongly dependent on additives and that these increase with increasing salinity (Table 2) caused by changed micelle-counterion interaction in presence of varying concentrations of the added salts.

3.3. Effect of Added Salt on the *cmc* of Aqueous C₁₆MImCl

Addition of each of the salt to C₁₆MImCl solution was found to cause a reduction in the *cmc* value from what is observed in salt-free solution. Further, the higher the amount of the added salt, the more is the reduction in the *cmc*. An interpretation of the observed decrease in the *cmc* values upon addition of a salt may be provided on the basis of a model put forward by Davis and Rideal⁶⁴, later modified by Borwankar and Wasan.⁶⁵ This model pictures the Stern layer comprising of the surfactant ions with counterions constituting the diffuse part of the electrical double layer, *i.e.*, the Guoy-Chapman layer. The added salt ions squeeze the electrical double layer and, consequently, induce the shielding of the electrostatic repulsion among the polar head groups; this results in a marked reduction in the *cmc* compared to that of the salt-free system.

Anions have been found to have pronounced influence on the *cmc* of aqueous C₁₆MImCl solutions. In particular, in presence of a given amount of an added sodium salt, the values of the *cmc* of C₁₆MImCl are found to decrease in the order: Cl⁻ > Br⁻ > PO₄³⁻ > SO₄²⁻ (*cf.* Table 1)

indicating that the ability of these ions to promote self-aggregation of C₁₆MImCl increase in the reverse order: SO₄²⁻ > PO₄³⁻ > Br⁻ > Cl⁻.

In this context, it would be interesting to examine the relevance of the “Hoffmeister Series” or the “Lyotropic Series” in the light of the effect of the salt ions on the micellization of C₁₆MImCl in aqueous solutions. The Hoffmeister or the Lyotropic series for the efficiency of the salting out effect of the anions of a lyophilic substance from a colloidal solution which is controlled by ionic hydration follows the order ²⁰: SO₄²⁻ > PO₄³⁻ > Cl⁻ > Br⁻.

A rationale for the observed trend may be sought by invoking the idea of ionic hydration. Generally, the more the hydration of the ions, the less is their efficacy to neutralize the charges on the micelle surface, and hence the less is the reduction of the *cmc* in their presence. Now, the extent of ionic hydration has been shown to decrease in the order ⁶⁶: PO₄³⁻ > SO₄²⁻ > Cl⁻ > Br⁻ and hence the *cmc* should follow the order: Br⁻ < Cl⁻ < SO₄²⁻ < PO₄³⁻, which is not in accordance with the experimental observation here.

In presence of a given concentration of the added electrolytes, the ionic strength of the solution varies in the order: PO₄³⁻ > SO₄²⁻ > Cl⁻ = Br⁻. This indicates that squeezing of the electrical double layer and consequent shielding of the electrostatic repulsion among the polar head-groups would also follow the same order. Hence the *cmc* of C₁₆MImCl should follow the order: Cl⁻ = Br⁻ > SO₄²⁻ > PO₄³⁻. This is also not in accordance with what observed experimentally.

Thus, neither the extent of hydration of the added anions nor the effect of the ionic strength of the added salt solutions could explain the observed order of the *cmc* values of aqueous C₁₆MImCl in the investigated salt solutions.

The apparent departure from the Hoffmeister series may be a consequence of basic difference between the two processes. Micelle formation is governed simultaneously by the electrostatic and hydrophobic effects, while the salting out of polymers and hydrocolloids is mainly controlled by the dehydration⁶⁷ of soluble polymers and hydrocolloids. Hence a strict adherence to this series is not expected for aqueous C₁₆MImCl in presence of different salts. Such a non-compliance of the Hoffmeister effect has also been reported earlier for other amphiphile-salt solutions.^{20, 45} Additional factors must, therefore, be identified to account for the salt effect on micellization: (a) One possible reason for the observed discrepancy may be sought in specific interaction between the added counter-anions and the micelle.⁵⁰ The effect of counterion specificity on the physical properties of micelle formation is, however, not well understood yet ⁶⁸, (b) Another factor might be the locally varying dielectric constant which has

not been taken into account in the theories of micellar solutions. The immediate neighbourhood of the micelle may exhibit a considerably different dielectric constant than the bulk water thus influencing the micelle-counterion interaction, (c) Effect of the added anions on the water structures, *i.e.*, structure-making / structure-breaking capabilities of these ions might also contribute to their relative influences on the micellization behavior in aqueous C₁₆MImCl solutions. Further studies are, therefore, required to clarify this aspect.

3.4. Effect of temperature on *cmc*

Influence of temperature on the *cmc* of aqueous C₁₆MImCl as well as C₁₆MImCl-salt solutions has been investigated in presence of two different salt concentrations, namely 0.001 and 0.005 mol·kg⁻¹ and has been demonstrated in Table 1. With the increase in temperature, the *cmc* values in aqueous C₁₆MImCl, C₁₆MImCl-NaCl, C₁₆MImCl-NaBr, and C₁₆MImCl-Na₂SO₄ solutions increase monotonically. For C₁₆MImCl-Na₃PO₄ system, on the other hand, the *cmc* is found to pass through a minimum on elevation of temperature. Literature reports on the temperature-dependence of *cmc* in other amphiphile solutions without or with a minimum are also available.^{16,39,45} An explanation may be sought in the differential effect of temperature on the dehydration of the polar head and the apolar tail of the amphiphile which contributes differently to the variation of *cmc* with temperature. There are two opposite factors contributing^{16,39,45} to this anomaly in the *cmc* trends: (a) the desolvation of water molecules from surfactant hydrophilic groups at lower temperature, leading to earlier micellization, (b) the breakdown of water structure from the surfactant hydrophobic tails, which is unfavourable in the process of micellization at higher temperature.

For aqueous C₁₆MImCl as well as for C₁₆MImCl-NaCl, C₁₆MImCl-NaBr, and C₁₆MImCl-Na₂SO₄ systems, the results indicate that the latter effect (dehydration of hydrophobic tail) predominates within the investigated temperature range, and the *cmc* values of these systems increase with temperature. It can, however, be hypothesized that a minimum could possibly occur at some temperature below 298.15 K where the former effect (dehydration of imidazolium head groups) is expected to be decisive. For C₁₆MImCl-Na₃PO₄ system, however, below 303.15 K, the former effect takes the leading role, while beyond this critical temperature the latter effect controls the aggregation process of C₁₆MImCl in presence of Na₃PO₄.

3.5. Thermodynamics of micellization

Standard free energy of micellization ΔG_m^0 can be calculated using the following equation based on the mass action model of micellization¹⁰:

$$\Delta G_m^0 = RT(1 + \beta) \ln x_{cmc} \quad (4)$$

where, x_{cmc} is the *cmc* expressed in terms of mole fraction. The parameter β in the above expression refers to the fraction of free energy required to condense the counter ions onto the monomer head groups during the process of micellization to reduce the repulsion.

The corresponding standard enthalpy of micellization (ΔH_m^0) can be obtained from the following equation:

$$\Delta H_m^0 = -RT^2 \left[(1 + \beta) \left(\frac{\partial \ln x_{cmc}}{\partial T} \right)_P - \ln x_{cmc} \left(\frac{\partial \beta}{\partial T} \right)_P \right] \quad (5)$$

When the β values do not vary appreciably with temperature, Eq. (5), as a first approximation, reduces to

$$\Delta H_m^0 = -RT^2 \left[(1 + \beta) \left(\frac{\partial \ln x_{cmc}}{\partial T} \right)_P \right] \quad (6)$$

The values of $(\partial \ln x_{cmc} / \partial T)_P$ were obtained from the slopes of the second order polynomial fitting of $\ln x_{cmc}$ vs. T profiles (shown in Fig. S1, supplementary section). The standard entropy of micellization (ΔS_m^0) can then be calculated using the following Gibbs-Helmholtz equation:

$$\Delta G_m^0 = \Delta H_m^0 - T \Delta S_m^0 \quad (7)$$

The ΔG_m^0 , ΔH_m^0 and ΔS_m^0 values for the micellization of aqueous C₁₆MImCl solutions in presence of all the salts investigated are shown in Table 2 and Fig. 6. ΔH_m^0 values for the micellization of C₁₆MImCl are always found to be relatively more negative in presence of the added salts than those in salt-free aqueous solution.⁶³ ΔH_m^0 values calculated from Eq. 6 are always found to be negative in presence of two different concentrations (0.001 and 0.005 mol·kg⁻¹) of all the added salts (Table 1) indicating an exothermic nature of micellization prevailing in these systems. Further, micellization processes become more exothermic in the higher temperature region or in presence of higher salt concentration. The relatively larger negative ΔH_m^0 values found for 0.005 mol·kg⁻¹ Na₂SO₄ (cf. Table 2) as a function of temperature as compared to the other salt solutions is probably due to the estimation of ΔH_m^0 using Eq. (5), as the β values are significantly temperature-dependent in this system (cf. Table 3). There are two factors which might contribute to the enthalpy of micellization and its variation with temperature^{16,69}: (a) a positive contribution is attributed to the release of water molecules from hydration layer around the hydrophilic heads and the hydrophobic tails of the amphiphile molecules due to breakdown of the electrostatic attraction of counterions with coions, and secondly, (b) transfer of the hydrophobic tails from aqueous phase to the micellar core and regenerate the H-bonding of water molecules around the micelles leading to negative contribution to ΔH_m^0 . As the temperature increases, the first factor becomes less prominent as the degree of H-bonding around the surfactant monomers diminishes at higher

temperatures. ΔH_m^0 values did not exhibit any specific trend with respect to the added anions except in the high temperature region, where negative ΔH_m^0 increases in the order: $\text{Cl}^- < \text{Br}^- < \text{SO}_4^{2-} < \text{PO}_4^{3-}$. Micellization of $\text{C}_{16}\text{MImCl}$ is more exothermic in presence of Br^- than in presence of Cl^- at the salt concentration of $0.001 \text{ mol}\cdot\text{kg}^{-1}$ throughout the entire investigated temperatures, whereas an opposite trend is observed when added salt concentration is $0.005 \text{ mol}\cdot\text{kg}^{-1}$ upto 313.15 K (*cf.* Table 2, Fig. 6). From Fig. 6(b), it is evident that, ΔH_m^0 values show a sharp decline ranging from positive to negative values when the micellization is studied at $0.005 \text{ mol}\cdot\text{kg}^{-1}$ NaBr compared to its lower concentration. A relatively larger contribution in terms of negative ΔH_m^0 values has been observed in presence of PO_4^{3-} at higher temperatures, whereas ΔH_m^0 values remained almost invariant with temperature in presence of for both salt concentrations investigated (*cf.* Figs. 6 (a) and 6(b)). The ΔH_m^0 values in presence of SO_4^{2-} are found to be intermediate between those in presence of Cl^- and PO_4^{3-} (*cf.* Fig.6 (a)). Table 2 demonstrates that the entropy of micellization (ΔS_m^0) is in the majority of cases are positive, and that ΔS_m^0 decreases as the temperature increases. Aqueous $\text{C}_{16}\text{MImCl-Na}_3\text{PO}_4$ solutions exhibit both positive and negative entropy values, with the negative values found at high temperature (*cf.* Table 2). The positive ΔS_m^0 values may be attributed⁴² to the breakdown of the ice-berg structure due to removal of hydrophobic tail to the micellar core, and to the increase of the degrees of rotational freedom of the hydrophobic tails inside the core. The negative ΔS_m^0 values could have arisen from the restoration of water structure around the amphiphile, and this effect becomes more important than the above two effects at elevated temperatures. The ΔG_m^0 values are found to be more negative in presence of electrolytes than those observed in aqueous solutions⁶³ indicating greater spontaneity of micellization in presence of salts with a concomitant reduction in the *cmc*s values (*cf.* Table 2). Improved spontaneity of micellization has also been observed as the salinity of the solutions increases except for $\text{C}_{16}\text{MImCl-Na}_2\text{SO}_4$ systems in the low temperature regions. The ΔG_m^0 values in $\text{C}_{16}\text{MImCl-salt}$ solutions are found to be slightly dependent on temperature ($\text{C}_{16}\text{MImCl-Na}_2\text{SO}_4$ system is an exception) (Table 2, Figs. 6(a)-(b)) probably due to close compensation of $T\Delta S_m^0$ and ΔH_m^0 values. A comparison of the ΔH_m^0 and $T\Delta S_m^0$ values for $\text{C}_{16}\text{MImCl-salt}$ systems indicates that the micellization process is entropy-driven in presence of $0.001 \text{ mol}\cdot\text{kg}^{-1}$ NaCl throughout the entire range of temperature, while enthalpy takes the lead in micelle formation in presence of $0.001 \text{ mol}\cdot\text{kg}^{-1}$ NaBr (*cf.* Table 2). In presence of $0.005 \text{ mol}\cdot\text{kg}^{-1}$ NaCl or NaBr, the micellization is, however, enthalpy driven at the higher temperatures. Similar behavior has also been observed for $0.001 \text{ mol}\cdot\text{kg}^{-1}$ Na_2SO_4 as well as for all concentrations of

Na₃PO₄, where the trivalent additive enhances the enthalpy contribution over entropy contribution significantly (*cf.* Table 2) at higher temperatures during micellization. Finally, it can be stated that, in this present work micellization of C₁₆MImCl is enthalpy driven at higher temperature, whereas the entropy play significant role at lower temperature, in presence of the investigated salts. Such observation underscoring the importance of both hydrophobic and electrostatic interactions during micellization in presence of added salts has also been reported earlier.³¹

An empirical equation often used^{43,44,62,70} for correlating ΔH_m^0 and ΔS_m^0 to determine the compensation temperature (T_{com}) describing the dehydration of hydrophobic part of surfactants,

$$\Delta H_m^0 = \Delta H_m^{0*} + T_{com}\Delta S_m^0 \quad (8)$$

here ΔH_m^{0*} , intrinsic enthalpy gain, reflects the solute-solute interaction and it has been described as chemical part for micelle formation in terms of association of the hydrophobic part to the micellar core.^{43,44,62,70} T_{com} values have been calculated for C₁₆MImCl in presence of different concentration of electrolytes using ΔH_m^0 vs. ΔS_m^0 profile (Fig.S2, in the supplementary section), and are summarized in Table 2. The quality fit has always been excellent, the squares of the correlation coefficients lying between 0.98 and 0.99. The compensation temperature for the micellization of aqueous C₁₆MeImCl has been reported to be 280 K.⁶³ For the micellization of aqueous C₁₆MImCl in presence of the electrolytes investigated here, the compensation temperatures are found to be between 270 and 301 K. It has been suggested earlier that the T_{com} value in aqueous solution is expected to lie between 270 and 294 K for processes dominated by hydration.⁷¹ The observed values of T_{com} are, therefore, very close to these values. However, relatively low T_{com} value observed in presence of 0.001 mol·kg⁻¹ NaBr (223 K) might be due to the difference of the bulk structural property of the solution from that of the water in this particular system. It is, however, worth mentioning that the linearity of the ΔH_m^0 vs. ΔS_m^0 plots should not be over-interpreted⁷², though this linearity is observed quite frequently.

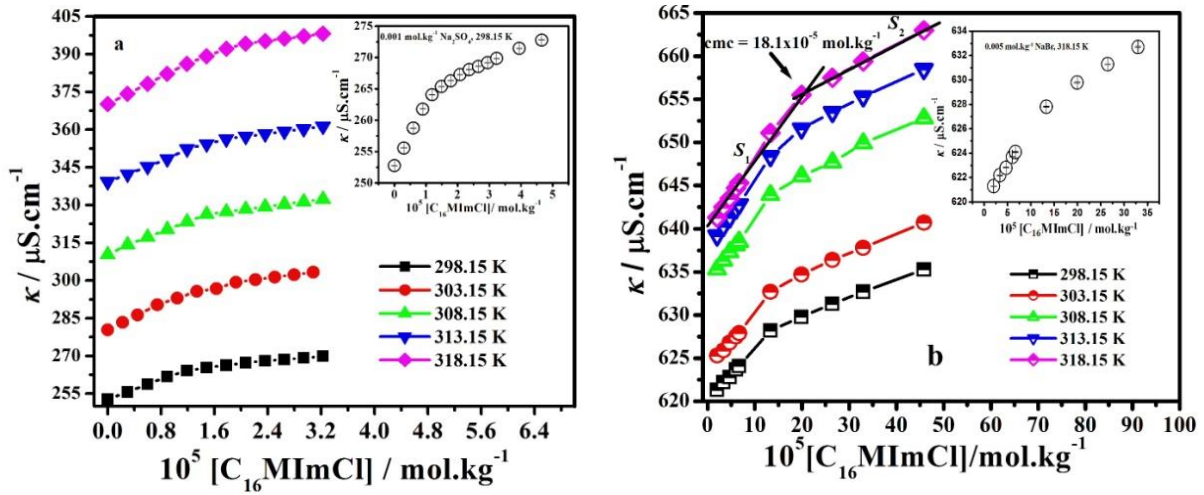


Fig. 2. Specific conductance (κ) vs. concentration of $C_{16}MImCl$ in presence of (a) $0.001 \text{ mol.kg}^{-1} \text{ Na}_2\text{SO}_4$, and (b) $0.005 \text{ mol.kg}^{-1} \text{ NaBr}$ at five different temperatures. Error bars are given at the inset.

3.6. Interfacial properties for the micellization of $C_{16}MeImCl$ in presence of salts

The excess surface concentration (Γ_{max}) and the minimum area per surfactant molecules (A_{min}) at the air/water interface have been obtained using the Gibbs adsorption equation^{63,73}:

$$\Gamma_{max} = - \frac{1}{2.303iRT} \lim_{c \rightarrow cmc} \left(\frac{\partial \gamma}{\partial \log c} \right) \quad (9)$$

$$A_{min} = \frac{10^{18}}{N_A \Gamma_{max}} \quad (10)$$

where, i is the number of species per surfactant monomer, R the universal gas constant, N_A the Avogadro number, $(\partial \gamma / \partial \log c)$ is the slope of tensiometric isotherm (cf. Fig. 3) at cmc , and, T the temperature in Kelvin scale. The values of n have been calculated for the surfactant-salt solutions using the equation put forward by Matijevic and Pethica [74]: $i = 1 + cmc / (cmc + m_e)$, where, m_e is the concentration of electrolytes in molality unit. The Γ_{max} and A_{min} values computed through Eqs. (9) and (10) have been recorded in Table 3. The Γ_{max} values of $C_{16}MImCl$ in aqueous solution have been found to be 2.04 at 298.15K.⁶³ The variations of Γ_{max} of $C_{16}MImCl$ in presence of different salts have not always been found to be regular with the molality of the surfactant, revealing sometimes a minimum (Fig. S3 in the supplementary section). Such phenomenon has also been observed for the micellization of CTAB in presence of NaBr at low salt concentration.⁷⁵ The calculated Γ_{max} values of $C_{16}MImCl$ in presence of different concentrations of NaBr have been found to be greater than that of aqueous solution, while addition of NaCl reveals an opposite trend beyond $0.001 \text{ mol.kg}^{-1}$. The reduction of Γ_{max} in presence of higher amount of added NaCl may be attributed to an enhanced repulsion among

the Cl⁻ ions at the interface³³ thus disfavoring the charge neutralization of C₁₆MIm⁺. On the other hand, greater charge neutralization of C₁₆MIm⁺ ions facilitated by the Br⁻ ions leads to larger adsorption of imidazolium head groups with concomitant decrease in A_{min} . Two opposing effects have been believed to operate³³ at the air/water interface with increasing ionic strength of the medium: i) electrostatic charge neutralization of surfactants at the interface and compression of the double layer leading to larger adsorption, and ii) van der Waals repulsion of surfactant tails and electrostatic repulsion of surfactant head groups due to incomplete charge neutralization, which slow down the adsorption process. The present observations indicate that when the concentration of added NaCl is low, the second factor predominates, whereas at high concentration of NaCl the first factor controls the adsorption process. The divalent SO₄²⁻ ions can easily neutralize the C₁₆MIm⁺ ions at the interface at relatively low concentration (0.001 mol.kg⁻¹) and its Γ_{max} value is larger than that in presence of NaBr of identical salinity. PO₄³⁻ ions show the same behavior as do the Cl⁻ ions (shown in Fig. S3, supplementary section) despite its trivalent character. Higher hydrophobicity of the two larger added anions (over the entire concentration range of PO₄³⁻ ions, and within a relatively moderate concentration range of SO₄²⁻ ions) keeps them apart from the interface with significant lowering of the adsorption of C₁₆MIm⁺ ions leading to a low Γ_{max} and a high A_{min} .

The geometrical shape of micelles formed in surfactant solutions can be conveniently predicted by a parameter, known as the packing parameter (P), defined by Israelachvili as [76]

$$P = \frac{v}{l_c A} \quad (11)$$

where v is the volume of the hydrophobic hydrocarbon chain assuming it to be fluid and incompressible, l_c the maximum effective length of that chain, and A the surface area of the surfactant monomer head-group. The values of l_c (in nm) and v (in nm³) of a saturated hydrocarbon chain bearing C_n number of carbon atoms have been calculated using the Tanford formulas with the following equations⁷⁷

$$l_c = (0.154 + 0.1265C_n) \quad (12)$$

$$v = (0.0274 + 0.0269C_n) \quad (13)$$

The exact determination of head group area (A) on the micellar surface is quite difficult.⁷⁸ We have, therefore, used A_{min} values (obtained from tensiometry) instead of A in Eq. 11 as suggested in the literature.^{78,79} P values, thus obtained are listed in Table 3. For spherical micelles, $P \leq 0.333$; for nonspherical shape, $0.333 < P < 0.5$; for vesicles and bilayers, $0.5 < P < 1$; and for inverted structures, $P > 1$. From Table 3, it is evident that C₁₆MImCl forms spherical micellar aggregates in presence of varying concentrations of NaCl, NaBr, Na₂SO₄ and Na₃PO₄

investigated here, except in presence of 0.02 mol.kg^{-1} NaBr. Although the predictions made here is solely based on the validity of the Israelachvili model ⁷⁶, a plausible molecular rationale of which could be provided. We may infer that the strong binding tendency of Br^- ion could convert the spherical micelles of $\text{C}_{16}\text{Mim}^+$ ions into rod-like micelles in presence of the highest amount of added NaBr. Compared with Br^- ions, other added ions are more highly hydrated ⁶⁶, and thus are less effective in penetrating and shielding the charge of the surfactant aggregates. Efficient shielding of the charge on the aggregates in presence of 0.02 mol.kg^{-1} NaBr by reducing the electrostatic repulsion among the ionic charges on micelles results in a larger reduction of the ionic head-group area, and hence an increase in the P value beyond 0.33. That is, only the least hydrated Br^- ion when present in a large amount can bind the cationic micelle to an amount large enough to stabilize a rod-like micelle. Such salt-induced transition of the shape of ionic micelles has also been observed earlier.⁸⁰⁻⁸² However, scattering experiments would be useful to provide a direct proof which, at present, is not possible for the lack of facility. We contemplate to take up the matter in a future occasion.

The efficiency of interfacial adsorption of any given amphiphile solution can be conveniently expressed by a parameter pC_{20} defined as

$$pC_{20} = -\log C_{20} \quad (14)$$

where C_{20} is the concentration of the amphiphile which reduces the surface tension of the solution by $20 \text{ mN}\cdot\text{m}^{-1}$. The pC_{20} values for aqueous $\text{C}_{16}\text{MimCl}$ solutions in absence and in the presence of different salt solutions are listed in Table 3. A higher pC_{20} value is indicative of a higher adsorption efficiency of the surfactant at the interface and more efficiency in reducing the surface tension. The results indicate that addition of salt to aqueous $\text{C}_{16}\text{MimCl}$ solutions leads to a reduction in the adsorption efficiency of the surfactant.

The surface pressure at the cmc (π_{cmc}) was calculated using the following equation

$$\pi_{cmc} = \gamma_0 - \gamma_{cmc} \quad (15)$$

where γ_0 and γ_{cmc} are the surface tension of pure solvent and that for the pure and mixed surfactants at their cmc respectively. The π_{cmc} values for aqueous $\text{C}_{16}\text{MimCl}$ solutions in absence and in the presence of different salt solutions are recorded in Table 3. This parameter indicates the maximum reduction of surface tension caused by the dissolution of surfactant molecules and hence becomes a measure for the effectiveness of the surfactant to lower the surface tension of the solvent medium. Addition of the investigated salts to the aqueous $\text{C}_{16}\text{MimCl}$ solutions caused an enhancement of the effectiveness of the surfactant in reducing the surface tension compared to the salt-free solutions.

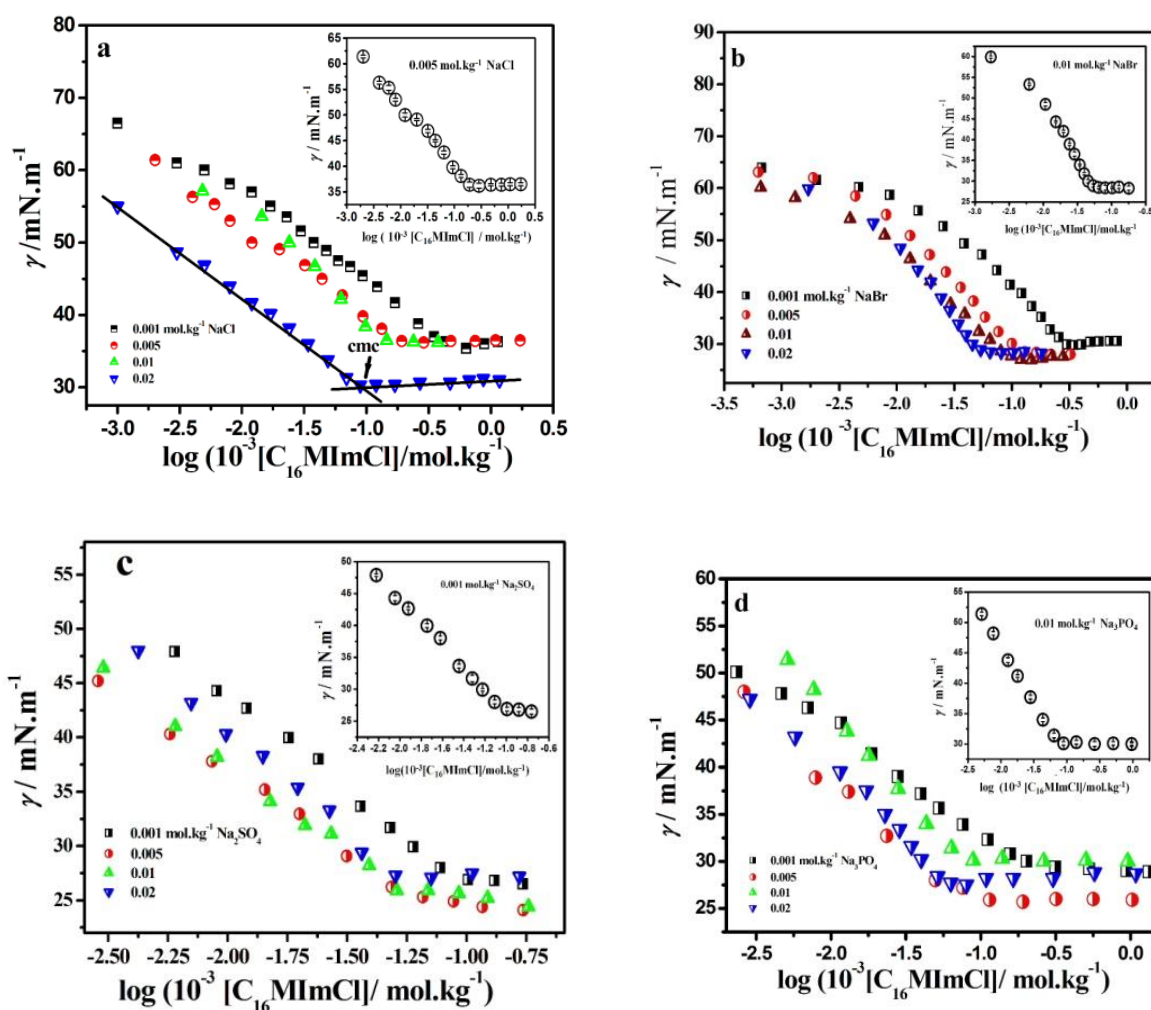


Fig. 3. Tensiometric isotherms of aqueous $C_{16}MImCl$ in presence of (a) $NaCl$, (b) $NaBr$, (c) Na_2SO_4 , and (d) Na_3PO_4 . The error bars are shown in the inset in each case.

3.7. Isothermal titration calorimetry (ITC)

All cmc values and ΔH_m^0 values (within the brackets) measured by ITC at 298.15 K for the micellization of $C_{16}MImCl$ in presence of different salts are listed in Table 2. Calorimetric titration curves along with the heat-flow results for aqueous $C_{16}MImCl$ in absence and in presence of salts at different concentrations have been shown in Fig. 4

Profiles showing the variation of the standard enthalpies of dilution (ΔH_{dil}^0) per mole of surfactant added per injection with the concentration of the $C_{16}MImCl$ reveal three distinct regions¹⁷: one in the premicellar region (I), where dilution of surfactant solution (having

concentration ≈ 10 times the *cmc* as mentioned in experimental section), leads to micellar break up into monomers; another in the post micellar region (III), where dilution of both the micelles and free monomers takes place; and one in the middle (II) between the above two regions, where a sharp decrease occurs in the enthalpogram due to the dissociation of a fraction of micelles into free monomers. In particular, these plots are more or less “sigmoidal” in nature and the inflection point in the intermediate region of these enthalpograms provides a measure of the *cmc*.^{10, 17, 52, 58-61} The *cmc* values have, however, been more precisely determined from the optimum of the plot of the first derivative of the enthalpy change as a function of the surfactant concentration.⁶⁰ In presence of salts both exo and endothermic processes were obtained for the micellization of C₁₆MeImCl. In presence of investigated salts, the enthalpograms shown initial increase or decrease in their pattern, and finally become almost constant at high surfactant concentration (*cf.* Fig. 4). The *cmc* values thus obtained agree well with the *cmcs* calculated by other methods, *i.e.*, conductometry, tensiometry and steady state anisotropy techniques. For salt-containing surfactant solutions, these two regions can be identified as the pre- and postmicellar regions respectively.

The intersection of the vertical line passing through the *cmc* and the premicellar line is the initial enthalpy of dilution [ΔH_{dil}^0 (initial)] while that of this vertical line with the postmicellar line provides a measure of the final enthalpy of dilution [ΔH_{dil}^0 (final)] as shown in Fig. 4. For some investigated systems (0.01 mol.kg⁻¹ NaBr, 0.001 mol.kg⁻¹ Na₂SO₄, and 0.005 mol.kg⁻¹ Na₂SO₄), however, the initial enthalpy of micellization was considered to be equal to the heat of the first injection assuming complete demicellization as suggested by Anderson et al. and Chadha et. al.⁸³⁻⁸⁴ The heat change due to micellization (ΔH_{obs}^0) is then given by the difference between ΔH_{dil}^0 (initial) and ΔH_{dil}^0 (final) values.

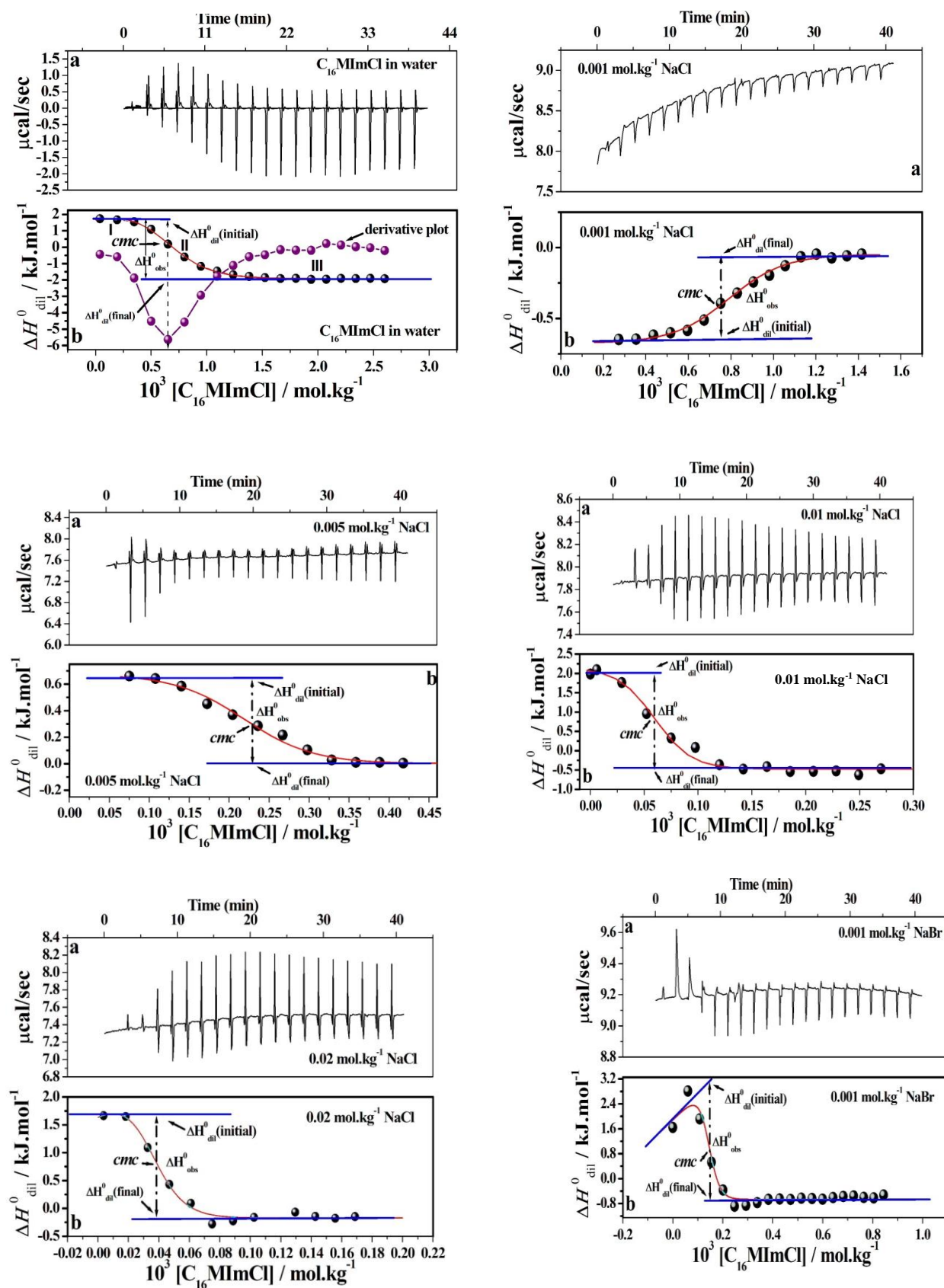
In some of the cases the data obtained here did not represent a plateau in the premicellar region, rather a linear variation of ΔH_{dil}^0 as a function of surfactant concentration with a definite slope was observed. Similar behavior has also been reported earlier for other surfactant solutions.^{58, 59, 85-89} Further, for some solutions the enthalpy values at high concentrations have been found to reach a plateau below zero. These results are in accordance with what observed earlier^{10, 52} where for some surface active ionic liquids at high concentrations the enthalpy values have been reported to reach a plateau well above ($\sim +2.5$ kJ.mol⁻¹) or below (~ -2.0 kJ.mol⁻¹) zero *instead of tending to zero*.

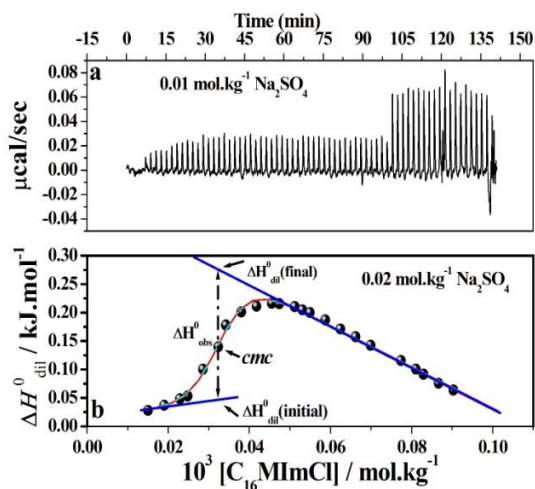
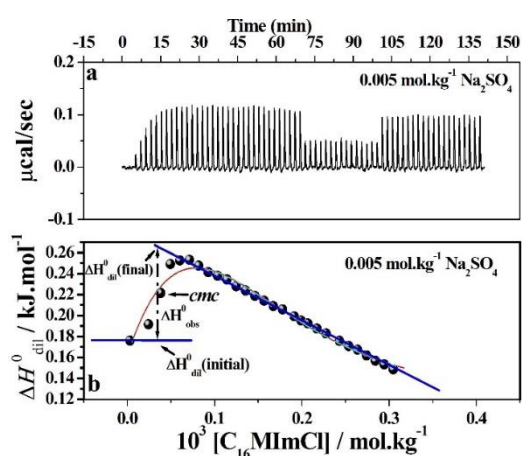
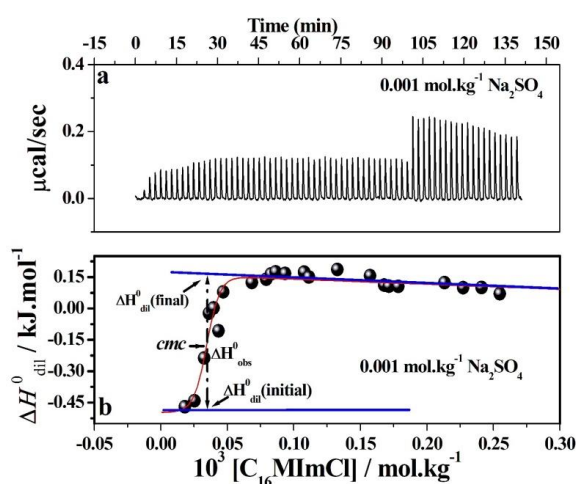
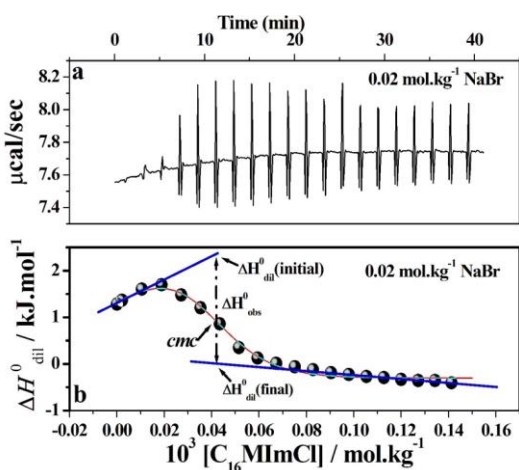
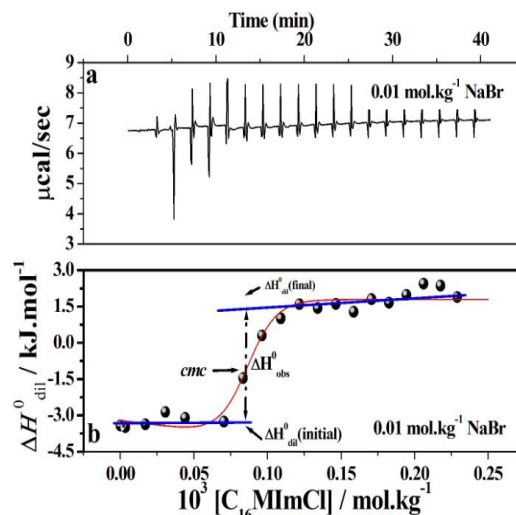
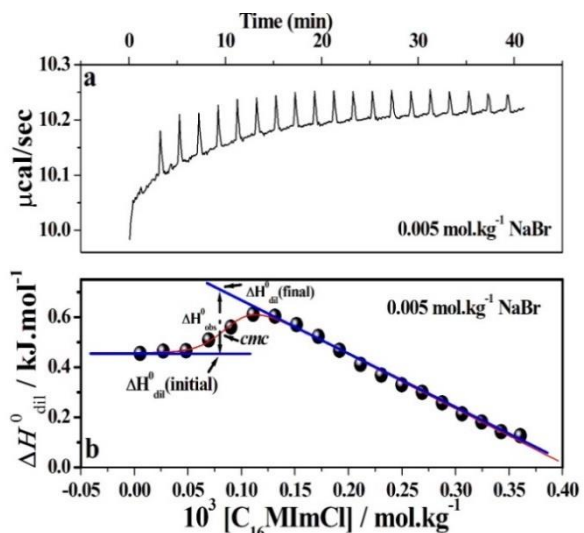
The enthalpies of micellization (ΔH_{m}^0) can be obtained from the following empirical equation^{52, 60},

$$\Delta H_m^0 = \frac{\Delta H_{\text{obs}}^0 c_T}{c_T - cmc} \quad (17)$$

where c_T is the initial concentration of stock surfactant solution. Micellization of $C_{16}\text{MImCl}$ in aqueous solution is exothermic ($\Delta H_m^0 = -3.34 \text{ kJ}\cdot\text{mol}^{-1}$) and the cmc has been found to be $0.70 \times 10^{-3} \text{ mol}\cdot\text{kg}^{-1}$ at 298.15 K. Seoud *et al.*¹⁷ also investigated the micellization of $C_{16}\text{MImCl}$ and they found a ΔH_m^0 value of $-2.75 \text{ kJ}\cdot\text{mol}^{-1}$ and a cmc of $0.99 \times 10^{-3} \text{ mol}\cdot\text{L}^{-1}$. Thus, there is a good agreement between the values obtained in this study and those reported earlier. Addition of salts greatly influences the thermodynamics of the micellization of $C_{16}\text{MImCl}$ (*cf.* Fig. 5, Table 2). In presence of $0.001 \text{ mol}\cdot\text{kg}^{-1}$ NaCl, micellization is found to be endothermic ($\Delta H_m^0 = +0.56 \text{ kJ}\cdot\text{mol}^{-1}$), while for higher salinity it becomes exothermic, the enthalpy of micellization reaching a plateau within the limits of experimental error (*cf.* Fig. 5). On the other hand, in presence of the lowest amount of added NaBr, micellization is exothermic ($\Delta H_m^0 = -3.65 \text{ kJ}\cdot\text{mol}^{-1}$) which then becomes endothermic and passes through a maximum ($+4.16 \text{ kJ}\cdot\text{mol}^{-1}$) at $0.01 \text{ mol}\cdot\text{kg}^{-1}$ (Fig. 5). Luczak *et al.*⁵² also observed both positive and negative enthalpy changes during while studying the micellization of 1-decyl-3-methylimidazolium chloride in presence of KBr at 298.15K. Micellization of $C_{16}\text{MImCl}$ both in presence of Na_2SO_4 and Na_3PO_4 shows overall endothermicity at all electrolyte concentrations, the process being more endothermic in presence of Na_3PO_4 . Enthalpy of micellization, as discussed in section 3.1, can be enlightened by two compromising factors. It is known that a cavity needs to be formed within the water structure to accommodate the micellar aggregate, and the addition of kosmotropes strengthens the water structure⁵². So, more energy is required to break the water structure in presence of the added kosmotropes compared to the kosmotrope-free situation, and consequently positive contribution to enthalpy factor increases and hence micellization becomes less exothermic in presence of these kosmotropes. Na_2SO_4 and Na_3PO_4 being the higher order kosmotropes produce greater endothermicity than the other two salts (NaCl and NaBr) except an unusual observation in presence of $0.01 \text{ mol}\cdot\text{kg}^{-1}$ NaBr. Due to the higher charge to radius ratio of hydrated Br^- ion compared to that of the Cl^- ion, Br^- ions easily replace Cl^- ions from the Stern layer of micelle³³ due to electrostatic reason and bind more easily with $C_{16}\text{MIm}^+$. The relatively large crowding of Br^- ions in the Stern layer when NaBr concentration is sufficiently high might progressively destabilize the micelle, and contribute less to negative enthalpy. Beyond a threshold concentration ($0.01 \text{ mol}\cdot\text{kg}^{-1}$) of Br^- ion, to gain stability, some Cl^- ions might diffuse into the Stern layer, and finally micellization becomes exothermic (Fig.5) at $0.02 \text{ mol}\cdot\text{kg}^{-1}$ salt concentration. ΔH_m^0 values obtained by ITC measurements, however, deviate from those (van't

Hoff enthalpies) obtained from the mass action model (*cf.* Section 3.1), though the relative trends are the same (*cf.* Table 2). Similar observations have also been reported earlier⁴⁵.





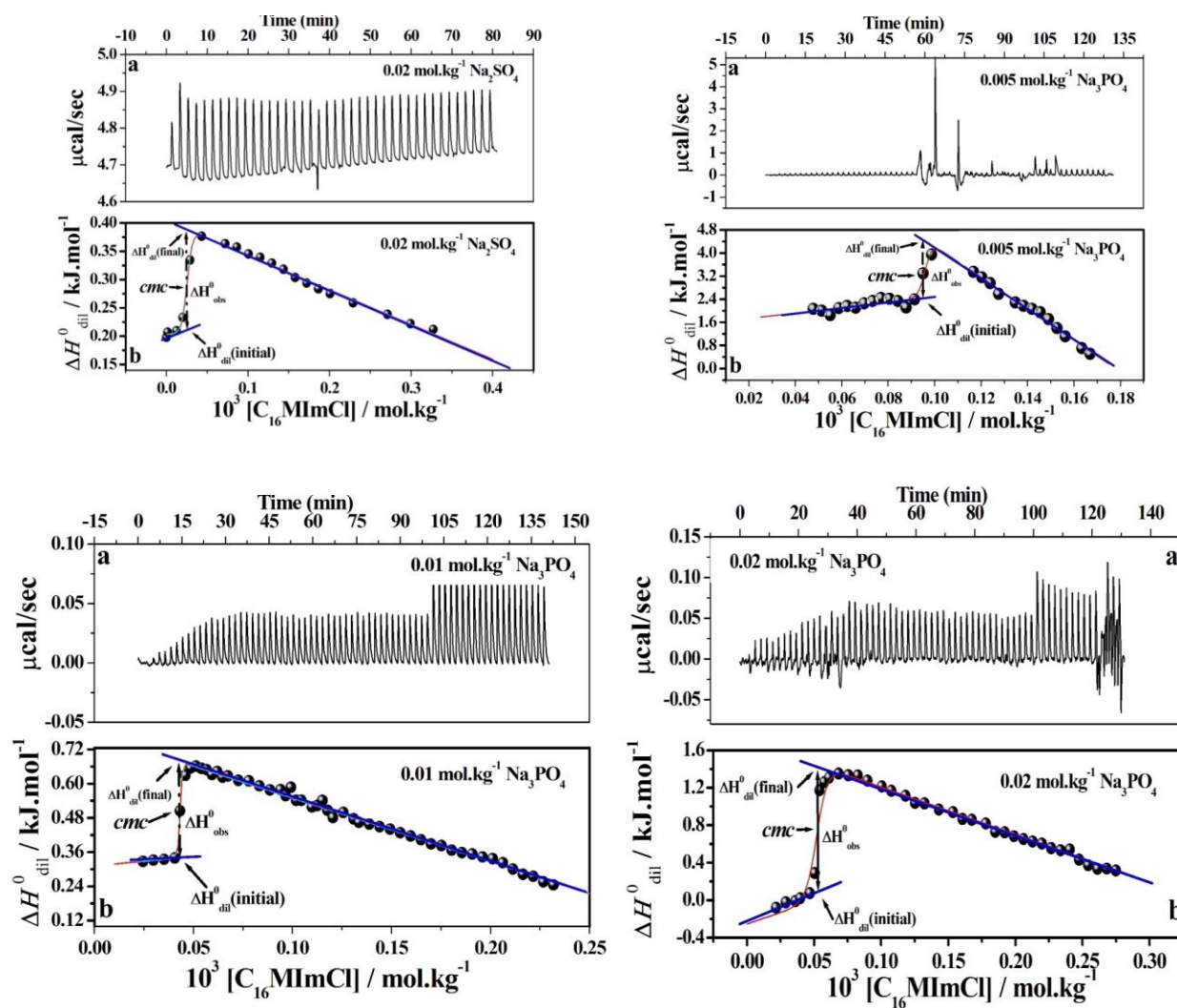


Fig. 4. Calorimetric titration curves of $C_{16}MImCl$ in water and in presence of different salts with four different concentrations (0.001 , 0.005 , 0.01 and 0.02 mol.kg^{-1}). (For each plot: top row (a): raw calorimetric traces (heat flow vs. time), bottom row (b): integration of peaks with thermodynamic parameters).

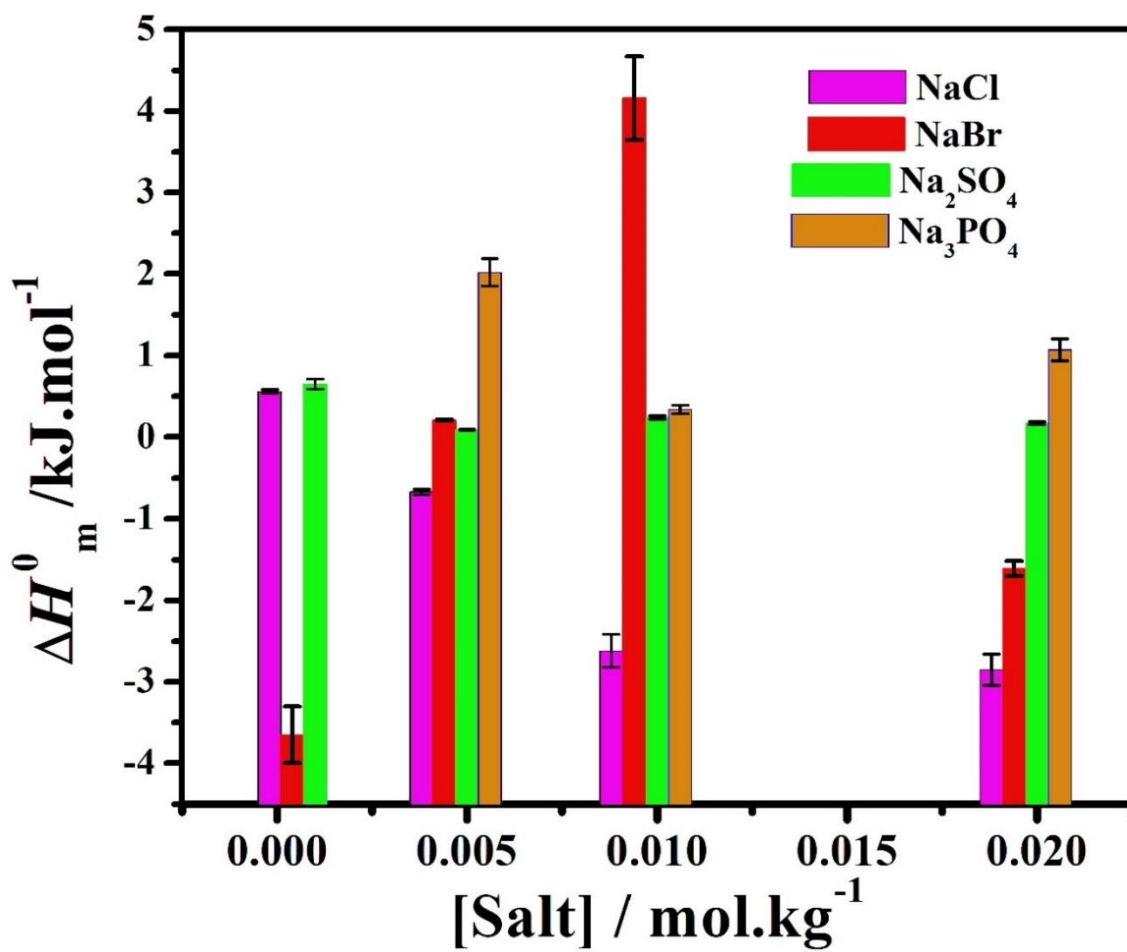


Fig. 5. Variation of calorimetric enthalpies (ΔH_m^0) in different C₁₆MImCl-salt solutions as a function of salt concentrations at 298.15K. Error bars are given for each

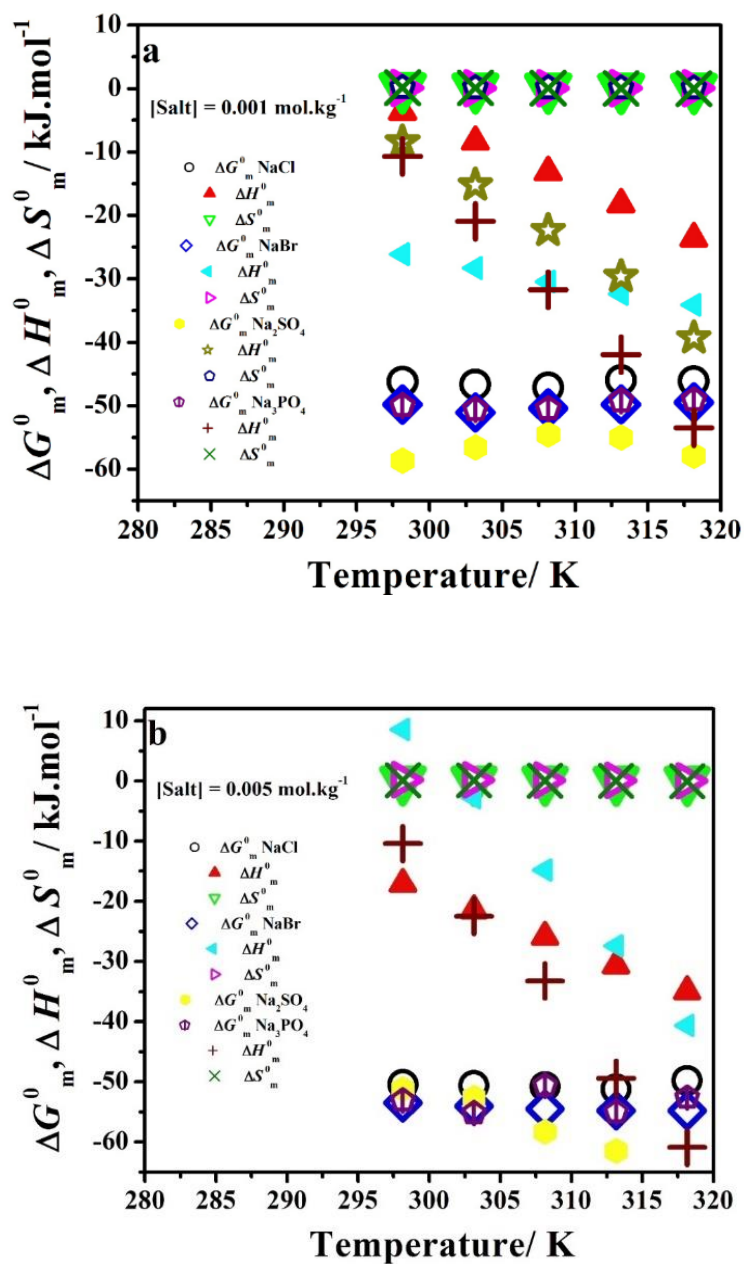


Fig. 6. Thermodynamic parameters derived from mass action model using conductometry at different temperatures for the micellization of C₁₆MImCl in the presence of two different concentrations of the added salts: (a) 0.001 mol.kg⁻¹, and (b) 0.005 mol.kg⁻¹

3.8. Steady state anisotropy(r), steady state and time resolved fluorescence quenching: cmc s, micropolarity (I_1/I_3), life time (τ), Stern-Volmer quenching constant (K_{SV}), and, aggregation number (N_a)

Fig.7(a) displays the steady state anisotropy (r) values as a function of surfactant molality (m) in presence of the four different salts each having a concentration of $0.001 \text{ mol.kg}^{-1}$. The plots show the similar trend: with the addition of surfactant, r values decrease gradually and finally reach a plateau beyond a certain inflection point [54]. The intersection of the two linear profiles above and below that inflection has been identified as the cmc (Fig.7 (a)). The solubility of DPH in water as well as in salt solutions is very low. Hence, prior to the addition of surfactant, DPH molecules remain self-aggregated^{53,54} impeding their rotational movement which results in a high value of anisotropy. Now, initial addition of surfactant to DPH solutions causes dissolution of the probe molecules leading to a gradual reduction in the anisotropy values. After commencement of surfactant aggregation, DPH molecules enters the hydrophobic micellar core of lower microviscosity^{53,54}, and after that anisotropy remains invariant with added surfactant concentration. The cmc values obtained from anisotropy measurements agree well with those calculated from conductometric and tensiometric methods (*cf.* Table 1).

The ratio of intensity of the first vibrational peak to that of the third of pyrene (I_1/I_3) has been widely used to determine the solvent polarity of pyrene environment^{46,90,91}. The ratio is 1.87 in water and 0.58 in cyclohexane⁹². The polarity of the pyrene environment increases as the I_1/I_3 ratio increases. Micropolarity (I_1/I_3) in the micellar region, which is an indicator of the feasibility of micellization, has been plotted as a function of the concentration of the added salts for all $C_{16}MeImCl$ -salt solutions in Fig. 7(b). Pyrene usually gets solubilized near the palisade layer of the micelle accompanied with some water molecules, and micropolarity senses the water penetration in this layer^{46,93}. From Fig.7(b), it is clear that with the increase in salt concentration, micropolarity in the micellar region decreases within the error range, and the ratio I_1/I_3 changes marginally in the second or third decimal place (*cf.* Table 4).The change in the value of I_1/I_3 with increasing salt concentrations in presence of Na_2SO_4 and Na_3PO_4 is, however, found to be relatively higher indicating that micellization of $C_{16}MImCl$ becomes more feasible in presence of these salts the more their concentrations.

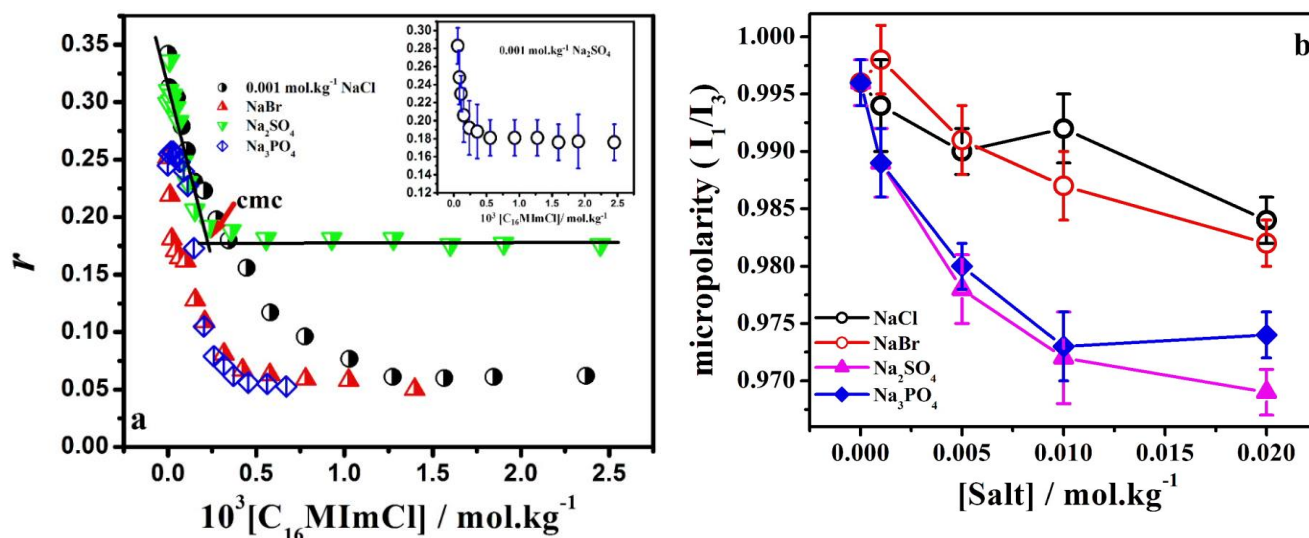


Fig. 7. (a) Steady state fluorescence anisotropy (r) vs. concentration of $C_{16}MImCl$ in presence of different salts (each with a concentration of $0.001 \text{ mol.kg}^{-1}$) at 298.15 K . Error bars are shown for the $C_{16}MImCl$ - Na_2SO_4 system. (b) A comparative plot of micropolarity (I_1/I_3) of micelle (surfactant concentration: $10 \times 10^{-3} \text{ mol.kg}^{-1}$) solubilized pyrene environment vs. concentration of added salts. Error bars are shown.

The fluorescence probe, pyrene, has a lower fluorescence life time than the residence time of CPC (an immobile quencher)⁹³. Under these circumstances, the equation based on the proposed kinetic model of Gratzel and Tachiya^{94,95} can be transformed into the following form^{46, 55-57, 96, 97}

$$I(t) = I(0) \exp \left[-\frac{t}{\tau_0} - n \{ 1 - \exp(-k_q t) \} \right] \quad (18)$$

where $I(t)$ and $I(0)$ are the fluorescence intensities of pyrene at time t and zero respectively; τ_0 and τ are the pyrene life times in the micellar atmosphere in the absence and in presence of CPC respectively, and τ is defined as the reciprocal of the intramolecular first order quenching rate constant (k_q) with one quencher molecule in or on the micelle. In Eq. (18), n is the ratio of the molal concentration of the quencher $[Q]$ added to the surfactant solution to that of the micelle, and is given by

$$n = N_a \frac{[Q]}{[S] - cmc} \quad (19)$$

where N_a is the aggregation number determined from time resolved fluorescence quenching (TRFQ) method, $[S]$ and cmc are the initial surfactant concentration (here, $12 \times 10^{-3} \text{ mol.kg}^{-1}$) and corresponding cmc (the average values of $cmcs$ from Table 1 were used for the determination of N_a). The values of n have been obtained from a fitting of the Eq.19 by

nonlinear least squares method (χ^2 test) for each quencher concentration in presence of different salt solutions with the help of IBH DAS-6 decay analysis software stated in the experimental procedure (section 2.2.3). The values of n have been kept here within 2 for theoretical consideration⁹⁸ and have been taken the average for all quencher concentration in each set of salts.

Aggregation number (N_D) has also been calculated from the steady state fluorescence quenching (SSFQ) measurements, assuming static quenching of probe in the micellar medium with the following equation^{18, 99-103}:

$$\ln \frac{F_0}{F} = \frac{[Q]N_D}{[S]-cmc} \quad (20)$$

where F_0 and F are the fluorescence intensities of pyrene in absence and in the presence of CPC, respectively. Other terms in Eq. 20 have their usual significance, as already discussed above.

Stern-Volmer equation can be used to determine the equilibrium bimolecular quenching constant (K_{SV}) of pyrene by CPC which in case of static quenching takes the following form¹⁰⁴:

$$\frac{F_0}{F} = 1 + K_{SV}[Q] \quad (21)$$

In case of dynamic quenching Eq. (20) may be written as¹⁰⁵

$$\frac{\tau_0}{\langle\tau\rangle} = 1 + K_{SV}[Q] = 1 + k_q\tau_0[Q] \quad (22)$$

where $\langle\tau\rangle$ and k_q average lifetime in presence of quencher and the first order intramolecular quenching constant.

Static and Dynamic quenching both show a linear dependence on quencher concentration $[Q]$ when plotted F_0/F and $\tau_0/\langle\tau\rangle$ against $[Q]$ respectively. Sometimes static and dynamic can occur simultaneously. Fig. 8(b) compares the F_0/F vs. $[Q]$ profiles with $\tau_0/\langle\tau\rangle$ vs. $[Q]$ profiles for some representative $C_{16}MImCl$ -salt solutions. Upward curvatures (second order polynomial dependence) in the steady state fluorescence quenching plots (F_0/F vs. $[Q]$) demonstrate that quenching of pyrene in micellar environment in presence of electrolytes are both static and dynamic in nature. This statement was further proved by the dissimilarly in the values of F_0/F and $\tau_0/\langle\tau\rangle$ for the same $[Q]$. Linear time-resolved fluorescence quenching plots ($\tau_0/\langle\tau\rangle$ vs. $[Q]$) accompanied with non-zero slope confirms dynamic quenching of pyrene in presence of CPC in the micellar environment of aqueous $C_{16}MImCl$ -salt solutions investigated here. So coupled influences of both the dynamic and static quenching have been operated. Such a

combined effect has also been reported earlier where quenching of anthracene fluorescence by CPC in SDS micelle environment has been investigated¹⁰⁵.

Stern-Volmer constant (K_{sv}) values calculated from Eq. (20) have been listed in Table 5. Also included in this table are the k_q values calculated using the K_{sv} values along with the unquenched life times (τ_0). In absence of the quencher, the decay curve of pyrene is single-exponential, whereas these are bi-exponential in presence of CPC^{55-57, 96} for aqueous surfactant and for all surfactant-salt solutions. This means, pyrene can be accessible by CPC in two different regions of micelle. These bi-exponential plots provide two sets of life time values (τ_1 and τ_2 ; *cf.* Table S1). Average life time values ($\langle\tau\rangle$) for all the sets in presence of CPC have been considered here, and are shown in Table S1. Quenching plots [$\log(\text{count})$ vs. time] of pyrene in micellar environment of $C_{16}\text{MImCl}$ by CPC for all the salts (concentration: $0.001 \text{ mol.kg}^{-1}$) have been shown in Fig. S4 of the supplementary section. Fig. 8(a) demonstrates the variation of life time as a function of the concentration of the added salts in absence of the quencher. The observed pyrene lifetime (136 ns) agrees fairly well with the literature values of the lifetimes (108-119 ns) in various aqueous cationic micellar solutions¹⁰⁶. The lifetime reflects the accessibility of chloride ions into the different micelles to quench the pyrene. The present observation thus indicates that pyrene was quenched by the chloride ions in slightly different ways depending on the nature of the surfactant. The life time values in absence of the quencher (τ_0) are found to vary within the range of 99-154 ns for aqueous $C_{16}\text{MImCl-NaBr}$ solutions, while for aqueous $C_{16}\text{MImCl-NaCl}$, $C_{16}\text{MImCl-Na}_2\text{SO}_4$, and $C_{16}\text{MImCl-Na}_3\text{PO}_4$ systems τ_0 values are found to be relatively higher (143-160 ns) probably due to an increase in the hydrophobicity in micellar region resulting from the decrease in the micropolarity in the later cases (*cf.* Table 4). Relative lifetime values of pyrene in micellar media in presence of different electrolytes at 0.02 mol.kg^{-1} have been shown at the inset of Fig. 8(a). Pyrene while diffusing into the micelle in NaBr solution quenched by Br^- ions¹⁰⁷ in the vicinity of Stern layer, manifested in lower life time values at high ionic strength of Br^- which was reflected in the high K_{sv} values with increasing Br^- (*cf.* Table 5) comparing with the other salts. The adsorbed Cl^- ions around $C_{16}\text{MIm}^+$ may be replaced by other anions in presence of different added electrolytes which lead to a varying quenching of the excited state.¹⁰⁷ The variation in lifetime thus indicates that pyrene was quenched in different ways depending on the nature of the added salts.

The values of the Stern-Volmer constants (K_{sv}) are always found to be greater than those in water (Table 5). Micellar aggregation numbers have been obtained both from SSFQ (N_a) and TRFQ (N_D) methods, and are listed in Table 5. The aggregation number values obtained with TRFQ

method are always found to be higher than those obtained with the SSFQ method. That the TRFQ method produces higher values of the aggregation numbers of a number of gemini surfactants has also been reported earlier by Tehrani-Bagha *et al.*¹⁰⁶ Addition of any of the investigated salts results in an increase in the aggregation number of C₁₆MImCl micelles (*cf.* Table 5). The aggregation numbers of C₁₆MImCl micelles in presence of the salts have been found to increase in the order: NaCl \approx Na₂SO₄ < NaBr < Na₃PO₄. The present study revealed an approximate linear relationship between the aggregation number and the hydrodynamic diameters of C₁₆MImCl micelles in presence of NaBr, Na₂SO₄, and Na₃PO₄ while this is not the case in the presence of NaCl indicating that the micelles are less compact in the latter case compared to the former cases.

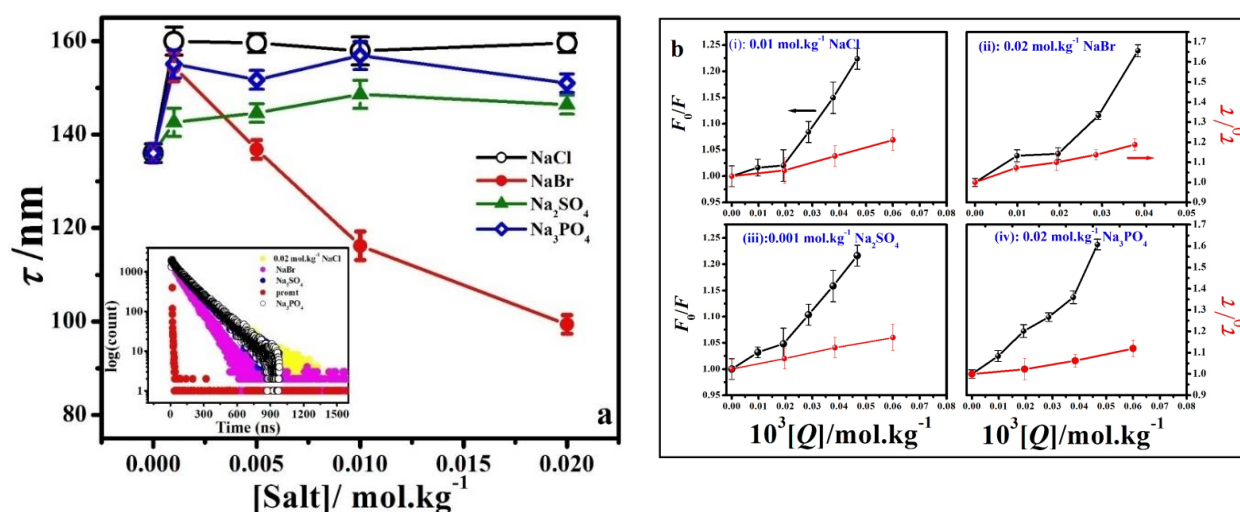


Fig. 8. (a) Life time (τ) of solubilized pyrene in micelle (surfactant concentration: 12×10^{-3} mol.kg⁻¹) in water and in different salt solutions vs. salt concentration. Error bars are also shown. The inset depicts a comparative decay curve of pyrene in micellar medium in presence of different salts each with a concentration of 0.02 mol.kg⁻¹ without quencher. (b) F_0/F (black) and τ_0/τ (red) vs. CPC concentration in presence different salts.

3.9. Zeta potential (ζ) and hydrodynamic radius (R_h) from DLS

The Zeta potential (ζ) defines the potential of the diffused electrical double layer of the ionic micellar aggregates. It provides a measure of the extent of electrostatic repulsion between aggregates with like charges in solution. The magnitude of Zeta potential also gives an estimate of the stability of colloidal systems.¹⁰⁸ In the present study, the magnitude of ζ has been found to decline for C₁₆MImCl micelles as the concentration of each of the added salt increases. The influence of the concentration of the added salt on ζ is consistent with the classical electrical double layer theory, according to which an increase in salt concentration causes a reduction of the thickness of the electrical double layer (Gouy-Chapman layer) and consequently there is a

decrease in Zeta potential (*cf.* Table 4 and Fig. 9). The stability of the system decreases with the decrease of ζ and it is generally considered that the instability window in terms of ζ varies within +30 mV to -30 mV. From Fig. 9, it is evident that the highest ζ values are obtained in presence of NaCl and the least in presence of Na₂SO₄. Bivalent and trivalent anions have reduced ζ significantly as these anions compress electrical double layer more effectively. This trend in ζ is similar to that what we find for the *cmc* values in presence of the investigated salts. (*cf.* Table 1). It is evident from Table 4 and Fig. 9 that the hydrodynamic radius (R_h) of C₁₆MImCl micelles increases with the increase of salt concentration. Presence of different salts affect the R_h values of C₁₆MImCl micelles differently, and the following sequence of these values have been found in presence of the investigated salts: NaCl > Na₃PO₄ > NaBr > Na₂SO₄. Representative plots of the number (%) vs. size (nm) of the C₁₆MImCl micelles in presence of 0.02 mol.kg⁻¹ of all the salts have been included in the supplementary section (Fig. S5) for better understanding of the size distribution of the micellar aggregates in salt medium.

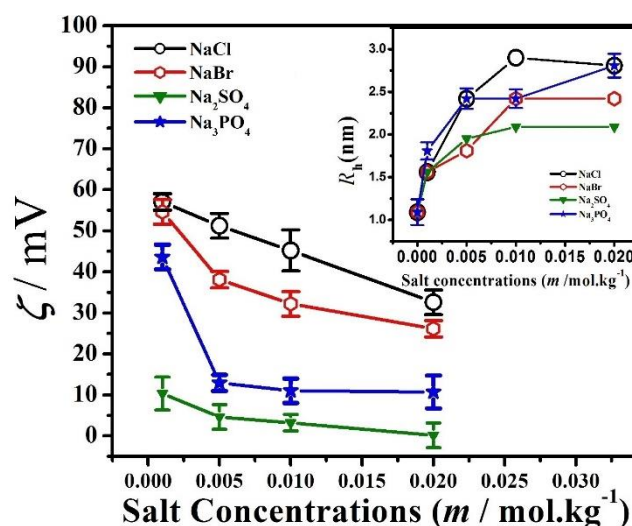


Fig. 9. Zeta potential (ζ) of C₁₆MImCl micelle in water and in different salt solutions (surfactant concentration: 6×10^{-3} mol.kg⁻¹) vs. salt concentration. Error bars are given. At the inset: the hydrodynamic diameter (D_h) of micelle (surfactant concentration: 6×10^{-3} mol.kg⁻¹) vs. salt concentration profile. Error bar for one system is given and the error bars for other systems are same.

4. Conclusions

A comprehensive study on the factors affecting the micellization of a surface-active ionic liquid, 1-hexadecyl-3-methylimidazolium chloride, in presence of different alkali metal salts in aqueous solutions unravelled the nature of the subtle interactions prevailing in these solutions. Since surfactant-salt mixtures have enormous potential in biological, technological,

medical and pharmaceutical formulations, in enhanced oil recovery etc. for the purpose of improved solubilization, suspension and dispersion, it is anticipated that the information obtained here might help modulate the properties of the 1-hexadecyl-3-methylimidazolium chloride micelles, in particular, and other surface-active ionic liquids in general. This study signifies the importance of conductometry, tensiometry, spectrofluorimetry, isothermal titration calorimetry and dynamic light scattering in conjunction with judicious choice of appropriate theoretical models to elucidate the behaviour of surface-active ionic liquid micellar solutions.

Table 1. Critical micellar concentration (*cmc*) of aqueous C₁₆MimCl in absence and presence of various salts with varying molal concentrations using conductometry (cond.), tensiometry (ST), steady state fluorescence anisotropy (FA), isothermal titration calorimetry (ITC) within the temperature range 298.15 K to 318.15 K^a

Added salt conc. (mol.kg ⁻¹)	T (K)	10 ⁴ <i>cmc</i> (mol.kg ⁻¹)				
		cond.	ST	FA	ITC	Average
C₁₆MimCl in water						
0	298.15	8.55, 8.76, ^a 8.60 ^b	8.28, 9.55 ^a	9.06	7.70, 9.90 ^b	8.80
	303.15	9.42, ^a 8.82 ^c	9.71 ^a	-	-	9.32
	308.15	9.49, ^a 9.10 ^b	10.17 ^a	-	-	9.59
	313.15	9.95, ^a 9.26 ^c	10.93 ^a	-	-	10.0
	318.15	10.63, ^a 10.10 ^b	11.07 ^a	-	-	10.6
C₁₆MimCl in NaCl solution^d						
0.001	298.15	5.99	6.32	5.40	6.67	6.09
	303.15	6.02	-	-	-	-
	308.15	6.40	-	-	-	-
	313.15	6.59	-	-	-	-
	318.15	7.18	-	-	-	-
0.005	298.15	2.29	1.99	2.23	2.10	2.15
	303.15	2.68	-	-	-	-
	308.15	2.72	-	-	-	-
	313.15	2.70	-	-	-	-
	318.15	3.37	-	-	-	-
0.010	298.15	-	1.32	1.09	0.60	1.00
0.020	298.15	-	0.91	0.91	0.54	0.79
C₁₆MimCl in NaBr solution^d						
0.001	298.15	3.29	2.97	3.39	1.10	2.70
	303.15	3.42	-	-	-	-
	308.15	3.95	-	-	-	-
	313.15	4.60	-	-	-	-

	318.15	4.94	-	-	-	-
0.005	298.15	1.46	1.27	1.47	0.91	1.30
	303.15	1.47	-	-	-	-
	308.15	1.48	-	-	-	-
	313.15	1.58	-	-	-	-
	318.15	1.81	-	-	-	-
0.010	298.15	-	1.21	0.77	0.81	0.93
0.020	303.15	-	0.53	0.48	0.45	0.49
C₁₆MimCl in Na₂SO₄ solution^d						
0.001	298.15	1.28	1.01	1.52	0.43	1.06
	303.15	1.31	-	-	-	-
	308.15	1.41	-	-	-	-
	313.15	1.53	-	-	-	-
	318.15	1.70	-	-	-	-
0.005	298.15	1.07	0.58	0.98	0.40	0.65
	303.15	1.25	-	-	-	-
	308.15	1.28	-	-	-	-
	313.15	1.37	-	-	-	-
	318.15	-	-	-	-	-
0.010	298.15	-	0.51	0.70	0.34	0.52
0.020	303.15	-	0.50	0.65	0.23	0.46
C₁₆MimCl in Na₃PO₄ solution^d						
0.001	298.15	2.33	2.20	2.25	-	2.26
	303.15	2.29	-	-	-	-
	308.15	2.67	-	-	-	-
	313.15	3.01	-	-	-	-
	318.15	3.46	-	-	-	-
0.005	298.15	1.16	0.90	1.27	0.96	1.07
	303.15	0.87	-	-	-	-
	308.15	1.47	-	-	-	-
	313.15	1.51	-	-	-	-
	318.15	1.71	-	-	-	-
0.010	298.15	-	0.80	0.81	0.57	0.73
0.020	303.15	-	0.75	0.75	0.52	0.67

^aRef. [63].

^bRef. [17].

^cRef. [18].

^dCalculated in this present work.

Table 2. Degree of counterion binding (β), Gibbs free energy of micellization from mass action model (ΔG_m^0), enthalpy of micellization (ΔH_m^0) / from ITC (within the bracket), entropy of micellization (ΔS_m^0), compensation temperature (T_{com}), intrinsic enthalpy gain (ΔH_m^{0*}) in absence and presence of different salt solutions within the temperature range 298.15 K to 318.15 K^a

[Salt] (mol.kg ⁻¹)	<i>T</i> (K)	β	ΔG_m^0 (kJ.mol ⁻¹)	ΔH_m^0 (kJ.mol ⁻¹)	ΔS_m^0 (kJ.mol ⁻¹ .K ⁻¹)	<i>T</i> _{com} (K)	ΔH_m^{0*} (kJ.mol ⁻¹)	$\left \frac{T\Delta S_m^0}{\Delta G_m^0} \right $
C₁₆MimCl in water^b								
0	298.15	0.50	-41.04	-6.94	0.11	-	-	-
	303.15	0.49	-41.26	-9.40	0.10	-	-	-
	308.15	0.48	-41.56	-11.99	0.09	-	-	-
	313.15	0.47	-41.74	-14.69	0.08	-	-	-
	318.15	0.46	-41.85	-17.52	0.07	-	-	-
C₁₆MimCl in NaCl solution^c								
0.001	298.15	0.63	-46.2	-3.63(0.56)	0.14	-	-	0.92
	303.15	0.62	-46.7	-8.36	0.13	-	-	0.82
	308.15	0.59	-46.3	-13.2	0.11	278	-43.3	0.71
	313.15	0.57	-46.3	-18.2	0.09	-	-	0.61
	318.15	0.56	-46.4	-23.6	0.07	-	-	0.49
0.005	298.15	0.64	-50.4	-17.1(-0.67)	0.11	-	-	0.66
	303.15	0.64	-50.6	-21.5	0.09	-	-	0.57
	308.15	0.62	-50.8	-25.9	0.08	279	-48.4	0.49
	313.15	0.61	-51.2	-30.6	0.06	-	-	0.40
	318.15	0.57	-49.8	-34.9	0.05	-	-	0.29
0.010	298.15	-	-	(-2.62)	-	-	-	-
0.020	298.15	-	-	(-2.85)	-	-	-	-
C₁₆MimCl in NaBr solution^c								
0.001	298.15	0.67	-49.8	-26.1(-3.65)	0.08	-	-	0.47
	303.15	0.66	-50.2	-28.3	0.07	-	-	0.43
	308.15	0.64	-49.8	-30.4	0.06	223	-44.2	0.39
	313.15	0.61	-49.0	-32.3	0.05	-	-	0.34
	318.15	0.57	-48.2	-34.1	0.04	-	-	0.29
0.005	298.15	0.68	-53.5	8.57(0.21)	0.21	-	-	1.00
	303.15	0.67	-54.0	-2.79	0.17	301	-53.8	0.95
	308.15	0.66	-54.5	-14.8	0.13	-	-	0.73
	313.15	0.65	-54.8	-27.4	0.08	-	-	0.49
	318.15	0.64	-54.8	-40.6	0.04	-	-	0.26
0.010	298.15	-	-	(4.16)	-	-	-	-
0.020	298.15	-	-	(-1.61)	-	-	-	-
C₁₆MimCl in Na₂SO₄ solution^c								
0.001	298.15	0.79	-57.6	-8.41(0.65)	0.16	-	-	0.85
	303.15	0.76	-57.4	-15.2	0.14	-	-	0.73
	308.15	0.74	-57.4	-22.4	0.11	299.6	-57.1	0.61
	313.15	0.71	-56.9	-29.6	0.09	-	-	0.48
	318.15	0.78	-	-59.7	-39.3	0.06	-	-
0.005	298.15	0.57	-51.2	-38.6 ^b (0.09)	-	-	-	-
	303.15	0.58	-52.6	-148.8 ^b	-	-	-	-

	308.15	0.70	-58.3	-266.6 ^b				
	313.15	0.83	-61.5	-388.3 ^b				
0.010	298.15	-	-	(0.24)				
0.020	298.15	-	-	(0.17)				
C₁₆MimCl in Na₃PO₄ solution^c								
0.001	298.15	0.63	-50.0	-10.7	0.13	-	-	0.78
	303.15	0.62	-50.6	-20.9	0.09	-	-	0.58
	308.15	0.61	-50.5	-31.7	0.06	291	-49.0	0.37
	313.15	0.56	-49.2	-41.9	0.02	-	-	0.15
	318.15	0.55	-49.1	-53.5	-0.01	-	-	0.09
0.005	298.15	0.64	-53.1	-10.4(2.02)	0.14	-	-	0.80
	303.15	0.64	-55.2	-22.5	0.11	-	-	0.59
	308.15	0.54	-50.6	-33.2	0.06	297	-53.1	0.34
	313.15	0.65	-55.0	-49.4	0.02	-	-	0.10
	318.15	0.57	-52.6	-60.9	-0.03	-	-	0.16
0.010	298.15	-	-	0.34	-	-	-	-
0.020	298.15	-	-	1.07	-	-	-	-

^a ΔH_m^0 calculated using Eq. (5).

^b ΔH_m^0 , ΔS_m^0 , and ΔG_m^0 values taken from Ref. [63] for the micellization of C₁₆MimCl in water.

^cCalculated in this study

Table 3. Surface excess at air/water interface (Γ_{cmc}), minimum area per surfactant monomer at air/water interface (A_{min}), efficiency of interfacial adsorption (pC_{20}), surface pressure at the cmc (π_{cmc}), and micellar packing parameters (P) in absence and in presence of different salts with varying concentrations at 298.15 K.

Added salt	[Salt] (mol·kg ⁻¹)	$10^3\pi_{cmc}$ (J·m ⁻²)	$10^6\Gamma_{cmc}$ (mol·m ⁻²)	A_{min} (nm ² ·molecule ⁻¹)	pC_{20}	P
NaCl	0	28.7	1.95	0.85	3.40	0.25
	0.001	30.5	1.28	1.29	1.11	0.16
	0.005	30.8	1.76	0.94	1.56	0.22
	0.010	32.8	1.82	0.91	1.47	0.23
	0.020	33.4	1.54	1.08	2.06	0.19
NaBr	0.001	34.3	2.36	0.70	1.14	0.30
	0.005	35.6	2.53	0.66	1.58	0.32
	0.010	37.2	2.60	0.64	1.78	0.33
	0.020	36.3	3.15	0.53	1.84	0.40
Na ₂ SO ₄	0.001	29.0	2.28	0.72	1.52	0.29
	0.005	31.0	1.74	0.95	1.92	0.19
	0.010	31.0	1.15	1.44	1.98	0.16
	0.020	32.7	1.90	0.87	2.00	0.23
Na ₃ PO ₄	0.001	29.7	1.15	1.15	1.55	0.14
	0.005	31.1	1.11	1.49	1.87	0.14
	0.010	30.0	1.50	1.10	1.70	0.19
	0.020	33.0	1.39	1.19	2.02	0.18

Table 4. Experimental values of hydrodynamic radius (R_h), Zeta potential (ζ) and micropolarity (I_1/I_3) in different C₁₆MImCl-salt solutions at 298.15K.

Added salt	[Salt] (mol·kg ⁻¹)	R_h (nm)	ζ (mV)	I_1/I_3
NaCl	0	-	-	0.996 ± 0.0008
	0.001	1.56 ± 0.03	57.0 ± 2	0.996 ± 0.0009
	0.005	2.42 ± 0.02	51.2 ± 3	0.994 ± 0.0010
	0.010	2.90 ± 0.04	45.2 ± 2	0.992 ± 0.0008
	0.020	2.80 ± 0.02	32.6 ± 3	0.992 ± 0.0008
NaBr	0.001	1.56 ± 0.02	54.6 ± 3	0.996 ± 0.0010
	0.005	1.81 ± 0.04	38.1 ± 2	0.998 ± 0.0008
	0.010	2.42 ± 0.03	32.2 ± 2	0.991 ± 0.0007
	0.020	2.42 ± 0.04	26.1 ± 1	0.987 ± 0.0010
Na ₂ SO ₄	0.001	1.56 ± 0.03	10.3 ± 2	0.996 ± 0.0008
	0.005	1.95 ± 0.02	4.62 ± 1	0.989 ± 0.0007
	0.010	2.09 ± 0.04	3.19 ± 0.8	0.978 ± 0.0009
	0.020	2.09 ± 0.02	0.14 ± 0.5	0.972 ± 0.0010
Na ₃ PO ₄	0.001	1.81 ± 0.01	43.6 ± 3	0.996 ± 0.0010
	0.005	2.42 ± 0.04	12.9 ± 2	0.989 ± 0.0007
	0.010	2.42 ± 0.02	11.0 ± 0.7	0.980 ± 0.0010
	0.020	2.81 ± 0.03	10.7 ± 0.5	0.973 ± 0.0009

Table 5. Stern-Volmer quenching constant (K_{SV}), bimolecular quenching constant (k_q), aggregation number by steady state quenching method (N_a) and time resolved fluorescence quenching method (N_D) of pyrene of micelle solution (12×10^{-3} mol.kg⁻¹) with CPC at 298.15 K

Added salt	[salt] (mol.kg ⁻¹)	$10^{-3}K_{sv}$ (mol ⁻¹ .kg)	$10^{-10}k_Q$ (s ⁻¹)	N_a	N_D
NaCl	0	0.84	0.62	48 ± 5	91±4
	0.001	1.93	1.21	74± 5	-
	0.005	2.35	1.47	81± 4	104±6
	0.010	2.26	1.43	-	102±6
	0.020	1.43	0.89	95± 5	128±4
NaBr	0.001	1.66	1.08	-	96± 5
	0.005	2.36	1.73	-	109±5
	0.010	2.27	1.95	-	109±5
	0.020	2.99	3.01	-	117±7
Na ₂ SO ₄	0.001	1.38	0.97	64 ± 5	93±7
	0.005	1.52	1.05	74± 5	103±6
	0.010	2.11	1.42	86± 6	105±9
	0.020	2.05	1.40	92± 4	131±5
Na ₃ PO ₄	0.001	2.10	1.35	61 ± 5	101±6
	0.005	1.91	1.25	74± 4	109±5
	0.010	2.29	1.46	99± 6	110±4
	0.020	1.88	1.25	117± 6	155±8

Supplementary Section

Studies on the self-aggregation, interfacial and thermodynamic properties of a surface active imidazolium-based ionic liquid in aqueous solution: Effects of salt and temperature.

Fig. S1: $(d\ln X_{cmc}/dT)$ vs. Temperature (T) plot for the micellization of $C_{16}MImCl$ in presence two different salt concentrations.

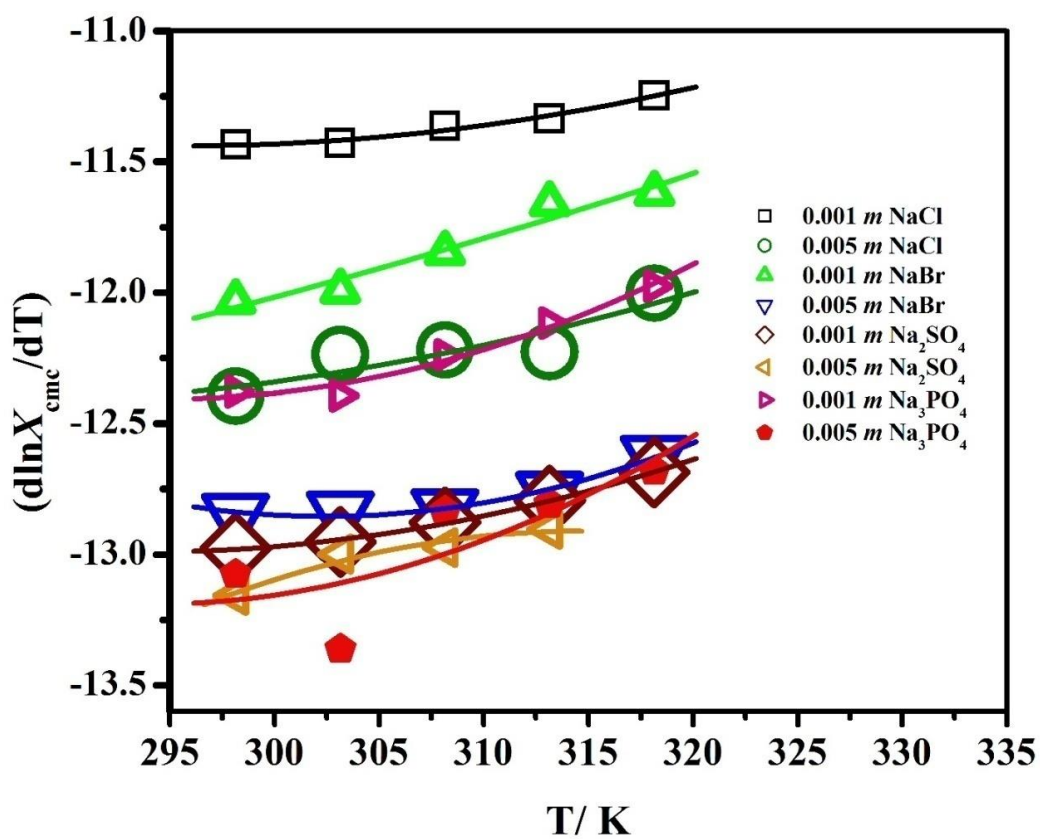


Fig. S2: Enthalpy vs. Entropy compensation plot for the micellization of C₁₆MImCl in presence of water and different salt concentrations

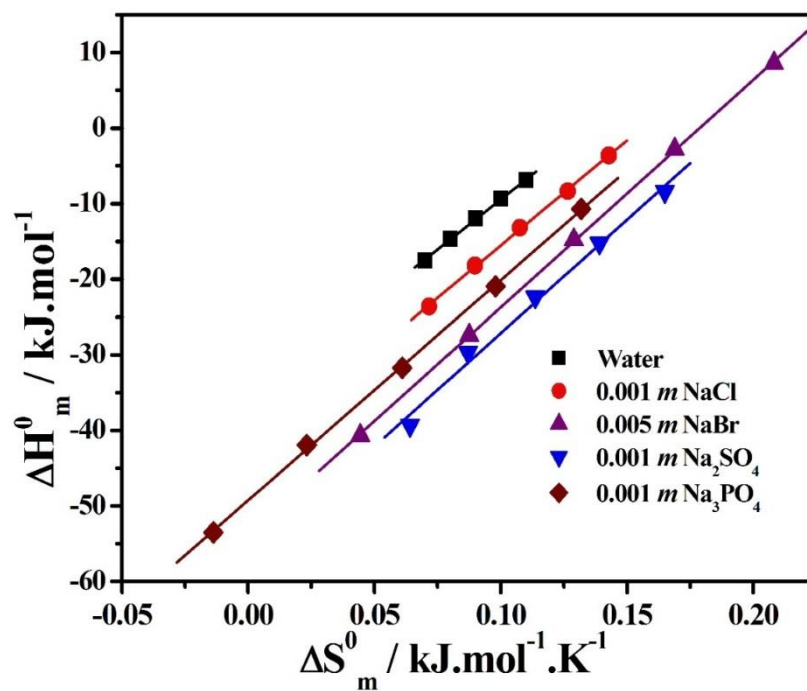


Fig. S3: Γ_{cmc} vs. molality (m) plot for the micellization of C₁₆MImCl in presence different salt concentrations.

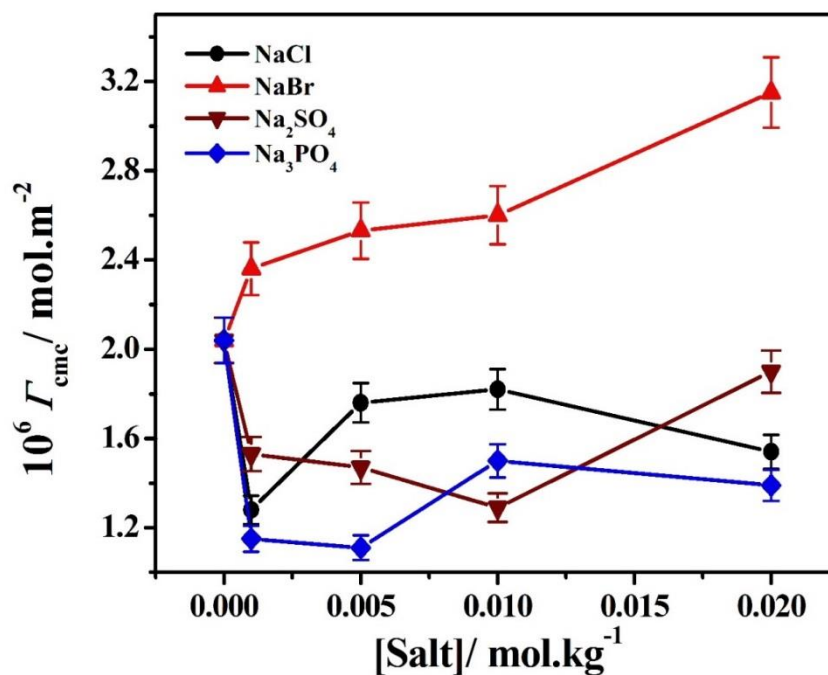


Fig. S4: Time resolved quenching of pyrene by CPC in micellar environment of $C_{16}MImCl$ in presence of different salts (a: $NaCl$, b: $NaBr$, c: Na_2SO_4 , d: Na_3PO_4) at $0.001\ m$ concentration. Concentrations of CPC [CPC] have been given in the individual plots.

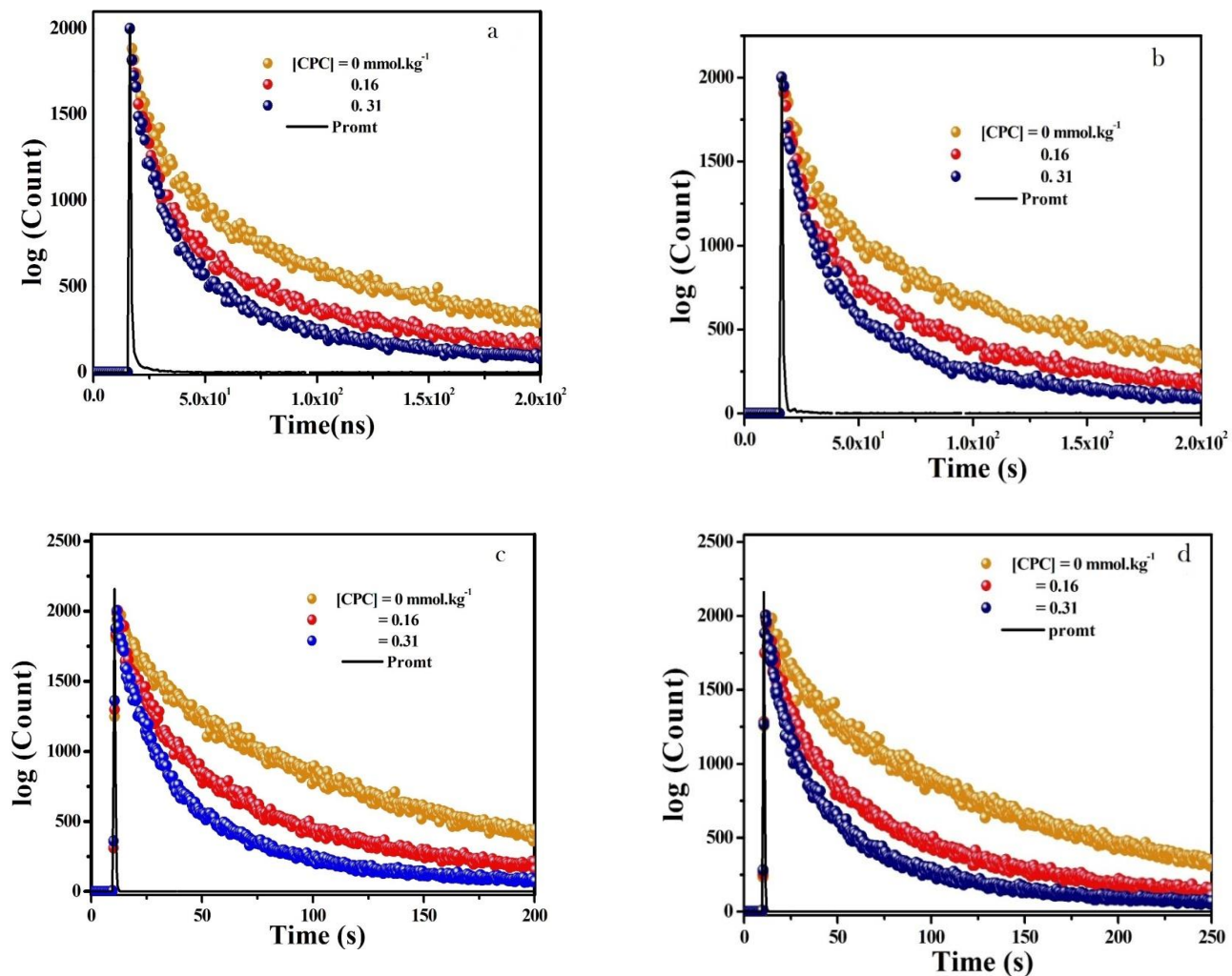


Fig. S5: Intensity (%) vs. size (nm) profile for the micellization of C₁₆MImCl in presence salts of 0.01 m; a: NaCl, b: NaBr, c: Na₂SO₄, d: Na₃PO₄

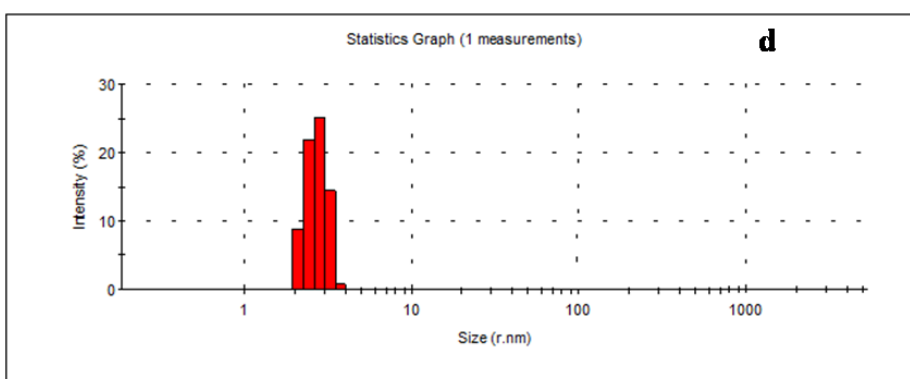
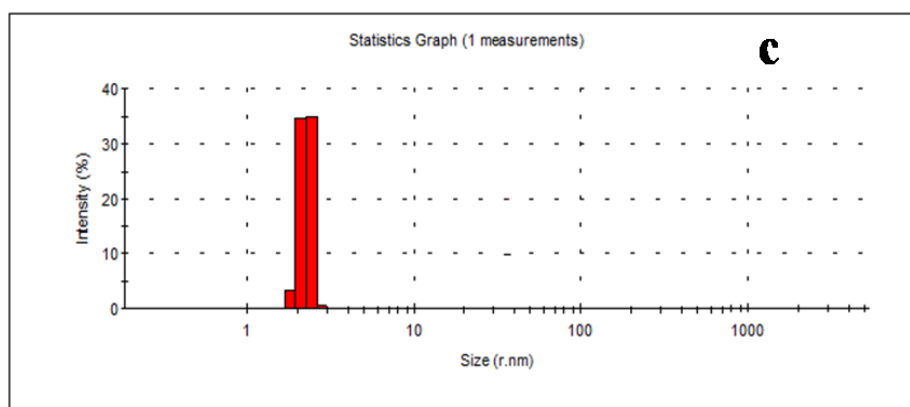
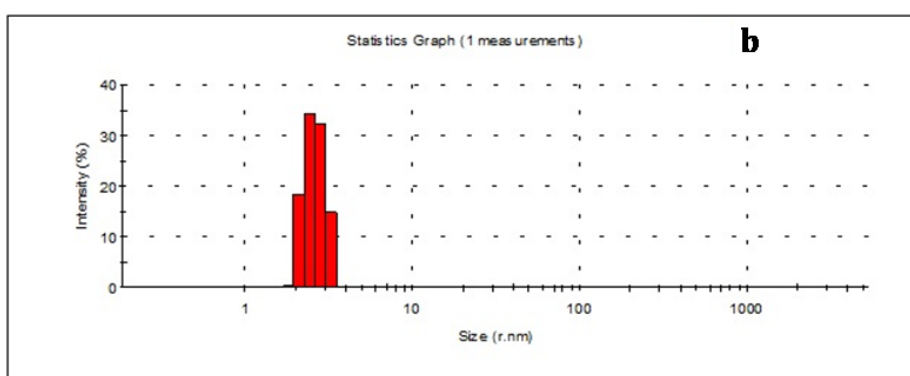
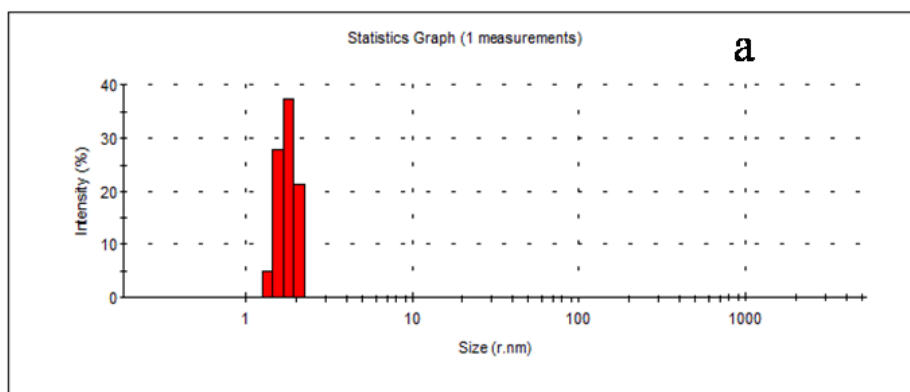


Table S1. Time resolved fluorescence quenching data of pyrene on C₁₆MImCl solution (12mmolal) with CPC as quencher at 298.15 ± 0.1 K^a

<i>m</i>	Water/Salts	[CPC] 10 ⁻³ <i>m</i>	(τ_0)/ τ_1 ns	<i>b</i> ₁	τ_2 ns	<i>b</i> ₂	< τ > ns	χ^2
0	Water	0.00	(136)	100.0			136.0	1.25
		0.16	31.7	24.64	148.1	75.36	119.4	1.05
		0.31	32.2	36.31	151.5	63.69	108.2	1.05
0.001	NaCl	0	(160)	100.0			160.0	1.13
		0.16	29.0	31.30	155.3	68.70	115.8	1.17
		0.31	31.1	39.28	146.4	60.72	101.1	1.11
	NaBr	0	(154.4)	100.0			154.4	1.17
		0.16	32.8	25.30	157.3	74.70	125.8	1.05
		0.31	31.3	40.40	145.9	59.60	99.61	1.10
	Na ₂ SO ₄	0.00	(142.6)	100			142.6	1.22
		0.16	38.24	30.90	150.8	69.10	116.0	1.02
		0.31	33.08	48.46	143.3	51.54	89.87	1.00
Na ₃ PO ₄	0	(155.0)	100			155.1	1.20	
	0.16	36.6	29.03	154.6	70.97	120.3	1.06	
	0.31	31.09	44.21	141.2	55.79	92.50	1.07	
0.005	NaCl	0	(159.6)	100.0			159.6	1.05
		0.16	36.0	24.52	154.1	75.48	125.1	1.06
		0.31	28.6	45.49	144.8	54.51	91.92	1.05
	NaBr	0	(136.8)	100.0			136.8	1.08
		0.16	35.3	30.34	132.6	69.66	103.0	1.09
		0.31	34.0	50.25	120.9	49.75	77.29	1.13
	Na ₂ SO ₄	0	(144.6)	100			144.6	1.16
		0.06	85.0	35.0	155.3	65.0	130.7	1.03
		0.31	33.67	51.61	133.9	48.39	98.44	1.02
	Na ₃ PO ₄	0	(151.7)	100			151.7	1.01
		0.16	47.84	34.77	165.2	65.23	124.3	1.07
		0.31	39.44	53.38	152.8	46.62	92.31	1.17
0.01	NaCl	0	(157.9)	100.0	0		157.9	1.27
		0.16	28.9	33.61	152.2	66.39	110.7	1.16
		0.31	30.5	43.80	140.9	56.20	92.55	1.18
	NaBr	0	(116.2)	100.0	0		116.2	1.14
		0.16	36.70	33.07	112.7	66.93	87.57	1.11
		0.31	29.3	44.76	97.55	55.24	67.03	1.07
	Na ₂ SO ₄	0	(148.9)	100.0			148.9	1.07
		0.16	41.38	35.12	147.5	64.88	110.3	1.08
		0.31	33.18	51.27	124.7	48.73	77.79	1.01
	Na ₃ PO ₄	0	(156.9)	100.0			156.9	0.99
		0.16	45.1	33.8	160.8	66.2	121.7	1.15
		0.31	34.91	47.81	139.4	52.19	89.45	1.06
0.02	NaCl	0	(159.6)	100.0	0		159.6	1.05
		0.16	29.8	33.45	155.7	66.55	113.6	1.27
		0.31	34.6	46.46	139.1	53.54	90.54	1.10
	NaBr	0	(99.4)	100.0	0		99.40	1.17
		0.16	27.2	29.89	91.20	70.11	72.06	1.09
		0.31	25.9	49.22	73.41	50.78	50.06	1.07
	Na ₂ SO ₄	0	(146.4)	100			146.4	1.25
		0.16	44.29	39.74	150.9	60.26	108.6	1.08
		0.31	33.89	55.37	130.9	44.63	77.22	1.10
	Na ₃ PO ₄	0	(151.0)	100.0			151.0	1.12
		0.16	44.07	31.78	158.6	68.22	122.2	1.00
		0.31	39.03	50.31	148.4	49.69	93.37	1.03

^a τ_0 values (within the first bracket) indicate life time when the quencher concentration is 0 mmol.kg⁻¹. Standard relative uncertainties (u_r): $u_r(\langle\tau\rangle) = 0.4$

References:

1. T. Welton, *Green Chem.*, 2011, **13**, 225.
2. M. J. Rosen, *Surfactants and interfacial Phenomenon*, 3rd ed, John Wiley, New York (2004).
3. D. Varade, T. Joshi, V. K. Aswal, P. S. Goyal, P. A. Hassan, P. Bahadur, *Colloids Surf., A*, 2005, **259**, 95-101.
4. B. Dong, X. Zhao, L. Zheng, J. Zhang, N. Li, T. Inoue, *Colloids Surf., A*, 2008, **317**, 666-672.
5. N. Vlachy, M. Drechsler, J. M. Verbavatz, D. Touraud, W. Kunz, *J. Colloid Interface Sci.*, 319, **2008**, 542-548.
6. M. Sammalkorpi, M. Karttunen, M. Haataja, *J. Phys. Chem. B*, 2009, **113**, 5863-5870.
7. A. Jusufi, A. P. Hynninen, M. Haataja, A. Z. Panagiotopoulos, *J. Phys. Chem. B*, 2009, **113**, 6314- 6320.
8. K. Maiti, D. Mitra, S. Guha, S. P. Moulik, *J. Mol. Liq.*, 2009, **146**, 44-51.
9. L. Abezgauz, K. Kuperkar, P. A. Hassan, O. Ramon, P. Bahadur, D. Danino, *J. Colloid Interface Sci.*, 2010, **342**, 83-92.
10. F. Geng, J. Liu, L. Zheng, L. Yu, Z. Li, G. Li and C. Tung, *J. Chem. Eng. Data*, 2010, **55**, 147-151.
11. N. Li, S. Zhang, L. Zheng, B. Dong, X. Li and L. Yu, *Phys. Chem. Chem. Phys.*, 2008, **10** 4375- 4377.
12. J. Łuczak, J. Hupka, J. Thöming, C. Jungnickel, *Colloids Surf. A*, 2008, **329**, 125- 133.
13. P. D. Galgano, O. A. E. Seoud, *J. Colloid Interface Sci.*, 2011, **361**, 186–194.
14. M. Ao, P. Huang, G. Xu, X. Yang, Y. Wang, *Colloid. Polym. Sci.*, 2009, **287**, 395-402.
15. B. Dong, N. Li, L. Zheng, Li Yu, and T. Inoue, *Langmuir*, 2007, **23**, 4178-4182.
16. J. Łuczak, C. Jungnickel, M. Joskowska, J. Thöming, J. Hupka, *J. Colloid Interface Sci.*, 2009, **336**, 111-116.
17. P. D. Galgano, O. A. E. Seoud, *J. Colloid Interface Sci.*, 2010, **345**, 1–11.
18. S. Das, S. Ghosh, and B. Das, *J. Chem. Eng. Data*, 2018, **63**, 3784–3800.
19. Md. S. Alam, A. Mandal, A. B. Mandal, *J. Chem. Eng. Data*, 2011, **56**, 1540-1546.
20. B. Naskar, A. Dan, S. Ghosh, V. K. Aswal, S. P. Moulik, *J. Mol. Liq.*, 2012, **170**, 1–10.
21. G. A. Cooney, C. C. Obunwo, *IOSR J. Appl. Chem. (IOSR-JAC)*, 2014, **7**, 34-38.
22. M. A. Rub, *J. Mol. Liq.*, 2020, **298**, 112049
23. S. V. Koroleva, A.I. Victorov, *Phys. Chem. Chem. Phys.*, 2014, **16**, 17422-17425.
24. Md. Akram, I. A. Bhat, A. K. Berekute, Kabir-ud-Din, *J. Ind. Eng. Chem.*, 2016, **40**, 161-167.
25. S. Kumar, A. Mandal, *Appl. Surf. Sci.*, 372 (2016) 42-51.
26. J. N. Tian, B. Q. Ge, Y. F. Shen, Y. X. U. He, Z. X. Chen, *J. Agric. Food Chem.*, 2016, **64**, 1977-1988.
27. E. Feitosa, M. R. S. Brazolinn, R. M. Z. G. Naal, M. P. F. De Moreis Del Lama, J. R. Lopes, W. Loh, M. Vasilescu, *J. Colloid Interface Sci.*, 2006, **299**, 883-889.
28. M. Benrraou, B. L. Bales, R. Jana, *J. Phys. Chem. B*, 2003, **107**, 13432-13440.
29. G. V. Jensen, R. Lund, J. Gummel, T. Narayanan, and J. S. Pedersen, *Angew. Chem. Int. Ed.* 2014, **53**, 11524-11528.
30. H. Hooshyar and R. Sadeghi, *J. Chem. Eng. Data*, 2015, **60**, 983–992.
31. Md. M. Alama, S. Rana, M. A. Rub, Md. A. Hoque, S. E. Kabir, A. M. Asiri, *J. Mol. Liq.* 2019, **278**, 86–96.
32. J. Mao, J. Tian, W. Zhang, X. Yang, H. Zhang, C. Lin, Y. Zhang, Z. Zhang, J. Zhao, *Colloids Surf., A*, 2019, **578**, 123619.
33. G. Para, E. Jarek, P. Warszynski, *Colloids Surf. A*, 2005, **261**, 65–73.
34. D. Kumar, S. Hidayathulla, M. A. Rub, *J. Mol. Liq.* 2018, **271**, 254-264.
35. S. Mahbub, Md. L. Mia, T. Roy, P. Aktera, A. K. M. R. Uddin, M. A. Rub, Md. A. Hoque, and, A. M. Asiri, *J. Mol. Liq.* 2020, **297**, 111583.
36. S. Mahbub, M. A. Rub, Md. A. Hoque, D. Kumar, *J Phys Org Chem.*, 2019, **32**, e3967.

37. J. Tan, J. Shao, C. Tian, Z. Liao, P. Yan, *J. Surfactants Deterg.* 2019, **22**, 125–130.
38. H. Okuda, *Colloids Surf.*, 1987, **27**, 187-200.
39. H. Demissie, R. Duraisamy, *Water Research*, 2016, **5**, 208-214.
40. S. Ozeki, and S. Ikeda, *Bull. Chem. Soc. Jpn.* 1980, **53**, 1832-1836.
41. R. Li, Q. Zhang, X. Pei, D. Xie, B. Song, *Colloids Surf., A* 2020, **585**, 124114.
42. M. Rahman, M. A. Khan, M. A. Rub, M. A. Hoque, A. M. Asiri, *J. Chem. Eng. Data*, 2017, **62**, 1464–1474.
43. O. Owoyomi, J. F. Olorunyomi, O. E. Olaoye, *Phys. Chem. Res.*, 2017, **5**, 531-540.
44. Md. A. Hoque, Md. R. Molla, Md. R. Amin, Md. M. Alam, Md. F. Hossain, M. A. Rub, *J. Solution Chem.*, 2019, **48**, 105–124.
45. I. Chakraborty and S. P. Moulik, *J. Phys. Chem. B* 2007, **111**, 3658-3664.
46. N. Patra, D. Ray, V. K. Aswal, and S. Ghosh, *ACS Omega*. 2018, **31**, 9256–9266.
47. A. A. Dar, G. M. Rather, S. Ghosh, A. R. Das, *J. Colloid Interface Sci.*, 2008, **32**, 572-581.
48. A. Pal, M. Saini, *J. Surfactants Deterg.*, 2019, **22**, 491-499.
49. H. Wang, Q. Feng, J. Wang, and H. Zhang, *J. Phys. Chem. B*, 2010, **114**, 1380–1387.
50. E. Ghasemian, M. Najafi, A. A. Rafati, Z. Felegari, *J. Chem. Thermodyn.*, 2010, **42**, 962- 966.
51. H. Kumar and C. Chadha, *J. Chem. Eng. Data*, 2015, **60**, 2937-2950.
52. J. Łuczak, M. Markiewicz, J. Thöming, J. Hupka, C. Jungnickel, *J. Colloid Interface Sci.*, 2011, **362**, 415–422.
53. U. Subuddhi, A. K. Mishra, *Colloids Surf., B* 2007, **57**, 102–107.
54. X. Zhang, J. K. Jackson, H. M. Burt, *Biophys.* 1996, **31**, 145-150.
55. A. Malliaris, J. Lang and R. Zana, *J. Chem. SOC., Faraday Trans. I* 1986, **82**, 109-118.
56. M. Pisárčik, F. Devínsky, M. Pupák, *Open Chem.*, 2015, **13**, 922–931.
57. R. G. Alargova, I. I. Kochijashky, M. L. Sierra, and R. Zana, *Langmuir*, 1998, **14**, 5412-5418.
58. K. Beyer, D. Leine, A. Blume, *Colloids Surf., B*, 2006, **49**, 31–39.
59. W. Loh, C. Brinatti, K. C. Tamb, *Biochim. Biophys. Acta*, 2016, **1860**, 999–1016.
60. A. Kessler, B. Zeeb, B. Kranz, O. M. Aguirre, L. Fischer, *Rev. Sci. Instrum.*, 2012, **83**, 105104.
61. P. R. Majhi and S. P. Moulik, *Langmuir*, 1998, **14**, 3986-3990.
62. M. Prasad, I. Chakraborty, A. K. Rakshit, S. P. Moulik, *J. Phys. Chem. B*, 2006, **110**, 9815–9821.
63. B. Das, D. Ray, R. De, *Carbohydr. Polym.*, 2014, **113**, 208–216.
64. J. T. Davis, E. K. Rideal, *Interfacial Phenomena*, Academic Press: New York, 1963.
65. R. P. Borwankar, D. T. Wasan, *Chem. Eng. Sci.*, 1988, **43**, 1323-1337.
66. Y. Marcus, *J. Chem. Soc., Faraday Trans.*, 1991, **87**, 2995-2999.
67. B. Naskar, A. Dan, S. Ghosh, S.P. Moulik, *Carbohydr. Polym.*, 2010, **81**, 700–706.
68. V. K. Aswal, P. S. Goyal, *Phys. ReV. E*, 2000, **61**, 2947-2953.
69. G. Pilcher, M. N. Jones, L. Espada, and H. A. Skinner, *J. Chem. Thermodyn.*, 1969, **1**, 381- 392.
70. Sk. Md. Ahsan, A. Hossain, M. D. Hoque, Md. A. Khan, M. Abdullah, *Indian J. Chem., Sect A*, 2016, **55**, 160-169.
71. S. B. Sulthana, S. G. T. Bhat, A. K. Rakshit, *Langmuir*, 1997, **13**, 4562–4568.
72. R. R. Krug, W. C. Hunter, R. A. Grieger, *J. Phys. Chem.*, 1976, **80**, 2335–2341.
73. S. Glasstone, *Text Book of Physical Chemistry*, 2nd ed. Macmillan, London, 1960.
74. E. Matijevic, B. Pethica, *Trans. Faraday Soc.*, 1958, **54**, 1382–1389.
75. G. Gunnarsson, J. Jönsson, and, H. Wennerström, *J. Phys. Chem.*, 1980, **84**, 3114–3121.
76. J. N. Israelachvili, In *Intermolecular and surface forces* (London: Academic Press), 2nd ed.; 1991, **17**, 370.
77. C. Tanford, *The Hydrophobic Effect*, 2nd ed.; Wiley-Interscience: New York (1980).
78. T. Chakraborty, S. Ghosh, *Colloid Polym Sci.*, 2007, **285**, 1665–1673.
79. S. Ghosh, T. Chakraborty, *J. Phys. Chem. B*, 2007, **111**, 8080–8088.
80. S. Ozeki, S. Ikeda, *Bull. Chem. Soc. Jpn.*, 1981, **54**, 552-555.

81. E.W. Anacker, H.M. Ghose, *Phys. Chem.*, 1963, **67**, 1713-1716.
82. S. Ozeki, S. Ikeda, *J. Colloid Interf. Sci.*, 1982, **87**, 424-435.
83. S.L. Anderson, D. Rovnyak, and T.G. Strein, *Chirality*, 2016, **28**, 290-298.
84. C. Chadha, G. Singh, G. Singh, H. Kumar, T.S. Kang, *RSC. Adv.*, 2016, **6**, 38238-38251.
85. P.A.R. Pires, O. A. El Seoud, *Progr Colloid Polym Sci.*, 2006, **133**, 131–141.
86. S. Shimizu, P. A. R. Pires, W. Loh, O. A. El Seoud, *Colloid Polym Sci.*, 2004, **282**, 1026–1032.
87. S. Shimizu, P. A. R. Pires, and O. A. El Seoud, *Langmuir*, 2004, **20**, 9551-9559.
88. T. Mehrian, A. de Keizer, A. J. Korteweg, J. Lyklema, *Colloids Surf. A*, 1993, **71**, 255-267.
89. K. Bijma, J. B. F. N. Engberts, M. J. Blandamer, P. M. Cullis, P. M. Last, K. D. Irlam, and, L. G. Soldi, *J Chem Soc Faraday Trans.*, 1997, **93**, 1579-1584.
90. L. Piñeiro, M. Novo, and W. A. Soufi, *Colloid Interface Sci.*, 2015, **215**, 1-12.
91. S. Das, S. Mondal, S. Ghosh, *J. Chem. Eng. Data*, 2013, **58**, 2586–2595.
92. D. C. Dong, M. A. Winnik, *Can. J. Chem.*, 1984, **62**, 2560-2565.
93. H. Hoffman, R. Nagel, G. Platz and W. Ulbricht, *Colloid Polym. Sci.*, 1976, **254**, 812-834
94. P. P. Infelta, M. Gratzel and J. K. Thomas, *J. Phys. Chem.*, 1974, **78**, 190-195.
95. M. Tachiya, *Chem. Phys. Lett.*, 1975, **33**, 289-292.
96. M. M. Velázquez and Silvia M. B. Costa, *Journal of the Chemical Society, Faraday Transactions*, 1990, **86**, 4043-4048.
97. L. Wattebled, A. Laschewsky, A. Moussa, J. Habib-Jiwan, *Langmuir*, 2006, **22**, 2551– 2557.
98. M. Almgren, J. Erik, L. froth, J. V. Stam, *J. Phys. Chem.*, 1986, **90**, 4431-4437.
99. S. Ghosh, *J. Colloid Interface Sci.*, 2001, **24**, 128-138.
100. S. P. Moulik, S. Ghosh, *J. Mol. Liq.*, 1997, **72**, 145-161.
101. C. Das, T. Chakraborty, S. Ghosh, B. Das, *Colloid and Polymer Science*, 2008, **286**, 1143- 1155.
102. D. Tikarika, B. Kumar, S. Ghosh, A. K. Tiwari, S. K. Saha, N. Barbero, P. Quagliotto, K. K. Ghosh, *J. Nanofluids*, 2013, **2**, 316-324.
103. C. Das, T. Chakraborty, S. Ghosh, B. Das, *Colloid J.*, 2010, **72**, 788-798.
104. J. R. Lakowicz, *Principles of Fluorescence Spectroscopy*, Plenum: New York, (1999).
105. A. R. Soemo and J. E. Pemberton, *J. Fluoresc.*, 2014, **24**, 295–299.
106. A.R. Tehrani-Bagha, J. Kärnbratt, J.-E. Löfroth, K. Holmberg, *J. Colloid Interface Sci.*, 2012, **376**, 126–132.
107. M. Grätzel and J. K. Thomas, *JACS*, 1973, **95**, 6885-6889.
108. M. A. Cassidy, G. G. Warr, *J. Phys. Chem.*, 1996, **100**, 3237-3240.

Chapter-III

A Detailed Assessment on
The Interaction of Sodium
Alginate with A Surface-
Active Ionic Liquid and A
Conventional Surfactant: A
Multi technique Approach

A detailed assessment on the interaction of sodium alginate with a surface-active ionic liquid and a conventional surfactant: a multitechnique approach ‡

Abstract:

Investigation has been made on the interaction of a biodegradable anionic polyelectrolyte, sodium alginate (NaAlg) with two oppositely charged cationic surfactants, 1-hexadecyl-3-methyl imidazolium chloride ($C_{16}MImCl$) and 1-hexadecyl triphenylphosphonium bromide ($C_{16}TPB$), former is a Surface-Active Ionic Liquid (SAIL) and latter a conventional surfactant over a wide concentration regime of polyelectrolyte. Dual influence of electrostatic and hydrophobic interactions plays in this investigation when mixing surfactants to oppositely charged polyelectrolyte. A number of different experimental techniques, e.g., conductometry, tensiometry, steady state and time resolved spectrofluorimetry, turbidimetry, isothermal titration calorimetry (ITC), dynamic light scattering (DLS), attenuated total reflection (ATR), high resolution transmission electron microscopy (HR-TEM) and fluorescence microscopy have been implemented to get comprehensive information originated from the interaction of oppositely charged polyelectrolyte and surfactants. Tensiometry study reveals the existence of several conformations of NaAlg influenced by different concentrations of surfactants titrated to it and these are abbreviated as, critical aggregation concentration (cac), saturated concentration of polymer-surfactant complex (C_s) and finally extended critical micelle concentration (C_m^*) due to aggregation of surfactant itself, appeared in chronological order from low to high concentrations of surfactants. Apart from tensiometry, these above concentrations have been well found and the values are well comparable when investigating polyelectrolyte-surfactant interaction by other physicochemical techniques also. Irreversible phase separation of oppositely charged polyelectrolyte-surfactant complex (PS-complex) occurs at higher polyelectrolyte concentration investigated here for both the surfactants in the vicinity of cac for $C_{16}MImCl$ and near C_m^* for $C_{16}TPB$ and finally persists after further addition of surfactants above the formation of free micelles. Several bulk and interfacial parameters, viz., Gibbs free energy of micellization (ΔG_m^0), enthalpy of micellization (ΔH_m^0), entropy of micellization (ΔS_m^0), degree of counterion binding (β), surface excess at cmc (Γ_{max}), area minimum (A_{min}), surface pressure at cmc (π_{cmc}), pC_{20} , packing parameter (P), hydrodynamic radius (r) and aggregation number (N_a) of two surfactants both in presence and absence of NaAlg have been calculated for these investigated systems. Characterization of NaAlg, both surfactants and their individual complexes were performed using FTIR-ATR. DLS shows the distribution of size of polymer surfactant complexes over a wide range of surfactant concentrations at a fixed polyelectrolyte concentration, while HR-TEM study reveals not only the size of agglomerated clusters of PS-complex and also its shapes. Images of NaAlg-surfactant complexes were also captured using fluorescence microscopy in solution phase. Strong PS-complex in presence of $C_{16}MImCl$ has been reported here over $C_{16}TPB$.

(‡ Published in *Phys. Chem. Chem. Phys.*, 24, (2022) 13738-13762)

1. Introduction:

Surfactants form a specific type of aggregate in both aqueous and non-aqueous solvents at a threshold concentration, called critical micelle concentration (cmc)¹⁻³. Significant attentions have been paid for decades till now⁴⁻¹⁴ on the oppositely charged polyelectrolyte with different conventional surfactant systems for their complexation ability and rich aggregation behaviour

in aqueous solution by considering emerging applications in cosmetic and paint industries, and also in enhanced oil recovery process. This complexation ability originates from the coulombic attraction between the oppositely charged polyions and surfactant monomers as well as the hydrophobic attraction among the apolar chain of surfactants, hydrophobic moieties of polyelectrolytes and tails of surfactants. Recently,¹⁵⁻¹⁹ some interests grow on the interaction of carbohydrate type polyelectrolytes with surface active ionic liquids (SAIL) in aqueous solution¹⁵⁻¹⁹. Carbohydrate based polymers gain special attraction for their biocompatible, biodegradable and low immunogenic nature^{17, 20, 21} and on the other hand, SAILs can improve mechanical, thermal and electrochemical properties of materials in addition with polymers in industrial arenas. For example, ILs have been used as curing agents²², modifier of glass temperature transition²³, conducting agent in polymer electrolytes film²⁴ as well as building blocks of polymer matrix²⁵, as plasticizers for polysaccharides²⁶ and also as heterogeneous catalyst in conjugation with polyelectrolyte²⁷. Moreover, easy tune of hydrophobic moieties and also counterions make the ionic liquids ('designer solvents') attractive in recent scenario over conventional surfactants²⁸. Sodium Alginate (NaAlg), an anionic biodegradable polysaccharide has been synthesized from marine brown algae containing 1-4 linked α -L-guluronic (G) and β -D-mannuronic (M) acid residues arranged in an irregular blockwise pattern of varying proportions of GG, MG, and MM blocks., widely used^{12, 17, 20, 22, 29} in medical, pharmaceutical industry for the purpose of gelling agents and in food industries as a stabilizer and thickener^{21, 29}. This anionic polyelectrolyte (block copolymers) has enormous uses for the production of bio films, bandages, beads, nanoparticles, and microcapsules by recognising its significant biocompatible stable gelling properties^{29, 30} which is obtained mainly by incorporation of surfactants and inorganic salts (K_2CO_3 , $CaCO_3$ etc.) at much higher NaAlg concentration with different proportions, investigated in previous literatures.^{20, 31, 32} Keeping in mind these several uses of NaAlg in medical, pharmaceutical and food industry, a systematic study on the interaction of NaAlg with various surfactants in aqueous solution also with other additives have much needed at wide concentration range of NaAlg both for the purpose of industrial as well as academic interest. Off late, although a significant amount of research work have been devoted to elucidate the physicochemical parameters for another biodegradable polyelectrolyte, sodium carboxymethylcellulose (NaCMC) with imidazolium SAILs in aqueous solution by researchers^{16, 18, 19, 33-35}, a comprehensive physicochemical investigation on the interaction of NaAlg with imidazolium ionic liquids in aqueous solution at low to moderately high polyelectrolyte concentration scarcely found in literature¹⁷.

In this present study, investigation has been performed on the aggregation phenomena and their thermodynamics of a cationic SAIL 1-hexadecyl-3-methylimidazolium chloride ($C_{16}MeImCl$), and a conventional surfactant, 1-hexadecyl triphenylphosphonium bromide ($C_{16}TPB$) in aqueous solution in absence as well as in presence of NaAlg as a function of polyelectrolyte concentration as probed by tensiometry, conductometry, isothermal titration calorimetry (ITC), steady state and time resolved fluorimetry and dynamic light scattering at 298.15 K. Characterization of NaAlg-surfactant complexes (PS-complex) were performed using FTIR-ATR technique. Fluorescence imaging and high-resolution transmission electron microscopy (HR-TEM) were used for the visual impression of polyelectrolyte surfactant complex (PS-complex) mediated by NaAlg with different surfactants investigated here, and also determining its size and shape. Two surfactants having different head groups and same number of carbon chain have been selected to gain better insight on the effect of different head groups with NaAlg in aqueous solution, also comparing the effect of SAIL to the conventional surfactant on NaAlg.

2. Experimental section:

2.1. Materials and solution preparation:

1-Hexadecyl-3-methylimidazolium chloride monohydrate [$C_{16}MImCl$] was purchased from Acros Organics (Germany) and 1-hexadecyl triphenylphosphoniumbromide ($C_{16}TPB$), 98% has been procured from Alfa Aesar (India), a part of Thermo Fisher Scientific. Alginic acid sodium salt (NaAlg) from brown algae (W201502) was obtained from Sigma Aldrich (USA). All the samples are used without further purification. Structures of polyelectrolyte and surfactants are displayed in Fig. 1. Reagent grade (ACS reagent, $\geq 99.0\%$) NaCl, fluorescence probe, pyrene (98%), cetylpyridinium chloride (CPC) and 1,6-diphenyl-1,3,5-triene (DPH) were purchased from Sigma Aldrich (USA) and used as received.

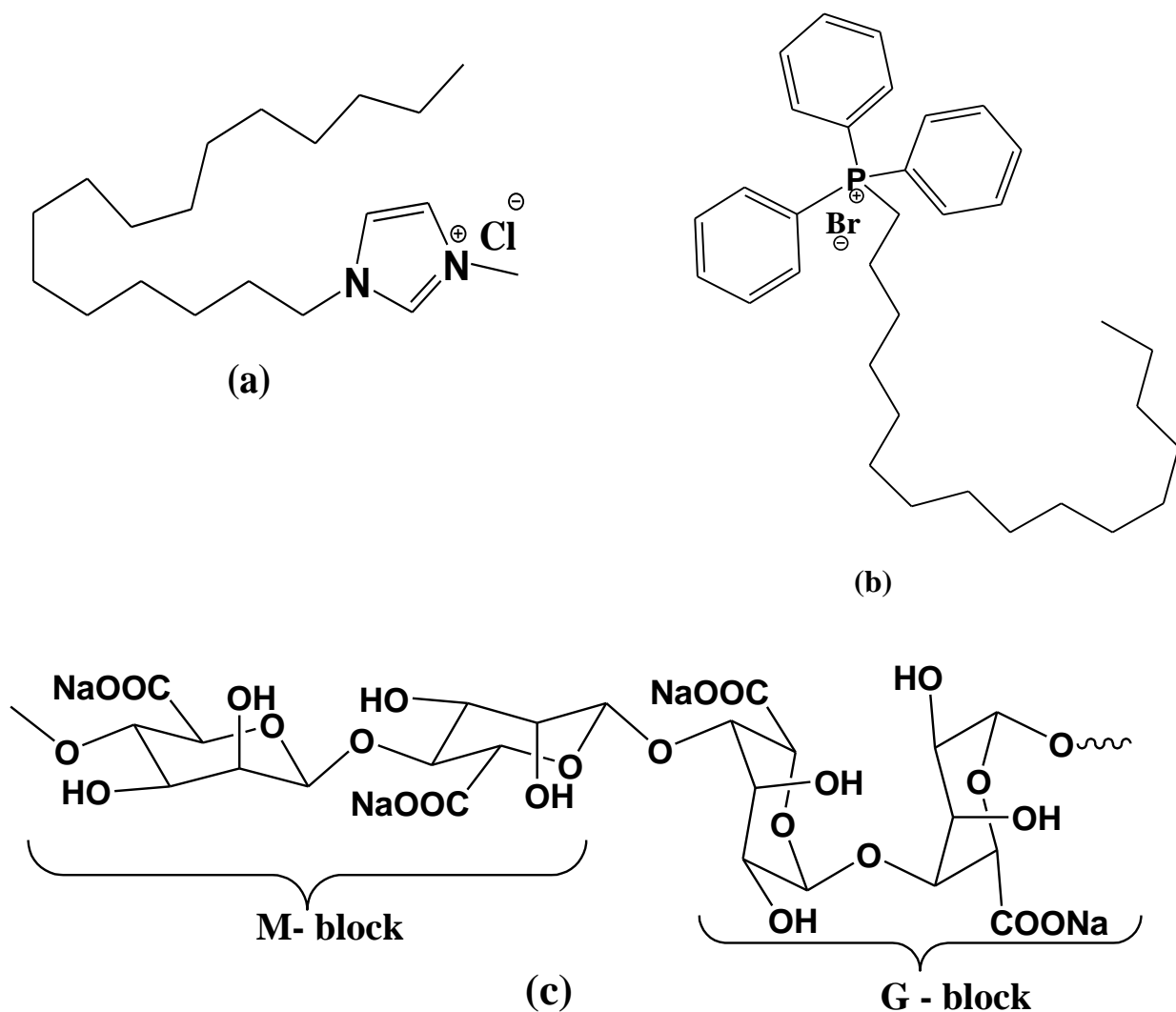


Figure 1. Structures of C₁₆MImCl (a), C₁₆TPB (b) and NaAlg (c)

All solutions are prepared in triply distilled water of specific conductance $\sim 1.0 \mu\text{S}/\text{cm}$ throughout the experiments at 298.15K. Concentration of NaAlg was chosen as 0.001, 0.005 and 0.01% (w/v) in this investigation. Polyelectrolyte concentration was fixed throughout the experiments during the titration of each surfactant to it. All the physicochemical parameters were measured after addition of stock surfactant solution to the corresponding polyelectrolyte solution of same concentration progressively with 5-10 min intervals (in short equilibration time) after proper stirring. No further modifications of any physicochemical properties with time are observed for all polyelectrolyte concentrations.

2.2. Methods:

2.2.1. Tensiometry:

A calibrated Krüss-K8 tensiometer (Germany) was used to determine surface tension at air water interface by du Noüy ring detachment method at 298.15 K. A clean platinum ring was used for this purpose. This ring has been cleaned using deionized water and acetone successively and burned briefly until glowing in ethanol flame prior to each measurement. A measured amount of 5 mL aqueous polyelectrolyte solutions (different % w/v) was taken in a double jacket container attached with a thermostatic water bath to maintain the desired temperature with an accuracy of ± 0.1 K. Stock surfactant solutions were prepared ~ 15 times above the cmcs^{19, 36-38}; shown in Table 1 & Table 2. in respective solvents (different % w/v polyelectrolyte solution) and added to the double jacket container by a Hamiltonian micro syringe and stirred well after each addition and kept for 5 minutes before taken the data. The same procedure has been followed for studying micellization of surfactants in aqueous solution also (cf. Figure. 2A (a) for C₁₆MImCl and Fig 2B (b) for C₁₆TPB.). Two or three consecutive readings of surface tension were taken for a particular addition of surfactant into polyelectrolyte solution by a syringe for better reproducibility. Surface tension of distilled water used for preparation of different solutions was found to be 70.8 mN.m⁻¹ with the precision of ± 1 mN.m⁻¹ at 298.15 K. The concentrations of NaAlg in this present study have been chosen (maximum concentration = 0.1 gm/L or, 4.6×10^{-4} mol saccharide unit/L) in such a manner that, NaAlg cannot show significant surface activity adopting extra complexity in tensiograms upon addition of surfactants. It has been observed that, surface activity of NaAlg in aqueous solution does not increase significantly even as high as of its 2×10^{-3} mol saccharide unit/L concentration at 298.15 K³⁹. Moreover, such low concentration of NaAlg deduces the possibility of polyion-polyion interaction between the alginate backbones. Representative plots of surface tension (γ) vs. log [surfactant] / mM of two surfactants at different wt% of NaAlg medium with individual inflection points (discussed elsewhere in this manuscript) were shown in Figure.3. Different interfacial parameters in presence and absence of NaAlg for both the surfactants calculated are displayed in Table 3.

2.2.2. Conductometry:

A conductivity meter (304, Systronics, India) equipped with a glass electrode (cell constant 1.0 cm⁻¹) was used for the measurement of conductance. Glass electrode was dipped in a double jacket glass container. This glass container was connected with a thermostatic water bath to maintain the solution temperature to a fixed value, 298.15 \pm 0.1K. Different % w/v of

polyelectrolyte solution (7 mL) kept in the glass container and surfactants prepared in same concentration in respective polyelectrolyte solutions, as those stated in section 2.2.1., were added from a Hamiltonian microsyringe and specific conductance values were measured. The same work has also been performed for studying micellization in aqueous solution for the two surfactants. Cmc's have been measured from the well specified inflection points represented at the specific conductance (κ) vs. total surfactant concentration plots for two pure surfactants (cf. Figure 2A (b), 2B (b)). Representative plots of specific conductance (μS) vs. [surfactant]/ mM of two surfactants at different wt% of NaAlg medium with individual inflection points (cf. Table 1 and 2, discussed elsewhere in this manuscript) were shown in Figure 4.

2.2.3. Turbidimetry:

Turbidimetry experiment was performed by using a Shimadzu 1601 UV-VIS spectrophotometer (made in Japan) at 298.15 ± 0.1 K. Baseline correction was done using different wt% of NaAlg prepared in deionized water prior to each experiment. Different wt % of NaAlg solution (2.5 mL) was taken in the cuvette for the measurement of transmittance. In the cuvette, surfactants were added using micro syringe and determined % transmittance (% T) between the wavelengths range from 200-800 nm. Plots containing absorbance ($100-\%T$) at 400 nm (average value of wavelength taken) vs. concentration of surfactants with different turbidimetry points in presence of NaAlg were displayed in Fig. 5 and values are shown in Tables 1 and 2.

2.2.4. Spectrofluorimetry:

Steady state spectrofluorimetry technique was carried out using a Perkin-Elmer LS 55 (USA) fluorescence spectrofluorimeter attached with Peltier facility at 298.15K with an accuracy of $\pm 0.02\text{K}$. Measured amount of 2.5 mL solution of different wt% of polyelectrolyte was taken in transparent quartz cuvette and prepared surfactant solution (~ 15 times above cmc in aqueous solution) in respective wt% of polyelectrolyte was added with a Hamilton micro syringe. Pyrene was used as a fluorescence probe excited at 335 nm with 14 nm band pass, while emission was monitored between wavelength ranges of 350- 550 nm with emission band pass of 4 nm. Pyrene excimer emission (occurred here nearly at 467 nm) along with monomeric vibrational peaks in presence of 0.005% (w/v) NaAlg with variation of concentration of both surfactants have been displayed in Fig. 6A and 6B. Ratio of first ($I_1 = 374$ nm) to third ($I_3 = 384$ nm) vibrational peak of pyrene (I_1/I_3) vs. [surfactant] in absence and presence of NaAlg

have been represented in Fig. 2A(c), 2B(c) and Fig. 7 (a-f) respectively. Probe concentration (1×10^{-4} mM) was kept fixed in both cuvette and syringe.

Time resolved fluorescence experiments have been performed by means of Horiba–Jobin–Yvon Fluoro Cube lifetime arrangement using time-correlated single photon counting (TCSPC) technique at 298.15 K. A Nano LED (IBH, UK) of 330 nm was used as excitation source of pyrene. Emission was monitored at 374 nm corresponding to pyrene first vibronic peak using TBX photon detection module. Decay profiles (at the inset of Fig. 8A and 8B) of pyrene in pure polyelectrolyte and in presence of surfactants titrating into it were fitted and analysed with the support of IBH DAS-6 software by nonlinear least square iterative method to minimize residual values (χ^2 values close to 1). The experimental procedure was same as those stated in steady state method. Lamp profile was collected using micellar aqueous solution of SDS, which is used as a scatter in place of sample. Average lifetime ($\langle \tau \rangle$) was calculated from the bi exponential iterative fitting in presence of surfactants using the pre-exponential factors (a_1, a_2) and decay times (τ_1, τ_2) with the assist of following equation:

$$\langle \tau \rangle = a_1 \tau_1 + a_2 \tau_2 \quad (1)$$

The values of a_1, a_2 and τ_1, τ_2 were given in Table S1 (refer to the supplementary section). Pyrene concentration was fixed to 1×10^{-4} throughout the measurements. Here 0.005 % (w/v) of NaAlg was used for TCSPC measurement.

2.2.5. Isothermal titration calorimetry:

Isothermal Titration Calorimetry (ITC) was executed with the help of a GE, MicroCal ITC₂₀₀ (Malvern, UK) microcalorimeter equipped with a thermostatic arrangement. Experimental temperature was maintained at 298.15 K with a precision of ± 0.02 K. In this investigation, surfactant solutions were prepared 10-15 times above their cmcs (cf. Table 1), those measured by conductometry and tensiometry in aqueous polyelectrolyte solution of different weight fractions. Deionised water and different aqueous % (w/v) NaAlg solution (200 μ L) taken in calorimeter cell and surfactant solutions was titrated (initially 0.5 μ L, then 2 μ L; total 20 injections) at a time interval of 120s using a micro syringe. Polyelectrolyte concentrations were fixed both at cell and in the syringe. Raw data were analysed by OriginTM 7.0 software in terms of μ cal/s vs. Time (min) [such plots regarding both surfactants shown in Fig. 9e & 9f in presence of 0.001% (w/v) NaAlg] after the subtraction of integrated baseline which was performed by taking deionized water in reference cell and polyelectrolytes with different

concentrations at the sample container (cell) prior to each experiment. Enthalpies of micellization (ΔH^0_m) determined (cf. Table.4.) from the normalised integration data plot (kcal.mol⁻¹ per mole of injectant vs. concentration of surfactant [Surf]; cf. Fig. 9(c) and 9(d)) obtained by the software with assistance of instrument generated data in terms of $\mu\text{cal/s}$ vs. Time (min) (cf. Fig. 9(e) and 9(f)). Cmc's were measured for all the systems from kcal.mol⁻¹ of injectant vs. [Surf] plots [shown in, Fig. 9] designated by arrow. Cmc values [Table 1 and 2] determined by ITC found well similarities with those obtained by other techniques for two surfactants both in presence and absence of different polyelectrolyte concentrations. ITC profiles of pure surfactants in aqueous solution were displayed in Fig. 2A (d) and 2B (d).

2.2.6. FTIR-ATR spectroscopy:

FT-IR spectra were performed using a Perkin Elmer (model no. spectrum Two) FTIR spectrometer using attenuated total reflectance (ATR) technique. A LiTiO₃ detector has been used to measure spectra. Small amount of samples was taken in diamond plate and pressure was adjusted and performed measurements between the ranges of 500-4000 cm⁻¹ wavelength. NaAlg, surfactants and NaAlg-surfactant complexes were characterized (shown in Fig. 10A and 10B). To prepare polyelectrolyte surfactant complex, 2mL 0.08% (w/v) of NaAlg has been mixed with 1.28 mL 15 mM surfactants (both C₁₆MImCl and C₁₆TPB separately in two vials) prepared in 0.01% (w/v) NaAlg. Phase separation occurred after addition and these were well sonicated at room temperature. The resultant polyelectrolyte-surfactant complexes were dried under vacuum.

2.2.7. Viscosity:

Average viscometric molecular weight (M_v) of NaAlg was determined with the help of an ubbelohde viscometer fitted in a thermostatic water bath at 298.15 K in the medium of 0.1 M NaCl, used as solvent. Using Mark–Houwink equation, viscosity average molecular weight of sodium alginate was found to be 123.19 kDa at 298.15K. Detailed procedure⁴⁰⁻⁴³ and the relevant values for determination of M_v have been shown in supplementary section (Fig.S1). Ratio of mannuronic (M) to guluronic (G) acid (M/G) was found to be 0.45 obtained⁴⁴ from absorption intensity values at 1123 and 1025 cm⁻¹ respectively in FTIR profile of pure alginate (Fig.10). The intense band at 1025 cm⁻¹ (Fig.10) clearly suggests that NaAlg used in this study contains high amount of guluronic acid.

2.2.8. Dynamic Light Scattering (DLS):

DLS measurement was performed using a Nano ZS Zetasizer (Malvern, UK) measuring at 90° angle with an exposure of He-Ne laser having wavelength (λ) of 632.8 nm at 298.15 K under thermostatic control. Experimental NaAlg solution (0.01% w/v) of 1mL was taken in a fluorescence cell and both surfactants were added using micropipette. Each time the solution was thoroughly mixed after addition of surfactant prior to each measurement. Experiments were repeated twice for reproducibility. Computer generated % Intensity vs. Size (r .nm) plots in presence of 0.01% (% w/v) of NaAlg for varying the concentration of both surfactants were presented in Fig. S2 in the supplementary section.

2.2.9. High Resolution (HR) transmission electron microscopy (TEM):

TEM images of sodium alginate associated with surfactants were obtained using a JEOL JEM 2010 (Tokyo, Japan) high resolution transmission electron microscope (HRTEM) operating at 200 kV. One small drop of a solution was prepared in 0.01% (w/v) NaAlg for both the surfactants, where surfactant concentration exceeded individual C_m^* values. This drop was placed onto a gold-coated copper grid, and it was then kept overnight on dried silica gel prior to the measurement being taken.

2.2.10. Fluorescence microscopy:

Fluorescence images were taken from Olympus inverted fluorescence microscope (model-IX73: one deck system). DPH was used as a fluorophore, prepared in absolute EtOH and taken in less turbid solutions containing NaAlg (0.01% w/v) and both surfactants individually above 2-3 times of C_m^* . Final DPH concentration remains 0.1 mM in surfactant containing polymer solutions. DPH containing polyelectrolyte-surfactant solutions were kept overnight prior to measurements. Fluorescence images were taken using FITC filter attached to the instrument with 100X zooming.

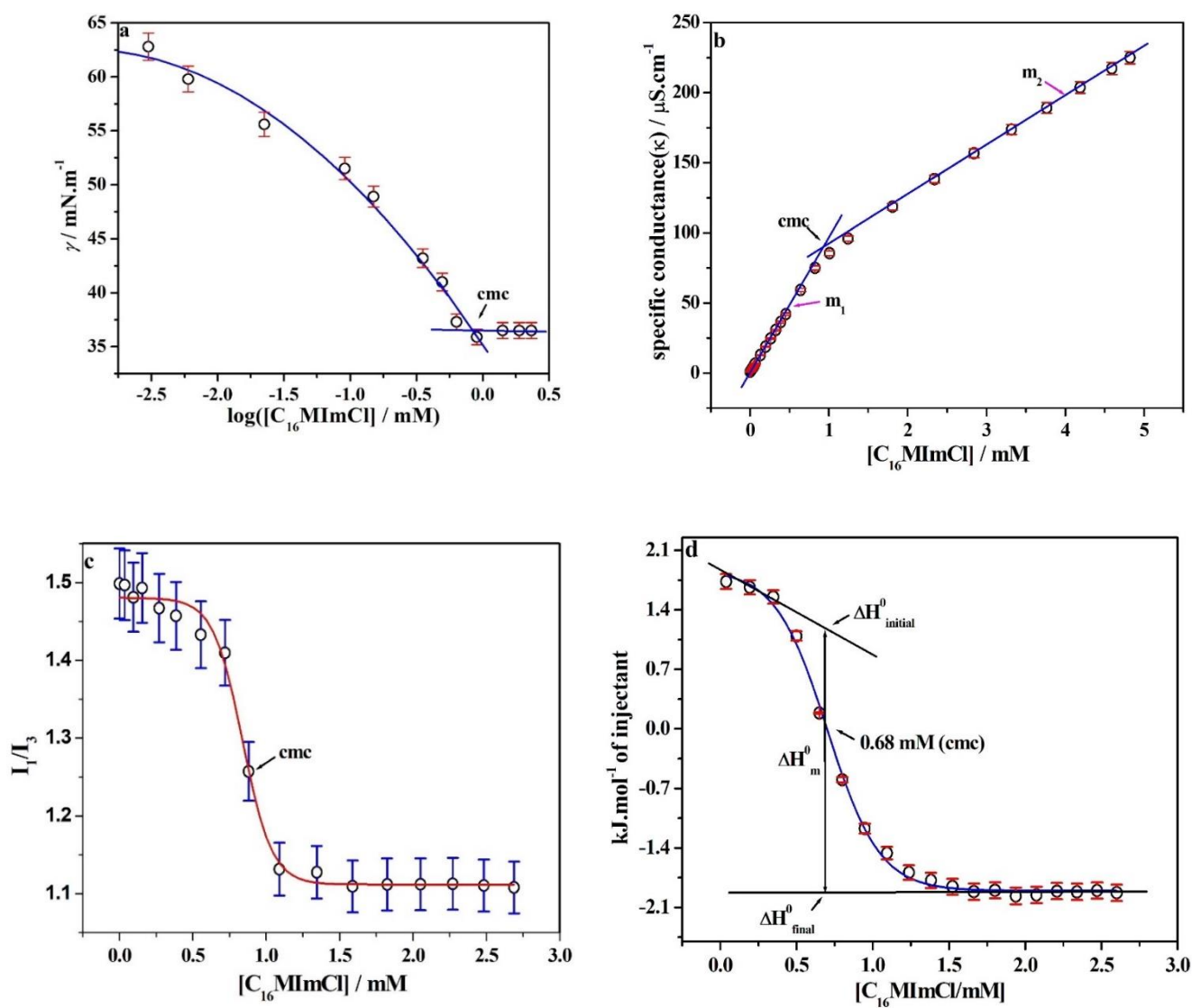


Fig. 2A: cmc of C₁₆MImCl determined by several experimental techniques: Tensiometry (a), Conductometry (b), spectrofluorimetry (c) and ITC (d). Error bar is given in each plot.

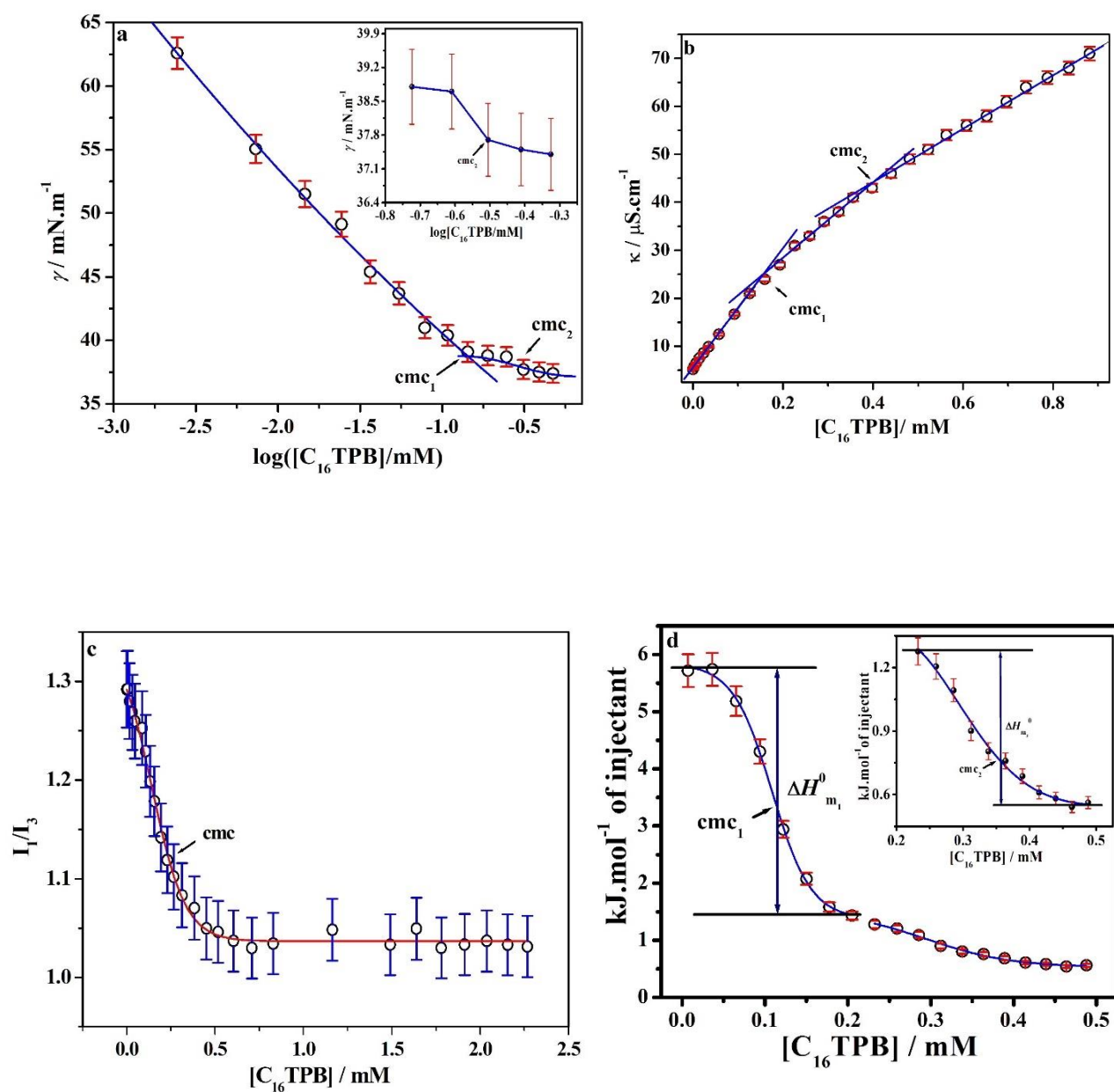


Fig. 2B: cmc of $C_{16}TPB$ determined by several experimental techniques: Tensiometry (at the inset: zoomed view of cmc_2) (a), Conductometry (b), spectrofluorimetry (c) and ITC (at the inset: zoomed view of cmc_2) (d). Error bar have been introduced

3. Results and discussions:

3.1. Tensiometry: Surface active and inactive polyelectrolyte-surfactant complex formation, Effect of polyelectrolyte concentrations, Interfacial and bulk parameters:

Critical micelle concentration (cmc) of a pure surfactant has been unambiguously determined from surface tension (γ) vs. \log [surfactant] profiles by taking a sharp break point (cf. Fig. 2) which designates the onset of micellization. Surface tension profiles of two pure surfactants have been displayed in Fig. 2A (a) for $C_{16}MImCl$ and 2B (a) for $C_{16}TPB$. The appearance of these two tensiometric profiles of both surfactants differs in the premicellar regions. Existence of second cmc (cmc_2) for the micellization of $C_{16}TPB$ have been found earlier^{36, 38} by means of conductance measurement. Although cmc_2 of $C_{16}TPB$ was not focused by tensiometric technique earlier³⁸, here second break (cmc_2) for pure $C_{16}TPB$ may have been obtained after precise investigation and zooming in small changes of surface tension (from 38.8 to 37.4 $mN.m^{-1}$, at the inset of Fig. 2B(a)) in this region after cmc_1 . The second micellar transition (cmc_2) as the existing micelles those appeared in first inflection region might have undergone secondary aggregation or change in shape and size⁴⁵. These small changes in γ may be due to the fact that tensiometric technique (interfacial properties) lost its significance in its lowering regions at high surfactant concentration in the bulk. Besides the found cmc_2 value of $C_{16}TPB$ is quite similar to those obtained by the other techniques (viz. conductometry, ITC; cf. Table 2). On the other hand, pure $C_{16}MImCl$ shows only one sharp break point in the tensiometry profile (Fig. 2A (a)). Apart from tensiometry, pure $C_{16}MImCl$ also shows only one inflection point determined by other methods (refer to Table 1). Tensiometric profile of pure $C_{16}MImCl$ initially decreases slightly with sparsely surfactant populated at air/water interface, while for $C_{16}TPB$, amphiphile molecules co-operatively get populated from the very low concentration of surfactant.

In presence of polyelectrolyte NaAlg, the situation is quite complex. Tensiograms (Fig 3A & 3B) exhibit several inflection points during studying micellization of both $C_{16}MImCl$ and $C_{16}TPB$ respectively in presence of varying concentration (% w/v) of sodium alginate due to strong electrostatic interaction between anionic NaAlg with cationic surfactants in the premicellar regime.

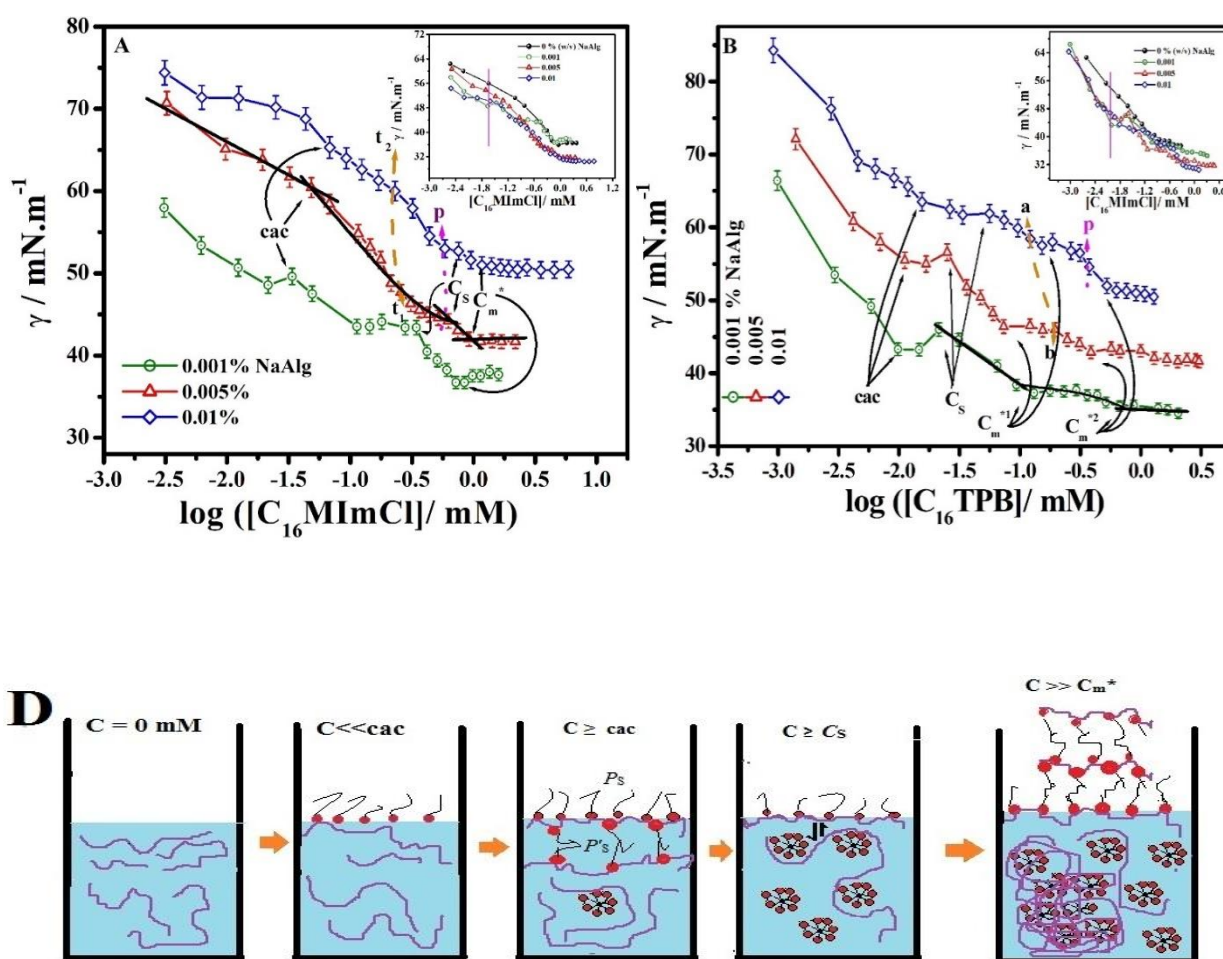


Fig. 3. Tensiometry profiles of (A) γ vs. $\log ([\text{surfactant}]/C)$ for the micellization of $C_{16}\text{MImCl}$; (B) $C_{16}\text{TPB}$ in presence of different wt% (w/v) of sodium alginate. Each tensiogram has been shifted 10 units upward for better visualization of break points. At the inset: comparative plots of surfactants in aqueous and in presence of different % (w/v) of NaAlg without changing the scale. Error bars are given in surface tension plots (D) Schematic diagram of different species was found due to interaction of oppositely charged polyelectrolyte and surfactants. At the inset of fig 3A & 3B: comparable line diagrams for tensiometric profiles of surfactants in presence and absence of NaAlg without shifting the data towards surface tension axes.

The decreasing pattern of pre micellar regions of surfactants in presence of NaAlg resemble with the alginate free tensiometry profiles (cf. Fig. 2A (a) & 2B(b)) of respective pure surfactants. It has been seen from the inset of Fig. 3A and 3B that, surface tension values decrease rapidly at the low surfactant concentration in presence of NaAlg in contrast with alginate free pure one. The decrement is more produced in 3B in case of $C_{16}\text{TPB}$ at all NaAlg concentration. This initial decrease in surface tension clearly indicates some sort of modification in terms of surface activity of surfactants adopted in presence of sodium alginate. Degen *et. al.*¹² have been shown the significant increase in interfacial thickness due to

formation of thin monolayer at liquid–gas interface upon addition of low concentration of surfactants (CTAB, DTAB and TTAB) on 0.1 g/ml NaAlg aqueous solution as compared with NaAlg free surfactant solution of same surfactant concentrations by X- ray reflectivity technique. The pattern of tensiograms for all alginate concentrations in presence of respective surfactant/NaAlg found to be more or less similar and different for different surfactants investigated here. With addition of C₁₆MImCl in 0.001% NaAlg solution surface tension initially decreases followed by a slight hump observed which is associated with another linear rapid decrease in tensiometric profile on further addition of ILs. Initial decrease is mainly attributed to the pure IL adsorption on the air –water interface; then on further addition of C₁₆MImCl, second decrease in tensiometric profile is observed due to formation surface active NaAlg - C₁₆MIm⁺ complex owing to electrostatic reason along with monomeric adsorption. This small hump has been reasonably chosen as the threshold concentration corresponding to the onset of surface-active polyelectrolyte-surfactant complex formation at the interface, called critical aggregation concentration (cac). Adsorption of IL on NaAlg backbone at the interface leads to the increase of hydrophobicity of the complex and they preferably populate at Langmurian interface. On further addition of IL, there occurs a large plateau after the formation of surface active anionic NaAlg- C₁₆MIm⁺ complex. Formation of plateau is attributed to the non-surface active NaAlg-C₁₆MIm⁺ complex associated with the formation of small micellar aggregates of C₁₆MImCl wrapped by alginate backbone (necklace like conformation). This phenomenon is observed at a concentration, called polymer saturation concentration, C_S, (displayed in Fig. 3A). After that IL molecules again repopulate at air water interface leading to the decrease in the value of surface tension again and finally, free micelle of C₁₆MImCl is formed after complete saturation of interface at a particular surfactant concentration called extended critical micelle concentration (C_m^{*}) just like cmcs of pure surfactants. After that, surface tension does not vary with surfactant concentrations. Formation of large plateau has been stated above was also documented in previous study due to formation of surface-active polyelectrolyte surfactant (IL) complex (AHX/ C_nMImBr system, n = 12, 14, and 16), by de Freitas *et. al.*¹⁷ at lower polyelectrolyte concentration (0.01 g L⁻¹ of AHX). Sometimes, maxima have also been reported (previously reported systems, NaCMC/C₁₆MImCl¹⁹, NaCMC/C_nMImBr (n = 14 and 16)¹⁸) in this region after cac due to dislodging of polyelectrolyte-surfactant complex from air-water interface to bulk. Unlike 0.001% (w/v) NaAlg, different behaviours were observed in the tensiograms while studying the interaction of IL with higher concentration (0.005% and 0.01%) of NaAlg. From Fig. 3A, it has been seen

that in both 0.005% and 0.01% of NaAlg, addition of IL initially decreases surface tension mildly, beyond which surface active NaAlg-C₁₆MIm⁺ complex is formed (at cac) leading to stiff nonlinear decrease in surface tension profiles until the completion of non-surface active NaAlg-C₁₆MIm⁺ complex (at C_S) at bulk. The nonlinear decrease is also due to the hydrophobic interactions between the NaAlg backbones wrapped with ILs and small micelle-like aggregates of ILs. Such type of appearance in tensiometric profiles of oppositely charged polyelectrolyte and surfactant have been shown by our group¹⁰. Widths of plateaus were gradually shortened from 0.001% to 0.005% NaAlg concentration and finally remain disappear at 0.01% NaAlg. The disappearance of plateau at high alginate concentration might be attributed to the increase of NaAlg population at the interface leading to increase of the stability of surface active polyelectrolyte-surfactant complex for the greater ease of electrostatic interaction between oppositely charged NaAlg and ILs and hindered the early formation of necklace type conformations at bulk. Screening of small IL aggregates neutralizes the surface charge density of NaAlg backbone leading to appearance of turbidity and finally, increased hydrophobicity due to formation of larger IL aggregates wrapping in NaAlg backbone and also inter chain interaction between NaAlgs leading to coacervation. These coacervates may be partially soluble in micellar medium of IL near C_m^{*}. At low NaAlg concentration (0.001% w/v) no noticeable turbidity was found during the whole course of addition of IL, whereas, for 0.005 and 0.01% NaAlg, visual coacervates appear after cac and partial phase separation appeared near C_S. Threshold concentration for the first appearance of coacervate was displayed in the tensiograms of 0.005 and 0.01% NaAlg in conjugation with IL by a both side double headed arrow connecting a solid line between t₁ and t₂ and phase separation zone presented by a dotted curve indicating the symbol p (cf. Fig. 3A). Phase separation in presence of 0.005 and 0.01% NaAlg with IL is transient in nature and converted to complex coacervates after further addition of ILs. We cannot detect the threshold concentrations where maximum turbidity appeared visually which in terms is obtained by turbidimetry measurement (refer to Sec. 3.1). These coacervates were slightly soluble in micellar medium after C_m^{*} manifested in turbidity profiles (cf. Fig. 5(a), (b) and (c)). Both turbidity and phase separations were appeared at relatively lower IL concentrations when the increase of the concentration of NaAlg from 0.005 to 0.01% (w/v) due to the increased hydrophobicity in solution. The tensiometric profiles of C₁₆MImCl in presence of 0.001, 0.005 and 0.01% (w/v) concentrations of NaAlg with the different inflection points, cac, C_S and C_m^{*} are presented clearly in Fig. 3A.

Addition of C₁₆TPB into NaAlg differs appreciably (cf. Fig. 3A) from the profile of C₁₆MImCl, especially at low surfactant concentration regime. With the increase of the concentration of C₁₆TPB, surface tension rapidly decreases initially, after that increases in the tensiometric profiles in presence of 0.001 and 0.005% NaAlg, whereas a large plateau appears in presence of 0.01% NaAlg. Initial surfactant concentrations at which surface tension values increase, are termed here as c_{ac} and C_s respectively. Formation of maximum values of surface tension can be explained in terms of Taylor *et. al.*^{46,47} regarding the stability between P_s and P'_s complexes (see Fig. 3D) referred to the surface active polyelectrolyte- surfactant complex and another surface-active polymer-surfactant complex binds on to the underside of P_s complex respectively. As C₁₆TPB head groups, containing three bulky phenyl groups, bind weakly to the NaAlg, surface activity due to P_s complex was somewhat compromised comparing with free C₁₆TPB monomers adsorption manifested in the absence of decayed tensiometric trends (cf. Fig.3B) after free surfactants adsorption at low surfactant concentration; those present in the tensiograms of C₁₆MImCl in presence of NaAlg (cf. Fig. 3A). Moreover, instability in P_s and later P'_s dislodges polyelectrolyte-surfactant complex in bulk from the interface as a consequence of formation of bulk necklace type conformation (stated above), forming maxima at C_s at 0.001 and 0.005% NaAlg solution. Surplus of polyelectrolytes at 0.01% NaAlg injects little stability in P'_s as the availability of more charged site is introduced with increasing NaAlg concentration, resulting to the formation of large plateau appeared without maximum. Schematic diagram has been displayed compiling all the conformations of NaAlg originated from the interaction with surfactants along with free surfactant aggregates with notations discussed here in Fig. 3C. After complete saturation of NaAlg backbone by means of small micelle like aggregates (at C_s , cf. Fig. 3B) of C₁₆TPB covering, free C₁₆TPB again populate at interface up to a certain concentration where free micelle formation (first extended cmc) occurred at C_m^{*1} . This process repeats itself as the increase of free monomer again forms second inflection point corresponding to the formation of another aggregates, which may be changed in shape and size relative to former aggregates, at C_m^{*2} . The extended second cmcs (C_m^{*2}) of C₁₆TPB in presence of NaAlg were clearly visible in Fig. 3B. Moreover, it has been seen from Fig. 3B that, the sharp inflections appear in the region of first cmc at low polyelectrolyte concentrations, whereas, at high alginate content, prominent second inflection point (C_m^{*2}) appears. First visible coacervate was appeared during the addition of C₁₆TPB to alginate solution after C_m^{*1} in presence of 0.005% NaAlg, whereas turbidity appears near C_m^{*1} at 0.01% alginate concentration. Transient phase separation of polyelectrolyte-surfactant (C₁₆TPB)

complex only occurred after C_m^{*2} in presence of 0.01% of NaAlg. The concentration zone where visual turbidity first appeared was denoted by a curved line of ab. The appearance of late coacervates in presence of C_{16} TPB as compared with C_{16} MImCl clearly indicates weak electrostatic interaction operating in the complexation process of NaAlg- C_{16} TPB combination comparing with NaAlg- C_{16} MImCl system. The turbidity that appeared at near C_m^{*1} for 0.005 and 0.01% NaAlg solution might be slightly soluble in micellar aggregates of C_{16} TPB. Phase separated complexes comprise of 0.01% NaAlg with C_{16} TPB are further converted to complex coacervates before C_m^{*2} on further addition of C_{16} TPB and are negligible soluble in micellar medium manifested in turbidimetric plots (cf. Fig. 5(f)). Solubilization of these polyelectrolyte-surfactant complexes occurs either in partially dissociated or rearranged form³⁵ into micellar hydrophobic core. The tensiometric profiles of C_{16} TPB in presence of 0.001, 0.005 and 0.01% (w/v) concentrations of NaAlg with the different inflection points, cac, C_s and C_m^* are clearly depicted in Fig. 3B.

The appearance of minima and subsequent maxima in the γ isotherms is not a rare phenomenon⁴⁸. The existence of a surface tension peak or a pleatu have also been recorded for the oppositely charged polyelectrolytes-conventional surfactant systems: PDADMAC–SDS system⁴⁹ and NaPSS–DTAB system^{46,47} respectively in between the region of cac and C_s . This phenomena in case of oppositely charged polyelectrolyte in combination with surfactant also have been explained by Ábraham *et al.* as the transient states to the pseudo equilibrium isotherm⁵⁰. In fact, the study of oppositely charged polyelectrolyte-surfactant system, PDADMAC–SDS system by Campbell *et al.*⁵¹ after aging the samples to three days (time dependent investigation) showed the different pattern of surface tension isotherms with time. This observation of Campbell *et al.* leads to the expiation that the depletion of surface active polyelectrolyte-surfactant complexes take place from interface to balk and settled down in form of precipitation after aging which is manifested in cliff edge peak in surface tension isotherm⁵¹, which is also reflected in peak height at which surface tension suddenly rises. To defined these types of systems properly Guzman *et al.* concluded that, it is necessary to leave the mixtures to stabilize for 24-48 hours before taking any measurement⁵². However, in present study, the appearance of maximum in the surface tension isotherms (0.001 and 0.005% NaAlg in presence of C_{16} TPB) show small in magnitude with absence of significant phase separation in between cac and C_s and it has been seen that the turbidity values remains more or less constant after aging to 48 hours and no precipitations settled down. Kinetically trapped oppositely charged polyelectrolyte-surfactant complexes sometimes have been formed due to

fast mixing of polyelectrolytes with surfactants as a consequence of non-equilibrium mixing as pointed out in previous literature⁵³. Moreover, it has also found that, more or less same turbidimetry data was found for the set of solutions at same concentration (which concentration have been studied in surface tension measurements) of surfactants at 0.005% (w/v) of NaAlg by using the both mixing protocols (slow and fast) rule out the possibility of kinetically trapped NaAlg-surfactant complex for the both investigated systems. Similar observation have been found for the mixing of sodium poly[(vinyl alcohol)-co-(vinyl sulfate)] with DTAB not forming any kinetically trapped complex⁵⁴.

The values of cac , C_S and C_m^* as well as pure cmcs are presented in Tables 1 and 2 for $C_{16}MImCl$ and $C_{16}TPB$ respectively. From Table 1, it has been seen that C_m^* of $C_{16}MImCl$ gradually increases with the increase in proportion of NaAlg as compared with its pure state indicating delayed micellization in presence of NaAlg. This observation has been recorded in previous literatures^{10, 13} for oppositely charged polyelectrolyte and cationic surfactants and explained in terms of increase of charge centres with the increasing proportion of polyelectrolyte and consequent increase of the number of surfactant monomers to neutralize them before reaching C_m^* . For this reason, cac and later C_S also increase with increasing the concentration of NaAlg during the addition of IL shown in Table 1. On the other hand, a slight decrease in C_m^{*1} and C_m^{*2} values is observed at 0.005% NaAlg in presence of $C_{16}TPB$ while comparing C_m^* by other techniques (cf. Table 2.) discussed in the latter sections. Similar observation has been reported formerly in HTAB + 0.005% NaPSS, TTAB + 0.005% DX and NaPSS, DDGB + 0.005% NaCMC systems by conductometric measurements⁵⁵. Same type of minimum point was also observed while determining C_S at the intermediate NaAlg concentration for $C_{16}TPB$ at 0.005% NaAlg solution in this study. Probably, the difference of head groups between $C_{16}MImCl$ and $C_{16}TPB$ is responsible for such type of difference during micellization in presence of same wt % of NaAlg, former shows a straight forward increasing pattern in C_m^* (Table 1) and later a minimum point is found in both C_m^* (cf. Table 2).

From tensiometric isotherms (cf. Fig. 3A and 3B), the efficiency of surface adsorption of surfactant monomers of both $C_{16}MImCl$ and $C_{16}TPB$ has been measured at cmc or C_m^* in terms of surface excess (Γ_{cmc}) in presence and absence of NaAlg using Gibbs adsorption equation¹⁷:

$$\Gamma_{cmc} = \frac{1}{2.303nRT} \lim_{C \rightarrow cmc(C_m^*)} \frac{d\gamma}{d \log C} \text{ mol.m}^{-2} \quad (2)$$

Here, n is the number of species dissociated per monomer of surfactants adsorbed at interface. The value of n is 2 for both the surfactants. R is the universal gas constant and T is the temperature in Kelvin scale. $(d\gamma/d \log C)$ was defined as the slope at cmc or C_m^* . $(d\gamma/d \log C)$

was determined from the tensiograms (cf. Fig. 2A (a), 2B (a) for pure surfactants and Fig. 3 in presence of alginate) by taking γ with corresponding \log [surfactant] values upto cmc/C_m^* and fitted them with second order polynomials ($Y = A + B_1X + B_2X^2$) of fairly good R^2 values displayed in the supplementary section (Fig. S3). Coefficients of A, B_1 and B_2 values for all the systems were given in Table S2 (Supplementary Section). In principle, the bulk concentration (c) of surfactants should be replaced by the chemical activity, (a)⁵⁶ for the corresponding surfactant using the equation, $a = \gamma C$, where, γ activity coefficient of corresponding surfactants both in presence and absence of NaAlg in different wt% aqueous solution. It has been stated that, for dilute system, concentration of surfactants must be in the order of ~ 1 mM, while for nonideal system surfactant concentration in the order of ~ 100 mM⁵⁷. In this present study, investigated surfactant concentration mentioned within the limit of ideal range. Under these circumstances, Eq. 2 can be reasonably used as an approximation as γ nearly independent in this investigated concentration range⁵⁸. In case of $C_{16}TPB$, the values of γ have been taken with corresponding $\log [C_{16}TPB]$ values upto cmc_1 for pure $C_{16}TPB$ and C_m^{*1} in presence of different wt% of NaAlg for determination of Γ_{cmc} and hence, it has been designated here as Γ_{cmc}^1 (refer to Table 3). Three bulky triphenyl containing phosphonium groups with relatively less charge density of pure $C_{16}TPB$ did not allow it for preferable adsorption on air-solution interface over $C_{16}MImCl$, while latter has relatively smaller head group size manifested in lower Γ_{cmc} value of $C_{16}TPB$ than $C_{16}MImCl$ as seen in Table 3. The values of Γ_{cmc} and Γ_{cmc}^1 of both surfactants in presence of NaAlg have lower magnitude while comparing with their pure states shown in Table 3 in aqueous solution. The values of Γ_{cmc} of $C_{16}MImCl$ in comparison with NaAlg-free aqueous solution initially decreases rapidly at 0.001% (w/v) NaAlg solution, increases slightly at 0.005% NaAlg solution, beyond which further decrease occurs at 0.01% NaAlg concentration. The same observations have been found in case of $C_{16}TPB$ with increasing NaAlg concentration. Initial huge decrement of Γ_{cmc} or Γ_{cmc}^1 of $C_{16}MImCl$ and $C_{16}TPB$ respectively at lower NaAlg concentration (0.001% w/v) is due to lesser population of surfactants present at interface than bulk due to electrostatic interaction of oppositely charged surfactants with NaAlg. However, both increase and decrease occurred at larger extent in Γ_{cmc}^1 profile for $C_{16}TPB$ over the entire NaAlg concentrations comparing with the same in presence of $C_{16}MImCl$ (See Table 3.). The increase in Γ_{cmc}^1 or Γ_{cmc} of $C_{16}TPB$ and $C_{16}MImCl$ respectively at 0.005% (w/v) NaAlg solution, shown in Table 3.; former is due to the increasing adsorption of $C_{16}TPB^+$ monomers at the interface after clearance or depletion of surface active polyelectrolyte surfactant complex

from interface to bulk after C_s to some extent, and latter is due to the formation of surface active polymer complex in larger extent after cac.

Guzman, Thomas, Eastoe, Penfold, and others⁵⁹⁻⁶⁴ have been shown that, neutron reflection (NR) and Gibbs surface excess method using surface tension (ST) have given the similar satisfactory results to wide variety of nonionic surfactant, including polymer or polydisperse system in the proximity of cmc or at lower concentration beyond cmc. The consistency of two methods suggests that, the surface have been saturated near completely before cmc. The major discrepancy arises in case of ionic surfactants, especially for anionic surfactant, where, it has been seen that, ST underestimates Γ_{cmc} values in comparison with NR⁶⁵. Moulik et. al.⁶⁶ have calculated Γ_{cmc} for ionic surfactants using the second order polynomial fitting of γ -log [Surfactant] plots taking the data of γ from the very beginning (surfactant concentration nearly equal to zero) upto cmc using Gibbs equation (Eq. 2). They found that, taking reliable data for γ values of SDS from another source [Addison and Hutchinson et. al.⁶⁷], calculated Γ_{cmc} using ST method found quite similarly than those found by NR. Although NR have been used as an excellent technique for determination of Γ_{cmc} ⁵⁹⁻⁶⁴, ST method using polynomial fitting give Γ_{cmc} values which have fair representability to NR for ionic surfactants and they⁶⁶ pointed out the apparent discrepancy for determine Γ_{cmc} by NR to ST in terms of impurity present in surfactant or lacuna in measurement of experimental data. So, it is reasonable to use Eq. 2. for determination of $\Gamma_{cmc}/\Gamma_{cmc}^1$ in absence of NR facility.

Minimum area of surfactant monomers (A_{min}) at air-water interface can be obtained using the following equation:

$$A_{min} = \frac{10^{18}}{N_a \Gamma_{cmc}} nm^2 / \text{molecule} \quad (3)$$

A_{min} has the reverse order with Γ_{cmc} , as the minimum surface area of surfactants increases; decrease in surface coverage is possible in terms of decrease in Γ_{cmc} and also vice versa. The term A_{min}^1 was denoted for the $C_{16}TPB$ in presence and absence of NaAlg whereas A_{min} for $C_{16}MImCl$. The values of A_{min} and A_{min}^1 have been presented in Table 3.

Efficiency of adsorption of amphiphiles on air-water interface in presence and absence of various wt% (w/v) of NaAlg have been defined by the parameter, $p^{C_{20}}$,

$$p^{C_{20}} = -\log_{10} C_{20} \quad (4)$$

The term C_{20} has been defined as the concentration at which reduction of surface tension of amphiphiles is 20 mN m⁻¹. Higher $p^{C_{20}}$ values indicate high efficiency of adsorption of amphiphiles at air – water interface and consequently more reduction of surface tension. Higher

$p^{C_{20}}$ value of pure C₁₆TPB compare with C₁₆MImCl indicates high efficiency of adsorption of C₁₆TPB at air-water interface. From Table 3, it has been seen that, adsorption of both surfactants was overall enhanced in presence of NaAlg and increases at high NaAlg contents. Surface pressure at cmc/ C_m^* (π_{cmc}) can be defined by the expression given below:

$$\pi_{cmc} = \gamma_S - \gamma_{cmc (or) C_m^*} \quad (5)$$

where, γ_S is the surface tension of pure solvents (deionised water, different wt% (w/v) of NaAlg in deionised water) and $\gamma_{cmc (or) C_m^*}$ is the surface tension of pure surfactants at cmc in aqueous solution or surface tension of surfactants at cmc (C_m^*) in presence of varying wt % (w/v) of NaAlg.

The symbol of γ_{cmc} with two superscripts 1 and 2 designate γ_{cmc} at cmc₁ and cmc₂ or C_m^{*1} and C_m^{*2} respectively for surfactants both in pure state and in presence of polyelectrolytes. From Table 3, it is seen that, π_{cmc} denotes the effectiveness of amphiphiles to reduce surface tension of a solvent medium while dissolute in it. The values of π_{cmc} of C₁₆MImCl and C₁₆TPB in presence and absence of NaAlg have been displayed in Table 3. Superscripts 1 and 2 denote first and second cmcs or first and second C_m^* respectively whichever is applicable. From Table 3, it is seen that C₁₆MImCl is more effective in reducing surface tension at C_m^* in its pure state as compared with C₁₆TPB in aqueous solution and improved effectiveness in reducing surface tension at C_m^* observed in presence of NaAlg for both the surfactants.

The geometrical shape of micelle can be defined by a parameter, called packing parameter (P), which was defined by Israelachvili⁶⁸ as,

$$P = \frac{v}{l_c A} \quad (6)$$

v and l_c were defined as the volume of the hydrocarbon chain of surfactant assuming it to be fluid and incompressible and maximum effective length of that hydrophobic chain, respectively. A is the area of the surfactant head groups forming micellar surface at the bulk. As the exact determination of A is difficult (depends on several external conditions, viz., temperature, local micropolarity, additives etc.), already stated in our previous literatures^{2, 3, 69}, we have approximately used A_{min} instead of A for determination of packing parameters. v and l_c were determined using the following formulae defined by Tanford⁷⁰,

$$l_c = (0.154 + 0.1265C_n) \text{ nm} \quad (7)$$

$$v = (0.0274 + 0.0269C_n) \text{ nm}^3 \quad (8)$$

where, C_n is the no of carbon atoms in saturated hydrocarbon chain of surfactants. It is stated that, $P \leq 0.333$, for spherical micelles; for non spherical micelles, $0.333 < P < 0.5$; for vesicles and bilayers, $0.5 < P < 1$; $P > 1$, denotes inverted structures. Calculated packing parameter values were presented in Table 3 which clearly indicates the forming micelles are spherical in nature for both $C_{16}MImCl$ and $C_{16}TPB$ in aqueous solution in presence and absence of different wt% of NaAlg. As Γ_{cmc} and corresponding A_{min} values are calculated at cmc_1 for pure $C_{16}TPB$ and at C_m^{*1} of $C_{16}TPB$ in presence of NaAlg, here P^1 is chosen to define packing parameters for $C_{16}TPB$ in absence and presence of NaAlg.

3.2. Conductometry; Transportation properties of conformers, Degree of counterion binding and Gibbs free energy of micellization:

Electrical conductance study provides the evidence of different conformers mediated by polyelectrolytes and surfactants in terms of ions transportation properties of charged species. Conductometry profiles of pure surfactants exhibits sharp inflection at cmc (cf. Fig. 2A (b) & 2B (b)). Initially, free monomers increase with the increase of the concentration of surfactants; increase the charged species (both monomers and counterions) to increase electrical conductance progressively which attribute to the steep slope (designated as m_1) obtained in specific conductance (κ) vs. concentration profiles (Fig. 2A (b)) in the pre micellar region. In the post micellar regime, free monomers are associated to form micellar aggregates with counterion condensation onto micellar surface; less transportation of relatively bulk micelles results in the decrease in κ attributed to relatively decreasing slope (designated as m_2) than those obtained in pre micellar regime. Intersection point between two lines (m_1 and m_2) designates the onset of micellization, called cmc. Degree of counter ion dissociation (α) from the micellar surface can be expressed as the ratio of slope of post micellar (m_2) to pre micellar (m_1) slope. On the other hand, degree of counter ion binding (β) can be expressed as^{2, 3, 10, 14, 16-19}.

$$\beta = 1 - \frac{m_2}{m_1} \quad (9)$$

Only one inflection with two different slopes (m_1 and m_2 ; cf. Fig. 2A (b)) was obtained for pure $C_{16}MImCl$. Two inflections with three distinct different slopes of decreasing magnitude were obtained [Fig. 2B (b)] for pure $C_{16}TPB$ conductometrically due to the formation of both cmcs, termed as cmc_1 and cmc_2 ; first cmc (cmc_1) is the threshold concentration where the free monomers aggregate to form micelle like structures, while latter inflection point (cmc_2) may be due to the change in micellar shape and size. Both cmc values of $C_{16}TPB$ have been documented in the literature with the help of conductance measurement^{36, 38}. Here, both β_1

(degree of counterion binding at cmc_1) and β_2 (degree of counterion binding at cmc_2) have been calculated for $C_{16}TPB$. Degree of counterion binding for $C_{16}MImCl$ has been designated as β . The process is same for the determination of β_1 and β_2 as those applied in the determination of β . The values of $cmcs$, β , β_1 and β_2 for the micellization of both the surfactants in presence and absence of NaAlg have been displayed in Tables 1 and 2.

The plot of κ vs. [surfactant] show several break points apart from $cmcs$ (for polyelectrolyte surfactant complex it has been termed as extended cmc or C_m^*) due to the interaction of oppositely charged NaAlg with the surfactants.

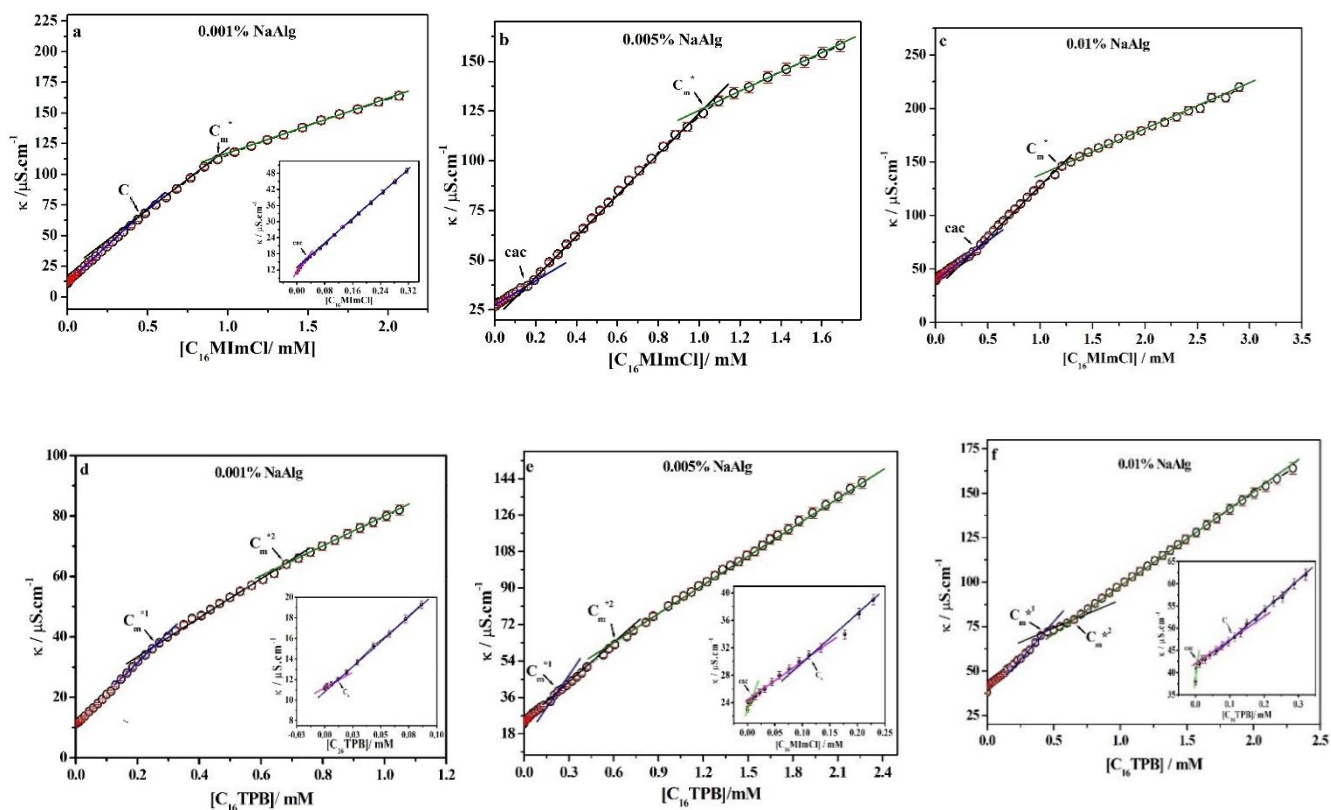


Fig. 4. Specific conductance (κ) vs. concentration of surfactant ([surfactant]), designated by open circle (\circ). Plots are presented in a sequential way: a, b and c for titration of $C_{16}MImCl$ in presence of 0.001, 0.005 and 0.01 % (w/v) of NaAlg respectively, whereas, d, e and f for titration of $C_{16}TPB$ in presence of 0.001, 0.005 and 0.01 % (w/v) of NaAlg respectively (At the inset of few diagrams: displaying cac , C_s or both clearly, whichever obtained). Error bars are given in different plots.

Introduction of $C_{16}MImCl$ into 0.001% NaAlg solution produces three break points with four distinct slopes of decreasing magnitude (cf. Fig. 4(a)) in conductometric profile. First break point with well-defined variation of specific conductance segments (at the inset of Fig. 4a) in this region, corresponds to cac due to the formation of NaAlg- IL complex (adsorption of $C_{16}MIm^+$ on to the anionic backbone of NaAlg) having relatively lesser transport properties

than free surfactant monomers which is attributed to the decrease in slope in κ vs. $[C_{16}MImCl]$ profile than the initial one. Faint variation in slope (cf. Fig. 4a) near the second break point (defined as C_S) proves the necklace type complex which comprises of NaAlg backbone with smaller micellar aggregates of ILs hardly affecting κ ; only the depletion of counterions¹⁰ due to wrapping of micellar aggregates with NaAlg backbone causes little variation in slopes. Beyond C_S , free micelles are formed by ILs, after prominent third break, called extended critical micelle concentration (C_m^*) like cmc of pure surfactants. This prominent third break in the vicinity of C_m^* appears due to the condensation of depleted counterions onto the micellar surface and follows the formation of less mobile free micellar aggregates of $C_{16}MImCl$. In presence of 0.005 and 0.01% NaAlg in comparison with 0.001% NaAlg, only variation occurred at low concentration of $C_{16}MImCl$. At higher NaAlg concentration (0.005% and 0.01% w/v), initially there is an ascending part with lower slope (figs. 4(b) and 4(c)) observed due to the formation of sufficient amount of $C_{16}MIm^+$ adsorbing onto anionic NaAlg site; the slopes tend to a stiff rise after a certain IL concentration due to the formation of sufficient coacervate. At that time, NaAlg-ILs complexes partially screen out from the solution and free monomer population increases upon further addition of ILs, which in term increases κ stiffly. At higher NaAlg concentrations (0.005, and 0.01%), the first break is denoted as cac (see Figs. 4(b) & 4(c)). In presence of 0.005 and 0.01% NaAlg, no inflection points are observed at the region of C_S as the increasing population of polyelectrolyte-surfactant complex (small surfactant aggregates wrapping along polyelectrolytes backbone) at high polyelectrolyte content media nullify the counterions depletion effect after C_S ; hardly produce any detectable change in conductometric profiles (cf. Fig. 4(b) and (c)) until free micelles of $C_{16}MImCl$ were formed, after the complete saturation of NaAlg backbone leading to phase separation ('p' zone, shown in Fig.3A) at C_m^* . The cac values of $C_{16}MImCl$ obtained by conductometric method in presence of 0.005 and 0.01% NaAlg were found relatively greater than those determined by tensiometry (Sec. 3.1.). Such observations have been documented in previous literatures^{10, 14} investigating the other oppositely charged polyelectrolyte surfactant systems. Possible reason for this disparity is that tensiometric technique detects the onset of formation of surface active NaAlg- $C_{16}MIm^+$ complex earlier, while conductometric technique shows significant change until the turbidity is formed in large amount. The cac values of $C_{16}MImCl$ found in conductometric method in presence of 0.005 and 0.01% NaAlg can be compared only with the first turbidity point (T_1) appeared in Turbidimetric experiments (see. Table1) discussed.

For C₁₆TPB, conductometric profile (Fig. 4(d)) in presence of 0.001% NaAlg show three distinct break points with four different slopes, while for the other two concentrations of NaAlg (0.005% and 0.01%), four distinct break points have been observed with five different slopes. First break point in presence of 0.001% of NaAlg in conjugation with C₁₆TPB corresponds to C_s. The break point cac have been not found in presence of 0.001% NaAlg with C₁₆TPB as the electrostatic interaction between carboxylate anion of NaAlg with C₁₆TP⁺ have lesser in magnitude than SAIL in conjugation with NaAlg stated in tensiometry section. From the inset of Fig. 4(d), it is evident that initially κ increases very slightly then increase steadily (reversal of slope in the conductometric profile). Initial slight increase is due to the formation of least amount of less mobile NaAlg- C₁₆TP⁺ complex as the interaction of C₁₆TP⁺ with NaAlg is somewhat lesser than C₁₆MIm⁺. As a result, although negligible amounts of free surfactant monomers along with small micellar aggregates are wrapped along the polymer backbones, but free surfactant monomers were adequate in solution medium to increase κ steadily after C_s. As [C₁₆TPB] increases, conductance increases steadily until free monomers form free micelles; occurring second break in conductometric profile (Fig. 4 (d)) and the corresponding break point is associated with significant change of slopes found in conductometric plot termed as first extended cmc (C_m^{*1}). Post micellar slope has slightly lesser in magnitude than pre-micellar slope (Fig. 4(d)) near C_m^{*1} due to formation of less mobile C₁₆TPB micelle. After C_m^{*1}, micelles formed by free monomers change its shape and size upon further addition of C₁₆TPB resulting to the formation of third inflection with negligible change in κ . The concentration of C₁₆TPB where the third break point is found has been termed as second extended micelle concentration (C_m^{*2}). At higher alginate concentrations (0.005 and 0.01% w/v), however, surplus polyelectrolytes forced some amount of C₁₆TPB monomers to be associated to some extent on to NaAlg backbone leading to formation of cac which appeared to the first break points shown at the inset of Fig. 4(e) and 4(f). Change in slopes below and above cac at 0.01% (w/v) is quite prominent (compare Fig 4(e) and 4(f); shown at the inset of both figures) than those found in 0.005% (w/v) in presence of C₁₆TPB clearly indicating feasibility of surfactant head groups attached on to alginate backbone at higher polyelectrolyte content. Reversal of slopes is also found for 0.005 and 0.01% (w/v) of NaAlg in conjugation with C₁₆TPB near the region of C_s (shown at the inset of Fig. 4(e) and 4(f)) like Fig. 4(d)). First visual turbidity was appeared in presence of 0.01% and 0.005% NaAlg in conjugation with [C₁₆TPB] closed to C_m^{*1} values calculated by tensiometric method (Table 2). The value of C_m^{*1} calculated from the inflections shown in κ vs. [C₁₆TPB] profiles (Fig. 4(e) & 4(f)). This was found relatively larger at 0.005

and 0.01% (w/v) than those obtained from tensiometry (shown in Table 2) as the break points were appeared in conductometry until sufficient turbidity formed in the medium leading to change in slope below and after of C_m^{*1} . The change in slopes in κ vs. $[C_{16}TPB]$ profile near C_m^{*1} is found more prominent at 0.01% (w/v) than 0.005% (w/v) probably due to the formation of maximum coacervates near C_m^{*1} in presence of 0.01% NaAlg upon addition of $C_{16}TPB$ which has also been concluded in turbidimetry plot (designated by Φ_m ; Fig. 5 (f)) and also displayed in Table 2. The trend for variation in C_m^{*1} with the variation of NaAlg in presence of $C_{16}TPB$ is consistent with tensiometry (cf. Table 2). From Fig. 5 (f) it is evident that, post micellar slope is found in greater magnitude than premicellar slope (reversal of slopes) in vicinity of C_m^{*2} in presence of 0.01% polyelectrolyte concentration, while reverse is obtained in presence of 0.005% (cf. Fig. 5(e)) in vicinity of C_m^{*2} . The different nature of slopes above and below the C_m^{*2} with increasing the concentration of NaAlg from 0.005 to 0.01% medium clearly indicates the polyelectrolyte assisted change in topology of free surfactant micelles during second micellization process. Like cacs, the values of C_m^{*2} calculated by conductometric method for NaAlg + $C_{16}TPB$ system are also found larger than those calculated by tensiometry (cf. Table 2).

Degree of counter ion binding (β) onto micellar surface formed by $C_{16}MImCl$ monomers have more or less increasing trend with slight variation upon increase the concentration of NaAlg displayed at the parenthesis (shown in Table 1.). The same observation has been found previously for AHX or ALG/ C_nMIMBr ($n = 12, 14, \text{ and } 16$) system¹⁷. On the other hand, β_1 for $C_{16}TPB$ initially increased at 0.001% (w/v) NaAlg comparing with alginate free medium and decreased significantly at high alginate concentrations (0.005 and 0.01%), while β_2 was found lower value as compared with alginate free $C_{16}TPB$ and also with β_1 . Degree of counter ion binding was found larger for $C_{16}MImCl$ than compared with $C_{16}TPB$ both in pure state as well in all polyelectrolyte concentrations (Table 1). This clearly indicates that chloride ions are partially associated to greater extent onto $C_{16}MImCl$ micelles than the bromide ions on to micellar surface of $C_{16}TPB$. Difference of degree of counterion binding onto the two different surfactant micelles manifested in the aggregation number (N_a , cf. Table 3) both in presence and absence of NaAlg discussed later in this manuscript.

Standard Gibbs free energy of micellization (ΔG_m^0) for the pure surfactants in aqueous medium as well as in presence of different concentrations of NaAlg can be expressed as:

For, free surfactants forming micelles in aqueous medium,

$$\Delta G_m^0 = (1 + \beta)RT \ln X_{cmc} \quad (10)$$

X_{cmc} is the cmc in molefraction unit. R is the universal gas constant and T denotes the temperature in Kelvin scale. For C₁₆TPB, having two cmcs (cmc_1 and cmc_2) and corresponding β_1 at cmc_1 and β_2 at cmc_2 , ΔG_m^0 be replaced to ΔG_m^0 (1) and ΔG_m^0 (2) respectively to the equation 10.

For, surfactants in presence of NaAlg in aqueous medium,

$$\Delta G_m^0 = (1 + \beta)RT \ln X_{C_m^*} \quad (11)$$

For C₁₆TPB, C_m^* is replaced to equation 11 by C_m^{*1} and C_m^{*2} and corresponding β by β_1 and β_2 respectively. The value of ΔG_m^0 has been replaced by ΔG_m^0 (1) and ΔG_m^0 (2) for the first and second micellization to equation 11.

The values of ΔG_m^0 were displayed for individual pure surfactants and in presence of different wt% (w/v) of NaAlg in Table 4. From Table 4., it is evident that, negative values of ΔG_m^0 (1) initially increases at 0.005% NaAlg medium (more spontaneous) compared with pure surfactant in aqueous medium for the first micellization of C₁₆TPB, beyond which decreases steadily up to 0.01% NaAlg medium. The values of ΔG_m^0 (2) decrease regularly, i.e., less spontaneous process with increase in polyelectrolyte concentrations for the second micellization process. For C₁₆MImCl, micellization process is more spontaneous in presence of NaAlg and spontaneity increases overall at higher concentration of NaAlg (cf. Table 4).

3.3. Turbidimetry; Determination of onset and maximum turbidity exactly compare with visual impressions, Solubilization of polyelectrolyte-surfactant complexes in to micellar medium, Effect of polyelectrolyte concentration:

Turbidimetric profiles ((100-T%) vs. [surfactant]) for NaAlg-C₁₆MImCl and NaAlg- C₁₆TPB were displayed in Fig. 5 (a-c) and Fig. 5(d-f) respectively. T₁, T₂ and T_m (displayed in Table 1.) represented here first, second and maximum turbidimetric points respectively that appear from low to high surfactant concentrations of C₁₆MImCl chronologically interacting with NaAlg. Alike, C₁₆MImCl + NaAlg systems, the notion Φ with the subscripts 1, 2 and m also designates the same turbidimetric significance for C₁₆TPB + NaAlg systems (cf. Table 2.) from low to high C₁₆TPB concentrations respectively.

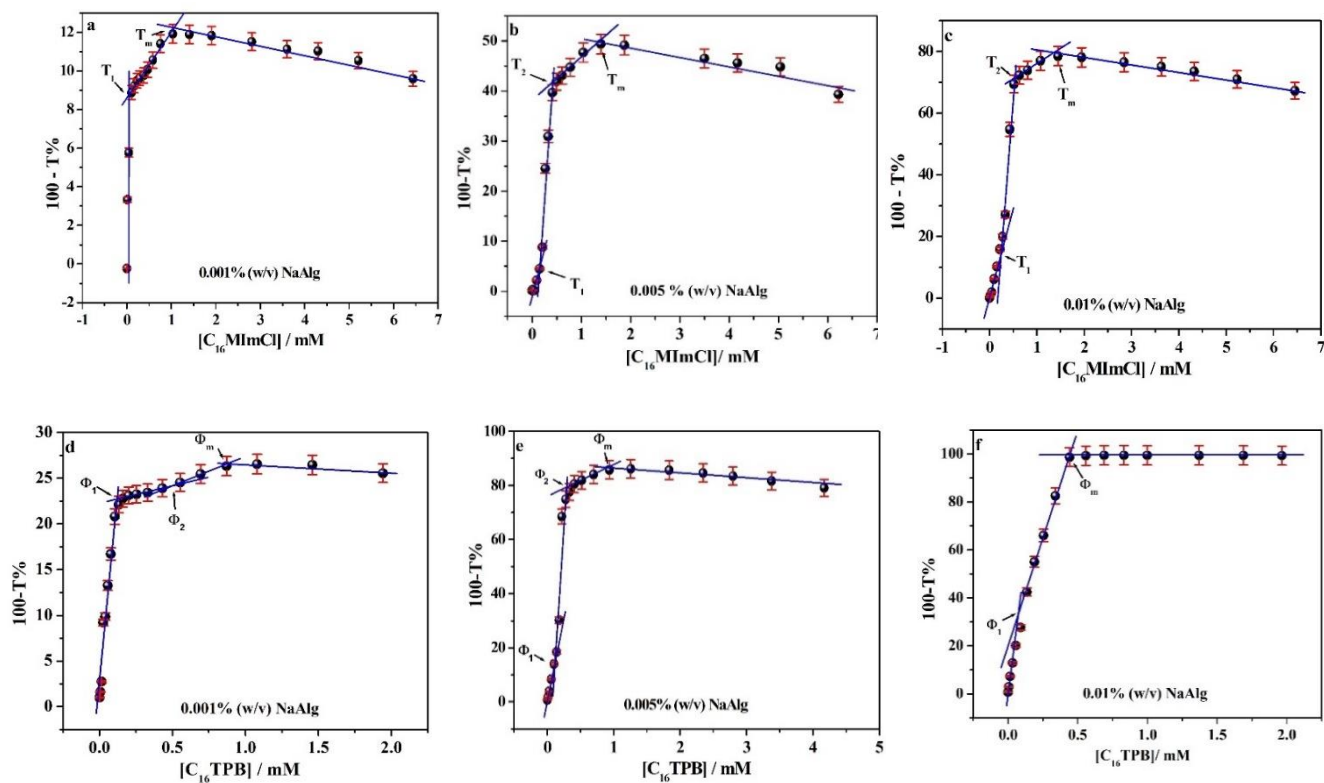


Fig. 5. Turbidimetric profiles for the interaction of each of $C_{16}MImCl$ and $C_{16}TPB$ with different wt % of NaAlg (0.001% (a)/(d), 0.005%(b)/(e) and 0.01%(c)/(f)).

From Fig. 5(a), it is evident that, turbidity (a little bit, maximum turbidity approaches to 12%) increases steeply upto 0.04 mM concentration of $C_{16}MImCl$, corresponding to the first inflection point (T_1); beyond which turbidity slightly increases upto 1.07 mM of $[C_{16}MImCl]$ (maximum Turbidity point, T_m) following with slight decrease in turbidity due to slight solubilization of it in micellar environment. From Table 1, it is seen that T_1 in presence of 0.001% (w/v) NaAlg has similarity to cac found by other techniques. In 0.005% NaAlg medium upon addition of $C_{16}MImCl$ (cf. Fig. 5 (b)), little turbidity appears different upto 0.167 mM of IL concentration corresponding to first inflection point, T_1 . Then step increase in turbidity arises in solution medium up to 0.41 mM of surfactant concentration where second inflection point (T_2) appeared, while for 0.01% (w/v) NaAlg medium, both T_1 and T_2 have the relatively larger turbidity content comparing to the turbidity axes (100-T%) of Fig. 5 (b) with Fig. 5(c). Concentration of $C_{16}MImCl$ corresponding to T_1 has the similarity with cac , those found by conductometric measurements and also relatively larger in magnitude than those found by other techniques (cf. Table 1). T_2 values found for the interaction of 0.005 and 0.01% (w/v) in conjugation with $C_{16}MImCl$ are relatively lesser than those found in terms of C_S obtained by

tensiometry (cf. Table 1). For $C_{16}MImCl + NaAlg$ system, inflections due to maximum turbidity (T_m) are relatively greater to the C_m^* found by other techniques (viz. conductometry, tensiometry and fluorimetry (discussed latter)) and sufficiently larger than C_m^* found by isothermal titration calorimetry (ITC) measurements (also discussed later) shown in Table 1. Like 0.001% (w/v) NaAlg medium, it is seen that turbidity appeared in solution in presence of 0.005 and 0.01% (w/v) NaAlg are also soluble in micellar environments after T_m which are found in turbidimetric profiles of Fig. 5(b) and 5(c) respectively. This observation has the similarity with the former studied systems like, NaCMC/CTAB combination in conjugation with NaBr¹⁰, and NaCMC/ $C_{12}mimBr/ NaBr$ ³⁵.

Turbidimetric profiles in presence of 0.001% and 0.005% NaAlg in conjugation with $C_{16}TPB$ (cf. Fig. 5(d) and 5(e)) have the similarity with $C_{16}MImCl$ in presence of alginate concentrations. Different inflection points in terms of Φ have been shown in Fig. 5(d), (e) and (f) and also recorded in Table 2. For $C_{16}TPB$ in presence of 0.001% (w/v) NaAlg (cf. Fig. 5(d)), slight turbidity appeared up to 0.11 mM of $[C_{16}TPB]$ corresponding to the first inflection point denoted as Φ_1 which has the close similarity with C_m^{*1} found by tensiometry as well as fluorimetry and ITC measurements (cf. Table 2.) under identical condition. After Φ_1 , turbidity slightly increases to maximum at Φ_m . In between Φ_1 and Φ_m , another inflection was found designated as second turbidimetry point (Φ_2). Steep increase in turbidity is observed up to second inflection point (Φ_2 , cf. Fig. 5(e)) in the solution of 0.005% NaAlg in presence of $C_{16}TPB$ and intensity of turbidity is found larger as compared with $C_{16}MImCl$ (cf. Fig. 5(b)) under identical condition. Like 0.001% NaAlg solution in conjugation with $C_{16}TPB$, Φ_1 value in presence of 0.005% (w/v) NaAlg also has well similarity with C_m^{*1} values those found by other techniques, like, tensiometry, fluorimetry and ITC (cf. Table 2.). The Φ_2 values are found in between C_m^{*1} and C_m^{*2} those assigned by conductometry and fluorimetry (cf. Table 2.) in presence of 0.001 and 0.005% (w/v) of NaAlg in conjugation with $C_{16}TPB$, whereas Φ_m values are found greater than C_m^{*2} obtained by conductometry (cf. Table.2.). In presence of 0.01% (w/v) NaAlg (Fig.5 (f)), turbidity is found maximum at $[C_{16}TPB] = 0.44$ mM and even to a greater extent (turbidity approaches to 100%) as compared with other two lower alginate concentrations (0.001 and 0.005% w/v) and also larger than that of the highest alginate concentration (0.01%) in presence of $C_{16}MImCl$. The Φ_1 value for 0.01% NaAlg + $C_{16}TPB$ system is found similar to C_s obtained by conductometry under similar condition and Φ_m is close to C_m^{*1} assigned by conductometry (Table 2); C_m^{*2} , calculated by tensiometry, fluorimetry and ITC techniques (Table 2). The maximum turbidity (Φ_m) appeared at relatively lower

C_{16} TPB concentration in presence of 0.01% (w/v) NaAlg due to the greater ease of hydrophobicity assisted by surplus of NaAlg and also by the micelles which wrapped along polyelectrolyte backbones leading to formation of agglomerated complex.

3.4. Spectrofluorimetry: *Variation of micropolarity (I_1/I_3) due to change of local environment of Pyrene, determination of aggregation number of surfactants in presence and absence of different wt% of NaAlg, time resolved study for 0.005% (w/v) of NaAlg in presence of both surfactants titrimetrically:*

3.4 (a). Steady state fluorimetry:

Fluorescence intensity ratio of first (I_1) to third (I_3) vibronic peak of pyrene (I_1/I_3) or ‘micropolarity index’ has been used extensively⁷¹⁻⁷⁶ to sense micropolarity in the immediate neighbouring medium of it. For instance, I_1/I_3 value of pyrene in hydrocarbon solvent is 0.6, for ethanol, it is 1.1 and for water the value is 1.6⁷⁶. The behaviour of pure surfactants in aqueous solution containing fixed pyrene concentration and variation of [surfactant] have been displayed in Fig 2A (c) and 2B (c) for C_{16} MImCl and C_{16} TPB respectively with the assistance of (I_1/I_3) vs. [surfactant] plots. From Fig 2A(c), the observation is initial plateau like appearance at low surfactant concentration, rapid decrease in I_1/I_3 at intermediate surfactant concentration and following by saturation occurring with nearly same I_1/I_3 with magnitude less than 1.0 above cmcs, while for C_{16} TPB (cf. 2B(c)), rapid decrease in micropolarity is observed from the very low surfactant concentration and finally remains saturated in I_1/I_3 nearly equal to 1.02.

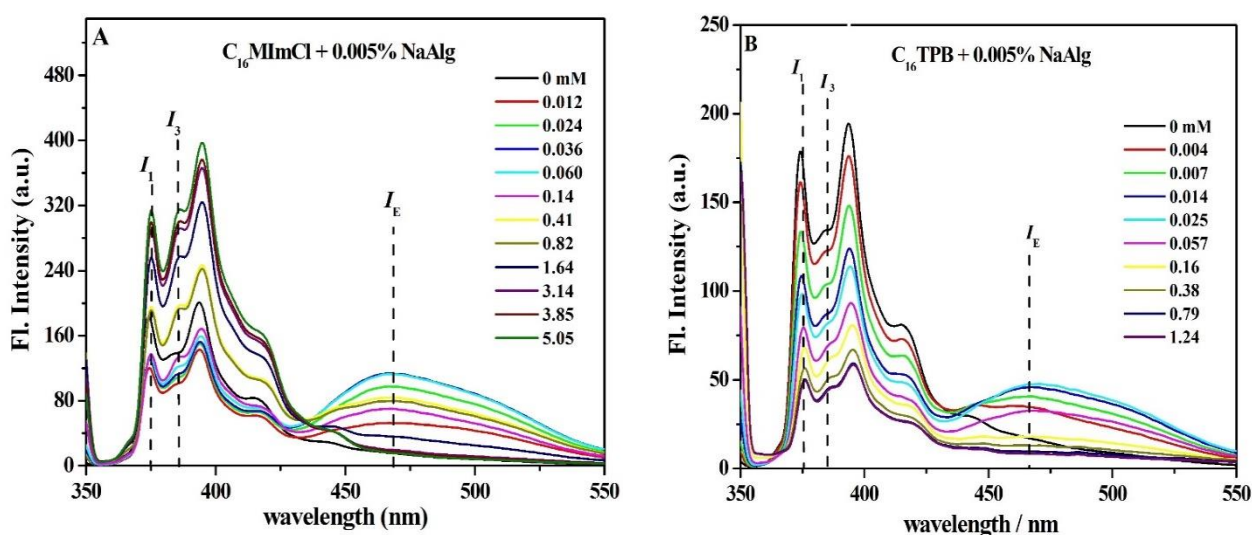


Fig. 6. Fluorescence intensity vs. wavelength profiles of pyrene in presence of 0.005% (w/v) NaAlg in conjugation with different concentrations of C_{16} MImCl (A) and C_{16} TPB (B).

I_1/I_3 vs.[surfactant] profiles (Fig 2A/2B (c)) for pure surfactants have been fitted with a decreasing sigmoidal Boltzmann equation of sufficiently fair R^2 values ($R^2 \sim 0.99$) and cmcs have been assigned ^{14, 18, 75} from the middle of sigmoid (indicating by a heavy arrow). Passage of pyrene molecule from aqueous phase to hydrophobic micellar environments show the sigmoid pattern of micropolarity index (I_1/I_3) of pyrene around cmc as the concentration of surfactant increases. For micellization of pure surfactants, at low surfactant concentrations with few numbers of surfactant monomers, pyrenes are little soluble in aqueous environment but not associated with each other. Increasing concentration of surfactants form some pre-micellar aggregates form which can draw pyrene molecules to hydrophobic environment (rapid decrease of micropolarity) associated with pyrene excimer formation⁷⁷ due to availability of pyrene molecules at close proximity following the formation of free micelles. At high surfactant concentrations, the number of micelles increases in solution and pyrenes were redistributed in each micellar medium, scarcely change micropolarity and also pyrene excimer disappears⁷⁷. Pyrene excimer has been shown in presence of surfactant polyelectrolyte system of oppositely charged species at very low surfactant concentration (even lower than cac) due to migration of pyrene molecules in the hydrophobic domain offered by tails of surfactants attached to the polyelectrolyte backbone⁷³. In this way, due to formation of hydrophobic pockets, pyrene molecules come together in pair and increase excimer intensity and consequently, decrease in monomer emission intensity at low surfactant concentration. Here, formation of pyrene excimer for our present system at all NaAlg concentrations below cac. Different pattern observed in fluorescence profiles of pyrene for $C_{16}MImCl$ and $C_{16}TPB$ in conjugation with NaAlg. We have shown fluorescence intensity vs. wavelength profiles (cf. Fig. 6) compasses in between 350-550 nm in presence of 0.005% (w/v) sodium alginate in conjugation with both $C_{16}MImCl$ (cf. Fig 6A) and $C_{16}TPB$ (cf. Fig. 6B). Excimer emission (I_E) was recorded around 467 nm, while first (I_1) and third (I_3) monomer peaks appeared at 374 and 385 nm respectively. Profound differences have been observed between Fig. 6A and 6B with increasing concentration of each surfactant. In case of $C_{16}MImCl$ (cf. Fig 6A), it is seen that fluorescence intensity initially of pyrene monomer initially drops at 0.012 mM of [$C_{16}MImCl$] with concomitant increase its excimer around 467 nm. After that, monomer emission hardly changes but excimer emission increases significantly upto 0.06 mM [$C_{16}MImCl$] and that concentration is slightly higher than the recorded cac value (cf. Table1.) which is measured by pyrene micropolarity technique. Upon further increase of the concentration of $C_{16}MImCl$ monomer, emission increases and finally, saturates around 0.81 mM of [$C_{16}MImCl$]. In the range of 0.14 to 0.82, excimer emission shows its nearly constant values and C_s has been recorded (Table 1).

With further increase of $[C_{16}MImCl]$ monomer, emission increases significantly and finally saturates with the disappearance of excimer. In case of $C_{16}TPB$ monomer, pyrene emission decreases with concomitant increase in excimer up to 0.025 mM of $[C_{16}TPB]$. After that, decrease of monomer emission occurs with decrease in excimer intensity upon further addition of surfactants and finally excimer disappears at sufficiently high surfactant concentration and monomer emission comes to saturation. Continuous decrease in pyrene monomer intensity with increase of concentration of $C_{16}TPB$ is possibly due to the quenching of pyrene by three benzene rings attached to tertiary P cation. This quenching of pyrene as the increase of $C_{16}TPB$ also manifested in rapid decrease in life time ($\langle \tau \rangle$), cf. Table S1) with increasing concentration of $C_{16}TPB$ in presence of 0.005% (w/v) NaAlg medium. Pyrene micropolarity (I_1/I_3) has been displayed in Fig. 7 by varying the concentration of both surfactants in presence of different weight % of NaAlg.

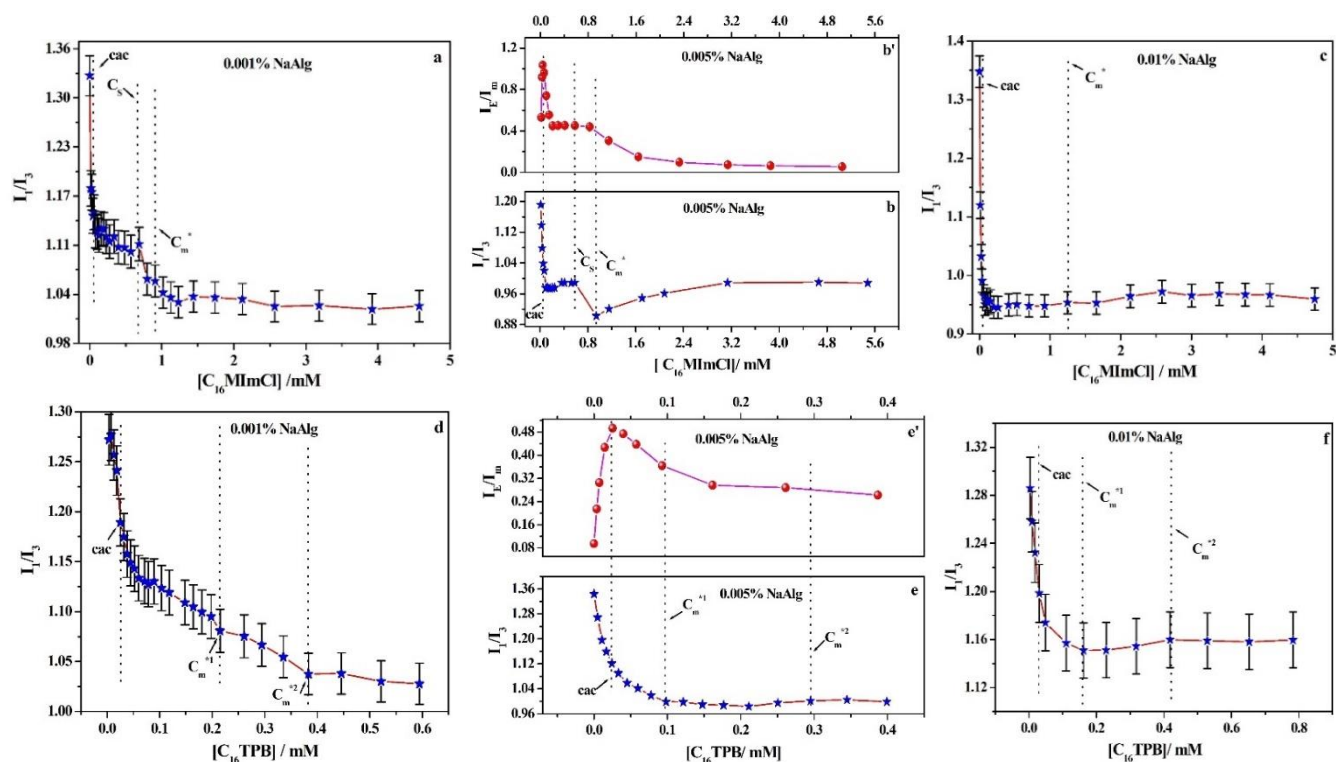


Fig. 7. Micropolarity (I_1/I_3) index vs. concentration of surfactant with different concentrations of NaAlg. Plots were designated as: I_1/I_3 vs. $[C_{16}MImCl]$ in presence of different wt% of NaAlg (a. 0.001%, b. 0.005% and c. 0.01%) & I_1/I_3 vs. $[C_{16}TPB]$ in presence of difference wt% of NaAlg (d. 0.001%, e. 0.005% and f. 0.01%). cac , C_s and C_m^* , whichever found, have been designated by dotted lines for both systems. Pyrene excimer emission (I_E) has been monitored at 467 nm and monomer emission (I_m) monitored at 474 nm corresponding to first vibrational peak of pyrene. Error bars are given

Unlike initial plateau like appearance formed in case of pure C₁₆MImCl (Fig. 2A(c)) at low surfactant concentration, initial steady decrease is observed in presence of NaAlg irrespective of concentration end to a nearly equal I₁/I₃ region which persists in presence of 0.01% (w/v) NaAlg (cf. Fig. 7 (c)) upon further addition of C₁₆MImCl, but found to be another decreasing in the I₁/I₃ values beyond complete saturation in presence of 0.001% (Fig. 7(a)) and 0.005% (Fig. 7b). From Fig. 7 (a), it is evident that, sigmoid pattern was observed in the second decreasing portion just like micropolarity vs. concentration profiles of pure C₁₆MImCl (cf. Fig. 2A(c)), while sigmoidal appearance deviates from ideality in presence 0.005% NaAlg (Fig. 7b) and finally, disappears at high alginate concentration (cf. Fig. 7(c)). First inflections of all the plots (cf. Fig. 7(a), 7(b) and 7(c)) where rapid change occurs are defined as cac; after that, second break point corresponding to C_S is found in presence of 0.001 and 0.005% NaAlg, whereas no observation of C_S has found in presence of 0.01% NaAlg. The C_m^{*} value in presence of 0.001% polyelectrolyte is defined from the middle of the second decreasing region (Fig. 7(a)), while it is rather an inflection point found in presence of 0.005 and 0.01% NaAlg. After C_m^{*} in presence of 0.005 and 0.01% (w/v) NaAlg in conjugation with C₁₆MImCl (cf. Fig. 7(b) and 7(c)), slight increase in I₁/I₃ values have been observed which is attributed to sensing of pyrene to polar environment for the formation of coacervate screening out partially from solution. The C_m^{*} values show well similarities for C₁₆MImCl in presence of different wt % of alginate with the other methods, such as, conductometry and tensiometry; while, cac and C_S values are resembled to tensiometry technique (Table 1). On the other hand, sharp decrease has been shown in micropolarity vs. concentration profiles (Fig. 7(d), 7(e) and 7(f)) at the low concentration region of C₁₆TPB. Middle points of the profiles (cf. Fig. 7(d), 7(e) and 7(f)) have been taken as cac for all the alginate concentrations in presence of C₁₆TPB and for second and third inflections designation have been given as C_m^{*1} and C_m^{*2} comparing to the tensiometry results (cf. Table 1). For 0.001% NaAlg in presence of C₁₆TPB, micropolarity decreases gradually till the formation of second cmc (C_m^{*2}), while for other two alginate concentrations saturation occurred near first cmcs (C_m^{*1}). From Fig. 7f, it is evident that, slight increase in micropolarity has been occurred after first cmcs (C_m^{*1}) and remain constant near second cmcs (C_m^{*2}). This slight increase in micropolarity is probably due to the turbidity effect corresponding to the slight change in pyrene microenvironment as displayed in the high alginate content medium. Nearly ideal micropolarity vs. concentration plots were appeared at low alginate concentrations (cf. Fig. 7(a), 7(b) and 7(d)) of both the surfactants as presented by Turro *et. al.*⁷⁶. A comparative representation (cf. Fig. 7(b) and 7(e)) has been presented in terms

of I_E/I_m (ratio of intensity of pyrene excimer to monomer ratio, cf. Fig. 7(b') and 7(e')) along with I_1/I_3 within the same concentration range of individual surfactants in presence of 0.005% (w/v) of NaAlg. I_E/I_m ratio has been used as a tool to determine cac and cmc in previous literature⁷². Initial decrease in micropolarity with corresponding increase in pyrene excimer to monomer ratio (I_E/I_m) has been occurred and it finally approaches to a peak which is nearly equal to the cac (shown by the dotted line, cf. Fig 7(b) and 7(e)) found in the present study. The appearance of peak near cac is due to the formation of micelle like microdomains which were attached on oppositely charged polyelectrolyte backbones and keep pyrenes to close proximity leading to formation of pyrene excimer (cf. Fig. 6A and 6B). After peak formation, ratio of I_E/I_m of pyrene diminishes rapidly, after that a plateau was formed (cf. Fig. 7(b')) upto ~ 1 mM [$C_{16}MImCl$] close to the extended cmc (C_m^*) of $C_{16}MImCl$. Further increase [$C_{16}MImCl$], I_E/I_m decreases and finally show saturation at high surfactant concentration (cf. Fig. 7(b')). For $C_{16}TPB$, in presence of 0.005% (cf. Fig.7e'), a peak is also observed in I_E/I_m value near cac, beyond which I_E/I_m decreases and finally go to saturation near C_m^{*2} . On the contrary with the earlier observation⁷², no peak is formed near C_m^* for both the surfactants in presence of 0.005% NaAlg.

Mean aggregation number (N_a) of both surfactants in absence and presence of NaAlg at different wt % has been determined using steady state fluorescence quenching of pyrene by CPC used as quencher. To perform it, a set of fresh surfactant solutions both in presence and absence of NaAlg has been prepared. 2.5 ml of each solution is taken in a cuvette and CPC is added by means of titration. Concentration of pyrene was fixed both in cuvette and in CPC solution. Intensity of pyrene in absence of quencher has been designated as I_0 and in presence of CPC designated as I are depicted in equation 12,

$$\ln \frac{I_0}{I} = \frac{N_a[CPC]}{[surfactant] - cmc(C_m^*)} \quad (12)$$

Here, [surfactant] is the concentration of surfactant either $C_{16}MImCl$ or $C_{16}TPB$ prepared in same concentration (~ 10 mM) both in aqueous and NaAlg solutions. Average values of cmc and C_m^* have been calculated from Tables 1 and 2 for the calculation of aggregation number for pure $C_{16}MImCl$ in aqueous solution and surfactants in presence of different wt% of NaAlg respectively. In case of $C_{16}TPB$, we have used average cmc_2 or C_m^{*2} in the denominator of equation 12. In this context, $\ln \frac{I_0}{I}$ vs. [CPC] profiles (refer to supplementary section, Fig. S4) have been displayed for both surfactants either in pure or in presence of difference wt% of

NaAlg. Aggregation numbers (N_a) have been displayed in Table 3. From this Table, it is evident that, N_a values of $C_{16}MImCl$ increase in presence of NaAlg and later decrease at 0.01 % w/v NaAlg medium. On the other hand, for $C_{16}MImCl$, aggregation number increases with the increase of alginate concentration within the investigated concentration range of polyelectrolyte. Increase of aggregation number of both surfactants in presence of NaAlg is probably due to the increase in hydrophobicity near the micellar surface, while in presence of 0.01% (w/v) NaAlg in conjugation with $C_{16}MImCl$ lowering in aggregation number may be owing to increase of hydrophilicity near micellar interface leading to effective phase separation of polyelectrolyte-surfactant complex. Moreover, increase in aggregation number for $C_{16}MImCl$ both in presence and absence of NaAlg than $C_{16}TPB$ probably due to the steric hindrance of three bulky phenyl head groups of $C_{16}TPB$. Loosely packed micelles penetrate some water molecules interior to the micelle⁷⁴ of $C_{16}TPB$ in comparison with $C_{16}MImCl$ manifested in relatively greater micropolarity (I_1/I_3) in the micellar region of $C_{16}TPB$ than $C_{16}MImCl$ both in aqueous solution (comparing Fig. 2A(c) with 2B(c)) and also in presence of different wt % of NaAlg (comparing Fig. 7a, with 7d; Fig. 7(b) with 7(e) and Fig. 7(c) with 7(f)).

3.4 (b). Time resolved fluorimetry:

Time resolved emission of pyrene may be the indirect tool to determine cac , C_5 and C_m^* for polyelectrolyte- surfactant systems. Titration of two investigated surfactants was performed at 0.005% (w/v) of NaAlg medium keeping pyrene concentration fixed same as steady state measurements. From Table S1, it is evident that log (count) vs. time (ns) profile (shown at the inset in Fig. 8A and B) for pure NaAlg (0.005% w/v) in conjugation with probe pyrene shows single exponential pattern (single lifetime (τ_1) value is close to 123.5 ns), while in presence of surfactants bi-exponential patterns have been observed (two lifetime values τ_1 and τ_2 , cf. Table S1). Average life times ($\langle\tau\rangle$) vs. concentration of both surfactants ($C_{16}MImCl$ and $C_{16}TPB$) have been displayed in Fig. 8.

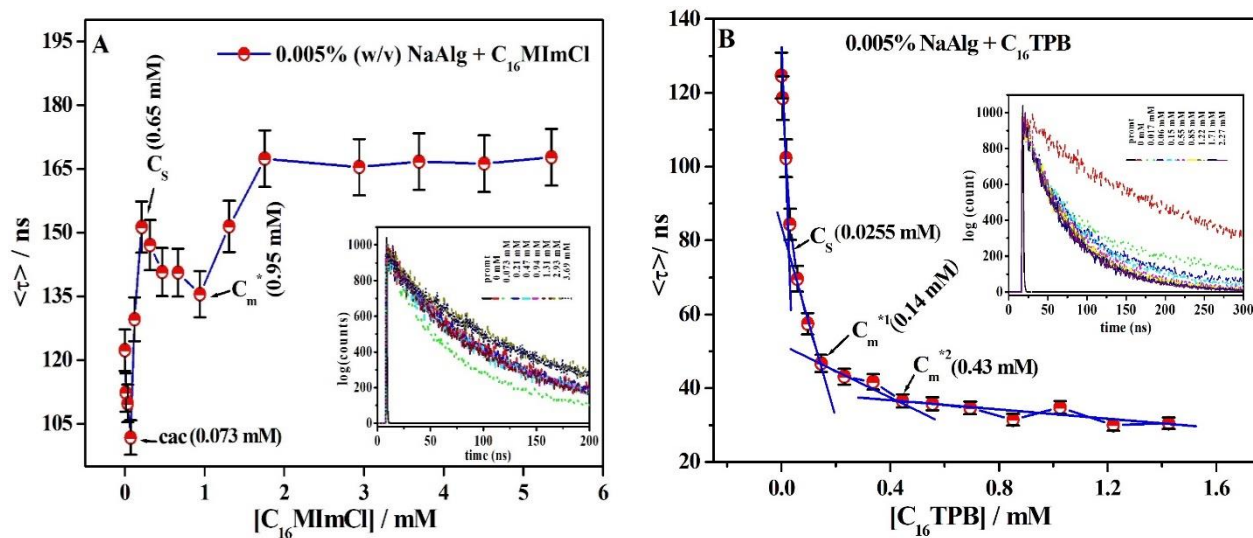


Fig. 8. $\langle \tau \rangle$ vs. [surfactant] profiles in presence of $C_{16}MImCl$ (A) and $C_{16}TPB$ (B) at 0.005% w/v of NaAlg: at the inset; log (count) vs. time (ns) profiles for respective surfactants. Error bars are included in each diagram.

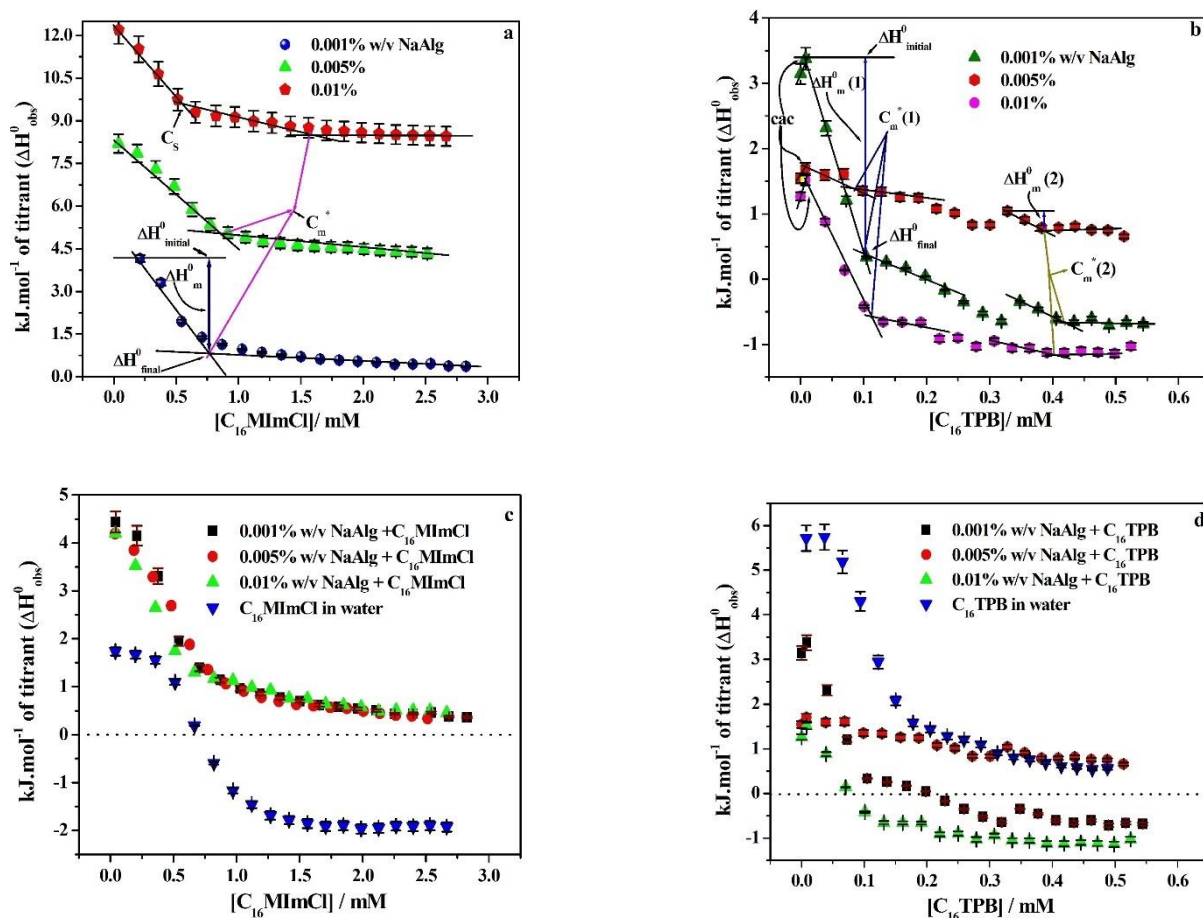
From Fig. 8A, it is probable that, $\langle \tau \rangle$ initially decreases from 123.5 ns to 101.8 ns at nearly 0.07 mM of $[C_{16}MImCl]$ which is close to cac, those calculated by steady state measurement and also by tensiometry for the same system (cf. Table 1). Pyrene excimer was formed due to electrostatic complexation between oppositely charged polyelectrolyte and surfactants forming hydrophobic domains which ensure two pyrene molecules in close proximity. Beyond the minimum, $\langle \tau \rangle$ increases to a maximum due to the redistribution of pyrene molecules from one polyelectrolyte- surfactant complex to another and prevents its close proximity. There is again decrease in $\langle \tau \rangle$ values after the maximum probably due to some close proximity of pyrene molecules again for the formation of premicellar aggregates on to polyelectrolytes backbone (C_s) following the formation of free micelles of surfactants at C_m^* . After C_m^* , both polyelectrolytes and surfactants were diluted and equally distributed among the species formed in the solution due to stabilization of pyrene molecules in hydrophobic domains and finally, increase of $[C_{16}MImCl]$ did not change pyrene lifetime. Concentration of $C_{16}MImCl$ indicating C_s and C_m^* (cf. Fig. 8A) are quite similar to those found by tensiometry and steady state fluorimetry [cf. Table 1]. On the other hand, increase of $[C_{16}TPB]$ stepwise decrease $\langle \tau \rangle$ gradually (Fig. 8B) and finally remains unchanged (28.6-35.9 ns, cf. Table S1.) after 0.5 mM of $[C_{16}TPB]$. This gradual decrease in $\langle \tau \rangle$ was probably due to the quenching of pyrene molecules by phenyl moieties of $C_{16}TPB$ which overshadowed the effect of pyrene excimer found during the surfactant induced conformational change of NaAlg in presence of $C_{16}MImCl$

(cf. Fig. 8A). Several break points were obtained in $\langle\tau\rangle$ vs. $[C_{16}TPB]$ profile (cf. Fig. 8B) and these are designated as C_s , C_m^{*1} and C_m^{*2} from low to high surfactant concentration corresponding to the similar inflections with those found in tensiometry and cac , C_m^{*1} and C_m^{*2} obtained by steady state measurement (cf. Table 2.).

3.5. Isothermal Titration Calorimetry (ITC): *Enthalpy of micellization and Entropy of micellization*

ITC plays a very important role to investigate heat changes (standard enthalpy of micellization, ΔH_m^0) due to conformational changes of polyelectrolyte mediated by oppositely charged surfactants in solution as well as free micelle formation between the surfactant monomers. ITC profiles (heat injection (ΔH_{obs}^0) in $\text{kJ}\cdot\text{mol}^{-1}$ vs. [surfactant]) of pure surfactants have been reported in Fig. 2A (d) for $C_{16}MImCl$ and 2B(d) for $C_{16}TPB$ respectively. ITC profile for pure surfactants shows sigmoidal pattern and these are fitted with Boltzmann-sigmoidal equation⁷⁸ and the values of cmc have been taken^{3, 79, 80} from the inflection of fitted plots intermediated of sigmoidal region (designated by the heavy arrows). Evaluation of second cmc (cmc_2) has been performed for $C_{16}TPB$ in aqueous solution by zooming the region in between 0.2 – 0.5 mM of $[C_{16}TPB]$ shown at the inset of Fig. 2B (d). All cmcs for pure surfactants determined by ITC technique have been presented in Tables 1 and 2. Standard enthalpy of micellization (ΔH_m^0) of pure surfactants has been calculated by simply taking the subtraction between ΔH_{final}^0 to $\Delta H_{initial}^0$ ($\Delta H_m^0 = \Delta H_{final}^0 - \Delta H_{initial}^0$), which are the enthalpy changes at two extremes of sigmoidal profiles shown in Fig. 2A/2B (d). The values of ΔH_m^0 are calculated by above method have been presented in Table 4. For $C_{16}TPB$ both values of enthalpy of micellization were obtained and these are designated as $\Delta H_m^0(1)$ and ΔH_m^0 corresponding to heat change for two micellization for cmc_1 and cmc_2 respectively. From Table 4, it has been seen that $\Delta H_m^0(1)$ for $C_{16}TPB$ is relatively higher in negative magnitude (more exothermic) than ΔH_m^0 of $C_{16}MImCl$. Bulky head groups containing three phenyl rings of $C_{16}TPB$ are easily dehydrated compared to the imidazolium head groups of $C_{16}MImCl$, i.e., less energy has been required to promote $C_{16}TPB$ comparing with $C_{16}MImCl$ to aqueous phase into micellar interior, more exothermic the enthalpy of micellization for $C_{16}TPB$. After the formation of first micelle, enthalpy change is negligible for the second one during cmc_2 probably owing to change in micellar shape and size manifested in less negative $\Delta H_m^0(2)$ value (cf. Table 4.) both in presence and absence of NaAlg in conjugation with $C_{16}TPB$. In presence of different wt % of NaAlg, enthalpograms are no longer sigmoid in nature and therefore, the C_m^* values have been taken from the intersection points of two linear segments before and after C_m^* shown in Fig. 9

(a) and 9 (b). Although the break point near C_m^* for $C_{16}MImCl + 0.01\%$ NaAlg system is not prominent, a sharp breakpoint is also formed (cf. Fig. 9 (a)) before C_m^* for that system at lower surfactant concentration which was close to C_s determined tensiometrically. In presence of NaAlg at different wt % solution, enthalpograms resemble to its polyelectrolyte free profiles of pure surfactants (cf. 9(c) and 9 (d)), except the enthalpy values are quite different in between alginate free and alginate containing solution during the course of surfactant additions. Such difference of dilution of micelles clearly indicates there some conformational change of polyelectrolytes³³ as the free surfactant monomer. From Fig. 9(c), it is evident that, almost no change is observed during the titration of $C_{16}MImCl$ in different wt % solution of NaAlg but change is found to pure $C_{16}MImCl$ in aqueous solution. At low $[NaAlg]$ the enthalpogram shows more endothermic nature than pure surfactant and also endothermicity persists in post micellar regime. More endothermic contribution at low surfactant concentration is probably due to the electrostatic binding of $C_{16}MImCl$ on to the backbone of NaAlg with consequent break down of water molecules around NaAlg backbone. Similar observation³³ has been found in for $C_{16}mimBr$ in 1 g/L NaCMC medium in comparison with $C_{16}mimBr$ in aqueous solution.



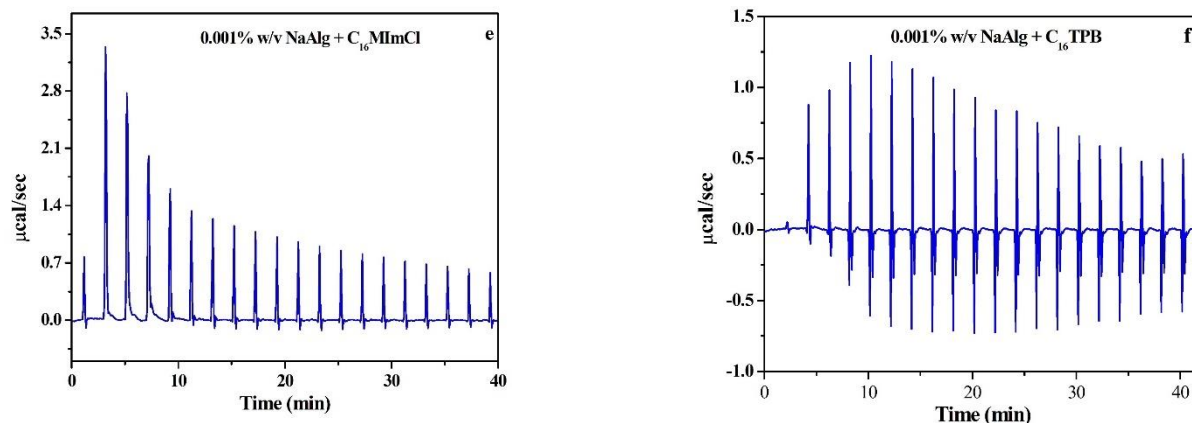


Fig. 9. 9(a). ITC profile for $C_{16}MImCl$ in presence of different wt% of NaAlg (enthalpograms are shifted to 4 units upward for better representation); 9(b). ITC profile for $C_{16}TPB$ in presence of different wt% of NaAlg; 9(c) and 9(d). Combined enthalpogram of $C_{16}MImCl$ and $C_{16}TPB$ respectively, in presence and absence of NaAlg for comparison purpose; 9 (e) and (f). Raw calorimetric traces (heat flow vs. Time) for $C_{16}MImCl$ and $C_{16}TPB$ respectively in presence of 0.001% (w/v) NaAlg medium.

After free micelle formation, no further heat change was observed as the medium contained only micelles, manifested in tending to zero of the enthalpograms (Fig. 9(c)) except for the micellization of pure $C_{16}MImCl$ where constant negative heat change has been observed at the post micellar region. It has been reported^{78,79} that for some surface active ionic liquid, constant enthalpy values have been observed in post micellar region above and below to zero without tending to zero. Again, enthalpograms of $C_{16}TPB$ in conjugation with different wt% of NaAlg show less endothermic in nature (Fig. 9(d)) at low $[C_{16}TPB]$ when compared with enthalpogram of free $C_{16}TPB$ in aqueous solution. This observation clearly indicates the weak binding of oppositely charged $C_{16}TP^+$ with NaAlg backbone which has been assigned in tensiometry section. Faint inflections (cf. Fig. 9(b)) have been observed at low concentration of $C_{16}TPB$ designated as cac displayed in Table 2. Representative diagram of raw calorimetric traces ($\mu cal/s$ vs. Time (min)) for $C_{16}MImCl$ and $C_{16}TPB$ in conjugation with 0.001% (w/v) NaAlg has been presented in Fig. 9(e) and 9(f) respectively. Enthalpy of micellization (ΔH_m^0) for the surfactants in presence of different wt % NaAlg has been calculated by the procedure discussed above for pure surfactants in aqueous solution. The values of cac , C_s and C_m^* are found for the present two surfactants in presence of different wt % of NaAlg by ITC measurement shown in Tables 1 and 2. It has been seen from Table 1 that, C_m^* values for $C_{16}MImCl$ in aqueous solution and in presence of 0.001 and 0.005% NaAlg media are found comparatively lower than those found in presence of other techniques, while for 0.01% NaAlg

medium, C_m^* is relatively higher than the prediction of other techniques. The values of enthalpy of micellization (ΔH_m^0) for $C_{16}MImCl$ and $C_{16}TPB$ in conjugation with NaAlg have been reported in Table 4 denoting exothermic in nature. Two enthalpies of micellization ($\Delta H_m^0(1)$, and $\Delta H_m^0(2)$) for $C_{16}TPB$ corresponding to two cmcs have been presented here in Table 4. This shows that, with increase of the concentration of NaAlg in conjugation with $C_{16}TPB$, negative $\Delta H_m^0(1)$ decreases gradually from -4.31 to -0.31 $\text{kJ}\cdot\text{mol}^{-1}$ at 0.005% NaAlg. Beyond which negative $\Delta H_m^0(1)$ increases again in presence of 0.01% NaAlg, while negative second enthalpy of micellization ($\Delta H_m^0(2)$) decreases with increase [NaAlg]. On the other hand, negative ΔH_m^0 decreases from -3.52 to -3.35 at 0.005 % NaAlg concentration in conjugation with $C_{16}MImCl$ and decreases sharply in presence of 0.01% NaAlg medium. Unlike to the earlier observation for $C_{16}TPB$, no minimum is found for the ΔH_m^0 trending for $C_{16}MImCl$ within the investigated concentration range of NaAlg (from 0 to 0.01%).

Here, standard entropy of micellization (ΔS_m^0) has been calculated taking the values of ΔG_m^0 which have been discussed in previous section and ΔH_m^0 using Gibbs-Helmholtz equation:

$$\Delta G_m^0 = \Delta H_m^0 - T\Delta S_m^0 \quad (13)$$

Micellization of $C_{16}MImCl$ and $C_{16}TPB$ is spontaneous (positive ΔS_m^0) shown in Table 4. Positive ΔS_m^0 increases (more spontaneous) with increase of NaAlg concentration in presence of $C_{16}MImCl$, while less spontaneous in presence of $C_{16}TPB$ for both micellization process (both entropy of micellization designated as $\Delta S_m^0(1)$ and $\Delta S_m^0(2)$ respectively) with increase of the concentration of NaAlg (cf. Table 4). Contribution of $T\Delta S_m^0$ over ΔG_m^0 has been found $\geq 90\%$ (cf. Table 4), which indicates micellization of $C_{16}MImCl$ and $C_{16}TPB$ in presence and absence of different wt % of NaAlg driven by entropy factor.

3.6. FTIR-ATR spectroscopy: Characterization of NaAlg-surfactant complexes in conjugation with pure NaAlg, $C_{16}MimCl$ and $C_{16}TPB$

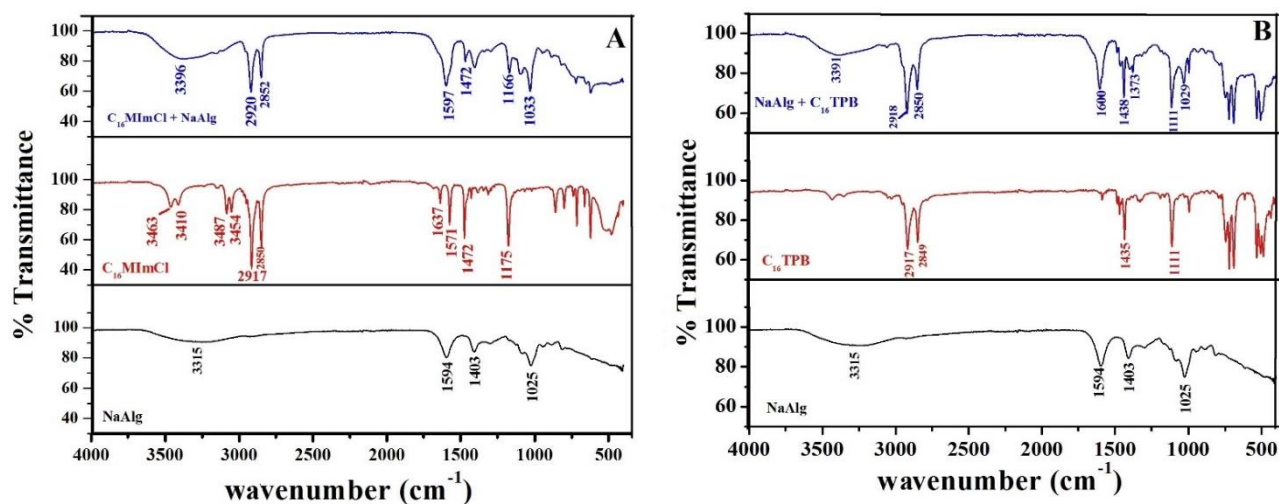


Fig. 10. Comparative profiles of % transmittance vs. wavenumber (cm^{-1}) for $C_{16}MimCl$ (A) and $C_{16}TPB$ (B). Three panels of each figure have been designated as: lower panel for NaAlg, middle panel for pure surfactant and upper panel for NaAlg-surfactant complex. Complex formation of NaAlg with $C_{16}MimCl$ and $C_{16}TPB$ has been done in 0.01% (w/v) NaAlg solution.

Characteristic absorption bands of NaAlg (both the lower panel of Fig. 10A and 10B) around 3315, 1594, 1403 and 1025 cm^{-1} correspond to stretching of hydroxyl (-OH) group, asymmetric stretching vibration of COO- group, symmetric stretching vibration of COO- group and elongation of C-O-C group in between the two adjacent residues respectively⁸⁰⁻⁸².

ATR spectrum of $C_{16}MimCl$ (middle panel of Fig. 10A) shows characteristics absorption peaks around 3087 and 3054 cm^{-1} due to the stretching vibration of aromatic H of imidazolium ring. Strong absorption peaks around 2117 and 2850 cm^{-1} are found due to the stretching vibration of alkyl-H in the 16-carbon long chain. Absorption peaks at 1571 and 1472 cm^{-1} are due to the vibrations of C=C and C=N of imidazolium ring respectively. Absorption Peaks at 3463 and 1637 cm^{-1} are owing to presence of free hydroxyl group (trapped H_2O molecules due to water of hydration attached to pure $C_{16}MimCl$). Absorption peak at 3410 cm^{-1} is due to the H bonded $H\cdots OH$ stretching vibration between water molecules⁸³.

ATR spectrum of $C_{16}TPB$ has been shown in Fig. 10B (middle panel). Asymmetric and symmetric stretching vibration of - CH_2 group containing 16-carbon alkyne chain are found

around 2917 and 2849 cm^{-1} respectively⁸⁴. Peak around 1435 cm^{-1} is due to the $-\text{CH}_2$ bending vibration.

Solid polyelectrolyte-surfactant complexes were formed due to 1:1 charge neutralization between cationic surfactant head groups of surfactants with negatively charged COO^- groups on to NaAlg backbone at moderately high surfactant concentration well above CNC (critical neutralization concentration)⁸⁵. ATR spectrum of NaAlg- $\text{C}_{16}\text{MImCl}$ complex has been shown in Fig. 10(A) (upper panel). Absorption peaks at low wavenumber region ($<1000 \text{ cm}^{-1}$, fingerprint region) are found less intense and sometimes disappeared in complex than those found in pure $\text{C}_{16}\text{MImCl}$, i.e., pure $\text{C}_{16}\text{MImCl}$ loss its individual identity in complex. Inclusion of new peak at 1033 cm^{-1} was found in alginate- $\text{C}_{16}\text{MImCl}$ complex which was not found in the spectrum of pure $\text{C}_{16}\text{MImCl}$. The intense peak at 1033 cm^{-1} is close to the relatively less intense peak of 1025 cm^{-1} which is found in pure NaAlg spectrum attributed to elongation of C-O-C of NaAlg requiring higher energy in presence of IL. Intense peak at 1175 cm^{-1} found in pure $\text{C}_{16}\text{MImCl}$ profile is transformed to less intense peak found at 1166 cm^{-1} in presence of NaAlg- $\text{C}_{16}\text{MImCl}$ complex. Intense peak at 1472 cm^{-1} for pure $\text{C}_{16}\text{MImCl}$ becomes less intense in presence of $\text{C}_{16}\text{MImCl}$ -NaAlg complex. Peaks at 1571, 1637, 3054, 3087, 3410 and 3463 cm^{-1} found in $\text{C}_{16}\text{MImCl}$ profile remain absent in the profile of NaAlg- $\text{C}_{16}\text{MImCl}$, while peak at 1597 cm^{-1} and the broad peak (peak centre at 3396 cm^{-1}) with shifting of values and change in intensities carry the identity of pure NaAlg to the complex comprise of NaAlg- $\text{C}_{16}\text{MImCl}$. On the other hand, fingerprint region in presence of NaAlg- C_{16}TPB complex remains more or less intact comparing with pure C_{16}TPB . Peak positions at 1111, 2917 and 2849 cm^{-1} in presence of pure C_{16}TPB (middle panel of Fig. 10B) remain unchanged at the ATR spectrum of complex made by NaAlg + $\text{C}_{16}\text{MImCl}$ (upper panel of Fig. 10B) and peak intensity remains same in both the profiles. ATR peak at 1435 cm^{-1} for pure C_{16}TPB changed to slightly high energy peak at 1438 cm^{-1} found in complex. Strong absorption peak at 1600 cm^{-1} appeared in NaAlg- C_{16}TPB complex which was seen at 1594 cm^{-1} in pure NaAlg profile. Broad peak around 3391 cm^{-1} masks the other small intensity peak within 3000-3500 cm^{-1} found in case of pure C_{16}TPB has observed for the polyelectrolyte-surfactant complex. Overall, it has been said by scrutinizing the comparative ATR- profiles of NaAlg, surfactants and their complexes that formation of complexes have made by inclusion of surfactants to polyelectrolyte backbone.

3.7. Dynamic Light Scattering (DLS), HR-TEM and fluorescence microscopy:

We have applied here first mixing procedure⁸⁶ when surfactants are added to NaAlg solution for the measurement of hydrodynamic radius (r) of NaAlg-surfactant complex. Diagrams of average hydrodynamic radius (r) vs. [surfactant] have been represented in Fig. 11(A) and 11(B) for C₁₆MImCl and C₁₆TPB respectively in presence of 0.01% (w/v) of NaAlg.

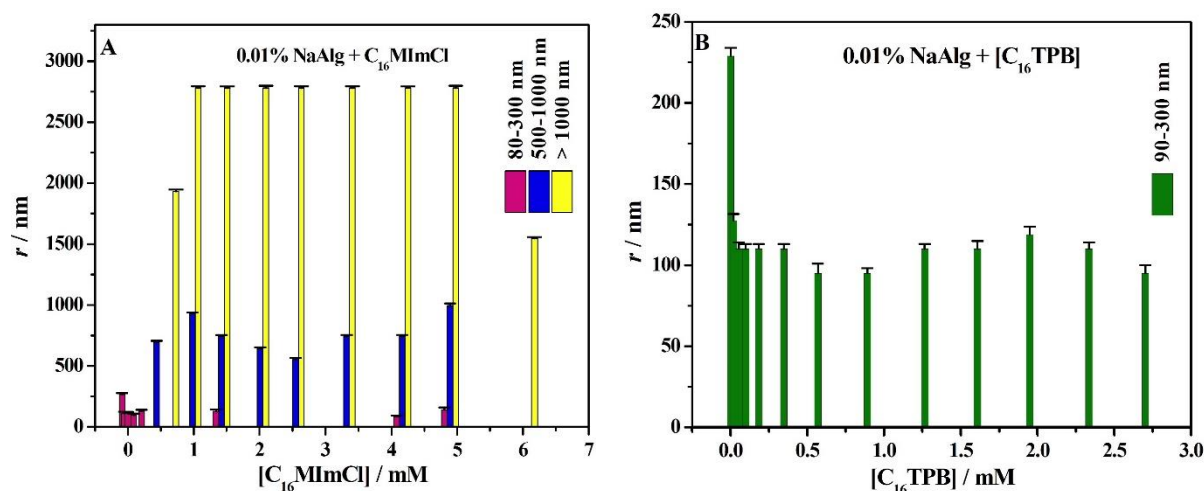


Fig. 11. Average hydrodynamic radius (r) vs. [surfactant] for C₁₆MImCl (A) and C₁₆TPB (B) in presence of NaAlg (0.01% w/v). Error bars are given at each diagram.

Wide range of mean hydrodynamic radius (r) distribution has been shown for C₁₆MImCl + NaAlg system (Fig. 11(A)) at and above 0.98 mM concentration of C₁₆MImCl due to existence of several polyelectrolyte-surfactant species present in the medium. Initially, below 0.98 mM, size of free NaAlg (229 -265 nm) decreases upon increase of C₁₆MImCl upto 0.18 mM of [C₁₆MImCl] probably due to the charge neutralization on polyelectrolyte backbone by positively charged surfactant monomers which in terms decrease intramolecular repulsion in the polyelectrolytes and shrink polyelectrolyte hydrodynamic diameter bound with surfactants. After that, r increases again from 0.3 mM to 0.7 mM due to attachment of small premicellar aggregates containing C₁₆MImCl monomers onto NaAlg backbone (necklace conformers). After C_m^* ([C₁₆MImCl] \geq 0.98 mM), three types of distributions present in medium: (i) $r > 1000$ nm due to formation of agglomerated species comprise of free micelles of C₁₆MImCl intercalated in necklace type conformers of polyelectrolytes., (ii) Complete charge neutralisation of polyelectrolyte is often not found throughout the polyelectrolyte backbone. Such incompletely neutralized polyelectrolytes adsorb on the free micellar surface due to electrostatic reason which is manifested in species formed in solution having radius in between 500 – 1000 nm., and thirdly, (iii) some polyelectrolyte-surfactant complexes break down in

solution and absorb in micellar medium forming complex of relatively less hydrodynamic radius (80-140 nm). On the other hand, single size distribution has been observed at different $[C_{16}TPB]$ in the range between 90 to 250 nm (cf. 11(B)) within the size limit of DLS instrument. Hydrodynamic radii of free NaAlg drop from ~ 230 nm to 127 nm when $[C_{16}TPB]$ increases from 0 to 0.018 mM. The decrease in r is probably due to charge neutralization in polyelectrolyte chains stated above. Further increase in surfactant concentration from 0.05 mM to 1.6 mM, r hardly changes (95-110 nm) shown in Fig. 11(B). We have not found higher sized species for the interaction of $C_{16}TPB$ with NaAlg after C_m^* , those found in presence of $C_{16}MImCl$ in conjugation with NaAlg. This observation suggests that weak interaction prevailed in presence of NaAlg with $C_{16}TPB$ than $C_{16}MImCl$. Same observation has also found by other investigated techniques discussed above. Polydispersity index (PDI) values (cf. Fig S2) of NaAlg (0.01% w/v)-surfactant interacted complexes are lower than the free NaAlg (0.01% w/v), but the values are within the limit of monodispersity (<0.7). Furthermore, it was seen from Fig. S2 that PDI values of NaAlg + $C_{16}MImCl$ systems (even greater at high $C_{16}MImCl$ concentration) have greater than NaAlg + $C_{16}TPB$ systems indicating less monodisperse character of NaAlg + $C_{16}MImCl$ system (multiple size distribution with variation of surfactant concentration) character than $C_{16}TPB$ in conjugation with NaAlg. HR- TEM images of polyelectrolyte-surfactant complexes have been shown in Fig. 12.

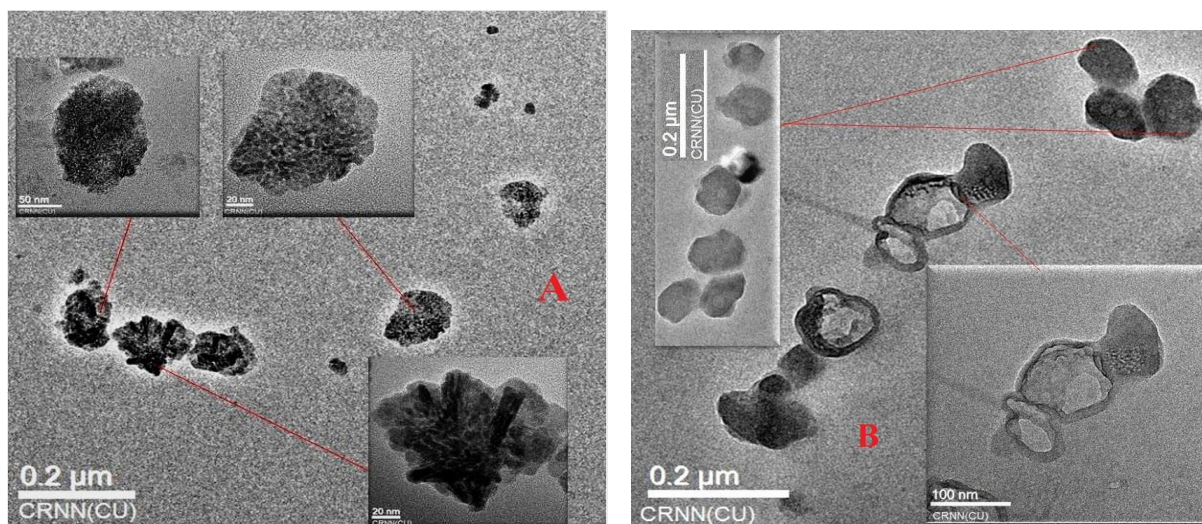


Fig. 12. Complex formation between NaAlg (0.01% w/v) with $C_{16}MImCl$ (A) and $C_{16}TPB$ (B).

NaAlg (0.01% w/v) + $C_{16}MImCl$ complexes (Fig. 12(A)) show non uniform globular like structure with radius varying between the range of 50-65 nm associated with small globular fragments (10-25 nm). Larger aggregates are not found for NaAlg - $C_{16}MImCl$ complex above

100 nm radius, those found using DLS measurement in solution phase. For NaAlg (0.01% w/v) + C₁₆TPB system (Fig. 12B), complexes look like different morphology, such as, non-uniform unpolished stone shaped coacervates (average radius within the range of 30-45 nm) along with single and fused ring like appearance structure. Average radii of these single and fused ring-shaped complexes (Fig. 12B) are found around 55 and 100 nm respectively. Less aggregated ring-shaped complex has been found in coacervates formed by 0.01% NaAlg with C₁₆TPB clearly indicating less association of NaAlg with C₁₆TPB in compared to C₁₆MImCl.

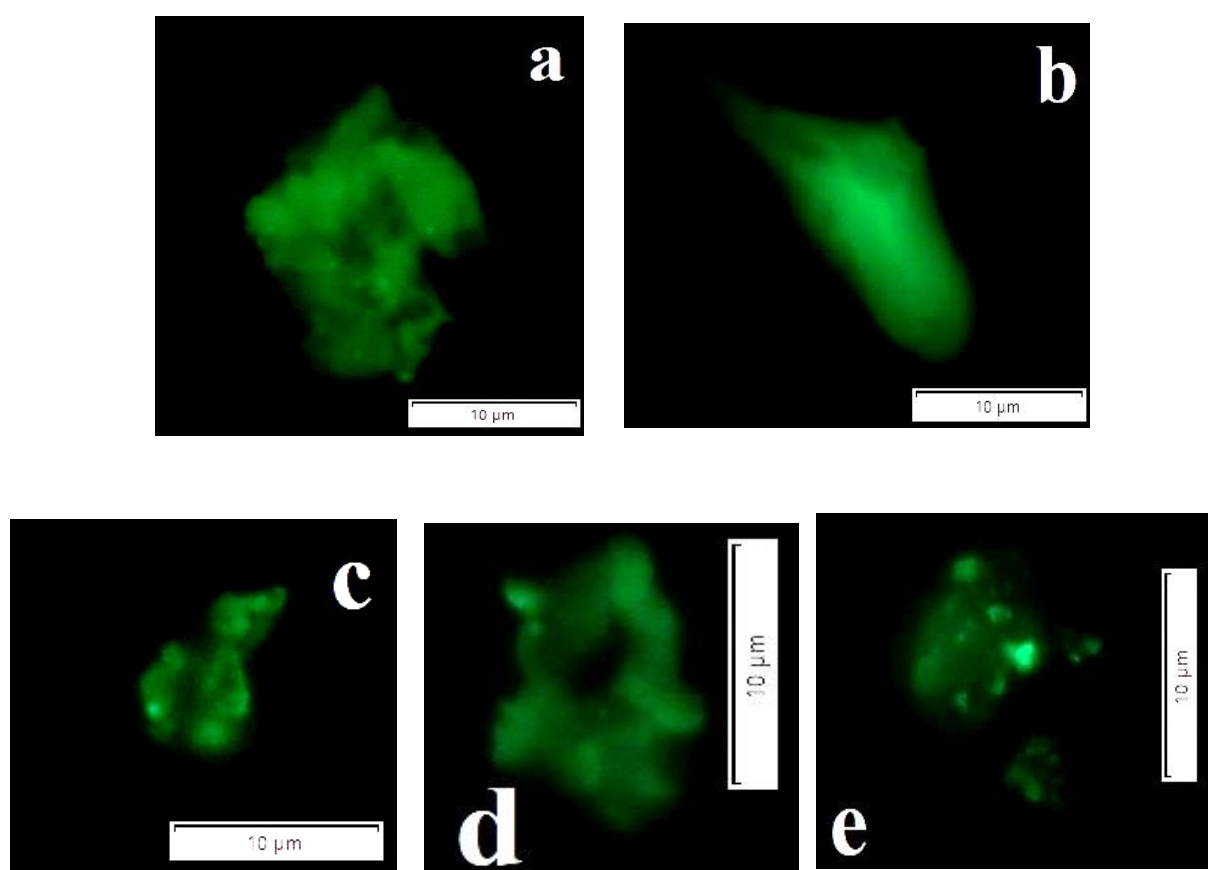


Fig. 13. Fluorescence microscopy images of polyelectrolyte-surfactant complexes: NaAlg (0.01% w/v) + C₁₆MImCl (a,b) and NaAlg (0.01%) + C₁₆TPB (c,d, and e). Scale bar = 10μm.

Non uniform cluster of polyelectrolyte surfactant complexes (NaAlg concentration fixed at 0.01% w/v) in coacervate form of relatively larger size have been found in Fig. 13. Clusters formed by NaAlg with C₁₆MImCl are found relatively denser (Fig. 13 (a), (b)) than NaAlg + C₁₆TPB system (Fig. 13(c), (d) and (f)) by observing the fluorescence intensity of DPH probes (bright green spots) attached to the micellar aggregates wrapped by NaAlg chains in

agglomerated form. Polyelectrolyte-surfactant clusters are found in different shapes (Fig. 13). As DPH selectively strains the micelles inside the aggregated complexes, free NaAlg structure cannot be detected. No smaller aggregates (< 1000 nm) are observed in fluorescence microscopic study.

Table1. Tabulated values of cmc for pure C₁₆MImCl in aqueous solution and cac, C_s and C_m* values appeared at different concentrations of C₁₆MImCl in presence of 0.001, 0.005 and 0.01% (w/v) of NaAlg in aqueous solution by different experimental techniques employed here at 298.15 K. †

[NaAlg] % w/v	Conductometry			tensiometry			fluorimetry			ITC			Turbidimetry		
	cac mM	C _s mM	cmc / C _m *(β) mM	cac mM	C _s mM	cmc/ C _m * mM	cac mM	C _s mM	cmc/C _m * mM	cac mM	C _s mM	cmc /C _m * mM	T ₁ mM	T ₂ mM	T _m mM
0			0.85(0.51) 0.876 (0.50) ^a 0.860 ^b			0.83 0.955 ^a			0.72			0.68 0.99 ^b			
0.001%	0.030	0.43	0.92(0.57)	0.033	0.35	0.85	0.044	0.34	0.85	-	-	0.74	0.04	-	1.07
0.005%	0.140	-	1.06(0.61)	0.049	0.62	0.88	0.051	0.65	0.97	-	-	0.86	0.167	0.41	1.34
0.01%	0.36	-	1.18(0.59)	0.069	0.76	1.14	0.062	-	1.24	-	0.65	1.55	0.26	0.54	1.36

a. Ref. [19]

b. Ref. [37]

†Standard uncertainties in terms of cac, C_s and C_m* / cmc are $\pm 0.01\%$, $\pm 0.005\%$ and $\pm 0.02\%$ respectively.

Table 2. Tabulated values of cmc_1 , and cmc_2 for pure $C_{16}TPB$ in aqueous solution and cac , C_s and C_m^{*1} , C_m^{*2} values appeared at different concentrations of $C_{16}TPB$ in presence of 0.001, 0.005 and 0.01% (w/v) of NaAlg in aqueous solution by different experimental techniques employed here at 298.15 K.[†]

[NaAlg] % w/v	conductometry				Tensiometry			fluorimetry			ITC			Turbidimetry		
	Cac mM	C _s mM	cmc ₁ /cmc ₂ or C _m ^{*1} /C _m ^{*2} mM	β_1/β_2	cac	C _s	cmc ₁ /cmc ₂ or C _m ^{*1} /C _m ^{*2} mM	Cac	C _s	cmc ₁ /cmc ₂ or C _m ^{*1} /C _m ^{*2} mM	cac	C _s	cmc ₁ /cmc ₂ or C _m ^{*1} /C _m ^{*2} mM	Φ_1 mM	Φ_2 mM	Φ_m mM
0	-	-	0.16/0.39 0.20/0.42 ^c 0.14/0.34 ^d	0.28/0.37 0.32/0.54 ^c 0.308/0.52 ^d			0.12/0.31 0.24/- ^c			0.14/-			0.12/0.36 0.11/- ^d			
0.001%	-	0.022	0.24/0.67	0.33/0.18	0.009	0.026	0.13/0.53	0.013	0.023	0.14/0.33	0.008	-	0.11/0.41	0.12	0.49	0.98
0.005%	0.007	0.02	0.21/0.59	0.07/0.20	0.011	0.025	0.10/0.40	0.024	-	0.09/0.30	0.007	-	0.09/0.38	0.11	0.29	0.91
0.01%	0.009	0.117	0.43/0.63	0.02/-	0.015	0.056	0.15/0.52	0.026	-	0.16/0.42	0.008	-	0.13/0.42	0.073	-	0.44

c. Ref. [38]

d. Ref. [36]

[†]Standard uncertainties of cac , C_s and C_m^*/cmc are $\pm 0.01\%$, $\pm 0.03\%$ and $\pm 0.02\%$ respectively.

Table 3. Interfacial and bulk parameters of surfactants measured in absence and presence of varying concentration of NaAlg (0.001, 0.005 and 0.01% w/v) in aqueous solution at 298.15 K. †

[NaAlg] % w/v	C ₁₆ TPB							C ₁₆ MimCl						
	10 ⁶ Γ _{cmc} ¹ mol.m ⁻²	10 ³ A _{min} ¹ nm ² /molecule	π _{cmc} ¹ /π _{cmc} ²	γ _{cmc} ¹ /γ _{cmc} ² mN.m ⁻¹	P ¹	pC ₂₀	N _a	10 ⁶ Γ _{cmc} mol.m ⁻²	10 ³ A _{min} nm ² /molecule	π _{cmc}	γ _{cmc} mN.m ⁻¹	P	pC ₂₀	N _a
0	0.93	1.78	27.6/29.2	39.1/37.5	0.117	1.49	8±5	1.15	1.46	30.6	36.4	0.144	0.58	49±6
0.001%	0.11	15.4	30.4/34.2	37.3/33.5	0.013	1.93	9±6	0.44	3.77	29.0	31.3	0.056	0.46	60±4
0.005%	0.69	2.40	29.3/32.8	36.4/32.9	0.087	1.95	16±6	0.97	1.71	33.2	31.7	0.121	0.79	59±5
0.01%	0.04	41.1	28.1/33.6	37.5/32.0	0.005	1.92	18±5	0.93	1.79	32.1	30.9	0.115	0.91	44±7

†Standard uncertainties of Γ_{cmc}, A_{min}, π_{cmc} and pC₂₀ are ± 0.04%, ± 0.04%, ± 0.02% and ± 0.03% respectively.

Table 4. Thermodynamic parameters for the micellization of C₁₆MimCl and C₁₆TPB determined in absence and presence of varying concentrations of NaAlg (0.001, 0.005 and 0.01% w/v) in aqueous solution at 298.15 K. †

[NaAlg]	C ₁₆ TPB				C ₁₆ MimCl			
	ΔG ⁰ _{m(1)/ΔG⁰_{m(2)} kJ.mol⁻¹}	ΔH ⁰ _{m(1)/ΔH⁰_{m(2)} kJ.mol⁻¹}	ΔS ⁰ _{m(1)/ΔS⁰_{m(2)} kJ.K⁻¹.mol⁻¹}	$\left \frac{T\Delta S_m^0}{\Delta G_m^0} \right $ (1)/(2)	ΔG ⁰ _m kJ.mol ⁻¹	ΔH ⁰ _m kJ.mol ⁻¹	ΔS ⁰ _m kJ.K ⁻¹ .mol ⁻¹	$\left \frac{T\Delta S_m^0}{\Delta G_m^0} \right $
0	-40.9/-40.4	-4.31/-0.73	0.123/0.133	0.89/0.98	-41.8	-3.52	0.128	0.92
0.001%	-42.3/-34.0	-3.03/-0.25	0.132/0.113	0.92/0.99	-43.2	-3.47	0.133	0.92
0.005%	-34.6/-35.1	-0.31/-0.25	0.115/0.117	0.99/0.99	-43.9	-3.35	0.136	0.93
0.01%	-31.3/-28.8	-2.38/-0.11	0.097/0.096	0.92/0.99	-42.8	-0.59	0.142	0.99

†Standard uncertainties of ΔG⁰_m, ΔH⁰_m and ΔS⁰_m are ± 0.04%, ± 0.03%, ± 0.04% respectively

Conclusions:

We have tried to shed light on the interaction of oppositely charged surfactants with polyelectrolyte probed by different experimental techniques in this manuscript. Difference of head groups of two surfactants is responsible for different extents of interaction with the carboxylate groups of M and G residues of NaAlg. Presence of bulky head groups of C₁₆TPB containing triphenyl attached to phosphonium cation makes it less accessible to COO⁻ groups of NaAlg over imidazolium cations of C₁₆MImCl, while C₁₆TPB enhances hydrophobicity in NaAlg medium forming greater amount of coacervates comparing with C₁₆MImCl + NaAlg systems. Existence of second cmc has been found clearly in presence of C₁₆TPB in aqueous solution by conductometry, ITC and fluorimetric techniques while, that cmc of C₁₆TPB is clearly detectable in presence of higher NaAlg concentration medium by tensiometry and conductometric techniques. Micellization process in presence of both surfactants is exothermic in presence of different wt% of NaAlg and overall decrease in exothermicity is observed with increase of polyelectrolyte concentration. The values of cac, C_S and C_m^{*} for two surfactants in corporation with different wt% (w/v) of NaAlg are estimated by different experimental techniques which have well similarity to each other. ATR spectra of polyelectrolyte-surfactant complex reveal the incorporation of surfactants into polyelectrolyte. DLS study reveals the hydrodynamic radii of NaAlg-surfactant complexes with variation of surfactant concentrations, while HR-TEM study reveals not only size but also shape of NaAlg-surfactant complexes. Fluorescence microscopy study detects relatively larger aggregates of NaAlg-surfactant complexes.

Supplementary Section

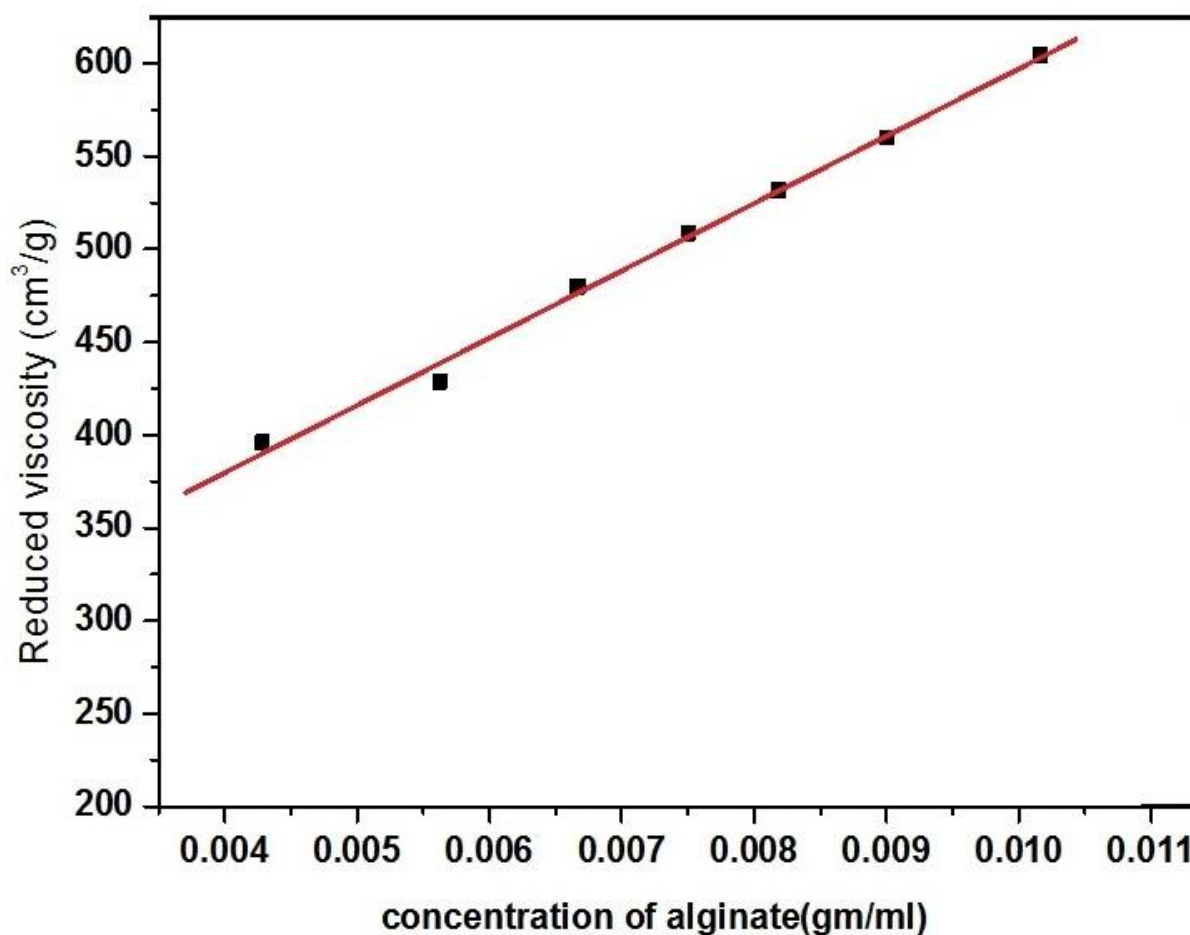
Table S1. Fitting parameters and lifetimes (τ_1 , τ_2 and $\langle\tau\rangle$) for different time resolved decay plots calculated using IBH DAS-6 software by nonlinear least square iterative method in presence of two different surfactants with their different concentrations in presence and absence of 0.005% (w/v) NaAlg.

[NaAlg] = 0.005% (w/v)						
[C ₁₆ MImCl]/ mM	a ₁	a ₂	τ_1	τ_2	$\langle\tau\rangle$	χ^2
0			123.5		123.5	1.05
0.012	13.5	86.5	32.57	124.8	112.3	1.06
0.036	16.9	83.0	36.07	124.8	109.8	1.01
0.073	23.1	76.9	39.14	120.6	101.8	0.99
0.121	34.4	65.6	64.38	163.9	129.6	0.99
0.211	35.2	64.8	75.76	192.3	151.3	1.01
0.318	30.4	69.6	70.39	180.6	147.1	1.13
0.469	29.7	70.3	69.44	170.9	140.7	1.08
0.668	37.6	62.3	74.51	180.5	140.6	1.03
0.943	27.9	72.0	67.64	161.9	135.5	0.95
1.310	11.1	88.9	52.62	163.8	151.5	1.06
1.756	17.1	82.9	83.42	184.7	167.4	1.06
2.939	4.38	95.6	55.35	170.4	165.4	1.03
3.690	9.17	90.8	81.80	175.3	166.7	0.99
4.510	3.18	96.8	40.71	170.3	166.2	1.02
5.353	6.96	93.0	82.24	174.1	167.7	1.02
[NaAlg] = 0.005% (w/v)						
[C ₁₆ TPB]/ mM	a ₁	a ₂	τ_1	τ_2	τ_{av}	χ^2
0			123.5		123.5	1.05
0.005	6.80	93.2	16.89	125.9	118.5	1.03
0.017	20.6	79.4	21.50	123.3	102.3	1.01
0.032	37.6	62.4	27.43	118.8	84.38	1.01
0.058	52.2	47.8	29.65	113.3	69.65	1.05
0.097	65.8	34.2	32.04	106.3	57.47	1.05
0.146	71.3	28.7	32.11	82.93	46.72	1.12
0.232	74.1	25.9	33.14	71.71	43.15	1.14
0.338	74.9	25.0	32.05	70.67	41.72	0.95
0.446	80.3	19.7	32.14	54.52	36.54	1.06
0.555	53.9	46.1	25.80	47.49	35.79	1.09
0.695	74.4	25.6	27.72	54.82	34.65	1.06
0.852	24.2	75.8	18.55	35.59	31.46	1.16
1.025	79.0	20.9	26.81	64.89	34.79	1.03
1.220	11.4	88.6	17.47	31.60	29.98	0.97
1.424	74.1	25.9	26.31	42.58	30.52	1.05
1.707	8.98	91.0	10.27	30.57	28.75	1.09
1.965	11.9	88.0	12.61	31.34	29.09	1.11
2.274	12.5	87.5	19.99	29.84	28.60	1.08

Table S2. Coefficients of A, B₁ and B₂ values derived from the fitting of $Y = A + B_1 \cdot X + B_2 \cdot X^2$ of γ vs. log [surfactant] plots given in Fig. S3.

[NaAlg] % w/v	C ₁₆ TPB			C ₁₆ MImCl		
	A	B ₁	B ₂	A	B ₁	B ₂
0	30.4	-8.67	1.16	34.8	-19.8	-3.94
0.001	41.8	7.78	5.12	37.5	-7.55	-0.004
0.005	43.2	-1.06	3.00	39.9	-16.6	-1.72
0.01	61.9	7.49	4.86	50.8	-15.6	-2.53

Fig. S1. Plot of reduced viscosity (cm³/gm) vs. concentration of alginate (gm/ml) at 298.15 K at a fixed NaCl concentration (0.1 M) #



Intrinsic viscosity $[\eta]$ of a polyelectrolyte can be determined in salt medium using Huggins equation:

$$\frac{\eta_{sp}}{C_P} = [\eta] + k_H[\eta]^2 C_P$$

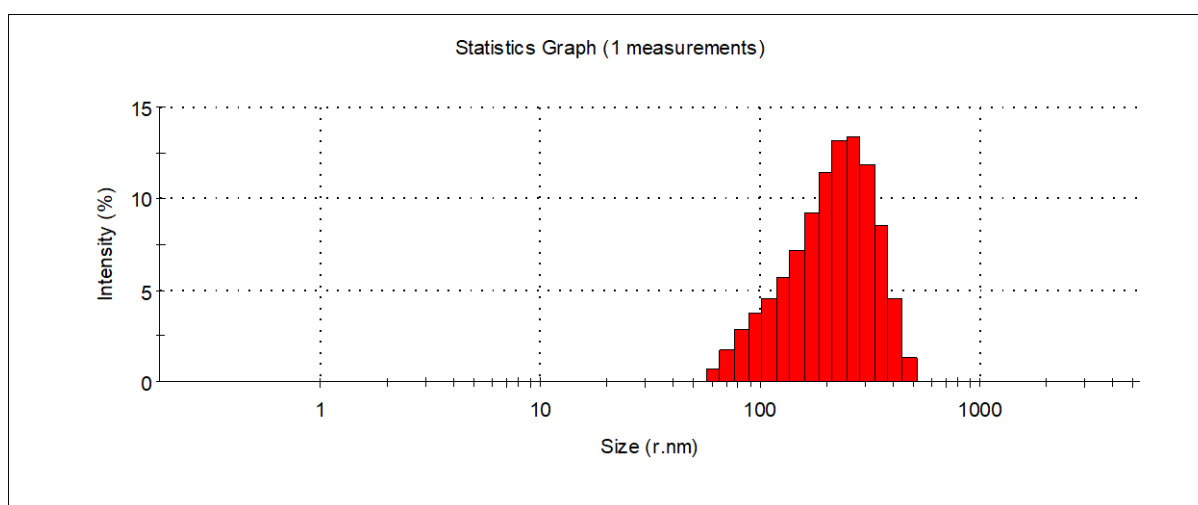
where, η_{sp} is the specific viscosity and C_P is the concentration of NaAlg (gm/ml). k_H is the Huggins constant. $\frac{\eta_{sp}}{C_P}$, termed as reduced viscosity in cm^3/g unit. A stock NaAlg solution was prepared in 0.1 M NaCl solution and progressively added to a 0.1 M NaCl solution taken in an ubbelohde viscometer fitted in a thermostatic water bath at 298.15 K and flow times were measured in triplicate after each addition of stock NaAlg. Reduced viscosity vs. concentration of alginate was plotted (shown in above). Intrinsic viscosity determined for NaAlg is $235 \text{ cm}^3/\text{gm}$ at 298.15 K and 0.1 M NaCl medium. Average viscometric molecular weight (M_v) of NaAlg was determined using Mark–Houwink equation:

$$[\eta] = K M_v^\alpha$$

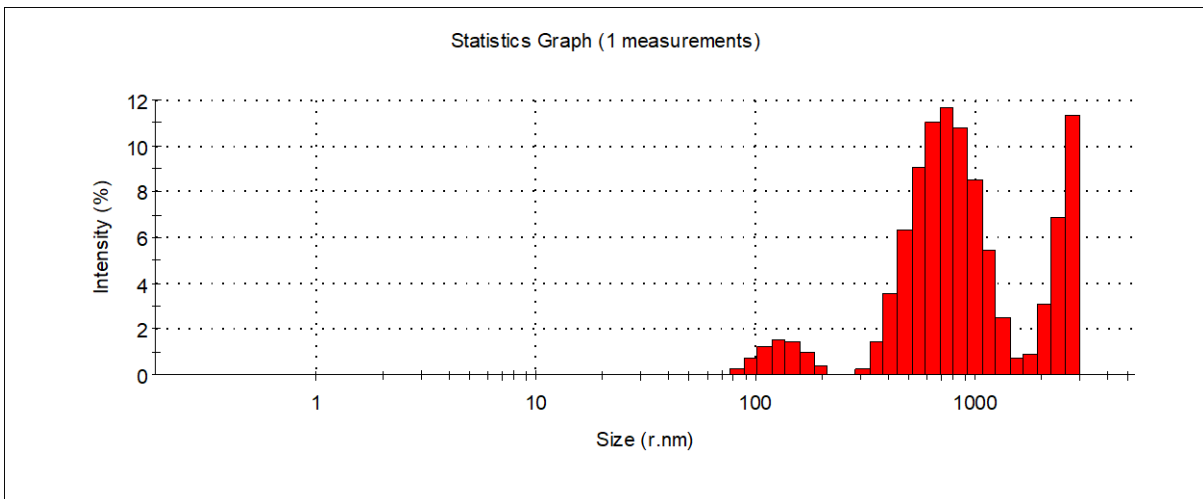
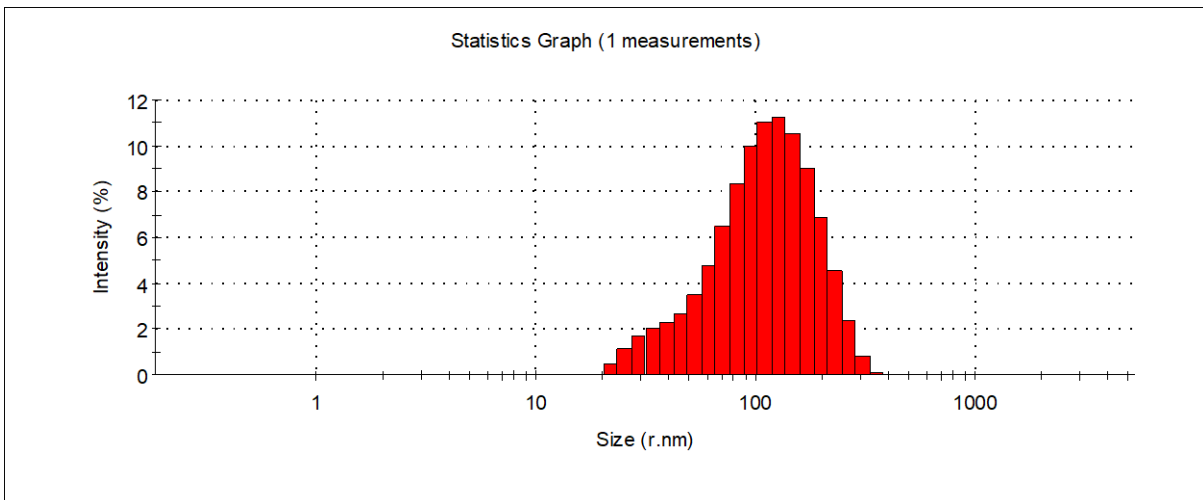
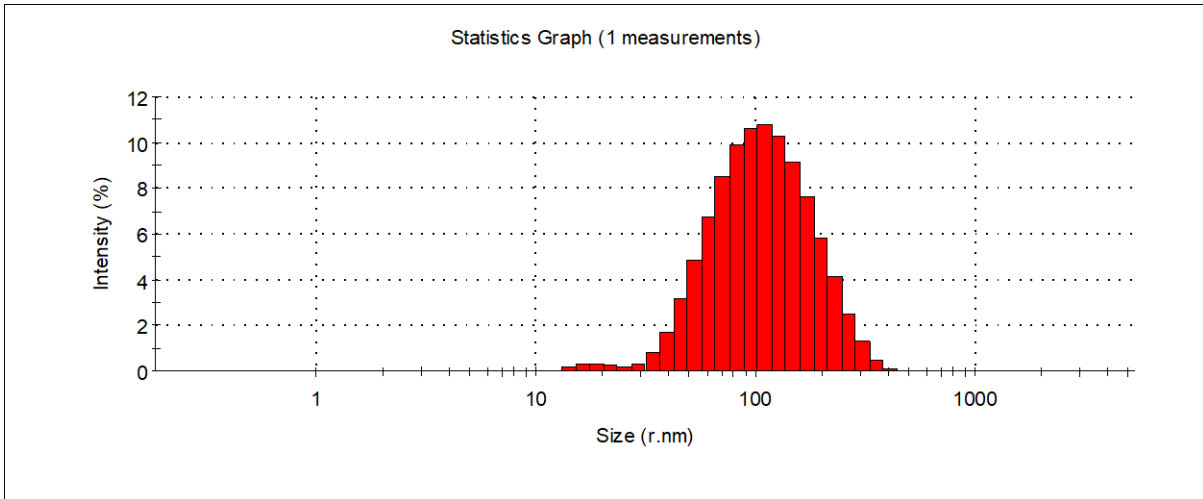
K and α are constants and characteristic of the medium, temperature and polymer. K and α values are taken from Clementi *et al.* [41], and Masuelli M. A. *et al.* [42]. $K = 0.0023 \text{ cm}^3/\text{gm}$, $\alpha = 0.984$.

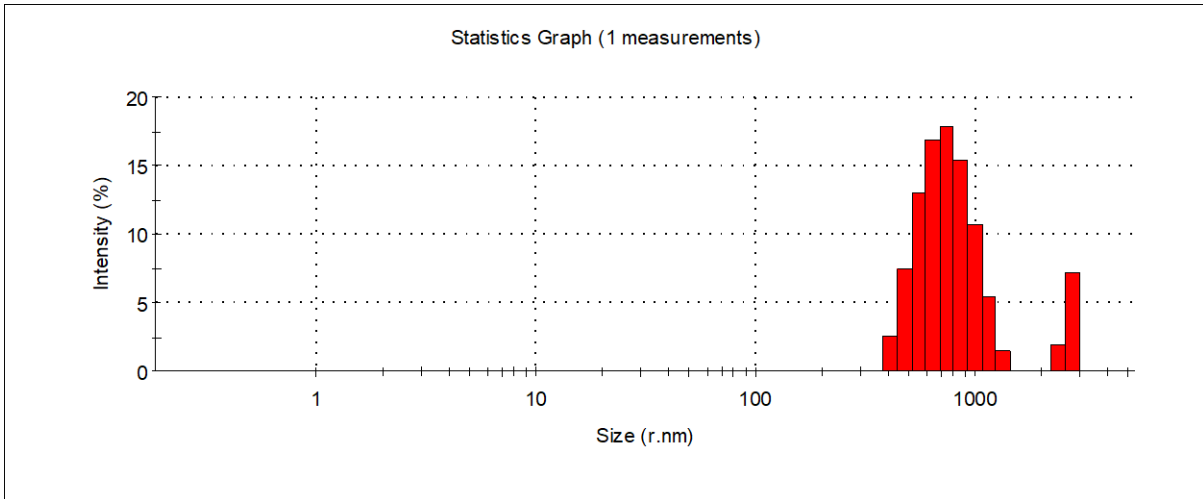
Fig.S2. Plot of % Intensity vs. hydrodynamic diameter of pure NaAlg (0.01% w/v) and with varying the concentrations of C₁₆MImCl (A) and C₁₆TPB (B) added to it. Concentrations of surfactants have been shown at the bottom of each plot. PDI values are given within a bracket beside each figure caption.

A



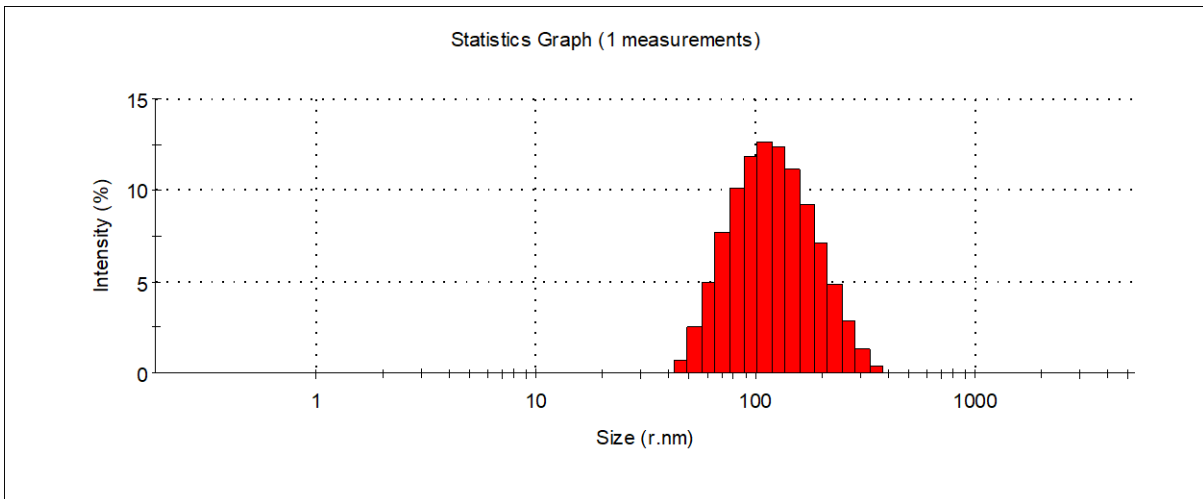
Free NaAlg 0.01% (PDI = 0.668)



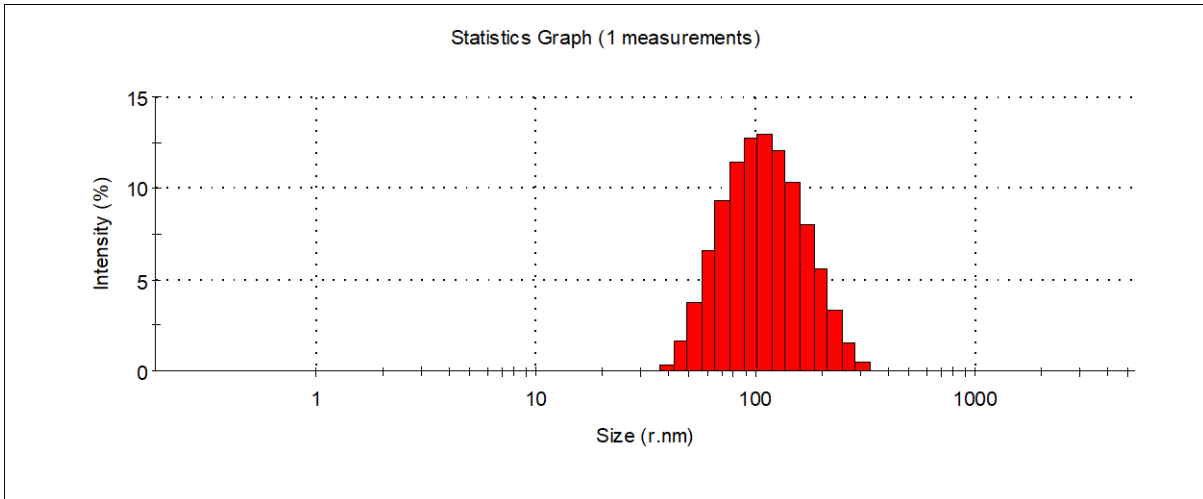


NaAlg 0.01% + 3.32 mM C₁₆MImCl (0.490)

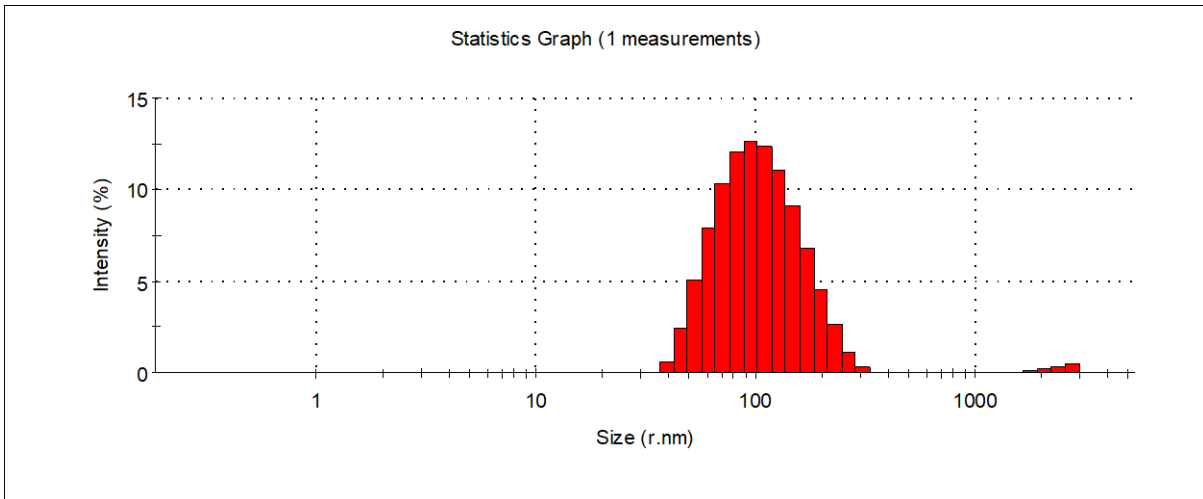
B



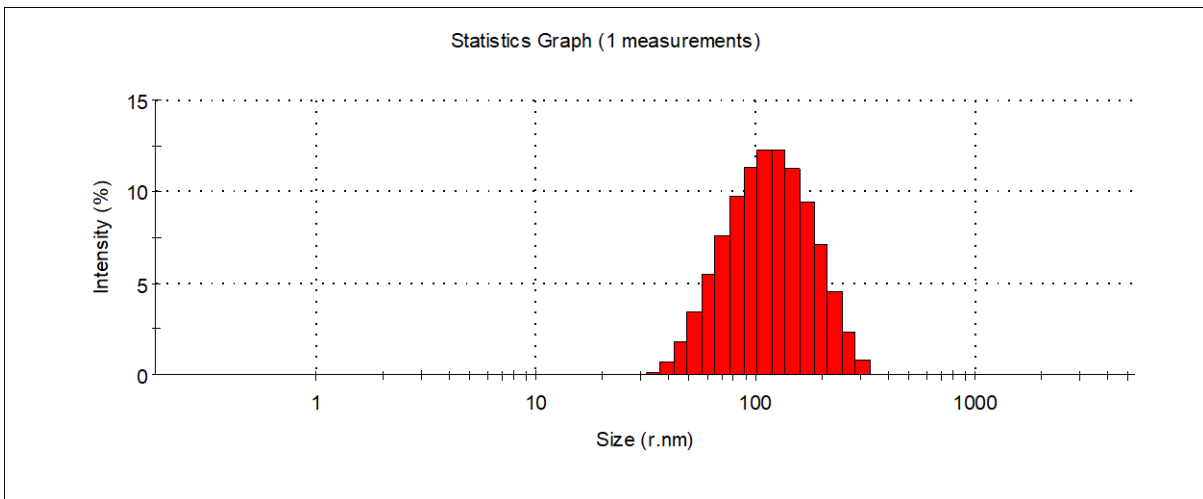
NaAlg 0.01% + 0.05 mM C₁₆TPB (PDI = 0.184)



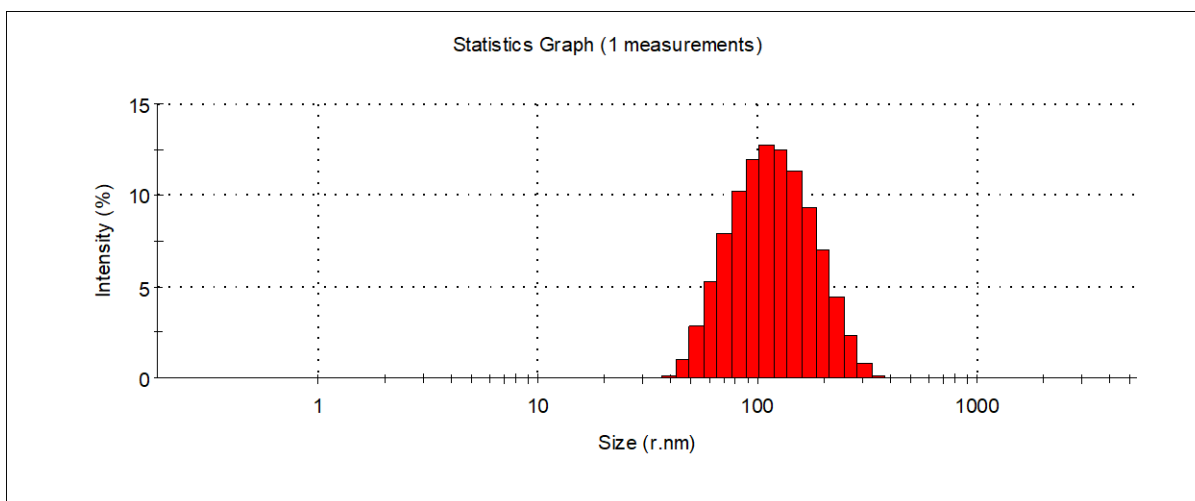
NaAlg 0.01% + 0.18 mM C₁₆TPB (PDI = 0.186)



NaAlg 0.01% + 0.89 mM C₁₆TPB (PDI = 0.197)



NaAlg 0.01% + 1.95 mM C₁₆TPB (PDI = 0.150)



NaAlg 0.01% + 2.33 mM C16TPB (PDI = 0.181)

Fig. S3. γ with corresponding $\log[\text{surfactant}]$ values up to cmc/C_m^* and fitted them with second order polynomials [a: free C₁₆MImCl, b: free C₁₆TPB, c: C₁₆MImCl + 0.001% (w/v) NaAlg, d: C₁₆MImCl + 0.005% (w/v) NaAlg, e: C₁₆MImCl + 0.01% (w/v) NaAlg, f: C₁₆TPB + 0.001% (w/v) NaAlg, g: C₁₆TPB + 0.005% (w/v) NaAlg, h: C₁₆TPB + 0.01% (w/v) NaAlg]

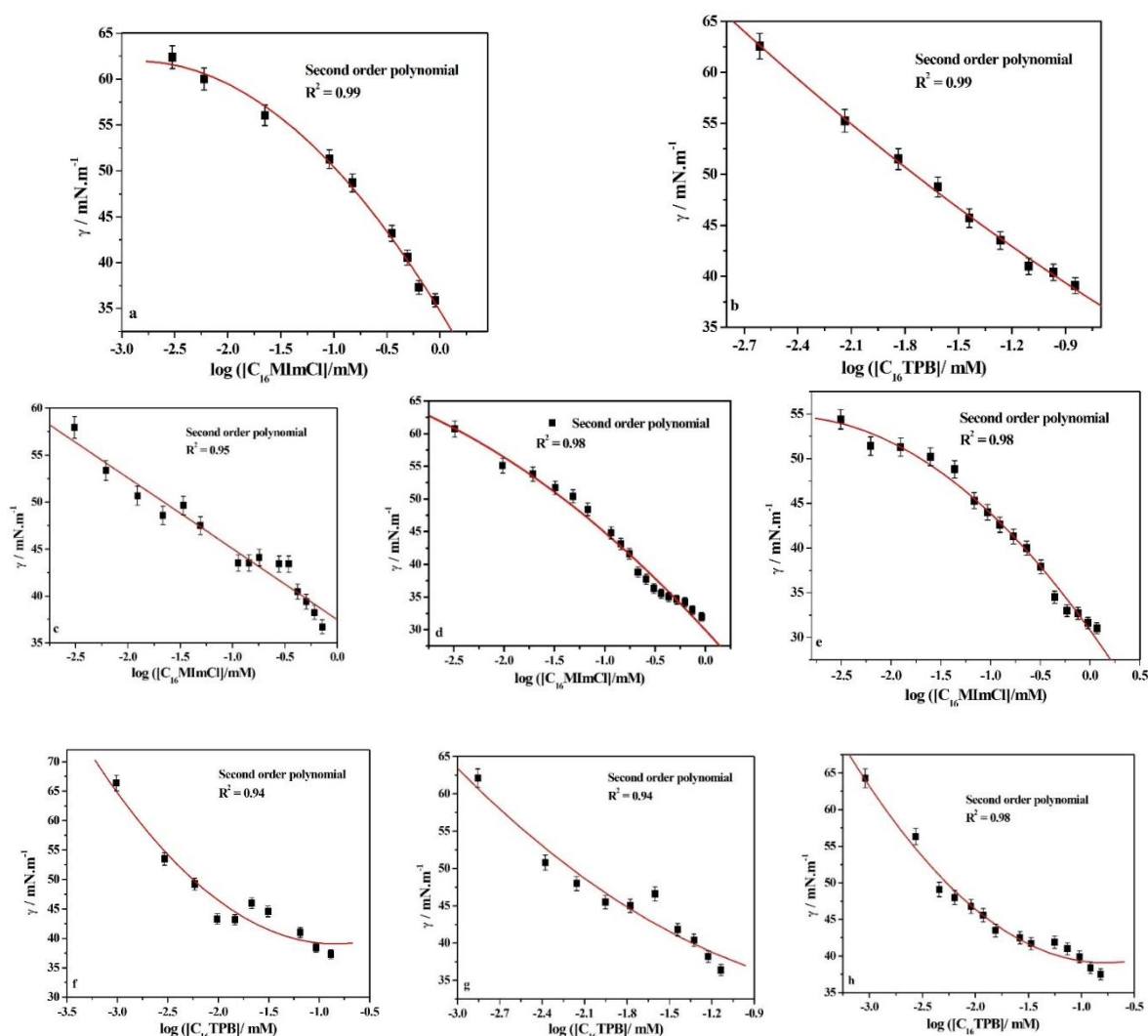
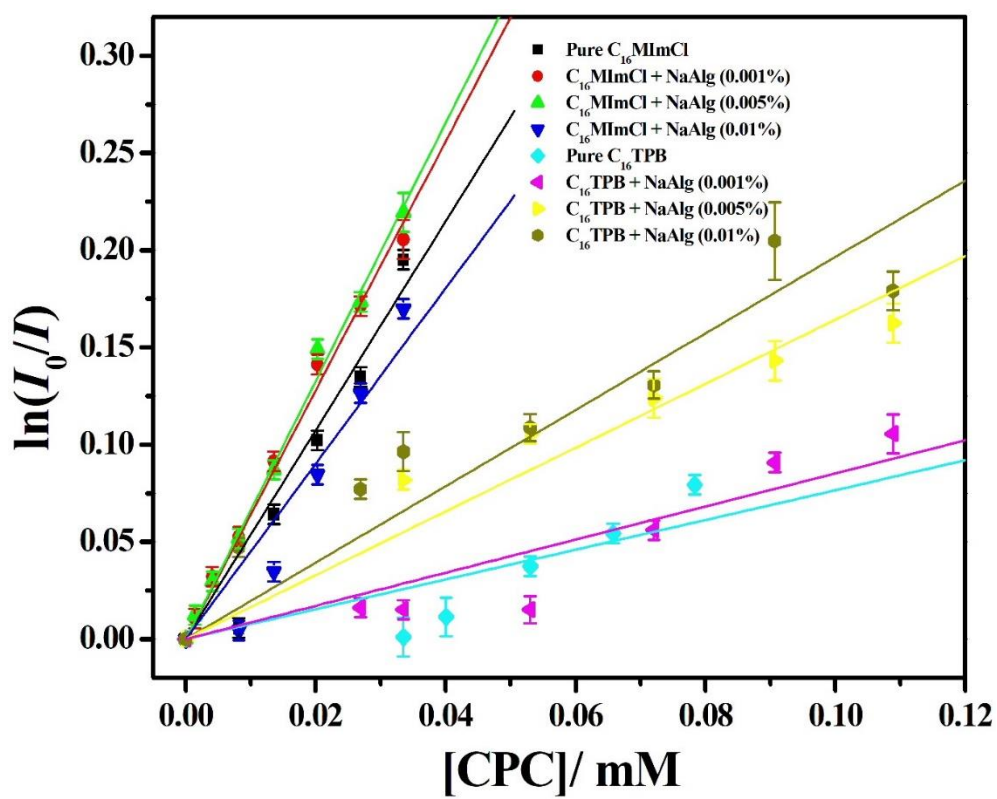


Fig. S4. $\ln(I_0/I)$ vs. [CPC] in presence of two different surfactants in presence and absence of NaAlg with varying wt %. Surfactant concentrations have been fixed to ~ 10 mM for each system showing in the legend.



References:

1. S. Das, S. Mondal and S. Ghosh, *Journal of Chemical & Engineering Data*, 2013, **58**, 2586-2595.
2. S. Das, S. Ghosh and B. Das, *Journal of Chemical & Engineering Data*, 2018, **63**, 3784-3800.
3. S. Das, N. Patra, A. Banerjee, B. Das and S. Ghosh, *Journal of Molecular Liquids*, 2020, **320**, 114497.
4. E. D. Goddard and R. B. Hannan, *Journal of the American Oil Chemists' Society*, 1977, **54**, 561-566.
5. T. Nylander, Y. Samoshina and B. Lindman, *Advances in Colloid and Interface Science*, 2006, **123-126**, 105-123.
6. J. C. T. Kwak, *Polymer-surfactant systems*, CRC Press 2020.
7. E. D. Goddard, *Journal of Colloid and Interface Science*, 2002, **256**, 228-235.
8. K. Holmberg, B. Jönsson, B. Kronberg and B. Lindman, *Polymers in Aqueous Solution*, Wiley-Blackwell 2002.
9. K. Kogej, *Advances in colloid interface science*, 2010, **158**, 68-83.
10. T. Chakraborty, I. Chakraborty and S. Ghosh, *Langmuir*, 2006, **22**, 9905-9913.
11. A. Dan, S. Ghosh and S. P. Moulik, *Carbohydrate polymers*, 2010, **80**, 44-52.
12. P. Degen, M. Paulus, E. Zwar, V. Jakobi, S. Dogan, M. Tolan and H. Rehage, *Surface Interface Analysis*, 2019, **51**, 1051-1058.
13. S. Ghosh, A. Mal, T. Chakraborty, G. C. De and D. G. Marangoni, *J Surface Sci Technol*, 2016, **32**, 107-114.
14. A. Mal, A. Saha, G. Dinda and S. Ghosh, *Journal of Molecular Liquids*, 2020, **299**, 112153.
15. T. Singh, S. Boral, H. Bohidar and A. Kumar, *Journal of Physical Chemistry B*, 2010, **114**, 8441-8448.
16. D. Ray, S. Das, R. De and B. Das, *J Carbohydrate polymers*, 2015, **125**, 255-264.
17. D. V. de Freitas, B. L. Kuhn, C. R. Bender, A. M. F. Lima, M. de Freitas Lima, M. J. Tiera, C. L. Kloster, C. P. Frizzo and M. A. Villetti, *J Journal of Molecular Liquids*, 2020, **297**, 111734.
18. A. Pal and S. Yadav, *J Journal of Molecular Liquids*, 2017, **241**, 584-594.
19. B. Das, D. Ray and R. De, *Carbohydrate polymers*, 2014, **113**, 208-216.
20. S. Jabeen, O. A. Chat, M. Maswal, U. Ashraf, G. M. Rather and A. A. Dar, *J Carbohydrate polymers*, 2015, **133**, 144-153.
21. J. Yang, J. Zhao and Y. Fang, *Carbohydrate research*, 2008, **343**, 719-725.
22. M. Ghaemy and S. Sadjady, *Journal of applied polymer science*, 2006, **100**, 2634-2641.
23. A. A. Silva, S. Livi, D. B. Netto, B. G. Soares, J. Duchet and J.-F. Gérard, *Polymer*, 2013, **54**, 2123-2129.
24. A. Noda and M. Watanabe, *Electrochimica Acta*, 2000, **45**, 1265-1270.
25. S. Livi, J.-F. Gérard and J. Duchet-Rumeau, *Chemical Communications*, 2011, **47**, 3589-3591.
26. A. Sankri, A. Arhaliass, I. Dez, A. C. Gaumont, Y. Grohens, D. Lourdin, I. Pillin, A. Rolland-Sabaté and E. Leroy, *Carbohydrate Polymers*, 2010, **82**, 256-263.
27. X. Wu, M. Wang, Y. Xie, C. Chen, K. Li, M. Yuan, X. Zhao and Z. Hou, *J Applied Catalysis A: General*, 2016, **519**, 146-154.
28. M. Blesic, M. H. Marques, N. V. Plechkova, K. R. Seddon, L. P. N. Rebelo and A. Lopes, *Green Chemistry*, 2007, **9**, 481-490.
29. A. M. Stephen, *Food polysaccharides and their applications*, CRC press 1995.
30. A. Haug and B. Larsen, *Acta chem. scand*, 1967, **21**, 691-704.

31. L. Lu, X. Liu, L. Dai and Z. Tong, *Biomacromolecules*, 2005, **6**, 2150-2156.
32. R. Seale, E. R. Morris and D. A. Rees, *Carbohydrate Research*, 1982, **110**, 101-112.
33. J. Liu, Q. Zhang, Y. Huo, M. Zhao, D. Sun, X. Wei, S. Liu and L. Zheng, *J Colloid Polymer Science*, 2012, **290**, 1721-1730.
34. G. Singh, G. Singh and T. S. Kang, *J Physical Chemistry Chemical Physics*, 2018, **20**, 18528-18538.
35. J. Liu, L. Zheng, D. Sun and X. Wei, *Colloids Surfaces A: Physicochemical Engineering Aspects*, 2010, **358**, 93-100.
36. M. Prasad, S. Moulik, A. MacDonald and R. Palepu, *The Journal of Physical Chemistry B*, 2004, **108**, 355-362.
37. P. D. Galgano and O. A. El Seoud, *Journal of Colloid Interface Science*, 2010, **345**, 1-11.
38. G. Basu Ray, S. Ghosh and S. P. Moulik, *Journal of Chemical Sciences*, 2010, **122**, 109-117.
39. V. G. Babak, E. A. Skotnikova, I. G. Lukina, S. Pelletier, P. Hubert and E. Dellacherie, *Journal of colloid and interface science*, 2000, **225**, 505-510.
40. Helmiyati and M. Aprilliza, *IOP Conference Series: Materials Science and Engineering*, 2017, **188**, 012019.
41. R. Houwink, *Journal für Praktische Chemie*, 1940, **157**, 15-18.
42. F. Clementi, M. Mancini and M. Moresi, *Journal of food engineering*, 1998, **36**, 51-62.
43. M. A. Masuelli and C. O. Illanes, *Open Science Publishing*, 2014.
44. M. Filippov and R. Kohn, *Chem zvesti*, 1974, **28**, 817-819.
45. Y. Shi, H. Q. Luo and N. B. Li, *Spectrochimica Acta Part A: Molecular and Biomolecular Spectroscopy*, 2011, **78**, 1403-1407.
46. D. Taylor, R. Thomas, J. Hines, K. Humphreys and J. Penfold, *Langmuir*, 2002, **18**, 9783-9791.
47. D. J. F. Taylor, R. K. Thomas, P. X. Li and J. Penfold, *Langmuir*, 2003, **19**, 3712-3719.
48. D. J. F. Taylor, R. K. Thomas and J. Penfold, *Advances in colloid and interface science*, 2007, **132**, 69-110.
49. R. A. Campbell, P. A. Ash and C. D. Bain, *Langmuir*, 2007, **23**, 3242-3253.
50. Á. Abraham, R. A. Campbell and I. Varga, *Langmuir*, 2013, **29**, 11554-11559.
51. R. A. Campbell, A. Angus-Smyth, M. Yanez Arteta, K. Tonigold, T. Nylander and I. Varga, *The Journal of Physical Chemistry Letters*, 2010, **1**, 3021-3026.
52. E. Guzmán, S. Llamas, A. Maestro, L. Fernández-Peña, A. Akanno, R. Miller, F. Ortega and R. G. Rubio, *Advances in colloid and interface science*, 2016, **233**, 38-64.
53. E. Guzmán, L. Fernández-Peña, F. Ortega and R. G. Rubio, *Current Opinion in Colloid & Interface Science*, 2020, **48**, 91-108.
54. K. Bodnár, E. Fegyver, M. s. Nagy and R. b. Mészáros, *Langmuir*, 2016, **32**, 1259-1268.
55. M. S. Bakshi and S. Sachar, *Colloid Polymer Science*, 2004, **282**, 993-999.
56. C. Wang and H. Morgner, *Physical Chemistry Chemical Physics*, 2014, **16**, 23386-23393.
57. L. Martínez-Balbuena, A. Arteaga-Jiménez, E. Hernández-Zapata and C. Márquez-Beltrán, *Advances in colloid and interface science*, 2017, **247**, 178-184.
58. K. G. Baikerikar and R. S. Hansen, *Langmuir*, 1991, **7**, 1963-1968.
59. S. W. An, J. R. Lu, R. K. Thomas and J. Penfold, *Langmuir*, 1996, **12**, 2446-2453.
60. J. D. Hines, R. K. Thomas, P. R. Garrett, G. K. Rennie and J. Penfold, *The Journal of Physical Chemistry B*, 1997, **101**, 9215-9223.
61. A. Downer, J. Eastoe, A. R. Pitt, J. Penfold and R. K. Heenan, *Colloids and Surfaces A: Physicochemical and Engineering Aspects*, 1999, **156**, 33-48.

62. G. Andersson, T. Krebs and H. Morgner, *Physical Chemistry Chemical Physics*, 2005, **7**, 136-142.
63. J. Eastoe, A. Paul, A. Rankin, R. Wat, J. Penfold and J. R. P. Webster, *Langmuir*, 2001, **17**, 7873-7878.
64. S. B. Sulthana, S. G. T. Bhat and A. K. Rakshit, *Langmuir*, 1997, **13**, 4562-4568.
65. H. Xu, P. X. Li, K. Ma, R. K. Thomas, J. Penfold and J. R. Lu, *Langmuir*, 2013, **29**, 9335-9351.
66. I. Mukherjee, S. P. Moulik and A. K. Rakshit, *Journal of Colloid and Interface Science*, 2013, **394**, 329-336.
67. C. C. Addison and S. K. Hutchinson, *J Chem Soc*, 1948, **1**, 943-948.
68. J. N. Israelachvili, *Intermolecular and Surface Forces*, Elsevier Science 2011.
69. T. Chakraborty and S. Ghosh, *Colloid Polymer Science*, 2007, **285**, 1665-1673.
70. C. Tanford, *The hydrophobic effect : formation of micelles and biological membranes*, New York (N.Y.) : Wiley 1980.
71. A. A. Dar, A. Garai, A. R. Das and S. Ghosh, *The Journal of Physical Chemistry A*, 2010, **114**, 5083-5091.
72. M. G. Neumann, C. C. Schmitt and E. T. Iamazaki, *Carbohydrate research*, 2003, **338**, 1109-1113.
73. M. G. Neumann and M. J. Tiera, *Pure applied chemistry*, 1997, **69**, 791-796.
74. P. Yan, C. Jin, C. Wang, J. Ye and J.-X. Xiao, *Journal of colloid interface science*, 2005, **282**, 188-192.
75. J. Aguiar, P. Carpena, J. Molina-Bolivar and C. C. Ruiz, *Journal of Colloid Interface Science*, 2003, **258**, 116-122.
76. N. J. Turro, B. H. Baretz and P. L. Kuo, *Macromolecules*, 1984, **17**, 1321-1324.
77. L. Piñeiro, M. Novo and W. Al-Soufi, *Advances in Colloid and Interface Science*, 2015, **215**, 1-12.
78. F. Geng, J. Liu, L. Zheng, L. Yu, Z. Li, G. Li and C. Tung, *Journal of Chemical & Engineering Data*, 2010, **55**, 147-151.
79. J. Łuczak, M. Markiewicz, J. Thöming, J. Hupka and C. Jungnickel, *Journal of Colloid and Interface Science*, 2011, **362**, 415-422.
80. R. Pereira, A. Tojeira, D. C. Vaz, A. Mendes and P. Bártolo, *International Journal of Polymer Analysis and Characterization*, 2011, **16**, 449-464.
81. M. Aprilliza, Characterization and properties of sodium alginate from brown algae used as an ecofriendly superabsorbent, 2017.
82. S. Hua, H. Ma, X. Li, H. Yang and A. Wang, *International Journal of Biological Macromolecules*, 2010, **46**, 517-523.
83. E. Thomas, D. Thomas, S. Bhuvaneswari, K. P. Vijayalakshmi and B. K. George, *Journal of Molecular Liquids*, 2018, **249**, 404-411.
84. S. Li, P. Xing, Y. Hou, J. Yang, X. Yang, B. Wang and A. Hao, *Journal of Molecular Liquids*, 2013, **188**, 74-80.
85. N. Khan and B. Brettmann, *Polymers*, 2019, **11**, 51.
86. A. Naderi, P. M. Claesson, M. Bergström and A. Dédinaité, *Colloids and Surfaces A: Physicochemical and Engineering Aspects*, 2005, **253**, 83-93.

Chapter-IV

Physicochemical and Spectroscopic Study on the Interaction of a Novel azabenzocrown Dye with Different Surfactants

Physicochemical and Spectroscopic Study on the Interaction of a Novel Azabenzocrown Dye with Different Surfactants

Abstract:

Interaction of a novel azabenzocrown ether (H₂DTC) with different kinds of surfactants such as, conventional anionic (SDS), cationic (DTAB), gemini cationic (16-4-16), ionic liquid (C₁₆MImCl) and non-ionic (Tween-60) has been investigated at the wide range of surfactant concentrations (premicellar, micellar and post micellar regime) in 15% (V/V) EtOH-water medium at 298.15 K. Several physicochemical techniques, viz., tensiometry, steady state fluorimetry, UV-VIS spectroscopy was employed. H₂DTC show several inflection points in surface tension, steady state fluorimetry and absorption profiles with variation of [surfactant] from very low to high, apart from critical micelle concentration (cmc). Equilibrium binding constants (K_b) for the binding of H₂DTC with micellar environment, partition coefficient values for H₂DTC (K_x) in micellar to solvent phase, molar absorptivity of H₂DTC in absence (ϵ_0) and presence (ϵ) of micellar solution, Gibbs energy of binding (ΔG_b^0), Gibbs energy of partition (ΔG_p^0) for H₂DTC in solvent to micellar phase have been evaluated in this present study. It has been seen that H₂DTC strongly binds with micelles of Tween-60 than the anionic and cationic surfactants and correspond K_x values are found higher for micelle medium of non-ionic surfactant. On the other hand, ϵ value of H₂DTC found lower in micellar Tween-60, whereas, it is found high in cationic and anionic micellar medium comparing with the pure solvent (15% V/V EtOH-water). Negative Gibbs binding and negative values of partition coefficient clearly indicates the spontaneity of both these processes. The binding of H₂DTC with Tween-60 micelles is greater than the other surfactants.

1. Introduction:

An enormous attention has been focused for the synthesis of azacrown compounds in past and preceding years. The azacrowns show intermediate complexation properties in between those crowns bind with only oxygens, which have strong intake affinity towards alkali and alkaline earth metal ions, and those of the all-nitrogen bound cyclams which strongly bind with heavy-metal cations inside in its cavity due to less electronegativity and strong complexing ability of N over O atom. These have important uses as artificial receptors in molecular recognition processes¹ and, in some cases, complexation of anions which have close similarity with the ions participate in definite biological systems.²⁻⁴ Thus, the introduction of biological entities into the crown ether macromolecules has provided researcher an even greater insight into biological ionophores, such as macrolide antibiotics, cyclic peptides etc.^{5,6} These crown based macrocycles have also an enhanced complexing ability for ammonium salts^{7,8} through H-bonding⁹⁻¹² and for transition-metal ions^{8,13} over the crowns containing only oxygen atom. Extensive numbers of azacrowns have been synthesized; among them, benzoazacrowns have been studied broadly on its complexation affinity towards main group and also transition metal

ions since its discovery in the mid-1970s.¹⁴⁻¹⁷ Surfactant mediated assemblies in solution medium have great potential applications in routine life. The simplest assemble is termed as micelle and the corresponding surfactant concentration abbreviated as critical micelle concentration (cmc).¹⁸ These micellar properties are affected by influence of several additives, i.e, non-polar and polar organic compounds, small amount of electrolytes etc.¹⁸ Recently, increasing effort is being emphasized to the study of the assimilation or solubilization of neutral molecules into micelle in aqueous solution. Although a lot of studies have already reported on the complexation properties of crowns with various cations, anions and neutral organic molecules, less attention has been devoted on the interaction of crowns with surface active agents¹⁹⁻²³ in both pre and post micellar regime and majority of them (surfactants) are anionic in nature. The inclusion of crown macromolecule to the surfactants during micellization results to the formation of inclusion complex mediated by crown cavity with oppositely charged counterions or simply association with monomeric and aggregated form of surfactants with crowns, and as a result, these crowns alter the adsorption of surfactants at interfaces and also influence in bulk micellization. On the other hand, the partition, absorption and emission properties of azacrown are influenced by surfactants in both monomeric and micellar solution. In this connection, a comprehensive investigation has been executed on the interaction of a synthesized chromophoric dihydroxy dibenzoaza-crown (1,16-dihydroxy-tetraaza-30-crown-8) with arbitrarily chosen surfactants [conventional cationic (dodecyltrimethylammonium bromide, DTAB) and anionic (sodiumdodecyl sulfate, SDS), cationic gemini (butanediyl-1,4-bis(dimethylcetylammmonium bromide),16-4-16), surface active ionic liquid (1-hexadecyl-3-methylimidazolium chloride, C₁₆MImCl) and non-ionic surfactant (polyoxyethylene sorbitan monostearate, Tween-60] covering all the classes in 15% EtOH-water medium at 298.15K. Tensiometry, UV-VIS spectroscopy and steady state spectrofluorimetry techniques were employed to elucidate the interaction between crown with surfactants both at the surface and in the bulk.

2. Experimental Section:

2.1. Materials:

DTAB, Tween-60 (HLB = 14.9), N, N-Dimethylhexadecylamine, 1,4-Dibromobutane, and Ethyl acetate were purchased from Merck (Sigma Aldrich), India and these are used without any further purification. SDS was obtained from SRL, India (assay min 85%) and used as received. C₁₆MImCl, 98%, monohydrate was purchased from Acros Organics (Germany) and used as received. Acetone (certified ACS) was purchased from Fisher Scientific (Germany).

Absolute Ethanol (EMSURE® ACS, for analysis, was purchased from Merck, Germany) and deionised water with a specific conductance of $0.98 \mu\text{S}\cdot\text{cm}^{-1}$ were used to prepare the experimental solutions. The gemini surfactant, 16-4-16 was synthesized in our laboratory (See below). H₂DTC was received as a gifted sample from Dr. Amrita Saha, Department of Chemistry, Jadavpur University. Structures of different surfactants and H₂DTC have been shown in Fig. 1.

2.2. Synthesis of butanediyl-1,4-bis (dimethylcetylammonium bromide) [16-4-16]:

Cationic gemini surfactant, 16-4-16 has been synthesized in our laboratory using the protocol mentioned by Menger et. al.²⁴ N,N-Dimethylhexadecylamine (2.67 g, 9.93 mmol) was added to a 5 ml dry acetone in a small clean round flask. After that, 1,4-Dibromobutane (1 g, 4.63 mmol) was added drop wise to the flask with continuous stirring by a mechanical stirrer and this mixture was finally brought for refluxing for 18 hours. During refluxing, white product was separated out from the solution. After cooling the refluxing mixture, 20 ml acetone was added and continuously stirred followed by decantation of supernatant liquid. This washing procedure was followed 2 - 3 times. After that, crude product was filtered and further washed with cold diethyl ether and dried with a rotary evaporator at moderate temperature. Product was recrystallized with ethanol and ethyl acetate and characterized by ¹H NMR. The calculated Yield was: 1.89 g (54%).

¹H NMR (400 MHz, DMSO-d₆, Fig.S1 in the supplementary) δ ppm: 3.25-3.32 (quart. N(+)-CH₂) (m, 8H), 3.00 (quart.N(+)-CH₃) (s, 12H), 1.65 (spacer-CH₂-CH₂-) (m, 4H), 1.24 (long chain-CH₂) (m, 52H), 0.85 (long chain terminal-CH₃) (t, 6H, J = 6.5 Hz).

2.3. Determination of molar absorptivity coefficient of H₂DTC and preparation of experimental Solutions:

Required weighted H₂DTC was dissolved in 15% EtOH-water under sonication at room temperature until soluble (maximum solubility range: ~ 0.15 mg H₂DTC in 1 ml 15% EtOH-water). Molar absorptivity of the H₂DTC (ϵ_0) in 15% v/v EtOH-water medium was calculated using rearranged Beer-Lambert equation: $\epsilon_0 = A/lC$, where A , l and C represent absorbance at a given wavelength corresponding to maximum absorbance (238, 356 and 423 nm, cf. Fig. S2(a) and S2(b)), the length of cuvette and concentration of H₂DTC, respectively. The calculated ϵ_0 values have been found to be 12000, 2531 and 2867 L mol⁻¹ cm⁻¹ at 238, 356 and 423 nm wavelength respectively corresponding to maximum absorbance (λ_{abs}^{max}) at 298.15K respectively. Detailed discussions have been given in results and discussions section in this

manuscript. Appearance of three absorbance peaks of dye molecules in 15% EtOH-water medium are probably due to $n \rightarrow \pi^*$ transition between nonbonding electron of N and $-N=C-$ group present in H₂DTC (for $\lambda_{abs}^{max} = 356$ and 423 nm; relatively less intensity (cf. Fig. S2(b)) with H-bonding type interaction between phenolic $-OH$ and azo group hampering $n \rightarrow \pi^*$ transitions; while relatively larger absorbance intensity is observed at 238 nm probably due to $\pi \rightarrow \pi^*$ transition. All surfactant solutions were prepared 15 times above their aqueous cmcs²⁵⁻⁴³ and also cmc values are evaluated in aqueous solution in the present study by different techniques shown elsewhere (cf. Table 1). Determined cmc values in this work in aqueous solution at 298.15 K are in good agreements with the literatures²⁵⁻⁴³, [Ref. for SDS²⁵⁻³¹; DTAB³²⁻³⁹; 16-4-16⁴⁰; C₁₆MImCl³⁹; Tween-60⁴¹⁻⁴³. All surfactants (same weightage as those taken for aqueous solution for tensiometry and later for spectrometry, 15 times the cmc values those calculated in tensiometric method) were dissolved in 15% EtOH-water both in presence and absence of H₂DTC and cmc values were evaluated and displayed in Table 1. Respective concentration of H₂DTC remains fixed both in the solutions containing only H₂DTC and surfactants with H₂DTC (Stock Solutions) for all the measurements. All experiments were performed at 298.15 K.

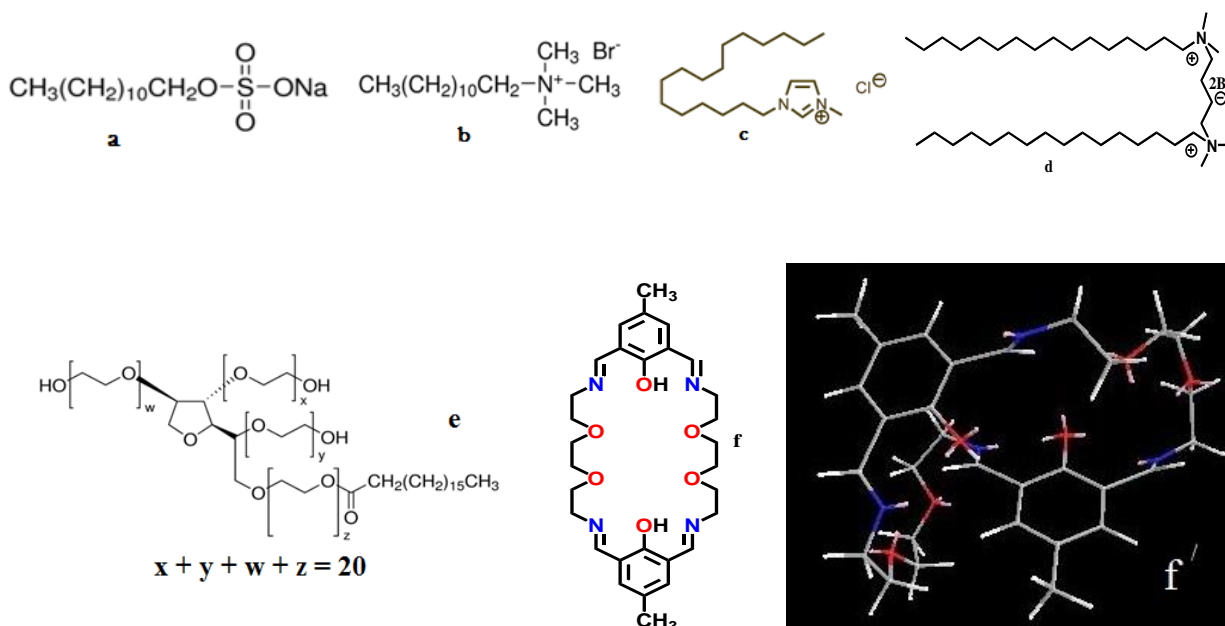


Fig.1. Structure of surfactants & H₂DTC: SDS (a), DTAB (b), C₁₆MImCl (c), 16-4-16 (d), Tween-60 (e), and H₂DTC (f: line structure, f': stick representation of H₂DTC (optimized)).

3. Methods Employed:

3.1. Tensiometry:

A calibrated Krüss-K8 tensiometer (Made in Germany) was used to determine surface tension at air water interface by du Noüy ring detachment method at 298.15K. A clean platinum ring was used for this purpose. This ring has been cleaned using deionized water and acetone successively and burned briefly until glowing in ethanol flame prior to each measurement. Pure ethanol and ethanol (15%) solubilised H₂DTC (concentration ~ 0.15 mM) were taken in a double jacket container attached with a thermostatic water bath to maintain the desired temperature with an accuracy of ± 0.1 K. Stock surfactant solutions were added to the double jacket container by a Hamiltonian micro syringe and stirred well after each addition and kept for 5 minutes before taken the data. Two or three consecutive readings of surface tension were taken for a particular addition of surfactant by syringe for better reproducibility. Surface tension of distilled water used for preparation of solution was found to be 70.8 mN.m⁻¹ with the precision of ± 1 mN.m⁻¹ at 298.15 K. Representative plots of surface tension (γ) vs. log [surfactant/ mM] were shown in Fig. 2. Several inflection points were identified and those were also verified by other methods (Spectrophotometry (Fig. 3.), and Fluorimetry (Fig. 4.))

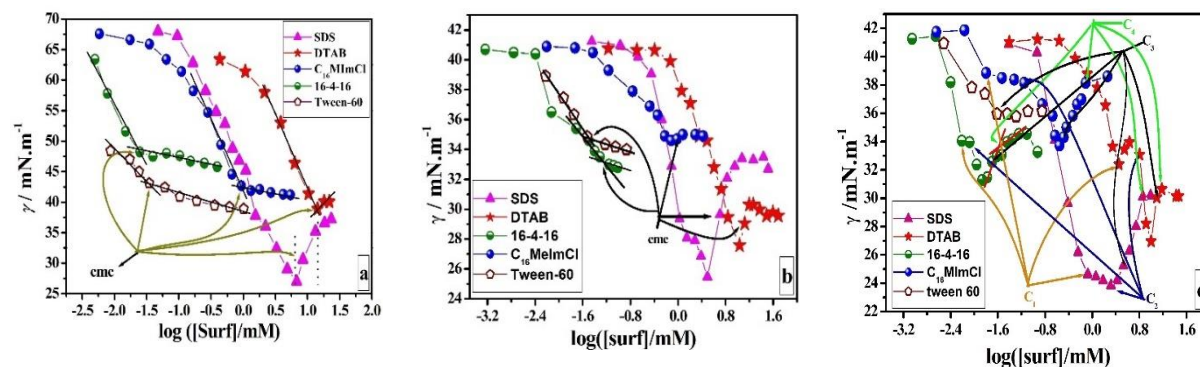


Fig.2. Plot of Surface tension (γ) vs. log ([surf]/ mM): Surfactants in aqueous solution (a), different surfactants employed here in 15% EtOH-water in absence (b), and presence (c) of H₂DTC. Cmc's and several inflection points (C₁, C₂, C₃ and C₄) have been specified.

3.2. Spectrophotometry:

Spectrophotometry was conducted using a Shimadzu UV-VIS spectrophotometer (made in Japan) attached with a thermostatic water bath to maintain 298.15 \pm 0.15 K. Initially, base line was done using the solvent (15% EtOH-water). 2.5 mL of H₂DTC (~ 0.13 mM) prepared in 15% EtOH-water was taken in a quartz cuvette of 1 cm path length and surfactant solutions

(Prepared in ~15 times above their cmcs those calculated in tensiometry) were prepared in same concentration of H₂DTC, added with a Hamiltonian micro syringe and spectrum was recorded (cf. Fig.3.).

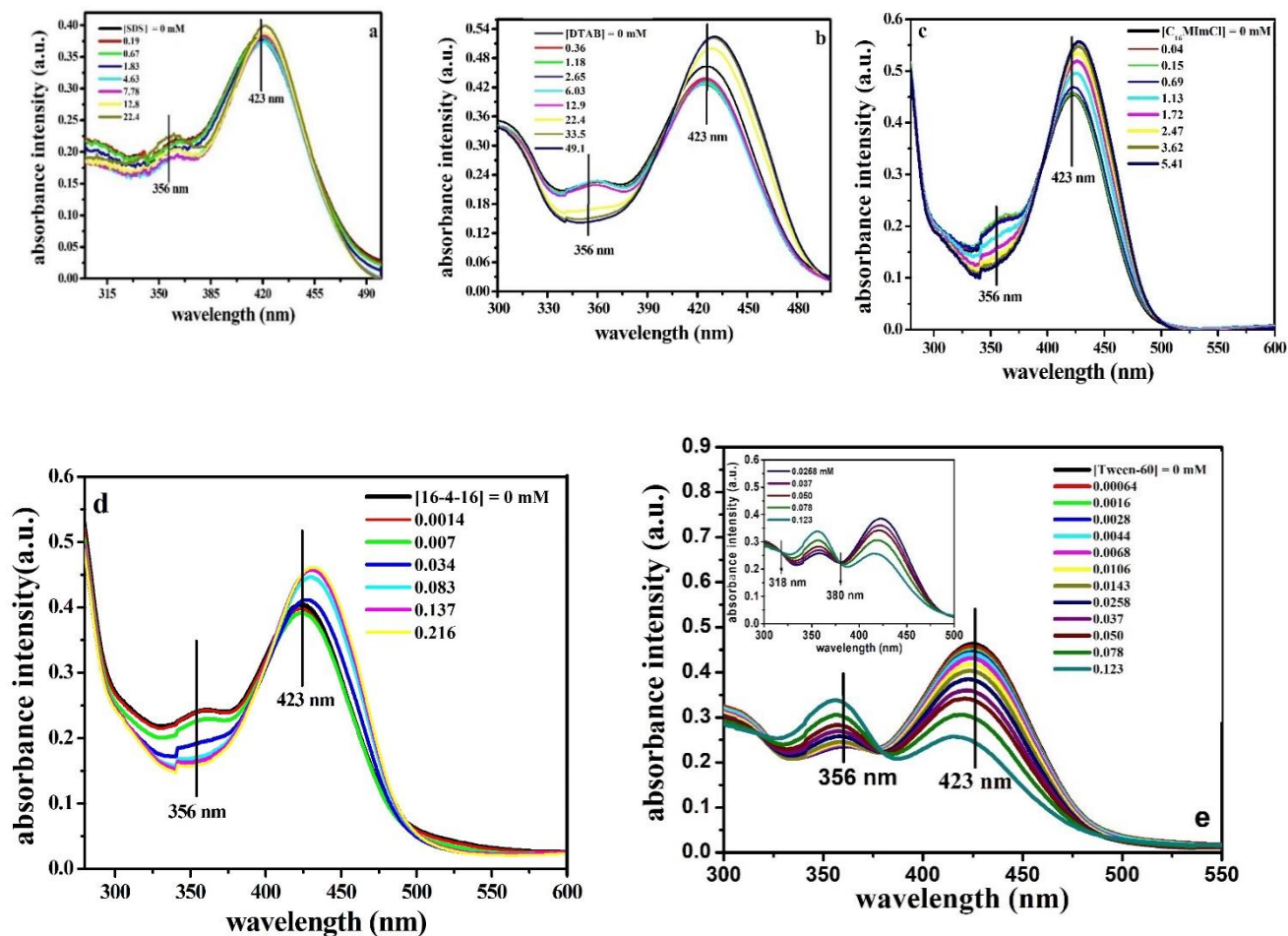


Fig.3. UV-VIS spectroscopy of H₂DTC (0.13 mM) upon addition of surfactants: SDS (a), DTAB (b) and C₁₆MimCl (c), 16-4-16 (d) and Tween 60 (e) in 15% EtOH-water medium.

3.3. Spectrofluorimetry:

A Perkin-Elmer LS 55 (USA) fluorescence spectrofluorometer attached with a Peltier have been used for steady state measurements at 298.15 ± 0.1 K. Spectroscopic behaviour of H₂DTC was observed in 15% EtOH-water at the excitation wavelength of 421 nm with 14 nm band pass. While emission monitored between 450 – 650 nm with a width of 4 nm band pass, emission maxima (λ_{max}) of H₂DTC was measured at 527 nm. Surfactants were added using a microsyringe to H₂DTC and the spectrum was measured (cf. Fig. 4). Same concentration of H₂DTC and same experimental procedure has been followed that stated in photometry section. Spectra were recorded in Fig.4.

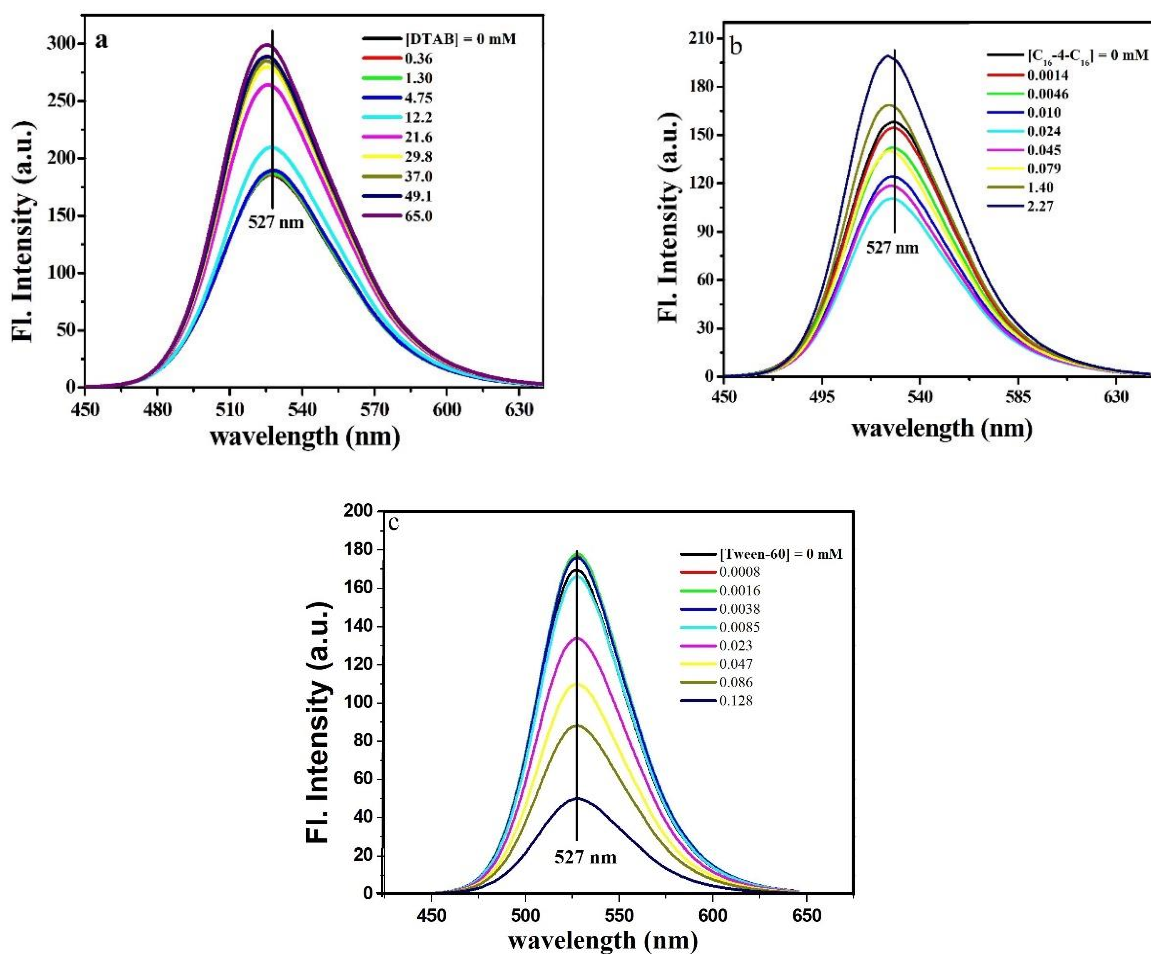


Fig.4. Fluorescence spectra of H₂DTC (0.09 mM) upon addition of surfactants: DTAB (a), C₁₆-4-C₁₆ (b) and Tween-60 (c) in 15% EtOH-water medium.

4. Results and Discussions:

4.1. Micellization of surfactants in aqueous, 15% EtOH-water solvent in absence and presence of H₂DTC by tensiometry

The variation of surface tension (γ) vs. \log [surf] profiles were exhibited in Fig. 2. for different surfactants in aqueous (a), in 15% EtOH-water (b) and in H₂DTC (0.15 mM) medium dissolved in 15% EtOH-water used as solvent (c). It is well known that amphiphiles residing at the air-water interface reduce γ significantly, and finally, remain invariant of surfactant concentration after the onset of micelle formation (cf. Fig 2a.). The inflection point obtained in the surface tension profiles for surfactants in aqueous solution was shown in Fig. 2a, and that concentration was termed as critical micelle concentration (cmc). Two intersecting linear slopes with different magnitude have been assigned (cf. Fig. 2) in this context and often used^{44, 45} to determine cmcs. Cmc values of surfactants in aqueous solution are displayed in Table 1.

Determination of cmc for SDS in aqueous solution is found difficult due to the existence of a minimum (Fig. 2(a)). During the addition of SDS solution in water, initially, surface tension decreases and finally a plateau is appeared followed by a sharp minimum. The minimum appears due to the n-dodecanol impurity^{25, 26, 44}, which is more surface active, found mostly in technical grade SDS samples. The more surface active n- dodecanol reduces the surface tension more even after the surface is saturated by SDS and finally, it is solubilised in SDS micelle causing a minimum. Even the minimum point has been reported for laboratory grade SDS ($\geq 98\%$ purity) due to auto hydrolysis of SDS forming n- dodecanol during the process of micellization.^{25, 44} From the minimum formation to the appearance of plateau is designated in between two dotted lines shown in Fig.2a. Same observation in the tensiometry profile (Fig.2b.) of SDS in 15% EtOH-water is also observed. To determine the cmc of SDS, the convenient concentration is used immediate after the concentration where minimum in γ is observed. Although a number of researchers have taken the minimum point in tensiometry profile to designate cmc in case of SDS, we have adopted the aforesaid method and also found excellent similarities with those obtained from literatures²⁵⁻²⁷ and in accord with the cmc determined by spectrometry (Table 1) in this present investigation. In 15% (v/v) ethanol content medium, cmc value of SDS is found to be 5.08mM, lower than that obtained in aqueous solution. This clearly indicates that EtOH would not act as a cosolvent at its 15% (v/v) volume fraction solution during the micellization of SDS while for the micellization of other cationic surfactants investigated here, increment of cmc is observed (Table 2) in 15% EtOH-water medium comparing with aqueous system (Table 1). The decrease of cmc in presence of SDS at 15% EtOH- water medium would be explained in terms of decrease of interfacial energy between the solvent and micelles by the adsorption of EtOH molecules on micellar surface attributed to greater micelle stability.⁴⁶ It has been reported that at its low concentration, EtOH behaves like a cosolvent and at higher concentration, cosurfactant nature predominates and in this consequence, a manifestation of minima in cmc trend^{47, 48} is observed for a particular (both anionic and cationic) surfactant at varying EtOH volume fractions.

Cmc of Tween-60 is found around 0.035 mM when studying micellization both in aqueous and 15% EtOH-water medium. The exact similarity in cmc of Tween-60 in both media is probably due to H- bonding interaction of polyoxyethylene hydrophilic moiety with water molecules and such interaction hinders EtOH molecules to influence the micellization of Tween-60. Similar observation was found by Gokturk et. al.⁴⁹, while micellization of TX100 was investigated in aqueous and ethanol-water medium.

From Fig. 2. It is found that, γ values of surfactants in presence of 15% EtOH-water decreases. The γ values in 15% EtOH-water is found to be 40 – 42 mN.m⁻¹ without surfactants attributed to the surface activity of the solvent itself. The decrease of surface tension in alcohol-water medium with respect to deionized water is also reported in previous literatures. Surface tension at cmc (γ_{cmc} , cf. Table 3) of surfactants decreases in presence of 15% EtOH-water when compare with aqueous medium.

Presence of slight minima in the tensiometric profile of DTAB and C₁₆MImCl is also observed and can be explained in terms of intercalation of EtOH molecule into micelles followed by more surface activity of EtOH along with these surfactants.

Interesting observation is obtained in the tensiometric profiles (Fig.2c.) of surfactants, except Tween-60, in presence of 0.15 mM H₂DTC in 15% EtOH water medium.

Several breaks are obtained in the tensiometric profiles in presence of H₂DTC except the non-ionic Tween. We have termed these break points as C₁, C₂, C₃ and C₄ (shown in Fig. 2c) from low to high surfactant concentration regions in sequential order. Each point probably has distinct significance. During the addition of surfactants into H₂DTC solution, the concentration of H₂DTC is kept constant in both media. Here, monolayer formation is possible at a particular surfactant concentration (termed as C₁), then an interpretation with H₂DTC probably occurred at the break point (C₂); after that, micelle formation by the surfactant monomers occurred (that concentration is cmc, here we termed as C₃ for studying of micellization in presence of H₂DTC) and finally, termination of the interaction at a particular concentration (C₄) associated with solubilisation of bound H₂DTC with surfactants along with EtOH were observed owing to the system coming from surface to the micelle region. In presence of 15% (v/v) ethanol, less population of surfactant monomers has been observed (confirmed by less surface coverage of monomers at cmc, discussed elsewhere in this section) at air-water interface. There is the greater tendency of ethanol molecules to reside on the surface by disruption of the H- bonded structure of water and at the same time, they attract hydrophobic H₂DTC molecules along with them to the less polar surface by means of some hydrogen bonding interaction. When the surfactants are added to the solution, surface tension gradually decreases as the surfactants reside on the surface replacing some ethanol/water molecules due to its greater surface activity than solvents, until a concentration of surfactants (C₁) reached when some bulk monomer population facilitate some sort of interaction with H₂DTC at the bulk. The mode of this interaction is different for different kind of surfactants. Until the completion of interaction mediated by surfactants and H₂DTC, we obtained a plateau in the tensiogram (Fig. 2c), that means, at that region (from C₁ to C₂) surfactants do not reside on surface. After C₂, further

addition of surfactants reduces surface tension and form micelles (at C₃) followed by a deep (except for SDS, which shows a plateau (Fig. 3c), here plateau and deep occurred in same region), After that, added surfactant monomers form micelle, increase the aggregation number and at the same time, H₂DTC is dissolved in micellar region which is associated with EtOH coming from interface, increase the surface tension. Finally, saturation of surface (at C₄) takes place and the whole process ends to completion and after C₄ there is no noticeable change of surface tension upon further addition of surfactants. The mode of interaction of anionic and cationic surfactants with H₂DTC is mostly ionic type (non covalent interaction) in nature at pre-micellar region, as there is not shown any such break except at cmc, while studying micellization of non-ionic Tween-60 in presence of H₂DTC.

The lone pairs of crown are oriented to the exterior in hydrophilic region, whereas, interior orientation is observed at the hydrophobic region.⁵⁰ Anionic surfactant, SDS has Na⁺ counterion, which is encapsulated in H₂DTC cavity at relatively high surfactant concentration, as the increasing hydrophobicity restricts the lone pairs orienting into the cavity of H₂DTC. The plateau in the tensiometric profile of SDS at its high concentration comparing with other cationic surfactants obtained supports aforesaid explanation with the experimental point of view. Dodecyl sulphate anions interact with Na⁺, those encapsulated by H₂DTC forming 1:1 SDS-H₂DTC complex⁵¹ (detailed in sec 4.2,) due to electrostatic reason. Cationic surfactants (DTAB, C₁₆MeImCl, and, 16-4-16) with quaternary ammonium head groups have the possibility to interact with the benzene rings through cation- π interaction as quaternary ammonium groups cannot be capable of forming H-bonds with N and O atoms. Although cation- π interaction predominates in the gas phase, there are few published literatures demonstrating the interaction occurred in solution phase⁵² Cation- π interaction plays fundamental role for the recognition of quaternary ammonium cations in biological system.⁵⁰ As their needs no such orientation of H₂DTC in terms of lone pairs, that are required for SDS, there is the possibility for cationic surfactants easily binding with H₂DTC at relatively lower surfactant concentrations (see the values of C₁ and C₂ in Table 1)

Maximum surface excess (Γ_{max}) at the air/water interface can be calculated using the Gibbs adsorption equation⁵³ as given below:

$$\Gamma_{max} = -\frac{1}{2.303nRT} \lim_{c \rightarrow cmc} \left(\frac{\partial \gamma}{\partial \log c} \right) \text{ mol. m}^{-2} \quad (1)$$

Γ_{max} can be defined as how much the air/water interface can be covered by surfactants which reduce the surface tension of solvent at cmc, γ is the surface tension in mN.m⁻¹ unit, c is the total surfactant concentration in solution and n , R and T are the number of species per surfactant

molecule at air/water interface, universal gas constant and temperature at Kelvin scale respectively. The number of species (n) participating at the air/ water interface for SDS, DTAB and $C_{16}MeImCl$ is 2; for 16-4-16 it is 3 and for nonionic surfactant, the value is 1. Variation of γ with the function of $\log C$ up to the cmc in 15% ethanol-water medium and in presence and absence of H_2DTC dissolved in 15% ethanol are displayed in Fig. S3 (a) & (b) (in the supplementary section). This can be best fitted by second order polynomial by scrutinizing the regression (R^2 factor, Table S1 in the supplementary section, found good correlation) analysis using the following equation:

$$\gamma = A + B_1 \log C + B_2 (\log C)^2 \quad (2)$$

where C is the concentration of surfactants. In equation 2, A , B_1 and B_2 values are the constants for particular surfactants outlined in Table S1 (in the supplementary section). These estimated values used to execute Γ_{max} (cf. Table 3.) by taking the first derivative of equation 2 to obtain $\frac{\partial \gamma}{\partial \log C}$ at cmc. From Table 3, it is quite evident that Γ_{max} decreases in presence of 15% EtOH solvent comparing with aqueous medium significantly in presence of all surfactants. This would be explained in terms of association of EtOH on the surface decreasing polarity by destructing water structure at interface. Further slight reduction in presence of H_2DTC is probably due to association of some H_2DTC with EtOH by H-bonding type interaction, which further hampered the association of hydrophilic head groups of surfactant monomers to reside on the surface.

Minimum area per surfactant monomer (A_{min}) can be calculated using the following equation⁴¹:

$$A_{min} = \frac{10^{18}}{N_a \Gamma_{max}} \text{ nm}^2 \text{ molecule}^{-1} \quad (3)$$

Surface pressure at cmc (π_{cmc}) can be obtained using the following equation:

$$\pi_{cmc} = \gamma_0 - \gamma_{cmc} \quad (4)$$

where γ_0 and γ_{cmc} are the surface tension values of pure solvent and at cmc of the solution.

Efficiency of interfacial adsorption can be predicted by evaluating $P^{C_{20}}$ which is defined how much the decrease of γ of the solution by adsorption of the surfactants on the interface. C_{20} values are defined empirically from the tensiograms (Fig.3) by the reduction of surface tension to 20 mN.m^{-1} upon addition of surfactants. $P^{C_{20}}$ is expressed by the following way:

$$P^{C_{20}} = -\log C_{20} \quad (5)$$

Packing parameter (P) deals with the micellar geometry predicted by Israelachvili⁵⁴ by the following equation:

$$P = \frac{v}{l_c A} \quad (6)$$

where l_c is the maximum effective length of hydrophobic tail of a monomer, A is surface area of head group of surfactant monomer and v is the hydrophobic chain volume assuming to be an incompressible fluid. Both l_c and v of a saturated hydrocarbon chain of carbon number C_n , can be evaluated using Tanford formulae⁵⁵:

$$l_c = 0.154 + 0.1265 C_n \text{ nm} \quad (7)$$

$$v = 0.0274 + 0.0269 C_n \text{ nm}^3 \quad (8)$$

C_n values are 12 for SDS and DTAB, for $C_{16}\text{MeImCl}$, 16-4-16 and Tween 60, the values are 16.

As the exact determination of the head group area (A) of surfactants on micellar surface is quite difficult, A_{\min} values those obtained from tensiometry have been used instead of A . The packing parameter values for the investigated surfactants both in presence and absence of H_2DTC predicted by empirical equation of Israelachvili⁵⁴ is given below:

$$P = \frac{v}{l_c A_{\min}} \quad (9)$$

for spherical micelles, $P \leq 0.333$; for nonspherical shape, $0.333 < P < 0.5$; for vesicles and bilayers, $0.5 < P < 1$; and for inverted structures, $P > 1$.

4.2. Investigation of interaction of surfactants with H_2DTC in presence of 15% EtOH probed by photometry and fluorimetry

The analysis of UV-VIS spectra of H_2DTC in presence of different surfactants in 15% v/v EtOH-water medium has been performed by taking $\lambda_{\text{abs}}^{\text{max}}$ at 356 nm and 423 nm respectively in this manuscript. H_2DTC shows significant red shift in the UV-VIS spectra in presence of all cationic surfactants (423 to 428 nm for DTAB (Fig. 3b), 423 to 439 nm for $C_{16}\text{MImCl}$ (Fig. 3c), and for 16-4-16, the shifting of wave length from 423 to 431 nm (Fig. 3d) after cmc, while relatively less red shift was obtained for SDS (spectral shift from 423 to 427 nm, cf. Fig. 3a) in UV-VIS spectra. On the other hand, in presence of Tween 60, significant blue shift (423 to 416 nm) was observed at post micellar region in the UV-VIS profile (Fig. 3e) when monitoring $\lambda_{\text{abs}}^{\text{max}}$ at 423 nm and 356 nm. In presence of cationic surfactants, H_2DTC absorbance intensity was decrease (except $C_{16}\text{MImCl}$, where less decline of absorbance intensity was observed at premicellar region) to a certain value followed by a large increase observed in micellar region

when monitoring λ_{abs}^{max} at 423 nm as a function of surfactant concentration (cf. Fig. 3b, c and d). The initial small decrease in absorbance intensity at low concentration of surfactant is attributed to the formation of weakly interacting complex of H₂DTC with surfactant monomers; after that, increase of surfactant concentration leads to formation of micelle. After micelle formation, weakly bound H₂DTC releases free surfactant monomers and bound to micelles due to hydrophobic interaction, resulting increase in absorbance intensity (cf. Fig. 3b, c and d)⁵⁶,⁵⁷ associated with red shifting and exciting the intensity of free H₂DTC. Similar type of observation was reported us in the absorbance spectra of Safranin T by adding surface active ionic liquid.⁵⁸ The change of absorbance intensity decreases with increase of concentration of all cationic surfactants at 356 nm of H₂DTC and decrease in intensity is more pronounced at the post micellar region of these surfactants. In case of SDS, the change of absorbance intensity is negligible though the same type of observation is found for cationic surfactants at 423 nm after cmc of SDS (cf. Fig.3a) and decrease of absorbance intensity is also less pronounced at 356 nm. Strong inclusion complex like, SDS-H₂DTC (stated earlier in tensiometry section) is mostly present in solvent and hardly allows the formation of free H₂DTC in solution medium and the binding of H₂DTC in interior of SDS-micelle. No shifting in wavelength is observed at 356 nm for all cationic and anionic surfactants. Gradual decrease is observed in the H₂DTC abs. intensity in presence of Tween 60 with concomitant blue shift at 423 nm, while concomitant increase of absorbance intensity is found at 356 nm also with blue shift (spectral shift from 356 to 360 nm, cf. Fig. 3e). All these observations in H₂DTC spectra in presence of varying concentrations of different surfactants reveal prominent interaction of cationic and non-ionic surfactants with H₂DTC specially, in the micellar region due to penetration of dye into the micelle interior; while for SDS, a strong inclusion complex probably formed with H₂DTC at free solvent or at the outer sphere (stren layer) of micelle. Local environment of H₂DTC decides the the shifting of its absorbance maximum at different surfactant solutions with varying surfactant concentrations. The reason for red shifting of H₂DTC in presence of anionic and cationic surfactants may be explained in terms of less energy gap between non-bonding (n-orbital) and anti-bonding (π^*) molecular orbitals of H₂DTC in less polar environment and increase of intensity of H₂DTC after cmc of surfactants (both cationic and anionic) due to positioning of dye in micellar core⁵⁹ and therefore, solubilizing the dye to micelle leading to more or less same absorbance intensity. Nonionic Tween-60 in presence of H₂DTC in 15% v/v EtOH-water medium shows isosbestic points at $\lambda_{abs}^{max} = 318$ and 380 nm at the post micellar region (shown at the inset of Fig. 3e). The blue shifted spectra of H₂DTC were

obtained at 356 and 423 nm with conjugation of isosbestic point at post micellar region of Tween-60 due to the formation of H – aggregated structure of H₂DTC in parallel arrangement.⁶⁰ Absorbance at 423 nm vs. [surfactants] has been given in Fig. 5.

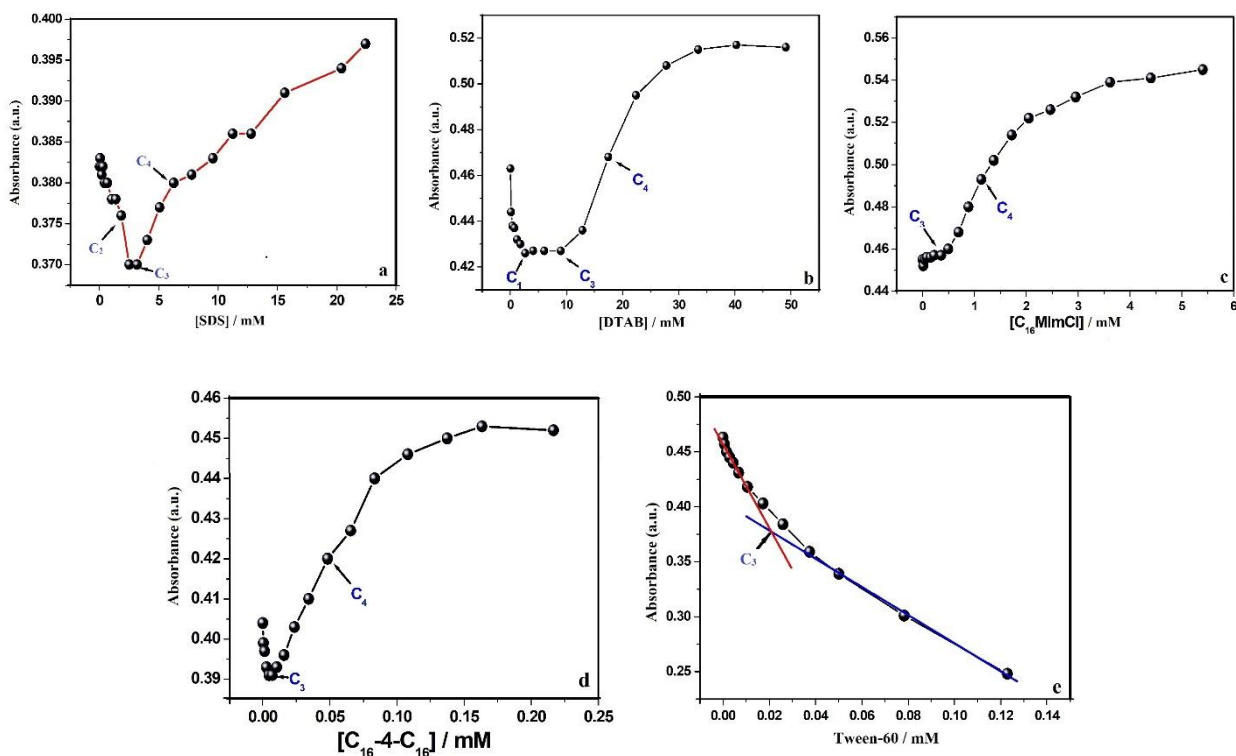


Fig. 5. absorbance intensity at 423 nm vs. concentration of surfactants profiles of H₂DTC (0.09 mM) upon addition of surfactants: SDS (a), DTAB (b), C₁₆MImCl (c), C₁₆-4-C₁₆ (d) and Tween-60 (e) in 15% EtOH-water medium.

Except Tween 60, all the plots in Fig. 5 show a sigmoidal nature in the micellar region which revealed the dynamic equilibrium in terms of partition of H₂DTC between bulk solution and micellar region. Several inflection points were designated in Fig. 5 and found close similarity those obtained from tensiometry (see Table 3). The decrease of absorbance intensity of H₂DTC in presence of Tween 60 at all concentration ranges and slight decrease of intensity in presence of cationic and anionic surfactants clearly indicates the interaction of H₂DTC with different surfactants. The equilibrium reaction for the binding of dye to the micelles can be written as⁶¹:



where K_b is the binding constant, DS_m and D are the concentrations of bound and free dye (H₂DTC), respectively, and S_m is the concentration of micellized surfactant. Binding constant can be determined using the Benesi Hildebrand equation.⁶² This equation is used in the following modified form for the dye surfactant micelle system⁶³, given below in Eq. 12:

$$\frac{d [D]_0}{A-A_0} = \frac{1}{\varepsilon-\varepsilon_0} + \frac{1}{(\varepsilon-\varepsilon_0)K_b S_m} \quad (12)$$

where d is the optical path length of the solution, A and A_0 are the absorbance values of dye in the presence and absence of surfactant, respectively, ε and ε_0 are the molar absorptivity of dye fully bound to micelles determined in large excess of the micelles and the molar absorptivity of dye in aqueous solution without surfactant, respectively. $[S_m]$ is equal to the difference between the total surfactant concentration and the *cmc* of surfactant solution containing dye. In this work, constant concentration of H₂DTC [0.308 mM] has been maintained throughout the addition of surfactants. The *cmc* values of each surfactants containing H₂DTC have been taken by averaging the three methods (tensiometry, spectrophotometry and spectrofluorimetry). The term $\frac{d [D]_0}{A-A_0}$ was plotted as a function of $1/[S_m]$ (shown in Fig. S4) according to Eq. 12 using the absorbance values at the maximum absorption wavelength of the micelle-bound H₂DTC (at 423 nm) in order to find the K_b and ε (Shown in Table 4). From Table 4, it is evident that binding of H₂DTC with cationic surfactant micelles are greater than SDS and for non-ionic, maximum binding is observed. Among the cationic micelles, for 16-4-16 gemini, K_b was observed greater than DTAB and C₁₆MImCl. On the other hand, molar extinction coefficient of H₂DTC in fully bound micellar medium (ε) also shows greater value for cationic surfactants than SDS, and the ε values in micellar medium are shown to exceed than the ε_0 of H₂DTC found in without micelle bound environment except for Tween -60, where ε value of H₂DTC is minimum even than ε_0 at 423 nm. Partition coefficient, K_c , is an important parameter to determine the partition of dye between the micellar and to the solvent phases. It can be calculated from the following equation⁶⁴:

$$\frac{1}{A-A_0} = \frac{1}{K_c(A-A_0)^*[D]_0+[S]_m} + \frac{1}{(A-A_0)^*} \quad (13)$$

where $(A - A_0)^*$ is the differential absorbance at the infinity of surfactant concentration where all H₂DTC molecules are assumed to be formed aggregates with the surfactant. The K_c values were obtained from the intercepts and slopes of the plots of $\frac{1}{A-A_0}$ versus $1/([D]_0 + [S]_m)$ have been shown in Fig. S5. K_c is defined as partition constant. Dimensionless partition coefficient, K_x is defined as the ratio of mole fraction of dye in micellar phase to mole fraction of dye in aqueous phase related with K_c as $K_x = K_c \times n_w$, where n_w is the molarity of water at 298.15 K representing the number of moles of water per dm³. The calculated K_c and K_x values are shown in Table 4. From Table 4, it is evident that, K_c and K_x values for cationic surfactants are greater than anionic SDS. Among the cationic surfactants, the values of K_c and K_x of H₂DTC are found

to be the following increasing order, $C_{16}MImCl > 16-4-16 > DTAB$. H_2DTC shows greater partition in Tween-60 micellar medium than the cationic and anionic micelles (cf. Table 4). Increase in the values of K_b and K_x can be attributed to the lower *cmc*, enhanced hydrophobicity and increased affinity of dye towards micelle.⁵⁶ Gibbs energies, i.e., the free energy of binding (ΔG_b) and free energy of partition (ΔG_p) can be calculated using the following equations 14 and 15:

$$\Delta G_b = -RT \ln K_b \quad (14)$$

$$\Delta G_p = -RT \ln K_p \quad (15)$$

From Table 4 it is evident that negative ΔG_b increases in terms of binding of H_2DTC with the different surfactant micelles showing the increasing trend, like, $SDS < DTAB < C_{16}MImCl < 16-4-16 < Tween-60$. So, the binding of H_2DTC with surfactant micelles is spontaneous in the present investigating systems. This trend somewhat changes in the negative ΔG_p values [cf. Table 4], showing similar pattern in the case of K_c and K_x . It has been seen that, binding of H_2DTC with the surfactant micelles are more spontaneous than partition of H_2DTC to the micellar core.

Fluorescence studies reveal the possible environmental transition of H_2DTC in the surfactant medium at both low and high concentration. It is seen that like absorbance,

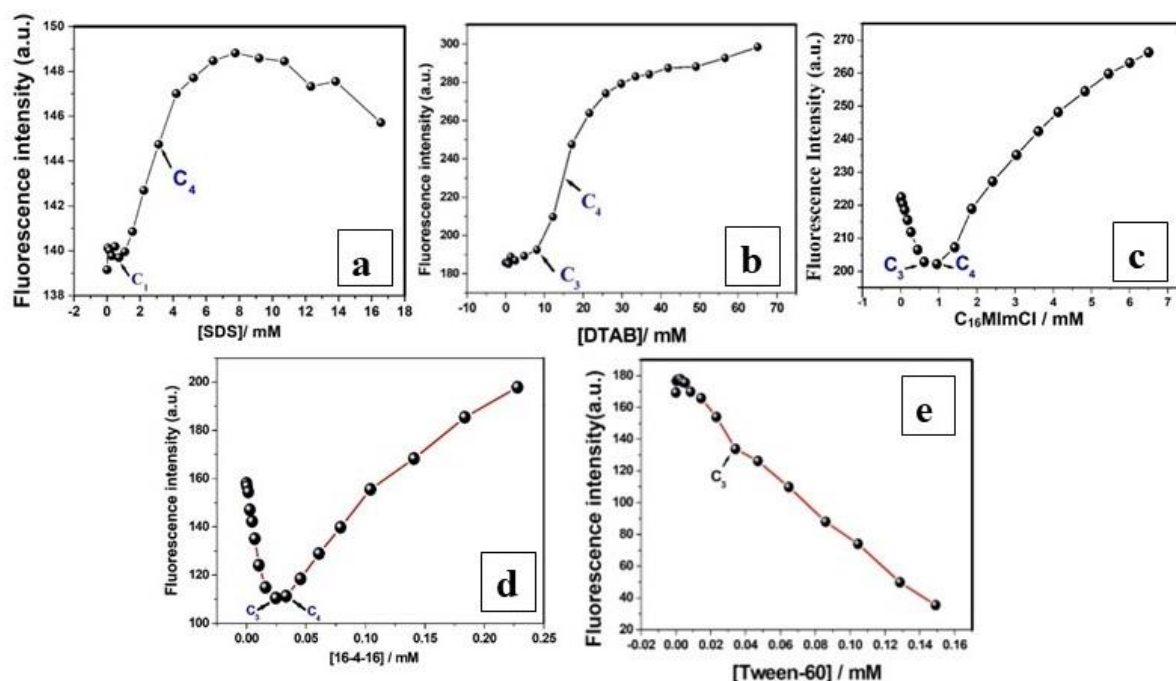


Fig.6. Fluorescence intensity at 527 nm vs. concentration of surfactants profiles of H_2DTC (0.09mM) upon addition of surfactants: SDS (a), $C_{16}MImCl$ (b), and Tween-60 (c), DTAB (d) and 16-4-16 (e) in 15% EtOH-water medium.

fluorescence intensity of H₂DTC does not change significantly in case of SDS, but the more profound sigmoidal nature is observed in fluorescence intensity plot [cf. Fig. 6(a)]. Blue shift in fluorescence spectra is observed for all anionic and cationic surfactants except Tween 60, where a regular decrease in fluorescence intensity were observed, revealing the transfer of H₂DTC in the hydrophobic core of micelle at high surfactant concentration

5. Conclusions:

Interaction of H₂DTC with different varieties of surfactants has been studied with the help of tensiometry and spectrometry. Binding constant determination using Benesi- Hildebrand equation shows its limitation as both increasing and decreasing patterns of λ_{max} are observed with variation of [surfactant] in absorbance and fluorescence spectroscopy of H₂DTC. Specific types interaction between the H₂DTC with different surfactants can only be achieved by other sophisticated experimental techniques, like ITC and also from DFT, will be undertaken as a future scheme.

Table 1. Critical micelle concentration (cmc) values of different investigated surfactants in aqueous solution at 298.15 K by tensiometry (S.T.), spectrophotometry (S.P.), spectrofluorimetry (S.F.) and isothermal titration calorimetry (ITC) ^{a,b,c,d}

Surfactants	Critical micelle concentration / mM		
	S.T.	S.P.	S.F.
SDS	8.45 ^a , 8.10 ^{[25]b} , 7.98 ^{[26]b} , 8.60 ^{[27]b} ,	8.10 ^{[28]b} (p-DMAB probe), 8.26 ^{[29]b} 7.09 ^{[35]b} (Pyrene absorbance method)	7.28 ^{[26]b} 8.304 ^{[31]b} 7.05 ^{[35]b} (Pyrene I ₁ /I ₃ method)
DTAB	12.07 ^a , 14.6 ^{[32]b}	15.3 ^{[35]b} (Pyrene absorbance method)	14.9 ^{[35]b} 15.1 ^{[38]b} (Pyrene I ₁ /I ₃ method)
C ₁₆ MImCl	0.86 ^a , 0.83 ^a		
16-4-16	0.021 ^a , 0.0272 ^{[40]c} ,		
Tween 60	0.036 ^a , 0.022 ^{[41]b} 0.021 ^{[42]b}	0.0209 ^{[42]b} (I ₂ absorbance method) 0.0210 ^{[43]b} (Safranine-T absorbance method)	0.020 ^{[43]b} (using Safranine-T)

- Found in this study
- Taken from literatures. References are given within the parenthesis.
- cmc at 303.15 K
- cmc at 300.15K

Table 2. Interfacial properties evaluated from tensiometry measurement for all the surfactants investigated here in aqueous, 15% (v/v) EtOH and in H₂DTC prepared in 15% (v/v) EtOH at 298.15±0.1 K. ^a

surfactants	solvents	γ_{cmc} mN.m ⁻¹	$10^6\Gamma_{max}$ mol.m ⁻²	A_{min} nm ² .molecule ⁻¹	$10^3\pi_{cmc}$ J.m ⁻²	$p^{C_{20}}$	P
SDS	water	30.6±0.2	2.17	0.76	42.2	0.287	0.27
	EtOH	29.6±0.3	0.94	1.84	17.4		0.11
	H ₂ DTC	25.2±0.2	0.64	2.59	21.6		0.08
DTAB	water	38.9±0.3	2.74	0.61	31.2	0.719	0.35
	EtOH	29.0±0.5	1.09	1.54	10.2		0.14
	H ₂ DTC	30.0±0.4	0.89	1.86	11.6		0.11
C ₁₆ MeImCl	water	35.9±0.3	1.56	1.06	28.4	0.674	0.16
	EtOH	34.7±0.3	0.54	3.06	6.70		0.06
	H ₂ DTC	34.3±0.4	0.46	3.63	0.70		0.05
16-4-16	water	48.5±0.3	1.80	0.92	24.2	1.780	0.08
	EtOH	33.5±0.3	0.41	4.05	7.30		0.04
	H ₂ DTC	32.5±0.5	0.66	2.50	8.70		0.07
Tween-60	water	43.1±0.2	0.95	1.75	27.5	0.993	0.12
	EtOH	34.8±0.3	0.43	3.87	12.6		0.05
	H ₂ DTC	35.8±0.5	0.26	6.47	11.5		0.03

^a. Error limits for Γ_{max} , A_{min} , π_{cmc} , $p^{C_{20}}$ and P are ±3, ±4, ±3, ±3 and ±4 % respectively.

Table 3. Various concentrations (C_1 , C_2 , C_3 and C_4) determined during micellization of surfactants in presence of H_2DTC solubilised in 15% EtOH-water at 298.15 K from several techniques employed^a.

Surfactants	Critical concentrations												
	Tensiometry					Spectrophotometry				Spectrofluorimetry			
	15% EtOH	H_2DTC				H_2DTC				H_2DTC			
	cmc (mM)	C_1	C_2	C_3	C_4	C_1	C_2	C_3	C_4	C_1	C_2	C_3	C_4
SDS	5.08	0.841	2.08	3.36	7.21	-	1.83	2.90	5.94	0.72	-	-	3.11
DTAB	15.75	2.23	6.33	12.4	15.1	2.49	-	12.7	17.4	-	7.88	-	14.6
$C_{16}MImCl$	1.15	0.016	0.07	0.33	0.77	-	-	0.36	1.13	-	-	0.57	0.95
16-4-16	0.069	0.006	0.008	0.02	0.03	-	-	0.007	0.05			0.018	0.03
Tween-60	0.035	-	-	-	0.024	-	-	-	0.025	-		0.034	

a. Error limits for the critical concentrations; within the brackets, the techniques are mentioned: $\pm 5\%$ (tensiometry), $\pm 4\%$ (isothermal titration calorimetry), $\pm 4\%$ (spectrophotometry), and $\pm 5\%$ (fluorimetry)

Table 4. Molar absorptivity of H₂DTC in absence (ϵ_0) and presence (ϵ) of micellar solution prepared in 15% v/v EtOH-water medium, binding constant (K_b), partition constant (K_c), partition coefficient (K_x), Gibbs energy of binding (ΔG_b^0), Gibbs energy of partition (ΔG_p^0) for H₂DTC/surfactant system^a

Surfactants	ϵ_0 (M ⁻¹ .cm ⁻¹) of H ₂ DTC (15% v/v EtOH-H ₂ O) $\lambda_{\text{abs(max)}} = 423$ nm	ϵ (M ⁻¹ .cm ⁻¹) of H ₂ DTC in micellar solution (15% v/v EtOH-H ₂ O) $\lambda_{\text{abs(max)}} = 423$ nm	$K_b \times 10^{-3}$ (M ⁻¹)	$K_c \times 10^{-2}$ (M ⁻¹)	$K_x \times 10^{-4}$ (M ⁻¹)	ΔG_b^0 (kJ.mol ⁻¹)	ΔG_p^0 (kJ.mol ⁻¹)
SDS	2867 ± 172	2969 ± 171	0.02 ± 0.004	0.62 ± 0.025	0.34 ± 0.02	-7.63	-10.2
DTAB		3080 ± 184	0.19 ± 0.01	1.79 ± 0.072	0.99 ± 0.05	-13.1	-12.9
C ₁₆ MImCl		3151 ± 189	4.44 ± 0.22	15.5 ± 0.620	8.63 ± 0.43	-20.8	-18.2
16-4-16		3056 ± 183	42.8 ± 2.14	3.95 ± 0.178	2.20 ± 0.12	-26.4	-14.8
Tween-60		2172 ± 130	70.9 ± 3.50	18.6 ± 0.824	10.3 ± 0.57	-27.7	-18.7

a. Error limit for ΔG_b^0 and ΔG_p^0 are ±5 and ±6% respectively

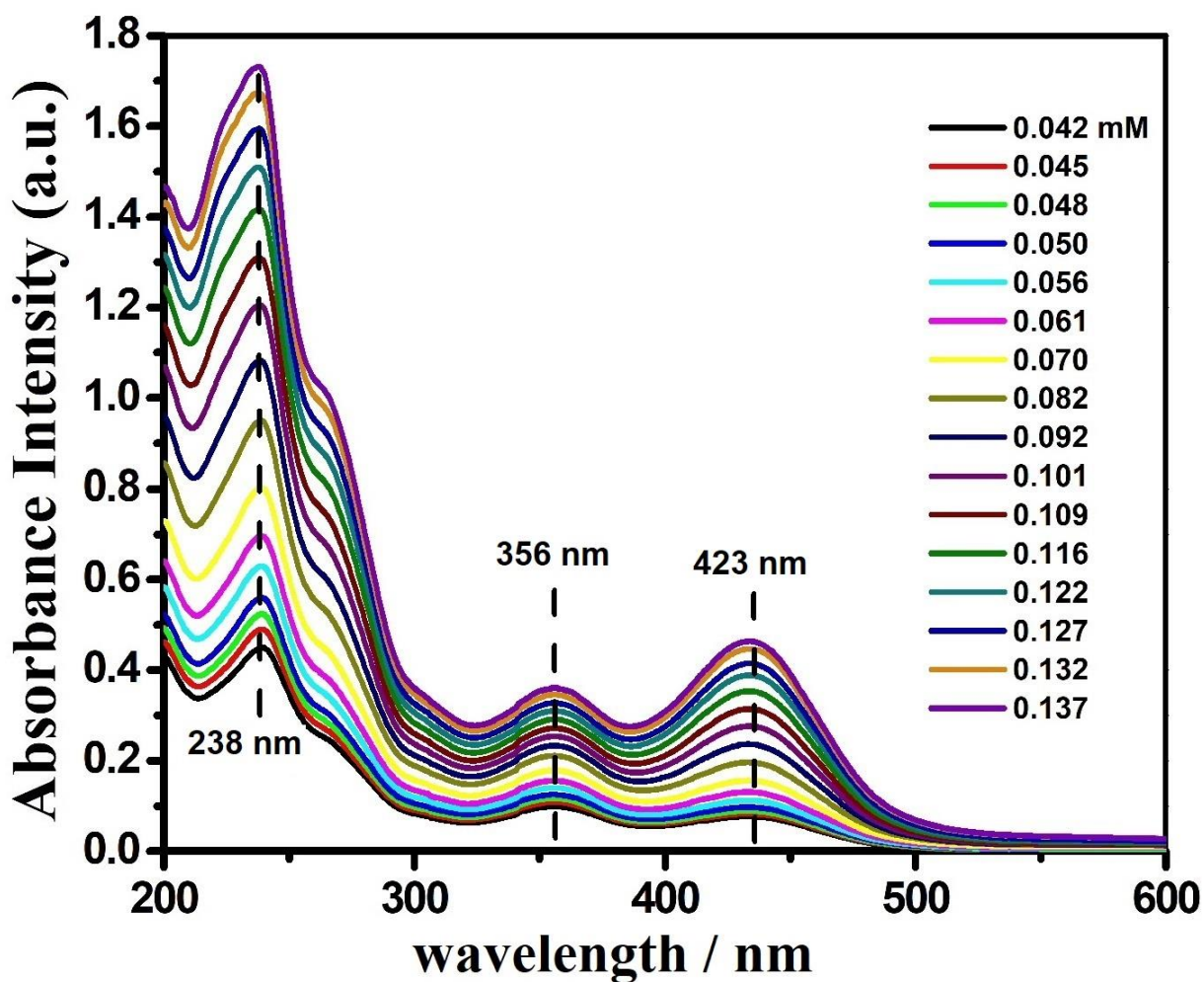


Fig. S2 (a). Absorbance Intensity vs. wavelength as a function of concentration of H₂DTC [H₂DTC] in mM unit in 15% EtOH-water medium at 298.15K.

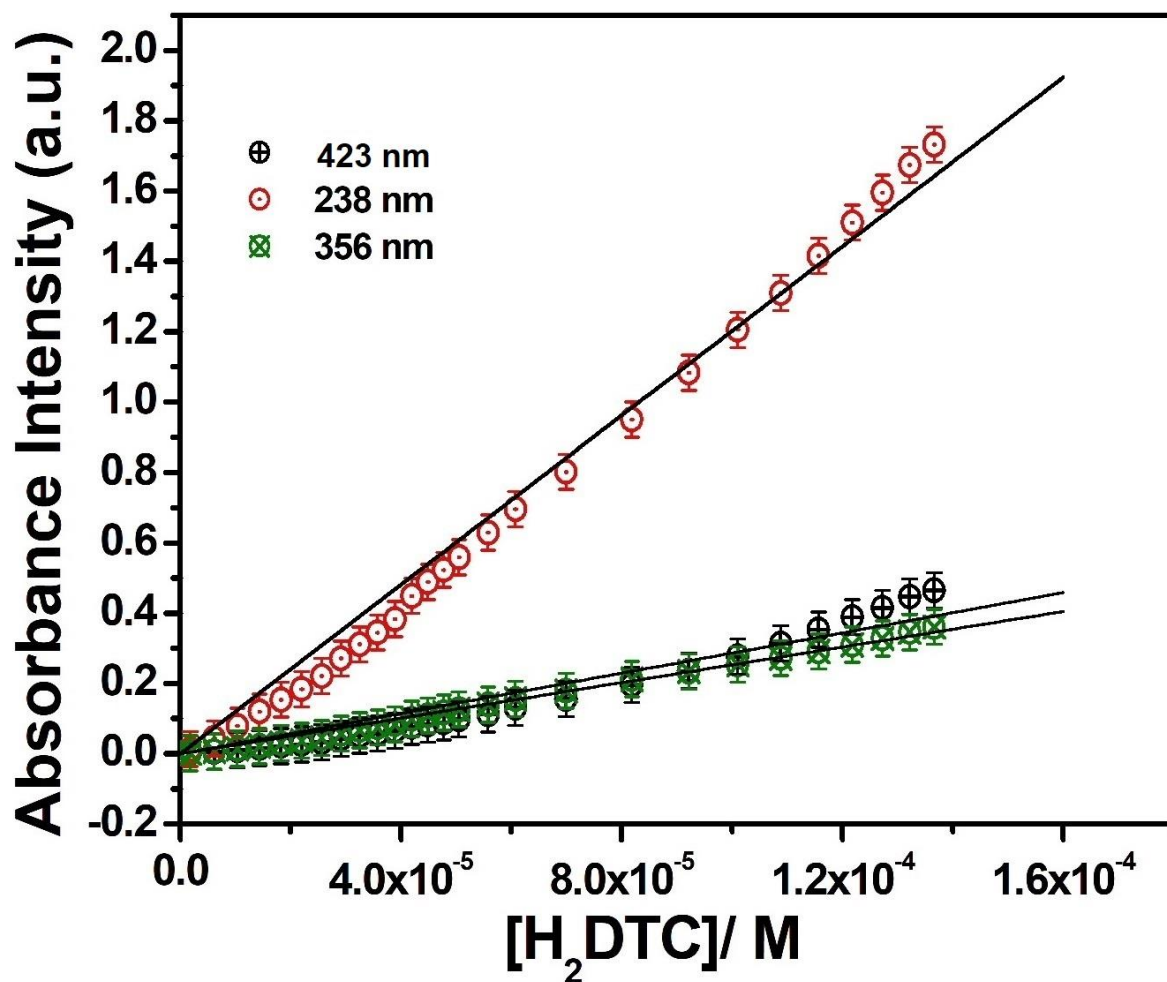


Fig. S2 (b): Linear dependence of absorbance intensity vs. concentration of H₂DTC [H₂DTC] at different absorbance wavelength in 15% EtOH-water medium at 298.15K.

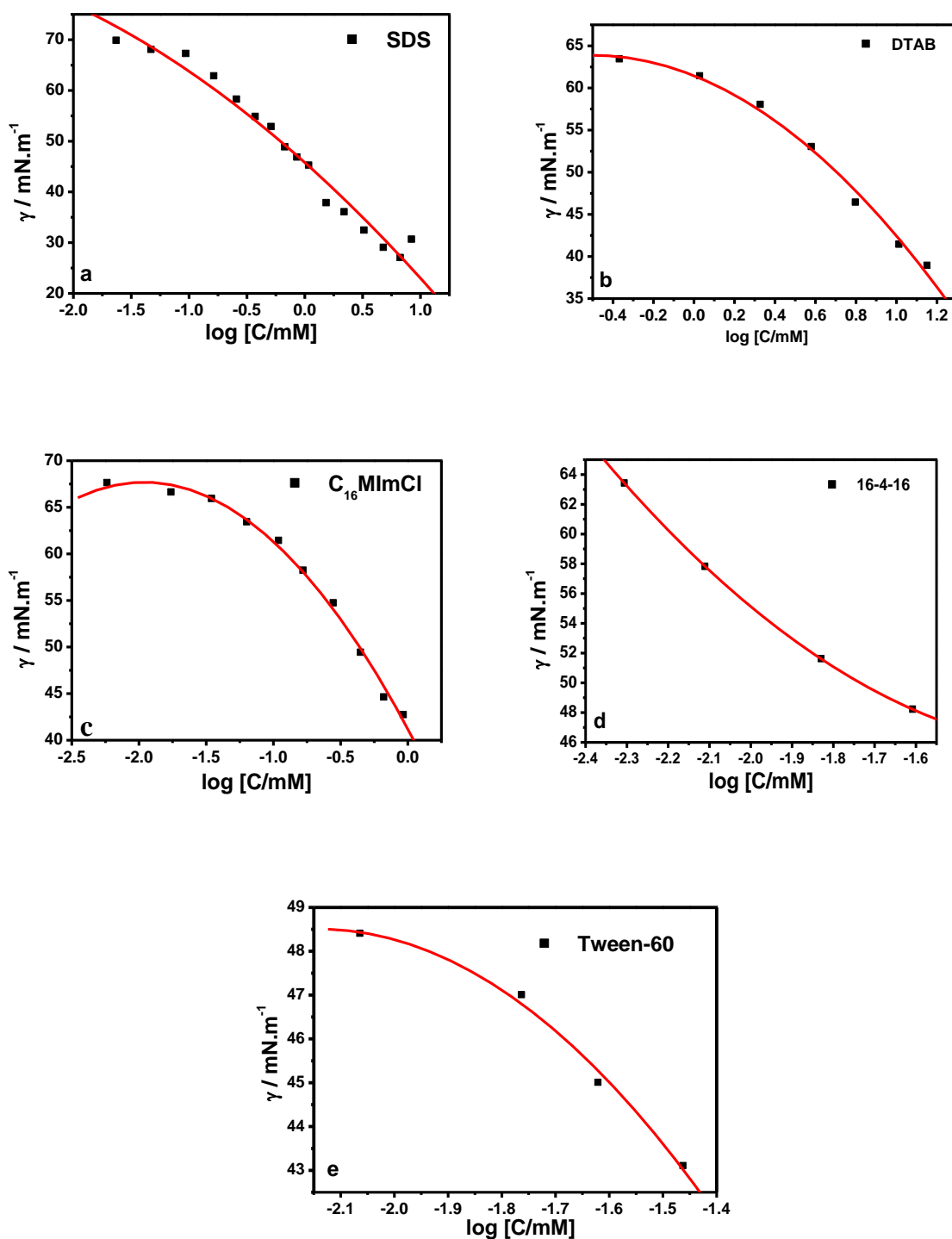


Fig. S3 (a): Surface tension (γ) vs. $\log [C/\text{mM}]$ plots with fitting of experimental data by second order polynomial equation [$\gamma = A + B_1 \log C + B_2 (\log C)^2$] for different surfactants (a. SDS, b. DTAB, c. $\text{C}_{16}\text{MImCl}$, d. 16-4-16 and e. Tween-60) at 15% v/v EtOH-water medium in absence of H_2DTC .

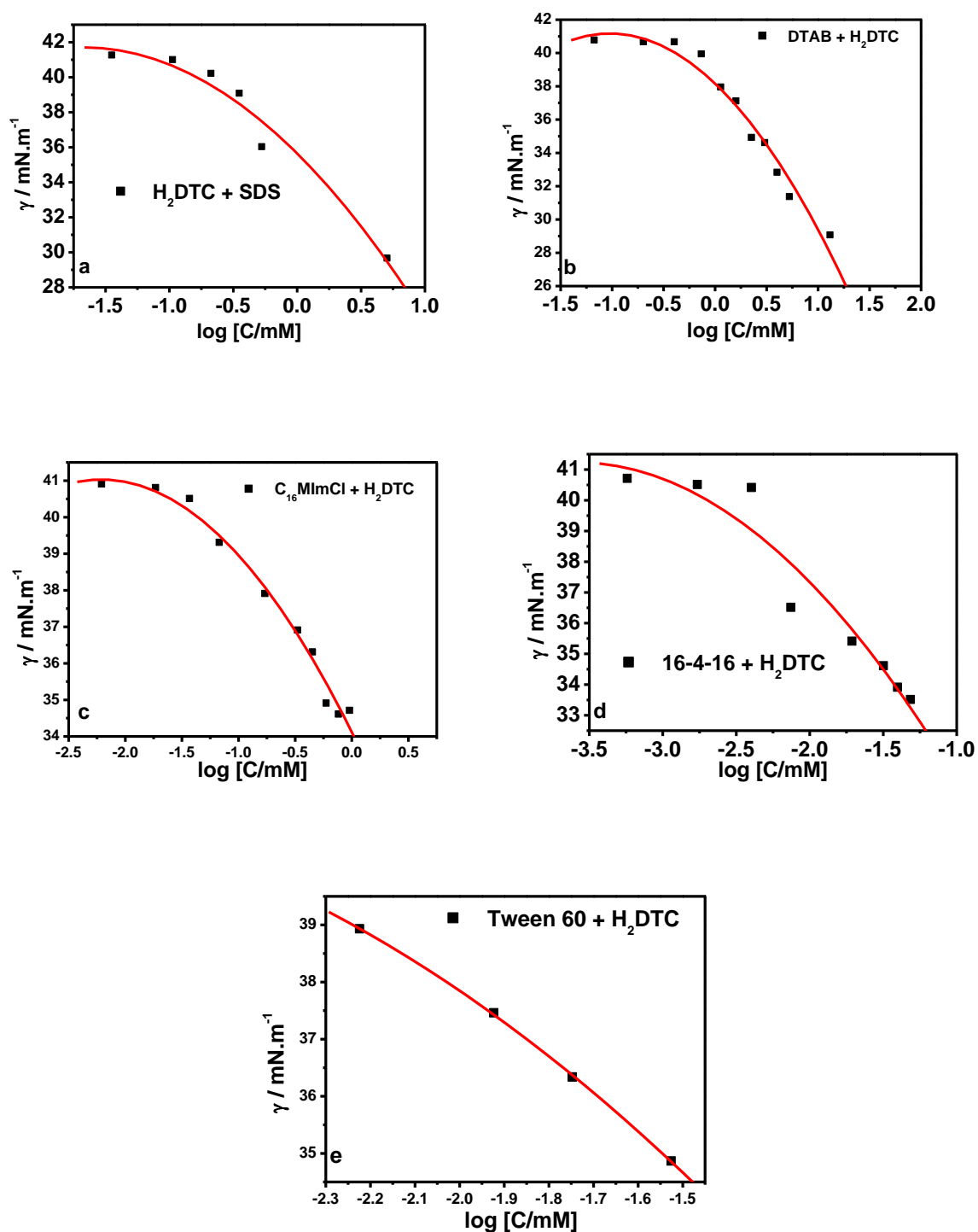


Fig. S3 (b): Surface tension (γ) vs. $\log [C/\text{mM}]$ plots with fitting of experimental data by second order polynomial equation [$\gamma = A + B_1 \log C + B_2 (\log C)^2$] for different surfactants (a. SDS, b. DTAB, c. $\text{C}_{16}\text{MimCl}$, d. 16-4-16 and e. Tween-60) at 15% v/v EtOH-water medium in presence of H_2DTC .

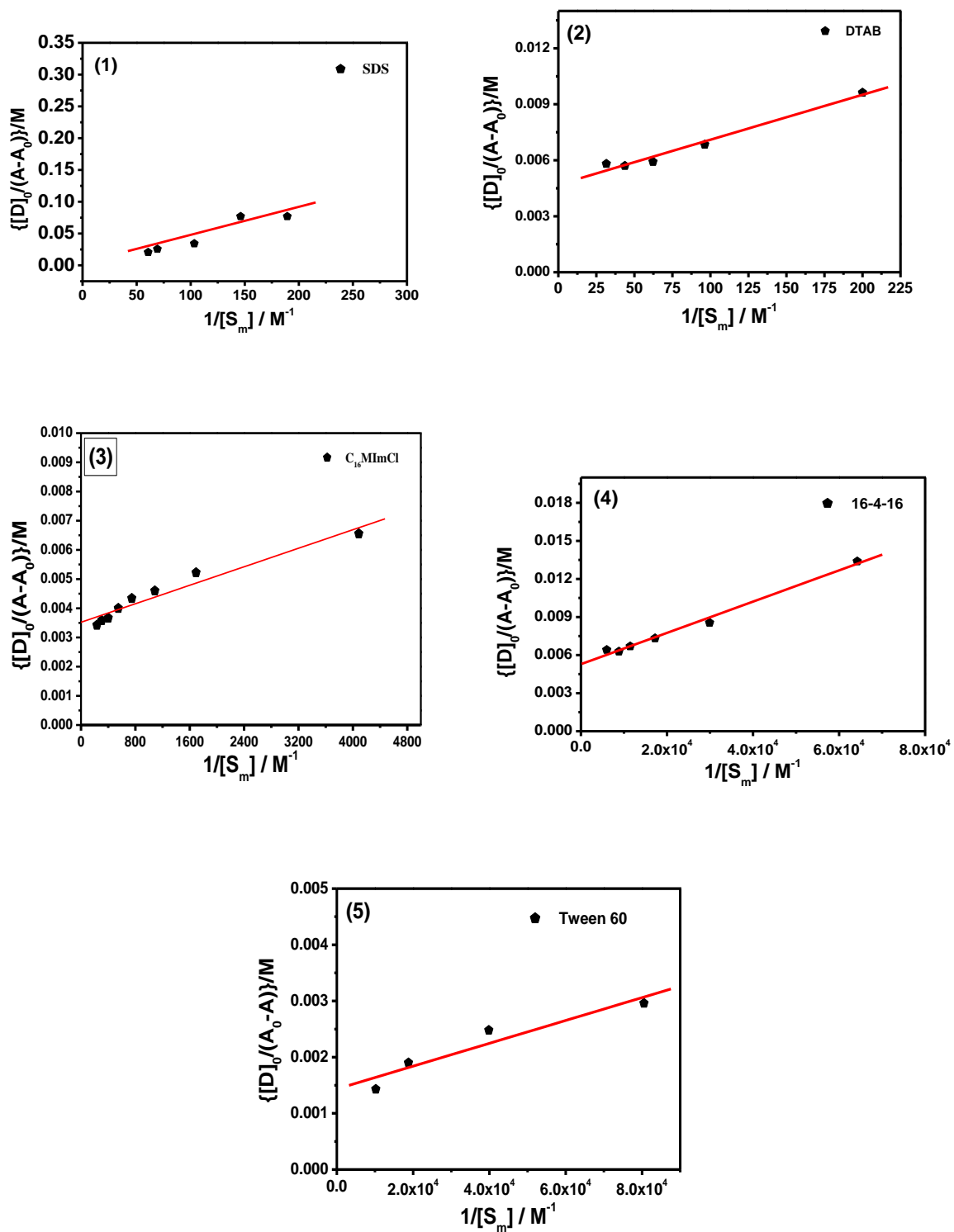


Fig. S4: Plot of $[D]_0/(A-A_0)$ vs. $1/[S_m]$ for the interaction of H_2DTC with different surfactants: SDS (Fig.1), DTAB (Fig.2), $C_{16}MImCl$ (Fig.3), 16-4-16 (Fig.4) and Tween 60 (Fig. 5).

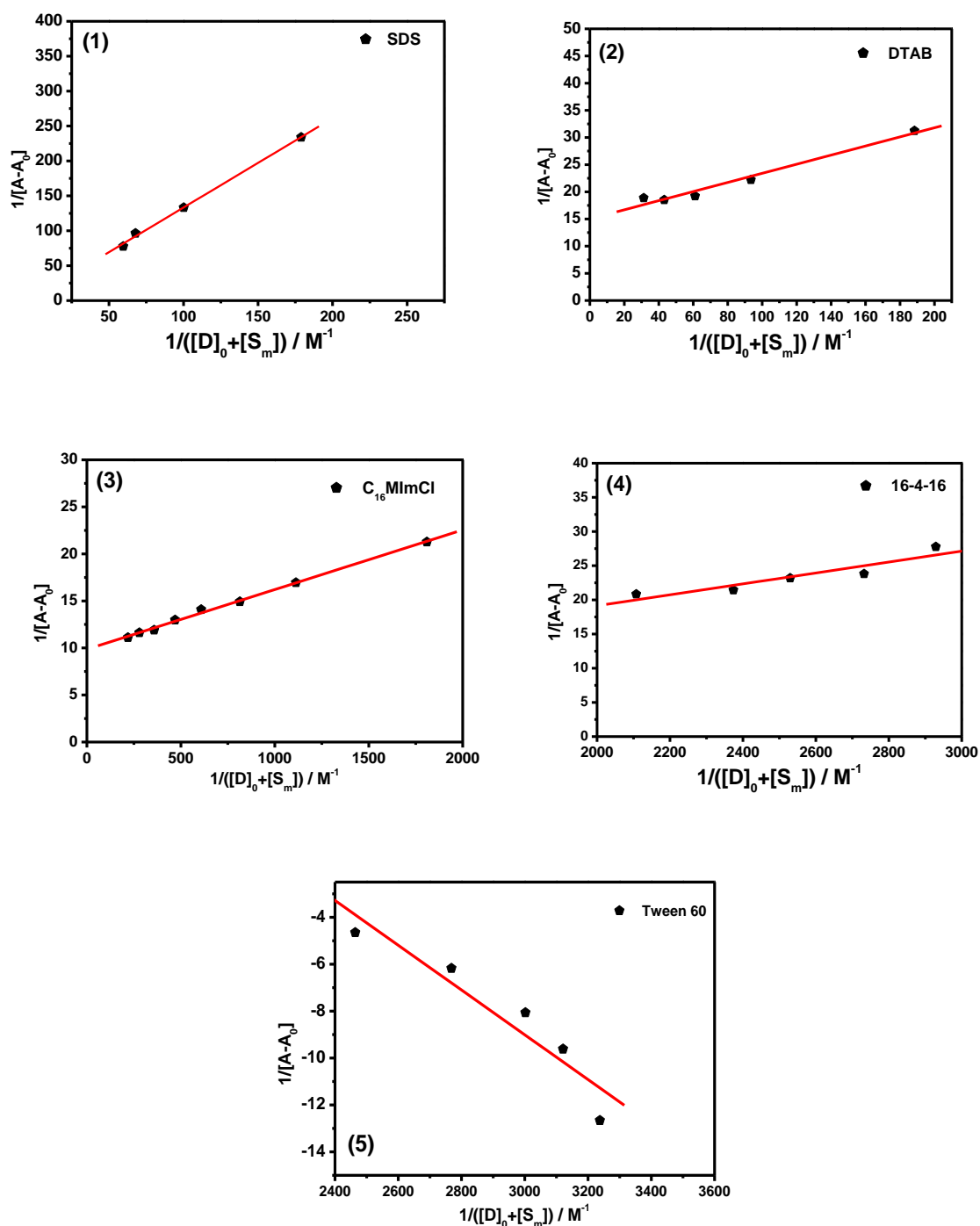


Fig. S5: Plot of $1/(A-A_0)$ vs. $1/([D]_0 + [S_m])$ for the interaction of H_2DTC with different surfactants in 15% v/v EtOH-water medium at 298.15 K; plots are given for different surfactants: SDS (Fig.1), DTAB (Fig.2), $C_{16}MImCl$ (Fig.3), 16-4-16 (Fig.4) and Tween 60 (Fig. 5).

In presence of 15% v/v EtOH in absence of H₂DTC				
Surfactants	A	B ₁	B ₂	R ²
SDS	45.8	-20.4	-2.41	0.97
DTAB	61.4	-9.58	-9.43	0.99
C ₁₆ MImCl	41.2	-26.9	-6.87	0.99
16-4-16	63.5	31.4	13.5	1.00
Tween-60	-5.98	-50.8	-11.8	0.99
In presence of 15% v/v EtOH in presence of H₂DTC				
Surfactants	A	B ₂	B ₃	R ²
SDS	35.6	-7.24	-2.16	0.97
DTAB	38.2	-5.89	-2.88	0.97
C ₁₆ MImCl	34.1	-6.25	-1.41	0.99
16-4-16	21.4	-11.1	-1.54	0.94
Tween-60	18.8	-13.7	-2.09	0.99

Table S1. List of Fitting parameters of γ vs. \log [surfactant] before cmc for different surfactants in presence of H₂DTC in 15% EtOH-water medium using second order polynomial. γ vs. \log [surfactant] plots where [Surfactants] \leq cmc were given in Fig. S3 (a) and S3 (b).

References:

1. I. O. Sutherland, *Pure and applied chemistry*, 1989, **61**, 1547-1554.
2. M. W. Hosseini, J. M. Lehn, S. R. Duff, K. Gu and M. P. Mertes, *The Journal of Organic Chemistry*, 1987, **52**, 1662-1666.
3. J. M. Lehn, *Inclusion Compounds*, 1985, **227**, 849-859.
4. P. G. Yohannes, M. P. Mertes and K. B. Mertes, *Journal of the American Chemical Society*, 1985, **107**, 8288-8289.
5. *Proceedings of the Fifth USSR-FRG Symposium on Chemistry of Peptides and Proteins, Odessa, USSR, May 16–20, 1985*, De Gruyter 2019.
6. S. Omura, *Macrolide antibiotics: chemistry, biology, and practice*, Academic press 2002.
7. J. M. Lehn and P. Vierling, *Tetrahedron Letters*, 1980, **21**, 1323-1326.
8. R. M. Izatt, J. S. Bradshaw, S. A. Nielsen, J. D. Lamb, J. J. Christensen and D. Sen, *Chemical Reviews*, 1985, **85**, 271-339.
9. S. Kado and K. Kimura, *Journal of the American Chemical Society*, 2003, **125**, 4560-4564.
10. R. C. Helgeson, J. M. Timko and D. J. Cram, *Journal of the American Chemical Society* 1973, **95**, 3023-3025.
11. G. W. Gokel and B. J. Garcia, *Tetrahedron Letters*, 1977, **18**, 317-320.
12. J. S. Bradshaw, M. L. Colter, Y. Nakatsuji, N. O. Spencer, M. F. Brown, R. M. Izatt, G. Arena, P. K. Tse, B. E. Wilson and J. D. Lamb, *J. Org. Chem.:(United States)*, 1985, **50**.
13. G. Melson, *Coordination chemistry of macrocyclic compounds*, Springer Science & Business Media 2012.
14. J. Lockhart, A. Robson, M. Thompson, S. D. Furtado, C. Kaura and A. J. J. o. t. C. S. Allan, *Perkin Transactions 1*, 1973, 577-581.
15. J. C. Lockhart and M. E. Thompson, *Journal of the Chemical Society, Perkin Transactions 1*, 1977, 202-204.
16. C. J. Pedersen and H. K. Frensdorff, *Angewandte Chemie International Edition in English*, 1972, **11**, 16-25.
17. S. A. G. Hogberg and D. J. Cram, *The Journal of Organic Chemistry*, 1975, **40**, 151-152.
18. S. Das, S. Mondal and S. Ghosh, *Journal of Chemical Engineering Data* 2013, **58**, 2586-2595.
19. R. Singh and R. Garg, *E-Journal of Chemistry*, 2010, **7**, 578-582.
20. R. Garg, R. Singh and S. Mehta, *Asian Journal of Research in Chemistry*, 2010, **3**, 71-77.
21. E. Caponetti, D. Chillura-Martino and L. Pedone, *Langmuir*, 2004, **20**, 3854-3862.
22. E. Vikingstad and J. Bakken, *Journal of Colloid and Interface Science*, 1980, **74**, 8-15.
23. N. Gol'dshleger, I. Kalashnikova, V. Baulin and A. Y. Tsivadze, *Protection of Metals, Physical Chemistry of Surfaces* 2011, **47**, 471-477.
24. F. M. Menger, J. S. Keiper and V. Azov, *Langmuir*, 2000, **16**, 2062-2067.
25. I. M. Umlong and K. Ismail, *Colloids and Surfaces A: Physicochemical and Engineering Aspects*, 2007, **299**, 8-14.
26. M. Milanović, V. Krstonošić, L. Dokić, M. Hadnađev and T. Dapčević Hadnađev, *Journal of Surfactants and Detergents*, 2015, **18**, 505-516.
27. J. Dey, N. Sultana, S. Kumar, V. K. Aswal, S. Choudhury and K. Ismail, *Rsc Advances*, 2015, **5**, 74744-74752.
28. H. Demissie and R. Duraisamy, *J. Sci. Innov. Res*, 2016, **5**, 208-214.
29. L. J. Waters, T. Hussain and G. M. B. Parkes, *The Journal of Chemical Thermodynamics*, 2012, **53**, 36-41.
30. S. Dai, K. C. Tam and L. Li, *Macromolecules*, 2001, **34**, 7049-7055.
31. A. M. Khan and S. S. Shah, *Journal of dispersion science and technology*, 2008, **29**, 1401-1407.
32. S. K. Shah, S. K. Chatterjee and A. Bhattarai, *Journal of Molecular Liquids*, 2016, **222**, 906-914.

33. S. K. Mehta, K. K. Bhasin, R. Chauhan and S. Dham, *Colloids and Surfaces A: Physicochemical and Engineering Aspects*, 2005, **255**, 153-157.
34. M. J. Suárez and V. Mosquera, *Physical Chemistry Chemical Physics*, 1999, **1**, 3583-3587.
35. G. B. Ray, I. Chakraborty and S. P. Moulik, *Journal of colloid and interface science*, 2006, **294**, 248-254.
36. S. P. Stodghill, A. E. Smith and J. H. O'Haver, *Langmuir*, 2004, **20**, 11387-11392.
37. W. Tong, Q. Zheng, S. Shao, Q. Lei and W. Fang, *Journal of Chemical & Engineering Data*, 2010, **55**, 3766-3771.
38. S. Chauhan, K. Singh, M. S. Chauhan and K. Sharma, *Journal of Molecular Liquids*, 2018, **258**, 163-171.
39. S. Das, S. Ghosh and B. Das, *Journal of Chemical & Engineering Data*, 2018, **63**, 3784-3800.
40. I. A. Khan, R. Mohammad, M. S. Alam and D. Kabir ud, *Journal of Dispersion Science and Technology*, 2009, **30**, 1486-1493.
41. D. M. Ćirin, M. M. Poša and V. S. Krstonošić, *Industrial & engineering chemistry research*, 2012, **51**, 3670-3676.
42. S. K. Hait and S. P. Moulik, *Journal of Surfactants and Detergents*, 2001, **4**, 303-309.
43. P. K. Khatua, S. Ghosh, S. K. Ghosh and S. C. Bhattacharya, *Journal of dispersion science and technology*, 2005, **25**, 741-748.
44. S.-Y. Lin, Y.-Y. Lin, E.-M. Chen, C.-T. Hsu and C.-C. Kwan, *Langmuir*, 1999, **15**, 4370-4376.
45. G. Sharma and A. Z. Naqvi, *Colloids and Surfaces A: Physicochemical and Engineering Aspects*, 2011, **385**, 63-71.
46. A. F. H. Ward, *Proceedings of the Royal Society of London. Series A. Mathematical and Physical Sciences*, 1940, **176**, 412-427.
47. L. G. Ionescu, L. S. Romanesco and F. Nome, *Surfactants in solution*, 1984, **2**, 789.
48. R. Zana, *Advances in Colloid and Interface Science*, 1995, **57**, 1-64.
49. S. Göktürk and U. Var, *Curr. Res. Chem*, 2011, **3**, 49-61.
50. A. Späth and B. König, *Beilstein journal of organic chemistry*, 2010, **6**, 32.
51. E. Caponetti, D. C. Martino, M. A. Floriano, R. Triolo and G. D. Wignall, *Langmuir*, 1995, **11**, 2464-2470.
52. J. P. Gallivan and D. A. Dougherty, *Journal of the American Chemical Society*, 2000, **122**, 870-874.
53. T. D. Gurkov, D. T. Dimitrova, K. G. Marinova, C. Bilke-Crause, C. Gerber and I. B. Ivanov, *Colloids and Surfaces A: Physicochemical and Engineering Aspects*, 2005, **261**, 29-38.
54. J. N. Israelachvili, *Intermolecular and surface forces*, Academic press 2011.
55. C. Tanford, *The hydrophobic effect: formation of micelles and biological membranes 2d ed*, J. Wiley. 1980.
56. S. Irshad, H. Sultana, M. Usman, M. Saeed, N. Akram, A. Yusaf and A. Rehman, *Journal of Molecular Liquids*, 2021, **321**, 114201.
57. S. Tunç, O. Duman and B. Kancı, *Dyes and Pigments*, 2012, **94**, 233-238.
58. N. Patra, B. Mandal and S. Ghosh, *Industrial & Engineering Chemistry Research*, 2017, **56**, 10044-10052.
59. R. Hosseinzadeh, R. Maleki, A. A. Matin and Y. Nikkhahi, *Spectrochimica Acta Part A: Molecular and Biomolecular Spectroscopy*, 2008, **69**, 1183-1187.
60. E. G. McRae and M. Kasha, *The Journal of Chemical Physics*, 1958, **28**, 721-722.
61. K. K. Rohatgi-Mukherjee, R. Chaudhuri and B. B. Bhowmik, *Journal of colloid and interface science*, 1985, **106**, 45-50.
62. H. A. Benesi and J. H. J. Hildebrand, *Journal of the American Chemical Society*, 1949, **71**, 2703-2707.
63. S. Göktürk and M. Tunçay, *Spectrochimica Acta Part A: Molecular and Biomolecular Spectroscopy*, 2003, **59**, 1857-1866.
64. S. Göktürk and R. Y. Talman, *Journal of solution chemistry*, 2008, **37**, 1709-1723.

Chapter-V

Addressing the Interaction of
Stem Bromelain with
different anionic Surfactants,
below, at and above CMC in
Phosphate Buffer at pH 7:
Physicochemical,
Spectroscopic & Molecular
docking Study

Addressing the Interaction of Stem Bromelain with different anionic Surfactants, below, at and above the critical micelle concentration (cmc) in Phosphate Buffer at pH 7: Physicochemical, Spectroscopic, & Molecular docking Study

ABSTRACT

This paper attempts to reveal the interaction and structural stability of stem Bromelain (BM) in presence of two different types of anionic surfactants (one type is bile salts, NaC and NaDC and others are the conventional anionic surfactants, SDDS and SDBS), below, at and above the critical micelle concentration in aqueous phosphate buffer medium (pH 7). Several biophysical techniques have been executed here. Several physicochemical parameters like, surface excess (Γ_{cmc}), minimum areas of surfactants at air water interface (A_{min}) are calculated from tensiometry both in absence and presence of BM. Several inflection points (C_1 , C_2 and C_3) have been found in tensiometry profile of surfactants in presence of BM due to the conformational change of BM assisted by surfactants. Similar observation also found in isothermal titration calorimetry (ITC) profiles where the enthalpy of micellization (ΔH_{obs}^0) of surfactants in absence and presence of BM have calculated. Steady state fluorescence spectra at 298 K reveal the quenching of tryptophan emission of BM in presence of bile salts/surfactants with blue shifting below the free micelle formation followed by the determination of binding constant (K_b) of BM with surfactants, bimolecular quenching constant (k_q), free energy of binding (ΔG_b^0) of bile salts/surfactants with BM have been calculated exploiting steady state fluorescence technique. It is observed that, the binding of NaC with BM is greater than any other surfactants investigated here, while Stern-Volmer quenching constant (K_{sv}) is found greater in presence of SDBS. From steady state and time resolved fluorescence study it is observed that static quenching of tryptophan is functional in presence of bile salts/surfactants. Circular Dichroism (CD) study shows the stability of secondary structure of BM in presence of NaC and NaDC below C_3 , while BM lost its structural stability even at very low surfactant concentration of SDDS and SDBS. The molecular docking studies have also been substantiated for better understanding the interaction of BM with the surfactants.

1. Introduction:

Proteins are the major and most abundant component of living body contributing in several biological activities. Little change in normal biological environment causes adverse effect to the protein activity, disrupting (denature) protein structure by way of unfolding¹. The interaction of surfactants with proteins has manifold applications in the field of biology, cosmetic and pharmaceutical industry, medicine etc. by recognizing significant impact of surfactants on physicochemical, rheological and detergency properties². Several studies have been witnessed in past and preceding years for studying the interaction of surfactants with globular proteins in presence and absence of additives³⁻²¹. Among them, most of the studies reveal that surfactant binds to single protein, unfolds or disrupts native structure of proteins^{5,19-23}. The comprehensive physicochemical investigations between globular proteins with surfactants are found very few in literature^{2, 9-12,16, 24-30}. In fact, the physicochemical study of proteases (which hydrolyse proteins to amino acid or other compounds) with surfactants have been seen limited in literature^{2, 9, 10, 25-26}. Proteases are the new class of proteins used widely

in the detergent industry in conjugation with traditional surfactants for the cleaning and removal of various proteinaceous stains ^{2, 9, 25}. It is seen that, binding of ionic surfactants is greater than non-ionic surfactants and among ionic surfactants, anionic surfactants (the most studied surfactant, sodium dodecyl sulphate (SDS)) may drastically change the conformation of proteins ^{1, 31-34}.

Naturally occurring amphiphilic molecules, especially bile salts sodium cholate (NaC) and sodium deoxycholate (NaDC) (Scheme 1a) are produced in the human liver and released into duodenum during food intake for the solubilization and absorption of fats ^{35, 36}. Bile salts aggregation is more complex in nature as compared to that of conventional surfactants which form simple micelles³⁷. Several methods have been applied to understand the self-aggregation behaviour of bile salts. The most widely accepted model amongst them, proposed by Small *et. al.* ^{38, 39} stated the formation of primary aggregates (generally 2–10 monomeric units) at lower bile salt concentration region driven by the hydrophobic interaction among the monomers of bile salts. The hydrophilic groups on the other hand, are believed to be oriented outward in the primary aggregates ^{38, 39}. However, at higher bile salt concentrations, the primary aggregates get clustered to form secondary aggregates believed to be elongated rodlike morphology ^{38, 39}. Bile salts have been used in several steps during protein purification process, e.g., selective membrane solubilization, reconstitution of proteins, and, chromatographic separation ^{40, 41}. Due to the several utilities of bile salts, the interaction of different types of proteins with the bile salt surfactants gain utmost interest although found inadequate in literature ⁴²⁻⁴⁶.

Anionic surfactant namely, sodium dodecyl benzenesulfonate (SDBS) (Scheme 1a) resembles the lipid molecules which is present in biological membranes and thus assisted as model system ⁴⁷. Anionic surfactants having similarity with the lipid molecules have the property of amyloid-like fibrils formation in several proteins ⁴⁸. Khan *et. al.* reported on investigation ⁴⁷ that the insulin fibrillation using SDBS probed by the optical spectroscopy and microscopy. Recently, Wajira *et. al.* ⁴⁹ reported the denaturation effect of SDBS on water and fat adsorption properties of canola protein isolates to improve mechanical and tensile strength of protein-based plastics. Negatively-charged sulfate moiety of SDBS (behave like head group of surfactants) attached to hydrophobic aliphatic chain, contains 18 carbon atoms and also an attachment with a benzene ring. SDBS is commonly used in chemical, biochemical, and industrial applications ⁵⁰. Several studies have been reported in recent years regarding the interaction of SDBS with digestive protease *Candida rugosa* lipase ⁵¹, equine heart haemoglobin ⁵², BSA ⁵³ etc. An amino acid based anionic surfactant, Sodium-N-dodecanoyl sarcosinate (SDDS) (Scheme 1a), has

numerous commercial and biological utility owing to its capability for the formation of particle emulsions in addition to its low toxicity and fair biodegradability. It can also be recommended for one of the components of tooth paste for controlling dental caries in order to strengthen tooth enamel from acid dissolution by recognising SDDS's upright foaming property^{54, 55, 56}. To the best of our knowledge, very few reports have been documented for studying the interaction of SDDS with different proteins; of which the recent documentation have been found in literature⁵⁷⁻⁵⁹.

Stem Bromelain (BM), (Scheme 1b) containing a single polypeptide chain, is composed of 212 amino acid residues with a molecular mass of 23.8 kDa specified in previous literature⁶⁰. Bromelain can be extracted from either the pulp, stem, core, or peel of pine apple which is found at huge abundance in tropical and subtropical countries⁶¹. The structure of BM contains 6 phenylalanine (Phe), 14 tyrosine (Tyr), 5 tryptophan (Trp), 14 tyrosine (Tyr) with 3 disulfide bonds and a single free cysteine (Cys) residue⁶². It is found that optimum pH and temperature required for the activity of BM are in the range of 6.5–8.0 and 55–60°C, respectively⁶³. Bromelain has found substantial attention from a wide array of industrial areas, such as, food, cosmetic, dairy, pharmaceutical etc., owing to its proteolytic activity, and high commercial value^{64, 65}. Moreover, bromelain shows numerous therapeutic applications, such as, it can be used in the treatment of malignant cell growth, thrombophlebitis, angina pectoris, inhibition of platelet aggregation, digestive problem, osteoarthritis, post-surgical traumas and so on⁶⁶⁻⁶⁸. In the context of the enormous applications of bromelain, it is supposedly needed to understand the structural stability of BM while encountering with various surfactants both for academic and industrial points of view. Investigations in past and preceding years have been undertaken to elucidate the interaction of BM with cationic surfactants^{63, 68}, surface active ionic liquids^{60, 62, 69}, zwitterionic surfactants⁷⁰ at different pH media to observe proteolytic activity and surfactant-mediated amyloidogenesis property of BM. To the best of our knowledge, the interaction of BM with anionic surfactants is hardly found in literature⁷¹. This scenario demands the study of structural stability of BM in presence of different anionic surfactants including bile salt surfactants.

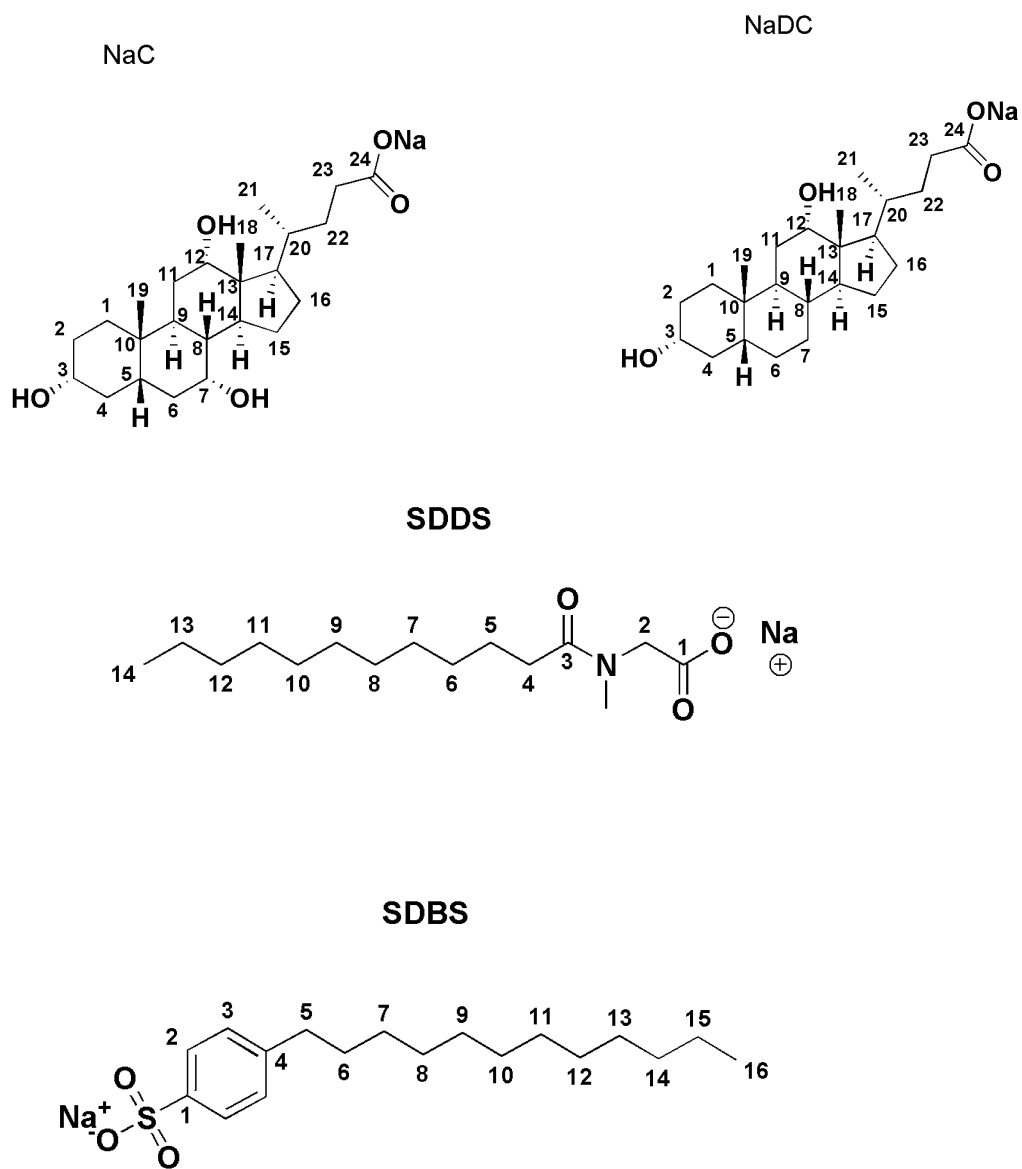
In this present study, our focus to explore the structural aspects of stem bromelain in presence of two bile salt surfactants, NaC and NaDC, two conventional anionic surfactants, SDDS and SDBS and also the investigation of those interactions by the physicochemical and photophysical processes. A comparative study of BM with the different bile salts and surfactants exploiting different techniques viz. tensiometry, isothermal titration calorimetry

(ITC), steady state absorption and fluorescence studies, time resolved fluorescence studies, circular dichroism (CD) studies have been carried out to understand the extent of stability of BM in presence of the bile salts and surfactants. Surface excess and area minimum of surfactants in absence and presence of BM, enthalpy of micellization, binding constant, bimolecular quenching constants followed by free energy of binding due to the interaction of BM with the surfactants have calculated and the critical concentrations of surfactants before and after micellization in presence of BM have also compared with the tensiometry and calorimetry data. The nature of quenching is tried to infer by the time resolved fluorescence quenching studies. The molecular docking studies have also been substantiated for better understanding the interaction of BM with the surfactants.

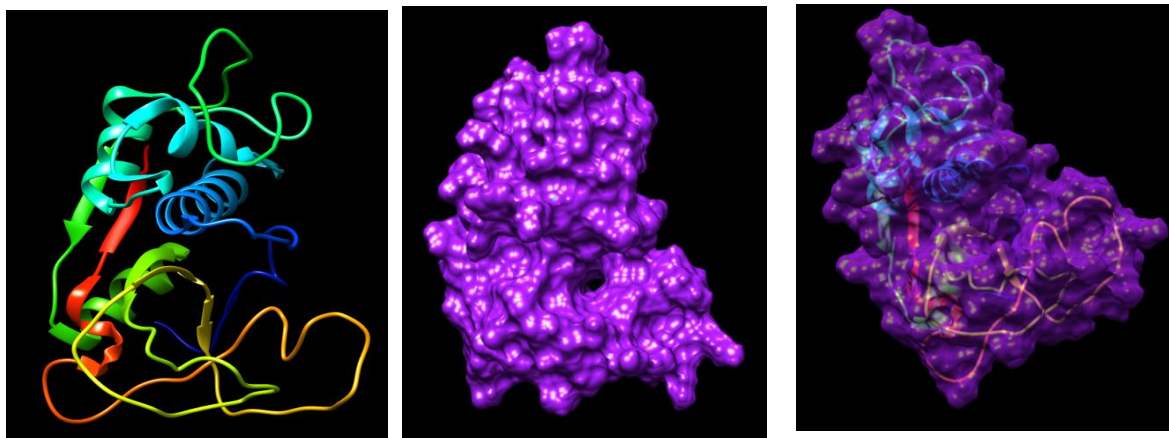
2. Experimental Section:

2.1. Materials and Sample Preparation:

Sodium cholate hydrate, 98% (NaC), sodium deoxycholate (NaDC), sodium dodecyl benzenesulfonate (SDBS), sodium lauroyl sarcosinate (SDDS) and bromelain (BM) from pineapple stem, B4882 were purchased from Sigma Aldrich. The detailed structures of these compounds are given in scheme 1(a) and (b). These chemicals were used as received without any further purification. Structure of surfactants were drawn by Avogadro software and optimized⁷² further to obtain the energy minimized structure (shown in Scheme 1a). Crystal structure of BM are given in Scheme 1(b). Phosphate buffer solution has been prepared at pH 7 using deionised water. Triply distilled water of specific conductance 0.99 $\mu\text{S}/\text{cm}$ was used throughout the experiments at 298.15K. For surface tension and isothermal titration calorimetry (ITC) measurements, BM was prepared at the concentration of 20 μM in pH 7 phosphate buffer. BM concentration was kept fixed at 10 μM in pH 7 phosphate buffer for spectrometry. Apart from spectrometry, BM concentration has been taken in 20 μM for the other measurements. Each surfactant was prepared at a surfactant concentration ≈ 15 times their *cmc* in pH 7 phosphate buffer at 298.15 K and have been used as a stock solution. Progressive addition method has been used in the dilution process of BM with that concentrated stock surfactant solutions in different experimental processes employed here. For different temperature variation processes, same surfactant stocks, which are prepared at 298.15 K, have been used assuming negligible expansion and compression of volume of such a low volume of stock solution at higher or lower temperature respectively.



Scheme. 1(a). Structure of surfactants drawn in Avogadro software



Scheme. 1(b). Crystal structures of Bromelain are obtained from protein data bank [PDB 1D: 1W0Q]

2.2. Methods employed:

2.2.1. Tensiometry:

A calibrated Krüss-K8 tensiometer (made in Germany) was cast off to determine surface tension at air water interface by du Noüy ring detachment method at 298.15 K. For this purpose, a platinum ring has been cleaned using deionized water and acetone successively and burned briefly until glowing in ethanol flame prior to experiment. A measured amount of 5 mL BM (20 μM) was prepared in phosphate buffer at pH 7 and taken in a double jacketed glass container attached with a thermostatic water bath to maintain the desired temperature (298.15 K) during experiment with an accuracy of ± 0.1 K. Stock surfactant solutions, which have been prepared, were added to the double jacketed container having BM by a Hamilton micro syringe and stirred well after each addition and kept for 5 minutes before taken surface tension value. Surface tension of phosphate buffer at pH 7 was found in the range between 65.6 to 70.8 $\text{mN}\cdot\text{m}^{-1}$ by considering the experimental error. On the other hand, surface tension value of 0.02 % w/v BM solution at the same pH was found to be 59 to 60 $\text{mN}\cdot\text{m}^{-1}$ (shown in Fig 1.). Relatively, little change in the value of surface tension of BM solution as compared with BM free buffer solution at pH 7 is due to the protease nature of BM (containing less α helix structure of BM) which is not usual for the other proteins containing well existence of α helix structure⁷³. Representative plots of surface tension (γ) vs. \log [surfactant]/ mM of different surfactants in presence and absence of BM in phosphate buffer at pH 7 with individual inflection points (discussed elsewhere in this manuscript) were shown in Fig. 1. Different interfacial parameters in presence and absence of BM for all the surfactants were displayed in Table 1.

2.2.2. Isothermal Titration Calorimetry (ITC):

ITC₂₀₀ (Malvern, UK) microcalorimeter was well equipped with a thermostatic arrangement. Experimental temperature was maintained at 298.15 K with a precision of ± 0.02 K. The concentration of BM for ITC measurements was 20 μM . Enthalpograms for the dilution of surfactants in presence and absence of BM in phosphate buffer medium of pH 7 have been presented in Fig. 2. The solutions of BM were taken in a calorimeter cell and surfactant solutions were added (initially 0.5 μL , then 2 μL ; total 20 injections) at a time interval of 120s using a micro syringe. Raw data were analysed by OriginTM 7.0 software with the help of $\mu\text{cal/s}$ vs. time (min) [given in Fig. 3] after the subtraction of integrated baseline which was performed by taking buffer solution in reference cell at the same experimental temperature. Enthalpies of micellization (ΔH_m^0) were determined (cf. Table. 2.) from the normalised integration data plot (kcal.mol^{-1} per mole of injectant vs. concentration of surfactant [Surf]; cf. Fig. 2) manually. Cmc values were calculated from enthalpograms and have been presented in Table 2.

2.2.3. Spectrophotometry:

Spectrophotometry was executed using a Shimadzu UV-vis spectrophotometer (made in Japan) attached with a thermostatic water bath to maintain 298.15 ± 0.15 K. Initially, base line correction was done using pH 7 phosphate buffer solution. Comparative spectra of BM in phosphate buffer at pH 7 in presence of different surfactants above critical micelle concentration have been presented in Fig. 4. BM shows absorbance maximum at 280 nm due to amino acid (AA) residues.

2.2.4. Spectrofluorimetry:

Steady state spectrofluorimetry was carried out using a Perkin-Elmer LS 55 (made in USA) spectrofluorometer attached with Peltier facility at 298.15 K with an accuracy of ± 0.02 K with excitation band pass fixed at 14 nm and emission band pass at 4 nm. Measured amount of 2.5 mL solution of BM (concentration is 10 μM) was taken in a quartz cuvette of 1 cm path length and stock surfactant solutions were added with a Hamilton micro syringe. Maximum emission wavelength of BM was found at 347 nm containing AA acid residues such as tryptophan (Trp), tyrosine (Tyr) and phenylalanine (Phe). Fluorescence intensity vs. wavelength (nm) of BM in presence of various surfactants were presented in Fig. 5.

Time resolved fluorescence experiments have been performed by means of Horiba-Jobin-Yvon Fluoro Cube lifetime arrangement using time-correlated single photon counting (TCSPC) technique at 298.15 K. A Nano LED (IBH, UK) of 280 nm was used as

excitation source of BM. Emission of BM was monitored at 347 nm using TBX photon detection module. Decay profiles were fitted and analysed with the support of IBH DAS-6 software by nonlinear least square iterative method to minimize residual values (χ^2 values close to 1). The experimental procedure was same as those stated in steady state method. Lamp profile was collected using micellar aqueous solution of SDS, which is used as a scatter in place of sample. Average lifetime (τ_{av}) was calculated from the bi exponential iterative fitting of BM in presence and absence of surfactants used in this present study with the help of the pre-exponential factors (a_1, a_2) and decay times (τ_{av}) with the assistance of following equation:

$$\tau_{av} = a_1\tau_1 + a_2\tau_2 \quad (1)$$

The values of a_1, a_2 and τ_1, τ_2 and τ_{av} of BM as a function of surfactant concentration for different surfactants have been presented in Table 4.

2.2.5. Circular Dichroism:

All the Circular Dichroism (CD) spectra were recorded on a Jasco model J-1500 spectrophotometer at 298.15 K. The final spectra of BM (5 μ M in phosphate buffer of pH 7) in absence of surfactants and with the variation of concentration of individual surfactant were obtained by averaging at least three consecutive scans. Baseline was corrected by subtracting the spectrum of the buffer (pH 7) from individual BM spectrum. CD spectra of BM were recorded in both far UV regions (total scanning range from 190 to 300 nm) in presence and absence of surfactants.

2.2.6. Docking Studies:

The crystal structure of BM was obtained from protein data bank (PDB ID: 1W0Q; cf. scheme. 1b) and the associated molecules were removed prior to the docking. The three-dimensional structures of SDBS, SDDS, NaC and NaDC were drawn in Avogadro software⁷² and optimized further to obtain the energy minimized structure. All the docking studies between Bromelain and the ligands (surfactants) were carried out using Auto Dock Vina software with centre at $x = -0.536$; $y = 2.928$; $z = 0.083$ and grid size of $54 \times 48 \times 48 \text{ \AA}$ ⁷⁴. The structure with the most the minimum energy value was selected and analysed using UCSF Chimera software⁷⁵.

2.2.7. Accessible surface area (ASA) calculations

The accessible surface area of a protein residue is a measure of the amount of solvent exposure of the residue when the protein is not bound with any molecules. Residues with high ASA are

generally found to lie on the surface of the protein whereas those lying within the core of the protein have low ASA values. When a ligand interacts with the protein, it attaches itself with certain amino acid residues (either through hydrophilic or hydrophobic interaction) thereby reducing the solvent exposure of those residues. Thus, by measuring the change in the accessible surface area (ΔASA) of the residues of the protein, it can be predicted which residues are most prone to interact with the ligand and the ligand binding region of the protein. The accessible surface area (ASA) of BM residues before and after docking with the ligands were obtained using NACCESS software and the change in the surface area values were calculated according to the equation, $\Delta ASA_i = ASA_{\text{free BM}} - ASA_{\text{BM+ligand}(i)}$, where $i = i^{\text{th}}$ ligand.

3. Result and discussions:

3.1. Interfacial and bulk property of surfactants in presence and absence of BM

BM show some surface activity at phosphate buffer of pH 7. (cf. Fig. 2). The study of surface tension of surfactants in phosphate buffer gives a break point which is the normal characteristics of surfactants after a certain concentration, called critical micelle concentration (cmc) (shown in Fig. 1). When surfactants added to BM solution (20 μM), the different break points were shown for surfactants in tensiometry profile (cf. Fig. 1) and these break points have been designated here as C_1 , C_2 and C_3 , from low to high surfactant concentrations respectively. C_3 corresponds to free micelles of surfactants having similarity with cmc both in presence and absence of BM. The first point (C_1) corresponds to the minimum (or the trough) and the second (C_2) indicated the maximum binding of the induced small surfactant micelles (or the crest) leading to unfolding of the native state of BM¹⁶. This binding interaction may be due to electrostatic and hydrophobic reason.³ It is seen from Fig. 1a (NaC) and 1b (NaDC) that, γ values for these two surfactants in presence of BM found well below as compare their BM free counterpart; tend to merge around cmc/C_3 ; after cmc/C_3 both profiles match to each other. In case of SDDS (Fig. 1c) and SDBS (Fig. 1d), γ values in presence of BM shows lower at initial surfactant concentration and the values match to the free BM profiles after C_1 . Initial depression of γ values clearly indicating the surface-active nature of stem bromelain and surface activity retains in presence of NaC and NaDC (Fig. 1a and b) upto cmc confirms the presence of surface-active surfactant – BM complex, while for NaC and NaDC, the depletion of surface-active species (BM-surfactant) from air/water surface to bulk at C_1 , result to produce similarity between the BM free and BM containing profiles (Fig. 1c and 1d). All the typical points originating from the interaction of BM with surfactants are displayed in Fig. 2. In presence of

NaC all three break points (C_1 , C_2 and C_3) have been found in tensiometry profile, but for SDDS and SDBS only C_1 and C_3 were found in tensiometry (Fig. 1c and 1d). NaDC shows only one inflection point (C_3) in tensiometry profile indicating formation of free micelle. All the values of C_1 , C_2 , cmc / C_3 are presented in Table 1. Although similar inflection points have been reported previously¹⁶ using tensiometry measurement, here the final break points (C_3) for all protein surfactant systems (see Table 1) cannot be termed as ‘extended cmc’, as the value of C_3 is found somewhat lesser than cmc for all surfactants. So, BM acts as an enhancer to reduce cmc of surfactants at this experimental condition and formed micelles incorporated with BM. Similar observation have been reported while studying trypsin in presence of bile salts⁴⁵.

From tensiometric isotherms (cf. Fig. 1), the efficiency of surface adsorption of surfactant monomers (NaC, NaDC, SDDS and SDBS) has been measured at cmc or C_3 in terms of surface excess ($\Gamma_{C_3}/\Gamma_{cmc}$) in presence and absence of BM using Gibbs adsorption equation:

$$\Gamma_{cmc} = \frac{1}{2.303nRT} \lim_{C \rightarrow cmc(C_3)} \frac{d\gamma}{d \log C} \text{ mol.m}^{-2} \quad (2)$$

here, n is the number of species dissociated per monomer of surfactants adsorbing at the air-solution/buffer interface. The value of n is 2 for both the surfactants. R is the universal gas constant and T is the temperature in Kelvin scale. The slope at cmc/ C_3 ($d\gamma/d \log C$) was determined from the tensiograms (cf. Fig. 1) by taking γ with corresponding $\log[\text{surfactant}]$ values upto cmc/ C_3 and fitted the values with second order polynomials of fairly good R^2 (0.99) values. It is seen from Table 2 that, Γ_{cmc} values of BM-surfactant system are relatively lesser than free surfactants (for NaC, NaDC) in pH-7 buffer medium, while, the reverse has been seen in case of SDDS and SDBS with same concentration of BM comparing with the micellization of SDDS and SDBS in phosphate buffer (pH 7).

Minimum area of surfactant monomers (A_{min}) at air-water interface can be obtained using the following equation:

$$A_{min} = \frac{10^{18}}{N_a \Gamma_{cmc}} nm^2 / \text{molecule} \quad (3)$$

A_{min} has the reverse order with Γ_{cmc} , as the minimum surface area of surfactants on the surface increases; decrease in surface coverage is possible in terms of decrease in Γ_{cmc} and also vice versa.

The surface pressure at the cmc (π_{cmc}) was calculated using the following equation

$$\pi_{cmc} = \gamma_0 - \gamma_{cmc} \quad (4)$$

where γ_0 and γ_{cmc} are the surface tension of surfactant in phosphate buffer at pH 7 and that for the surfactant in presence of buffer of pH 7 at the cmc respectively. This parameter indicates the measurement for the effectiveness of the surfactant to lower the surface tension of the solution medium (free buffer and free buffer in presence of BM). It is seen in Fig. 1 that π_{cmc} values of surfactants in presence of BM found lower than the BM free surfactants in aqueous phosphate buffer medium.

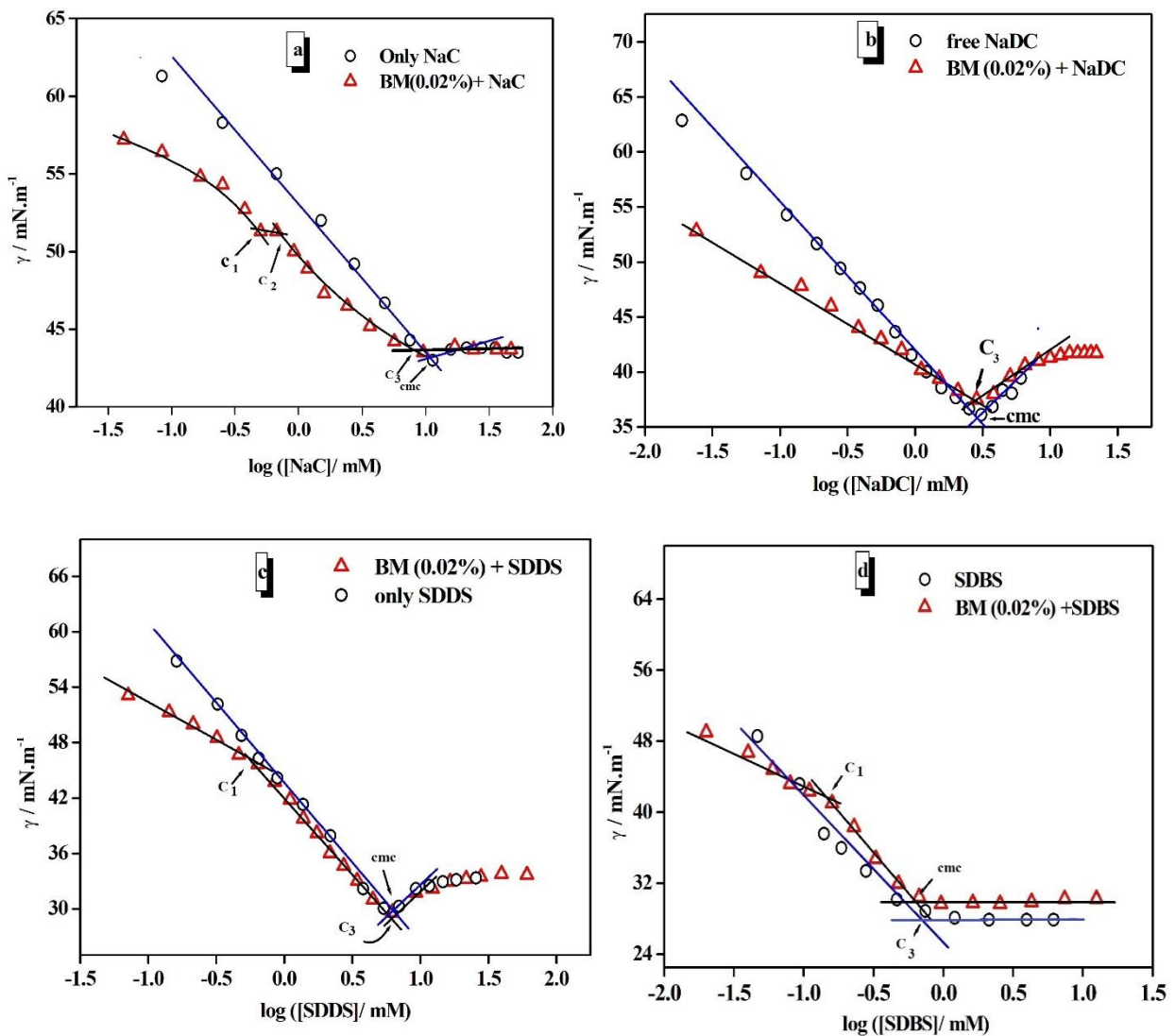


Fig. 1. Surface tension profiles (γ vs. \log [surfactant]) of NaC (a), NaDC (b), SDDS (c) and SDBS (d) at 298.15 K

Table 1. Critical concentrations (C_1 , C_2 and cmc or C_3) of surfactants, surface excess at cmc or C_3 (Γ_{cmc} or, Γ_{C_3}), surface pressure at cmc (π_{cmc}), area minimum (A_{min}) in presence and absence of BM in phosphate buffer of pH 7.0. BM concentration were fixed at 20 μM ^a

Systems	C_1	C_2	cmc/ C_3	$10^3\pi_{cmc}$ (J.m^{-2})	$10^6\Gamma_{cmc}/$ $10^6\Gamma_{C_3}$ (mol.m^{-2})	A_{min} ($\text{nm}^2.\text{molecule}^{-1}$)
NaC			11.3	21.3	1.02	1.63
BM + NaC	0.47	0.72	9.53	15.8	0.67	2.47
NaDC			3.09	31.1	1.34	1.23
BM + NaDC			2.82	18.8	0.73	2.26
SDDS			6.95	39.9	1.46	1.13
BM + SDDS	0.59		6.19	29.5	1.81	0.98
SDBS			0.82	42.1	0.69	2.56
BM + SDBS	0.15		0.77	29.7	1.71	0.97

^a Errors in $C_1 = \pm 3\%$, $C_2 = \pm 3\%$ and cmc/ $C_3 = \pm 5\%$ respectively.

3.2. Isothermal titration calorimetry:

A heat change (standard enthalpy of micellization of surfactant monomers, ΔH^0_{obs}) along with the conformational change of bromelain in presence of monomers has been analysed using ITC measurements. ITC profiles (heat injection (ΔH^0_{dil}) in kJ.mol^{-1} vs. [surfactant] in mM) of pure surfactants in presence and absence of BM in phosphate buffer of pH = 7 have been reported in Figure 2. ITC profiles of surfactants near the vicinity of cmc (pure surfactant in phosphate buffer of pH 7) or C_3 (surfactants in presence of BM in phosphate buffer pH 7) show sigmoid nature and therefore were fitted by Boltzmann-sigmoidal equation⁷⁶ and the corresponding cmc/ C_3 has been selected from the inflection of the sigmoidal fittings. The same procedure has been presented in previous literature¹². Standard enthalpy of micellization (ΔH^0_{obs}) of pure surfactants in presence and absence of BM has been calculated by simply taking the subtraction between ΔH^0_{final} to $\Delta H^0_{initial}$ ($\Delta H^0_{obs} = \Delta H^0_{final} - \Delta H^0_{initial}$), which are the enthalpy changes at two extremes of sigmoidal profiles (see Fig. 2). The straight lines were drawn (see in Fig. 2) through the transition region (cmc or C_3) in the enthalpograms met the pre- and post- cmc / C_3 dilution enthalpy designated by horizontal lines. The vertical distance was considered as the

enthalpy for the micellization process (ΔH^0_{obs} , given in Table 2)¹². Apart from NaC, all endothermic enthalpy changes have been observed (documented in Table 2). It is seen that for NaDC, SDDS and SDBS, the ΔH^0_{obs} values were found more positive in presence of bromelain than their pure states in phosphate buffer at 298.15 K. Exception has been found in the interaction of NaC in presence of BM where exothermic heat change has been observed ($\Delta H^0_{\text{obs}} = -0.11 \text{ kJ.mol}^{-1}$), although NaC in absence of BM shows the positive contribution of enthalpy change during micellization. Enthalpy change during micellization of pure NaC, NaDC, SDDS and SDBS in aqueous solution at 298.15 K has been documented in previous literatures.^{77, 56, 78} It is seen that, for NaC and NaDC, the experimental values of ΔH^0_{obs} in phosphate buffer (pH = 7) medium were found lower than the values in aqueous solution⁷⁷ at 298.15K, but both values are endothermic; whereas for SDDS, the enthalpy change of micellization (ΔH^0_{obs}) is found more or less similar at 298.15 K with same sign⁵⁶ in both aqueous and phosphate buffer (pH-7) medium. In case of SDBS, little endothermic heat change was observed in presence of phosphate buffer at pH 7, while exothermic heat change (-1.0 kJ.mol^{-1}) was observed previously.⁷⁸ Thus, it is obvious that, salinity as well as different nature and charge of surfactant monomers influence enthalpy of micellization by changing the ionic strength of the aqueous solution. Different break points (C_1 and C_2) at low and intermediated surfactant concentration apart from C_3 in presence of BM in enthalpogram profiles of NaC and SDBS (Fig. 2a and 2d) were found and the values of C_1 and C_2 (Table 2) have similarity with those calculated by tensiometry measurements. It is also seen that C_3 values of surfactants were found lower than the corresponding cmc of pure surfactants in absence of BM calculated by calorimetry (Table 2). Cmc/ C_3 values of surfactants in phosphate buffer medium in absence and presence of bromelain were found in fair agreement with those calculated by tensiometry (comparing Table 1 and 2).

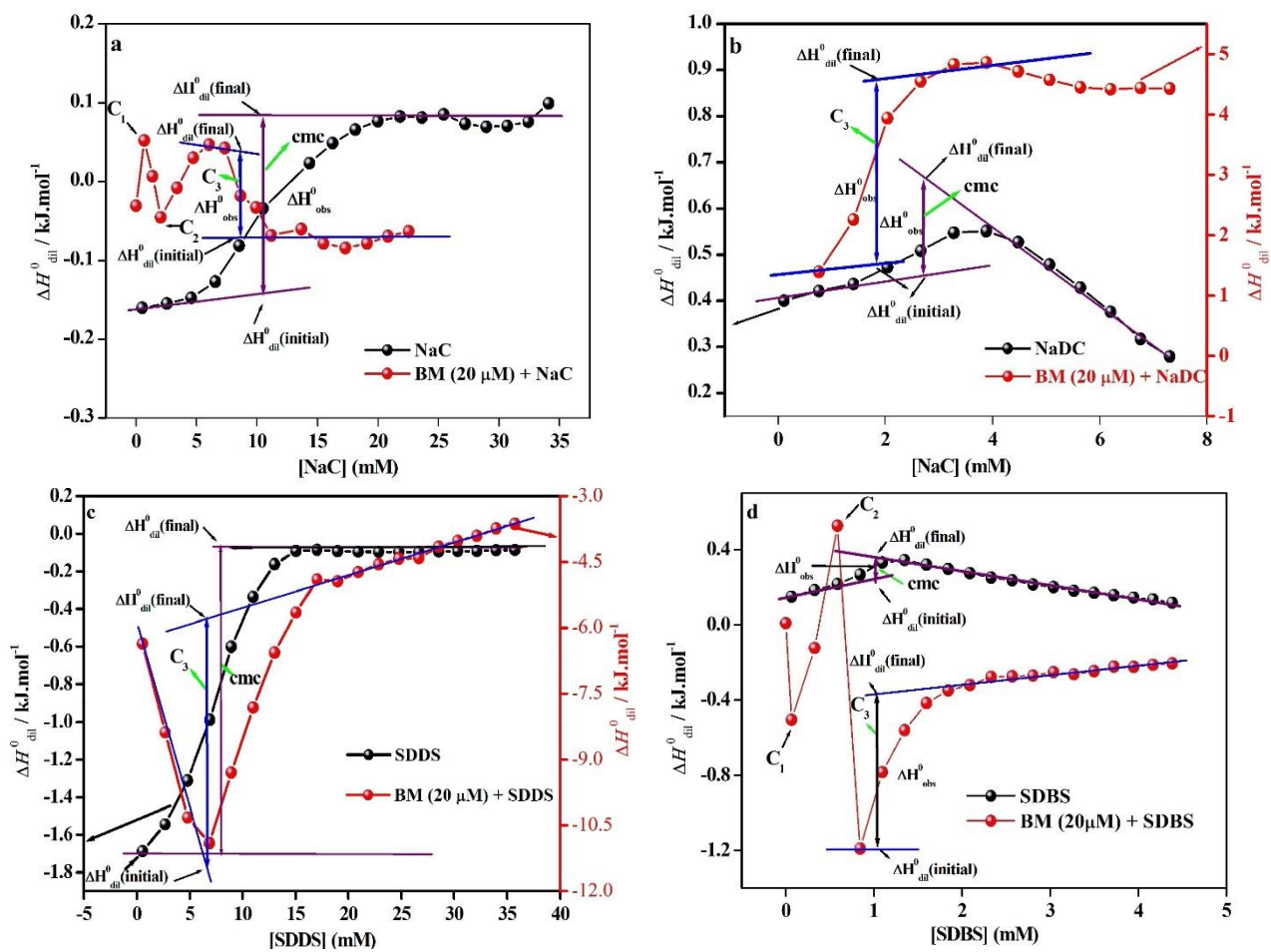


Fig. 2. Calorimetric titration curves of surfactants in Phosphate buffer (pH 7) in presence and absence of BM (20 μ M); surfactants are shown in different diagrams along with their interaction with BM: (a)NaC, (b)NaDC, (c) SDDS& (d)SDBS

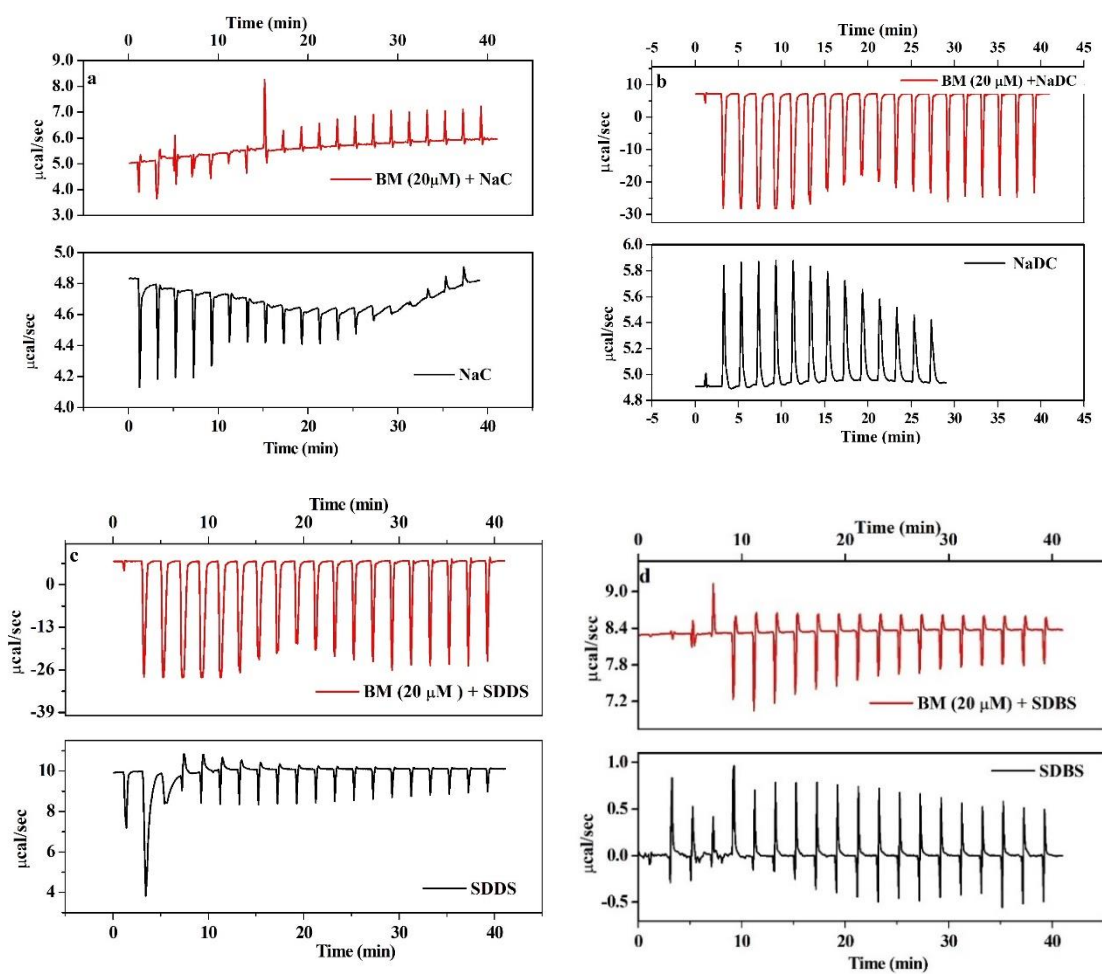


Fig. 3. Raw data (calorimetric traces) of ITC for different surfactants in presence and absence of different surfactants (a. NaC, b. NaDC, c. SDDS and d. SDBS). For each diagram (top compartment: calorimetric traces of surfactant in presence of BM, bottom compartment: calorimetric traces of surfactants in pH 7 aqueous phosphate buffer)

Table 2. Table for assessment of critical parameters (C_1 , C_2 and cmc/C_3) and enthalpy of micellization (ΔH^0_{obs}) of surfactants in presence and absence of BM in phosphate buffer (BM concentration was fixed at 20 μM) at pH 7 at 298.15 K^a.

Systems	C_1 mM	C_2 mM	C_3/ cmc mM	ΔH^0_{obs} kJ.mol ⁻¹
NaC			11.95	0.23
BM + NaC	0.55	2.04	8.58	-0.11
NaDC			2.52	0.21
BM + NaDC			1.83	3.05
SDDS			7.96	1.62
BM + SDDS			6.65	5.68
SDBS		-	1.02	0.11
BM + SDBS	0.048	0.60	1.00	0.82

^aErrors for the calculation of $\Delta H^0_{obs} = \pm 2\%$

3.3.UV-VIS absorbance and fluorescence study

3.3.1. Steady state absorption and emission studies at 298.15 K:

The interaction between the surfactants with biomolecular system could be well understood by the spectroscopic technique, viz., steady state absorption and emission studies at 298.15 K. The absorption spectra of stem bromelain (BM) (10 μM) and BM in presence of the varying concentrations of two bile salts, namely, NaC and NaDC and two surfactants, namely SDDS and SDBS were recorded in aqueous phosphate buffer of pH 7 at 298.15 K (**Fig.4**) A characteristic peak at around 280 nm is observed in each case which signifies the involvement of the Trp or Tyr residues in all the interactions. Also, it is observed that in each case, the intensity of the peak at around 280 nm increases with the gradual addition of surfactants (Fig not shown). A representative figure (**Fig. 4**) comprising absorption spectra of free BM and BM in presence of saturating concentration of bile salts and the surfactants respectively with the slight shift of the absorption maxima in all the BM-surfactant complexes. This could be proposed that step by step alteration in the microenvironment occurs due to the interaction of BM with the bile salts and the surfactants. For SDBS, however, the absorption pattern is

different indicating the perturbation of the microenvironment which is more sensitive in case of SDBS-bromelain interaction. Also, the C_3 is observed in each case due to the formation of free micelles and this proposition is also justified with the steady state fluorescence studies at 298.15 K (the break points are shown in F vs [surfactant] plots at the inset of Fig. 5) The values of C_3 which have been found by steady state fluorescence techniques for different surfactants in presence of BM show good similarity with those calculated by other techniques (tensiometry, ITC). Apart from C_3 , we also found the other break points in F vs [surfactant] plots for NaC, SDDS and SDBS and the corresponding [surfactant] are found close to the value of C_1 .

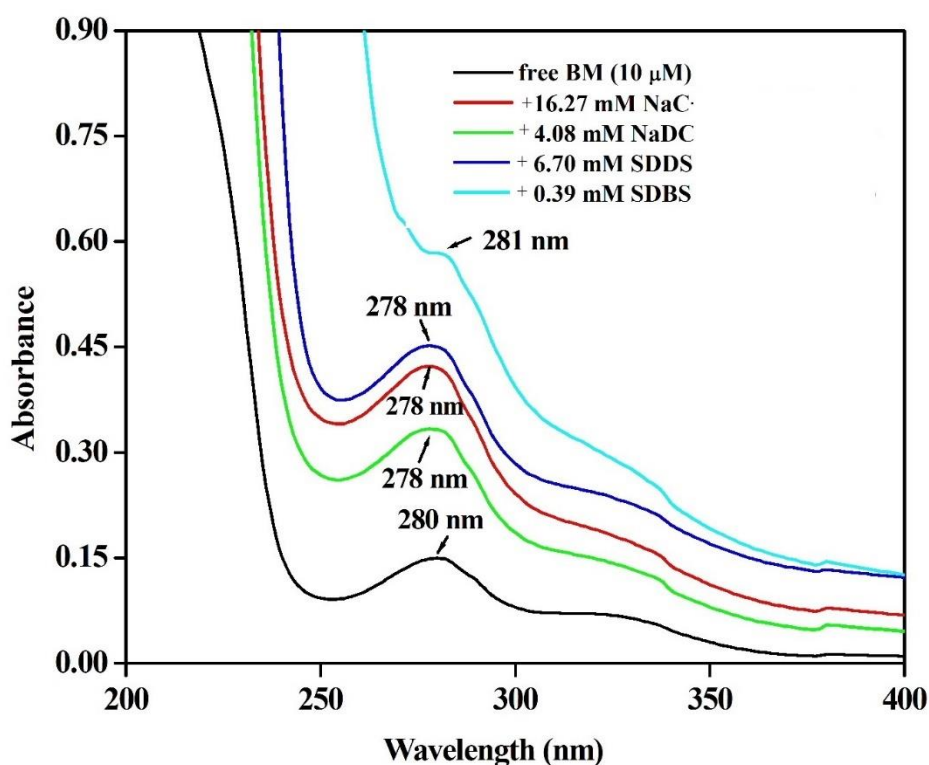


Fig. 4. Absorbance spectra of BM in free state and in presence of four different surfactants in buffer solution (pH 7) at 298.15 K

The steady state fluorescence spectra of bromelain in presence of two conventional surfactants and two bile salts have been carried out at 298.15 K (**Fig. 5**) monitoring the intrinsic fluorescence of Trp residue(s). Tyrosine (Tyr) and Phenylalanine (Phe) are also known as the natural fluorophore in proteins. Owing to a larger difference in quantum yield, lifetime and energy transfer from Phe to Tyr and Tyr to Trp for the fluorescence, only Trp molecule is responsible for fluorescence.⁷⁹⁻⁸⁴

Our present study on Bromelain is concerned on the interaction of the surfactants and bile salts in presence of five Trp residues (Trp 8, Trp 27, Trp 67, Trp 176 and Trp 180) in Bromelain. Interestingly, the environmental features of the Bromelain help one to find out the differential behaviour of emission of Bromelain in presence of different surfactants and bile salts. The widespread sequence homology of papain suggests that two Trp residues are located near the surface of the molecule and three tryptophans are buried in hydrophobic core of the molecule.^{62, 85, 86} The exposure of the buried residues to the protein surface leads to unfolding of the protein.

Steady state fluorescence spectra of intrinsic Trp residue(s) in free stem Bromelain (10 μ M) at 298.15 K show that λ_{max} of the emission at \sim 347 nm on excitation at 290 nm clearly matches with the earlier literature data.^{62,87} This emission maximum of free Bromelain molecule indicates that the emitting Trp residues(s) are in solvent exposed environment as the solvent exposed Trp residue(s) generally appears around 347 - 350 nm. Our focus is to study the interaction of Bromelain with two bile salts, viz. NaC and NaDC by the fluorescence spectra at 298.15 K shows the appreciable decrement of Trp emission with gradual addition of varying concentrations of both the bile salts, NaC and NaDC (Fig. 5) at 298.15 K in aqueous phosphate buffer of pH 7 at $\lambda_{\text{exc}}=290$ nm. The λ_{max} value of the emitting Trp residue(s) gradually shifted towards from 347 nm (free Bromelain) to 340 nm (for NaC) and 339 nm (for NaDC) (Fig. 5) clearly indicates the change of microenvironment of Trp residue(s) due to the interaction of NaC and NaDC. The blue shifted emissions of Trp residue(s) in both the cases specifically suggest that the less polar or more hydrophobic environment of Trp residue(s) experience after the interaction with the bile salt molecules.

The interaction of Bromelain with the two surfactants SDDS and SDBS has been also performed to visualize the alteration of the microenvironment of the Trp residue(s) in presence of two surfactants SDDS and SDBS and also compared to that with the bile salts NaC and NaDC respectively.

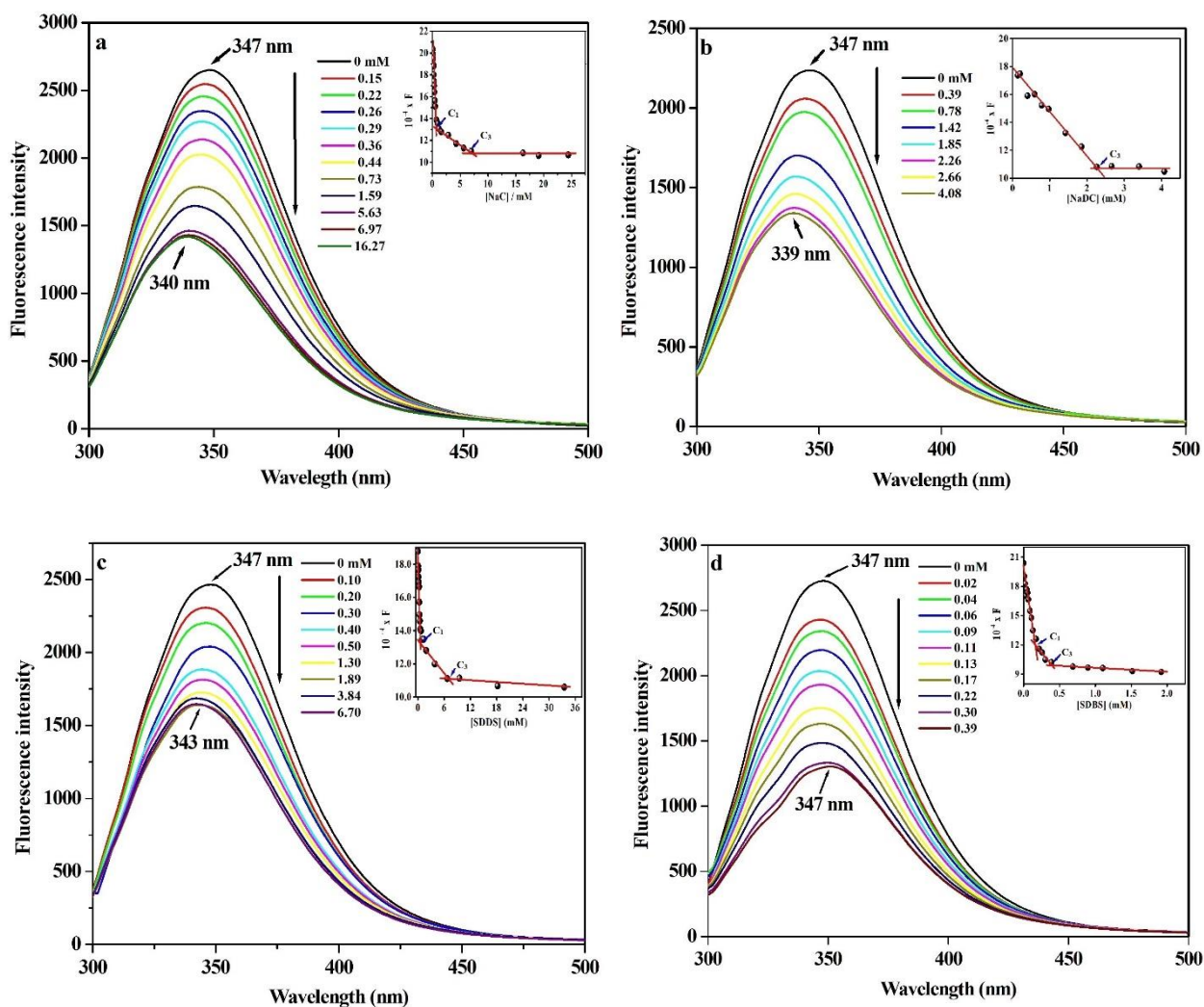


Fig. 5. Steady state fluorescence spectra of BM in presence of different surfactants (a: NaC, b: NaDC, c: SDDS and d: SDBS) at 298.15 K. Excitation wavelength = 280 nm; excitation and emission band pass = 10 and 5 nm, respectively, for each case. Inset: fluorescence area under the curve ($10^{-4} \times F$) vs. [surfactant] predicting different break points.

The gradual addition of two surfactants, SDDS and SDBS to the free stem bromelain (10 μ M) is responsible for quenching of the Trp fluorescence at 298.15 K in both the cases with excitation at 290 nm. (Fig. 5) In both the cases, the fluorescence quenching clearly imposes on the fact that SDDS and SDBS also interact appreciably with the Trp residue(s) of the Bromelain molecule. The λ_{max} of the emission of Trp residues in Bromelain is blue shifted to 343 nm for SDDS molecules inferring that the emitting Trp residue(s) of Bromelain molecule is blue shifted indicating somewhat the alteration of the microenvironment occurring in presence of SDDS molecule.(Fig. 5) Conversely, no peak shift is observed for the interaction of bromelain

with the SDBS molecule indicating no such change in the surrounding environment of emitting Trp residue(s) happening while interaction with the SDBS molecule. (Fig. 5)

The comparative nature of the interactions of stem bromelain with the bile salts and surfactants helps one to reach to the fact that the Trp residue(s) move towards more buried or hydrophobic region in case of bile salts as compared to that with the surfactant SDDS. The further time resolved fluorescence studies and docking studies corroborate with this connection (See next section).

The fluorescence quenching of Trp residue(s) of the bromelain molecule by the bile salts and surfactants is generally analysed by the following Stern-Volmer equation (Eq.2) ⁷⁹

$$F_0/F = 1 + K_{SV}[L] = 1 + k_q\tau_0[L] \quad (2)$$

where, F_0 and F are the fluorescence intensities of bromelain in the absence and the presence of the quencher (bile salts and surfactants). K_{SV} is the Stern-Volmer quenching constant, $[L]$ is the concentration of quencher compounds, NaC, NaDC, SDDS and SDBS, k_q is the bimolecular quenching rate constant, and $\langle\tau_0\rangle$ is the average fluorophore lifetime in the F_0 and F in Figure 5 are calculated using the area under the emission curve. The K_{SV} values for the different surfactant systems in conjugation with stem bromelain are summarized in Table 3.

Table 3. Stern- Volmer Quenching Constant (K_{SV}) and Bimolecular Quenching Constant (k_q) of the complex of surfactants and the bile salts with the Bromelain molecule in aqueous buffer (pH 7) at 298.15 K.

Systems (10 μ M BM in phosphate buffer pH 7 + surfactants)	λ_{max} (nm)	K_{SV} (M^{-1})	k_q ($M^{-1}s^{-1}$)	R^2
Free BM (10 μ M)	347	-	-	-
+NaC (16.27 mM)	340	6.00×10^2	1.69×10^{11}	0.975
+NaDC (4.08 mM)	339	1.77×10^2	0.50×10^{11}	0.962
+SDDS (6.70 mM)	343	6.68×10^2	1.89×10^{11}	0.983
+SDBS (0.39 mM)	347	30.35×10^2	8.59×10^{11}	0.954

The fluorescence quenching of bromelain due to binding with bile salts and surfactants could be investigated through static quenching and dynamic quenching processes. The formation of a stable complex between the protein and quencher usually occurs via static quenching process whereas the collisional encounters between the protein and quencher mostly occurs through dynamic quenching process.⁷⁹ The linearity of the Stern-Volmer equation may be ascribed to infer on the operational concept of the static and dynamic quenching process. All the bile salt and surfactant complexes with the bromelain molecule show the linear S-V plot indicating that the emitting Trp residue(s) of the proteins which are prompt to response mainly in the static quenching process over the dynamic quenching process⁷⁹ (Fig. 6 and Table 3). The fluorescence quenching parameters (Table 3) reveal that the fluorescence quenching is not so much significant for NaDC while it is more appreciable for SDBS. The time-resolved fluorescence studies could also be helpful to realize the nature of fluorescence quenching operational in all the complexes. (see next section, 3.3.2)

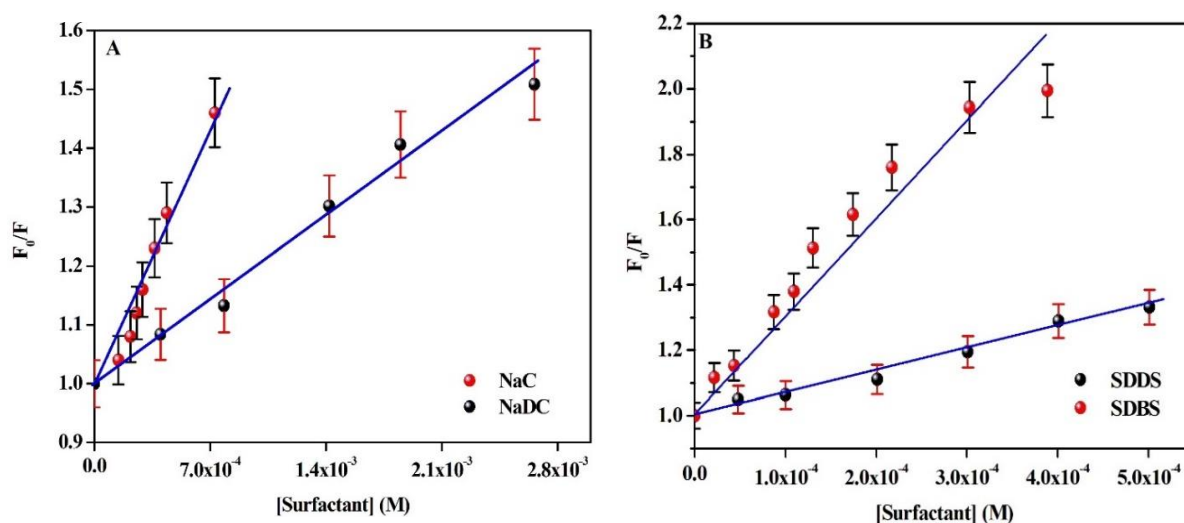


Fig. 6. Stern-Volmer (SV) plots for fluorescence quenching of BM with the different concentrations of (a) bile salts (NaC and NaDC) (b) surfactants (SDDS and SDBS) at 298.15 K. $\lambda_{exc}=280$ nm, [BM]= 10 μ M; Excitation band-pass = 10 nm and Emission band-pass = 5 nm.

3.3.2. Time-Resolved Fluorescence Studies at 298.15 K:

To understand the nature of the observed quenching of the fluorescence, the lifetime measurement by time-resolved fluorescence decay technique monitoring the emission maxima of Trp emission was performed at 298 K. The relevant lifetime data for all the complexes of

bromelain with the bile salt and surfactants are provided in Table 4., and Fig. 7 represents one representative decay profile of free BM and BM with varying concentrations of NaC in aqueous buffer of pH 7 at 298.15 K. Free protein shows biexponential decay with good χ^2 values in aqueous phosphate buffer of pH 7.

The data collected in Table 4 provide that BM is slightly perturbed with increasing concentration of the bile salts and surfactants. In all the cases, a comparatively constant lifetime values of BM are observed (Figure, Table 4) from the fluorescence decay and clearly implies that the static quenching process is predominant over the dynamic quenching process in all the cases.

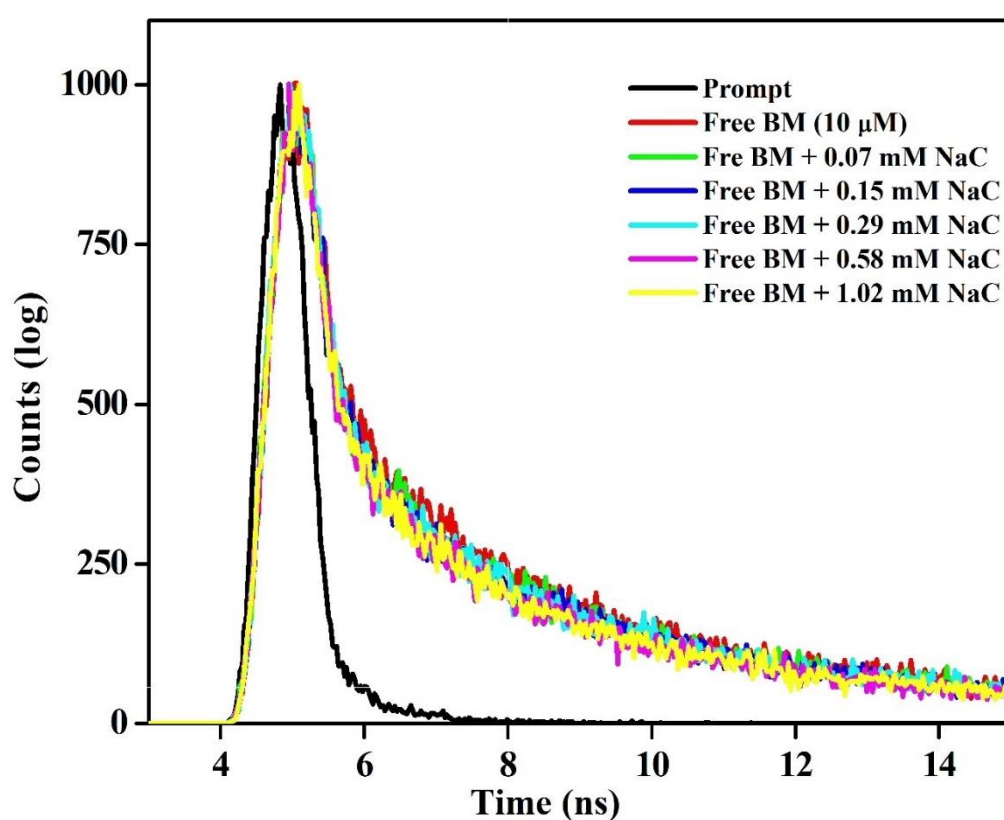


Fig. 7. Representative time resolved fluorescence decay profile of Free BM (10 μM) and its complex with varying concentration of bile salt, NaC in aqueous phosphate buffer (pH 7). $\lambda_{\text{exc}} = 280 \text{ nm}$, $\lambda_{\text{monitor}} = 335 \text{ nm}$. The excitation and emission band passes are 10 nm each.

However, a characteristic observation has been noted for the BM-NaDC complex where the shorter and longer component values of the lifetime along with the respective percent contribution of both the components keeping the average fluorescence lifetime of protein is almost constant (Table 4). The slight variation in both the component and also percent contribution pointed out (Table 4) that the microenvironment of Trp residue of BM near the

binding site of NaDC is perturbed to a greater extent as compared to that of other compounds viz., other bile salt and surfactants. This reflected in the fluorescence quenching study of BM-NaDC complex where the lowest K_{SV} as well as k_q value (Table 3) enables one to infer that the contribution of the surrounding environment of NaDC is prompt as compared to that of Trp residue(s) in BM those are responsible for quenching. Docking study also supports to analyse this observable fact.

Table 4. Singlet state lifetime data of BM (10 μ M) and its complexes with bile salts and surfactants in aqueous phosphate buffer (pH 7) at 298 K where $\lambda_{exc} = 280$ nm, $\lambda_{monitored} = 347$ nm.

[Bile salts/ Surfactants] (mM)	τ_1^a (ns)	τ_2^a (ns)	α_1 (%)	α_2 (%)	$\langle\tau\rangle$ (ns)	χ^2
Bromelain-NaC						
0	0.48	4.43	22.88	77.12	3.53	1.01
0.15	0.51	4.61	26.54	73.46	3.52	1.11
0.29	0.45	4.54	25.44	74.56	3.50	1.05
0.58	0.53	4.59	28.21	71.79	3.44	0.99
1.02	0.59	4.49	26.87	73.13	3.44	1.23
1.74	0.55	4.55	28.08	71.92	3.43	1.11
Bromelain-NaDC						
0	0.48	4.43	22.88	77.12	3.53 (= τ_0)	1.14
0.10	0.63	5.22	37.33	62.67	3.50	0.99
0.25	0.56	4.74	29.95	70.05	3.49	0.92
0.59	0.71	5.61	33.98	57.59	3.47	0.93
0.78	0.75	6.77	42.41	47.65	3.54	1.18
0.97	0.72	5.34	41.13	58.87	3.44	1.08
Bromelain-SDDS						
0	0.48	4.43	22.88	77.12	3.53 (= τ_0)	1.14
0.50	0.42	4.44	20.75	79.25	3.61	1.14
1.00	0.49	4.24	20.41	79.59	3.47	1.06
1.49	0.48	4.17	19.77	80.23	3.44	1.03
2.97	0.47	4.35	21.86	78.14	3.50	1.18
5.38	0.48	4.54	24.14	75.86	3.56	1.22
Bromelain-SDBS						
0	0.48	4.43	22.88	77.12	3.53 (= τ_0)	1.14
0.02	0.48	4.40	22.82	77.18	3.51	1.10
0.11	0.43	4.23	21.32	78.68	3.42	1.21
0.15	0.45	4.55	22.74	77.26	3.62	1.04
0.22	0.41	4.39	21.86	78.14	3.52	1.19
0.30	0.49	4.27	17.55	82.45	3.61	1.15

^a Error in the measurements is ± 0.1 ns.

3.3.3. Binding Data from Fluorescence Spectra:

The binding interaction between bromelain with the bile salts and the surfactants are quantitatively analysed by evaluating the binding constants (K_b) and the associated free-energy change (ΔG_b^0) for the interaction processes (Table 5) by the following Eqs.^{79, 88}

$$\log [(F_0 - F)/F] = \log K_b + n \log [Q] \quad (3)$$

$$\Delta G_b^0 = -RT \ln K_b \quad (4)$$

where F_0 and F represent the corrected fluorescence intensities of bromelain in absence and presence of quencher (bile salts and surfactants) molecule, respectively, T is the temperature in Kelvin scale, R is the universal gas constant, K_b is the binding constant of all of the complexes of bromelain, n is the number of binding sites, F_0 and F in all of the cases of Fig. 8 are calculated considering the area under the emission curve of the corrected fluorescence spectra. The double-logarithmic plots of $\log [(F_0 - F)/F]$ versus $\log [Q]$ of the complexes of bromelain with bile salts and surfactants are presented in Fig 8. The values of K_b and n along with the correlation coefficients (R^2) are listed in Table 5.

Several reports of the fluorescence quenching technique (using Eq. 3) are utilised for the determination of binding parameters^{79, 88, 89} and the quantitative determination of K_b and ΔG_b^0 by the equation (Eq. 3 and 4) depicts the equilibrium between free and bound units when they bind independently to a set of equivalent sites in a macromolecule.

Table 5. Binding Parameters of Bromelain (BM)- Surfactants at 298.15 K.

Systems (10 μ M BM in aqueous phosphate buffer at pH 7 + surfactants)	K_b (M^{-1})	R^2	N	ΔG_b^0 ($kJ.mol^{-1}$)
NaC	64.4×10^2	0.982	1.60	-21.7
NaDC	1.29×10^2	0.995	0.94	-12.1
SDDS	2.18×10^2	0.976	0.86	-13.3
SDBS	7.34×10^{-2}	0.981	0.82	-16.4

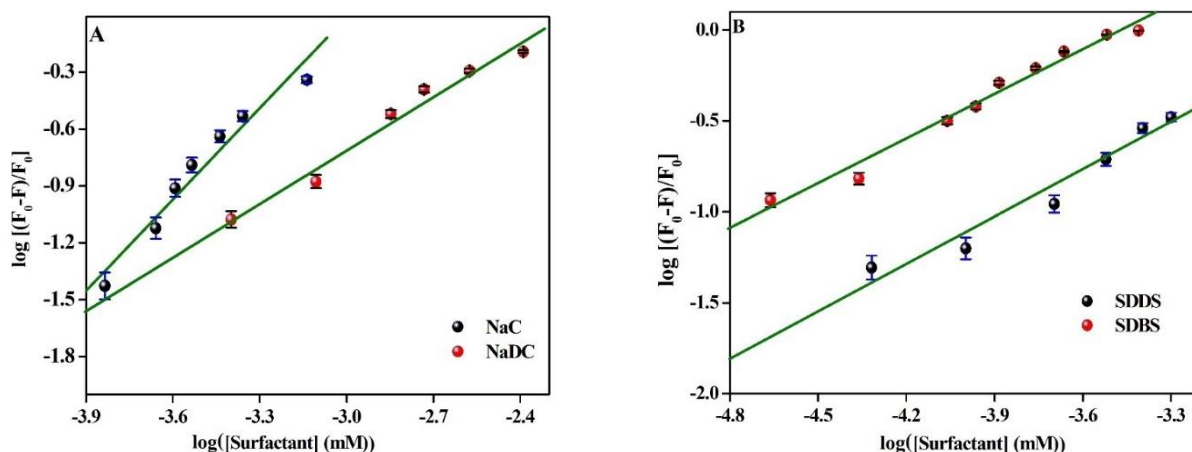


Fig. 8. Representative double logarithmic plot of $\log [(F_0-F)/F]$ vs. $\log [\text{Surfactant}]$ of BM with the different bile salts/surfactant concentration (A) NaC and NaDC, (B) SDDS and SDBS at 298.15 K where $\lambda_{\text{exc}} = 280 \text{ nm}$, $[\text{BM}] = 10 \mu\text{M}$; Excitation band pass = 10 nm and Emission band pass = 5 nm.

3.4. Circular Dichroism study:

Secondary structure of native BM shows two characteristic absorption band in far UV CD spectra, one at 208 nm (sharp band) and another at 222 nm (shallow band)^{79, 80} (cf. Fig.10, more clearly shown at the inset of Fig. 9a). These types of bands suggest BM lies in the $\alpha+\beta$ class of enzymes. The band at 208 nm stands for π to π^* transitions of the α -helix of native BM, while the band at 222 nm (shallow) is due to π to π^* transition for both α -helix and random coil of the protein. It is seen from Fig. 9 (a) and (b) that, the CD spectra of bromelain in presence of NaC and NaDC show negative ellipticity at all concentration of surfactants. Secondary structure of native BM retains at low and moderate concentration of both NaC and NaDC below their cmc. In presence of NaC, upto 3.46 mM, secondary structure remains intact and also both 208 and 222 nm bands. For NaDC, nearly 1.15 mM, similar observation was noted. This implies that at low surfactant concentration the secondary structure of BM somehow stabilized in comparison with its native state, while near and above cmc of the two surfactants (NaC and NaDC), the band at 208 nm shifts and 222 nm gradually disappears with negative ellipticity (Fig. 9 (a) and (b)). The shifting of 208 nm band with negative ellipticity is ascertained the disruption of secondary structure. It is also seen that the stability of secondary structure of BM is greater in presence of NaC rather NaDC.

The situation is quite different while studying the stability of secondary structure in presence of SDDS and SDBS (Fig. 9 (c) and (d)). Both in presence of SDDS and SDBS at low concentration, secondary structure of BM is stabilized compare with its native form. But after

that, at moderate and very high surfactant concentration (near to cmc or above cmc), the negative ellipticity gradually decreases, shifting of 208 nm peak and finally complete disruption of BM secondary structure. At higher concentrations of SDDS and SDBS, a fundamental modification is observed (Fig. 9 (a) and (d)) where simultaneous various kinds of distorted secondary structures such as 3π -helix, β -turn, and many other disordered structures can be prominently observed instead of α and β structures. Similar kind of observations have been reported in previous literatures.

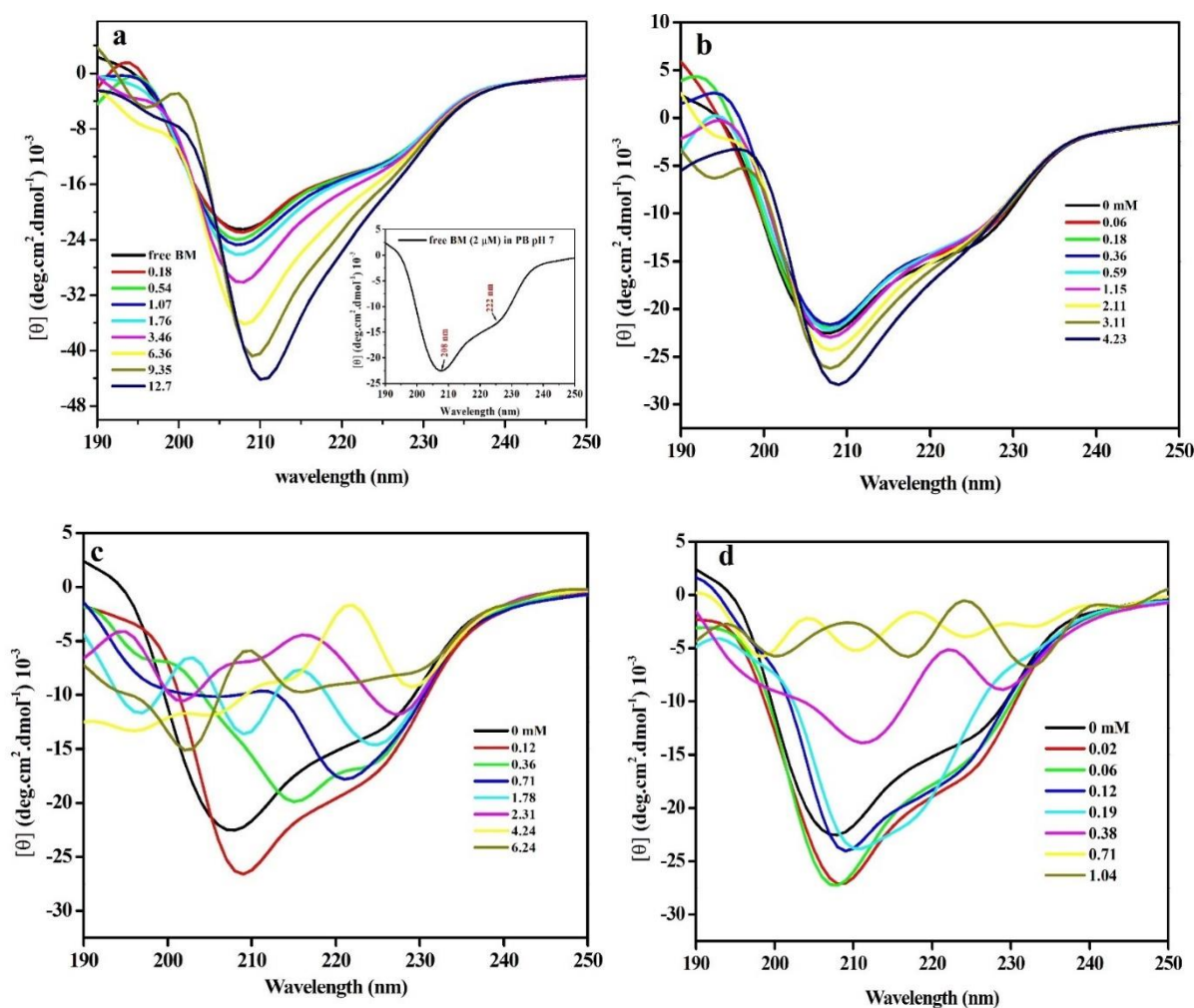


Fig. 9. Far UV- VIS CD-spectra analysis of BM (2 μ M) in phosphate buffer (pH 7) medium with varying concentration of surfactants: (a) NaC, (b) NaDC, (c) SDDS and (d) SDBS. Final concentration of surfactants was chosen nearly 1.5 times of cmc for NaC and NaDC, while for SDDS and SDBS, the final concentrations were chosen up to cmc in buffer medium.

3.5. Molecular Docking Studies:

Molecular docking studies have been employed to demonstrate the experimental data since the docking study aids to visualize the probable location of the compounds (bile salt surfactants and conventional surfactants) in the surrounding microenvironment of the Trp residue(s) of BM with the significant change in the parameters responsible for the molecular docking studies by the interaction between BM and bile salts/surfactants. The docked pose of BM and surfactants are presented in Fig. 10 (panel A) and the binding energy (ΔG) of bile salts/surfactants with BM have been given in Table 6 and out of 5 Trp residues (Trp8, 27, 67,176 and 180), Trp180 has been found to be closest Trp residue to the different atoms of surfactants (Table 6). Distance of tryptophan residue 180 (Trp 180) of BM from the different atoms of bile salts and surfactants obtained from the docked complexes are provided in Table 7 and shown in Fig. 10 (panel B).

Sodium cholate (NaC) and sodium deoxycholate (NaDC) are amphiphilic molecules which constitute an important constituent of the bile salt. The non-polar steroid part constitutes the hydrophobic part of the molecule whereas the carboxylic part forms the hydrophilic portion of the molecule. NaC binds predominantly in cavity 1 of BM but with much negative binding energy (Table 6) indicating highly stable interaction of the bile salt with BM. This is reflected in the binding constant as well as binding energy value of the BM with the surfactants obtained experimentally. Also, the closest distances of different atoms/groups bile salts from Trp 180 in Table 6 reveals that NaC/NaDC situated much closure to Trp 180 as compared to SDDS/SDBS which are reflected also in change in ASA values (Table 8). Nonpolar amino acid residues like Val (14, 17), Ala (30,33), Ile163 and aromatic residues like Phe29 and Tyr185 lies in close (around 3-4 Å) to the steroid moiety of NaC which stabilizes the interaction through hydrophobic interaction (Table 9, Fig. 11). This has been further supported by the significant changes in the ΔASA values (Table 8), which suggest that these residues are shielded upon interaction with the ligand and are less solvent exposed. The other hydrophobic residues like Trp180, Ile186, Ala136 and Phe140 also lie in close proximity (around 3.5 Å) to the aliphatic chain which may also take part in hydrophobic interaction (Table 7 and 9). Although π -stacking interaction is not possible for NaC/NaDC (unlike SDBS) but the higher ΔASA values of the residues (Table 8) may be accounted due to the greater surface area of NaC/NaDC (82.11 Å² / 81.99 Å²) over SDBS/SDDS (32.06 Å² / 42.04 Å²). Greater surface area of the ligand suggests that it would reduce the solvent exposure of the amino acids to a greater extent which also

supports the higher extent of protein ligand binding. In addition, the polar COOH part is can solved with H-bonding with the His158.

The binding energy of NaDC does not vary much as compared to NaC (Table 6), but the overall Δ ASA value is slightly higher for NaC than NaDC (Table 8). This may be due to the additional OH functional group in NaC which lies within a H-bond distance of ~ 4.5 Å from Tyr 185 (Table 9, Fig. 11) thereby reducing the solvent exposure of Tyr somewhat more than that in NaDC. However, the slightly higher stabilization for NaDC may be explained on the basis of hydrophobic interaction with the steroid moiety. Generally, the hydrophobic amino acids prefer to lie in close proximity to the hydrophobic steroid group, but the presence of polar OH group might affect the hydrophobic interaction. Similar situation can be observed for fullerene/fullerenol interaction with RNase A, where the protein ligand interaction is reduced upon addition of OH groups in fullerenol NaC has 3 -OH groups in the steroid part whereas NADC has 2, which makes the interaction more favourable for the former ligand with BM.

Table 6: Distance of tryptophan residue 180 (Trp 180) of BM from the different atoms of bile salts and surfactants obtained from the docked complexes.

Systems (Bile Salts/ Surfactants)	Protein Residue (Trp180)	Atom/ Group of bile salts and surfactants	Distance (Å)	ΔG in (kJ/mole)
NaC	C α -(Trp180)	H (CH ₃ -C21)	4.97	-41.2
	N indole ring-(Trp180)	O- (OOC24)	4.55	
NaDC	C α -(Trp180)	H (CH ₃ -C21)	6.18	-41.6
	N indole ring-(Trp180)	O- (OOC24)	4.33	
SDDS	C α -(Trp180)	O- (COOH)	9.23	-25.2
	N indole ring-(Trp180)	O- (COOH)	8.39	
SDBS	C α -(Trp180)	C4 (Phe ring)	10.96	-30.7
	N indole ring-(Trp180)	C4 (Phe ring)	10.95	

Table.7. Distance of different atoms of bile salts and surfactants and neighbouring different polar and non-polar residues of protein BM within a distance of $\sim 5\text{\AA}$ obtained from the docked complexes.

Systems (Bile Salts/ surfactants)	Atom (Protein Residue)	Atom/ group of bile salts and surfactants	Distance (\AA)
NaC	C α -(Val17)	H (OH-C3)	3.47
	C α -(Lys18)	O (OH-C12)	5.57
	C α -(Phe29)	H (CH3-C19)	4.11
	C α -(Ala33)	H (CH3-C19)	4.09
	C α -(Val160)	H (CH3-C18)	3.96
NaDC	C α -(Val17)	O (OH-C3)	3.47
	C α -(Lys18)	O (OH-C12)	5.40
	C α -(Phe29)	H (CH3-C19)	4.00
	C α -(Ala33)	H (CH3-C19)	4.05
	C α -(Val160)	H (CH3-C18)	4.19
SDDS	C α -(Val17)	N (N-CH3)	6.04
	C α -(Lys18)	N (N-CH3)	5.89
	C α -(Phe29)	O= (CO-N-CH3)	4.28
	C α -(Ala33)	H (C7)	3.66
	C α -(Val160)	N (N-CH3)	5.92
	C α -(Tyr185)	C (C14)	3.98
SDBS	C α -(Val17)	H (C15)	3.04
	C α -(Lys18)	O (SO3)	3.98
	C α -(Phe29)	C1 (Phe ring)	4.44
	C α -(Ala33)	HC1 (Phe ring)	4.28
	C α -(Val160)	H (C5)	3.64
	C α -(Tyr185)	H (C11)	3.26

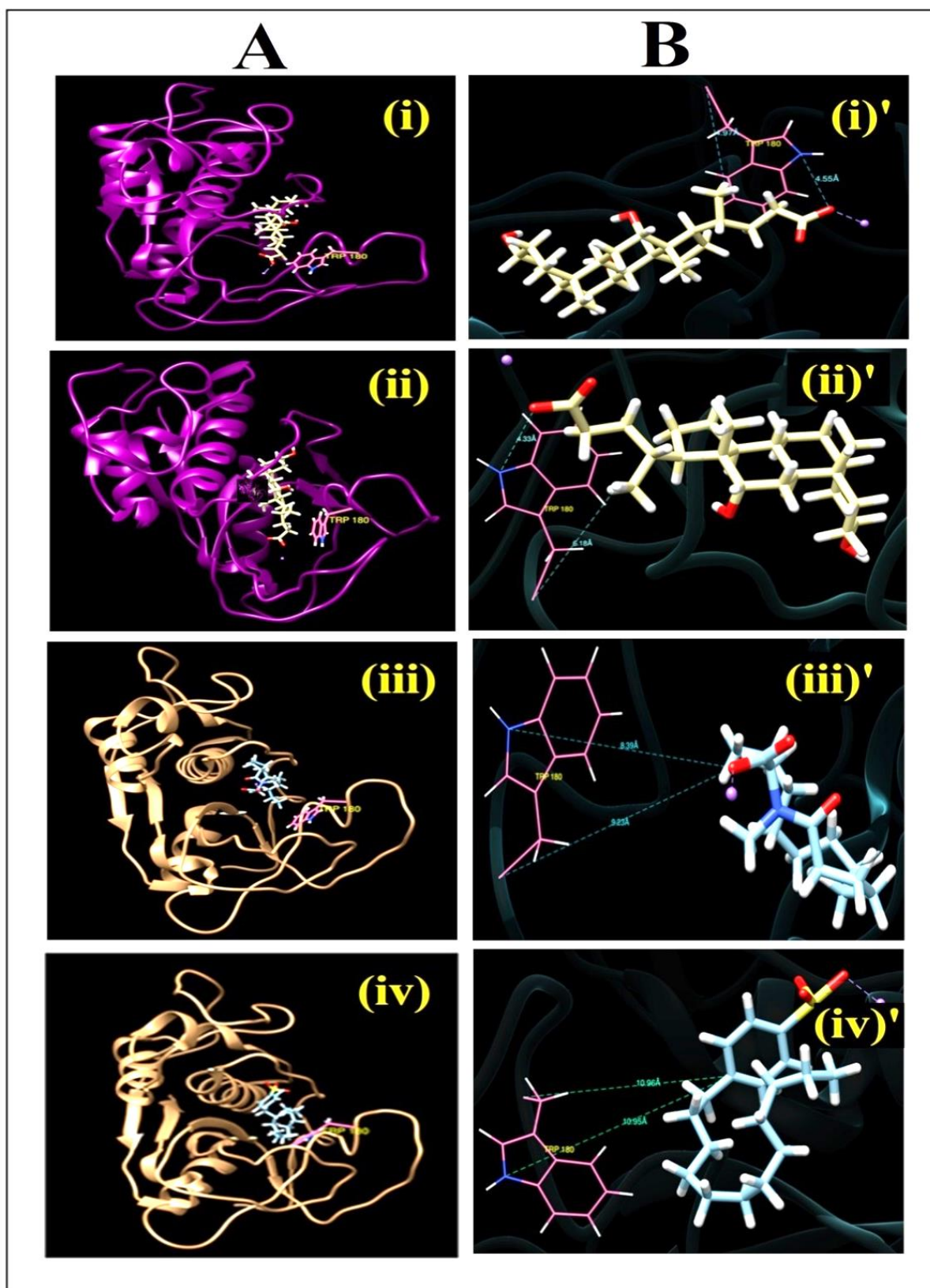


Fig.10. Panel A: Docked pose of the complexes of BM with the bile salts and the surfactants with BM: (i) NaC, (ii) NaDC, (iii) SDDS, (iv) SDBS.

Panel B: Distances (in Å) obtained from docked poses of Trp residue 180 of BM from the different atoms of bile salts and surfactants. (i)' NaC, (ii)' NaDC, (iii)' SDDS, (iv)' SDBS.

Table. 8. The changes in accessible surface area (Δ ASA, \AA^2) of the amino acid residues of docked complexes of BM with bile salt surfactants and conventional surfactants.

Protein Residue	NaC	NADC	SDDS	SDBS
	Δ ASA (\AA^2)	Δ ASA (\AA^2)	Δ ASA (\AA^2)	Δ ASA (\AA^2)
VAL 14	5.04	5.09	6.39	5.38
THR 15	5.59	5.87	9.51	8.54
SER 16	2.70	2.71	2.68	2.68
VAL 17	26.62	26.61	24.45	22.48
LYS 18	21.56	22.41	24.20	22.89
GLN 20	1.20	1.35	6.64	0.67
CYS 26	0.23	0.20	0.92	0.26
PHE 29	21.55	22.04	24.60	27.81
ALA 30	2.56	2.57	2.74	2.74
ILE 32	-	-	0.32	0.32
ALA 33	17.48	17.74	22.67	21.5
GLU 36	-	-	2.41	2.23
GLU 51	-	-	3.40	3.40
ALA 136	8.78	8.46	-	-
PHE 140	8.17	8.17	-	0.28
GLN 141	8.33	8.29	-	-
HIS 158	30.76	29.93	15.21	10.12
ALA 159	2.12	2.06	2.79	2.76
VAL 160	30.70	30.54	19.88	32.91
THR 161	16.55	15.90	16.15	21.8
ILE 163	11.36	11.12	11.65	11.76
TRP 180	40.35	40.93	-	9.69
GLY 184	17.38	17.20	11.42	15.09
TYR 185	17.61	14.48	19.22	21.95
ILE 186	6.19	6.12	1.21	13.12
Total	302.83	299.79	228.46	260.38

Table 9. Hydrogen bonding distances between bile salts and surfactants and different groups of polar and non-polar residues around tryptophan residue(s) of the docked complexes of protein BM with the bile salts and the surfactants

Systems (Bile Salts/ surfactants)	Protein Residue	Atom/ Group of bile salts and surfactants	H-Bond Distance* (Å)
NaC	HO-(Tyr185)	H (OH-C3)	2.8
	NH-amide (Val17)	O (OH-C3)	3.58
NaDC	O=C amide (Thr15)	H (OH-C3)	1.95
	O=C amide (Ser16)	H (OH-C3)	3.19
SDDS	H-N(ϵ) (His158)	O- (COOH)	2.36
	H-N(ϵ) (His158)	O= (COOH)	2.67
SDBS	HO- (Glu36)	O (SO ₃)	3.57
	HO- (Thr15)	O (SO ₃)	3.47
	NH-(Lys18)	O (SO ₃)	3.32
	NH-amide (Lys18)	O (SO ₃)	2.58

*(Strong H-bond: 1-2 Å; Weak: >3.5Å)

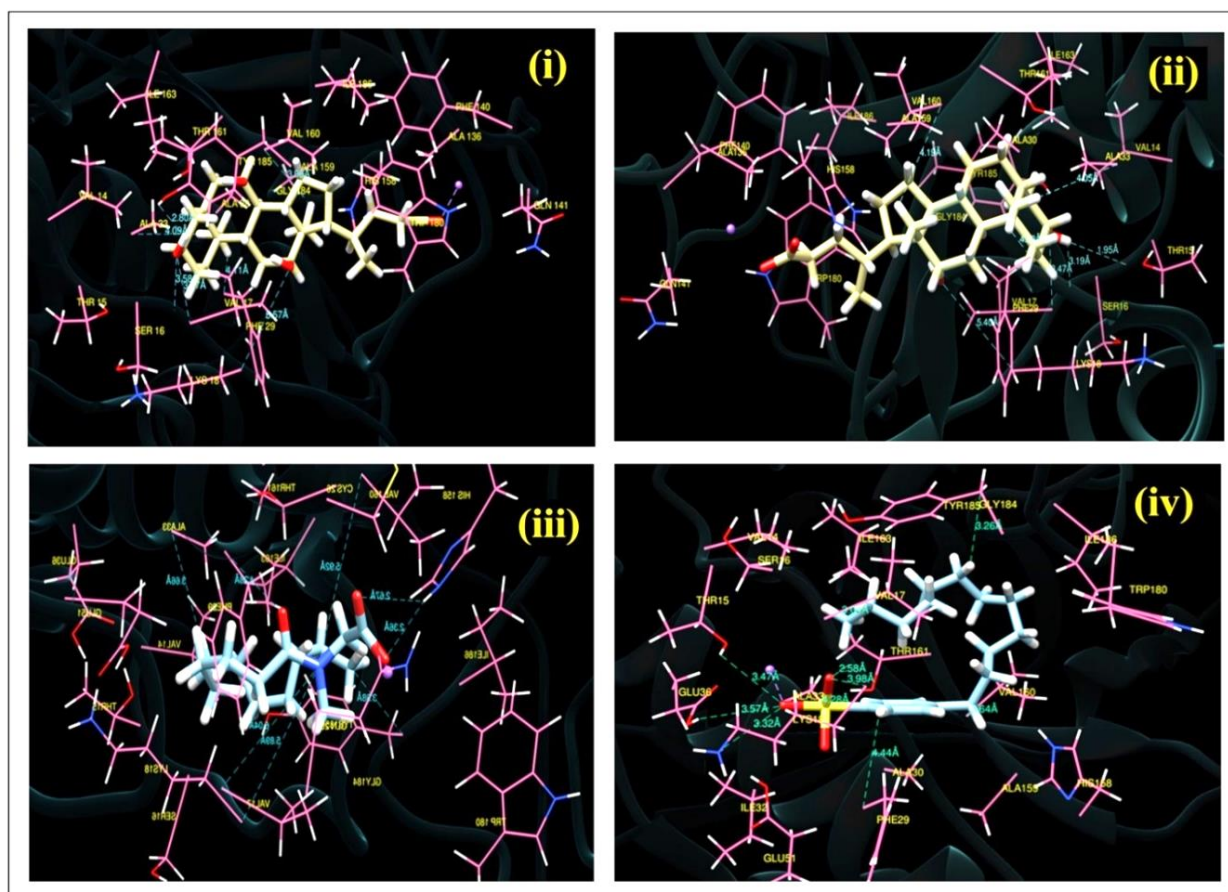


Fig. 11 H-Bonding distances between bile salts and surfactants from the different polar and non-polar residues around tryptophan residue(s) of protein BM of the docked complexes.

SDBS has an aliphatic dodecyl long chain along with a benzene sulfonic moiety which constitutes the hydrophobic part of the molecule. The docked structure of the BM-SDBS shows that the ligand binds to the surface of the protein (Fig. 10, panel A). The docked ligand is placed near the protein in such a way that the hydrophobic amino acid residues like Val14, Val17, Val160, Ile 163, Ile 186 lies at the close proximity near the aliphatic tail within a distance ranging from 1.5 Å (Ile186) to ~3.75 Å (Val17) [Table 7]. In addition, the aromatic amino acid residues like Phe29, Tyr185 and Trp180 is situated with 5 Å distance from the ligand. This suggests that the molecule is stabilized preferentially through hydrophobic interaction between the non-polar amino acid residues. Presence of Phe29 close to the phenyl ring of SDBS highlights the possibility of π -stacking interaction. Accessible surface area calculation (cf. Table 8) clearly shows significant change in surface area (Δ ASA) for the non-polar protein residues which indicates that these residues become less exposed to the solvent upon binding with the ligand. Apart from the above-mentioned residues, Ala30 and Ala33 shows noticeable

changes in surface area and it lies at a distance of ~ 4.5 Å from SDBS. However, it can be seen in Fig. 11 that certain polar residue like Thr15, Ser16, Lys18, Glu36 lies near the sulfonic moiety of SDBS out of which Gln36 and Thr15 can be involved in hydrogen bonding with the oxygen atom of $-\text{SO}_3^-$ (Table 9). The neighbouring ligands around SDBS indicates that the binding occurs preferentially in cavity-1 of BM with slight involvement of cavity-2 and the stabilization occurs primarily through hydrophobic interaction along with hydrogen bonding between the ligand and protein residues. Out of the five Trp residues in BM, SDBS and SDDS both lie close to Trp180 which can be also seen from the changes in the ΔASA values of Trp180 (see. Table 6 and 8)

The significance of the π -stacking interaction through the phenyl moiety in SDBS can be understood upon comparison with SDDS, since the latter is devoid of any phenyl part within the structure and the binding energy is almost 1.2 times lower as compared to the former (cf. Table 6). The aliphatic chain of SDDS is one carbon shorter than SDBS, but it binds almost in the similar region to SDBS, i.e., in cavity-1 and it stabilized the binding through hydrophobic interaction with the non-polar amino acid residues. As observed from the surface area calculation (Table 8), the ΔASA values for Val17 and Ala33 are somewhat higher for SDDS as compared to SDBS, however the ΔASA for Phe29, Ile163, Gly184, Tyr185 and Ile186 are significantly lower than the former. This may be due to the lack of phenyl moiety in SDDS which cannot promote sufficient hydrophobic interaction with the amino acid residues of BM, which in turn does not affect the solvent exposure of the residues significantly. One noticeable difference between SDBS and SDDS is the orientation of the ligand while binding to the protein surface since the $-\text{SO}_3^-$ is directed towards OH or NH_2 regions of Glu36, Thr15 and Lys18 whereas sarcosinate part [$-\text{N}(\text{CH}_3) - \text{CH}_2 - \text{COOH}$] of SDDS faces the opposite side thereby interacting more with Gln20 and His158 which is also supported by the higher ΔASA values of these residues in SDDS over SDBS (Table 8). This change in orientation of the polar part of SDDS may be due to the sarcosinate moiety which consist of a methyl group in addition of CH_2 group which prefer non-polar residues like Val17 (located at a distance of 2.27 Å) and Val160 (distance of around 3.37 Å) (Table 7). In addition, certain degree of stabilization is also obtained from the hydrogen bonding interaction between the SO_3^- group (SDBS) or COO^- group (SDDS) with the polar residues like Thr15, Lys18, Glu36, His158 (Table 9).

Conclusions:

In this study, an attempt has been made to elucidate the structural stability of stem bromelain (BM) with the possible interaction it shows two different kinds of anionic surfactant at 298.15 K. The interaction of different surfactants with stem bromelain at all concentration of surfactants: below, at and above of the cmc in phosphate buffer medium (pH 7) was investigated by several physicochemical methods, like, tensiometry and isothermal titration calorimetry. From tensiometry, several physicochemical parameters like, surface excess (Γ_{cmc}), minimum area of surfactants at air water interface (A_{min}) were calculated both in presence and absence of BM. Several inflection points (C_1 , C_2 and C_3) have been found in tensiometry profiles of surfactants in conjugation with BM. These break points were found due to the conformational change of BM assisted by surfactants. Similar observation was also found in isothermal titration calorimetry (ITC) profiles. Γ_{cmc} values of BM-surfactant system are relatively lesser than free surfactants (for NaC and NaDC) in pH-7 buffer medium, while, the reverse has been seen in case of SDDS and SDBS with same concentration of BM comparing with the micellization of SDDS and SDBS in phosphate buffer (pH 7). Enthalpy of micellization (ΔH^0_{obs}) of surfactants in presence and absence of BM were calculated. It is seen that for NaDC, SDDS and SDBS, the ΔH^0_{obs} values were found more positive in presence of BM than their pure states in phosphate buffer. Exception has been found in the interaction of NaC with BM, where exothermic heat change has been observed ($\Delta H^0_{obs} = -0.11 \text{ kJ.mol}^{-1}$), whereas, NaC in absence of BM shows the positive contribution of enthalpy change during micellization. Steady state fluorescence reveals the quenching of Trp. emission of BM in presence of all surfactants with blue shift below the free micelle formation. Binding constant (K_b) of BM with surfactants, bimolecular quenching constant (k_q), free energy of binding (ΔG_b^0) of surfactants with BM were calculated using steady state fluorescence method. It is observed that, the binding of NaC with BM is greater than any other surfactants investigated here, while Stern-Volmer quenching constant (K_{SV}) is found greater in presence of SDBS. From steady state and time resolved fluorescence study it is observed that, quenching of tryptophan in presence of surfactants are static in nature. Circular Dichroism (CD) study shows the stability of secondary structure of BM in presence of NaC and NaDC below C_3 , while BM lost its structural stability even at very low surfactant concentration of SDDS and SDBS. Molecular docking studies have been employed to visualize the probable location of the compounds (bile salt surfactants and conventional surfactants) in the surrounding microenvironment of the Trp residue(s) of BM. The binding energy (ΔG) of NaDC with BM does not vary much as compared to NaC, but the energy values are more negative than SDDS and SDBS.

References:

1. D. V. Volkin, 1989. *Minimizing protein inactivation. Protein Function. A practical approach*, 1-24.
2. S. Ghosh, *Colloids and Surfaces B: Biointerfaces*, 2008, **66**, 178–186.
3. D. Otzen, *Biochimica et Biophysica Acta (BBA)-Proteins and Proteomics*, 2011, **1814**, 562-591.
4. K.P. Ananthapadmanabhan, *Interactions of Surfactants with Polymers and Proteins*, CRC Press Inc., London, 1993 (Chapter 8).
5. C. Tanford, *The Hydrophobic effect: Formation of Micelles and Biological Membranes*, 2nd ed., Wiley–Interscience, New York, 1980 (Chapter 14).
6. A.K. Wright, M.R. Thompson, R.L. Miller, *Biochemistry*, 1975, **14**, 3224-3228.
7. G. Prieto, J.M. del Rio, M.I. Paz Andrade, F. Sarmiento, M.N. Jones, *Int. J. Biol. Macromol.*, 1993, **15**, 343-345.
8. J. Greener, B.A. Contestable, M.D. Bale, *Macromolecules*, 1987, **20**, 2490-2498.
9. S. Ghosh, *Colloids Surf. A: Physicochem. Eng. Aspects*, 2005, **264**, 6-16.
10. S. Ghosh, *Colloids Surf. B: Biointerfaces*, 2005, **41**, 209-216.
11. S. Ghosh, *J. Surf. Sci. Technol.*, 2003, **19**, 167-182.
12. T. Chakraborty, I. Chakraborty, S.P. Moulik, S. Ghosh, *J. Phys. Chem. B*, 2007, **111**, 2736-2746.
13. E. L. Gelamo, C. H. T. P. Silva, H. Imasato, and M. Tabak, 2002, **1594**, 84-99.
14. J. Abedin, S. Mahbub, M. M. Rahman, A. Hoque, D. Kumar, J. M. Khan, and A. M. El-Sherbeeney, 2021, **29**, 279-287.
15. G. Singh, T.S. Kang, *J. Phys. Chem. B*, 2015, **119**, 10573–10585.
16. B. Mandal, S. Mondal, A. Pan, S.P. Moulik, S. Ghosh, *Colloids and Surfaces A: Physicochem. Eng. Aspects*, 2015, **484**, 345–353.
17. R. J. Green, T. J. Su, H. Joy, and J. R. Lu., *Langmuir*, 2000, **16**, 5797-5805.
18. A. Chakraborty and S. Basak, *Colloids and Surfaces B: Biointerfaces.*, 2008, **63**, 83-90.
19. W.L. Mattice, J.M. Riser, D.S. Clark, *Biochemistry*, 1976, **15**, 4264–4272.
20. J. A. Reynolds, C. Tanford, *J. Biol. Chem.*, 1970, **245**, 5161–5165.
21. J. A. Reynolds, C. Tanford, *Proc. Natl. Acad. Sci.*, 1970, **66**, 1002–1007.
22. U Anand, S Mukherjee, *Biochimica et Biophysica Acta*, 2013, **1830**, 5394–5404.
23. S. Halder, S Kumari, R. Aggrawal, V. K. Aswal, and S. K. Saha, *Journal of Molecular Liquids* 2017, **243**, 369-379.
24. N. Ghosh, R. Mondal, S. Mukherjee, *Langmuir*, 2005, **31**, 1095–1104.
25. S. Ghosh, A. Banerjee, *Biomacromolecules*, 2002, **3**, 9–16.
26. S. Sinha, D. Tikariha, J. Larka, T. Yadav, S. Kumari, S. K. Saha, K. K. Ghosh, *J. Mol. Liq.*, 2016, **218**, 421-428.
27. T. Chakraborty, I. Chakraborty, S. P. Moulik, S. Ghosh, *Langmuir*, 2009, **25**, 3062-3074.
28. J. Zhu, L. Chen, X. Guo, *Colloids and Surfaces A*, 2020, **601**, 125029.
29. P. K. Misra, U. Dash, S. Maharana, *Colloids and Surfaces A: Physicochem. Eng. Aspects*, 2015, **483**, 36–44.
30. S. Dasmandal, A. Kundu, S. Rudra, A Mahapatra, *RSC Adv.*, 2015, **5**, 79107-79118.
31. J. Steinhardt, and J. A. Reynolds. *Multiple equilibria in proteins*. Academic Press, 2014.
32. C. A. Nelson, *J. Biol. Chem.*, 1971, **246**, 3895-3901.
33. J. Steinhardt, *Protein-Ligand Interactions*, edited by Horst Sund and Gideon Blauer, Berlin, Boston: De Gruyter, 2019, 422-434.
34. M. N. Jones, *Chem. Soc. ReV.*, 1992, **21**, 127-136.

35. J. M. Ridlon, D. J. Kang, P. B. Hylemon, *J. Lipid Res.*, 2006, **47**, 241–259.
36. O'Connor, C. J.; Wallace, R. G. Physico-Chemical Behavior of Bile Salts. *Adv. Colloid Interface Sci.* 1985, **22**, 1–111.
37. G. Li, L. B. Mc Gown, *J. Phys. Chem.*, 1994, **98**, 13711–13719.
38. D. M. Small, *In the Bile Salts*; P. P. Nair, D. Kritchevsky, Eds.; Plenum Press: New York, 1971; Vol. 1.
39. D. M. Small, S. A. Penkett, D. Chapman, *Biochim. Biophys. Acta*, 1969, **176**, 178–189.
40. T. Jones, J. P. Earnest, M. G. McNamee, *In Biological Membranes: Practical Approach*; J. B. C. Findlay, W. H. Evans, Eds.; IRL Press: Oxford, 1987.
41. T. Kamataki, K. Maeda, Y. Yamazoe, T. Nagai, R. Kato, *Biochem. Biophys. Res. Commun.* 1981, **103**, 1–7.
42. T. Saitoh, T. Fukuda, H. Tani, T. Kamidate, H. Watabane, *Anal. Sci.*, 1996, **12**, 569–573.
43. N Ghosh, R Mondal, S Mukherjee, *Langmuir*, 2015, **31**, 1095–1104.
44. S. De, S. Das, A. Girigoswami, *Colloids and Surfaces B: Biointerfaces*, 2007, **54**, 74–81.
45. M. H. Najar, O. A. Chat, P. A. Bhat, M. A. Mir, G. M. Rather, A. A. Dar, *Int. J. Biol. Macromol.*, 2021, **180**, 121–128.
46. Z. Yong, D. Yingjie, L. Ming, D. Q. M. Craig, L. Zhengqiang, *J. Colloid Interface Sci.*, 2009, **337**, 322–331.
47. J. M. Khan, A. Malik, P. Sen, A. Ahmad, A. Ahmed, A. Atiya, *Int. J. Biol. Macromol.*, 2020, **148**, 880–886
48. S. Bag, S. Chaudhury, D. Pramanik, S. D. Gupta, S. Dasgupta, *Proteins*, 2016, **84**, 1213–1223.
49. W. A. R. Manamperi, S. W. Pryor, *J Am Oil Chem Soc*, 2012, **89**, 541–549.
50. V. Sharma, P. C. López, O. Y. Osses, C. R. fuentes, A. Kumar, *J. Mol. Liq.*, 2018, **271**, 443–445
51. Rui Zhang, Y. Liu, X. Huang, M. Xu, R. Liu, W. Zong, *Sci. Total Environ.*, 2018, **622–623**, 306–315.
52. S Mondal, A Banerjee, B Das, *J. Mol. Liq.*, 2010, **301**, 112450.
53. Y. Liu, Y. Liu, R. Guo, *J Solution Chem*, 2011, **40**, 1140–1152.
54. M.R. Infante, A. Pinazo and J. Seguer, *Colloids Surf., A*, 1997, **49**, 123–124
55. L. S. Fosdick, *Science*, 1956, **123**, 988–989.
56. G.B Ray, S. Ghosh, S.P. Moulik, *J. Surfact. Deterg.*, 2009, **12**, 131–143.
57. S. Rudra, S. Dasmandal, A. Mahapatra, *J. Colloid Interface Sci.*, 2017, **496**, 267–277
58. S Mondal, ML Raposo, A Ghosh, G Prieto, *Colloids Surf. A: Physicochem. Eng. Asp.*, 2019, **577**, 167–174
59. B Mandal, S Ghosh, SP Moulik, *New J. Chem.*, 2016, **40**, 4617–4624
60. P.K.Kumar, I. Jha, A. Sindhu, P.Venkatesu, I. Bahadur, E. E.Ebenso, *J. Mol. Liq.*, 2020, 295, 111785
61. M. Bala, N. A. Ismail, M. Mel, M. S. Jami, H. M. Salleh, A. Amid, *Arch. Des Sci.*, 2012, 65, 369–399.
62. M. Bisht, I. Jha, P. Venkatesu, *Chemistry Select*, 2016, **1**, 3510 – 3519.
63. M Tian, J Zhu, J Guo, X Guo, *J Surfact Deterg*, 24, **2011**, 111–119
64. V. Rathnavelu, N. B. Alitheen, S. Sohila, S. Kanagesan, & R. Ramesh, *Biomedical reports*, 2016, **5**, 283–288.
65. Z. I. M. Arshad, A. Amid, F. Yusof, I. Jaswir, K. Ahmad & S. P. Loke, *Applied Microbiology and Biotechnology*, 2014, **98**, 7283–7297.
66. D. MacKay, A. L. Miller, *Altern. Med. Rev.*, 2003, **8**, 359–377.

67. W. Hu, A. M. Wang, S. Y. Wu, B. Zhang, S. Liu, Y. Bin Gou, J.M. Wang, *J. Trauma Inj. Infect. Crit. Care*, 2011, **71**, 966–972.
68. J. Shi, Q. Wang, D. Pan, T. Li & M. Jiang, *J. Biomol. Struct. Dyn.*, 2017, **35**, 1529-1546.
69. P. K. Kumar, I. Jha, P. Venkatesu, I. Bahadur, E. E. Ebenso, *J. Mol. Liq.* 2017, **246**, 178–186.
70. Y. Jiang, M. Tian, Y. Wang, W. Xu, X. Guo, *J. Mol. Liq.* 2021, **328**, 115439.
71. R. Bhattacharya, D. Bhattacharyya, *Biochim Biophys Acta*, 2009, **1794**, 698-708.
72. M. D. Hanwell, D. E. Curtis, D. C. Lonie, T. Vandermeersch, E. Zurek, G. R. Hutchison, *J. Cheminf.*, 2012, **4**, 1-17.
73. S. Mondal, A. Banerjee, B. Das., *J. Mol. Liq.*, 2020, **301**, 112450.
74. O. Trott, A. Olson, *J. Comput. Chem.* 2010, **31**, 455- 461.
75. E. F. Pettersen, T. D. Goddard, C. C. Huang, G. S. Couch, D. M. Greenblatt, E. C. Meng, T. E. Ferrin, *J. Comput. Chem.*, 2004, **25**, 1605-1612.
76. F. Geng, J. Liu, L. Zheng, L. Yu, Z. Li, G. Li and C. Tung, *Journal of Chemical & Engineering Data*, 2010, **55**, 147-151.
77. A. Maestre, P. Guardado, M. L. Moya, *J. Chem. Eng. Data*, 2014, **59**, 433–438
78. S. K. Hait, P. R. Majhi, A. Blume, and S. P. Moulik, *J. Phys. Chem. B*, 2003, **107**, 3650-3658.
79. J. R. Lakowicz, *Principles of Fluorescence Spectroscopy*, 3rd ed.; Springer: New York, 2006.
80. P. S. Sardar, S. S. Maity, S. Ghosh, J. Chatterjee, T. K. Maiti, S. Dasgupta, *J. Phys. Chem. B*, 2006, **110**, 21349–21356.
81. M. Mukherjee, P. S. Sardar, S. K. Ghorai, S. K. Samanta, A. S. Roy, S. Dasgupta, S. Ghosh, *J. Photochem. Photobiol., B*, 2012, **115**, 93–104.
82. S. Paul, N. Sepay, S. Sarkar, P. Roy, S. Dasgupta, P. S. Sardar, A. Majhi, *New J. Chem.* , 2017, **41**, 15392–15404.
83. P. S. Sardar, S. Samanta, S. S. Maity, S. Dasgupta, S. Ghosh, *J. Phys. Chem. B*, 2008, **112**, 3451–3461.
84. J. M. Berg, J. L. Tymoczko, L. Stryer, *In Biochemistry*, 5th ed.; Delvin, T. M., Ed.; W. H. Freeman and Co.: New York, 2002.
85. A. Ritonja, A. D. Rowan, D. J. Buttle, N. D. Rawlings, V. Turk, & A. J. Barrett, *FEBS Lett.*, 1989 **247**, 419–424
86. S. Habib, M. A. Khan, H. Younus, *The Protein J.*, 2007, **26**, 117–124
87. S. K. Haq, S. Rasheedi and R. H. Khan, *Eur. J. Biochem.*, 2002, **269**, 47–52
88. K. A. Connors, *Binding Constants: The Measurements of Molecular Complex Stability*; Wiley: New York, 1987.
89. I. M. Klotz, *Ann. N. Y. Acad. Sci.*, 1973, **226**, 18–35.
90. H.R. Maurer, *Cell. Mol. Life Sci.*, 2001, **58**, 1234–1245
91. A. Arroyo-Reyna, A. Hernandez-Arana, R. Arreguin-Espinosa, *Biochem. J.*, 1994, **300**, 107–110.

Summary and Conclusions

The interaction and self-aggregation of binary surfactants, 1-hexadecyl-3-methylimidazolium chloride (HDMimCl or can be written as, C₁₆MimCl), a Surface Active Ionic Liquid (SAIL) and dodecyltrimethylammonium bromide (DTAB) have been investigated in three desired temperatures (T = 303.15 K, 313.15 K and 323.15 K) and different stoichiometric mole fractions using conductometry, tensiometry, spectrofluorimetry, steady state fluorescence anisotropy and dynamic light scattering (DLS) techniques. From conductometry measurements, the bulk properties, like critical micellar concentrations (*cmc*s), degree of counterion binding (*g*), free energy of micellization (ΔG_M), enthalpy of micellization (ΔH_M) and entropy of micellization (ΔS_M) have been evaluated at three different temperatures. With the help of well-established models such as Clint, Rubingh and Motomura, ideal *cmc* in mixtures (*cmc*), interaction parameters (β^R), micellar mole fraction of components (*X*) and activity coefficients (*f*) of components have been calculated theoretically using conductometric *cmc*s of individual and mixed surfactants. Several interfacial parameters, like surface excess (Γ_{\max}), minimum monomer area (A_{\min}), surface pressure at *cmc* (π_{cmc}) and efficiency of adsorption of amphiphiles at air water interface (pC_{20}) of mixed and individual components have been calculated using tensiometry at 313.15 K. It is seen that the experimental *cmc*s of mixed surfactants differ significantly with *cmc* of individual one from both conductometry and tensiometric measurements. Spectrofluorimetry technique helps to determine the aggregation number (*N*). Zeta potential (ζ) values are calculated at different mole fractions of two investigated surfactants using dynamic light scattering. Spectrofluorimetry technique helps to determine the aggregation number (*N*) and anisotropy (*r*) using 1, 6-diphenyl-1, 3, 5-hexatriene (DPH) at different mole fractions of surfactants in both pure and mixed states. Anisotropy of DPH increases with increase of mole fraction of HDMimCl. Both aggregation number and hydrodynamic diameter increase at high DTAB content, while, zeta potential has the more positive value at higher mole fraction of HDMimCl. The critical micellar concentrations (*cmc*) of HDMimCl-DTAB mixtures demonstrate some negative deviation from the ideal behavior, implying a nonideal mixing. Mixed micelles of HDMimCl-DTAB are also characterized by negative interaction parameter values, i.e., the actual mixed micelles are thermodynamically more stable compared to hypothetical ideal state. Thermodynamic parameters indicate that the spontaneous process of micellization is entropically favourable for HDMimCl-rich mixtures while it is enthalpy-driven for DTAB-rich mixtures. The contributions from the electrostatic

attraction between the surfactant molecules, the steric effect, and the repulsive molecular interaction vary with the mixture composition. Evaluation of the packing parameter values indicate spherical shape of the micelles formed individual and mixed surfactant solutions. Aggregation number of the mixed micelles initially increase with the increase in the HDMimCl-content followed by a decrease in the HDMimCl-rich region. Hydrophobicity of the mixed micellar solutions increases with the increase in the amount of the HDMimCl in the binary surfactant mixtures.

The influence of four sodium salts (NaCl, NaBr, Na₂SO₄, and Na₃PO₄) on the self-aggregation, interfacial, and thermodynamic properties of a surface-active ionic liquid (1-hexadecyl-3-methylimidazolium chloride, C₁₆MimCl) has been explored in aqueous solutions by conductometry, tensiometry, spectrofluorimetry, isothermal titration calorimetry and dynamic light scattering (DLS). Analyses of the *cmc* values indicate that the anions of the added salts promote the self-aggregation of C₁₆MimCl in the order: Cl⁻ < Br⁻ < PO₄³⁻ < SO₄²⁻. Melting of iceberg, in general, governs the process of micellization of aqueous C₁₆MimCl in presence of the investigated salts within the investigated temperature range (298.15 - 318.15 K), while the dehydration of imidazolium head groups takes the leading role below 303.15 K for the C₁₆MimCl-Na₃PO₄ system. The results indicate that addition of salt leads to a greater spontaneity of micellization, and that exothermicity prevails in these systems. Differential effect of the salts on the interfacial properties of C₁₆MimCl has been interpreted on the basis of the coupled influence of the electrostatic charge neutralization of surfactants at the interface, and the van der Waals repulsion of surfactant tails and electrostatic repulsion of surfactant head groups. C₁₆MimCl has been shown to form spherical micelles in presence of varying amounts of NaCl, Na₂SO₄ and Na₃PO₄, while there occurs probably a transition in the micellar geometry from spherical to non-spherical shape when added NaBr concentration exceeds 0.01 mol.kg⁻¹. Fluorescence studies demonstrate that a combined quenching mechanism is operative for the quenching of pyrene fluorescence in the investigated C₁₆MimCl-salt systems. Micellar aggregation numbers obtained from Steady State Fluorescence Quenching method (SSFQ) have always been found to be somewhat smaller than those estimated from Time Resolved Fluorescence Quenching (TRFQ) method. The order of instability of the C₁₆MimCl-micelles ascertained from Zeta potential measurements confirms to what has been inferred from the *cmc* values. The hydrodynamic radii of C₁₆MimCl-micelles, obtained from DLS studies, have been found to increase with increasing salinity of the solutions. Bivalent and trivalent anions have reduced ζ significantly as these anions compress electrical double layer more effectively. This

trend in ζ is similar to that what we find for the *cmc* values in presence of the investigated salts. Presence of different salts affect the R_h values of $C_{16}MImCl$ micelles differently, and the following sequence of these values have been found in presence of the investigated salts: $NaCl > Na_3PO_4 > NaBr > Na_2SO_4$.

Investigation have been made on the interaction of a biodegradable polyelectrolyte, sodium alginate (NaAlg) with two oppositely charged cationic surfactants, 1-hexadecyl-3-methyl imidazolium chloride ($C_{16}MImCl$) and (1-Hexadecyl) triphenylphosphonium bromide ($C_{16}TPB$), while later a conventional surfactant over a wide concentration regime of polyelectrolyte (0.001, 0.005 and 0.01% w/v) at 298.15 K. Dual influence of electrostatic and hydrophobic interactions operates in this investigation when mixing surfactants to oppositely charged polyelectrolyte. A number of different experimental techniques, e.g., conductometry, tensiometry, steady state and time resolved spectrofluorimetry, turbidimetry, isothermal titration calorimetry (ITC), dynamic light scattering (DLS), attenuated total reflection (ATR), high resolution transmission electron microscope (HR-TEM) and fluorescence microscopy have been implemented to get comprehensive information originated from the interaction of oppositely charged polyelectrolyte and surfactants. Tensiometry study reveals the existence of several conformations of NaAlg influenced by different concentrations of surfactants titrated to it and these are abbreviated, critical aggregation concentration (*cac*), so-called ‘neckless’ type polymer-surfactant complex (C_s) and finally extended critical micelle concentration (C_m^*) due to aggregation of surfactant itself, appeared in chronological order from low to high concentration of surfactants. Apart from tensiometry, these above concentrations have been well found and the values are well comparable when investigating polyelectrolyte-surfactant interaction by other physicochemical techniques also. Irreversible phase separation of oppositely charged polyelectrolyte- surfactant complex (PS-complex) occurs at higher polyelectrolyte concentration investigated here for both the surfactants in the vicinity of *cac* for $C_{16}MImCl$ and near C_m^{*1} for $C_{16}TPB$ and finally remain persist after further addition of surfactants above the formation of free micelles. Several bulk and interfacial parameters, viz., Gibbs free energy of micellization (ΔG_m^0), enthalpy of micellization (ΔH_m^0), entropy of micellization (ΔS_m^0), degree of counterion binding (β), surface excess at *cmc* (Γ_{max}), area minimum (A_{min}), surface pressure at *cmc* (π_{cmc}), pC_{20} , packing parameter (P), hydrodynamic radii (*r*) and aggregation number (N_a) of two surfactants both in presence and absence of NaAlg have been calculated for these investigated systems. Characterization of NaAlg, both surfactants and their individual complexes were performed using FTIR-ATR. DLS show the

distribution of size of polymer surfactant complexes over a wide range of surfactant concentrations at a fixed polyelectrolyte concentration, while HR-TEM study revealed not only the size of agglomerated clusters of PS-complex and also its shapes. Images of NaAlg-surfactant complexes were also captured using fluorescence microscopy in solution phase. Strong PS-complex in presence of C₁₆MImCl has been reported here over C₁₆TPB. Presence of bulky head groups of C₁₆TPB containing triphenyl attached to phosphonium cation makes it less accessible to COO⁻ groups of NaAlg over imidazolium cations of C₁₆MImCl, while C₁₆TPB enhances hydrophobicity in NaAlg medium forming greater amount of coacervates comparing with C₁₆MImCl + NaAlg systems. Existence of second *cmc* has been found clearly in presence of C₁₆TPB in aqueous solution by conductometry, ITC and fluorimetric techniques while, that *cmc* of C₁₆TPB is clearly detectable in presence of higher NaAlg concentration medium by tensiometry and conductometric techniques. Micellization process in presence of both surfactants is exothermic in presence of different wt% of NaAlg and overall decrease in exothermicity is observed with increase of polyelectrolyte concentration. The values of *cac*, *C_s* and *C_m^{*}* for two surfactants in corporation with different wt% (w/v) of NaAlg are estimated by different experimental techniques which have well similarity to each other. ATR spectra of polyelectrolyte-surfactant complex reveal the incorporation of surfactants into polyelectrolyte.

Interaction of a novel azabenzocrown ether (H₂DTC) with different kinds of surfactants such as, conventional anionic (SDS), cationic (DTAB), gemini cationic (16-4-16), ionic liquid (C₁₆MImCl) and non-ionic (Tween-60) has been investigated at the wide range of surfactant concentrations (premicellar, micellar and post micellar regime) in 15% (V/V) EtOH-water medium at 298.15 K. Several physicochemical techniques, viz., tensiometry, steady state fluorimetry, UV-VIS spectroscopy was employed. H₂DTC show several inflection points in surface tension, steady state fluorimetry and absorption profiles with variation of [surfactant] from very low to high, apart from critical micelle concentration (*cmc*). Equilibrium binding constants (*K_b*) for the binding of H₂DTC with micellar environment, partition coefficient values for H₂DTC (*K_x*) in micellar to solvent phase, molar absorptivity of H₂DTC in absence (*ε₀*) and presence (*ε*) of micellar solution, Gibbs energy of binding (*ΔG_b⁰*), Gibbs energy of partition (*ΔG_p⁰*) for H₂DTC in solvent to micellar phase have been evaluated in this present study. It has been seen that H₂DTC strongly binds with micelles of Tween-60 than the anionic and cationic surfactants and correspond *K_x* values are found higher for micelle medium of non-ionic surfactant. On the other hand, *ε* value of H₂DTC found lower in micellar Tween-60, whereas, it is found high in cationic and anionic micellar medium comparing with the pure solvent (15%

V/V EtOH-water). Negative Gibbs binding and negative values of partition coefficient clearly indicates the spontaneity of both these processes. The binding of H₂DTC with Tween-60 micelles is greater than the other surfactants. K_x values for cationic surfactants are greater than anionic SDS. Among the cationic surfactants, the values of K_x of H₂DTC are found to be the following increasing order, C₁₆MImCl > 16-4-16 > DTAB. H₂DTC shows greater partition in Tween-60 micellar medium than the cationic and anionic micelles. Increase in the values of K_b and K_x for Tween-60 can be attributed to the lower *cmc*, enhanced hydrophobicity and increased affinity of dye towards micelle.

An attempt has been made to elucidate the structural stability of stem bromelain (BM) with the possible interaction it shows two different kinds of anionic surfactant at 298.15 K. The interaction of different surfactants with stem bromelain at all concentration of surfactants: below, at and above of the *cmc* in phosphate buffer medium (pH 7) was investigated by several physicochemical methods, like, tensiometry and isothermal titration calorimetry. From tensiometry, several physicochemical parameters like, surface excess (Γ_{cmc}), minimum area of surfactants at air water interface (A_{min}) were calculated both in presence and absence of BM. Several inflection points (C_1 , C_2 and C_3) have been found in tensiometry profiles of surfactants in conjugation with BM. These break points were found due to the conformational change of BM assisted by surfactants. Similar observation was also found in isothermal titration calorimetry (ITC) profiles. Γ_{cmc} values of BM-surfactant system are relatively lesser than free surfactants (for NaC and NaDC) in pH-7 buffer medium, while, the reverse has been seen in case of SDDS and SDBS with same concentration of BM comparing with the micellization of SDDS and SDBS in phosphate buffer (pH 7). Enthalpy of micellization (ΔH^0_{obs}) of surfactants in presence and absence of BM were calculated. It is seen that for NaDC, SDDS and SDBS, the ΔH^0_{obs} values were found more positive in presence of BM than their pure states in phosphate buffer. Exception has been found in the interaction of NaC with BM, where exothermic heat change has been observed ($\Delta H^0_{obs} = -0.11 \text{ kJ.mol}^{-1}$), whereas, NaC in absence of BM shows the positive contribution of enthalpy change during micellization. Steady state fluorescence reveals the quenching of Trp. emission of BM in presence of all surfactants with blue shift below the free micelle formation. Binding constant (K_b) of BM with surfactants, bimolecular quenching constant (k_q), free energy of binding (ΔG^0_b) of surfactants with BM were calculated using steady state fluorescence method. It is observed that, the binding of NaC with BM is greater than any other surfactants investigated here, while Stern-Volmer quenching constant (K_{SV}) is found greater in presence of SDBS. From steady state and time resolved

fluorescence study it is observed that, quenching of tryptophan in presence of surfactants are static in nature. Circular Dichroism (CD) study shows the stability of secondary structure of BM in presence of NaC and NaDC below C_3 , while BM lost its structural stability even at very low surfactant concentration of SDDS and SDBS. Molecular docking studies have been employed to visualize the probable location of the compounds (bile salt surfactants and conventional surfactants) in the surrounding microenvironment of the Trp residue(s) of BM. The binding energy (ΔG) of NaDC with BM does not vary much as compared to NaC, but the energy values are more negative than SDDS and SDBS.

Appendix

Basic Data

Chapter- I

1.1. Data of $\ln(I_0/I)$ with the variation of [CPC] at 298.15K. I_0 and I are the Fl. Intensity of Pyrene in absence and presence of CPC at different mole fractions of HDMimCl. Total [Surf] = 0.05 mol.kg⁻¹

[CPC]/ mol.kg ⁻¹	ln (I_0/I)								
	$\alpha_1/ 0.9$	0.8	0.7	0.6	0.5	0.4	0.3	0.2	0.1
0	0	0	0	0	0	0	0	0	0
2.99x10 ⁻⁵	0.022	0.063	0.042	0.004	0.032	0.041	0.060	0.042	0.037
5.94x10 ⁻⁵	0.064	0.110	0.104	0.051	0.057	0.065	0.111	0.076	0.070
8.87x10 ⁻⁵	0.113	0.162	0.147	0.094	0.100	0.103	0.163	0.124	0.100
1.18x10 ⁻⁴	0.162	0.201	0.197	0.136	0.132	0.134	0.212	0.155	0.169
1.46x10 ⁻⁴	0.217	0.254	0.230	0.179	0.172	0.170	0.273	0.227	0.195

1.2. Anisotropy data of Pyrene at various mole fractions of HDMimCl (α_1) at 298.15 K

α_1	Anisotropy (r)
0	0.025
0.1	0.026
0.2	0.028
0.3	0.025
0.4	0.029
0.5	0.030
0.6	0.032
0.7	0.038
0.8	0.039
0.9	0.041
1	0.045

Chapter-II

2.1. Specific conductance (κ) data with variation of $[C_{16}MImCl]$ at different temperatures in presence of $0.001 \text{ mol.kg}^{-1} \text{ Na}_2\text{SO}_4$

298.15 K		303.15 K		308.15 K		313.15 K		318.15K	
$10^5 [C_{16}MImCl] / \text{mol.kg}^{-1}$	$\kappa / \mu\text{S.cm}^{-1}$	$10^5 [C_{16}MImCl] / \text{mol.kg}^{-1}$	$\kappa / \mu\text{S.cm}^{-1}$	$10^5 [C_{16}MImCl] / \text{mol.kg}^{-1}$	$\kappa / \mu\text{S.cm}^{-1}$	$10^5 [C_{16}MImCl] / \text{mol.kg}^{-1}$	$\kappa / \mu\text{S.cm}^{-1}$	$10^5 [C_{16}MImCl] / \text{mol.kg}^{-1}$	$\kappa / \mu\text{S.cm}^{-1}$
0	253	0	280	0	310	0	339	0	370
0.3	256	0.23	283	0.3	314	0.3	342	0.3	374
0.6	259	0.45	286	0.6	317	0.6	345	0.6	378
0.9	262	0.75	290	0.9	320	0.9	348	0.9	382
1.19	264	1.04	293	1.19	323	1.19	352	1.19	386
1.49	265	1.34	296	1.49	326	1.49	354	1.49	389
1.78	266	1.63	297	1.78	327	1.78	356	1.78	392
2.07	267	1.92	299	2.07	328	2.07	357	2.07	394
2.36	268	2.22	300	2.36	329	2.36	358	2.36	395
2.65	269	2.51	301	2.65	330	2.65	359	2.65	396
2.94	269	2.8	302	2.94	331	2.94	360	2.94	397
3.23	270	3.09	303	3.23	332	3.23	361	3.23	398
3.94	271	3.37	304	3.94	334	3.94	363	3.94	400
4.65	273	3.66	305	4.65	336	4.65	365	4.65	402
		4.37	307						

2.2. Specific conductance (κ) data with variation of $[C_{16}MImCl]$ at different temperatures in presence of $0.005 \text{ mol.kg}^{-1} \text{ NaBr}$

298.15 K		303.15 K		308.15 K		313.15 K		318.15 K	
$10^5 [C_{16}MImCl] / \text{mol.kg}^{-1}$	$\kappa / \mu\text{S.cm}^{-1}$	$10^5 [C_{16}MImCl] / \text{mol.kg}^{-1}$	$\kappa / \mu\text{S.cm}^{-1}$	$10^5 [C_{16}MImCl] / \text{mol.kg}^{-1}$	$\kappa / \mu\text{S.cm}^{-1}$	$10^5 [C_{16}MImCl] / \text{mol.kg}^{-1}$	$\kappa / \mu\text{S.cm}^{-1}$	$10^5 [C_{16}MImCl] / \text{mol.kg}^{-1}$	$\kappa / \mu\text{S.cm}^{-1}$
0	620	0	623	0	633	0	638	0	640
2.01	621	2.01	625	2.01	635	2.01	639	2.01	641
3.34	622	3.34	626	3.34	636	3.34	640	3.34	643
4.68	623	4.68	627	4.68	637	4.68	641	4.68	644
6.01	624	6.01	628	6.01	638	6.01	642	6.01	645
6.68	624	6.68	628	6.68	639	6.68	643	6.68	645
13.3	628	13.3	633	13.3	644	13.3	648	13.3	651
19.9	630	19.9	635	19.9	646	19.9	652	19.9	656
26.4	631	26.4	636	26.4	648	26.4	654	26.4	658
33	633	33	638	33	650	33	655	33	659
45.8	635	45.8	641	45.8	653	45.8	659	45.8	663
64.8	639	64.8	645	64.8	657	64.8	663	64.8	668
83.5	644	83.5	649	83.5	662	83.5	668	83.5	673
101.8	648	101.8	654	101.8	667	101.8	673	101.8	678
125.6	653	125.6	659	125.6	673	125.6	679	125.6	685

2.3. Tensiometric data of C₁₆MImCl at different [NaCl] at 298.15 K

[NaCl] = 0.001 mol.kg ⁻¹		[NaCl] = 0.005 mol.kg ⁻¹		[NaCl] = 0.01 mol.kg ⁻¹		[NaCl] = 0.02 mol.kg ⁻¹	
[C ₁₆ MImCl]/ mmol.kg ⁻¹	γ/ mN.m ⁻¹	[C ₁₆ MImCl]/ mmol.kg ⁻¹	γ/ mN.m ⁻¹	[C ₁₆ MImCl]/ mmol.kg ⁻¹	γ/ mN.m ⁻¹	[C ₁₆ MImCl]/ mmol.kg ⁻¹	γ/ mN.m ⁻¹
0.000	66.3	0.000	67.4	0.000	61.4	0.000	63.2
0.001	66.5	0.002	61.4	0.005	57.1	0.001	55.0
0.003	61.0	0.004	56.3	0.014	53.6	0.003	48.7
0.005	60.0	0.006	55.3	0.024	50.0	0.005	46.9
0.008	58.1	0.008	53.0	0.038	46.7	0.008	44.0
0.012	57.0	0.012	50.0	0.062	42.2	0.012	41.7
0.017	55.0	0.020	49.1	0.098	38.4	0.017	40.2
0.023	53.5	0.032	46.9	0.145	36.5	0.024	38.2
0.030	51.6	0.044	45.0	0.239	36.3	0.034	36.0
0.038	50.0	0.064	42.7	0.376	36.2	0.049	33.8
0.048	48.9	0.094	39.8			0.069	31.3
0.059	47.5	0.133	38.1			0.089	30.3
0.074	46.7	0.192	36.4			0.119	30.4
0.093	45.4	0.288	36.2			0.169	30.4
0.122	43.9	0.476	36.4			0.269	30.7
0.169	41.7	0.748	36.4			0.469	30.7
0.261	38.8	1.090	36.5			0.669	31.0
0.349	37.0	1.716	36.5			0.869	31.2
0.434	36.3					1.169	31.0
0.632	35.4						
0.885	36.0						
1.139	36.3						

2.4. Tensiometric data of C₁₆MImCl at different [NaBr] at 298.15 K

[NaBr] = 0.001 mol.kg ⁻¹		[NaBr] = 0.005 mol.kg ⁻¹		[NaBr] = 0.01 mol.kg ⁻¹		[NaBr] = 0.02 mol.kg ⁻¹	
[C ₁₆ MImCl]/ mmol.kg ⁻¹	γ/ mN.m ⁻¹	[C ₁₆ MImCl]/ mmol.kg ⁻¹	γ/ mN.m ⁻¹	[C ₁₆ MImCl]/ mmol.kg ⁻¹	γ/ mN.m ⁻¹	[C ₁₆ MImCl]/ mmol.kg ⁻¹	γ/ mN.m ⁻¹
0.000	64.4	0.000	64.1	0.000	64.8	0.000	65.3
0.001	63.9	0.001	63.1	0.001	60.1	0.002	59.9
0.002	61.6	0.002	62.0	0.001	58.2	0.006	53.3
0.005	60.2	0.004	58.5	0.004	54.1	0.011	48.5
0.009	58.7	0.008	54.9	0.008	50.9	0.015	44.3
0.015	55.7	0.013	50.9	0.013	46.4	0.020	42.0
0.025	52.7	0.019	47.2	0.020	42.1	0.024	38.9
0.038	49.4	0.027	43.9	0.029	37.7	0.029	36.5
0.055	47.2	0.036	40.9	0.039	35.8	0.034	33.9
0.074	44.2	0.046	38.3	0.052	32.4	0.040	31.8
0.096	41.4	0.058	35.2	0.064	30.8	0.045	30.0
0.121	39.8	0.076	32.4	0.080	28.6	0.054	28.9
0.149	37.3	0.100	30.1	0.099	27.7	0.064	28.5
0.179	35.2	0.129	28.5	0.120	26.9	0.081	28.4
0.215	32.8	0.163	28.4	0.147	26.9	0.102	28.4
0.256	31.3	0.218	28.0	0.183	27.2	0.128	28.6

0.301	29.9	0.323	28.0	0.223	27.6	0.179	28.3
0.350	29.8			0.279	27.6		
0.403	29.9						
0.478	30.4						
0.574	30.5						
0.705	30.6						
0.825	30.6						

Fig. 2.5. Tensiometric data of C₁₆MImCl at different [Na₂SO₄] at 298.15 K

[Na ₂ SO ₄] = 0.001 mol.kg ⁻¹		[Na ₂ SO ₄] = 0.005 mol.kg ⁻¹		[Na ₂ SO ₄] = 0.01 mol.kg ⁻¹		[Na ₂ SO ₄] = 0.02 mol.kg ⁻¹	
[C ₁₆ MImCl]/ mmol.kg ⁻¹	γ/ mN.m ⁻¹	[C ₁₆ MImCl]/ mmol.kg ⁻¹	γ/ mN.m ⁻¹	[C ₁₆ MImCl]/ mmol.kg ⁻¹	γ/ mN.m ⁻¹	[C ₁₆ MImCl]/ mmol.kg ⁻¹	γ/ mN.m ⁻¹
0.000		0.000		0.000		0.000	
0.006	47.9	0.003	45.2	0.003	46.4	0.001	54.4
0.009	44.3	0.006	40.3	0.006	41	0.004	48
0.012	42.6	0.009	37.8	0.009	38.2	0.007	43.2
0.018	39.9	0.014	35.2	0.015	34.1	0.010	40.3
0.024	38	0.020	32.9	0.021	31.9	0.014	38.3
0.036	33.6	0.031	29.1	0.027	31.1	0.020	35.4
0.048	31.7	0.049	26.2	0.039	28.2	0.027	33.3
0.060	29.9	0.066	25.3	0.051	25.9	0.036	29.4
0.078	28	0.088	24.9	0.069	25.9	0.050	27.3
0.101	26.9	0.116	24.4	0.093	25.6	0.071	27.1
0.131	26.8	0.173	24.1	0.123	25.2	0.105	27.5
0.172	26.5	0.284	23.9	0.182	24.4	0.166	27.2
0.459	25.9			0.748	25.2	0.630	27.1
0.736	25.6			1.272	25	0.962	27.6
1.259	25.6						
1.744	25.6						

2.6. Tensiometric data of C₁₆MImCl at different [Na₃PO₄] at 298.15 K

[Na ₃ PO ₄] = 0.001 mol.kg ⁻¹		[Na ₃ PO ₄] = 0.005 mol.kg ⁻¹		[Na ₃ PO ₄] = 0.01 mol.kg ⁻¹		[Na ₃ PO ₄] = 0.02 mol.kg ⁻¹	
[C ₁₆ MImCl]/ mmol.kg ⁻¹	γ/ mN.m ⁻¹	[C ₁₆ MImCl]/ mmol.kg ⁻¹	γ/ mN.m ⁻¹	[C ₁₆ MImCl]/ mmol.kg ⁻¹	γ/ mN.m ⁻¹	[C ₁₆ MImCl]/ mmol.kg ⁻¹	γ/ mN.m ⁻¹
0.000	59.1	0.000	56.7	0.000	60.3	0.000	60.5
0.002	50.1	0.003	48.0	0.005	51.4	0.003	47.2
0.005	47.8	0.008	38.9	0.008	48.2	0.006	43.2
0.007	46.3	0.013	37.4	0.013	43.8	0.011	39.5
0.012	44.7	0.024	32.7	0.018	41.2	0.017	37.5
0.019	41.4	0.050	28.0	0.028	37.7	0.023	35.0
0.028	39.0	0.076	27.2	0.043	34.0	0.029	33.4
0.040	37.2	0.115	25.9	0.064	31.4	0.034	31.6
0.052	35.7	0.191	25.7	0.089	30.1	0.040	30.2
0.076	33.9	0.318	26.0	0.139	30.3	0.052	28.4
0.111	32.3	0.563	26.0	0.263	30.0	0.063	27.7
0.157	30.8	1.026	25.9	0.503	30.1	0.080	27.5
0.202	30.0	1.858	26.5	0.958	30.0	0.108	28.2
0.314	29.4					0.165	28.2
0.531	29.2					0.304	28.2
0.942	29.0					0.574	28.8
1.323	28.9					1.083	28.7
1.847	28.7						
2.320	28.7						

2.7. Calorimetric titration data of C₁₆MImCl in different [NaCl] in mol.kg⁻¹ at 298.15 K

Demucellization of C ₁₆ MImCl in different [NaCl] in mol.kg ⁻¹							
0.001		0.005		0.01		0.02	
[C ₁₆ MImCl]/ mM	ΔH ₀ ^m / kJ.mol ⁻¹	[C ₁₆ MImCl]/ mM	ΔH ₀ ^m / kJ.mol ⁻¹	[C ₁₆ MImCl]/ mM	ΔH ₀ ^m / kJ.mol ⁻¹	[C ₁₆ MImCl]/ mM	ΔH ₀ ^m / kJ.mol ⁻¹
0		0		0		0	
0.27	-0.648	0.075	0.661	0.006	2.097	0.004	1.664
0.35	-0.646	0.108	0.642	0.029	1.761	0.018	1.649
0.44	-0.618	0.140	0.585	0.052	0.956	0.033	1.093
0.52	-0.602	0.172	0.451	0.075	0.324	0.047	0.432
0.60	-0.585	0.204	0.369	0.098	0.083	0.061	0.091
0.67	-0.512	0.236	0.286	0.120	-0.364	0.075	-0.280
0.75	-0.394	0.267	0.217	0.142	-0.475	0.089	-0.224
0.83	-0.322	0.298	0.104	0.164	-0.414	0.102	-0.160
0.91	-0.243	0.328	0.027	0.186	-0.540	0.129	-0.068
0.98	-0.195	0.358	0.010	0.207	-0.537	0.143	-0.146
1.06	-0.128	0.388	0.011	0.228	-0.524	0.156	-0.178
1.13	-0.065	0.418	0.005				
1.20	-0.046						
1.27	-0.072						
1.35	-0.058						
1.42	-0.046						

2.8. Calorimetric titration data of C₁₆MImCl at different [NaBr] at 298.15 K

Demicellization of C ₁₆ MImCl in different [NaBr] in mol.kg ⁻¹							
0.001		0.005		0.010		0.020	
[C ₁₆ MImCl]/mM	$\Delta H_0^m / \text{kJ.mol}^{-1}$	[C ₁₆ MImCl]/mM	$\Delta H_0^m / \text{kJ.mol}^{-1}$	[C ₁₆ MImCl]/mM	$\Delta H_0^m / \text{kJ.mol}^{-1}$	[C ₁₆ MImCl]/mM	$\Delta H_0^m / \text{kJ.mol}^{-1}$
0		0		0		0	
0.060	2.811	0.005	0.455	0.003	-3.420	0.002	1.284
0.108	1.914	0.027	0.465	0.017	-3.489	0.011	1.366
0.155	0.527	0.048	0.466	0.031	-3.374	0.019	1.606
0.201	-0.367	0.069	0.509	0.044	-2.859	0.027	1.697
0.247	-0.885	0.090	0.560	0.070	-3.105	0.035	1.480
0.293	-0.859	0.111	0.611	0.083	-3.262	0.043	1.203
0.338	-0.772	0.131	0.604	0.096	-1.459	0.052	0.859
0.383	-0.664	0.152	0.570	0.109	0.301	0.059	0.350
0.427	-0.655	0.172	0.523	0.122	1.009	0.067	0.127
0.471	-0.668	0.192	0.468	0.134	1.596	0.075	0.013
0.514	-0.628	0.211	0.412	0.146	1.437	0.083	-0.060
0.557	-0.641	0.231	0.369	0.159	1.608	0.090	-0.123
0.599	-0.662	0.250	0.329	0.171	1.281	0.098	-0.188
0.641	-0.611	0.269	0.299	0.183	1.800	0.105	-0.228
0.683	-0.574	0.288	0.257	0.194	1.656	0.113	-0.271
0.724	-0.558	0.306	0.213	0.206	1.979	0.120	-0.294
0.764	-0.603	0.324	0.181	0.218	2.442	0.127	-0.332
0.804	-0.617	0.343	0.142	0.229	2.363	0.134	-0.356
0.843	-0.526	0.361	0.126	0.240	1.891	0.141	-0.355
						0.148	-0.405

2.9. Calorimetric titration data of C₁₆MImCl at different [Na₂SO₄] at 298.15 K

Demicellization of C ₁₆ MImCl in different [Na ₂ SO ₄] in mol.kg ⁻¹							
0.001		0.005		0.010		0.020	
[C ₁₆ MImCl]/mM	$\Delta H_0^m / \text{kJ.mol}^{-1}$	[C ₁₆ MImCl]/mM	$\Delta H_0^m / \text{kJ.mol}^{-1}$	[C ₁₆ MImCl]/mM	$\Delta H_0^m / \text{kJ.mol}^{-1}$	[C ₁₆ MImCl]/mM	$\Delta H_0^m / \text{kJ.mol}^{-1}$
0		0		0		0	
0.018	-0.470	0.003	0.176	0.015	0.028	0.001	0.207
0.025	-0.442	0.024	0.192	0.019	0.037	0.012	0.210
0.033	-0.237	0.038	0.221	0.023	0.048	0.020	0.233
0.036	-0.022	0.049	0.249	0.025	0.053	0.029	0.334
0.040	0.002	0.060	0.253	0.029	0.100	0.043	0.377
0.043	-0.107	0.071	0.253	0.032	0.140	0.072	0.364
0.047	0.079	0.082	0.248	0.034	0.178	0.086	0.357
0.069	0.125	0.093	0.241	0.038	0.201	0.101	0.345
0.079	0.140	0.093	0.241	0.042	0.211	0.115	0.339

0.083	0.165	0.103	0.238	0.046	0.216	0.129	0.329
0.086	0.175	0.114	0.234	0.047	0.216	0.144	0.318
0.094	0.167	0.125	0.228	0.051	0.211	0.158	0.304
0.108	0.173	0.136	0.224	0.053	0.205	0.172	0.294
0.111	0.150	0.146	0.219	0.055	0.200	0.186	0.284
0.133	0.186	0.157	0.214	0.059	0.187	0.200	0.275
0.157	0.157	0.167	0.209	0.062	0.171	0.229	0.259
0.168	0.112	0.178	0.206	0.066	0.158	0.271	0.239
0.171	0.106	0.191	0.199	0.070	0.142	0.299	0.222
0.178	0.105	0.199	0.195	0.077	0.116	0.327	0.212
0.213	0.124	0.207	0.192	0.081	0.101		
0.227	0.099	0.217	0.188	0.083	0.092		
0.241	0.100	0.228	0.183	0.087	0.076		
0.255	0.070	0.243	0.176	0.090	0.064		
		0.253	0.171				
		0.264	0.167				
		0.274	0.162				
		0.284	0.157				
		0.294	0.153				
		0.305	0.149				

2.10. Calorimetric titration data of C₁₆MImCl at different [Na₃PO₄] at 298.15 K

Demicellization of C ₁₆ MImCl in different [Na ₃ PO ₄] in mol.kg ⁻¹					
0.005		0.010		0.020	
[C ₁₆ MImCl]/mM	$\Delta H_0^m /$ kJ.mol ⁻¹	[C ₁₆ MImCl]/mM	$\Delta H_0^m /$ kJ.mol ⁻¹	[C ₁₆ MImCl]/mM	$\Delta H_0^m /$ kJ.mol ⁻¹
0		0		0	
0.048	2.064	0.025	0.327	0.022	-0.081
0.051	2.002	0.030	0.332	0.029	-0.023
0.055	1.851	0.035	0.335	0.036	-0.011
0.059	2.092	0.041	0.339	0.040	0.021
0.062	2.163	0.043	0.505	0.047	0.074
0.066	2.108	0.046	0.629	0.051	0.287
0.070	2.261	0.049	0.655	0.054	1.173
0.073	2.338	0.051	0.662	0.058	1.260
0.077	2.443	0.054	0.654	0.061	1.306
0.081	2.417	0.057	0.649	0.068	1.350
0.084	2.337	0.059	0.632	0.076	1.333
0.088	2.113	0.062	0.643	0.083	1.330
0.091	2.395	0.065	0.623	0.090	1.275
0.095	3.293	0.067	0.627	0.101	1.214
0.099	3.950	0.073	0.612	0.108	1.167
0.117	3.349	0.078	0.610	0.118	1.114
0.120	3.159	0.083	0.592	0.125	1.038

0.124	2.955	0.089	0.578	0.132	1.032
0.128	2.586	0.094	0.579	0.143	0.968
0.135	2.287	0.097	0.558	0.154	0.939
0.138	2.170	0.099	0.587	0.161	0.866
0.142	2.069	0.102	0.542	0.168	0.857
0.145	1.948	0.105	0.542	0.178	0.817
0.149	1.711	0.110	0.518	0.185	0.729
0.153	1.404	0.112	0.523	0.192	0.723
0.156	1.112	0.115	0.541	0.199	0.682
0.163	0.709	0.118	0.507	0.206	0.651
0.167	0.507	0.120	0.481	0.213	0.626
		0.126	0.499	0.220	0.603
		0.131	0.477	0.227	0.555
		0.134	0.464	0.234	0.532
		0.139	0.458	0.241	0.538
		0.144	0.449	0.247	0.431
		0.149	0.440	0.254	0.371
		0.154	0.428	0.261	0.334
		0.160	0.417	0.268	0.336
		0.165	0.404	0.275	0.316
		0.170	0.389	0.282	
		0.175	0.383		
		0.180	0.367		
		0.186	0.358		
		0.191	0.353		
		0.196	0.343		
		0.201	0.337		
		0.206	0.323		
		0.211	0.300		
		0.216	0.282		
		0.222	0.275		
		0.227	0.256		
		0.232	0.245		

2.11. Steady state fluorescence anisotropy (r) vs. concentration of $C_{16}MImCl$ in presence of different salts (each with a concentration of $0.001 \text{ mol.kg}^{-1}$) at 298.15 K .

[Salt] = 0.01 mol.kg^{-1}							
NaCl		NaBr		Na ₂ SO ₄		Na ₃ PO ₄	
10^3 [C ₁₆ MImCl] / mol.kg ⁻¹	r	10^3 [C ₁₆ MImCl] / mol.kg ⁻¹	r	10^3 [C ₁₆ MImCl] / mol.kg ⁻¹	r	10^3 [C ₁₆ MImCl] / mol.kg ⁻¹	r
0	0.342	0	0.252	0	0.299	0	0.245
0.007	0.313	0.011	0.219	0.004	0.310	0.006	0.255
0.022	0.303	0.022	0.181	0.009	0.336	0.017	0.257
0.050	0.304	0.045	0.171	0.017	0.301	0.029	0.257
0.079	0.279	0.067	0.165	0.026	0.306	0.044	0.254
0.107	0.258	0.100	0.162	0.043	0.295	0.067	0.248
0.150	0.231	0.155	0.128	0.060	0.283	0.090	0.240
0.206	0.223	0.209	0.109	0.085	0.248	0.113	0.227
0.275	0.198	0.317	0.081	0.111	0.230	0.147	0.173
0.344	0.180	0.423	0.067	0.153	0.206	0.204	0.105
0.447	0.156	0.579	0.063	0.236	0.192	0.261	0.079
0.580	0.117	0.781	0.059	0.358	0.188	0.317	0.071
0.777	0.096	1.025	0.058	0.556	0.181	0.372	0.062
1.029	0.077	1.398	0.050	0.929	0.181	0.455	0.056
1.273	0.061			1.276	0.181	0.563	0.055
1.566	0.060			1.599	0.176	0.671	0.053
1.846	0.061			1.901	0.177		
2.370	0.062			2.450	0.176		

2.12. Time resolved quenching data of Pyrene in presence of different [CPC] in presence of Na₂SO₄ and Na₃PO₄ ($0.001 \text{ mol.kg}^{-1}$) at 298.15 K

Time (ns)	prompt	Quenching of Pyrene in presence of CPC at $0.001 \text{ mol.kg}^{-1}$ concentration of Na ₂ SO ₄			Quenching of Pyrene in presence of CPC at $0.001 \text{ mol.kg}^{-1}$ concentration of Na ₃ PO ₄		
		[CPC] = 0 mmol.kg ⁻¹	[CPC] = 0.16 mmol.kg ⁻¹	[CPC] = 0.31 mmol.kg ⁻¹	[CPC] = 0 mmol.kg ⁻¹	[CPC] = 0.16 mmol.kg ⁻¹	[CPC] = 0.31 mmol.kg ⁻¹
		log (Count)	log (Count)	log (Count)	log (Count)	log (Count)	log (Count)
0.48	0	0	0	0	0	0	0
0.96	0	0	0	0	0	0	0
1.44	0	0	0	0	0	0	0
1.92	0	0	0	0	0	0	0
2.40	0	0	0	0	0	0	0
2.87	0	0	0	0	0	0	0
3.35	0	0	0	0	0	0	0
3.83	0	0	0	0	0	0	0
4.31	0	0	0	0	0	0	0
4.79	0	0	0	0	0	0	0
5.27	0	0	0	0	0	0	0
5.75	0	0	0	0	0	0	0

6.23	0	0	0	0	0	0	0
6.71	0	0	0	0	0	0	0
7.19	0	0	0	0	0	0	0
7.67	0	0	0	0	0	0	0
8.14	0	0	0	0	0	0	0
8.62	0	0	0	0	0	0	0
9.10	0	0	0	0	0	0	0
9.58	9	6	7	3	0	2	7
10.06	889	357	312	361	236	254	281
10.54	2160	1248	1298	1362	1258	1281	1267
11.02	893	1806	1835	1877	1750	1748	1882
11.50	158	1940	1989	2003	1980	2003	2001
11.98	39	2000	2005	1945	2002	1948	1961
12.46	10	1908	1840	1890	1926	1803	1793
12.94	2	1949	1923	1786	1870	1831	1843
13.41	1	1972	1806	1807	1925	1824	1781
13.89	1	1819	1730	1742	1826	1750	1724
14.37	0	1892	1893	1759	1832	1768	1692
14.85	0	1872	1895	1715	1981	1827	1767
15.33	0	1862	1646	1598	1785	1620	1705
15.81	0	1836	1605	1533	1768	1649	1614
16.29	1	1820	1701	1583	1846	1733	1583
16.77	0	1793	1654	1502	1800	1686	1495
17.25	0	1746	1550	1457	1681	1551	1466
17.73	0	1768	1586	1519	1872	1596	1516
18.21	0	1741	1564	1455	1770	1581	1476
18.68	0	1658	1567	1367	1725	--	1412
19.16	0	1777	1522	1445	1792	1534	1393
19.64	0	1768	1552	1420	1767	1513	--
20.12	0	1735	1518	1360	1640	1494	1391
20.60	0	1675	1475	1372	1673	1558	1355
21.08	0	1691	1513	1252	1808	1488	1319
21.56	0	1618	1510	1264	1754	1442	1274
22.04	0	1609	1418	1284	1631	1365	1191
22.52	1	1639	1465	1246	1763	1455	1306
23.00	0	1650	1451	1233	1645	1392	1259
23.48	0	1615	1382	1241	1609	1367	1176
23.95	0	1664	1376	1211	1633	1392	1246
24.43	0	1641	1459	1146	1603	1373	1233
24.91	0	1595	1392	1111	1669	1347	1087
25.39	0	1610	1340	1154	1677	1365	1136
25.87	0	1570	1382	1193	1629	1289	1165
26.35	0	1565	1313	1077	1592	1328	1005
26.83	0	1598	1241	1104	1638	1345	1142

27.31	0	1550	1332	1088	1609	1301	1135
27.79	0	1516	1283	1027	1426	1295	1006
28.27	0	1471	1327	1028	1619	1261	1004
28.74	0	1535	1199	973	1612	1216	1055
29.22	0	1490	1253	1020	1546	1257	1007
29.70	0	1524	1228	1005	1567	1263	1008
30.18	0	1518	1233	991	1582	1208	1023
30.66	0	1524	1284	943	1568	1166	958
31.14	0	1500	1137	907	1531	1118	981
31.62	0	1509	1134	924	1518	1185	975
32.10	0	1536	1136	902	1466	1167	950
32.58	0	1498	1100	958	1487	1075	935
33.06	0	1434	1149	909	1544	1177	935
33.54	0	1472	1146	889	1482	1130	940
34.01	0	1442	1121	898	1466	1141	855
34.49	1	1374	1070	837	1429	1106	869
34.97	0	1468	1102	828	1414	1062	854
35.45	0	1436	1068	811	1445	1053	829
35.93	0	1432	1083	805	1502	1058	830
36.41	0	1441	1074	824	1442	1048	831
36.89	0	1374	1049	823	1447	1057	774
37.37	0	1354	981	750	1436	1033	784
37.85	0	--	--	756	1433	1027	842
38.33	0	1359	1032	710	1417	1078	824
39.28	0	1407	1066	762	1458	1067	820
39.76	0	1393	1043	709	1372	1032	772
40.24	0	1369	1011	668	1395	992	760
40.72	0	1370	1000	719	1401	1011	816
41.20	0	1343	953	710	--	1013	744
41.68	0	1342	947	691	1344	958	719
42.16	0	1342	953	659	1372	981	733
42.64	0	1334	977	694	1370	955	730
43.12	0	1306	999	661	1299	948	692
43.60	0	1328	974	673	1386	942	682
44.08	0	1256	966	677	1372	953	662
44.55	0	1289	922	668	1272	917	696
45.03	0	1330	949	649	1376	989	712
45.51	0	1329	915	621	1291	930	678
45.99	0	1249	915	593	1399	909	653
46.47	0	1255	901	618	1280	886	659
46.95	0	1234	872	636	1316	880	635
47.43	0	1223	882	584	1324	895	654
47.91	0	1245	856	560	1222	857	666
48.39	0	1255	908	597	1411	849	635

48.87	0	1268	910	574	1308	794	676
49.35	0	1255	820	556	1265	817	659
49.82	0	1285	856	546	1265	874	659
50.30	0	1206	776	559	1274	828	615
50.78	0	1271	804	558	1257	854	606
51.26	0	1216	847	550	1281	821	604
51.74	0	1230	805	513	1220	877	621
52.22	0	1105	828	537	1204	776	595
52.70	0	1208	823	533	1246	863	562
53.18	0	1191	829	560	1188	771	574
53.66	0	1144	820	559	1230	780	578
54.14	0	1215	774	536	1256	819	558
54.62	0	1210	780	536	1170	795	625
55.09	0	1184	780	535	1220	802	575
55.57	0	1203	787	532	1258	768	520
56.05	0	1221	794	491	1204	772	522
56.53	0	1096	735	472	1240	767	549
57.01	0	1191	760	484	1191	744	487
57.49	0	1156	715	461	1267	742	536
57.97	0	1201	756	483	1217	803	478
58.45	0	1104	740	454	1215	770	506
58.93	0	1118	772	435	1192	747	546
59.41	0	1148	711	465	1149	791	528
59.89	0	1159	708	495	1209	736	488
60.36	0	1151	732	471	1191	762	505
60.84	0	1115	756	485	1105	747	521
61.32	0	1138	717	443	1194	725	481
61.80	0	1088	790	450	1248	726	465
62.28	0	1098	697	467	1154	738	503
62.76	0	1077	687	408	1164	709	509
63.24	0	1063	697	416	1179	737	433
63.72	0	1161	716	448	1151	678	479
64.20	1	1122	686	434	1175	695	441
64.68	0	1088	726	416	1088	691	450
65.16	0	1137	631	431	1147	710	460
65.63	0	1169	659	409	1121	712	428
66.11	0	1043	696	417	1158	725	453
66.59	0	1116	715	402	1148	648	416
67.07	0	1079	626	423	1109	669	402
67.55	0	1090	648	400	1103	641	438
68.03	0	1092	691	424	1127	675	442
68.51	0	1098	667	383	1113	636	446
68.99	0	1014	640	378	1143	686	443
69.47	0	1033	649	392	1122	679	419

69.95	0	1090	630	405	1031	643	439
70.43	0	1038	710	383	1180	677	440
70.90	0	1078	618	388	1076	663	445
71.38	0	1088	648	329	1075	618	388
71.86	0	1094	625	375	1038	635	415
72.34	0	1033	659	364	1164	599	436
72.82	0	997	639	364	1076	610	412
73.30	0	1014	585	358	1051	624	416
73.78	0	1034	610	360	1089	638	442
74.26	0	1029	606	345	1032	586	394
74.74	0	1030	577	347	1082	642	361
75.22	0	1000	555	352	1048	603	373
75.70	0	992	622	339	1071	605	404
76.17	0	973	566	367	1036	607	360
76.65	0	1025	579	367	1028	623	379
77.13	0	996	563	341	1034	589	367
77.61	0	991	544	329	1051	573	338
78.09	0	968	514	318	1009	576	357
78.57	0	957	560	331	960	583	348
79.05	0	924	533	314	1058	591	371
79.53	0	913	545	346	1012	572	360
80.01	0	990	550	306	1006	574	367
80.49	0	950	569	309	1015	534	379
80.96	0	975	586	289	1029	551	353
81.44	0	980	530	307	1003	569	370
81.92	0	994	508	325	955	538	318
82.40	0	920	533	309	987	542	337
82.88	0	928	542	293	1055	539	338
83.36	0	997	532	284	968	518	348
83.84	0	953	531	292	1030	547	331
84.32	0	952	524	283	985	541	333
84.80	0	926	539	287	987	564	298
85.28	0	957	527	274	1016	520	342
85.76	0	920	533	274	1059	546	322
86.23	0	963	513	294	939	568	340
86.71	0	914	523	284	967	508	331
87.19	0	950	499	294	954	526	309
87.67	0	953	503	278	919	510	326
88.15	0	918	516	270	1033	543	312
88.63	0	888	509	278	935	539	313
89.11	0	878	492	272	936	487	307
89.59	0	930	511	263	966	502	320
90.07	0	894	497	269	964	492	276
90.55	0	898	465	272	985	483	300

91.03	0	928	505	283	935	535	278
91.50	0	882	492	267	928	472	288
91.98	0	887	482	254	954	525	331
92.46	0	862	487	239	912	501	296
92.94	0	899	470	243	888	486	312
93.42	0	908	476	273	916	489	322
93.90	0	893	473	266	958	496	284
94.38	0	876	426	254	962	503	291
94.86	0	815	421	250	904	478	287
95.34	0	865	457	246	898	482	248
95.82	0	887	470	251	919	441	290
96.30	0	854	482	238	922	474	304
96.77	0	869	467	260	829	451	278
97.25	0	846	428	274	846	493	263
97.73	0	859	464	220	902	452	298
98.21	0	865	502	248	869	486	300
98.69	0	884	467	231	940	457	254
99.17	0	853	424	229	868	465	280
99.65	0	770	422	232	903	483	262
100.1	0	882	446	216	870	429	259
100.6	0	897	425	216	927	465	298
101.1	0	798	446	253	886	505	251
101.6	0	819	419	199	873	418	251
102.0	0	792	393	242	883	423	260
102.5	0	846	444	229	867	446	277
103.0	0	857	400	205	903	431	224
103.5	0	816	400	213	875	458	229
104.0	0	838	408	202	891	459	278
104.4	0	775	444	203	836	439	240
104.9	0	779	432	244	841	431	264
105.4	0	744	443	205	886	404	233
105.9	0	820	379	210	854	440	253
106.4	0	857	428	234	872	435	250
106.8	0	734	417	204	842	399	252
107.3	0	804	400	195	856	443	242
107.8	0	767	400	225	849	405	217
108.3	0	748	428	194	879	408	254
108.8	0	763	425	220	829	426	256
109.2	0	771	410	202	863	428	232
109.7	0	771	433	200	822	418	246
110.2	0	760	415	207	862	418	250
110.7	0	800	402	183	836	405	203
111.1	0	764	367	209	832	434	253
111.6	0	767	369	200	824	425	214

112.1	0	811	400	192	842	378	271
112.6	0	804	404	179	853	419	243
113.1	0	751	395	195	796	426	247
113.5	0	727	395	204	863	368	196
114.0	0	751	384	208	805	400	250
114.5	0	715	413	187	812	420	224
115.0	0	761	368	179	818	374	238
115.5	0	770	369	196	753	420	219
115.9	0	776	390	187	781	411	199
116.4	0	714	356	169	782	370	218
116.9	0	763	380	161	724	405	205
117.4	0	753	351	174	776	371	185
117.9	0	744	361	177	801	361	219
118.3	0	741	346	185	795	380	234
118.8	0	742	382	179	816	396	199
119.3	0	715	360	148	829	373	218
119.8	0	775	385	169	791	386	202
120.2	0	707	342	167	796	365	197
120.7	0	737	386	163	791	381	219
121.2	0	715	353	186	782	362	214
121.7	0	722	362	172	711	377	212
122.2	0	672	379	168	772	316	203
122.6	0	672	353	142	759	356	205
123.1	0	690	352	186	759	316	201
123.6	0	694	364	172	748	413	208
124.1	0	668	331	165	768	368	202
124.6	0	677	357	170	726	351	200
125.0	0	695	316	153	725	362	186
125.5	0	712	350	166	758	340	200
126.0	0	695	360	168	703	336	221
126.5	0	632	314	185	726	341	184
127.0	0	676	347	138	739	367	200
127.4	0	693	346	161	775	356	200
127.9	0	701	320	149	715	327	184
128.4	0	626	351	155	735	342	177
128.9	0	686	309	161	638	358	186
129.4	0	653	334	142	737	372	187
129.8	0	687	353	150	743	350	184
130.3	0	661	326	145	727	324	159
130.8	0	665	338	149	693	322	164
131.3	0	651	329	136	685	332	188
131.7	0	644	338	130	730	316	162
132.2	0	660	367	144	733	306	165
132.7	0	621	310	160	750	351	166

133.2	0	615	291	150	722	353	191
133.7	0	674	319	142	766	344	167
134.1	0	621	300	137	684	309	179
134.6	0	646	297	138	667	297	192
135.1	0	598	313	163	702	343	162
135.6	0	688	292	149	735	300	177
136.1	0	601	305	154	731	328	182
136.5	0	642	288	131	694	322	164
137.0	0	709	311	162	679	317	143
137.5	0	628	302	141	673	309	183
138.0	0	631	293	131	726	310	167
138.5	0	602	313	170	653	304	178
138.9	0	572	302	160	653	283	179
139.4	0	631	329	135	641	328	150
139.9	0	595	300	135	678	350	163
140.4	0	636	320	132	652	321	158
140.9	0	610	277	149	669	306	162
141.3	0	637	306	151	694	291	169
141.8	0	597	281	125	643	289	167
142.3	0	594	305	126	712	270	150
142.8	0	632	320	116	639	305	144
143.2	0	582	297	142	665	308	144
143.7	0	568	300	152	661	302	138
144.2	0	573	269	141	709	322	159
144.7	0	613	293	128	681	296	150
145.2	0	602	280	130	663	301	170
145.6	0	613	267	139	684	298	154
146.1	0	623	275	142	652	310	155
146.6	0	615	269	136	664	283	155
147.1	0	593	257	122	658	294	184
147.6	0	601	280	146	628	290	160
148.0	0	582	271	146	626	311	140
148.5	0	606	285	113	649	300	130
149.0	0	519	301	117	627	292	172
149.5	0	617	282	144	585	301	166
150.0	0	590	268	119	599	274	145
150.4	0	604	241	114	611	286	153
150.9	0	583	273	114	613	267	132
151.4	0	571	298	113	636	266	159
151.9	0	571	284	112	662	282	159
152.3	0	588	266	125	629	279	149
152.8	0	551	273	124	658	301	150
153.3	0	595	247	125	590	245	138
153.8	0	565	264	124	631	276	139

154.3	0	556	264	124	589	273	129
154.7	0	539	272	128	624	312	136
155.2	0	548	271	118	613	257	147
155.7	0	567	267	118	582	288	146
156.2	0	548	248	114	632	268	158
156.7	0	583	243	120	594	254	139
157.1	0	498	260	121	587	250	128
157.6	0	563	265	106	620	263	152
158.1	0	552	215	130	625	255	138
158.6	0	543	273	103	641	272	142
159.1	0	573	246	97	592	286	133
159.5	0	532	227	110	598	285	131
160.0	0	565	257	117	568	279	117
160.5	0	551	255	114	568	270	147
161.0	0	524	269	130	626	247	139
161.5	0	551	226	114	556	244	124
161.9	0	557	277	100	577	261	123
162.4	0	480	252	124	610	251	128
162.9	0	466	243	96	614	257	122
163.4	0	531	256	108	570	259	130
163.8	0	522	227	116	554	296	123
164.3	0	485	258	118	548	255	124
164.8	0	534	252	99	560	252	134
165.3	0	469	252	138	594	257	112
165.8	0	500	216	97	564	261	122
166.2	0	526	234	104	578	238	107
166.7	0	529	230	107	568	236	125
167.2	0	514	234	92	542	238	152
167.7	0	483	251	110	527	238	111
168.2	0	509	275	106	591	244	136
168.6	0	527	241	112	536	259	131
169.1	0	526	250	105	563	230	111
169.6	0	515	229	123	544	233	112
170.1	0	502	241	86	539	232	118
170.6	0	494	242	117	563	203	122
171.0	0	504	232	90	530	236	111
171.5	0	512	213	103	545	225	132
172.0	0	464	231	105	546	243	108
172.5	0	473	194	97	579	260	115
172.9	0	494	232	95	517	242	107
173.4	0	471	222	99	587	242	106
173.9	0	503	235	85	561	244	116
174.4	0	485	210	96	560	227	123
174.9	0	504	222	91	541	217	119

175.3	0	468	217	116	545	236	127
175.8	0	464	210	116	515	244	119
176.3	0	491	203	83	528	223	116
176.8	0	474	245	100	556	254	110
177.3	0	511	212	86	496	240	116
177.7	0	477	218	90	533	209	114
178.2	0	464	212	101	524	240	103
178.7	0	480	219	96	541	243	107
179.2	0	443	217	85	529	222	119
179.7	0	419	215	95	511	241	124
180.1	0	484	217	96	544	261	130
180.6	0	453	216	98	511	238	114
181.1	0	469	232	98	524	221	122
181.6	0	483	215	109	535	216	106
182.1	0	468	187	92	539	243	120
182.5	0	494	189	91	539	217	113
183.0	0	447	204	81	498	231	101
183.5	0	469	200	113	487	221	94
184.0	0	458	216	95	538	200	104
184.4	0	438	211	98	545	203	98
184.9	0	479	209	100	549	220	94
185.4	0	446	197	92	487	228	98
185.9	0	441	198	101	478	206	111
186.4	0	429	194	91	524	198	106
186.8	0	464	192	92	504	216	105
187.3	0	430	209	91	486	208	83
187.8	0	432	197	81	510	192	105
188.3	0	426	182	78	511	185	84
188.8	0	482	172	83	507	197	100
189.2	0	447	183	88	450	203	110
189.7	1	424	203	77	489	205	96
190.2	0	432	181	88	486	190	101
190.7	0	437	189	74	458	202	96
191.2	0	446	200	71	453	197	116
191.6	0	465	194	82	474	193	89
192.1	0	403	195	96	531	181	96
192.6	0	418	184	84	465	196	103
193.1	0	430	198	86	460	182	94
193.5	0	425	196	85	498	190	100
194.0	0	428	177	95	503	207	81
194.5	0	442	206	86	459	196	114
195.0	0	424	188	100	481	191	107
195.5	0	420	178	67	450	192	94
195.9	0	400	192	69	482	187	85

196.4	0	397	188	84	453	170	101
196.9	0	406	190	70	458	199	106
197.4	0	395	189	79	442	187	85
197.9	0	441	187	81	425	193	96
198.3	0	392	196	78	443	200	82
198.8	0	397	216	96	431	175	98
199.3	0	362	207	71	471	183	96
199.8	0	412	213	69	463	181	94
200.3	0	443	155	75	450	220	100
200.7	0	432	193	82	462	202	87
201.2	0	390	187	95	434	175	93
201.7	0	438	182	67	467	197	80
202.2	0	409	189	80	462	206	97
202.7	0	377	201	84	468	180	94
203.1	0	425	184	84	430	174	86
203.6	0	403	178	77	418	188	92
204.1	0	402	194	76	434	176	101
204.6	0	441	170	90	477	187	100
205.0	0	422	194	70	463	181	91
205.5	0	398	175	74	474	198	81
206.0	0	422	176	62	448	151	83
206.5	0	368	147	75	437	171	73
207.0	0	423	164	77	443	180	80
207.4	0	420	177	93	413	169	85
207.9	0	379	172	69	441	188	86
208.4	0	367	176	70	457	154	88
208.9	0	376	178	63	456	158	82
209.4	0	355	166	64	431	173	82
209.8	0	355	177	86	444	175	76
210.3	0	412	174	69	432	183	93
210.8	0	368	163	78	430	155	83
211.3	0	385	174	61	426	156	80
211.8	0	365	194	76	405	186	82
212.2	0	362	176	66	407	179	105
212.7	0	351	142	58	413	191	83
213.2	0	373	150	69	412	183	83
213.7	0	377	169	62	395	181	85
214.2	0	398	154	63	425	168	84
214.6	0	381	161	64	465	182	78
215.1	0	369	165	74	394	183	81
215.6	0	363	193	76	438	166	98
216.1	0	389	159	66	423	181	90
216.5	0	388	179	65	415	181	79
217.0	0	384	185	77	385	182	80

217.5	0	351	149	74	426	188	89
218.0	1	349	171	64	430	145	76
218.5	0	347	166	61	417	154	81
218.9	0	372	147	74	389	161	88
219.4	0	353	140	65	388	136	75
219.9	0	331	155	78	413	156	88
220.4	0	344	148	71	406	158	79
220.9	0	373	148	73	373	155	85
221.3	0	353	146	65	395	156	88
221.8	0	369	169	73	418	166	77
222.3	0	362	147	65	393	164	88
222.8	0	360	176	70	417	161	76
223.3	0	366	152	77	400	153	73
223.7	0	346	146	83	374	171	68
224.2	0	337	150	67	364	147	74
224.7	0	342	147	70	392	186	71
225.2	0	388	154	57	403	152	77
225.6	0	320	133	56	400	151	86
226.1	0	380	151	66	413	149	73
226.6	0	325	144	71	356	147	75
227.1	0	369	184	78	385	168	80
227.6	0	319	158	70	390	176	89
228.0	0	338	154	72	395	144	80
228.5	0	333	138	60	389	174	79
229.0	0	319	132	62	404	167	91
229.5	0	360	156	67	380	127	73
230.0	0	339	141	46	387	158	78
230.4	0	352	152	77	380	167	76
230.9	0	320	144	87	376	151	84
231.4	0	343	149	76	373	178	83
231.9	0	314	147	60	343	151	59
232.4	0	340	131	52	392	179	76
232.8	0	309	140	63	392	149	82
233.3	0	334	145	64	382	145	77
233.8	0	323	154	47	374	144	76
234.3	0	328	127	60	373	130	74
234.8	0	321	134	65	340	138	75
235.2	0	311	130	52	345	135	73
235.7	0	333	121	66	373	153	73
236.2	0	334	156	60	347	165	77
236.7	0	310	155	68	380	144	70
237.1	0	305	150	55	373	152	61
237.6	0	333	170	69	355	154	63
238.1	0	313	147	55	372	154	73

238.6	0	315	127	63	353	159	70
239.1	0	298	139	63	368	139	65
239.5	0	299	102	58	342	184	77
240.0	0	353	135	62	329	139	68
240.5	0	313	136	62	378	132	69
241.0	0	308	150	60	361	135	76
241.5	0	328	134	46	361	145	79
241.9	0	310	127	59	375	136	56
242.4	0	296	127	58	377	146	65
242.9	0	311	134	44	346	126	72
243.4	0	294	141	51	366	138	75
243.9	0	315	154	66	322	128	62
244.3	0	306	137	59	369	142	52
244.8	0	281	120	49	367	119	64
245.3	0	329	135	64	368	128	60
245.8	0	322	150	49	343	125	67
246.2	0	305	122	58	331	137	81
246.7	0	290	121	50	342	141	65
247.2	0	293	135	58	334	164	75
247.7	0	301	152	49	354	139	71
248.2	0	315	119	67	339	137	62
248.6	0	296	124	48	350	152	60
249.1	0	315	146	47	311	133	54
249.6	0	307	121	67	335	154	59
250.1	0	262	120	51	331	110	69
250.6	0	289	106	50	327	136	65
251.0	0	296	121	50	342	131	77
251.5	0	284	138	52	303	135	65
252.0	0	284	125	57	286	130	57
252.5	0	303	128	40	289	124	46
253.0	0	278	119	51	359	157	70
253.4	0	262	121	61	315	124	65
253.9	0	295	134	50	308	128	69
254.4	0	278	124	57	327	137	54
254.9	0	283	121	64	325	120	54
255.4	0	278	115	55	340	151	61
255.8	0	301	142	58	319	125	51
256.3	0	293	145	42	306	128	53
256.8	0	288	114	60	327	127	55
257.3	0	274	113	43	303	134	60
257.7	0	267	120	48	341	107	61
258.2	0	309	112	45	314	123	61
258.7	0	272	114	44	306	140	68
259.2	0	285	123	61	317	128	57

259.7	0	280	128	49	297	117	55
260.1	0	305	108	46	325	124	57
260.6	0	276	115	50	307	126	59
261.1	0	258	129	50	315	139	46
261.6	0	306	129	54	338	158	74
262.1	0	244	108	46	317	115	61
262.5	0	275	122	45	304	128	62
263.0	0	247	101	51	300	107	67
263.5	0	297	107	50	323	114	51
264.0	0	271	119	43	296	134	63
264.5	0	270	117	47	277	127	54
264.9	0	260	113	46	297	114	51
265.4	0	250	98	36	318	150	57
265.9	0	259	143	58	297	114	68
266.4	0	261	117	47	337	136	54
266.8	0	259	112	54	309	106	55
267.3	0	263	132	46	295	116	62
267.8	0	295	107	51	286	110	55
268.3	0	287	110	49	299	129	53
268.8	0	264	111	42	284	119	55
269.2	0	278	107	42	310	110	52
269.7	0	287	106	44	300	102	57
270.2	0	241	112	35	291	118	53
270.7	0	273	126	57	295	97	63
271.2	0	248	109	45	299	102	55
271.6	0	267	105	47	340	107	59
272.1	0	291	123	37	301	130	52
272.6	0	264	126	42	288	108	65
273.1	0	232	99	43	298	99	49
273.6	0	257	90	57	299	142	50
274.0	0	266	109	60	285	88	63
274.5	0	255	90	40	328	121	53
275.0	0	254	113	46	276	130	48
275.5	0	252	101	41	312	106	48
276.0	0	252	106	38	280	102	45
276.4	0	248	99	42	274	114	54
276.9	0	230	105	47	301	104	53
277.4	0	223	110	48	290	96	46
277.9	0	233	108	37	265	111	44
278.3	0	255	120	41	281	106	49
278.8	0	256	97	55	284	111	45
279.3	0	240	119	47	277	127	57
279.8	0	236	106	45	262	117	46
280.3	0	232	83	33	279	124	57

280.7	0	267	106	42	258	109	40
281.2	0	260	85	37	298	106	58
281.7	0	239	103	36	266	99	53
282.2	0	263	103	45	291	131	49
282.7	0	227	99	39	289	117	57
283.1	0	248	96	43	289	107	47
283.6	0	240	108	33	269	119	48
284.1	0	233	111	43	279	96	47
284.6	0	236	96	53	298	126	43
285.1	0	250	93	45	264	80	42
285.5	0	227	101	40	285	105	49
286.0	0	247	100	48	261	106	42
286.5	0	236	95	46	262	120	43
287.0	0	260	91	49	253	98	46
287.4	0	201	107	33	260	104	64
287.9	0	252	86	37	300	112	54
288.4	0	239	87	34	246	104	51
288.9	0	252	103	28	259	103	45
289.4	0	227	106	43	266	133	54
289.8	0	221	103	40	281	92	54
290.3	0	227	90	41	271	100	49
290.8	0	216	104	41	245	102	44
291.3	0	204	91	46	268	88	47
291.8	0	223	103	44	243	90	45
292.2	0	206	86	43	261	113	52
292.7	0	209	98	33	252	82	32
293.2	0	243	101	30	279	100	48
293.7	0	218	100	48	263	101	40
294.2	0	217	89	30	235	95	47
294.6	0	231	92	42	230	106	48
295.1	0	237	92	45	266	108	48
295.6	0	239	85	40	252	98	47
296.1	0	194	78	37	242	109	53
296.6	0	218	102	32	245	99	48
297.0	0	181	84	41	244	101	45
297.5	0	200	87	30	251	97	36
298.0	0	232	108	40	256	89	52
298.5	0	225	94	39	262	82	53
298.9	0	246	82	37	248	91	53
299.4	0	192	106	44	265	108	44
299.9	0	227	96	37	258	81	39
300.4	0	199	92	45	246	95	58
300.9	0	245	88	38	270	104	38
301.3	0	223	89	44	256	104	49

301.8	0	204	99	40	250	98	41
302.3	0	210	81	36	235	96	45
302.8	0	232	82	29	280	97	49
303.3	0	206	82	28	247	97	51
303.7	0	196	92	40	228	108	46
304.2	0	174	97	38	248	86	50
304.7	0	214	95	31	222	114	46
305.2	0	211	87	37	236	114	47
305.7	0	187	95	27	225	92	40
306.1	0	214	99	39	262	115	46
306.6	0	214	73	36	261	97	56
307.1	0	184	81	32	235	105	41
307.6	0	199	103	35	233	95	35
308.1	0	191	77	30	233	97	49
308.5	0	204	91	42	226	101	36
309.0	0	181	94	32	250	87	42
309.5	0	206	98	25	213	94	54
310.0	0	202	74	44	232	86	32
310.4	0	203	64	31	226	94	48
310.9	0	185	86	31	237	80	28
311.4	0	177	70	31	259	81	44
311.9	0	212	73	31	244	85	34
312.4	0	203	81	37	216	89	37
312.8	0	210	82	33	239	86	40
313.3	0	193	75	26	216	87	43
313.8	0	185	107	35	244	94	34
314.3	0	218	92	48	223	89	35
314.8	0	202	71	33	210	85	45
315.2	0	200	68	37	270	95	48
315.7	0	196	82	31	231	91	44
316.2	0	226	69	28	206	75	45
316.7	0	206	78	32	210	102	40
317.2	0	158	86	36	248	88	41
317.6	0	185	96	39	245	70	59
318.1	0	199	99	33	241	82	36
318.6	0	176	78	35	214	83	40
319.1	0	184	81	34	206	78	43
319.5	0	165	69	41	226	93	40
320.0	0	173	83	24	220	84	44
320.5	0	204	78	45	188	71	43
321.0	0	200	103	38	221	90	51
321.5	0	181	58	27	222	100	38
321.9	0	195	80	35	210	89	45
322.4	0	212	75	30	210	74	38

322.9	0	179	76	32	215	100	46
323.4	0	176	75	39	216	83	38
323.9	0	184	83	30	200	93	39
324.3	0	183	79	36	202	80	37
324.8	0	180	80	32	191	80	30
325.3	0	180	73	35	211	84	30
325.8	0	184	80	41	199	85	37
326.3	0	178	73	27	191	88	41
326.7	0	176	70	31	194	73	46
327.2	0	175	70	27	239	81	39
327.7	0	190	72	40	209	70	40
328.2	0	172	72	45	218	57	52
328.7	1	173	85	32	196	81	39
329.1	0	206	72	33	204	91	51
329.6	0	184	84	28	199	68	31
330.1	0	166	88	33	206	82	47
330.6	0	171	68	36	216	71	36
331.0	0	179	72	31	230	82	42
331.5	0	185	77	35	212	95	33
332.0	0	167	67	32	216	79	47
332.5	0	189	71	20	214	76	43
333.0	0	177	68	33	223	77	29
333.4	0	176	81	31	226	73	38
333.9	0	166	66	31	191	86	44
334.4	0	171	84	35	230	73	32
334.9	0	189	71	30	199	74	35
335.4	0	174	86	22	172	77	30
335.8	0	167	81	42	196	67	37
336.3	0	157	74	28	197	70	39
336.8	0	153	73	32	213	73	36
337.3	0	188	82	31	207	64	34
337.8	0	155	63	31	186	79	40
338.2	0	168	77	31	194	79	39
338.7	0	155	54	23	207	85	42
339.2	0	184	79	27	175	84	45
339.7	0	171	70	31	170	80	30
340.1	0	148	71	27	204	81	36
340.6	0	149	68	23	186	78	42
341.1	0	163	66	28	182	71	36
341.6	0	170	71	34	187	74	38
342.1	0	178	65	33	175	86	25
342.5	0	141	72	39	203	66	39
343.0	0	161	83	20	184	90	37
343.5	0	179	75	35	192	86	41

344.0	0	142	59	30	202	66	30
344.5	0	158	74	27	194	73	33
344.9	0	170	75	20	192	61	33
345.4	0	146	63	26	169	62	41
345.9	0	148	71	26	187	66	26
346.4	0	172	51	23	192	61	42
346.9	0	156	60	29	199	76	35
347.3	0	158	63	27	198	76	27
347.8	0	152	65	26	192	69	29
348.3	0	168	57	25	201	61	36
348.8	0	157	49	34	221	78	50
349.3	0	159	69	28	160	76	29
349.7	0	160	71	29	182	58	36
350.2	0	155	53	22	190	69	32
350.7	0	150	68	26	186	78	32
351.2	0	166	55	25	205	65	39
351.6	0	173	49	20	170	65	25
352.1	0	169	60	27	188	69	36
352.6	0	161	81	37	178	87	28
353.1	0	147	72	28	171	80	48
353.6	0	135	58	29	173	77	36
354.0	0	144	67	35	174	77	21
354.5	0	130	61	35	167	69	43
355.0	0	136	61	17	199	59	33
355.5	0	144	73	20	169	72	35
356.0	0	128	60	30	197	65	29
356.4	0	159	69	22	181	54	41
356.9	0	142	53	24	180	73	29
357.4	0	140	53	23	182	68	40
357.9	0	143	60	22	199	63	35
358.4	0	165	73	30	179	73	40
358.8	0	121	64	36	184	74	36
359.3	0	136	66	31	160	56	39
359.8	0	160	49	23	162	57	29
360.3	0	153	69	26	171	70	37
360.7	0	150	57	26	169	72	33
361.2	0	142	68	27	171	65	33
361.7	0	145	54	26	164	66	35
362.2	0	140	82	22	152	62	27
362.7	0	148	56	30	152	52	31
363.1	0	141	65	23	213	67	33
363.6	0	135	52	30	157	70	32
364.1	0	129	59	25	188	63	25
364.6	0	139	53	32	172	58	30

365.1	0	141	57	31	183	67	23
365.5	0	147	70	21	165	64	29
366.0	0	117	59	16	159	62	28
366.5	0	156	65	27	154	80	22
367.0	0	145	67	17	174	58	33
367.5	0	131	66	30	152	66	37
367.9	0	146	59	25	173	65	42
368.4	0	163	60	16	153	69	23
368.9	0	136	62	17	137	75	31
369.4	0	140	69	13	161	72	28
369.9	0	133	67	24	160	71	22
370.3	0	143	50	27	172	53	33
370.8	0	140	62	20	146	78	26
371.3	0	154	48	30	168	58	32
371.8	0	132	53	24	156	59	34
372.2	0	141	61	23	167	72	29
372.7	0	132	55	19	173	63	29
373.2	0	127	67	18	163	62	29
373.7	0	142	58	31	172	76	28
374.2	0	136	67	23	163	61	31
374.6	0	136	66	18	164	65	18
375.1	0	138	54	25	195	63	28
375.6	0	140	51	23	137	68	30
376.1	0	108	51	22	174	66	25
376.6	0	135	63	25	158	70	32
377.0	0	124	53	25	147	66	31
377.5	0	148	58	23	159	64	23
378.0	0	130	66	22	155	58	22
378.5	0	138	43	29	181	60	22
379.0	0	159	55	19	160	51	27
379.4	0	130	50	25	160	56	21
379.9	0	135	47	22	140	63	24
380.4	0	128	54	22	148	68	40
380.9	0	109	56	15	141	61	17
381.3	0	135	50	18	174	57	33
381.8	0	135	54	20	158	61	32
382.3	0	125	47	30	146	53	23
382.8	0	116	52	30	146	53	26
383.3	0	126	54	24	164	58	22
383.7	0	104	61	19	158	62	28
384.2	0	112	50	17	146	56	33
384.7	0	149	64	23	155	59	27
385.2	0	113	56	26	137	47	19
385.7	0	122	56	23	129	67	33

386.1	0	119	52	17	153	55	23
386.6	0	122	51	16	164	57	33
387.1	0	120	51	19	150	50	35
387.6	0	112	38	20	145	55	25
388.1	0	118	46	26	122	69	24
388.5	0	119	61	21	155	56	33
389.0	0	116	46	18	148	60	19
389.5	0	111	48	16	142	50	35
390.0	0	136	56	17	144	51	27
390.5	0	106	37	20	140	68	27
390.9	0	123	38	20	126	46	36
391.4	0	105	50	24	135	54	25
391.9	0	99	50	21	139	46	34
392.4	0	113	60	18	157	59	37
392.8	0	115	49	32	120	57	34
393.3	0	111	46	15	124	50	17
393.8	0	120	43	20	145	61	29
394.3	0	122	43	22	143	57	21
394.8	0	115	49	18	138	46	24
395.2	0	126	42	23	121	58	20
395.7	0	121	50	18	148	60	24
396.2	0	119	56	18	132	54	23
396.7	0	131	50	20	144	55	25
397.2	0	99	55	20	127	51	26
397.6	0	137	54	18	149	54	24
398.1	0	102	59	25	150	57	23
398.6	0	105	44	24	150	50	21
399.1	0	104	40	21	161	52	20
399.6	0	113	54	32	152	58	28
400.0	0	124	44	15	135	49	26
400.5	0	106	47	19	122	60	29
401.0	0	104	35	19	145	49	28
401.5	0	110	38	22	116	48	26
402.0	0	113	47	21	145	63	18
402.4	0	121	59	17	126	55	18
402.9	0	117	45	21	136	49	24
403.4	0	117	56	23	147	55	17
403.9	0	93	42	11	151	49	20
404.3	0	113	48	18	126	49	25
404.8	0	108	44	13	110	66	22
405.3	0	103	51	23	125	54	27
405.8	0	90	45	19	135	42	27
406.3	0	103	55	17	133	54	35
406.7	0	108	43	22	151	58	29

407.2	0	111	51	15	130	56	21
407.7	0	114	38	21	123	57	22
408.2	0	97	51	25	127	40	30
408.7	0	123	47	27	126	55	23
409.1	0	104	42	23	116	49	19
409.6	0	122	44	16	125	57	21
410.1	0	95	60	17	120	53	26
410.6	0	121	44	15	120	46	17
411.1	0	103	53	17	138	55	13
411.5	0	90	57	29	147	55	20
412.0	0	98	36	18	145	54	24
412.5	0	98	44	17	128	52	25
413.0	0	93	32	13	128	49	29
413.4	0	102	44	21	127	59	21
413.9	0	112	30	16	126	50	10
414.4	0	104	49	24	135	52	25
414.9	0	108	35	17	139	39	17
415.4	0	109	44	30	153	49	30
415.8	0	110	50	15	124	42	30
416.3	0	101	36	17	130	40	29
416.8	0	119	51	16	124	51	22
417.3	0	93	43	16	126	41	21
417.8	0	89	44	17	142	41	21
418.2	0	114	47	10	131	52	19
418.7	0	91	46	22	122	47	15
419.2	0	101	37	12	117	57	19
419.7	0	111	39	16	120	53	19
420.2	0	105	50	15	109	58	19
420.6	0	86	47	15	125	42	22
421.1	0	94	51	23	121	62	24
421.6	0	105	44	13	128	51	14
422.1	0	96	49	14	123	48	23
422.6	0	104	35	14	108	39	14
423.0	0	99	45	16	108	57	25
423.5	0	92	48	14	108	43	23
424.0	0	87	37	12	109	44	24
424.5	0	120	36	20	109	40	20
424.9	0	95	32	16	115	51	23
425.4	0	82	40	13	122	39	20
425.9	0	108	53	12	121	46	18
426.4	0	94	44	9	106	32	19
426.9	0	114	42	16	111	34	19
427.3	0	90	37	15	111	30	18
427.8	0	84	36	15	110	42	18

428.3	0	80	34	11	131	48	16
428.8	0	97	32	18	105	47	19
429.3	0	91	34	14	120	36	13
429.7	0	107	43	12	121	56	29
430.2	0	100	29	14	95	53	24
430.7	0	91	46	20	131	46	23
431.2	0	100	29	10	112	52	21
431.7	0	91	35	12	109	40	22
432.1	0	98	33	15	116	45	25
432.6	0	108	34	17	117	42	20
433.1	0	89	34	22	96	55	13
433.6	0	80	37	13	120	35	27
434.0	0	70	51	18	113	43	9
434.5	0	84	38	10	113	35	18
435.0	0	82	34	12	104	50	14
435.5	0	92	35	17	107	55	25
436.0	0	86	41	11	111	33	14
436.4	0	73	44	15	100	29	22
436.9	0	79	18	11	116	51	31
437.4	0	80	40	11	106	32	13
437.9	0	78	38	17	120	55	22
438.4	0	104	33	20	105	50	24
438.8	0	82	46	14	98	39	26
439.3	0	80	33	10	129	56	17
439.8	0	82	36	8	120	31	21
440.3	0	72	39	29	128	48	14
440.8	0	74	28	10	108	37	18
441.2	0	84	36	22	103	38	18
441.7	0	75	40	14	116	39	16
442.2	0	97	35	22	120	54	25
442.7	0	100	29	18	97	44	18
443.2	0	82	31	14	103	44	12
443.6	0	92	40	14	118	43	27
444.1	0	88	40	13	95	28	18
444.6	0	90	35	8	85	51	14
445.1	0	78	40	15	114	32	19
445.5	0	92	28	20	91	40	21
446.0	0	80	39	16	103	40	15
446.5	0	84	33	10	112	40	13
447.0	0	81	33	15	94	37	14
447.5	0	82	33	20	95	47	13
447.9	0	98	37	15	102	35	19
448.4	0	84	26	13	116	45	20
448.9	0	103	37	23	88	41	14

449.4	0	83	33	13	119	39	18
449.9	0	99	28	9	112	44	14
450.3	0	75	34	11	106	37	18
450.8	0	84	48	14	94	26	15
451.3	0	67	37	16	100	42	21
451.8	0	88	26	14	94	30	16
452.3	0	89	46	11	114	44	24
452.7	0	89	28	17	100	36	23
453.2	0	79	32	17	110	43	21
453.7	0	75	35	19	100	34	13
454.2	0	77	41	10	96	43	19
454.6	0	89	32	13	84	32	14
455.1	0	83	33	12	92	42	15
455.6	0	80	25	16	76	38	16
456.1	0	83	37	17	90	48	14
456.6	0	83	23	22	88	31	18
457.0	0	84	36	14	99	35	13
457.5	0	88	26	15	97	47	24
458.0	0	82	40	14	85	37	21
458.5	0	75	31	16	94	34	13
459.0	0	65	25	10	107	42	15
459.4	0	77	30	12	104	42	19
459.9	0	106	21	14	92	41	24
460.4	0	82	21	8	99	36	24
460.9	0	86	24	13	87	35	18
461.4	0	78	28	12	98	40	18
461.8	0	61	31	12	89	26	20
462.3	0	73	29	12	103	38	18
462.8	0	84	26	14	85	34	15
463.3	0	73	23	13	88	46	13
463.8	0	60	31	5	97	33	19
464.2	0	77	38	10	96	37	14
464.7	0	70	26	10	94	33	14
465.2	0	67	28	8	92	30	17
465.7	0	58	37	11	105	41	14
466.1	0	75	23	14	89	37	13
466.6	0	72	26	25	100	31	24
467.1	0	89	29	15	86	42	12
467.6	0	77	31	14	86	41	12
468.1	0	58	27	15	87	35	10
468.5	0	82	33	16	93	39	16
469.0	0	70	29	9	92	36	11
469.5	0	61	36	10	106	30	13
470.0	0	73	27	20	98	41	18

470.5	0	68	36	14	94	47	12
470.9	0	80	31	8	94	25	23
471.4	0	72	23	14	82	39	11
471.9	0	76	28	19	104	37	20
472.4	0	64	26	12	91	39	16
472.9	0	70	29	19	108	32	18
473.3	0	77	21	10	98	34	15
473.8	0	71	33	13	96	39	13
474.3	0	78	26	7	99	35	13
474.8	0	57	40	9	101	33	19
475.3	0	75	26	12	87	36	19
475.7	0	62	26	16	85	37	13
476.2	0	66	31	14	96	39	14
476.7	0	77	31	14	74	32	13
477.2	0	78	25	7	89	38	14
477.6	0	61	24	19	86	28	13
478.1	0	87	31	12	71	37	15
478.6	0	77	30	14	95	35	14
479.1	0	76	21	12	94	23	10
479.6	0	82	27	10	94	31	18
480.0	0	66	31	11	86	36	10
480.5	0	71	27	14	92	45	13
481.0	0	83	34	18	77	34	9
481.5	0	70	36	10	78	32	15
482.0	0	78	21	3	88	26	13
482.4	0	73	32	13	84	31	21
482.9	0	76	25	13	91	32	10
483.4	0	64	29	15	95	25	11
483.9	0	76	22	13	89	31	13
484.4	0	78	28	14	83	20	20
484.8	0	68	26	8	84	31	20
485.3	0	73	31	7	79	33	9
485.8	0	64	39	14	98	24	12
486.3	0	67	23	4	73	34	16
486.7	0	46	31	7	68	34	9
487.2	0	66	32	9	89	28	13
487.7	0	70	31	7	81	25	18
488.2	0	78	31	13	81	30	15
488.7	0	71	34	14	92	28	14
489.1	0	66	31	11	71	31	16
489.6	0	74	30	11	95	32	14
490.1	0	65	31	13	79	37	11
490.6	0	81	33	12	92	38	23
491.1	0	59	29	14	76	40	15

491.5	0	60	26	13	77	33	17
492.0	0	60	17	14	71	24	11
492.5	0	74	31	10	69	19	18
493.0	0	60	29	6	72	27	12
493.5	0	52	15	16	72	36	12
493.9	0	59	17	8	88	54	17
494.4	0	51	23	14	87	34	13
494.9	0	56	29	11	73	33	15
495.4	0	60	20	18	96	20	9
495.9	0	64	34	9	58	34	12
496.3	0	62	21	13	83	30	14
496.8	0	63	28	11	75	30	10
497.3	0	64	22	14	70	31	14
497.8	0	63	26	8	53	33	13
498.2	0	67	24	19	80	29	10
498.7	0	57	30	7	82	23	8
499.2	0	56	19	15	71	25	23
499.7	0	60	31	15	81	22	14
500.2	0	53	25	11	76	31	17
500.6	0	62	30	11	78	29	14
501.1	0	52	25	12	75	21	16
501.6	0	54	18	17	69	33	14
502.1	0	77	18	13	71	24	12
502.6	0	61	30	11	64	33	17
503.0	0	56	26	13	83	38	10
503.5	0	61	18	12	61	31	7
504.0	0	52	15	11	78	18	14
504.5	0	83	28	10	70	28	14
505.0	0	49	25	11	74	18	13
505.4	0	56	28	8	83	25	20
505.9	0	69	16	11	80	23	12
506.4	0	62	16	11	61	26	12
506.9	0	46	27	9	76	30	15
507.3	0	51	21	9	88	34	13
507.8	0	61	32	10	71	30	13
508.3	0	62	22	5	70	32	13
508.8	0	56	23	8	72	21	18
509.3	0	64	31	6	68	30	12
509.7	0	61	18	9	58	25	16
510.2	0	54	27	13	69	24	14
510.7	0	61	17	8	73	26	7
511.2	0	63	26	7	87	23	14
511.7	0	65	28	11	85	22	13
512.1	0	54	26	11	65	32	9

512.6	0	53	29	10	76	29	16
513.1	0	66	20	8	83	33	12
513.6	0	56	24	6	70	18	10
514.1	0	54	19	5	50	27	9
514.5	0	63	18	11	75	20	14
515.0	0	47	18	8	75	25	12
515.5	0	69	19	8	67	31	12
516.0	0	41	22	9	63	33	17
516.5	0	50	27	10	74	24	7
516.9	0	56	28	7	60	31	10
517.4	0	59	17	10	65	26	14
517.9	0	49	16	11	56	22	14
518.4	0	48	21	5	61	31	14
518.8	0	59	24	4	48	29	19
519.3	0	61	25	8	69	29	11
519.8	0	45	15	7	66	22	11
520.3	0	49	25	11	67	22	12
520.8	0	51	19	8	68	18	7
521.2	0	51	27	11	64	20	16
521.7	0	51	28	12	71	34	9
522.2	0	48	30	6	75	26	13
522.7	0	47	17	10	74	18	16
523.2	0	54	21	7	71	19	9
523.6	0	52	23	8	66	21	14
524.1	0	41	27	10	55	22	10
524.6	0	57	19	5	66	23	14
525.1	0	58	32	10	69	29	17
525.6	0	51	25	13	71	25	11
526.0	0	62	19	9	64	21	10
526.5	0	44	32	8	78	22	13
527.0	0	57	12	10	68	24	10
527.5	0	46	22	14	71	22	5
527.9	0	45	22	10	67	35	11
528.4	0	44	29	6	72	28	10
528.9	0	54	27	3	70	22	17
529.4	0	52	16	6	76	25	11
529.9	0	32	30	6	69	21	11
530.3	0	46	18	6	49	33	19
530.8	0	53	24	11	54	29	11
531.3	0	42	16	14	64	18	11
531.8	0	50	15	8	59	29	14
532.3	0	47	23	13	44	21	11
532.7	0	53	28	8	51	22	16
533.2	0	44	19	9	63	11	5

533.7	0	44	16	6	63	24	10
534.2	0	43	19	9	53	20	15
534.7	0	45	24	4	59	14	11
535.1	0	47	23	8	46	17	13
535.6	0	63	24	10	66	28	11
536.1	0	47	21	9	62	17	9
536.6	0	48	16	12	65	22	12
537.1	0	56	28	4	67	16	11
537.5	0	47	16	6	65	22	6
538.0	0	46	18	7	70	24	10
538.5	0	56	21	7	62	17	11
539.0	0	53	20	7	58	29	8
539.4	0	56	20	9	62	27	10
539.9	0	45	18	4	54	26	9
540.4	0	51	18	13	61	20	13
540.9	0	65	20	6	58	15	19
541.4	0	53	16	11	63	23	10
541.8	0	49	17	15	53	27	6
542.3	0	45	15	7	71	28	11
542.8	0	56	20	9	68	17	8
543.3	0	44	23	12	59	18	8
543.8	0	50	15	7	58	25	8
544.2	0	56	20	8	65	20	15
544.7	0	45	18	4	63	26	12
545.2	0	47	30	9	64	19	18
545.7	0	52	13	9	51	20	13
546.2	0	44	20	8	62	22	11
546.6	0	50	18	3	63	24	12
547.1	0	43	18	9	49	23	7
547.6	0	44	18	5	51	30	6
548.1	0	51	21	7	68	18	11
548.5	0	45	15	10	54	23	10
549.0	0	59	20	5	58	17	12
549.5	0	39	21	8	55	24	6
550.0	0	46	16	5	50	30	10
550.5	0	51	13	8	56	21	7
550.9	0	42	21	7	57	21	10
551.4	0	57	22	9	44	23	17
551.9	0	31	16	9	55	17	10
552.4	0	48	24	6	75	23	14
552.9	0	44	13	6	44	21	7
553.3	0	49	16	6	67	20	14
553.8	0	39	23	5	44	21	7
554.3	0	41	15	6	51	19	11

554.8	0	51	14	8	43	26	9
555.3	0	40	12	8	43	14	5
555.7	0	43	21	10	57	21	13
556.2	0	56	16	7	46	22	8
556.7	0	54	16	7	66	23	5
557.2	0	32	15	5	47	23	9
557.7	0	41	19	7	53	21	7
558.1	0	50	18	9	46	18	6
558.6	0	48	18	11	56	23	2
559.1	0	47	19	6	47	16	10
559.6	0	41	14	4	51	20	10
560.0	0	38	13	8	71	15	12
560.5	0	53	11	11	54	25	13
561.0	0	41	15	2	55	21	11
561.5	0	47	17	9	55	18	11
562.0	0	41	22	4	60	18	10
562.4	0	51	23	5	62	12	11
562.9	0	50	16	7	65	16	12
563.4	0	34	21	7	58	19	9
563.9	0	40	17	8	58	17	11
564.4	0	42	20	9	38	20	11
564.8	0	51	15	9	53	14	12
565.3	0	42	19	9	62	29	9
565.8	0	46	19	6	45	25	8
566.3	0	44	17	7	49	33	13
566.8	0	25	10	8	59	19	11
567.2	0	42	8	4	67	17	5
567.7	0	37	23	9	61	28	3
568.2	0	46	19	6	41	17	5
568.7	0	53	15	4	47	22	9
569.2	0	36	16	4	42	24	8
569.6	0	42	14	5	57	25	8
570.1	0	53	20	3	60	22	13
570.6	0	46	15	7	54	26	7
571.1	0	29	18	4	51	6	6
571.5	0	55	11	3	34	11	13
572.0	0	36	15	7	55	17	5
572.5	0	40	20	7	42	15	9
573.0	0	26	14	9	47	19	10
573.5	0	43	21	6	57	26	10
573.9	0	30	16	5	62	20	11
574.4	0	44	16	7	47	21	8
574.9	0	46	16	8	38	21	9
575.4	0	39	17	10	60	31	6

575.9	0	32	14	2	54	12	9
576.3	0	36	15	8	44	14	6
576.8	0	24	13	5	44	18	4
577.3	0	37	13	6	42	13	14
577.8	0	37	15	5	48	25	6
578.3	0	33	21	5	56	26	14
578.7	0	43	23	7	33	14	5
579.2	0	27	16	5	41	16	5
579.7	0	41	10	4	37	19	5
580.2	0	38	14	5	39	22	7
580.6	0	34	13	4	39	20	6
581.1	0	36	11	5	44	14	9
581.6	0	39	23	9	45	15	11
582.1	0	35	18	8	48	27	10
582.6	0	36	14	6	53	21	9
583.0	0	34	25	8	36	15	15
583.5	0	36	14	5	42	24	10
584.0	0	30	14	7	36	15	9
584.5	0	42	18	8	58	23	10
585.0	0	44	16	10	56	17	9
585.4	0	39	10	6	44	20	15
585.9	0	42	7	6	48	21	6
586.4	0	32	21	6	49	14	14
586.9	0	36	9	11	36	17	5
587.4	0	34	13	4	46	24	9
587.8	0	38	11	5	43	20	4
588.3	0	37	9	3	52	8	8
588.8	0	34	17	8	52	11	5
589.3	0	33	12	9	49	18	6
589.8	0	30	14	4	52	9	4
590.2	0	27	8	11	42	16	10
590.7	0	31	20	8	48	22	4
591.2	0	30	13	1	35	19	10
591.7	0	39	16	7	33	23	8
592.1	0	25	10	4	32	15	11
592.6	0	34	19	3	38	17	12
593.1	0	45	10	9	50	15	9
593.6	0	24	10	6	35	27	9
594.1	0	45	19	7	44	11	6
594.5	0	35	18	4	49	17	7
595.0	0	28	11	1	43	13	9
595.5	0	37	8	7	47	21	9
596.0	0	33	17	8	44	20	9
596.5	0	40	14	3	42	15	11

596.9	0	40	15	4	28	22	11
597.4	0	34	15	9	38	12	13
597.9	0	32	14	7	47	14	9
598.4	0	29	17	12	55	20	7
598.9	0	28	19	8	38	17	6
599.3	0	30	18	8	47	10	7
599.8	0	22	19	7	55	18	10
600.3	0	29	19	8	55	21	8
600.8	0	42	8	5	36	20	9
601.2	0	30	15	6	46	19	5
601.7	0	28	11	5	44	11	11
602.2	0	36	16	5	42	18	6
602.7	0	28	13	4	41	14	4
603.2	0	34	12	6	35	14	10
603.6	0	24	8	11	45	14	10
604.1	0	36	13	3	27	21	3
604.6	0	41	25	8	43	12	2
605.1	0	34	19	4	39	19	12
605.6	0	35	18	5	39	13	8
606.0	0	26	10	2	38	18	5
606.5	0	34	14	7	37	19	6
607.0	0	42	13	7	38	22	6
607.5	0	35	15	3	31	17	6
608.0	0	28	10	3	50	13	6
608.4	0	32	14	7	42	11	4
608.9	0	41	10	4	33	17	10
609.4	0	31	20	3	35	14	5
609.9	0	32	9	4	36	14	5
610.4	0	33	13	2	53	17	6
610.8	0	27	11	8	38	10	9
611.3	0	33	20	3	34	17	12
611.8	0	38	15	2	36	28	3
612.3	0	22	15	8	34	18	8
612.7	0	26	16	4	41	16	6
613.2	0	25	14	8	42	21	9
613.7	0	28	12	5	42	11	7
614.2	0	29	9	6	42	9	8
614.7	0	27	12	3	45	11	10
615.1	0	32	13	8	50	17	11
615.6	0	31	9	8	41	10	6
616.1	0	31	9	6	46	14	5
616.6	0	28	16	5	48	18	6
617.1	0	31	13	5	42	9	8
617.5	0	27	17	6	39	13	6

618.0	0	29	9	1	37	16	6
618.5	0	29	13	5	33	18	6
619.0	0	26	8	2	43	11	4
619.5	0	25	9	4	29	24	8
619.9	0	36	14	2	38	17	7
620.4	0	34	7	12	55	24	14
620.9	0	19	14	4	53	12	2
621.4	0	23	10	6	29	15	5
621.8	0	32	12	3	40	13	2
622.3	0	26	14	5	34	11	7
622.8	0	27	13	4	36	13	9
623.3	0	31	18	3	44	12	7
623.8	0	31	7	5	33	8	7
624.2	0	32	16	5	29	13	7
624.7	0	27	11	4	32	10	7
625.2	0	23	15	3	29	19	5
625.7	0	36	11	8	29	9	7
626.2	0	36	9	9	32	14	7
626.6	0	21	15	5	22	16	9
627.1	0	27	14	2	33	9	9
627.6	0	31	9	6	38	19	6
628.1	0	27	11	6	29	14	10
628.6	0	26	10	3	32	19	10
629.0	0	36	15	5	28	12	8
629.5	0	24	11	2	29	19	12
630.0	0	33	17	11	27	17	4
630.5	0	29	9	8	36	25	5
631.0	0	25	6	4	28	13	7
631.4	0	27	9	9	35	14	5
631.9	0	28	12	6	34	10	9
632.4	0	25	10	6	35	17	4
632.9	0	28	13	4	42	14	7
633.3	0	30	18	2	40	14	14
633.8	0	23	17	1	33	10	3
634.3	0	30	12	5	35	13	4
634.8	0	16	7	3	42	9	6
635.3	0	28	7	4	26	15	9
635.7	0	30	10	8	36	16	3
636.2	0	23	12	2	29	9	2
636.7	0	21	12	1	44	19	4
637.2	0	25	10	2	32	13	5
637.7	0	39	13	3	35	10	6
638.1	0	36	18	5	46	19	11
638.6	0	21	7	3	34	16	8

639.1	0	32	9	6	33	11	4
639.6	0	24	12	1	38	12	6
640.1	0	37	10	3	34	11	8
640.5	0	32	13	5	37	12	6
641.0	0	12	11	3	30	16	6
641.5	0	24	7	4	37	14	9
642.0	0	24	2	7	29	8	4
642.5	0	28	11	5	35	20	8
642.9	0	32	12	5	27	12	7
643.4	0	22	9	2	30	17	6
643.9	0	21	5	5	23	10	10
644.4	0	23	8	2	48	14	7
644.8	0	21	6	2	31	16	12
645.3	0	35	14	3	39	16	4
645.8	0	17	5	2	28	15	4
646.3	0	31	12	9	42	12	7
646.8	0	21	10	8	27	11	9
647.2	0	25	12	5	36	19	5
647.7	0	28	9	3	22	11	5
648.2	0	23	17	6	37	8	7
648.7	0	21	13	6	36	6	5
649.2	0	18	9	7	32	10	5
649.6	0	27	8	3	31	11	4
650.1	0	17	9	4	25	18	8
650.6	0	28	11	3	36	6	4
651.1	0	24	9	4	31	13	8
651.6	0	33	12	5	24	5	7
652.0	0	19	10	2	30	15	10
652.5	0	30	9	5	40	12	5
653.0	0	26	8	4	43	7	7
653.5	0	29	9	5	32	11	5
653.9	0	17	8	2	36	9	4
654.4	0	27	8	4	31	13	8
654.9	0	26	12	3	23	13	4
655.4	0	26	11	3	44	9	3
655.9	0	26	11	4	36	14	7
656.3	0	24	6	8	37	18	10
656.8	0	33	7	1	27	7	8
657.3	0	26	12	6	32	8	5
657.8	0	22	7	7	22	9	3
658.3	0	21	9	6	24	8	5
658.7	0	29	8	1	37	9	5
659.2	0	14	8	6	34	17	6
659.7	0	17	10	7	33	16	5

660.2	0	19	8	5	28	13	1
660.7	0	15	7	5	36	18	4
661.1	0	18	10	4	25	9	4
661.6	0	18	8	2	29	7	4
662.1	0	15	12	4	32	14	10
662.6	0	23	11	4	19	12	5
663.1	0	22	9	4	26	11	8
663.5	0	20	6	2	15	10	6
664.0	0	29	12	8	41	13	7
664.5	0	29	14	1	31	12	5
665.0	0	25	10	6	32	13	5
665.4	0	23	10	5	27	15	6
665.9	0	23	9	5	23	11	7
666.4	0	14	9	4	29	6	8
666.9	0	21	8	2	42	10	4
667.4	0	22	9	5	27	7	6
667.8	0	21	8	5	35	14	7
668.3	0	19	13	0	23	7	7
668.8	0	30	11	4	27	8	4
669.3	0	21	8	1	17	15	2
669.8	0	20	8	5	27	8	4
670.2	0	19	12	6	19	7	10
670.7	0	24	8	5	28	7	5
671.2	0	18	8	7	30	14	6
671.7	0	24	8	2	31	9	4
672.2	0	24	12	6	29	9	6
672.6	0	19	9	8	27	8	5
673.1	0	22	9	3	29	11	5
673.6	0	24	11	1	34	6	5
674.1	0	30	7	4	32	10	12
674.5	0	20	6	9	15	9	3
675.0	0	19	7	3	24	10	4
675.5	0	31	4	4	25	12	6
676.0	0	17	5	5	39	9	6
676.5	0	18	12	4	17	11	4
676.9	0	16	9	3	28	10	2
677.4	0	26	8	5	30	7	4
677.9	0	23	7	4	27	15	3
678.4	0	29	14	7	21	11	8
678.9	0	13	12	5	30	14	4
679.3	0	24	8	2	20	7	5
679.8	0	16	8	3	29	7	6
680.3	0	20	9	5	18	10	6
680.8	0	23	9	1	25	9	4

681.3	0	12	7	3	28	12	3
681.7	0	27	7	3	25	9	6
682.2	0	18	8	5	30	10	3
682.7	0	23	7	3	21	8	2
683.2	0	12	5	3	30	7	5
683.7	0	23	7	4	33	9	3
684.1	0	19	9	2	21	12	3
684.6	0	22	3	4	29	12	5
685.1	0	28	17	2	29	13	4
685.6	0	17	8	4	19	8	3
686.0	0	15	10	4	28	13	6
686.5	0	26	5	2	23	11	7
687.0	0	24	6	3	29	5	4
687.5	0	18	4	1	29	11	7
688.0	0	23	12	6	21	11	4
688.4	0	14	6	2	25	12	6
688.9	0	15	11	4	30	17	6
689.4	0	25	8	0	25	7	4
689.9	0	16	3	3	28	10	3
690.4	0	18	5	2	22	7	4
690.8	0	18	9	6	24	12	8
691.3	0	21	8	1	23	13	3
691.8	0	21	9	2	29	9	7
692.3	0	13	16	3	21	8	2
692.8	0	21	7	4	24	10	7
693.2	0	29	11	3	23	8	7
693.7	0	19	12	7	18	10	3
694.2	0	14	13	4	19	12	9
694.7	0	20	9	6	35	11	5
695.1	0	17	3	2	26	7	3
695.6	0	18	8	4	20	6	5
696.1	0	21	14	5	16	10	1
696.6	0	16	15	2	32	10	4
697.1	0	22	9	4	25	5	5
697.5	0	18	5	2	27	5	5
698.0	0	14	6	5	26	5	2
698.5	0	17	9	2	14	7	2
699.0	0	15	6	4	23	9	9
699.5	0	13	6	1	20	11	2
699.9	0	13	8	1	19	7	6
700.4	0	18	2	4	20	10	7
700.9	0	17	7	9	28	13	3
701.4	0	19	5	3	15	16	2
701.9	0	12	7	6	21	11	6

702.3	0	20	8	3	22	7	3
702.8	0	15	2	1	21	4	5
703.3	0	18	7	2	20	14	6
703.8	0	9	9	0	20	10	4
704.3	0	24	11	4	19	8	2
704.7	0	17	10	2	12	9	3
705.2	0	10	8	2	18	10	1
705.7	0	16	7	3	35	5	2
706.2	0	14	4	6	12	12	5
706.6	0	19	7	4	22	15	2
707.1	0	17	10	6	17	11	2
707.6	0	16	6	3	15	9	3
708.1	0	10	8	3	23	9	4
708.6	0	15	8	1	19	10	8
709.0	0	18	8	1	24	5	5
709.5	0	17	6	1	19	11	6
710.0	0	21	5	3	18	9	1
710.5	0	11	9	2	28	6	3
711.0	0	17	7	5	30	5	3
711.4	0	19	7	3	22	6	4
711.9	0	14	8	1	24	12	3
712.4	0	17	8	2	28	11	2
712.9	0	15	12	1	28	8	5
713.4	0	14	6	5	22	6	2
713.8	0	19	6	2	13	6	5
714.3	0	11	6	4	19	7	1
714.8	0	13	6	1	23	8	5
715.3	0	11	8	2	19	6	1
715.7	0	16	6	4	30	6	2
716.2	0	19	4	2	20	4	5
716.7	0	12	10	4	19	7	4
717.2	0	16	2	3	23	5	5
717.7	0	15	6	7	17	9	0
718.1	0	16	8	2	27	7	7
718.6	0	27	11	1	18	3	4
719.1	0	10	7	2	24	11	2
719.6	0	16	8	2	16	5	3
720.1	0	20	6	1	23	6	2
720.5	0	17	4	0	20	9	4
721.0	0	13	7	1	11	11	4
721.5	0	23	9	0	26	6	4
722.0	0	19	6	1	16	6	0
722.5	0	15	6	1	28	4	6
722.9	0	13	6	5	18	11	3

723.4	0	20	8	1	21	3	6
723.9	0	14	8	4	28	4	7
724.4	0	12	9	2	21	9	5
724.9	0	20	8	1	29	11	6
725.3	0	12	5	1	28	6	7
725.8	0	26	9	2	19	5	4
726.3	0	16	5	6	21	7	5
726.8	0	15	7	2	18	11	7
727.2	0	7	3	1	14	6	3
727.7	0	23	4	2	17	8	5
728.2	0	11	5	3	21	4	6
728.7	0	20	8	4	18	7	7
729.2	0	18	4	2	12	6	2
729.6	0	9	6	2	15	8	3
730.1	0	15	4	1	23	13	2
730.6	0	13	9	1	22	11	5
731.1	0	25	5	3	19	9	4
731.6	0	12	4	0	19	4	2
732.0	0	15	2	1	16	6	4
732.5	0	13	6	4	16	3	3
733.0	0	24	6	3	20	4	4
733.5	0	19	10	3	28	6	5
734.0	0	13	8	2	22	5	2
734.4	0	20	5	3	17	7	5
734.9	0	11	7	1	18	9	2
735.4	0	17	7	2	13	8	4
735.9	0	19	6	0	12	7	5
736.4	0	14	4	1	12	12	2
736.8	0	12	7	3	19	10	0
737.3	0	14	8	4	27	15	2
737.8	0	25	12	4	23	2	6
738.3	0	19	4	1	19	6	2
738.7	0	15	3	1	14	8	0
739.2	0	16	6	4	22	11	3
739.7	0	15	4	0	18	6	5
740.2	0	14	11	2	13	7	3
740.7	0	13	7	0	14	8	7
741.1	0	12	3	1	25	10	1
741.6	0	14	6	2	9	3	5
742.1	0	14	4	2	24	8	4
742.6	0	10	6	5	23	6	0
743.1	0	12	2	1	20	7	3
743.5	0	14	5	3	17	6	5
744.0	0	15	8	1	16	7	6

744.5	0	13	4	1	22	7	5
745.0	0	13	3	2	12	7	0
745.5	0	12	9	4	17	7	2
745.9	0	15	7	0	12	8	5
746.4	0	10	7	4	18	7	4
746.9	0	12	6	0	23	6	3
747.4	0	19	10	4	18	3	1
747.8	0	8	1	0	14	6	3
748.3	0	14	6	3	19	4	3
748.8	0	15	7	2	18	10	1
749.3	0	17	4	3	19	7	6
749.8	0	15	4	3	18	8	4
750.2	0	10	3	2	8	5	2
750.7	0	10	5	4	19	12	4
751.2	0	9	6	5	10	8	1
751.7	0	20	7	2	19	6	0
752.2	0	17	12	5	25	7	4
752.6	0	11	2	2	21	5	5
753.1	0	19	5	4	15	6	0
753.6	0	10	5	2	21	4	2
754.1	0	20	6	2	24	8	7
754.6	0	15	7	3	17	9	2
755.0	0	17	6	1	24	9	1
755.5	0	17	5	2	12	8	2
756.0	0	13	2	4	13	6	5
756.5	0	11	5	3	20	4	0
757.0	0	14	9	1	15	6	5
757.4	0	15	3	2	16	5	3
757.9	0	17	3	2	23	4	1
758.4	0	15	6	1	23	6	1
758.9	0	13	7	4	13	5	4
759.3	0	18	6	2	17	5	0
759.8	0	9	6	1	18	9	3
760.3	0	10	3	4	21	6	2
760.8	0	9	7	2	15	4	1
761.3	0	10	3	0	19	5	3
761.7	0	13	3	3	10	6	5
762.2	0	12	5	0	14	1	2
762.7	0	8	9	2	23	9	3
763.2	0	15	9	0	27	7	1
763.7	0	14	5	0	19	10	8
764.1	0	14	4	5	21	6	2
764.6	0	8	4	1	17	5	3
765.1	0	11	5	2	19	3	6

765.6	0	4	9	1	19	5	3
766.1	0	10	5	2	15	8	5
766.5	0	14	5	3	11	8	3
767.0	0	8	5	2	19	3	3
767.5	0	16	2	1	21	5	5
768.0	0	9	2	1	15	5	1
768.4	0	7	6	2	21	3	9
768.9	0	12	7	1	13	10	3
769.4	0	13	2	2	16	7	1
769.9	0	5	6	2	19	5	1
770.4	0	13	3	3	19	5	2
770.8	0	11	6	1	12	3	4
771.3	0	8	3	1	17	2	1
771.8	0	16	3	6	17	6	2
772.3	0	8	3	0	14	8	4
772.8	0	15	8	5	15	5	2
773.2	0	9	5	2	12	6	3
773.7	0	14	7	3	12	4	2
774.2	0	8	3	0	10	8	3
774.7	0	11	3	1	24	6	6
775.2	0	9	3	2	22	5	2
775.6	0	13	3	1	16	8	2
776.1	0	13	8	2	5	6	2
776.6	0	5	4	2	20	5	1
777.1	0	7	3	1	13	6	5
777.6	0	8	2	0	13	5	6
778.0	0	11	6	1	15	4	6
778.5	0	13	5	4	12	7	0
779.0	0	13	5	4	17	8	0
779.5	0	13	4	0	15	5	3
779.9	0	9	1	1	18	3	5
780.4	0	7	5	1	8	7	4
780.9	0	13	6	1	18	2	2
781.4	0	10	9	2	20	3	1
781.9	0	11	6	3	11	2	4
782.3	0	8	5	1	13	6	3
782.8	0	13	1	0	11	6	0
783.3	0	11	6	2	12	4	2
783.8	0	14	1	1	13	11	1
784.3	0	15	4	3	12	12	1
784.7	0	13	4	1	22	3	2
785.2	0	9	2	1	16	9	4
785.7	0	9	6	3	16	9	0
786.2	0	16	5	0	17	3	4

786.7	0	8	2	7	12	10	1
787.1	0	12	7	2	19	6	2
787.6	0	13	5	1	15	5	2
788.1	0	8	7	2	17	2	4
788.6	0	10	2	2	11	4	3
789.0	0	10	4	5	10	5	1
789.5	0	7	6	1	9	3	2
790.0	0	8	2	1	12	6	2
790.5	0	10	5	3	15	5	1
791.0	0	9	5	1	19	6	4
791.4	0	8	4	2	12	5	3
791.9	0	11	6	3	11	4	2
792.4	0	11	2	4	11	2	1
792.9	0	8	2	1	11	5	1
793.4	0	7	6	1	14	3	0
793.8	0	12	5	2	20	3	5
794.3	0	9	4	3	12	6	1
794.8	0	6	4	0	10	3	4
795.3	0	16	2	1	16	8	0
795.8	0	7	2	4	13	5	0
796.2	0	7	6	4	19	6	1
796.7	0	10	1	1	14	2	0
797.2	0	11	4	5	12	2	5
797.7	0	10	4	3	15	3	4
798.2	0	12	2	1	15	2	2
798.6	0	5	6	1	16	6	3
799.1	0	11	5	4	18	3	5
799.6	0	6	4	1	18	5	0
800.1	0	7	4	2	17	3	2
800.5	0	9	2	2	17	8	2
801.0	0	6	8	2	19	7	4
801.5	0	12	4	0	14	5	4
802.0	0	13	4	2	15	3	1
802.5	0	13	8	2	12	5	2
802.9	0	12	2	1	13	2	4
803.4	0	8	7	1	19	7	6
803.9	0	9	2	1	13	7	0
804.4	0	13	5	3	18	5	2
804.9	0	5	5	0	11	2	3
805.3	0	9	3	3	12	8	4
805.8	0	6	3	1	11	4	1
806.3	0	3	2	2	9	5	2
806.8	0	12	4	0	22	5	3
807.3	0	8	5	2	12	3	1

807.7	0	10	2	1	15	5	4
808.2	0	5	0	2	15	7	3
808.7	0	7	5	1	13	7	4
809.2	0	6	4	1	11	2	0
809.6	0	8	4	1	10	5	3
810.1	0	5	5	4	14	5	3
810.6	0	7	7	2	11	4	3
811.1	0	7	2	4	15	5	3
811.6	0	12	1	1	14	8	3
812.0	0	9	3	1	9	3	4
812.5	0	11	7	1	13	9	2
813.0	0	5	5	2	9	1	2
813.5	0	9	8	2	11	2	3
814.0	0	10	3	0	7	8	1
814.4	0	7	3	0	16	2	3
814.9	0	8	3	1	10	3	1
815.4	0	7	6	0	18	6	1
815.9	0	15	5	1	12	7	3
816.4	0	6	2	0	19	8	3
816.8	0	12	5	1	10	8	2
817.3	0	8	3	1	15	5	3
817.8	0	10	3	0	10	4	3
818.3	0	6	6	1	9	2	3
818.8	0	11	4	1	14	7	1
819.2	0	1	2	2	16	8	1
819.7	0	7	4	2	6	2	4
820.2	0	16	7	1	6	8	5
820.7	0	6	2	5	9	4	3
821.1	0	5	6	2	9	3	2
821.6	0	9	4	3	12	3	3
822.1	0	6	4	0	14	5	1
822.6	0	8	3	3	11	3	1
823.1	0	12	4	2	9	3	0
823.5	0	11	4	4	17	3	2
824.0	0	2	2	0	10	4	2
824.5	0	10	5	5	6	3	1
825.0	0	15	0	0	13	0	0
825.5	0	8	3	1	10	4	2
825.9	0	9	2	0	18	3	3
826.4	0	10	3	0	14	5	0
826.9	0	10	7	3	13	5	2
827.4	0	6	3	2	17	3	1
827.9	0	9	1	0	13	4	3
828.3	0	17	4	1	9	1	3

828.8	0	3	3	1	14	3	0
829.3	0	7	1	2	17	3	5
829.8	0	9	3	0	10	3	4
830.3	0	8	2	0	6	4	2
830.7	0	13	1	1	13	5	2
831.2	0	13	1	1	10	5	1
831.7	0	9	2	0	7	6	3
832.2	0	12	6	2	12	7	3
832.6	0	3	1	1	16	3	4
833.1	0	5	3	1	11	7	1
833.6	0	11	2	2	10	2	2
834.1	0	7	2	0	4	4	0
834.6	0	13	4	3	5	2	1
835.0	0	13	4	0	9	3	2
835.5	0	9	4	1	11	5	2
836.0	0	8	2	0	5	2	5
836.5	0	5	3	2	19	3	2
837.0	0	10	2	0	8	3	6
837.4	0	6	8	0	12	6	1
837.9	0	6	1	1	12	2	2
838.4	0	5	3	1	10	4	0
838.9	0	6	7	2	11	6	0
839.4	0	6	1	2	13	7	1
839.8	0	8	2	1	9	6	1
840.3	0	4	4	2	7	1	2
840.8	0	7	4	1	7	6	2
841.3	0	8	5	1	12	3	4
841.7	0	8	3	1	13	4	1
842.2	0	11	2	2	7	6	6
842.7	0	10	4	1	12	4	3
843.2	0	6	1	0	14	4	0
843.7	0	6	3	1	8	3	2
844.1	0	8	3	2	13	2	2
844.6	0	12	2	1	10	5	0
845.1	0	9	5	1	5	6	1
845.6	0	5	5	1	12	1	3
846.1	0	11	4	0	5	3	1
846.5	0	7	0	2	13	2	0
847.0	0	6	3	1	12	4	2
847.5	0	9	0	2	11	5	4
848.0	0	4	6	0	12	5	1
848.5	0	8	1	0	13	9	1
848.9	0	7	4	2	13	7	3
849.4	0	8	0	0	15	5	1

849.9	0	8	3	2	9	5	1
850.4	0	7	6	2	8	1	2
850.9	0	7	4	0	11	6	0
851.3	0	6	2	2	10	2	0
851.8	0	7	1	1	8	5	3
852.3	0	15	4	1	5	8	4
852.8	0	8	5	1	14	5	1
853.2	0	6	4	2	17	4	6
853.7	0	6	1	1	5	4	3
854.2	0	5	2	0	5	6	2
854.7	0	3	3	1	10	2	1
855.2	0	10	1	1	12	5	1
855.6	0	7	4	1	9	6	1
856.1	0	7	2	1	9	3	0
856.6	0	3	1	0	14	8	0
857.1	0	6	3	2	14	5	1
857.6	0	5	0	1	9	3	2
858.0	0	9	2	0	13	8	1
858.5	0	8	4	0	15	3	1
859.0	0	5	1	4	10	7	1
859.5	0	9	3	2	13	3	0
860.0	0	3	2	0	12	3	3
860.4	0	11	5	0	6	5	3
860.9	0	10	2	1	14	2	1
861.4	0	14	2	1	9	3	2
861.9	0	9	0	0	7	4	1
862.3	0	10	2	0	9	4	2
862.8	0	9	5	0	3	2	1
863.3	0	8	3	3	8	3	5
863.8	0	2	4	1	5	6	3
864.3	0	4	1	1	13	4	1
864.7	0	5	3	1	9	2	1
865.2	0	6	7	4	6	2	3
865.7	0	6	0	3	6	3	0
866.2	0	6	3	1	15	3	2
866.7	0	9	3	1	6	3	3
867.1	0	5	5	3	7	1	5
867.6	0	5	2	2	4	3	4
868.1	0	6	0	0	8	4	1
868.6	0	7	3	1	12	6	1
869.1	0	3	4	2	14	2	1
869.5	0	5	5	2	14	1	1
870.0	0	8	4	0	11	1	2
870.5	0	7	2	2	10	6	1

871.0	0	4	4	1	8	2	3
871.5	0	9	2	0	10	3	1
871.9	0	5	0	3	2	4	1
872.4	0	10	5	2	9	1	3
872.9	0	3	6	0	8	2	1
873.4	0	4	2	1	13	4	0
873.8	0	4	5	0	8	1	0
874.3	0	2	3	3	9	2	1
874.8	0	4	4	4	12	6	2
875.3	0	5	2	0	13	4	0
875.8	0	8	0	1	7	1	1
876.2	0	5	0	0	8	2	1
876.7	0	2	1	1	10	7	2
877.2	0	7	1	0	12	3	2
877.7	0	6	2	1	13	3	1
878.2	0	5	2	1	6	2	2
878.6	0	6	1	1	5	3	1
879.1	0	4	4	3	11	0	2
879.6	0	9	4	0	6	3	2
880.1	0	5	4	0	8	2	0
880.6	0	6	3	1	8	0	1
881.0	0	6	1	2	13	9	4
881.5	0	9	1	2	9	1	1
882.0	0	6	3	1	9	8	0
882.5	0	3	3	1	4	3	0
882.9	0	2	2	0	12	3	0
883.4	0	5	4	0	8	1	2
883.9	0	5	1	1	14	3	1
884.4	0	10	2	0	16	6	2
884.9	0	5	2	2	15	3	1
885.3	0	6	1	2	12	1	1
885.8	0	2	7	4	8	4	1
886.3	0	4	2	0	4	2	2
886.8	0	8	2	1	12	2	0
887.3	0	11	2	2	3	1	0
887.7	0	4	0	1	7	1	3
888.2	0	6	1	1	13	6	2
888.7	0	7	2	2	6	2	3
889.2	0	3	2	0	10	2	0
889.7	0	6	4	3	7	5	1
890.1	0	5	2	0	12	2	1
890.6	0	6	3	2	6	3	1
891.1	0	9	1	5	11	4	0
891.6	0	7	0	0	15	5	3

892.1	0	5	2	1	8	5	0
892.5	0	8	1	1	5	1	0
893.0	0	5	1	0	5	5	1
893.5	0	8	1	0	6	4	0
894.0	0	4	2	0	9	3	1
894.4	0	6	2	1	5	1	2
894.9	0	9	2	3	6	3	3
895.4	0	4	2	1	5	7	2
895.9	0	5	5	2	11	4	2
896.4	0	3	0	1	10	6	0
896.8	0	8	1	1	8	7	2
897.3	0	2	2	2	7	0	0
897.8	0	7	1	0	5	4	2
898.3	0	3	2	0	11	4	0
898.8	0	5	2	0	6	2	2
899.2	0	3	5	0	4	0	3
899.7	0	6	2	1	12	2	2
900.2	0	4	1	1	8	7	1
900.7	0	5	2	0	3	4	2
901.2	0	7	4	0	8	1	2
901.6	0	10	4	0	8	6	2
902.1	0	2	2	2	12	2	1
902.6	0	10	0	0	9	3	1
903.1	0	8	3	0	8	5	1
903.6	0	8	2	1	5	4	3
904.0	0	6	2	0	9	2	3
904.5	0	2	2	1	2	1	0
905.0	0	6	2	0	3	4	0
905.5	0	8	1	0	11	2	2
905.9	0	5	2	2	9	4	1
906.4	0	7	0	0	5	2	0
906.9	0	9	3	1	7	1	1
907.4	0	6	1	0	8	3	1
907.9	0	6	2	0	10	4	1
908.3	0	1	5	0	5	1	1
908.8	0	2	2	1	6	2	0
909.3	0	5	3	1	4	2	0
909.8	0	7	0	0	7	3	1
910.3	0	5	0	2	3	2	1
910.7	0	4	1	0	3	1	0
911.2	0	5	2	1	7	0	0
911.7	0	8	0	2	7	1	1
912.2	0	3	3	2	5	5	0
912.7	0	7	4	1	7	6	4

913.1	0	4	0	0	5	2	2
913.6	0	4	2	1	7	4	2
914.1	0	7	3	0	6	5	1
914.6	0	6	2	2	6	3	1
915.0	0	3	3	1	4	0	0
915.5	0	2	3	1	3	2	0
916.0	0	10	1	0	4	1	0
916.5	0	10	2	2	8	4	3
917.0	0	4	0	1	8	3	1
917.4	0	8	2	1	3	5	1
917.9	0	5	2	0	5	2	1
918.4	0	9	1	1	6	2	1
918.9	0	1	4	1	6	3	3
919.4	0	3	3	1	5	1	1
919.8	0	4	3	0	6	2	2
920.3	0	5	3	2	5	2	2
920.8	0	3	0	1	7	2	1
921.3	0	5	0	1	7	3	1
921.8	0	2	3	0	6	5	2
922.2	0	4	1	1	7	3	1
922.7	0	3	2	0	9	4	0
923.2	0	8	2	1	4	5	2
923.7	0	2	0	2	12	3	1
924.2	0	6	3	0	4	2	1
924.6	0	3	2	3	8	0	1
925.1	0	6	7	0	6	5	1
925.6	0	6	0	0	6	1	1
926.1	0	4	1	0	7	4	0
926.5	0	5	3	1	9	1	0
927.0	0	3	1	3	8	2	0
927.5	0	3	2	0	5	4	2
928.0	0	3	2	3	2	5	4
928.5	0	4	3	1	3	2	1
928.9	0	5	4	0	6	5	1
929.4	0	4	5	1	7	2	1
929.9	0	5	2	2	14	1	2
930.4	0	2	6	3	6	1	3
930.9	0	3	3	0	2	2	0
931.3	0	4	1	2	9	0	2
931.8	0	5	1	0	8	3	1
932.3	0	2	5	2	7	4	3
932.8	0	4	2	0	5	8	1
933.3	0	3	2	0	3	2	1
933.7	0	2	0	0	3	0	3

934.2	0	5	3	1	6	3	1
934.7	0	8	3	1	14	4	0
935.2	0	1	2	0	7	4	1
935.6	0	7	3	0	4	1	0
936.1	0	8	4	1	6	4	0
936.6	0	4	0	1	4	1	3
937.1	0	2	1	0	3	1	3
937.6	0	5	2	0	5	2	0
938.0	0	4	1	1	5	4	1
938.5	0	5	3	0	10	0	1
939.0	0	3	1	0	3	2	1
939.5	0	4	0	1	8	2	1
940.0	0	2	1	1	5	3	0
940.4	0	1	0	0	6	1	2
940.9	0	3	4	0	8	0	2
941.4	0	6	3	3	4	2	0
941.9	0	6	1	0	6	2	0
942.4	0	5	2	1	3	0	1
942.8	0	7	3	0	4	1	0
943.3	0	2	1	1	5	4	1
943.8	0	4	0	2	8	4	4
944.3	0	5	4	1	10	1	2
944.8	0	2	1	0	6	2	1
945.2	0	6	0	0	6	0	1
945.7	0	1	4	1	8	2	1
946.2	0	3	1	0	6	1	1
946.7	0	1	2	0	5	1	4
947.1	0	4	2	0	6	4	2
947.6	0	4	0	1	8	1	0
948.1	0	2	4	1	3	0	0
948.6	0	5	1	2	6	4	0
949.1	0	2	0	0	4	3	2
949.5	0	4	2	1	5	2	2
950.0	0	2	1	0	2	1	0
950.5	0	5	0	0	9	2	0
951.0	0	2	0	1	5	2	0
951.5	0	3	2	2	5	0	2
951.9	0	3	1	1	4	1	1
952.4	0	2	1	0	5	2	0
952.9	0	4	4	0	10	3	0
953.4	0	2	0	0	5	1	2
953.9	0	7	1	2	9	7	0
954.3	0	5	2	1	6	0	0
954.8	0	3	0	0	9	0	2

955.3	0	3	0	0	6	1	2
955.8	0	2	1	1	9	2	0
956.2	0	2	2	0	6	4	0
956.7	0	2	5	0	3	1	0
957.2	0	4	1	1	6	4	0
957.7	0	1	1	0	5	1	2
958.2	0	6	4	1	4	1	2
958.6	0	5	0	3	4	3	1
959.1	0	8	2	1	6	4	0
959.6	0	4	1	0	7	3	3
960.1	0	0	2	0	3	4	0
960.6	0	4	2	0	4	1	2
961.0	0	3	0	0	6	1	1
961.5	0	2	1	0	5	3	0
962.0	0	1	3	0	5	3	2
962.5	0	2	0	0	3	4	0
963.0	0	2	1	0	7	0	2
963.4	0	4	1	0	9	3	1
963.9	0	3	3	1	7	1	2
964.4	0	2	0	0	5	2	2
964.9	0	6	2	0	9	1	0
965.4	0	4	4	0	5	2	4
965.8	0	3	0	1	6	0	3
966.3	0	5	2	0	11	1	2
966.8	0	1	3	1	6	0	0
967.3	0	2	2	1	7	2	0
967.7	0	1	1	1	6	0	1
968.2	0	2	2	1	6	2	0
968.7	0	2	5	0	6	1	1
969.2	0	4	0	0	5	2	2
969.7	0	5	0	1	5	2	0
970.1	0	4	0	0	4	4	1
970.6	0	4	1	0	7	3	3
971.1	0	8	3	0	8	1	1
971.6	0	4	0	1	7	2	0
972.1	0	4	1	0	2	4	2
972.5	0	4	2	0	5	0	0
973.0	0	9	1	1	5	1	2
973.5	0	5	1	0	7	3	1
974.0	0	3	0	2	8	6	2
974.5	0	4	6	0	8	3	1
974.9	0	1	5	0	6	1	1
975.4	0	3	0	0	8	3	1
975.9	0	3	2	0	1	4	1
976.4	0	4	2	0	6	2	0

976.8	0	6	1	1	10	2	0
977.3	0	2	1	0	4	2	1
977.8	0	1	3	1	3	2	3
978.3	0	4	1	0	2	2	0
978.8	0	2	0	0	4	4	0
979.2	0	3	1	1	8	1	2
979.7	0	4	0	0	5	4	2
980.2	0	1	1	0	4	3	1
980.7	0	0	0	0	0	0	0
981.2	0	0	0	0	0	0	0

2.13. Data table of $\ln X_{cmc}$ at different salt concentrations with the variation of temperatures

T/K	$\ln X_{cmc}$ at different [Salt] with the variation of salt concentration with temperatures							
	0.001 m NaCl	0.005 m NaCl	0.001 m NaBr	0.005 m NaBr	0.001 m Na ₂ SO ₄	0.005m Na ₂ SO ₄	0.001 m Na ₃ PO ₄	0.005m Na ₃ PO ₄
298.15	-11.43	-12.40	-12.03	-12.85	-12.98	-13.16	-12.38	-13.08
303.15	-11.43	-12.24	-11.99	-12.84	-12.95	-13.00	-12.39	-13.36
308.15	-11.36	-12.22	-11.85	-12.83	-12.88	-12.97	-12.24	-12.84
313.15	-11.33	-12.23	-11.66	-12.76	-12.79	-12.90	-12.12	-12.81
318.15	-11.25	-12.00	-11.62	-12.62	-12.69		-11.98	-12.68

2.14. Steady state Stern Volmer data of Pyrene with variation of [CPC] concentration at different salt concentrations for NaCl, NaBr, Na₂SO₄ and Na₃PO₄ at 298.15 K

0.01 mol.kg ⁻¹ NaCl		0.02 mol.kg ⁻¹ NaBr		0.001 mol.kg ⁻¹ Na ₂ SO ₄		0.02 mol.kg ⁻¹ Na ₃ PO ₄	
10 ³ [CPC] / mol.kg ⁻¹	F ₀ /F	10 ³ [CPC] / mol.kg ⁻¹	F ₀ /F	10 ³ [CPC] / mol.kg ⁻¹	F ₀ /F	10 ³ [CPC] / mol.kg ⁻¹	F ₀ /F
0	1.00	0	1.00	0	1.00	0	1.00
0.010	1.02	0.010	1.13	0.010	1.03	0.010	1.08
0.019	1.02	0.020	1.14	0.019	1.05	0.019	1.20
0.029	1.08	0.029	1.33	0.029	1.10	0.029	1.27
0.038	1.15	0.038	1.66	0.038	1.16	0.038	1.36
0.047	1.22			0.047	1.22	0.047	1.61

2.15. Time resolved Stern Volmer data of Pyrene with variation of [CPC] concentration at different salt concentrations for NaCl, NaBr, Na₂SO₄ and Na₃PO₄ at 298.15 K

0.01 mol.kg ⁻¹ NaCl		0.02 mol.kg ⁻¹ NaBr		0.001 mol.kg ⁻¹ Na ₂ SO ₄		0.02 mol.kg ⁻¹ Na ₃ PO ₄	
10 ³ [CPC] / mol.kg ⁻¹	τ_0/τ	10 ³ [CPC] / mol.kg ⁻¹	τ_0/τ	10 ³ [CPC] / mol.kg ⁻¹	τ_0/τ	10 ³ [CPC] / mol.kg ⁻¹	τ_0/τ
0	1.00	0	1.00	0	1.00	0	1.00
0.020	1.01	0.010	1.07	0.020	1.02	0.020	1.02
0.038	1.04	0.019	1.10	0.038	1.04	0.038	1.06
0.060	1.07	0.029	1.14	0.060	1.06	0.060	1.12
		0.038	1.19				

2.16. Dynamic Light Scattering (DLS) data for C₁₆MImCl in presence of different [Salt] for NaCl, NaBr, Na₂SO₄ and Na₃PO₄ at 298.15 K

NaCl/0.01 m		NaBr / 0.01 m		Na ₂ SO ₄ /0.01 m		Na ₃ PO ₄ /0.01 m	
Size r(nm)	Mean Intensity %	Size r(nm)	Mean Intensity %	Size r(nm)	Mean Intensity %	Size r(nm)	Mean Intensity %
0.20	0.0	0.20	0	0.20	0	0.20	0
0.23	0.0	0.23	0	0.23	0	0.23	0
0.27	0.0	0.27	0	0.27	0	0.27	0
0.31	0.0	0.31	0	0.31	0	0.31	0
0.36	0.0	0.36	0	0.36	0	0.36	0
0.42	0.0	0.42	0	0.42	0	0.42	0
0.48	0.0	0.48	0	0.48	0	0.48	0
0.56	0.0	0.56	0	0.56	0	0.56	0
0.65	0.0	0.65	0	0.65	0	0.65	0
0.75	0.0	0.75	0	0.75	0	0.75	0
0.87	0.0	0.87	0	0.87	0	0.87	0
1.01	0.0	1.01	0	1.01	0	1.00	0
1.16	0.0	1.16	0	1.16	0	1.16	0
1.35	4.8	1.35	0	1.35	0	1.35	0
1.56	27.8	1.56	0	1.56	0	1.56	0
1.81	37.3	1.81	0.3	1.81	3.2	1.81	0
2.09	21.3	2.09	18.4	2.09	34.6	2.09	20.1
2.42	0.1	2.42	34.3	2.42	35	2.42	33.7
2.81	0.0	2.81	32.1	2.81	0.5	2.81	20.5
3.25	0.0	3.25	14.9	3.25	0	3.25	0
3.77	0.0	3.77	0	3.77	0	3.76	0
4.36	0.0	4.36	0	4.36	0	4.36	0
5.05	0.0	5.05	0	5.05	0	5.05	0
5.85	0.0	5.85	0	5.85	0	5.85	0
6.77	0.0	6.77	0	6.77	0	6.77	0
7.84	0.0	7.84	0	7.84	0	7.84	0
9.08	0.0	9.08	0	9.08	0	9.08	0
10.52	0.0	10.52	0	10.52	0	10.52	0
12.18	0.0	12.18	0	12.18	0	12.18	0

14.11	0.0	14.11	0	14.11	0	14.11	0
16.34	0.0	16.34	0	16.34	0	16.34	0
18.92	0.0	18.92	0	18.92	0	18.92	0
21.91	0.0	21.91	0	21.91	0	21.91	0
25.37	0.0	25.37	0	25.37	0	25.37	0
29.39	0.0	29.39	0	29.39	0	29.39	0
34.03	0.0	34.03	0	34.03	0	34.03	0
39.41	0.0	39.41	0	39.41	0	39.41	13.6
45.64	0.0	45.64	0	45.64	0	45.64	12.1
52.85	0.0	52.85	0	52.85	0	52.85	0
61.21	0.0	61.21	0	61.21	0	61.21	0
70.89	0.0	70.89	0	70.89	0	70.89	0
82.09	0.0	82.09	0	82.09	0	82.09	0
95.07	1.5	95.07	0	95.07	0	95.07	0
110.1	4.1	110.1	0	110.1	0	110.1	0
127.5	3.0	127.5	0	127.5	0	127.5	0
147.7	0.0	147.7	0	147.7	0	147.7	0
171.0	0.0	171.0	0	171.0	0	171.0	0
198.0	0.0	198.0	0	198.0	0	198.0	0
229.3	0.0	229.3	0	229.3	0	229.3	0
265.6	0.0	265.6	0	265.6	0	265.6	0
307.6	0.0	307.6	0	307.6	0	307.6	0
356.2	0.0	356.2	0	356.2	0	356.2	0
412.5	0.0	412.5	0	412.5	0	412.5	0
477.7	0.0	477.7	0	477.7	0	477.7	0
553.2	0.0	553.2	0	553.2	0	553.2	0
640.7	0.0	640.7	0	640.7	0	640.7	0
741.9	0.0	741.9	0	741.9	0	741.9	0
859.2	0.0	859.2	0	859.2	0	859.2	0
995.1	0.0	995.1	0	995.1	0	995.1	0
1152	0.0	1152	0	1152	0	1152	0
1335	0.0	1335	0	1335	0	1335	0
1545	0.0	1545	0	1545	0	1545	0
1790	0.0	1790	0	1790	0	1790	0
2073	0.0	2073	0	2073	0	2073	0
2400	0.0	2400	0	2400	0	2400	0
2780	0.0	2780	0	2780	0	2780	0
3219	0.0	3219	0	3219	0	3219	0
3728	0.0	3728	0	3728	0	3728	0
4317	0.0	4317	0	4317	0	4317	0
5000	0.0	5000	0	5000	0	5000	0

Chapter- III

3.1. Different experimental data (tensiometry, conductometry, fluorimetry, isothermal titration calorimetry) with the variation of [C₁₆MImCl] for the determination of cmc in aqueous solution at 298.15 K.

Surfacetension		Conductance		Fluorescence		ITC	
[C ₁₆ MImCl] / mM	γ / mN.m ⁻¹	[C ₁₆ MImCl] / mM	K / μ S.cm ⁻¹	[C ₁₆ MImCl] / mM	I ₁ /I ₃	[C ₁₆ MImCl] / mM	ΔH_m^0 / kJ.mol ⁻¹
0	66.5	0	0.91	0	1.498	0	
0.003	62.8	0.007	1.55	0.036	1.497	0.039	1.73
0.006	59.8	0.013	2.03	0.095	1.481	0.194	1.67
0.022	55.6	0.020	2.62	0.154	1.493	0.348	1.55
0.091	51.5	0.027	3.21	0.271	1.467	0.500	1.09
0.150	48.9	0.033	3.68	0.386	1.457	0.651	0.19
0.353	43.2	0.040	4.15	0.555	1.433	0.800	-0.60
0.495	41.0	0.046	5.03	0.720	1.410	0.948	-1.17
0.634	37.3	0.053	5.42	0.881	1.257	1.094	-1.46
0.904	35.9	0.060	6.32	1.091	1.132	1.238	-1.69
1.414	36.5	0.066	6.89	1.344	1.128	1.382	-1.78
1.889	36.5	0.132	12.88	1.588	1.109	1.523	-1.86
2.332	36.5	0.197	18.95	1.824	1.112	1.663	-1.92
		0.262	24.81	2.051	1.112	1.802	-1.90
		0.326	30.82	2.271	1.113	1.938	-1.97
		0.390	36.51	2.483	1.110	2.074	-1.95
		0.454	42.16	2.689	1.108	2.208	-1.91
		0.642	59.25			2.340	-1.92
		0.827	75.09			2.471	-1.90
		1.008	85.60			2.600	-1.93
		1.244	96.04				
		1.809	118.6				
		2.341	138.3				
		2.843	156.8				
		3.317	173.7				
		3.765	189.1				
		4.190	203.7				
		4.592	217.3				
		4.824	225.0				

3.2. Different experimental data (tensiometry, conductometry, fluorimetry, isothermal titration calorimetry) with the variation of [C₁₆TPB] for the determination of cmc at 298.15 K.

Surfacetension		Conductance		Fluorescence		ITC	
[C ₁₆ TPB]/ mM	γ / mN.m ⁻¹	[C ₁₆ TPB]/ mM	κ / μ S.cm ⁻¹	[C ₁₆ TPB]/ mM	I ₁ /I ₃	[C ₁₆ TPB]/ mM	ΔH_m^0 / kJ.mol ⁻¹
0	66.5	0	5.2	0	1.292	0	
0.002	62.6	0.002	5.8	0.005	1.292	0.007	5.717
0.007	55.1	0.007	6.5	0.016	1.280	0.036	5.741
0.015	51.5	0.014	7.5	0.031	1.269	0.065	5.186
0.024	49.1	0.023	8.6	0.046	1.260	0.094	4.302
0.036	45.4	0.035	9.9	0.087	1.253	0.122	2.941
0.054	43.7	0.058	12.5	0.107	1.229	0.150	2.077
0.078	41.0	0.092	16.7	0.132	1.199	0.178	1.583
0.108	40.4	0.126	21	0.157	1.179	0.205	1.434
0.143	39.1	0.160	24	0.194	1.142	0.232	1.276
0.189	38.8	0.193	27	0.230	1.119	0.259	1.205
0.246	38.7	0.226	31	0.266	1.102	0.286	1.092
0.312	37.7	0.259	33	0.313	1.083	0.312	0.901
0.388	37.5	0.292	36	0.383	1.070	0.338	0.804
0.472	37.4	0.324	38	0.451	1.050	0.364	0.759
		0.356	41	0.517	1.046	0.389	0.687
		0.398	43	0.604	1.037	0.414	0.610
		0.440	46	0.708	1.030	0.439	0.582
		0.481	49	0.829	1.034	0.464	0.541
		0.522	51	1.163	1.048	0.488	0.561
		0.563	54	1.490	1.033		
		0.608	56	1.639	1.049		
		0.652	58	1.779	1.030		
		0.697	61	1.912	1.033		
		0.740	64	2.037	1.037		
		0.788	66	2.156	1.033		
		0.835	68	2.268	1.031		
		0.881	71				

3.3. Tensiometry data of C₁₆MImCl in presence of different [NaAlg] at 298.15 K.

0.001% w/v NaAlg		0.005% w/v NaAlg		0.01% w/v NaAlg	
[C ₁₆ MImCl]/ mM	γ / mN.m ⁻¹	[C ₁₆ MImCl]/ mM	γ / mN.m ⁻¹	[C ₁₆ MImCl]/ mM	γ / mN.m ⁻¹
0	65.7	0	64.9	0	62.4
0.003	58.0	0.003	60.7	0.003	54.4
0.006	53.4	0.010	55.1	0.006	51.4
0.012	50.7	0.019	53.8	0.012	51.3
0.022	48.6	0.032	51.7	0.025	50.2
0.034	49.6	0.048	50.4	0.044	48.8
0.049	47.5	0.068	48.4	0.068	45.3
0.113	43.5	0.116	44.8	0.093	44.0
0.143	43.5	0.144	43.1	0.124	42.6
0.180	44.1	0.176	41.6	0.170	41.3
0.278	43.4	0.214	38.8	0.230	40.0
0.343	43.4	0.258	37.7	0.321	37.9
0.420	40.5	0.308	36.3	0.439	34.5
0.507	39.4	0.364	35.5	0.585	33.0
0.607	38.2	0.432	35.0	0.756	32.7
0.720	36.7	0.517	34.6	0.951	31.6
0.845	36.7	0.625	34.2	1.168	31.0
0.981	37.5	0.744	33.0	1.404	30.9
1.141	37.5	0.919	32.0	1.658	30.7
1.349	38.0	1.146	31.7	1.926	30.6
1.601	37.7	1.420	31.8	2.276	30.5
		1.684	31.7	2.716	30.7
		2.186	31.7	3.514	30.4
				4.541	30.4
				5.912	30.5

3.4. Tensiometry data of C₁₆TPB in presence of different [NaAlg] at 298.15 K

0.001% w/v NaAlg		0.005% w/v NaAlg		0.01% w/v NaAlg	
[C ₁₆ TPB]/ mM	γ / mN.m ⁻¹	[C ₁₆ TPB]/ mM	γ / mN.m ⁻¹	[C ₁₆ TPB]/ mM	γ / mN.m ⁻¹
0	67.7	0	65.7	0	65.6
0.001	66.4	0.001	62.1	0.001	64.3
0.003	53.5	0.004	50.8	0.003	56.3
0.006	49.2	0.007	48.0	0.005	49.1
0.010	43.3	0.011	45.5	0.006	48.0
0.015	43.2	0.017	45.0	0.009	46.8
0.021	46.0	0.025	46.6	0.012	45.6
0.031	44.6	0.036	41.8	0.015	43.5
0.065	41.0	0.047	40.4	0.026	42.5
0.093	38.4	0.060	38.2	0.034	41.7
0.131	37.3	0.073	36.4	0.056	41.9
0.177	37.6	0.121	36.5	0.074	41.0
0.231	37.5	0.154	35.9	0.096	39.9
0.292	37.7	0.194	36.0	0.122	38.4
0.360	37.0	0.247	34.6	0.152	37.5
0.435	37.0	0.311	34.0	0.186	38.0
0.515	36.0	0.387	32.9	0.264	36.8
0.666	35.5	0.568	33.4	0.312	36.5
0.875	35.6	0.673	33.0	0.375	34.6
1.393	35.2	0.997	33.1	0.523	32.0
1.671	35.0	1.290	32.1	0.628	31.4
2.047	34.5	1.639	31.9	0.759	31.3
		2.019	31.6	0.912	31.0
		2.409	31.9	1.079	30.9
		2.843	31.8	1.280	30.5
		3.031	31.6		

3.5. Conductometric data for C₁₆MImCl in presence of different [NaAlg] at 298.15 K

0.001% w/v NaAlg		0.005% w/v NaAlg		0.01% w/v NaAlg	
[C ₁₆ MImCl]/ mM	$\kappa/\mu\text{S.cm}^{-1}$	[C ₁₆ MImCl]/ mM	$\kappa/\mu\text{S.cm}^{-1}$	[C ₁₆ MImCl]/ mM	$\kappa/\mu\text{S.cm}^{-1}$
0.000	11	0.000	27	0.000	39
0.005	12	0.004	27	0.004	40
0.009	13	0.013	28	0.008	41
0.014	14	0.022	29	0.012	41
0.021	15	0.031	29	0.020	42
0.028	16	0.044	30	0.028	43
0.038	17	0.057	31	0.037	44
0.049	18	0.070	32	0.049	45
0.066	20	0.087	33	0.061	45
0.085	22	0.106	34	0.077	46
0.108	25	0.128	36	0.097	48
0.131	28	0.160	37	0.117	49
0.154	30	0.192	40	0.137	51
0.178	33	0.224	44	0.157	52
0.212	37	0.266	49	0.177	53
0.247	41	0.309	53	0.201	55
0.281	45	0.350	58	0.229	57
0.315	49	0.392	62	0.260	59
0.349	53	0.434	66	0.291	61
0.394	58	0.475	71	0.323	62
0.439	63	0.516	75	0.357	66
0.484	68	0.556	79	0.392	67
0.551	75	0.607	85	0.431	73
0.616	81	0.657	90	0.469	77
0.682	88	0.707	95	0.507	81
0.768	97	0.767	101	0.554	86
0.854	106	0.826	107	0.601	91
0.938	112	0.884	113	0.648	95
1.043	118	0.942	117	0.703	101
1.146	123	1.019	124	0.758	106
1.247	128	1.095	130	0.813	111
1.348	132	1.170	134	0.876	117
1.466	138	1.244	137	0.938	123
1.583	144	1.336	142	1.000	129
1.698	149	1.426	146	1.140	138
1.812	153	1.515	150	1.208	146
1.942	159	1.604	154	1.293	150
2.069	164	1.691	158	1.377	155
2.195	170	1.794	162	1.459	159
2.318	175	1.895	166	1.557	163
2.457	180	1.995	171	1.653	167

2.592	186	2.110	176	1.748	172
2.725	191	2.223	180	1.857	175
2.856	197	2.334	185	1.964	179
3.000	200	2.443	189	2.069	184
3.141	210	2.565	194	2.187	187
3.279	210	2.685	199	2.303	192
3.429	220	2.803	200	2.416	198
3.576	220	2.919	210	2.528	200
3.720	230	3.033	210	2.637	210
3.997	240	3.172	220	2.771	210
4.263	250	3.308	220	2.901	220
4.518	260				

3.6. Conductometric data for C₁₆TPB in presence of different [NaAlg] at 298.15 K

0.001% w/v NaAlg		0.005% w/v NaAlg		0.01% w/v NaAlg	
[C ₁₆ TPB]/ mM	κ / $\mu\text{S.cm}^{-1}$	[C ₁₆ TPB]/ mM	κ / $\mu\text{S.cm}^{-1}$	[C ₁₆ TPB]/ mM	κ / $\mu\text{S.cm}^{-1}$
0.000	11	0.000	23	0.000	38
0.002	11	0.002	24	0.002	41
0.006	12	0.004	24	0.006	42
0.012	12	0.005	24	0.011	42
0.019	13	0.009	25	0.018	43
0.029	14	0.015	25	0.028	43
0.043	15	0.022	25	0.041	44
0.058	17	0.031	26	0.060	45
0.072	18	0.045	27	0.078	46
0.086	19	0.058	28	0.096	47
0.101	21	0.076	29	0.114	48
0.115	22	0.094	30	0.132	49
0.129	24	0.112	31	0.149	51
0.147	26	0.134	32	0.176	52
0.166	28	0.177	34	0.202	54
0.184	30	0.203	37	0.228	56
0.203	32	0.229	39	0.254	57
0.226	34	0.254	40	0.288	60
0.248	36	0.288	42	0.321	62
0.271	38	0.321	44	0.363	66
0.297	40	0.354	46	0.404	70
0.324	42	0.386	48	0.453	72
0.350	44	0.422	51	0.500	73
0.376	46	0.532	57	0.547	75
0.407	47	0.570	60	0.601	77
0.437	49	0.608	62	0.654	79
0.466	51	0.689	66	0.706	82
0.500	53	0.733	69	0.757	85
0.533	55	0.818	73	0.811	88
0.570	57	0.866	76	0.863	91
0.606	59	0.967	81	0.919	94

0.642	61	1.019	84	0.973	97
0.682	64	1.070	86	1.032	100
0.721	66	1.121	88	1.091	103
0.760	68	1.170	91	1.148	106
0.798	70	1.225	93	1.204	109
0.839	72	1.278	96	1.258	112
0.880	74	1.330	99	1.318	115
0.920	76	1.381	101	1.376	118
0.964	78	1.437	103	1.433	121
1.006	80	1.491	106	1.489	124
1.048	82	1.545	108	1.570	128
1.348	96	1.597	111	1.648	132
1.392	98	1.648	114	1.724	136
1.434	100	1.698	116	1.822	141
1.479	102	1.771	119	1.916	146
1.524	104	1.842	123	2.006	150
1.567	106	1.933	127	2.093	154
1.613	107	2.020	131	2.176	158
1.658	109	2.104	135	2.296	164
1.702	111	2.185	139		
1.748	113	2.263	142		
1.793	115				
1.837	117				
1.884	119				
1.929	121				
1.973	123				
2.019	125				
2.065	126				
2.109	128				
2.155	130				
2.200	132				
2.244	133				
2.287	135				
2.330	137				
2.371	139				
2.412	140				
2.452	141				

3.7. Turbidimetry data for C₁₆MImCl in presence of different [NaAlg] at 298.15 K

0.001% w/v NaAlg		0.005% w/v NaAlg		0.01% w/v NaAlg	
[C ₁₆ MImCl]/ mM	100-%T	[C ₁₆ MImCl]/ mM	100-%T	[C ₁₆ MImCl]/ mM	100-%T
0	-0.2	0	0.2	0	0.1
0.013	3.3	0.012	0.3	0.013	0.8
0.044	5.8	0.042	0.2	0.044	1.9
0.106	8.9	0.090	2.2	0.093	6.2
0.167	9.2	0.149	4.5	0.155	10.2
0.228	9.5	0.208	8.8	0.216	15.9
0.289	9.6	0.267	24.5	0.277	20.0
0.379	9.8	0.325	30.9	0.337	27.1
0.468	10.1	0.411	39.7	0.426	54.7
0.585	10.6	0.496	41.8	0.515	69.4
0.757	11.4	0.608	43.1	0.631	72.3
1.035	11.9	0.773	44.7	0.802	73.9
1.407	11.9	1.039	47.7	1.078	77.0
1.907	11.8	1.396	49.4	1.449	78.5
2.810	11.5	1.875	49.2	1.946	78.1
3.600	11.1	3.498	46.5	2.843	76.5
4.300	11.0	4.168	45.6	3.630	75.0
5.208	10.5	5.040	44.8	4.326	73.5
6.438	9.6	6.220	39.3	5.231	70.9
				6.455	67.2

3.8. Turbidimetry data for C₁₆MImCl in presence of different [NaAlg] at 298.15 K

0.001% w/v NaAlg		0.005% w/v NaAlg		0.01% w/v NaAlg	
[C ₁₆ TPB]/ mM	100-%T	[C ₁₆ TPB]/ mM	100-%T	[C ₁₆ TPB]/ mM	100-%T
0.000	1.0	0.000	0.7	0.000	0.7
0.006	1.6	0.008	1.6	0.005	3.0
0.014	2.7	0.028	3.9	0.014	7.3
0.025	9.2	0.060	8.4	0.033	12.9
0.039	9.9	0.100	14.0	0.056	20.2
0.056	13.3	0.140	18.4	0.090	27.7
0.078	16.7	0.179	30.2	0.135	42.5
0.105	20.8	0.218	68.5	0.190	55.0
0.133	22.1	0.275	74.9	0.255	66.1
0.160	22.8	0.332	77.6	0.340	82.5
0.200	23.1	0.408	80.5	0.441	98.7
0.252	23.3	0.518	81.9	0.559	99.3
0.330	23.4	0.697	84.1	0.690	99.5
0.431	23.9	0.936	85.8	0.831	99.5
0.552	24.5	1.257	86.1	0.998	99.5
0.693	25.5	1.837	85.7	1.370	99.5
0.871	26.3	2.345	84.6	1.689	99.4
1.079	26.6	2.795	83.5	1.965	99.3
1.457	26.5	3.379	81.7		
1.942	25.6	4.170	79.1		

3.9. Fl. intensity data of Pyrene with variation of [C₁₆MImCl] in presence of 0.005% w/v NaAlg at 298.15 K

wavelength/ nm	0.005% w/v NaAlg																	
	[C ₁₆ MImCl] = 0 mM	0.012	0.024	0.036	0.060	0.096	0.140	0.200	0.290	0.410	0.580	0.820	1.140	1.640	2.320	3.140	3.850	5.050
350.0	3.27	11.1	14.8	19.1	25.8	39.7	54.8	84.2	131.9	136.1	136.9	138.5	135.2	129.4	118.3	107.5	99.6	88.6
350.5	2.78	8.9	11.9	15.4	20.7	31.8	43.5	66.8	105.1	108.6	109.1	109.8	107.5	102.5	94.3	85.9	79.5	70.6
351.0	2.33	6.9	9.1	11.8	16.0	24.5	33.2	50.8	80.2	83.2	83.2	83.4	81.9	77.7	72.0	65.8	60.9	54.0
351.5	1.93	5.1	6.8	8.8	11.8	18.1	24.3	37.0	58.7	61.1	60.9	60.6	59.8	56.5	52.7	48.5	44.8	39.6
352.0	1.60	3.7	4.9	6.3	8.5	12.9	17.1	26.0	41.4	43.1	42.8	42.3	41.9	39.4	37.2	34.4	31.7	28.1
352.5	1.35	2.7	3.5	4.5	6.0	9.0	11.7	17.7	28.2	29.4	29.1	28.7	28.6	26.7	25.5	23.7	21.9	19.4
353.0	1.18	2.0	2.6	3.2	4.3	6.3	8.0	12.1	19.1	19.8	19.6	19.3	19.3	18.0	17.4	16.2	15.0	13.4
353.5	1.09	1.6	2.0	2.4	3.2	4.5	5.7	8.4	13.1	13.5	13.4	13.3	13.2	12.5	12.1	11.3	10.5	9.5
354.0	1.05	1.3	1.6	1.9	2.5	3.4	4.1	6.1	9.2	9.5	9.4	9.4	9.4	9.0	8.7	8.1	7.7	7.1
354.5	1.06	1.2	1.4	1.6	2.1	2.7	3.2	4.7	6.9	7.1	7.1	7.0	7.1	6.8	6.7	6.2	6.0	5.6
355.0	1.11	1.1	1.3	1.5	1.9	2.4	2.8	3.9	5.7	5.8	5.8	5.8	5.8	5.8	5.6	5.3	5.2	4.8
355.5	1.18	1.1	1.3	1.5	1.8	2.3	2.7	3.7	5.2	5.3	5.3	5.2	5.3	5.3	5.2	5.0	4.8	4.5
356.0	1.28	1.1	1.4	1.5	1.8	2.3	2.6	3.6	5.1	5.2	5.1	5.1	5.2	5.3	5.1	4.9	4.8	4.5
356.5	1.38	1.2	1.4	1.6	1.9	2.4	2.7	3.6	5.2	5.3	5.2	5.2	5.3	5.4	5.2	5.0	4.9	4.7
357.0	1.50	1.3	1.5	1.7	2.0	2.5	2.8	3.7	5.3	5.4	5.3	5.3	5.4	5.5	5.4	5.2	5.1	4.9
357.5	1.64	1.4	1.6	1.8	2.1	2.6	2.9	3.8	5.5	5.5	5.4	5.4	5.6	5.7	5.6	5.5	5.3	5.2
358.0	1.80	1.5	1.8	1.9	2.2	2.7	3.0	3.9	5.6	5.7	5.6	5.5	5.8	5.9	5.9	5.7	5.6	5.5
358.5	2.00	1.6	1.9	2.1	2.4	2.9	3.1	4.1	5.7	5.8	5.7	5.7	5.9	6.1	6.1	5.9	5.9	5.8
359.0	2.25	1.8	2.1	2.2	2.5	3.0	3.3	4.2	5.9	5.9	5.8	5.8	6.1	6.4	6.4	6.3	6.2	6.1
359.5	2.57	2.0	2.3	2.5	2.7	3.2	3.5	4.4	6.1	6.1	6.0	6.1	6.3	6.7	6.7	6.7	6.6	6.5
360.0	2.99	2.3	2.6	2.7	3.0	3.5	3.7	4.7	6.4	6.5	6.3	6.4	6.7	7.1	7.2	7.2	7.1	7.0
360.5	3.51	2.6	2.9	3.1	3.3	3.8	4.0	5.0	6.8	6.9	6.7	6.8	7.1	7.6	7.7	7.8	7.7	7.7
361.0	4.14	2.9	3.3	3.5	3.7	4.2	4.4	5.5	7.3	7.4	7.2	7.3	7.6	8.3	8.5	8.6	8.6	8.5
361.5	4.89	3.4	3.9	4.0	4.2	4.7	4.9	6.0	8.0	8.1	7.9	8.0	8.4	9.2	9.4	9.6	9.6	9.6
362.0	5.76	3.9	4.5	4.6	4.8	5.4	5.5	6.7	8.9	9.0	8.8	8.8	9.3	10.3	10.6	10.9	10.9	11.0
362.5	6.74	4.5	5.2	5.4	5.6	6.1	6.2	7.6	9.9	10.0	9.8	9.8	10.5	11.7	12.1	12.4	12.5	12.7
363.0	7.80	5.2	5.9	6.2	6.4	7.0	7.1	8.5	11.1	11.2	11.0	11.0	11.8	13.2	13.7	14.2	14.4	14.7
363.5	8.93	6.0	6.8	7.0	7.3	7.9	8.1	9.6	12.4	12.5	12.4	12.3	13.2	15.0	15.6	16.2	16.5	16.8

364.0	10.08	6.8	7.6	7.9	8.3	9.0	9.1	10.8	13.9	13.9	13.8	13.7	14.8	17.0	17.7	18.4	18.8	19.2
364.5	11.21	7.6	8.5	8.8	9.2	10.1	10.2	11.9	15.3	15.4	15.3	15.2	16.5	18.9	19.8	20.6	21.1	21.6
365.0	12.32	8.3	9.3	9.7	10.2	11.2	11.3	13.1	16.9	17.0	16.8	16.6	18.1	20.9	22.0	22.9	23.4	24.1
365.5	13.39	9.1	10.1	10.5	11.2	12.2	12.3	14.3	18.3	18.5	18.2	18.0	19.7	22.8	24.0	25.0	25.6	26.4
366.0	14.54	9.9	10.9	11.4	12.2	13.3	13.3	15.4	19.7	19.8	19.6	19.3	21.1	24.7	25.9	26.9	27.6	28.6
366.5	15.88	10.8	11.9	12.3	13.2	14.2	14.2	16.4	21.0	21.1	20.7	20.5	22.5	26.2	27.6	28.6	29.4	30.5
367.0	17.91	12.1	13.2	13.5	14.3	15.3	15.1	17.4	22.3	22.3	21.9	21.6	23.7	27.7	29.2	30.2	31.0	32.3
367.5	21.01	13.9	15.0	15.3	15.8	16.7	16.3	18.6	23.8	23.6	23.3	22.9	25.1	29.4	30.9	32.0	32.9	34.2
368.0	25.80	16.6	17.8	17.9	18.0	18.7	18.0	20.3	25.7	25.5	25.1	24.7	27.1	31.7	33.3	34.5	35.5	36.9
368.5	32.89	20.5	22.0	21.8	21.2	21.5	20.5	22.8	28.7	28.4	27.9	27.4	30.1	35.1	37.0	38.4	39.5	41.0
369.0	42.72	26.0	27.9	27.2	25.8	25.8	24.3	26.7	33.1	32.8	32.3	31.7	34.7	40.4	42.8	44.5	45.9	47.5
369.5	55.57	33.2	35.7	34.4	32.2	31.8	29.7	32.4	39.8	39.5	38.7	38.1	41.6	48.7	51.7	53.8	55.5	57.4
370.0	71.30	42.4	45.5	43.7	40.7	39.8	37.1	40.3	49.2	48.9	47.8	47.2	51.6	60.6	64.5	67.2	69.2	71.7
370.5	89.25	53.1	57.1	54.9	51.1	50.0	46.5	50.6	61.7	61.3	60.0	59.3	64.8	76.5	81.6	85.2	87.7	91.0
371.0	108.60	65.2	70.0	67.5	63.3	62.1	58.0	63.3	77.3	76.8	75.2	74.3	81.5	96.6	103.2	107.9	111.1	115.5
371.5	128.03	77.6	83.5	80.9	76.5	75.5	71.0	77.8	95.6	94.9	93.1	92.0	101.1	120.4	128.6	134.8	138.8	144.5
372.0	146.19	89.9	96.6	94.2	90.1	89.8	85.0	93.6	115.7	114.7	112.7	111.3	122.8	146.6	156.8	164.6	169.5	176.9
372.5	161.73	100.9	108.5	106.6	103.2	103.8	98.9	109.5	136.3	135.0	132.9	131.2	145.2	173.7	185.7	195.3	201.3	210.5
373.0	173.55	109.9	118.3	117.0	114.7	116.5	111.9	124.5	155.9	154.2	152.0	150.1	166.6	199.5	213.4	224.8	231.8	242.8
373.5	181.05	116.2	125.2	124.9	123.8	127.2	122.9	137.4	172.8	171.0	168.5	166.7	185.4	222.0	237.7	250.7	258.7	271.2
374.0	184.10	119.8	129.2	129.7	130.1	135.0	131.2	147.3	185.8	184.0	181.4	179.6	200.2	239.7	256.7	271.1	279.8	293.4
374.5	182.91	120.4	130.1	131.5	133.2	139.5	136.1	153.7	194.1	192.3	189.5	188.0	209.9	251.2	269.2	284.5	293.6	307.9
375.0	178.34	118.7	128.4	130.4	133.3	140.8	137.7	156.2	197.3	195.8	192.7	191.6	214.1	256.1	274.6	290.4	299.5	314.2
375.5	171.36	115.0	124.7	127.1	130.7	139.1	136.2	155.1	195.8	194.5	191.5	190.6	213.2	255.0	273.3	289.2	298.1	312.5
376.0	163.28	110.3	119.7	122.3	126.4	135.2	132.3	151.2	190.7	189.5	186.6	185.9	208.2	248.8	266.6	282.3	290.6	304.5
376.5	155.03	105.2	114.1	116.7	121.1	129.8	126.9	145.4	183.3	182.1	179.5	178.8	200.4	239.4	256.4	271.3	279.2	292.5
377.0	147.43	100.4	108.8	111.2	115.6	123.9	121.0	138.8	175.1	173.8	171.4	170.6	191.2	228.4	244.4	258.5	266.0	278.8
377.5	141.10	96.3	104.1	106.2	110.5	118.3	115.4	132.5	167.1	165.8	163.5	162.7	182.3	217.7	232.7	246.0	253.3	265.4
378.0	136.36	93.2	100.4	102.4	106.3	113.6	110.7	127.2	160.6	159.2	156.8	156.1	174.6	208.5	222.7	235.4	242.6	254.1
378.5	133.15	91.2	97.8	99.7	103.4	110.1	107.4	123.5	156.0	154.4	152.0	151.3	169.0	201.6	215.5	227.6	234.8	245.8
379.0	131.31	90.1	96.3	98.2	101.6	108.1	105.5	121.3	153.4	151.8	149.3	148.7	165.7	197.5	211.2	222.9	230.2	241.0
379.5	130.51	89.8	95.6	97.6	100.8	107.4	104.8	120.6	152.7	151.0	148.4	147.9	164.5	196.0	209.7	221.3	228.6	239.1

380.0	130.64	90.1	95.7	97.9	101.0	107.8	105.2	121.1	153.4	151.8	149.2	148.6	165.5	196.8	210.5	222.3	229.5	239.9
380.5	131.34	90.7	96.3	98.6	102.0	109.0	106.4	122.6	155.3	153.7	151.2	150.6	167.8	199.3	213.2	225.2	232.4	242.7
381.0	132.40	91.7	97.3	99.8	103.4	110.9	108.3	124.9	158.3	156.6	154.1	153.4	171.1	203.3	217.3	229.4	236.9	247.3
381.5	133.56	93.0	98.5	101.2	105.3	113.3	110.8	127.9	161.9	160.3	157.8	156.9	175.5	208.3	222.5	234.9	242.5	253.2
382.0	134.80	94.3	100.0	102.9	107.6	116.0	113.7	131.4	166.2	164.7	162.1	161.1	180.5	214.2	228.8	241.5	249.2	260.5
382.5	135.95	95.6	101.6	104.7	110.1	119.1	116.9	135.4	171.0	169.6	166.9	165.8	186.2	220.8	235.9	248.9	257.0	268.8
383.0	136.95	97.0	103.2	106.5	112.7	122.2	120.4	139.6	176.3	175.0	172.2	171.0	192.3	227.9	243.7	257.0	265.5	278.0
383.5	137.65	98.3	104.7	108.3	115.2	125.3	123.8	143.8	181.7	180.4	177.7	176.3	198.4	235.1	251.5	265.3	274.1	287.3
384.0	138.05	99.3	106.1	109.8	117.6	128.3	127.0	147.8	186.9	185.6	182.9	181.4	204.2	241.8	258.9	273.4	282.3	296.1
384.5	138.28	100.1	107.3	111.1	119.5	130.8	129.7	151.2	191.4	190.2	187.6	185.9	209.3	247.8	265.3	280.5	289.4	303.6
385.0	138.48	100.7	108.1	112.1	121.0	132.7	131.8	153.9	195.1	193.9	191.1	189.5	213.3	252.5	270.4	286.0	295.1	309.5
385.5	138.68	101.1	108.6	112.8	121.9	134.0	133.1	155.7	197.6	196.3	193.5	192.0	215.9	255.6	273.6	289.7	298.7	313.2
386.0	139.15	101.6	109.1	113.3	122.4	134.8	133.8	156.7	198.9	197.7	194.8	193.3	217.2	257.2	275.3	291.6	300.3	314.9
386.5	140.11	102.2	109.6	113.8	122.8	135.1	134.1	157.0	199.3	198.0	194.9	193.6	217.4	257.5	275.7	291.9	300.5	315.0
387.0	141.70	103.2	110.4	114.5	123.1	135.3	134.1	156.9	199.0	197.7	194.5	193.4	217.0	257.1	275.2	291.2	299.8	314.2
387.5	144.09	104.6	111.6	115.5	123.7	135.5	134.2	156.7	198.6	197.2	194.0	192.9	216.5	256.6	274.6	290.3	298.7	313.3
388.0	147.26	106.6	113.4	117.0	124.6	136.1	134.5	156.9	198.7	197.0	193.8	192.7	216.4	256.5	274.4	289.9	298.4	313.1
388.5	151.25	109.2	115.7	119.0	126.1	137.1	135.4	157.6	199.4	197.4	194.4	193.1	217.2	257.4	275.3	290.7	299.1	314.0
389.0	156.12	112.3	118.6	121.6	128.2	138.8	136.8	159.2	201.0	198.9	196.0	194.6	219.1	259.6	277.5	292.8	301.4	316.3
389.5	161.69	115.9	122.0	124.8	130.9	141.1	139.0	161.5	203.7	201.5	198.6	197.0	222.1	263.1	281.2	296.6	305.4	320.5
390.0	167.81	119.8	125.8	128.3	134.0	144.0	141.8	164.6	207.5	205.3	202.4	200.6	226.1	267.8	286.3	301.9	310.9	326.3
390.5	174.23	124.0	130.0	132.2	137.7	147.6	145.1	168.4	212.1	210.0	207.0	205.2	231.1	273.8	292.8	308.6	317.9	333.5
391.0	180.72	128.3	134.3	136.3	141.6	151.6	148.8	172.6	217.3	215.5	212.3	210.5	236.9	280.6	300.2	316.5	326.1	341.9
391.5	186.94	132.5	138.5	140.4	145.7	155.8	152.8	177.2	222.9	221.4	218.0	216.2	243.2	288.1	308.3	325.1	335.1	351.3
392.0	192.41	136.3	142.5	144.2	149.6	160.0	156.8	181.9	228.9	227.3	223.8	222.0	249.7	295.9	316.5	334.2	344.3	361.2
392.5	196.76	139.5	145.8	147.6	153.2	164.1	160.6	186.6	234.7	233.0	229.5	227.7	256.1	303.6	324.6	343.1	353.3	371.0
393.0	199.71	141.8	148.4	150.2	156.1	167.5	163.9	190.7	240.1	238.2	234.5	232.8	262.1	310.8	332.2	351.4	361.6	380.1
393.5	201.01	143.0	149.9	152.0	158.3	170.2	166.4	194.2	244.6	242.4	238.6	237.1	267.2	316.9	338.5	358.5	368.6	387.9
394.0	200.45	143.1	150.3	152.6	159.5	171.8	168.1	196.6	247.8	245.4	241.6	240.2	271.0	321.2	343.2	363.5	373.6	393.7
394.5	197.96	141.8	149.5	152.0	159.5	172.1	168.6	197.7	249.6	246.9	243.0	241.9	273.0	323.7	345.7	366.0	376.1	396.9
395.0	193.69	139.2	147.4	150.0	158.2	171.1	167.7	197.1	249.4	246.5	242.8	241.9	273.0	323.6	345.7	365.7	375.9	396.9
395.5	187.88	135.7	144.1	147.0	155.7	168.8	165.8	195.0	247.1	244.2	240.7	240.0	270.9	320.9	342.9	362.3	372.6	393.5

396.0	180.85	131.2	139.8	142.9	152.1	165.1	162.6	191.2	242.9	240.0	236.8	236.1	266.5	315.6	337.2	356.0	366.3	386.8
396.5	173.03	126.1	134.7	138.0	147.4	160.5	158.3	186.2	236.8	234.0	231.3	230.5	260.1	308.0	329.0	347.1	357.3	377.1
397.0	164.87	120.7	129.0	132.5	141.9	154.9	153.0	179.9	229.2	226.6	224.3	223.3	251.9	298.5	318.5	336.0	346.0	364.9
397.5	156.84	115.3	123.0	126.8	136.0	148.9	147.1	172.9	220.6	218.2	216.1	215.0	242.5	287.4	306.6	323.5	333.2	350.9
398.0	149.21	109.9	117.1	121.2	129.9	142.6	141.0	165.4	211.4	209.3	207.2	206.1	232.3	275.4	293.8	310.1	319.3	336.0
398.5	142.18	104.9	111.4	115.7	124.1	136.4	134.7	158.0	202.0	200.1	198.1	197.1	221.9	263.3	280.8	296.5	305.1	321.0
399.0	135.87	100.2	106.3	110.6	118.5	130.4	128.5	150.8	192.8	191.3	189.1	188.3	211.8	251.3	268.0	283.2	291.3	306.4
399.5	130.29	95.9	101.7	105.9	113.4	124.9	122.8	144.0	184.3	182.9	180.7	180.1	202.4	240.0	256.2	270.7	278.2	292.8
400.0	125.35	92.1	97.6	101.8	108.9	119.9	117.7	137.9	176.6	175.4	173.0	172.5	194.0	229.7	245.2	259.2	266.2	280.4
400.5	121.05	88.8	94.1	98.1	104.9	115.4	113.1	132.6	169.7	168.6	166.2	165.9	186.6	220.6	235.5	248.9	255.5	269.5
401.0	117.21	85.8	91.1	94.8	101.3	111.3	109.0	128.0	163.8	162.6	160.3	160.1	180.1	212.6	227.0	239.8	246.3	260.1
401.5	113.80	83.3	88.5	91.9	98.2	107.8	105.5	124.0	158.8	157.6	155.4	155.1	174.5	205.8	219.7	232.0	238.5	251.9
402.0	110.71	81.1	86.2	89.4	95.5	104.7	102.6	120.7	154.5	153.3	151.2	150.7	169.8	199.8	213.5	225.4	231.8	244.9
402.5	107.97	79.1	84.2	87.1	93.2	102.1	100.0	117.8	150.8	149.6	147.5	147.0	165.6	194.8	208.2	219.9	226.2	238.9
403.0	105.51	77.3	82.5	85.1	91.2	99.7	97.8	115.3	147.6	146.5	144.3	143.8	161.9	190.4	203.7	215.2	221.4	233.7
403.5	103.19	75.6	80.9	83.4	89.4	97.7	95.9	113.0	144.8	143.8	141.6	141.1	158.7	186.7	199.9	211.2	217.3	229.0
404.0	100.94	74.0	79.3	81.7	87.7	96.0	94.2	111.0	142.3	141.4	139.1	138.7	155.9	183.4	196.4	207.6	213.6	224.6
404.5	98.89	72.6	77.9	80.2	86.3	94.4	92.6	109.0	140.0	139.2	136.9	136.5	153.3	180.5	193.3	204.2	210.1	220.8
405.0	96.93	71.3	76.5	78.9	84.9	93.0	91.1	107.2	137.9	137.1	134.9	134.6	150.8	177.8	190.3	200.9	206.8	217.2
405.5	95.01	70.0	75.1	77.5	83.6	91.5	89.6	105.5	135.9	135.1	133.0	132.7	148.5	175.2	187.5	197.8	203.7	213.7
406.0	93.20	68.8	73.7	76.4	82.3	90.2	88.2	103.9	133.9	133.1	131.2	130.7	146.3	172.7	184.6	194.7	200.4	210.4
406.5	91.50	67.7	72.4	75.2	81.1	88.8	86.8	102.3	131.9	131.0	129.4	128.7	144.1	170.1	181.7	191.6	197.2	207.1
407.0	89.93	66.6	71.2	74.2	79.9	87.4	85.5	100.8	129.8	129.0	127.5	126.6	142.0	167.4	178.7	188.5	194.0	203.8
407.5	88.50	65.6	70.1	73.1	78.8	86.0	84.2	99.2	127.8	126.9	125.7	124.6	139.9	164.7	175.8	185.4	190.8	200.3
408.0	87.14	64.7	69.1	72.1	77.7	84.7	82.9	97.7	125.8	124.8	123.7	122.6	137.9	161.9	172.8	182.3	187.8	196.9
408.5	85.96	63.9	68.2	71.0	76.6	83.4	81.7	96.2	123.7	122.8	121.7	120.6	135.8	159.1	169.8	179.2	184.6	193.5
409.0	84.98	63.2	67.5	70.2	75.6	82.2	80.5	94.7	121.8	120.8	119.7	118.7	133.8	156.4	166.7	176.0	181.5	190.3
409.5	84.18	62.7	66.9	69.4	74.6	81.1	79.3	93.3	120.0	118.9	117.7	117.0	131.8	153.7	163.9	172.9	178.4	187.2
410.0	83.58	62.2	66.4	68.8	73.8	80.1	78.3	91.9	118.2	117.2	115.9	115.3	129.8	151.4	161.2	170.1	175.5	184.4
410.5	83.18	61.9	66.0	68.3	73.1	79.2	77.4	90.7	116.6	115.7	114.1	113.7	127.9	149.2	158.8	167.5	172.6	181.8
411.0	82.90	61.6	65.7	68.0	72.6	78.4	76.6	89.6	115.2	114.3	112.7	112.3	126.3	147.4	156.6	165.2	170.1	179.4
411.5	82.83	61.5	65.6	67.8	72.2	77.7	76.0	88.6	114.0	113.1	111.5	111.1	124.8	145.8	154.7	163.3	167.9	177.3

412.0	82.82	61.3	65.5	67.7	71.9	77.2	75.5	87.8	113.0	112.1	110.5	110.1	123.6	144.4	153.1	161.6	166.1	175.5
412.5	82.86	61.3	65.5	67.5	71.7	76.7	75.1	87.2	112.1	111.3	109.7	109.3	122.5	143.2	151.8	160.3	164.6	173.9
413.0	82.99	61.3	65.6	67.4	71.6	76.4	74.8	86.6	111.4	110.6	109.2	108.6	121.7	142.1	150.6	159.1	163.4	172.5
413.5	83.16	61.5	65.7	67.4	71.6	76.3	74.6	86.1	110.8	110.0	108.8	108.2	121.0	141.1	149.7	158.2	162.3	171.3
414.0	83.29	61.6	65.8	67.4	71.6	76.2	74.4	85.7	110.2	109.5	108.4	107.7	120.3	140.3	148.9	157.3	161.4	170.1
414.5	83.41	61.7	66.0	67.3	71.5	76.3	74.2	85.4	109.6	109.1	108.0	107.3	119.6	139.5	148.1	156.6	160.5	169.0
415.0	83.32	61.8	66.1	67.4	71.5	76.3	74.0	85.0	109.2	108.7	107.7	106.9	118.9	138.7	147.3	155.8	159.7	168.1
415.5	83.11	61.8	66.3	67.4	71.5	76.2	73.8	84.6	108.8	108.4	107.4	106.5	118.2	138.1	146.6	155.1	158.8	167.2
416.0	82.63	61.7	66.2	67.4	71.4	76.1	73.6	84.2	108.5	108.1	106.9	106.1	117.6	137.4	145.8	154.2	158.0	166.4
416.5	81.92	61.5	66.1	67.4	71.3	75.9	73.4	83.8	108.2	107.8	106.5	105.7	117.1	136.7	145.0	153.2	157.2	165.6
417.0	81.05	61.2	65.9	67.3	71.2	75.6	73.1	83.4	107.9	107.5	106.0	105.3	116.6	136.0	144.1	152.1	156.3	164.7
417.5	79.97	60.7	65.6	67.1	71.0	75.3	72.7	82.9	107.6	107.1	105.5	104.8	116.1	135.2	143.1	150.9	155.3	163.6
418.0	78.70	60.1	65.0	66.7	70.7	74.9	72.1	82.2	107.0	106.5	104.9	104.1	115.4	134.1	141.9	149.6	154.2	162.1
418.5	77.29	59.3	64.3	66.1	70.2	74.4	71.3	81.6	106.2	105.8	104.1	103.3	114.6	132.8	140.5	148.1	152.6	160.4
419.0	75.67	58.3	63.4	65.4	69.6	73.8	70.5	80.8	105.1	104.7	103.2	102.3	113.5	131.3	138.9	146.3	150.8	158.3
419.5	73.91	57.2	62.4	64.6	68.9	72.9	69.5	79.8	103.8	103.5	102.0	101.1	112.1	129.4	137.0	144.3	148.5	155.8
420.0	71.90	55.9	61.2	63.5	67.9	71.9	68.4	78.6	102.2	102.0	100.6	99.6	110.4	127.2	134.7	141.9	145.7	152.8
420.5	69.64	54.5	60.0	62.4	66.7	70.7	67.2	77.3	100.4	100.3	98.9	98.0	108.4	124.5	132.0	139.1	142.5	149.5
421.0	67.25	53.0	58.6	61.2	65.5	69.3	65.9	75.7	98.3	98.3	96.8	96.0	106.0	121.5	128.8	135.7	138.7	145.6
421.5	64.70	51.5	57.1	59.9	64.1	67.7	64.5	73.9	96.0	96.0	94.5	93.9	103.3	118.1	125.2	131.8	134.7	141.5
422.0	62.10	49.9	55.6	58.5	62.5	66.0	62.9	71.9	93.4	93.5	91.9	91.4	100.4	114.3	121.3	127.4	130.2	136.9
422.5	59.53	48.4	54.1	57.2	61.0	64.2	61.2	69.7	90.7	90.7	89.1	88.7	97.2	110.3	117.0	122.8	125.5	131.9
423.0	57.02	46.9	52.6	55.7	59.3	62.3	59.3	67.4	87.9	87.6	86.1	85.8	93.8	106.0	112.4	117.8	120.6	126.6
423.5	54.68	45.5	51.3	54.3	57.7	60.4	57.4	64.9	85.0	84.5	83.1	82.8	90.3	101.7	107.7	112.6	115.5	121.2
424.0	52.45	44.0	50.0	52.9	56.2	58.5	55.4	62.4	81.9	81.4	80.1	79.7	86.8	97.3	102.9	107.4	110.3	115.5
424.5	50.35	42.7	48.9	51.6	54.7	56.6	53.4	60.0	78.9	78.3	77.2	76.7	83.2	92.9	98.1	102.3	105.1	110.0
425.0	48.40	41.5	47.9	50.5	53.4	55.0	51.6	57.6	75.9	75.4	74.4	73.8	79.8	88.7	93.3	97.3	100.0	104.4
425.5	46.54	40.4	46.9	49.6	52.2	53.5	49.9	55.4	73.1	72.6	71.8	71.1	76.6	84.7	88.8	92.6	95.1	99.2
426.0	44.85	39.5	46.2	48.7	51.2	52.2	48.4	53.5	70.5	70.2	69.3	68.6	73.6	80.8	84.5	88.2	90.4	94.4
426.5	43.32	38.6	45.5	48.1	50.3	51.0	47.0	51.7	68.2	68.0	67.1	66.4	70.8	77.3	80.5	84.1	86.1	89.9
427.0	41.95	37.8	44.9	47.6	49.6	50.0	45.8	50.3	66.2	66.0	65.1	64.5	68.3	74.1	77.0	80.4	82.2	85.9
427.5	40.81	37.1	44.5	47.3	49.2	49.2	44.8	49.0	64.5	64.3	63.4	62.8	66.1	71.3	73.8	77.1	78.7	82.2

428.0	39.83	36.6	44.2	47.1	48.9	48.4	43.9	47.9	63.2	62.9	61.8	61.4	64.2	68.8	71.1	74.1	75.6	79.0
428.5	38.96	36.1	44.0	47.1	48.7	47.8	43.3	47.1	62.0	61.6	60.6	60.3	62.6	66.7	68.8	71.4	72.9	76.1
429.0	38.19	35.7	43.9	47.2	48.7	47.4	42.8	46.3	61.0	60.6	59.6	59.2	61.2	64.9	66.7	69.1	70.4	73.5
429.5	37.44	35.5	44.0	47.3	48.8	47.2	42.4	45.8	60.1	59.8	58.8	58.4	60.1	63.3	65.0	67.1	68.3	71.2
430.0	36.70	35.4	44.2	47.6	48.9	47.1	42.1	45.3	59.4	59.2	58.2	57.6	59.1	61.9	63.3	65.2	66.4	69.2
430.5	36.00	35.3	44.4	47.9	49.2	47.2	41.9	45.0	58.8	58.7	57.8	57.0	58.3	60.6	61.8	63.5	64.7	67.4
431.0	35.33	35.1	44.6	48.3	49.4	47.4	41.7	44.8	58.3	58.3	57.5	56.6	57.7	59.3	60.4	62.0	63.2	65.8
431.5	34.74	35.1	44.9	48.7	49.8	47.7	41.7	44.6	58.0	58.1	57.3	56.3	57.1	58.2	59.1	60.6	61.7	64.3
432.0	34.19	35.0	45.1	49.2	50.2	48.0	41.6	44.4	57.7	57.9	57.2	56.1	56.6	57.2	57.8	59.3	60.4	62.9
432.5	33.64	35.0	45.4	49.7	50.7	48.3	41.7	44.3	57.5	57.7	57.0	55.9	56.1	56.2	56.6	58.0	59.1	61.5
433.0	33.14	34.9	45.8	50.3	51.2	48.6	41.7	44.2	57.5	57.5	56.9	55.8	55.7	55.2	55.5	56.8	57.8	60.0
433.5	32.70	35.0	46.2	50.8	51.8	48.9	41.8	44.1	57.5	57.4	56.7	55.8	55.3	54.4	54.5	55.6	56.6	58.6
434.0	32.26	35.1	46.7	51.5	52.5	49.2	42.0	44.0	57.5	57.4	56.6	55.7	54.9	53.6	53.5	54.4	55.4	57.2
434.5	31.90	35.2	47.3	52.2	53.2	49.5	42.2	44.0	57.6	57.3	56.5	55.7	54.6	52.8	52.6	53.2	54.3	55.9
435.0	31.58	35.4	47.9	53.0	53.9	49.9	42.4	44.1	57.6	57.2	56.6	55.8	54.4	52.1	51.7	52.1	53.2	54.5
435.5	31.30	35.6	48.7	53.9	54.7	50.4	42.7	44.2	57.8	57.3	56.7	55.8	54.1	51.4	50.8	51.1	52.1	53.3
436.0	31.07	35.9	49.6	54.9	55.6	50.9	43.0	44.5	57.9	57.4	56.9	56.0	53.9	50.9	50.0	50.1	51.0	52.3
436.5	30.83	36.2	50.5	55.9	56.4	51.6	43.4	44.7	58.1	57.7	57.2	56.2	53.8	50.3	49.2	49.2	50.1	51.3
437.0	30.60	36.6	51.4	57.0	57.4	52.3	43.8	45.1	58.4	58.0	57.5	56.5	53.8	49.8	48.5	48.4	49.2	50.4
437.5	30.42	37.0	52.3	58.2	58.5	53.0	44.3	45.5	58.8	58.6	57.9	56.9	53.8	49.4	47.9	47.6	48.4	49.7
438.0	30.24	37.4	53.2	59.4	59.6	53.8	44.8	45.9	59.3	59.3	58.4	57.3	54.0	49.0	47.3	47.0	47.7	49.1
438.5	30.12	37.9	54.2	60.7	60.8	54.6	45.3	46.4	59.8	60.0	58.9	57.8	54.2	48.7	46.9	46.5	47.1	48.5
439.0	30.05	38.3	55.1	62.0	62.0	55.5	45.9	47.0	60.5	60.8	59.5	58.3	54.5	48.5	46.4	46.1	46.6	47.9
439.5	30.01	38.8	56.1	63.4	63.3	56.5	46.5	47.6	61.1	61.5	60.2	58.9	54.9	48.4	46.1	45.7	46.1	47.5
440.0	29.98	39.3	57.2	64.7	64.6	57.5	47.2	48.3	61.9	62.3	61.0	59.5	55.2	48.4	45.9	45.5	45.7	47.1
440.5	29.93	39.8	58.3	65.9	65.8	58.7	47.9	49.0	62.6	63.0	61.7	60.1	55.7	48.4	45.7	45.2	45.3	46.7
441.0	29.84	40.4	59.4	67.2	67.1	60.0	48.6	49.7	63.4	63.7	62.5	60.8	56.1	48.5	45.6	45.0	45.0	46.3
441.5	29.72	40.9	60.6	68.5	68.4	61.2	49.4	50.4	64.2	64.4	63.3	61.6	56.5	48.5	45.6	44.7	44.7	45.9
442.0	29.54	41.5	61.8	69.8	69.7	62.4	50.2	51.1	65.0	65.3	64.0	62.4	56.9	48.5	45.5	44.4	44.4	45.5
442.5	29.35	42.0	63.0	71.2	71.0	63.5	51.0	51.7	65.9	66.1	64.7	63.2	57.3	48.5	45.4	44.1	44.2	45.2
443.0	29.14	42.4	64.2	72.7	72.4	64.6	51.7	52.4	66.7	67.0	65.4	64.0	57.8	48.5	45.3	43.8	43.9	44.8
443.5	28.94	42.8	65.3	74.1	73.8	65.6	52.4	52.9	67.6	67.9	66.1	64.7	58.3	48.5	45.1	43.5	43.6	44.5

444.0	28.69	43.1	66.5	75.6	75.2	66.6	53.2	53.5	68.4	68.7	66.9	65.4	58.8	48.5	44.8	43.2	43.3	44.1
444.5	28.41	43.4	67.6	77.0	76.6	67.7	53.8	54.0	69.2	69.4	67.7	66.0	59.2	48.5	44.5	42.9	43.0	43.6
445.0	28.06	43.7	68.6	78.4	77.9	68.7	54.5	54.5	70.1	70.1	68.5	66.7	59.7	48.5	44.1	42.5	42.5	43.1
445.5	27.70	44.0	69.7	79.8	79.2	69.7	55.1	55.0	70.8	70.6	69.2	67.4	60.2	48.4	43.7	42.1	42.0	42.5
446.0	27.28	44.4	70.7	81.1	80.4	70.7	55.8	55.5	71.4	71.2	69.9	68.1	60.6	48.2	43.2	41.6	41.4	41.7
446.5	26.82	44.7	71.7	82.3	81.6	71.7	56.4	56.0	72.0	71.8	70.5	68.7	60.8	48.0	42.8	41.1	40.7	41.0
447.0	26.32	45.0	72.6	83.6	82.8	72.6	57.0	56.5	72.6	72.4	71.1	69.3	61.0	47.6	42.3	40.4	39.8	40.1
447.5	25.87	45.2	73.6	84.8	84.0	73.5	57.7	57.0	73.0	72.9	71.5	69.8	61.0	47.2	41.7	39.6	38.9	39.2
448.0	25.40	45.5	74.5	86.0	85.3	74.3	58.3	57.5	73.5	73.4	71.9	70.3	61.0	46.7	41.1	38.8	38.0	38.2
448.5	24.92	45.7	75.6	87.2	86.5	75.2	58.9	57.9	73.9	73.8	72.3	70.6	60.8	46.1	40.3	37.8	37.0	37.2
449.0	24.43	45.9	76.6	88.3	87.7	76.0	59.5	58.2	74.3	74.1	72.6	70.9	60.6	45.5	39.5	36.7	35.9	36.1
449.5	23.98	46.1	77.6	89.5	88.9	76.8	60.0	58.5	74.6	74.3	72.8	71.1	60.5	44.9	38.5	35.6	34.7	34.9
450.0	23.53	46.3	78.6	90.7	90.0	77.6	60.4	58.8	74.9	74.5	73.1	71.4	60.3	44.2	37.6	34.4	33.5	33.7
450.5	23.06	46.5	79.4	91.9	90.9	78.3	60.8	59.0	75.1	74.7	73.4	71.6	60.2	43.6	36.6	33.3	32.3	32.4
451.0	22.59	46.7	80.1	93.1	91.9	79.0	61.2	59.3	75.3	74.9	73.6	71.8	60.0	43.0	35.6	32.2	31.2	31.2
451.5	22.18	47.0	80.8	94.2	92.9	79.6	61.7	59.6	75.6	75.2	73.8	72.0	60.0	42.5	34.7	31.1	30.1	30.1
452.0	21.83	47.3	81.5	95.3	93.9	80.3	62.1	59.8	75.9	75.6	74.1	72.3	59.9	41.9	33.9	30.1	29.1	29.0
452.5	21.50	47.6	82.2	96.4	94.9	81.1	62.5	60.0	76.2	75.9	74.4	72.4	59.8	41.3	33.1	29.2	28.3	27.9
453.0	21.19	47.9	83.0	97.4	96.0	81.8	62.9	60.3	76.6	76.2	74.8	72.6	59.8	40.6	32.4	28.4	27.5	27.0
453.5	20.91	48.2	83.9	98.4	97.1	82.6	63.3	60.5	77.0	76.5	75.2	72.8	59.7	40.1	31.8	27.7	26.7	26.1
454.0	20.67	48.5	84.9	99.5	98.1	83.5	63.6	60.7	77.4	76.8	75.7	73.1	59.8	39.5	31.2	27.0	26.0	25.3
454.5	20.42	48.8	85.8	100.5	99.2	84.3	63.9	61.0	77.9	77.1	76.2	73.4	59.9	39.1	30.7	26.3	25.3	24.5
455.0	20.16	49.0	86.7	101.6	100.2	85.0	64.2	61.4	78.3	77.3	76.6	73.7	60.0	38.7	30.2	25.8	24.6	23.8
455.5	19.94	49.2	87.6	102.6	101.1	85.7	64.6	61.9	78.8	77.7	77.0	74.0	60.2	38.4	29.8	25.3	24.0	23.1
456.0	19.76	49.5	88.5	103.5	102.1	86.3	65.0	62.3	79.1	78.2	77.3	74.5	60.4	38.2	29.4	24.8	23.4	22.5
456.5	19.60	49.8	89.3	104.4	103.0	87.0	65.5	62.7	79.5	78.7	77.6	74.9	60.7	38.1	29.1	24.4	22.9	22.0
457.0	19.45	50.1	90.1	105.2	103.9	87.6	66.0	63.1	79.9	79.2	77.9	75.3	60.9	38.0	28.8	24.1	22.5	21.4
457.5	19.30	50.4	90.9	105.9	104.7	88.2	66.5	63.4	80.2	79.7	78.2	75.7	61.1	37.9	28.5	23.7	22.1	21.0
458.0	19.15	50.7	91.7	106.6	105.4	88.8	66.9	63.7	80.6	80.1	78.5	76.0	61.3	37.8	28.3	23.5	21.8	20.6
458.5	18.98	50.8	92.3	107.3	106.1	89.5	67.4	64.0	80.9	80.5	78.8	76.4	61.4	37.7	28.1	23.2	21.6	20.2
459.0	18.78	51.0	93.0	108.0	106.7	90.1	67.8	64.3	81.3	80.9	79.3	76.7	61.6	37.7	27.9	23.0	21.4	19.9
459.5	18.57	51.0	93.5	108.7	107.3	90.7	68.1	64.6	81.7	81.2	79.7	77.0	61.8	37.5	27.7	22.8	21.1	19.6

460.0	18.33	51.2	93.9	109.3	107.9	91.3	68.4	64.8	82.1	81.5	80.1	77.4	61.9	37.4	27.5	22.6	20.9	19.4
460.5	18.11	51.3	94.3	109.9	108.4	91.8	68.6	65.0	82.4	81.9	80.4	77.8	62.0	37.4	27.2	22.4	20.7	19.2
461.0	17.91	51.5	94.6	110.5	108.9	92.3	68.8	65.2	82.7	82.2	80.8	78.1	62.2	37.3	26.9	22.1	20.4	19.0
461.5	17.73	51.8	94.9	111.0	109.4	92.6	68.9	65.4	83.0	82.5	81.1	78.5	62.3	37.2	26.7	21.9	20.1	18.7
462.0	17.57	52.0	95.3	111.5	109.9	92.9	69.1	65.5	83.2	82.7	81.3	78.8	62.4	37.2	26.5	21.6	19.8	18.5
462.5	17.42	52.2	95.7	111.9	110.5	93.2	69.2	65.7	83.4	82.9	81.5	79.0	62.5	37.1	26.2	21.3	19.6	18.2
463.0	17.27	52.3	96.0	112.3	110.9	93.6	69.4	65.8	83.6	83.0	81.7	79.1	62.6	37.1	26.0	21.0	19.3	17.9
463.5	17.12	52.3	96.3	112.6	111.4	93.9	69.5	65.9	83.8	83.2	81.8	79.2	62.7	37.0	25.8	20.8	19.1	17.6
464.0	16.94	52.4	96.6	112.8	111.8	94.2	69.6	66.0	83.9	83.3	81.9	79.2	62.7	36.9	25.7	20.6	18.9	17.3
464.5	16.76	52.4	96.9	113.0	112.1	94.5	69.7	66.1	83.9	83.4	82.0	79.3	62.7	36.8	25.6	20.4	18.8	17.0
465.0	16.58	52.5	97.1	113.2	112.4	94.7	69.8	66.1	83.9	83.5	82.0	79.2	62.6	36.7	25.5	20.2	18.6	16.8
465.5	16.40	52.5	97.2	113.4	112.6	94.8	69.9	66.1	83.9	83.5	82.0	79.3	62.5	36.6	25.4	20.1	18.4	16.6
466.0	16.25	52.6	97.3	113.5	112.7	94.8	70.0	66.2	83.9	83.5	82.1	79.3	62.4	36.4	25.3	20.0	18.2	16.4
466.5	16.08	52.6	97.4	113.5	112.8	94.7	70.0	66.2	84.0	83.5	82.1	79.3	62.2	36.3	25.2	19.9	18.0	16.3
467.0	15.94	52.6	97.4	113.5	112.7	94.7	70.1	66.1	84.1	83.6	82.2	79.4	62.2	36.1	25.0	19.8	17.8	16.2
467.5	15.83	52.6	97.4	113.4	112.7	94.6	70.1	66.1	84.2	83.8	82.3	79.5	62.2	36.0	24.9	19.7	17.7	16.0
468.0	15.70	52.6	97.3	113.3	112.7	94.5	70.1	66.1	84.3	83.9	82.4	79.6	62.2	35.8	24.7	19.6	17.5	15.9
468.5	15.56	52.5	97.3	113.1	112.6	94.6	70.1	66.1	84.4	84.0	82.4	79.7	62.3	35.7	24.6	19.5	17.4	15.8
469.0	15.42	52.5	97.3	112.9	112.5	94.6	69.9	66.0	84.3	84.1	82.4	79.7	62.5	35.7	24.5	19.4	17.3	15.6
469.5	15.28	52.4	97.3	112.8	112.3	94.6	69.7	66.0	84.2	84.1	82.3	79.6	62.5	35.6	24.3	19.3	17.2	15.5
470.0	15.13	52.4	97.2	112.8	112.2	94.6	69.5	65.9	84.1	84.0	82.3	79.5	62.6	35.6	24.2	19.2	17.1	15.4
470.5	14.98	52.4	97.2	112.8	112.1	94.5	69.3	65.8	84.0	83.7	82.2	79.4	62.6	35.5	24.1	19.1	17.0	15.3
471.0	14.80	52.4	97.0	112.8	111.9	94.3	69.2	65.7	83.8	83.4	82.0	79.2	62.4	35.5	24.0	19.0	16.9	15.2
471.5	14.62	52.4	96.8	112.8	111.8	94.1	69.0	65.6	83.6	83.2	82.0	79.0	62.2	35.4	23.9	18.9	16.8	15.1
472.0	14.46	52.4	96.5	112.7	111.8	93.8	68.9	65.4	83.4	82.9	81.9	78.9	61.9	35.3	23.9	18.7	16.7	15.0
472.5	14.28	52.3	96.2	112.5	111.6	93.5	68.8	65.3	83.2	82.7	81.7	78.8	61.6	35.2	23.8	18.6	16.6	14.8
473.0	14.12	52.3	95.9	112.2	111.3	93.3	68.6	65.1	83.0	82.5	81.5	78.6	61.3	35.0	23.7	18.4	16.5	14.7
473.5	13.94	52.3	95.5	111.8	111.0	93.1	68.3	64.9	82.8	82.4	81.3	78.5	61.0	34.9	23.5	18.3	16.4	14.6
474.0	13.78	52.2	95.3	111.4	110.6	92.9	68.1	64.8	82.5	82.2	81.1	78.4	60.8	34.7	23.4	18.1	16.3	14.4
474.5	13.62	52.1	95.0	111.0	110.3	92.7	67.8	64.7	82.3	82.0	80.9	78.3	60.6	34.5	23.2	17.9	16.1	14.3
475.0	13.44	52.1	94.8	110.6	109.9	92.5	67.5	64.5	82.1	81.7	80.6	78.2	60.5	34.2	23.1	17.7	16.0	14.2
475.5	13.26	52.0	94.6	110.2	109.5	92.3	67.3	64.3	81.8	81.5	80.4	78.0	60.3	34.0	22.9	17.5	15.8	14.0

476.0	13.10	51.9	94.4	109.7	109.3	92.1	67.1	64.1	81.5	81.3	80.2	77.8	60.1	33.8	22.7	17.3	15.6	13.8
476.5	12.94	51.8	94.3	109.4	109.0	91.9	67.0	63.9	81.2	81.1	79.9	77.5	59.8	33.6	22.5	17.2	15.4	13.7
477.0	12.78	51.6	94.0	109.1	108.6	91.6	66.8	63.6	80.9	80.8	79.6	77.1	59.6	33.4	22.3	17.1	15.2	13.5
477.5	12.62	51.4	93.6	108.8	108.3	91.3	66.5	63.2	80.5	80.5	79.3	76.6	59.3	33.2	22.1	16.9	15.0	13.3
478.0	12.46	51.2	93.3	108.5	107.9	91.0	66.2	62.9	80.2	80.2	78.9	76.2	59.1	33.0	21.8	16.8	14.8	13.0
478.5	12.32	51.0	93.0	108.2	107.4	90.6	65.8	62.5	79.9	79.8	78.6	75.8	58.8	32.8	21.6	16.6	14.6	12.9
479.0	12.16	50.7	92.7	107.9	107.1	90.1	65.5	62.1	79.5	79.4	78.3	75.4	58.6	32.5	21.4	16.5	14.4	12.7
479.5	11.99	50.6	92.3	107.7	106.6	89.8	65.1	61.8	79.1	79.0	78.0	75.0	58.4	32.3	21.2	16.3	14.2	12.5
480.0	11.82	50.4	92.0	107.4	106.3	89.4	64.8	61.5	78.8	78.5	77.6	74.6	58.1	32.1	21.1	16.1	14.1	12.4
480.5	11.68	50.4	91.6	107.0	105.9	89.0	64.6	61.2	78.4	78.1	77.2	74.2	57.8	31.9	20.9	15.9	13.9	12.2
481.0	11.53	50.4	91.2	106.6	105.6	88.7	64.4	61.0	78.1	77.8	76.8	73.9	57.5	31.7	20.8	15.7	13.7	12.1
481.5	11.40	50.3	90.8	106.2	105.2	88.4	64.2	60.7	77.7	77.4	76.4	73.5	57.2	31.5	20.6	15.5	13.6	11.9
482.0	11.27	50.3	90.4	105.7	104.8	88.1	64.0	60.4	77.3	77.1	76.0	73.2	56.8	31.4	20.4	15.3	13.4	11.8
482.5	11.15	50.2	90.0	105.2	104.4	87.8	63.8	60.1	77.1	76.9	75.5	72.9	56.4	31.2	20.2	15.1	13.3	11.6
483.0	11.03	50.0	89.7	104.7	104.0	87.5	63.5	59.7	76.8	76.6	75.2	72.7	56.1	31.0	20.1	15.0	13.1	11.4
483.5	10.89	49.8	89.4	104.1	103.7	87.1	63.2	59.3	76.5	76.3	74.8	72.5	55.9	30.9	19.9	14.9	13.0	11.3
484.0	10.72	49.6	89.1	103.6	103.2	86.7	62.8	58.9	76.3	76.0	74.5	72.3	55.6	30.7	19.7	14.8	12.9	11.1
484.5	10.57	49.4	88.8	103.2	102.8	86.3	62.4	58.6	76.0	75.7	74.2	72.1	55.4	30.6	19.6	14.7	12.8	11.0
485.0	10.41	49.2	88.5	102.8	102.3	85.8	62.0	58.3	75.7	75.3	73.9	71.8	55.1	30.4	19.4	14.6	12.8	10.9
485.5	10.27	49.0	88.0	102.3	101.8	85.4	61.7	58.0	75.2	74.9	73.7	71.5	54.8	30.3	19.3	14.5	12.7	10.8
486.0	10.13	48.8	87.5	101.9	101.3	85.1	61.3	57.7	74.8	74.5	73.4	71.1	54.5	30.2	19.2	14.3	12.6	10.6
486.5	10.04	48.7	86.9	101.5	100.7	84.7	61.0	57.4	74.3	74.0	73.1	70.8	54.2	30.0	19.0	14.2	12.5	10.5
487.0	9.98	48.5	86.4	101.0	100.2	84.4	60.7	57.2	73.9	73.6	72.8	70.4	53.9	29.8	18.9	14.1	12.4	10.4
487.5	9.94	48.4	85.9	100.5	99.8	84.1	60.4	56.9	73.5	73.1	72.5	69.9	53.7	29.5	18.9	14.0	12.2	10.3
488.0	9.88	48.2	85.4	100.1	99.3	83.7	60.0	56.6	73.1	72.6	72.1	69.6	53.4	29.3	18.8	13.9	12.1	10.2
488.5	9.81	48.1	85.0	99.7	98.9	83.3	59.6	56.4	72.8	72.2	71.7	69.2	53.2	29.1	18.6	13.8	11.9	10.1
489.0	9.74	48.0	84.7	99.3	98.5	82.8	59.1	56.1	72.5	71.8	71.3	68.8	52.9	28.9	18.5	13.7	11.8	10.0
489.5	9.64	47.8	84.5	98.9	98.1	82.3	58.8	55.9	72.2	71.5	70.8	68.4	52.6	28.7	18.4	13.6	11.7	9.9
490.0	9.53	47.7	84.1	98.5	97.6	81.9	58.4	55.5	71.9	71.1	70.4	68.1	52.3	28.6	18.2	13.5	11.7	9.8
490.5	9.44	47.5	83.7	98.1	97.1	81.5	58.2	55.1	71.5	70.8	70.0	67.8	52.0	28.4	18.0	13.3	11.6	9.7
491.0	9.35	47.4	83.3	97.6	96.6	81.2	57.9	54.8	71.1	70.5	69.6	67.5	51.6	28.3	17.8	13.2	11.5	9.6
491.5	9.30	47.2	82.8	97.1	96.2	80.9	57.6	54.4	70.6	70.2	69.2	67.1	51.3	28.1	17.7	13.1	11.4	9.5

492.0	9.25	47.1	82.3	96.7	95.7	80.6	57.3	54.1	70.1	69.9	68.9	66.7	50.9	27.8	17.6	13.0	11.2	9.4
492.5	9.21	46.9	81.8	96.2	95.2	80.3	57.0	53.7	69.7	69.6	68.6	66.3	50.6	27.6	17.4	12.9	11.1	9.4
493.0	9.19	46.8	81.4	95.7	94.7	79.9	56.7	53.4	69.3	69.3	68.2	65.9	50.3	27.4	17.4	12.8	11.0	9.3
493.5	9.15	46.6	81.0	95.3	94.1	79.5	56.3	53.1	69.0	69.0	67.8	65.5	50.0	27.1	17.3	12.7	10.9	9.3
494.0	9.09	46.4	80.6	94.8	93.6	79.1	56.0	52.8	68.6	68.7	67.4	65.1	49.8	27.0	17.2	12.6	10.9	9.3
494.5	9.01	46.2	80.3	94.3	93.1	78.6	55.7	52.5	68.3	68.3	67.0	64.8	49.6	26.8	17.0	12.5	10.8	9.2
495.0	8.92	45.9	79.9	93.7	92.6	78.2	55.5	52.2	68.0	67.9	66.6	64.6	49.4	26.7	16.9	12.5	10.7	9.2
495.5	8.82	45.6	79.5	93.2	92.1	77.7	55.2	52.0	67.6	67.5	66.2	64.3	49.2	26.6	16.8	12.4	10.7	9.1
496.0	8.71	45.3	79.1	92.5	91.7	77.3	54.9	51.7	67.2	67.1	65.9	64.0	48.9	26.5	16.7	12.4	10.6	9.0
496.5	8.61	45.0	78.7	91.9	91.2	76.8	54.6	51.5	66.7	66.7	65.6	63.6	48.7	26.4	16.7	12.3	10.5	8.9
497.0	8.53	44.8	78.3	91.3	90.7	76.3	54.2	51.2	66.3	66.4	65.4	63.3	48.3	26.2	16.6	12.3	10.4	8.8
497.5	8.47	44.5	77.9	90.8	90.2	75.8	53.9	51.0	65.9	66.2	65.2	62.9	48.0	26.1	16.5	12.2	10.3	8.7
498.0	8.40	44.3	77.5	90.3	89.7	75.3	53.5	50.7	65.5	65.8	65.0	62.5	47.6	25.9	16.4	12.1	10.3	8.7
498.5	8.33	44.0	77.1	90.0	89.1	74.8	53.1	50.3	65.2	65.4	64.7	62.2	47.3	25.7	16.3	12.0	10.2	8.6
499.0	8.27	43.7	76.7	89.6	88.5	74.3	52.8	50.0	64.8	65.0	64.4	61.8	47.0	25.5	16.1	11.9	10.2	8.5
499.5	8.20	43.4	76.4	89.2	88.0	73.8	52.4	49.6	64.4	64.5	63.9	61.5	46.8	25.3	15.9	11.7	10.2	8.5
500.0	8.12	43.1	75.9	88.8	87.5	73.3	52.1	49.2	64.0	64.0	63.5	61.1	46.5	25.1	15.8	11.6	10.1	8.4
500.5	8.05	42.8	75.4	88.3	87.0	72.8	51.8	48.8	63.6	63.4	62.9	60.7	46.2	24.9	15.6	11.5	10.0	8.3
501.0	7.98	42.6	75.0	87.6	86.5	72.4	51.5	48.4	63.2	63.0	62.3	60.3	45.9	24.7	15.5	11.5	9.9	8.2
501.5	7.94	42.3	74.5	87.0	86.0	71.9	51.2	48.2	62.8	62.5	61.8	59.7	45.6	24.6	15.3	11.4	9.8	8.1
502.0	7.89	42.1	74.0	86.3	85.4	71.5	50.9	47.9	62.4	62.1	61.3	59.2	45.3	24.4	15.3	11.4	9.7	8.1
502.5	7.85	41.9	73.6	85.6	84.9	71.1	50.5	47.6	62.2	61.7	60.9	58.6	44.9	24.3	15.2	11.3	9.6	8.0
503.0	7.82	41.6	73.1	84.9	84.2	70.7	50.1	47.3	61.8	61.3	60.5	58.2	44.6	24.1	15.1	11.2	9.5	8.0
503.5	7.77	41.4	72.6	84.2	83.5	70.3	49.7	47.1	61.4	60.8	60.1	57.8	44.3	24.0	15.1	11.1	9.4	7.9
504.0	7.72	41.1	72.0	83.7	82.9	69.9	49.2	46.8	61.0	60.4	59.8	57.4	44.0	23.8	14.9	11.0	9.3	7.8
504.5	7.66	40.9	71.4	83.1	82.3	69.5	48.8	46.4	60.6	59.9	59.3	57.2	43.7	23.7	14.8	10.9	9.3	7.8
505.0	7.59	40.6	70.8	82.6	81.7	69.0	48.3	46.1	60.1	59.5	58.9	56.9	43.4	23.6	14.7	10.7	9.3	7.7
505.5	7.51	40.3	70.1	82.0	81.1	68.6	47.8	45.8	59.5	59.2	58.4	56.6	43.1	23.4	14.6	10.6	9.2	7.6
506.0	7.42	40.1	69.5	81.4	80.6	68.1	47.5	45.4	59.0	58.9	58.0	56.3	42.8	23.3	14.4	10.6	9.1	7.6
506.5	7.32	39.8	68.8	80.8	80.1	67.5	47.1	45.1	58.4	58.5	57.5	55.9	42.5	23.1	14.3	10.5	9.0	7.5
507.0	7.22	39.4	68.2	80.1	79.4	66.9	46.7	44.7	57.9	58.2	57.1	55.5	42.1	22.9	14.2	10.5	8.9	7.4
507.5	7.12	39.1	67.7	79.4	78.8	66.2	46.4	44.3	57.4	57.7	56.7	55.1	41.7	22.7	14.1	10.5	8.8	7.4

508.0	7.01	38.7	67.1	78.8	78.1	65.6	46.1	44.0	56.9	57.1	56.2	54.5	41.4	22.5	14.0	10.4	8.7	7.3
508.5	6.92	38.3	66.6	78.1	77.5	65.0	45.8	43.6	56.5	56.6	55.8	54.0	41.0	22.2	13.9	10.4	8.6	7.2
509.0	6.82	38.0	66.1	77.4	76.8	64.4	45.4	43.3	56.0	55.9	55.3	53.5	40.6	22.0	13.8	10.3	8.6	7.2
509.5	6.72	37.6	65.6	76.8	76.1	63.9	45.0	42.9	55.5	55.4	54.8	53.0	40.2	21.9	13.7	10.2	8.5	7.1
510.0	6.62	37.3	65.1	76.1	75.4	63.3	44.6	42.5	55.1	54.8	54.3	52.5	39.9	21.7	13.5	10.1	8.5	7.1
510.5	6.53	36.9	64.5	75.3	74.7	62.7	44.1	42.0	54.6	54.4	53.8	52.1	39.5	21.6	13.4	10.0	8.4	7.0
511.0	6.44	36.6	63.9	74.6	74.0	62.1	43.7	41.5	54.1	54.0	53.3	51.6	39.2	21.4	13.3	9.9	8.4	7.0
511.5	6.37	36.2	63.3	73.8	73.1	61.5	43.2	40.9	53.6	53.6	52.8	51.1	38.9	21.2	13.1	9.8	8.3	6.9
512.0	6.31	35.9	62.7	73.0	72.2	60.8	42.7	40.4	53.0	53.2	52.2	50.6	38.6	21.0	13.0	9.7	8.2	6.8
512.5	6.25	35.6	62.0	72.3	71.4	60.2	42.2	39.9	52.5	52.8	51.7	50.2	38.2	20.8	12.8	9.6	8.1	6.8
513.0	6.20	35.2	61.3	71.5	70.6	59.5	41.7	39.4	51.9	52.3	51.1	49.7	37.9	20.6	12.7	9.4	8.0	6.7
513.5	6.12	34.9	60.6	70.8	69.8	58.9	41.2	39.0	51.3	51.7	50.7	49.2	37.5	20.4	12.6	9.3	7.9	6.6
514.0	6.04	34.5	59.9	70.1	69.0	58.2	40.7	38.6	50.8	51.1	50.3	48.8	37.2	20.2	12.5	9.2	7.8	6.5
514.5	5.96	34.2	59.2	69.3	68.3	57.5	40.3	38.3	50.2	50.4	49.8	48.4	36.8	20.1	12.4	9.1	7.8	6.5
515.0	5.87	33.9	58.5	68.5	67.6	56.8	39.9	38.0	49.7	49.9	49.3	47.9	36.4	19.9	12.2	9.0	7.7	6.4
515.5	5.78	33.5	57.8	67.7	67.0	56.1	39.4	37.6	49.1	49.3	48.9	47.4	36.1	19.7	12.0	8.9	7.7	6.3
516.0	5.70	33.1	57.2	66.9	66.2	55.4	39.0	37.2	48.6	48.7	48.4	46.9	35.6	19.5	11.9	8.9	7.6	6.2
516.5	5.62	32.7	56.5	66.1	65.5	54.6	38.5	36.7	48.1	48.2	47.8	46.4	35.2	19.3	11.7	8.8	7.5	6.2
517.0	5.56	32.3	55.8	65.3	64.7	53.9	38.0	36.2	47.6	47.8	47.2	45.9	34.7	19.1	11.6	8.8	7.4	6.1
517.5	5.47	31.9	55.0	64.6	63.8	53.2	37.5	35.8	47.0	47.3	46.6	45.3	34.3	18.8	11.4	8.7	7.3	6.1
518.0	5.37	31.4	54.3	63.8	62.9	52.5	37.0	35.3	46.5	46.8	46.0	44.7	33.9	18.6	11.3	8.6	7.2	6.0
518.5	5.28	31.0	53.6	63.0	62.0	51.8	36.5	34.8	45.9	46.2	45.3	44.1	33.6	18.4	11.2	8.5	7.1	6.0
519.0	5.18	30.6	52.9	62.2	61.1	51.1	36.0	34.4	45.3	45.6	44.7	43.6	33.2	18.1	11.1	8.4	7.0	5.9
519.5	5.10	30.2	52.2	61.4	60.2	50.4	35.6	34.0	44.7	45.0	44.1	43.0	32.9	17.9	11.0	8.2	7.0	5.9
520.0	5.03	29.8	51.5	60.5	59.4	49.8	35.2	33.6	44.1	44.3	43.6	42.5	32.5	17.6	10.9	8.1	6.9	5.8
520.5	4.97	29.4	50.8	59.6	58.7	49.2	34.7	33.2	43.5	43.7	43.2	42.0	32.1	17.4	10.8	8.0	6.8	5.7
521.0	4.91	29.1	50.1	58.7	57.9	48.6	34.2	32.8	42.9	43.1	42.7	41.5	31.7	17.2	10.7	7.9	6.8	5.7
521.5	4.85	28.7	49.4	57.7	57.1	47.9	33.7	32.3	42.3	42.6	42.2	41.0	31.2	17.0	10.5	7.8	6.7	5.6
522.0	4.78	28.2	48.6	56.8	56.3	47.2	33.2	31.8	41.8	42.0	41.7	40.5	30.7	16.9	10.4	7.7	6.6	5.6
522.5	4.71	27.8	47.8	55.9	55.4	46.6	32.7	31.3	41.2	41.4	41.2	39.9	30.3	16.7	10.3	7.6	6.5	5.5
523.0	4.63	27.4	47.0	55.0	54.5	45.9	32.1	30.7	40.6	40.9	40.5	39.4	29.8	16.5	10.2	7.5	6.4	5.4
523.5	4.57	27.0	46.2	54.2	53.6	45.1	31.6	30.2	39.9	40.3	39.9	38.8	29.4	16.3	10.1	7.4	6.3	5.4

524.0	4.51	26.7	45.5	53.3	52.8	44.4	31.1	29.8	39.3	39.7	39.3	38.2	29.0	16.1	9.9	7.3	6.2	5.3
524.5	4.45	26.3	44.9	52.6	52.1	43.6	30.5	29.3	38.7	39.1	38.7	37.7	28.6	15.8	9.8	7.2	6.2	5.2
525.0	4.40	26.0	44.3	51.8	51.3	42.9	30.0	28.8	38.1	38.5	38.0	37.1	28.2	15.6	9.7	7.1	6.1	5.1
525.5	4.33	25.7	43.6	51.1	50.5	42.2	29.5	28.4	37.6	38.0	37.4	36.5	27.8	15.4	9.6	7.0	6.0	5.0
526.0	4.25	25.3	42.9	50.3	49.6	41.5	29.0	28.0	37.0	37.4	36.8	36.0	27.3	15.2	9.4	7.0	6.0	5.0
526.5	4.17	24.9	42.2	49.5	48.7	40.8	28.5	27.6	36.5	36.8	36.2	35.4	26.9	14.9	9.3	6.9	5.9	4.9
527.0	4.08	24.5	41.5	48.6	47.8	40.2	28.0	27.2	36.0	36.2	35.6	34.9	26.5	14.8	9.2	6.8	5.8	4.8
527.5	4.01	24.1	40.7	47.7	46.8	39.5	27.6	26.8	35.4	35.7	35.0	34.3	26.1	14.6	9.0	6.7	5.7	4.8
528.0	3.94	23.6	40.0	46.7	45.9	38.8	27.2	26.3	34.8	35.1	34.5	33.8	25.6	14.4	8.9	6.7	5.6	4.7
528.5	3.88	23.2	39.2	45.9	45.1	38.1	26.8	25.9	34.3	34.5	33.9	33.2	25.2	14.1	8.7	6.6	5.6	4.7
529.0	3.82	22.8	38.5	45.0	44.4	37.4	26.3	25.4	33.7	33.9	33.4	32.7	24.8	13.9	8.6	6.5	5.5	4.6
529.5	3.76	22.5	37.8	44.2	43.7	36.7	25.9	24.9	33.1	33.3	32.9	32.1	24.5	13.6	8.5	6.5	5.5	4.6
530.0	3.71	22.1	37.1	43.4	42.9	35.9	25.4	24.4	32.4	32.8	32.3	31.5	24.0	13.4	8.4	6.4	5.4	4.5
530.5	3.65	21.8	36.5	42.7	42.2	35.2	24.9	23.9	31.8	32.2	31.8	30.9	23.7	13.2	8.3	6.3	5.3	4.5
531.0	3.58	21.4	35.8	41.9	41.5	34.5	24.4	23.5	31.2	31.7	31.3	30.3	23.3	13.0	8.2	6.2	5.3	4.5
531.5	3.52	21.1	35.2	41.2	40.7	33.8	23.9	23.1	30.6	31.2	30.7	29.7	22.9	12.8	8.1	6.1	5.2	4.4
532.0	3.46	20.7	34.5	40.5	39.9	33.2	23.4	22.7	30.0	30.6	30.1	29.2	22.5	12.5	7.9	6.0	5.1	4.3
532.5	3.40	20.4	33.9	39.7	39.1	32.7	22.9	22.3	29.5	30.0	29.6	28.7	22.1	12.3	7.8	5.9	5.0	4.2
533.0	3.33	20.1	33.3	39.0	38.4	32.2	22.5	21.9	28.9	29.4	29.0	28.2	21.7	12.1	7.7	5.8	4.9	4.2
533.5	3.24	19.7	32.7	38.3	37.7	31.7	22.1	21.6	28.4	28.8	28.4	27.7	21.2	11.9	7.6	5.7	4.8	4.1
534.0	3.17	19.4	32.0	37.6	36.9	31.1	21.7	21.2	27.9	28.2	27.9	27.2	20.8	11.6	7.4	5.7	4.7	4.0
534.5	3.10	19.0	31.4	36.8	36.2	30.6	21.4	20.7	27.4	27.6	27.4	26.7	20.4	11.4	7.3	5.6	4.7	3.9
535.0	3.04	18.6	30.8	36.1	35.5	30.0	21.0	20.3	26.9	27.0	26.9	26.2	20.0	11.2	7.2	5.5	4.6	3.9
535.5	2.99	18.3	30.2	35.3	34.7	29.5	20.7	20.0	26.4	26.5	26.4	25.7	19.7	11.0	7.0	5.4	4.6	3.8
536.0	2.96	17.9	29.5	34.6	34.0	28.9	20.3	19.6	25.9	26.0	26.0	25.2	19.4	10.8	6.9	5.3	4.5	3.8
536.5	2.93	17.5	28.9	33.9	33.4	28.3	20.0	19.3	25.4	25.5	25.6	24.7	19.1	10.6	6.8	5.2	4.5	3.8
537.0	2.91	17.2	28.3	33.2	32.7	27.7	19.7	19.0	25.0	25.1	25.1	24.2	18.8	10.4	6.7	5.1	4.4	3.7
537.5	2.87	16.9	27.7	32.5	32.1	27.1	19.3	18.7	24.6	24.7	24.7	23.8	18.5	10.2	6.6	5.1	4.4	3.7
538.0	2.83	16.6	27.2	31.9	31.5	26.5	19.0	18.4	24.1	24.4	24.2	23.3	18.2	10.0	6.5	5.0	4.3	3.6
538.5	2.78	16.3	26.7	31.3	31.0	26.0	18.6	18.1	23.7	24.0	23.8	22.9	17.9	9.9	6.4	5.0	4.3	3.5
539.0	2.74	16.0	26.2	30.7	30.4	25.4	18.3	17.8	23.3	23.6	23.4	22.5	17.6	9.8	6.3	4.9	4.2	3.5
539.5	2.68	15.7	25.7	30.1	29.8	24.9	17.9	17.5	22.9	23.2	23.0	22.1	17.3	9.6	6.1	4.9	4.1	3.4

540.0	2.62	15.3	25.2	29.6	29.3	24.4	17.6	17.2	22.5	22.8	22.6	21.7	17.0	9.5	6.0	4.8	4.0	3.4
540.5	2.56	15.0	24.7	29.0	28.7	23.9	17.3	16.9	22.1	22.3	22.2	21.3	16.7	9.4	5.9	4.7	4.0	3.4
541.0	2.50	14.6	24.2	28.4	28.1	23.5	17.0	16.5	21.7	21.8	21.8	20.9	16.4	9.2	5.9	4.6	3.9	3.3
541.5	2.44	14.4	23.7	27.9	27.5	23.0	16.6	16.2	21.3	21.4	21.4	20.5	16.1	9.0	5.8	4.5	3.8	3.3
542.0	2.41	14.1	23.2	27.3	26.9	22.6	16.3	15.9	20.9	21.0	21.0	20.2	15.8	8.9	5.7	4.4	3.8	3.3
542.5	2.38	13.9	22.8	26.7	26.3	22.1	16.0	15.6	20.5	20.6	20.6	19.9	15.5	8.7	5.7	4.4	3.7	3.2
543.0	2.37	13.7	22.3	26.1	25.8	21.7	15.7	15.3	20.1	20.2	20.2	19.6	15.2	8.5	5.6	4.3	3.7	3.2
543.5	2.35	13.5	21.9	25.6	25.3	21.2	15.3	15.0	19.7	19.9	19.9	19.3	14.9	8.4	5.5	4.2	3.7	3.1
544.0	2.33	13.2	21.4	25.1	24.8	20.8	15.0	14.7	19.4	19.5	19.6	19.0	14.6	8.2	5.5	4.2	3.6	3.1
544.5	2.30	13.0	21.0	24.6	24.4	20.4	14.7	14.5	19.1	19.2	19.2	18.7	14.3	8.1	5.4	4.1	3.6	3.0
545.0	2.26	12.7	20.6	24.2	23.9	20.0	14.4	14.2	18.7	18.9	18.9	18.4	14.0	8.0	5.3	4.1	3.5	3.0
545.5	2.20	12.4	20.2	23.8	23.5	19.8	14.1	13.9	18.4	18.6	18.5	18.0	13.8	7.8	5.2	4.0	3.5	3.0
546.0	2.16	12.1	19.9	23.3	23.1	19.5	13.9	13.7	18.1	18.2	18.2	17.7	13.6	7.7	5.1	3.9	3.4	2.9
546.5	2.11	11.9	19.5	22.9	22.6	19.2	13.7	13.4	17.8	17.9	17.8	17.3	13.3	7.5	5.1	3.9	3.4	2.9
547.0	2.07	11.6	19.2	22.5	22.1	19.0	13.4	13.2	17.6	17.5	17.4	17.0	13.1	7.4	5.0	3.9	3.3	2.8
547.5	2.03	11.5	18.9	22.1	21.6	18.6	13.1	13.0	17.3	17.2	17.1	16.6	12.9	7.3	4.9	3.8	3.3	2.8
548.0	1.99	11.3	18.6	21.6	21.2	18.3	12.9	12.7	17.0	16.9	16.8	16.3	12.7	7.2	4.9	3.8	3.3	2.7
548.5	1.95	11.1	18.3	21.2	20.8	17.9	12.7	12.5	16.7	16.6	16.5	16.1	12.4	7.1	4.7	3.7	3.2	2.7
549.0	1.91	10.9	17.8	20.7	20.6	17.6	12.5	12.2	16.3	16.3	16.2	15.8	12.2	7.1	4.6	3.7	3.2	2.7
549.5	1.86	10.6	17.3	20.4	20.5	17.2	12.3	12.0	15.8	16.0	15.9	15.6	11.9	7.1	4.4	3.6	3.1	2.8
550.0	1.81	10.2	16.7	20.1	20.5	16.8	12.2	11.7	15.3	15.6	15.5	15.3	11.6	7.1	4.2	3.5	3.0	2.9
550.5	1.77	9.8	16.0	19.9	20.7	16.5	12.2	11.5	14.7	15.3	15.2	15.1	11.3	7.1	4.0	3.4	2.9	3.0

3.10. Micropolarity (I_1/I_3) values of pyrene with variation of [Surf] at different NaAlg concentration at 298.15 K

0.001% w/v NaAlg		0.005% w/v NaAlg		0.01% w/v NaAlg		0.001% w/v NaAlg		0.005% w/v NaAlg		0.01% w/v NaAlg	
[C ₁₆ MImCl] / mM	I_1/I_3	[C ₁₆ MImCl] / mM	I_1/I_3	[C ₁₆ MImCl] / mM	I_1/I_3	[C ₁₆ TPB] / mM	I_1/I_3	[C ₁₆ TPB] / mM	I_1/I_3	[C ₁₆ TPB] / mM	I_1/I_3
0	1.33	0	1.34	0	1.35	0	1.35	0	1.34	0	1.32
0.02	1.18	0.01	1.19	0.01	1.12	0.004	1.27	0.005	1.27	0.004	1.29
0.03	1.18	0.02	1.14	0.03	1.03	0.008	1.28	0.011	1.20	0.009	1.26
0.05	1.14	0.04	1.08	0.04	0.99	0.013	1.26	0.017	1.16	0.018	1.23
0.06	1.15	0.06	1.04	0.06	0.97	0.019	1.24	0.024	1.12	0.031	1.20
0.08	1.12	0.07	1.02	0.08	0.95	0.025	1.19	0.033	1.09	0.049	1.17
0.10	1.12	0.10	0.98	0.10	0.96	0.032	1.18	0.045	1.06	0.111	1.16
0.13	1.12	0.12	0.98	0.12	0.95	0.038	1.16	0.060	1.04	0.162	1.15
0.16	1.13	0.15	0.97	0.15	0.96	0.045	1.15	0.078	1.02	0.229	1.15
0.19	1.13	0.18	0.97	0.20	0.95	0.052	1.14	0.098	1.00	0.318	1.15
0.23	1.12	0.21	0.98	0.26	0.95	0.06	1.13	0.122	1.00	0.418	1.16
0.28	1.11	0.25	0.98	0.41	0.95	0.071	1.13	0.148	0.99	0.528	1.16
0.34	1.12	0.37	0.99	0.53	0.95	0.079	1.13	0.177	0.99	0.653	1.16
0.40	1.10	0.41	0.99	0.70	0.95	0.089	1.13	0.211	0.98	0.783	1.16
0.48	1.10	0.53	0.99	0.92	0.95	0.104	1.12	0.250	1.00		
0.57	1.10	0.58	0.99	1.25	0.95	0.118	1.12	0.295	1.00		
0.69	1.11	0.94	0.90	1.66	0.95	0.148	1.11	0.345	1.01		
0.80	1.06	1.16	0.92	2.14	0.96	0.164	1.11	0.399	1.00		
0.91	1.06	1.71	0.95	2.58	0.97	0.181	1.10				
1.02	1.04	2.08	0.96	3.00	0.97	0.198	1.10				
1.13	1.04	3.14	0.99	3.39	0.97	0.215	1.08				
1.23	1.03	4.66	0.99	3.76	0.97	0.261	1.08				
1.44	1.04	5.48	0.99	4.11	0.97	0.294	1.07				
1.74	1.04			4.75	0.96	0.335	1.06				
2.12	1.03					0.383	1.04				
2.57	1.02					0.446	1.04				
3.18	1.03					0.521	1.03				
3.92	1.02					0.594	1.03				
4.57	1.02										

3.11. Micropolarity (I_1/I_3) values of pyrene with variation of [Surf] in aqueous medium at 298.15 K

[C ₁₆ MImCl]/ mM	I_E/I_m	[C ₁₆ TPB]/ mM	I_E/I_m
0	0.115	0	0.095
0.012	0.531	0.004	0.215
0.024	0.919	0.007	0.305
0.036	1.036	0.015	0.427
0.060	0.961	0.025	0.493
0.096	0.740	0.040	0.474
0.144	0.554	0.058	0.438
0.203	0.449	0.093	0.364
0.291	0.452	0.162	0.296
0.406	0.452	0.261	0.288
0.576	0.451	0.387	0.262
0.824	0.440		
1.141	0.305		
1.640	0.150		
2.325	0.097		
3.136	0.073		
3.851	0.063		
5.052	0.055		

3.12. Average lifetime ($\langle\tau\rangle$) of Pyrene in presence and absence of C₁₆MImCl and C₁₆TPB (variation of surfactant concentrations) in 0.005% w/v NaAlg solution at 298.15 K.

0.005% w/v NaAlg			
[C ₁₆ MImCl] / mM	$\langle\tau\rangle$	[C ₁₆ TPB] / mM	$\langle\tau\rangle$
0	122.3	0	124.7
0.01	112.3	0.0048	118.6
0.04	109.8	0.0168	102.3
0.07	101.8	0.0317	84.4
0.12	129.6	0.0585	69.7
0.21	151.3	0.0968	57.5
0.32	147.1	0.1463	46.7
0.47	140.8	0.2320	43.1
0.67	140.6	0.3378	41.7
0.94	135.5	0.4458	36.5
1.31	151.5	0.5559	35.8
1.76	167.4	0.6949	34.7
2.94	165.4	0.8522	31.5
3.69	166.7	1.0249	34.8
4.51	166.2	1.2207	30.0
5.35	167.7	1.4248	30.5

3.13. Average hydrodynamic radius (r) of Pyrene in presence and absence of C₁₆MImCl and C₁₆TPB (variation of surfactant concentrations) in 0.005% w/v NaAlg solution at 298.15 K.

[C ₁₆ MImCl] / mM	Hydrodynamic radius (r) in nm unit in presence of 0.01% w/v of NaAlg		
	< 500 nm	500-1000 nm	>500 nm
0	265.6	-	-
0.030	110.1	-	-
0.089	110.1	-	-
0.178	95.07	-	-
0.294	127.5	-	-
0.436	--	694	--
0.645	--	--	1931
0.980	--	927	2780
1.423	127.5	742	2780
2.010	--	641	2780
2.548	--	553	2780
3.322	--	742	2780
4.164	82.09	742	2780
4.892	138	995	2780
6.090	--	--	1545

0.01% w/v NaAlg	
[C ₁₆ TPB] / mM	r / nm
0	229
0.018	127.5
0.054	110
0.098	110
0.184	110
0.347	110
0.569	95.07
0.891	95.07
1.265	110
1.608	110
1.949	118.7
2.335	110
2.702	95.1

3.14. Calorimetric data of [C₁₆MImCl] at different concentration of NaAlg at 298.15 K.

0.001% w/v NaAlg		0.005% w/v NaAlg		0.01% w/v NaAlg	
[C ₁₆ MImCl]/ mM	ΔH^0_{obs} kJ.mol ⁻¹	[C ₁₆ MImCl]/ mM	ΔH^0_{obs} kJ.mol ⁻¹	[C ₁₆ MImCl]/ mM	ΔH^0_{obs} kJ.mol ⁻¹
0	--	0	--	0	--
0.211	4.152	0.038	4.195	0.040	4.196
0.378	3.307	0.188	3.851	0.199	3.523
0.543	1.948	0.337	3.292	0.357	2.646
0.707	1.387	0.484	2.687	0.513	1.745
0.869	1.135	0.629	1.880	0.667	1.295
1.030	0.967	0.774	1.351	0.820	1.170
1.188	0.858	0.916	1.064	0.971	1.129
1.345	0.769	1.058	0.909	1.121	0.986
1.501	0.702	1.197	0.778	1.269	0.928
1.654	0.616	1.336	0.698	1.416	0.759
1.806	0.582	1.473	0.633	1.561	0.755
1.957	0.542	1.608	0.604	1.705	0.644
2.106	0.504	1.742	0.570	1.847	0.618
2.253	0.436	1.874	0.551	1.987	0.579
2.398	0.441	2.005	0.493	2.126	0.487
2.542	0.458	2.135	0.446	2.263	0.510
2.684	0.377	2.263	0.409	2.399	0.505
2.824	0.364	2.389	0.392	2.533	0.505
		2.514	0.339	2.665	0.453
		2.638	--	2.796	--

3.15. Calorimetric data of [C₁₆TPB] at different concentration of NaAlg at 298.15 K.

0.001% w/v NaAlg		0.005% w/v NaAlg		0.01% w/v NaAlg	
[C ₁₆ TPB]/ mM	ΔH^0_{obs}	[C ₁₆ TPB]/ mM	ΔH^0_{obs}	[C ₁₆ TPB]/ mM	ΔH^0_{obs}
0.000		0.000		0.000	
0.008	3.144	0.008	1.546	0.008	1.266
0.041	3.375	0.038	1.700	0.039	1.513
0.073	2.311	0.069	1.595	0.070	0.883
0.105	1.207	0.099	1.610	0.101	0.138
0.136	0.335	0.128	1.352	0.131	-0.418
0.167	0.259	0.158	1.342	0.161	-0.652
0.198	0.171	0.187	1.257	0.191	-0.656
0.229	0.045	0.216	1.245	0.221	-0.660
0.259	-0.168	0.244	1.079	0.250	-0.913
0.289	-0.349	0.273	1.014	0.279	-0.897
0.319	-0.523	0.301	0.834	0.307	-1.032
0.348	-0.647	0.328	0.834	0.336	-0.946
0.377	-0.347	0.356	1.043	0.363	-1.052
0.406	-0.456	0.383	0.912	0.391	-1.056
0.434	-0.607	0.409	0.786	0.418	-1.124
0.462	-0.657	0.436	0.789	0.445	-1.125
0.490	-0.601	0.462	0.811	0.472	-1.100
0.517	-0.711	0.488	0.756	0.499	-1.119
0.544	-0.660	0.513	0.751	0.525	-1.137
0.571	-0.685	0.538	0.657	0.550	-1.026

3.16. Quenching of pyrene by [CPC] at aqueous micellar solution (both C₁₆MImCl and C₁₆TPB) in presence and absence of NaAlg (0.001, 0.005 and 0.01 % w/v) at 298.15 K.

Quenching of pyrene by CPC in presence of aqueous micellar and micellar solution in presence of NaAlg							
C ₁₆ MImCl in water		C ₁₆ MImCl in 0.001% w/v NaAlg		C ₁₆ MImCl in 0.005% w/v NaAlg		C ₁₆ MImCl in 0.01% w/v NaAlg	
[CPC]/ mM	ln(I ₀ /I)	[CPC]/ mM	ln(I ₀ /I)	[CPC]/ mM	ln(I ₀ /I)	[CPC]/ mM	ln(I ₀ /I)
0.000	0.000	0.000	0.000	0.000	0.000	0.000	0.000
0.008	0.006	0.001	0.011	0.001	0.012	0.008	0.004
0.014	0.064	0.004	0.032	0.004	0.030	0.014	0.035
0.020	0.102	0.008	0.053	0.008	0.052	0.020	0.085
0.027	0.135	0.014	0.092	0.014	0.087	0.027	0.126
0.034	0.195	0.020	0.141	0.020	0.149	0.034	0.170
		0.027	0.171	0.027	0.173		
		0.034	0.205	0.034	0.219		
C ₁₆ TPB in water		C ₁₆ TPB in 0.001% w/v NaAlg		C ₁₆ TPB in 0.005% w/v NaAlg		C ₁₆ TPB in 0.01% w/v NaAlg	
[CPC]/ mM	ln(I ₀ /I)	[CPC]/ mM	ln(I ₀ /I)	[CPC]/ mM	ln(I ₀ /I)	[CPC]/ mM	ln(I ₀ /I)
0.000	0.000	0.000	0.000	0.000	0.000	0.000	0.000
0.034	0.001	0.027	0.016	0.008	0.077	0.008	0.047
0.040	0.011	0.034	0.015	0.027	0.106	0.027	0.077
0.053	0.037	0.053	0.015	0.034	0.082	0.034	0.096
0.066	0.054	0.072	0.056	0.053	0.106	0.053	0.109
0.078	0.079	0.091	0.091	0.072	0.124	0.072	0.131
		0.109	0.106	0.091	0.143	0.091	0.205
				0.109	0.162	0.109	0.179

3.17. Specific viscosities of NaAlg with variation of its concentration in 0.1 M NaCl solution at 298.15 K

[NaAlg] / gm.mol ⁻¹	specific viscosity (cm ³ /g)
0.010	606
0.009	562
0.008	533
0.007	509
0.007	480
0.006	431
0.004	396

3.18. Hydrodynamic radius data vs. Mean Intensity in conjugation with NaAlg with C₁₆MImCl. Different concentrations of C₁₆MImCl have been used.

Hydrodynamic radius of NaAlg ([NaAlg] = 0.01% w/v) in pure state and in presence of different [C ₁₆ MImCl] in mM					
r/nm	Pure NaAlg	[C ₁₆ MImCl] = 0.09 mM	[C ₁₆ MImCl] = 0.30 mM	[C ₁₆ MImCl] = 1.42 mM	[C ₁₆ MImCl] = 3.32 mM
	Mean Intensity %	Mean Intensity %	Mean Intensity %	Mean Intensity %	Mean Intensity %
0.20	0.0	0.0	0.0	0.0	0.0
0.23	0.0	0.0	0.0	0.0	0.0
0.27	0.0	0.0	0.0	0.0	0.0
0.31	0.0	0.0	0.0	0.0	0.0
0.36	0.0	0.0	0.0	0.0	0.0
0.42	0.0	0.0	0.0	0.0	0.0
0.48	0.0	0.0	0.0	0.0	0.0
0.56	0.0	0.0	0.0	0.0	0.0
0.65	0.0	0.0	0.0	0.0	0.0
0.75	0.0	0.0	0.0	0.0	0.0
0.87	0.0	0.0	0.0	0.0	0.0
1.01	0.0	0.0	0.0	0.0	0.0
1.16	0.0	0.0	0.0	0.0	0.0
1.35	0.0	0.0	0.0	0.0	0.0
1.56	0.0	0.0	0.0	0.0	0.0
1.81	0.0	0.0	0.0	0.0	0.0
2.09	0.0	0.0	0.0	0.0	0.0
2.42	0.0	0.0	0.0	0.0	0.0
2.81	0.0	0.0	0.0	0.0	0.0
3.25	0.0	0.0	0.0	0.0	0.0
3.77	0.0	0.0	0.0	0.0	0.0
4.36	0.0	0.0	0.0	0.0	0.0
5.05	0.0	0.0	0.0	0.0	0.0
5.85	0.0	0.0	0.0	0.0	0.0
6.77	0.0	0.0	0.0	0.0	0.0
7.84	0.0	0.0	0.0	0.0	0.0
9.08	0.0	0.0	0.0	0.0	0.0
10.52	0.0	0.0	0.0	0.0	0.0
12.18	0.0	0.0	0.0	0.0	0.0
14.11	0.0	0.1	0.0	0.0	0.0
16.34	0.0	0.3	0.0	0.0	0.0
18.92	0.0	0.3	0.0	0.0	0.0
21.91	0.0	0.3	0.5	0.0	0.0
25.37	0.0	0.2	1.2	0.0	0.0
29.39	0.0	0.3	1.7	0.0	0.0
34.03	0.0	0.8	2.1	0.0	0.0
39.41	0.0	1.7	2.3	0.0	0.0
45.64	0.0	3.1	2.7	0.0	0.0

52.85	0.0	4.9	3.5	0.0	0.0
61.21	0.7	6.8	4.8	0.0	0.0
70.89	1.8	8.5	6.5	0.0	0.0
82.09	2.9	9.9	8.3	0.2	0.0
95.07	3.8	10.7	10.0	0.7	0.0
110.10	4.6	10.8	11.0	1.2	0.0
127.50	5.6	10.3	11.3	1.5	0.0
147.70	7.2	9.2	10.6	1.4	0.0
171.00	9.3	7.6	9.0	1.0	0.0
198.00	11.5	5.9	6.9	0.4	0.0
229.30	13.1	4.1	4.5	0.0	0.0
265.60	13.4	2.5	2.4	0.0	0.0
307.60	11.8	1.3	0.8	0.3	0.0
356.20	8.5	0.5	0.1	1.4	2.0
412.50	4.6	0.1	0.0	3.6	6.1
477.70	1.3	0.0	0.0	6.3	10.8
553.20	0.0	0.0	0.0	9.0	14.5
640.70	0.0	0.0	0.0	11.0	15.6
741.90	0.0	0.0	0.0	11.7	13.9
859.20	0.0	0.0	0.0	10.8	10.0
995.10	0.0	0.0	0.0	8.5	5.3
1152.00	0.0	0.0	0.0	5.4	1.7
1335.00	0.0	0.0	0.0	2.5	0.0
1545.00	0.0	0.0	0.0	0.8	0.0
1790.00	0.0	0.0	0.0	0.9	0.0
2073.00	0.0	0.0	0.0	3.1	1.5
2400.00	0.0	0.0	0.0	6.9	6.0
2780.00	0.0	0.0	0.0	11.3	12.8
3219.00	0.0	0.0	0.0	0.0	0.0
3728.00	0.0	0.0	0.0	0.0	0.0
4317.00	0.0	0.0	0.0	0.0	0.0
5000.00	0.0	0.0	0.0	0.0	0.0
Hydrodynamic radius of NaAlg ([NaAlg] = 0.01% w/v) in pure state and in presence of different [C ₁₆ TPB] in mM					
r.nm	[C ₁₆ TPB] = 0.05 mM	[C ₁₆ TPB] = 0.18mM	[C ₁₆ TPB] = 0.89 mM	[C ₁₆ TPB] = 1.95 mM	[C ₁₆ TPB] = 2.33 mM
	Mean Intensity %	Mean Intensity %	Mean Intensity %	Mean Intensity %	Mean Intensity %
0.20	0.0	0.0	0.0	0.0	0.0
0.23	0.0	0.0	0.0	0.0	0.0
0.27	0.0	0.0	0.0	0.0	0.0
0.31	0.0	0.0	0.0	0.0	0.0
0.36	0.0	0.0	0.0	0.0	0.0
0.42	0.0	0.0	0.0	0.0	0.0
0.48	0.0	0.0	0.0	0.0	0.0
0.56	0.0	0.0	0.0	0.0	0.0
0.65	0.0	0.0	0.0	0.0	0.0

0.75	0.0	0.0	0.0	0.0	0.0
0.87	0.0	0.0	0.0	0.0	0.0
1.01	0.0	0.0	0.0	0.0	0.0
1.16	0.0	0.0	0.0	0.0	0.0
1.35	0.0	0.0	0.0	0.0	0.0
1.56	0.0	0.0	0.0	0.0	0.0
1.81	0.0	0.0	0.0	0.0	0.0
2.09	0.0	0.0	0.0	0.0	0.0
2.42	0.0	0.0	0.0	0.0	0.0
2.81	0.0	0.0	0.0	0.0	0.0
3.25	0.0	0.0	0.0	0.0	0.0
3.77	0.0	0.0	0.0	0.0	0.0
4.36	0.0	0.0	0.0	0.0	0.0
5.05	0.0	0.0	0.0	0.0	0.0
5.85	0.0	0.0	0.0	0.0	0.0
6.77	0.0	0.0	0.0	0.0	0.0
7.84	0.0	0.0	0.0	0.0	0.0
9.08	0.0	0.0	0.0	0.0	0.0
10.52	0.0	0.0	0.0	0.0	0.0
12.18	0.0	0.0	0.0	0.0	0.0
14.11	0.0	0.0	0.0	0.0	0.0
16.34	0.0	0.0	0.0	0.0	0.0
18.92	0.0	0.0	0.0	0.0	0.0
21.91	0.0	0.0	0.0	0.0	0.0
25.37	0.0	0.0	0.0	0.0	0.0
29.39	0.0	0.0	0.0	0.0	0.0
34.03	0.0	0.0	0.0	0.1	0.0
39.41	0.0	0.3	0.7	0.7	0.1
45.64	0.8	1.6	2.4	1.8	1.1
52.85	2.5	3.8	5.0	3.4	2.9
61.21	5.0	6.5	7.9	5.4	5.3
70.89	7.7	9.3	10.4	7.6	7.9
82.09	10.2	11.5	12.0	9.7	10.2
95.07	11.9	12.8	12.7	11.3	11.9
110.1	12.6	13.0	12.3	12.2	12.7
127.5	12.3	12.1	11.0	12.2	12.5
147.7	11.1	10.3	9.1	11.3	11.3
171.0	9.3	8.0	6.8	9.4	9.4
198.0	7.1	5.5	4.5	7.1	7.0
229.3	4.8	3.3	2.6	4.6	4.5
265.6	2.8	1.6	1.1	2.3	2.3
307.6	1.4	0.5	0.3	0.8	0.8
356.2	0.4	0.0	0.0	0.0	0.1
412.5	0.0	0.0	0.0	0.0	0.0

477.7	0.0	0.0	0.0	0.0	0.0
553.2	0.0	0.0	0.0	0.0	0.0
640.7	0.0	0.0	0.0	0.0	0.0
741.9	0.0	0.0	0.0	0.0	0.0
859.2	0.0	0.0	0.0	0.0	0.0
995.1	0.0	0.0	0.0	0.0	0.0
1152	0.0	0.0	0.0	0.0	0.0
1335	0.0	0.0	0.0	0.0	0.0
1545	0.0	0.0	0.0	0.0	0.0
1790	0.0	0.0	0.1	0.0	0.0
2073	0.0	0.0	0.2	0.0	0.0
2400	0.0	0.0	0.3	0.0	0.0
2780	0.0	0.0	0.5	0.0	0.0
3219	0.0	0.0	0.0	0.0	0.0
3728	0.0	0.0	0.0	0.0	0.0
4317	0.0	0.0	0.0	0.0	0.0
5000	0.0	0.0	0.0	0.0	0.0

Chapter –IV

4.1. Tensiometry data for SDS, DTAB, C₁₆MImCl, 16-4-16 and Tween-60 in aqueous medium at 298.15 K

Surface tension in aqueous solution									
[SDS]/ mM	γ / mN.m ⁻¹	[DTAB]/ mM	γ / mN.m ⁻¹	[C ₁₆ MImCl]/ mM	γ / mN.m ⁻¹	[16-4-16]/ mM	γ / mN.m ⁻¹	[Tween- 60]/ mM	γ / mN.m ⁻¹
0.00	72.8	0.00	70.1	0.00	70.6	0.000	69.8	0.000	70.6
0.05	68.0	0.43	63.4	0.01	67.6	0.005	63.4	0.009	48.4
0.09	67.2	1.07	61.4	0.02	66.6	0.008	57.8	0.017	47.0
0.16	62.8	2.13	58.0	0.03	65.9	0.015	51.6	0.024	45.0
0.26	58.2	3.82	53.0	0.06	63.4	0.025	48.2	0.035	43.1
0.38	54.8	6.30	46.4	0.11	61.4	0.040	47.5	0.060	42.4
0.52	52.8	10.33	41.4	0.17	58.2	0.064	48.0	0.103	40.9
0.68	48.8	14.22	38.9	0.28	54.7	0.103	47.6	0.189	40.2
0.86	46.8	18.01	40.1	0.45	49.4	0.152	46.7	0.358	39.5
1.09	45.2	21.68	40.1	0.67	44.6	0.248	46.4	0.608	39.2
1.54	37.8			0.93	42.7	0.391	45.8	1.013	38.9
2.21	36.0			1.31	41.9				
3.28	32.4			1.80	42.1				
4.82	29.0			2.68	41.6				
6.74	27.0			4.18	41.3				
8.45	30.6			5.41	41.2				
13.24	35.2								
18.30	36.6								
23.25	37.2								

4.2. Tensiometry data for SDS, DTAB, C₁₆MImCl, 16-4-16 and Tween-60 in 15% EtOH-water medium at 298.15 K

Surface tension in 15% v/v EtOH medium									
[SDS]/mM	γ / mN.m ⁻¹	[DTAB]/mM	γ / mN.m ⁻¹	[16-4-16]/mM	γ / mN.m ⁻¹	[C ₁₆ MImCl]/mM	γ / mN.m ⁻¹	[Tween-60]/mM	γ / mN.m ⁻¹
0.000	41.0	0.00	41.0	0.000	40.8	0.000	41.4	0.00	41.0
0.036	41.2	0.07	40.8	0.001	40.7	0.006	40.9	0.01	38.9
0.107	41.0	0.20	40.7	0.002	40.5	0.019	40.8	0.01	37.5
0.213	40.2	0.41	40.7	0.004	40.4	0.037	40.5	0.02	36.3
0.355	39.1	0.74	39.9	0.007	36.5	0.068	39.3	0.03	34.9
0.531	36.0	1.14	37.9	0.020	35.4	0.172	37.9	0.06	34.3
0.778	32.9	1.61	37.1	0.032	34.6	0.335	36.9	0.09	34.2
1.058	29.4	2.27	34.9	0.040	33.9	0.453	36.3	0.14	34.0
1.406	28.1	3.06	34.6	0.049	33.5	0.599	34.9		
1.923	27.9	4.03	32.8	0.070	33	0.769	34.6		
2.436	26.9	5.32	31.4	0.083	32.9	0.964	34.7		
3.112	25.5	6.89	29.5	0.097	32.8	1.206	35.0		
5.087	29.6	10.84	27.6			1.959	35.0		
6.677	32.1	13.18	29.1			2.638	34.9		
8.970	32.9	15.73	30.3						
11.870	33.4	18.47	30.3						
18.419	33.3	23.66	30.0						
27.205	33.5	30.81	29.6						
32.728	32.7	39.33	29.8						
		48.60	29.6						

4.3. Tensiometry data for SDS, DTAB, C₁₆MImCl, 16-4-16 and Tween-60 in 15% EtOH-water medium in presence of H₂DTC at 298.15 K

Surface tension in 15% v/v EtOH medium in presence of H ₂ DTC									
[SDS]/mM	γ / mN.m ⁻¹	[DTAB]/mM	γ / mN.m ⁻¹	[16-4-16]/mM	γ / mN.m ⁻¹	[C ₁₆ MImCl]/mM	γ / mN.m ⁻¹	[Tween-60]/mM	γ / mN.m ⁻¹
0.000	40.7	0.00	40.4	0.000	40.7	0.000	40.7	0.000	42.1
0.038	40.9	0.04	41.0	0.001	41.3	0.002	41.8	0.003	40.9
0.115	40.3	0.12	41.2	0.002	41.5	0.007	41.9	0.009	37.8
0.231	34.1	0.27	41.1	0.004	38.2	0.016	38.8	0.015	37.4
0.384	29.7	0.51	39.9	0.006	34.1	0.030	38.5	0.024	36.0
0.575	26.2	0.82	38.8	0.008	34.0	0.048	38.4	0.036	36.0
0.841	24.6	1.21	37.8	0.011	32.4	0.070	38.1	0.051	35.8
1.144	24.4	1.67	36.6	0.014	31.3	0.142	36.6	0.081	36.1
1.520	24.2	2.21	33.7	0.017	31.5	0.212	35.8	0.140	36.1
2.079	23.8	2.83	32.4	0.020	32.6	0.234	34.4		
2.634	24.2	3.51	33.5	0.024	33.0	0.278	33.7		
3.364	25.2	4.26	34.0	0.029	33.1	0.329	34.3		

4.264	26.3	6.35	33.1	0.04	34.0	0.364	35.0		
5.500	28.0	8.17	28.2	0.04	34.2	0.469	35.8		
7.219	30.1	9.95	27.0	0.06	34.5	0.552	36.6		
9.698	30.2	12.40	30.1	0.08	34.5	0.654	37.0		
		15.11	30.7	0.12	33.3	0.774	38.1		
		26.41	30.2			1.809	38.6		
		29.30	30.2						

4.4. Absorbance data of H₂DTC at different SDS concentration at 298.15 K

absorbance of H ₂ DTC in different wavelength upon addition of different concentration of SDS in mM unit								
Wavelength/ nm	[SDS]= 0 mM	0.19	0.67	1.83	4.03	7.78	12.78	22.42
300.0	0.22	0.22	0.22	0.21	0.19	0.18	0.19	0.19
300.5	0.22	0.22	0.22	0.21	0.19	0.18	0.19	0.19
301.0	0.22	0.22	0.22	0.21	0.19	0.18	0.18	0.19
301.5	0.22	0.22	0.22	0.21	0.19	0.18	0.18	0.19
302.0	0.21	0.22	0.22	0.20	0.18	0.18	0.18	0.19
302.5	0.22	0.22	0.21	0.20	0.18	0.18	0.18	0.19
303.0	0.22	0.22	0.21	0.20	0.18	0.18	0.18	0.19
303.5	0.21	0.22	0.21	0.20	0.18	0.18	0.18	0.19
304.0	0.21	0.22	0.21	0.20	0.18	0.18	0.18	0.19
304.5	0.22	0.22	0.21	0.20	0.18	0.18	0.18	0.19
305.0	0.21	0.22	0.21	0.20	0.18	0.18	0.18	0.19
305.5	0.21	0.22	0.21	0.20	0.18	0.18	0.18	0.19
306.0	0.22	0.22	0.21	0.20	0.18	0.18	0.18	0.19
306.5	0.22	0.22	0.22	0.20	0.18	0.18	0.18	0.19
307.0	0.22	0.22	0.22	0.20	0.18	0.18	0.18	0.19
307.5	0.21	0.22	0.22	0.20	0.18	0.18	0.19	0.19
308.0	0.22	0.22	0.21	0.20	0.18	0.18	0.18	0.20
308.5	0.22	0.22	0.21	0.20	0.18	0.18	0.18	0.19
309.0	0.22	0.22	0.21	0.20	0.18	0.18	0.18	0.19
309.5	0.22	0.21	0.21	0.20	0.18	0.18	0.18	0.19
310.0	0.21	0.21	0.21	0.20	0.18	0.18	0.18	0.19
310.5	0.21	0.21	0.21	0.20	0.18	0.18	0.18	0.19
311.0	0.21	0.21	0.21	0.20	0.18	0.18	0.18	0.19
311.5	0.21	0.21	0.21	0.20	0.18	0.18	0.18	0.19
312.0	0.21	0.21	0.21	0.20	0.18	0.18	0.18	0.19
312.5	0.21	0.21	0.21	0.20	0.18	0.18	0.18	0.19
313.0	0.21	0.21	0.21	0.20	0.18	0.18	0.18	0.19
313.5	0.21	0.21	0.21	0.20	0.18	0.18	0.18	0.19
314.0	0.21	0.21	0.21	0.20	0.18	0.18	0.18	0.19
314.5	0.21	0.21	0.21	0.20	0.18	0.18	0.18	0.19
315.0	0.21	0.21	0.21	0.20	0.18	0.17	0.18	0.19
315.5	0.21	0.21	0.20	0.20	0.18	0.17	0.18	0.19
316.0	0.20	0.21	0.20	0.20	0.17	0.18	0.18	0.19
316.5	0.20	0.21	0.20	0.19	0.17	0.18	0.18	0.19
317.0	0.20	0.20	0.20	0.19	0.17	0.17	0.17	0.19
317.5	0.20	0.20	0.20	0.19	0.17	0.17	0.18	0.19
318.0	0.20	0.21	0.20	0.19	0.17	0.17	0.18	0.19
318.5	0.20	0.21	0.20	0.19	0.17	0.17	0.18	0.18

319.0	0.20	0.20	0.20	0.19	0.17	0.17	0.18	0.19
319.5	0.20	0.20	0.20	0.19	0.17	0.17	0.18	0.19
320.0	0.20	0.20	0.20	0.19	0.17	0.17	0.18	0.19
320.5	0.20	0.20	0.20	0.19	0.17	0.17	0.17	0.19
321.0	0.20	0.20	0.20	0.19	0.17	0.17	0.17	0.18
321.5	0.20	0.20	0.20	0.19	0.17	0.17	0.18	0.18
322.0	0.20	0.20	0.20	0.19	0.17	0.17	0.18	0.18
322.5	0.20	0.20	0.20	0.19	0.17	0.17	0.18	0.18
323.0	0.20	0.20	0.20	0.19	0.17	0.17	0.18	0.18
323.5	0.20	0.20	0.20	0.19	0.17	0.17	0.17	0.18
324.0	0.20	0.20	0.20	0.18	0.17	0.17	0.17	0.18
324.5	0.20	0.20	0.20	0.18	0.16	0.17	0.17	0.18
325.0	0.20	0.19	0.20	0.18	0.16	0.17	0.17	0.18
325.5	0.19	0.19	0.19	0.18	0.16	0.16	0.17	0.18
326.0	0.19	0.20	0.19	0.18	0.16	0.17	0.17	0.18
326.5	0.19	0.19	0.19	0.18	0.16	0.17	0.17	0.18
327.0	0.19	0.19	0.19	0.18	0.16	0.16	0.17	0.18
327.5	0.19	0.19	0.19	0.18	0.16	0.16	0.17	0.18
328.0	0.19	0.19	0.19	0.18	0.16	0.17	0.17	0.18
328.5	0.19	0.19	0.19	0.18	0.16	0.17	0.17	0.18
329.0	0.19	0.19	0.19	0.18	0.16	0.17	0.17	0.18
329.5	0.19	0.19	0.19	0.18	0.16	0.17	0.17	0.18
330.0	0.19	0.19	0.19	0.18	0.16	0.17	0.17	0.18
330.5	0.19	0.19	0.19	0.18	0.16	0.17	0.17	0.18
331.0	0.19	0.19	0.19	0.18	0.16	0.16	0.17	0.18
331.5	0.19	0.19	0.19	0.18	0.16	0.16	0.17	0.18
332.0	0.19	0.19	0.19	0.18	0.16	0.16	0.17	0.18
332.5	0.19	0.19	0.19	0.18	0.16	0.16	0.17	0.18
333.0	0.19	0.19	0.19	0.18	0.16	0.17	0.17	0.18
333.5	0.19	0.19	0.19	0.18	0.16	0.17	0.17	0.19
334.0	0.19	0.19	0.19	0.18	0.16	0.16	0.17	0.19
334.5	0.20	0.19	0.19	0.18	0.16	0.16	0.17	0.19
335.0	0.19	0.19	0.19	0.18	0.16	0.17	0.17	0.19
335.5	0.19	0.20	0.19	0.18	0.16	0.17	0.17	0.19
336.0	0.19	0.19	0.19	0.18	0.16	0.17	0.17	0.19
336.5	0.20	0.20	0.19	0.18	0.16	0.17	0.17	0.19
337.0	0.20	0.20	0.19	0.18	0.16	0.17	0.17	0.19
337.5	0.20	0.20	0.19	0.18	0.16	0.17	0.17	0.19
338.0	0.19	0.20	0.19	0.18	0.17	0.17	0.17	0.19
338.5	0.19	0.20	0.19	0.18	0.17	0.17	0.18	0.19
339.0	0.20	0.20	0.19	0.18	0.16	0.17	0.18	0.19
339.5	0.20	0.20	0.19	0.18	0.17	0.17	0.18	0.19
340.0	0.20	0.20	0.19	0.18	0.17	0.17	0.18	0.20
340.5	0.20	0.20	0.20	0.18	0.16	0.17	0.18	0.20
341.0	0.19	0.19	0.19	0.17	0.16	0.17	0.18	0.20
341.5	0.18	0.18	0.19	0.17	0.16	0.17	0.18	0.19
342.0	0.19	0.19	0.18	0.18	0.16	0.17	0.18	0.19
342.5	0.19	0.19	0.18	0.18	0.16	0.17	0.17	0.19
343.0	0.19	0.19	0.19	0.18	0.16	0.17	0.18	0.19
343.5	0.19	0.19	0.19	0.18	0.17	0.16	0.18	0.20
344.0	0.19	0.19	0.19	0.18	0.17	0.17	0.18	0.20
344.5	0.18	0.19	0.19	0.18	0.17	0.17	0.18	0.20
345.0	0.19	0.19	0.19	0.18	0.17	0.17	0.18	0.20

345.5	0.19	0.19	0.19	0.18	0.17	0.17	0.18	0.20
346.0	0.19	0.19	0.19	0.18	0.17	0.17	0.18	0.20
346.5	0.19	0.20	0.19	0.19	0.17	0.17	0.18	0.20
347.0	0.20	0.20	0.20	0.19	0.17	0.18	0.18	0.21
347.5	0.20	0.20	0.20	0.19	0.17	0.18	0.18	0.21
348.0	0.20	0.20	0.19	0.18	0.17	0.18	0.18	0.21
348.5	0.20	0.20	0.20	0.19	0.18	0.18	0.19	0.21
349.0	0.20	0.20	0.20	0.19	0.18	0.18	0.19	0.21
349.5	0.20	0.20	0.20	0.19	0.18	0.18	0.19	0.21
350.0	0.20	0.20	0.20	0.19	0.17	0.18	0.19	0.21
350.5	0.20	0.20	0.20	0.19	0.18	0.18	0.19	0.22
351.0	0.20	0.20	0.20	0.19	0.18	0.18	0.20	0.22
351.5	0.20	0.20	0.20	0.19	0.18	0.19	0.19	0.22
352.0	0.20	0.20	0.20	0.19	0.18	0.19	0.19	0.22
352.5	0.20	0.20	0.20	0.20	0.18	0.19	0.20	0.22
353.0	0.21	0.21	0.20	0.20	0.18	0.19	0.20	0.22
353.5	0.21	0.21	0.20	0.20	0.18	0.19	0.20	0.22
354.0	0.21	0.21	0.20	0.20	0.18	0.19	0.20	0.22
354.5	0.21	0.21	0.21	0.20	0.19	0.19	0.20	0.22
355.0	0.21	0.21	0.21	0.20	0.19	0.19	0.20	0.22
355.5	0.21	0.21	0.21	0.20	0.18	0.19	0.20	0.22
356.0	0.21	0.21	0.21	0.20	0.19	0.19	0.20	0.22
356.5	0.21	0.21	0.21	0.20	0.19	0.19	0.20	0.22
357.0	0.21	0.21	0.21	0.20	0.19	0.19	0.20	0.22
357.5	0.21	0.22	0.21	0.20	0.19	0.19	0.20	0.23
358.0	0.21	0.22	0.21	0.20	0.19	0.19	0.20	0.23
358.5	0.22	0.21	0.21	0.20	0.19	0.19	0.20	0.22
359.0	0.22	0.22	0.21	0.21	0.19	0.19	0.20	0.23
359.5	0.22	0.22	0.21	0.21	0.19	0.19	0.20	0.23
360.0	0.22	0.22	0.21	0.21	0.19	0.19	0.20	0.23
360.5	0.22	0.21	0.21	0.21	0.19	0.19	0.20	0.23
361.0	0.22	0.21	0.21	0.21	0.19	0.19	0.20	0.22
361.5	0.22	0.21	0.22	0.21	0.19	0.19	0.20	0.22
362.0	0.22	0.22	0.22	0.21	0.19	0.19	0.20	0.22
362.5	0.22	0.22	0.21	0.21	0.19	0.20	0.20	0.23
363.0	0.22	0.22	0.22	0.21	0.19	0.20	0.20	0.23
363.5	0.22	0.22	0.22	0.21	0.19	0.19	0.20	0.22
364.0	0.22	0.22	0.22	0.21	0.19	0.19	0.21	0.23
364.5	0.22	0.22	0.22	0.21	0.19	0.19	0.20	0.22
365.0	0.22	0.22	0.22	0.20	0.19	0.19	0.20	0.22
365.5	0.22	0.22	0.21	0.20	0.19	0.19	0.20	0.22
366.0	0.22	0.22	0.22	0.21	0.19	0.19	0.20	0.22
366.5	0.22	0.22	0.22	0.21	0.19	0.19	0.20	0.22
367.0	0.22	0.22	0.21	0.21	0.19	0.19	0.20	0.22
367.5	0.22	0.22	0.21	0.21	0.19	0.19	0.20	0.22
368.0	0.22	0.22	0.22	0.21	0.19	0.19	0.20	0.22
368.5	0.22	0.22	0.22	0.21	0.19	0.19	0.20	0.22
369.0	0.22	0.22	0.22	0.20	0.19	0.19	0.20	0.21
369.5	0.22	0.22	0.21	0.20	0.19	0.19	0.20	0.21
370.0	0.22	0.22	0.22	0.21	0.19	0.19	0.20	0.21
370.5	0.22	0.22	0.22	0.21	0.19	0.19	0.20	0.22
371.0	0.22	0.22	0.21	0.21	0.19	0.19	0.20	0.21
371.5	0.22	0.22	0.21	0.21	0.19	0.19	0.19	0.21

372.0	0.22	0.22	0.22	0.21	0.19	0.19	0.19	0.21
372.5	0.22	0.22	0.22	0.21	0.19	0.19	0.20	0.21
373.0	0.22	0.22	0.22	0.21	0.19	0.19	0.20	0.21
373.5	0.22	0.22	0.22	0.21	0.19	0.19	0.20	0.21
374.0	0.22	0.22	0.22	0.21	0.19	0.19	0.20	0.21
374.5	0.22	0.22	0.22	0.21	0.19	0.19	0.20	0.21
375.0	0.22	0.22	0.22	0.21	0.19	0.19	0.20	0.21
375.5	0.22	0.22	0.22	0.21	0.19	0.19	0.20	0.21
376.0	0.22	0.23	0.22	0.21	0.20	0.19	0.19	0.21
376.5	0.22	0.23	0.22	0.21	0.20	0.19	0.19	0.21
377.0	0.23	0.23	0.22	0.21	0.19	0.19	0.19	0.21
377.5	0.23	0.23	0.22	0.21	0.20	0.19	0.20	0.21
378.0	0.23	0.23	0.22	0.21	0.20	0.20	0.20	0.21
378.5	0.23	0.23	0.22	0.22	0.20	0.19	0.20	0.21
379.0	0.23	0.23	0.23	0.22	0.20	0.19	0.20	0.21
379.5	0.23	0.23	0.23	0.22	0.20	0.20	0.20	0.21
380.0	0.23	0.23	0.23	0.22	0.20	0.20	0.20	0.21
380.5	0.23	0.23	0.23	0.22	0.20	0.20	0.20	0.21
381.0	0.24	0.24	0.23	0.22	0.20	0.20	0.20	0.21
381.5	0.24	0.24	0.23	0.22	0.21	0.20	0.20	0.21
382.0	0.24	0.24	0.24	0.23	0.21	0.20	0.20	0.21
382.5	0.24	0.24	0.24	0.23	0.21	0.20	0.20	0.21
383.0	0.24	0.24	0.24	0.23	0.21	0.20	0.21	0.21
383.5	0.24	0.24	0.24	0.23	0.21	0.21	0.21	0.22
384.0	0.25	0.24	0.24	0.23	0.22	0.21	0.21	0.22
384.5	0.25	0.25	0.24	0.24	0.22	0.21	0.21	0.22
385.0	0.25	0.25	0.25	0.24	0.22	0.21	0.21	0.22
385.5	0.25	0.25	0.25	0.24	0.22	0.21	0.22	0.22
386.0	0.25	0.25	0.25	0.24	0.22	0.22	0.22	0.23
386.5	0.26	0.26	0.25	0.24	0.23	0.22	0.22	0.23
387.0	0.26	0.26	0.26	0.25	0.23	0.22	0.22	0.23
387.5	0.26	0.26	0.26	0.25	0.23	0.22	0.23	0.23
388.0	0.26	0.26	0.26	0.25	0.23	0.23	0.23	0.23
388.5	0.27	0.26	0.26	0.25	0.23	0.23	0.23	0.24
389.0	0.27	0.27	0.26	0.25	0.24	0.23	0.23	0.24
389.5	0.27	0.27	0.27	0.26	0.24	0.23	0.23	0.24
390.0	0.27	0.27	0.27	0.26	0.24	0.24	0.24	0.25
390.5	0.28	0.28	0.27	0.26	0.24	0.24	0.24	0.25
391.0	0.28	0.28	0.28	0.27	0.25	0.24	0.24	0.25
391.5	0.28	0.28	0.28	0.27	0.25	0.24	0.25	0.25
392.0	0.28	0.28	0.28	0.27	0.25	0.25	0.25	0.25
392.5	0.28	0.28	0.28	0.27	0.26	0.25	0.25	0.26
393.0	0.29	0.29	0.28	0.28	0.26	0.25	0.25	0.26
393.5	0.29	0.29	0.29	0.28	0.26	0.26	0.26	0.26
394.0	0.29	0.29	0.29	0.28	0.26	0.26	0.26	0.27
394.5	0.30	0.30	0.29	0.28	0.27	0.26	0.26	0.27
395.0	0.30	0.30	0.29	0.29	0.27	0.26	0.27	0.27
395.5	0.30	0.30	0.30	0.29	0.27	0.27	0.27	0.27
396.0	0.30	0.30	0.30	0.29	0.27	0.27	0.27	0.28
396.5	0.31	0.31	0.30	0.29	0.28	0.27	0.27	0.28
397.0	0.31	0.31	0.30	0.30	0.28	0.27	0.28	0.28
397.5	0.31	0.31	0.31	0.30	0.28	0.28	0.28	0.29
398.0	0.31	0.31	0.31	0.30	0.29	0.28	0.28	0.29

398.5	0.32	0.32	0.31	0.30	0.29	0.28	0.29	0.29
399.0	0.32	0.32	0.32	0.31	0.29	0.29	0.29	0.30
399.5	0.32	0.32	0.32	0.31	0.30	0.29	0.29	0.30
400.0	0.32	0.32	0.32	0.31	0.30	0.30	0.30	0.30
400.5	0.33	0.33	0.32	0.32	0.30	0.30	0.30	0.30
401.0	0.33	0.33	0.33	0.32	0.30	0.30	0.30	0.31
401.5	0.33	0.33	0.33	0.32	0.31	0.30	0.30	0.31
402.0	0.33	0.33	0.33	0.32	0.31	0.30	0.31	0.32
402.5	0.34	0.34	0.33	0.33	0.31	0.31	0.31	0.32
403.0	0.34	0.34	0.34	0.33	0.31	0.31	0.31	0.32
403.5	0.34	0.34	0.34	0.33	0.32	0.31	0.32	0.32
404.0	0.34	0.34	0.34	0.33	0.32	0.32	0.32	0.33
404.5	0.35	0.35	0.34	0.33	0.32	0.32	0.32	0.33
405.0	0.35	0.35	0.35	0.34	0.32	0.32	0.33	0.33
405.5	0.35	0.35	0.35	0.34	0.33	0.33	0.33	0.34
406.0	0.35	0.35	0.35	0.34	0.33	0.33	0.33	0.34
406.5	0.35	0.35	0.35	0.34	0.33	0.33	0.33	0.34
407.0	0.36	0.36	0.35	0.35	0.34	0.33	0.34	0.35
407.5	0.36	0.36	0.36	0.35	0.34	0.34	0.34	0.35
408.0	0.36	0.36	0.36	0.35	0.34	0.34	0.34	0.35
408.5	0.36	0.36	0.36	0.35	0.34	0.34	0.35	0.35
409.0	0.36	0.36	0.36	0.36	0.34	0.34	0.35	0.36
409.5	0.36	0.37	0.36	0.36	0.35	0.35	0.35	0.36
410.0	0.37	0.37	0.37	0.36	0.35	0.35	0.35	0.36
410.5	0.37	0.37	0.37	0.36	0.35	0.35	0.36	0.36
411.0	0.37	0.37	0.37	0.36	0.35	0.36	0.36	0.37
411.5	0.37	0.37	0.37	0.36	0.35	0.36	0.36	0.37
412.0	0.37	0.37	0.37	0.36	0.36	0.36	0.36	0.37
412.5	0.37	0.37	0.37	0.37	0.36	0.36	0.37	0.37
413.0	0.38	0.37	0.37	0.37	0.36	0.36	0.37	0.38
413.5	0.38	0.38	0.37	0.37	0.36	0.36	0.37	0.38
414.0	0.38	0.38	0.37	0.37	0.36	0.37	0.37	0.38
414.5	0.38	0.38	0.38	0.37	0.36	0.37	0.37	0.38
415.0	0.38	0.38	0.38	0.37	0.37	0.37	0.37	0.39
415.5	0.38	0.38	0.38	0.37	0.37	0.37	0.38	0.39
416.0	0.38	0.38	0.38	0.37	0.37	0.37	0.38	0.39
416.5	0.38	0.38	0.38	0.37	0.37	0.38	0.38	0.39
417.0	0.38	0.38	0.38	0.38	0.37	0.38	0.38	0.39
417.5	0.38	0.38	0.38	0.38	0.37	0.38	0.38	0.39
418.0	0.38	0.38	0.38	0.38	0.37	0.38	0.39	0.40
418.5	0.38	0.38	0.38	0.38	0.37	0.38	0.39	0.40
419.0	0.38	0.38	0.38	0.38	0.37	0.38	0.39	0.40
419.5	0.38	0.38	0.38	0.38	0.37	0.38	0.39	0.40
420.0	0.38	0.38	0.38	0.38	0.37	0.38	0.39	0.40
420.5	0.38	0.38	0.38	0.38	0.37	0.38	0.39	0.40
421.0	0.38	0.38	0.38	0.38	0.37	0.38	0.39	0.40
421.5	0.38	0.38	0.38	0.38	0.37	0.38	0.39	0.40
422.0	0.38	0.38	0.38	0.37	0.37	0.38	0.39	0.40
422.5	0.38	0.38	0.38	0.37	0.37	0.38	0.39	0.40
423.0	0.38	0.37	0.38	0.37	0.37	0.38	0.39	0.40
423.5	0.38	0.37	0.37	0.37	0.37	0.38	0.39	0.40
424.0	0.37	0.37	0.37	0.37	0.37	0.38	0.39	0.40
424.5	0.37	0.37	0.37	0.37	0.37	0.38	0.39	0.40

425.0	0.37	0.37	0.37	0.37	0.37	0.38	0.38	0.40
425.5	0.37	0.37	0.37	0.36	0.37	0.38	0.38	0.39
426.0	0.37	0.37	0.37	0.36	0.36	0.38	0.38	0.39
426.5	0.37	0.36	0.36	0.36	0.36	0.37	0.38	0.39
427.0	0.36	0.36	0.36	0.36	0.36	0.37	0.38	0.39
427.5	0.36	0.36	0.36	0.36	0.36	0.37	0.38	0.39
428.0	0.36	0.36	0.36	0.36	0.36	0.37	0.37	0.39
428.5	0.36	0.36	0.36	0.35	0.36	0.37	0.37	0.38
429.0	0.36	0.35	0.35	0.35	0.35	0.36	0.37	0.38
429.5	0.35	0.35	0.35	0.35	0.35	0.36	0.37	0.38
430.0	0.35	0.35	0.35	0.35	0.35	0.36	0.37	0.38
430.5	0.35	0.35	0.35	0.34	0.35	0.36	0.36	0.37
431.0	0.35	0.35	0.35	0.34	0.34	0.36	0.36	0.37
431.5	0.34	0.34	0.34	0.34	0.34	0.35	0.36	0.37
432.0	0.34	0.34	0.34	0.34	0.34	0.35	0.35	0.37
432.5	0.34	0.34	0.34	0.33	0.34	0.35	0.35	0.36
433.0	0.34	0.33	0.33	0.33	0.33	0.34	0.35	0.36
433.5	0.33	0.33	0.33	0.33	0.33	0.34	0.35	0.36
434.0	0.33	0.33	0.33	0.32	0.33	0.34	0.34	0.35
434.5	0.33	0.33	0.33	0.32	0.32	0.33	0.34	0.35
435.0	0.32	0.32	0.32	0.32	0.32	0.33	0.34	0.35
435.5	0.32	0.32	0.32	0.32	0.32	0.33	0.33	0.34
436.0	0.32	0.32	0.32	0.31	0.31	0.32	0.33	0.34
436.5	0.32	0.31	0.31	0.31	0.31	0.32	0.32	0.34
437.0	0.31	0.31	0.31	0.31	0.31	0.32	0.32	0.33
437.5	0.31	0.31	0.31	0.30	0.30	0.31	0.32	0.33
438.0	0.31	0.30	0.30	0.30	0.30	0.31	0.31	0.32
438.5	0.30	0.30	0.30	0.30	0.30	0.30	0.31	0.32
439.0	0.30	0.30	0.30	0.29	0.29	0.30	0.31	0.32
439.5	0.30	0.29	0.29	0.29	0.29	0.30	0.30	0.31
440.0	0.29	0.29	0.29	0.28	0.28	0.29	0.30	0.31
440.5	0.29	0.29	0.28	0.28	0.28	0.29	0.29	0.30
441.0	0.29	0.28	0.28	0.28	0.28	0.28	0.29	0.30
441.5	0.28	0.28	0.28	0.27	0.27	0.28	0.28	0.30
442.0	0.28	0.28	0.27	0.27	0.27	0.28	0.28	0.29
442.5	0.27	0.27	0.27	0.27	0.27	0.27	0.28	0.29
443.0	0.27	0.27	0.27	0.26	0.26	0.27	0.27	0.28
443.5	0.27	0.26	0.26	0.26	0.26	0.26	0.27	0.28
444.0	0.26	0.26	0.26	0.25	0.25	0.26	0.26	0.27
444.5	0.26	0.26	0.26	0.25	0.25	0.26	0.26	0.27
445.0	0.26	0.25	0.25	0.25	0.25	0.25	0.26	0.27
445.5	0.25	0.25	0.25	0.24	0.24	0.25	0.25	0.26
446.0	0.25	0.25	0.24	0.24	0.24	0.24	0.25	0.26
446.5	0.25	0.24	0.24	0.24	0.23	0.24	0.24	0.25
447.0	0.24	0.24	0.24	0.23	0.23	0.23	0.24	0.25
447.5	0.24	0.23	0.23	0.23	0.22	0.23	0.23	0.24
448.0	0.23	0.23	0.23	0.22	0.22	0.23	0.23	0.24
448.5	0.23	0.23	0.23	0.22	0.22	0.22	0.23	0.24
449.0	0.23	0.22	0.22	0.22	0.21	0.22	0.22	0.23
449.5	0.22	0.22	0.22	0.21	0.21	0.21	0.22	0.23
450.0	0.22	0.22	0.21	0.21	0.20	0.21	0.21	0.22
450.5	0.22	0.21	0.21	0.20	0.20	0.21	0.21	0.22
451.0	0.21	0.21	0.21	0.20	0.20	0.20	0.21	0.22

451.5	0.21	0.21	0.20	0.20	0.19	0.20	0.20	0.21
452.0	0.21	0.20	0.20	0.19	0.19	0.19	0.20	0.21
452.5	0.20	0.20	0.20	0.19	0.19	0.19	0.19	0.20
453.0	0.20	0.19	0.19	0.19	0.18	0.19	0.19	0.20
453.5	0.19	0.19	0.19	0.18	0.18	0.18	0.19	0.19
454.0	0.19	0.19	0.19	0.18	0.17	0.18	0.18	0.19
454.5	0.19	0.18	0.18	0.18	0.17	0.18	0.18	0.19
455.0	0.18	0.18	0.18	0.17	0.17	0.17	0.18	0.18
455.5	0.18	0.18	0.18	0.17	0.16	0.17	0.17	0.18
456.0	0.18	0.17	0.17	0.17	0.16	0.17	0.17	0.18
456.5	0.17	0.17	0.17	0.16	0.16	0.16	0.16	0.17
457.0	0.17	0.17	0.17	0.16	0.15	0.16	0.16	0.17
457.5	0.17	0.16	0.16	0.15	0.15	0.15	0.16	0.16
458.0	0.16	0.16	0.16	0.15	0.15	0.15	0.15	0.16
458.5	0.16	0.16	0.16	0.15	0.14	0.15	0.15	0.16
459.0	0.16	0.16	0.15	0.15	0.14	0.14	0.15	0.15
459.5	0.16	0.15	0.15	0.14	0.14	0.14	0.14	0.15
460.0	0.15	0.15	0.15	0.14	0.13	0.14	0.14	0.15
460.5	0.15	0.15	0.14	0.14	0.13	0.13	0.14	0.14
461.0	0.15	0.14	0.14	0.13	0.13	0.13	0.13	0.14
461.5	0.14	0.14	0.14	0.13	0.12	0.13	0.13	0.14
462.0	0.14	0.14	0.14	0.13	0.12	0.13	0.13	0.13
462.5	0.14	0.14	0.13	0.12	0.12	0.12	0.12	0.13
463.0	0.14	0.13	0.13	0.12	0.12	0.12	0.12	0.13
463.5	0.13	0.13	0.13	0.12	0.11	0.12	0.12	0.12
464.0	0.13	0.13	0.12	0.12	0.11	0.11	0.12	0.12
464.5	0.13	0.12	0.12	0.11	0.11	0.11	0.11	0.12
465.0	0.12	0.12	0.12	0.11	0.10	0.11	0.11	0.12
465.5	0.12	0.12	0.12	0.11	0.10	0.10	0.11	0.11
466.0	0.12	0.12	0.11	0.11	0.10	0.10	0.10	0.11
466.5	0.12	0.11	0.11	0.10	0.10	0.10	0.10	0.11
467.0	0.11	0.11	0.11	0.10	0.09	0.10	0.10	0.10
467.5	0.11	0.11	0.11	0.10	0.09	0.09	0.09	0.10
468.0	0.11	0.11	0.10	0.10	0.09	0.09	0.09	0.10
468.5	0.11	0.10	0.10	0.09	0.09	0.09	0.09	0.09
469.0	0.10	0.10	0.10	0.09	0.08	0.09	0.09	0.09
469.5	0.10	0.10	0.10	0.09	0.08	0.08	0.08	0.09
470.0	0.10	0.10	0.09	0.09	0.08	0.08	0.08	0.08
470.5	0.10	0.09	0.09	0.08	0.08	0.08	0.08	0.08
471.0	0.09	0.09	0.09	0.08	0.07	0.07	0.08	0.08
471.5	0.09	0.09	0.09	0.08	0.07	0.07	0.07	0.08
472.0	0.09	0.09	0.08	0.08	0.07	0.07	0.07	0.07
472.5	0.09	0.09	0.08	0.07	0.07	0.07	0.07	0.07
473.0	0.09	0.08	0.08	0.07	0.06	0.07	0.07	0.07
473.5	0.08	0.08	0.08	0.07	0.06	0.06	0.06	0.07
474.0	0.08	0.08	0.08	0.07	0.06	0.06	0.06	0.06
474.5	0.08	0.08	0.07	0.07	0.06	0.06	0.06	0.06
475.0	0.08	0.08	0.07	0.06	0.06	0.06	0.06	0.06
475.5	0.08	0.07	0.07	0.06	0.05	0.05	0.05	0.06
476.0	0.07	0.07	0.07	0.06	0.05	0.05	0.05	0.05
476.5	0.07	0.07	0.07	0.06	0.05	0.05	0.05	0.05
477.0	0.07	0.07	0.07	0.06	0.05	0.05	0.05	0.05
477.5	0.07	0.07	0.06	0.05	0.05	0.05	0.05	0.05

478.0	0.07	0.07	0.06	0.05	0.04	0.04	0.04	0.05
478.5	0.07	0.06	0.06	0.05	0.04	0.04	0.04	0.04
479.0	0.06	0.06	0.06	0.05	0.04	0.04	0.04	0.04
479.5	0.06	0.06	0.06	0.05	0.04	0.04	0.04	0.04
480.0	0.06	0.06	0.06	0.05	0.04	0.04	0.04	0.04
480.5	0.06	0.06	0.05	0.05	0.04	0.04	0.03	0.04
481.0	0.06	0.06	0.05	0.04	0.03	0.03	0.03	0.03
481.5	0.06	0.06	0.05	0.04	0.03	0.03	0.03	0.03
482.0	0.06	0.05	0.05	0.04	0.03	0.03	0.03	0.03
482.5	0.05	0.05	0.05	0.04	0.03	0.03	0.03	0.03
483.0	0.05	0.05	0.05	0.04	0.03	0.03	0.03	0.03
483.5	0.05	0.05	0.05	0.04	0.03	0.03	0.03	0.03
484.0	0.05	0.05	0.05	0.04	0.03	0.03	0.02	0.03
484.5	0.05	0.05	0.04	0.04	0.02	0.02	0.02	0.02
485.0	0.05	0.05	0.04	0.03	0.02	0.02	0.02	0.02
485.5	0.05	0.05	0.04	0.03	0.02	0.02	0.02	0.02
486.0	0.05	0.04	0.04	0.03	0.02	0.02	0.02	0.02
486.5	0.05	0.04	0.04	0.03	0.02	0.02	0.02	0.02
487.0	0.05	0.04	0.04	0.03	0.02	0.02	0.02	0.02
487.5	0.04	0.04	0.04	0.03	0.02	0.02	0.02	0.02
488.0	0.04	0.04	0.04	0.03	0.02	0.02	0.02	0.02
488.5	0.04	0.04	0.04	0.03	0.02	0.02	0.01	0.01
489.0	0.04	0.04	0.04	0.03	0.02	0.01	0.01	0.01
489.5	0.04	0.04	0.03	0.03	0.01	0.01	0.01	0.01
490.0	0.04	0.04	0.03	0.02	0.01	0.01	0.01	0.01
490.5	0.04	0.04	0.03	0.02	0.01	0.01	0.01	0.01
491.0	0.04	0.04	0.03	0.02	0.01	0.01	0.01	0.01
491.5	0.04	0.04	0.03	0.02	0.01	0.01	0.01	0.01
492.0	0.04	0.03	0.03	0.02	0.01	0.01	0.01	0.01
492.5	0.04	0.03	0.03	0.02	0.01	0.01	0.01	0.01
493.0	0.04	0.03	0.03	0.02	0.01	0.01	0.01	0.01
493.5	0.04	0.03	0.03	0.02	0.01	0.01	0.01	0.01
494.0	0.03	0.03	0.03	0.02	0.01	0.01	0.01	0.01
494.5	0.03	0.03	0.03	0.02	0.01	0.01	0.00	0.00
495.0	0.03	0.03	0.03	0.02	0.01	0.01	0.00	0.00
495.5	0.03	0.03	0.03	0.02	0.01	0.00	0.00	0.00
496.0	0.03	0.03	0.03	0.02	0.01	0.00	0.00	0.00
496.5	0.03	0.03	0.03	0.02	0.01	0.00	0.00	0.00
497.0	0.03	0.03	0.02	0.02	0.00	0.00	0.00	0.00
497.5	0.03	0.03	0.02	0.02	0.00	0.00	0.00	0.00
498.0	0.03	0.03	0.02	0.01	0.00	0.00	0.00	0.00
498.5	0.03	0.03	0.02	0.01	0.00	0.00	0.00	0.00
499.0	0.03	0.03	0.02	0.01	0.00	0.00	0.00	0.00
499.5	0.03	0.03	0.02	0.01	0.00	0.00	0.00	0.00
500.0	0.03	0.03	0.02	0.01	0.00	0.00	0.00	0.00

Table 4.5 Absorbance data of H₂DTC in presence of [Surfactant] in 15% v/v EtOH-water medium

absorbance of H ₂ DTC with variation of surfactant concentrations in 15% v/v EtOH-water medium									
SDS		DTAB		C ₁₆ MImCl		16-4-16		Tween-60	
[SDS]/ mM	absorbance	[DTAB]/mM	absorbance	[C ₁₆ MImCl]/ mM	absorbance	[16-4-16]/ mM	absorbance	[Tween-60]/ mM	absorbance
0.000	0.382	0.0000	0.463	0.0000	0.455	0.00000	0.404	0.0000	0.463
0.048	0.383	0.1196	0.444	0.0142	0.452	0.00047	0.399	0.0006	0.457
0.121	0.382	0.3584	0.438	0.0425	0.455	0.00140	0.397	0.0016	0.450
0.193	0.381	0.7150	0.437	0.085	0.456	0.00280	0.393	0.0029	0.445
0.290	0.382	1.1879	0.432	0.155	0.456	0.00465	0.391	0.0044	0.440
0.433	0.380	1.775	0.430	0.224	0.457	0.00695	0.391	0.0068	0.431
0.671	0.380	2.646	0.426	0.361	0.457	0.01036	0.393	0.0106	0.418
1.025	0.378	4.077	0.427	0.496	0.460	0.01596	0.396	0.0143	0.403
1.374	0.378	6.033	0.427	0.693	0.468	0.024	0.403	0.026	0.384
1.834	0.376	9.003	0.427	0.885	0.480	0.034	0.410	0.037	0.359
2.510	0.370	12.860	0.436	1.134	0.493	0.048	0.420	0.050	0.339
3.171	0.370	17.453	0.468	1.375	0.502	0.066	0.427	0.078	0.301
4.029	0.373	22.400	0.495	1.721	0.514	0.083	0.440	0.123	0.248
5.066	0.377	27.789	0.508	2.051	0.522	0.108	0.446		
6.261	0.380	33.467	0.515	2.467	0.526	0.137	0.450		
7.777	0.381	40.262	0.517	2.953	0.532	0.163	0.453		
9.557	0.383	49.085	0.516	3.618	0.539	0.217	0.452		
11.221	0.386			4.403	0.541				
12.780	0.386			5.406	0.545				
15.620	0.391								
20.396	0.394								
22.423	0.397								

4.6. Steady state emission data of H₂DTCat different concentrations of 16-4-16 at 298.15 K

Emission of H ₂ DTC in presence of different [16-4-16] in 15% v/v EtOH-water medium									
wavelength/ nm	0.000	0.001	0.005	0.010	0.024	0.045	0.079	1.400	2.270
450	0.474	0.442	0.431	0.358	0.256	0.268	0.270	0.279	0.263
450.5	0.477	0.446	0.439	0.373	0.286	0.275	0.275	0.291	0.301
451	0.485	0.454	0.449	0.386	0.312	0.285	0.283	0.304	0.335
451.5	0.499	0.465	0.463	0.401	0.333	0.299	0.296	0.318	0.363
452	0.520	0.485	0.479	0.419	0.350	0.315	0.315	0.336	0.383
452.5	0.547	0.513	0.498	0.440	0.366	0.334	0.338	0.355	0.399
453	0.578	0.546	0.523	0.461	0.379	0.356	0.359	0.373	0.412
453.5	0.613	0.583	0.550	0.483	0.393	0.377	0.377	0.391	0.424
454	0.650	0.620	0.580	0.510	0.412	0.395	0.390	0.407	0.436
454.5	0.691	0.659	0.611	0.540	0.433	0.412	0.403	0.424	0.451
455	0.736	0.699	0.646	0.570	0.456	0.426	0.416	0.440	0.471
455.5	0.785	0.740	0.688	0.605	0.481	0.442	0.431	0.460	0.497
456	0.837	0.785	0.736	0.642	0.509	0.458	0.452	0.483	0.525
456.5	0.891	0.838	0.786	0.682	0.539	0.478	0.477	0.513	0.560
457	0.943	0.897	0.841	0.722	0.570	0.503	0.506	0.547	0.601
457.5	0.995	0.959	0.897	0.764	0.603	0.537	0.537	0.584	0.647
458	1.049	1.022	0.954	0.808	0.641	0.574	0.571	0.623	0.692
458.5	1.106	1.088	1.009	0.855	0.681	0.619	0.609	0.666	0.735
459	1.169	1.155	1.061	0.901	0.723	0.663	0.652	0.710	0.776
459.5	1.241	1.224	1.117	0.952	0.765	0.711	0.700	0.758	0.819
460	1.323	1.294	1.183	1.007	0.813	0.759	0.754	0.807	0.860
460.5	1.415	1.373	1.255	1.066	0.867	0.809	0.812	0.862	0.910
461	1.507	1.462	1.339	1.132	0.920	0.862	0.875	0.923	0.970
461.5	1.602	1.561	1.429	1.204	0.978	0.921	0.935	0.988	1.040
462	1.699	1.666	1.526	1.285	1.042	0.981	0.994	1.054	1.121
462.5	1.796	1.776	1.630	1.373	1.113	1.045	1.053	1.125	1.211
463	1.897	1.889	1.737	1.469	1.188	1.110	1.115	1.200	1.307
463.5	2.005	2.008	1.845	1.569	1.263	1.176	1.182	1.282	1.410
464	2.121	2.125	1.956	1.672	1.343	1.247	1.253	1.371	1.513
464.5	2.249	2.244	2.068	1.776	1.428	1.324	1.332	1.468	1.615
465	2.391	2.366	2.192	1.885	1.515	1.409	1.425	1.577	1.719
465.5	2.544	2.497	2.321	1.997	1.605	1.502	1.524	1.694	1.821
466	2.707	2.640	2.453	2.116	1.700	1.599	1.632	1.813	1.935
466.5	2.873	2.791	2.592	2.236	1.808	1.701	1.748	1.929	2.058
467	3.048	2.952	2.745	2.367	1.920	1.806	1.867	2.049	2.192
467.5	3.225	3.128	2.907	2.501	2.037	1.911	1.996	2.169	2.344
468	3.407	3.314	3.077	2.635	2.164	2.022	2.126	2.292	2.513
468.5	3.591	3.513	3.245	2.770	2.295	2.140	2.261	2.423	2.694
469	3.784	3.716	3.430	2.914	2.430	2.269	2.404	2.569	2.887
469.5	3.989	3.925	3.624	3.069	2.561	2.412	2.554	2.736	3.083

470	4.208	4.144	3.821	3.237	2.703	2.564	2.713	2.925	3.296
470.5	4.437	4.365	4.025	3.411	2.860	2.728	2.885	3.129	3.515
471	4.683	4.595	4.241	3.609	3.026	2.912	3.067	3.352	3.740
471.5	4.941	4.838	4.480	3.824	3.204	3.103	3.258	3.589	3.980
472	5.227	5.102	4.738	4.050	3.403	3.306	3.462	3.844	4.243
472.5	5.533	5.390	5.003	4.286	3.621	3.514	3.676	4.111	4.533
473	5.856	5.703	5.293	4.535	3.854	3.731	3.899	4.389	4.841
473.5	6.196	6.029	5.600	4.799	4.085	3.956	4.135	4.677	5.167
474	6.548	6.377	5.918	5.080	4.321	4.185	4.392	4.981	5.524
474.5	6.911	6.735	6.241	5.371	4.566	4.417	4.672	5.298	5.896
475	7.284	7.105	6.581	5.690	4.817	4.677	4.981	5.628	6.287
475.5	7.659	7.481	6.938	6.026	5.074	4.953	5.313	5.968	6.694
476	8.063	7.873	7.322	6.369	5.343	5.251	5.671	6.332	7.118
476.5	8.498	8.292	7.720	6.718	5.642	5.565	6.048	6.726	7.581
477	8.958	8.747	8.144	7.065	5.963	5.899	6.442	7.149	8.074
477.5	9.448	9.225	8.591	7.424	6.297	6.249	6.845	7.597	8.591
478	9.961	9.733	9.056	7.799	6.645	6.611	7.265	8.074	9.152
478.5	10.505	10.274	9.534	8.195	7.008	6.971	7.689	8.590	9.743
479	11.069	10.835	10.037	8.633	7.393	7.357	8.130	9.130	10.374
479.5	11.636	11.402	10.552	9.108	7.791	7.761	8.581	9.697	11.035
480	12.233	11.975	11.103	9.607	8.204	8.193	9.063	10.285	11.715
480.5	12.852	12.578	11.676	10.131	8.644	8.640	9.574	10.901	12.429
481	13.495	13.213	12.272	10.659	9.103	9.117	10.120	11.543	13.192
481.5	14.166	13.868	12.894	11.198	9.590	9.619	10.691	12.210	13.979
482	14.849	14.542	13.539	11.740	10.091	10.157	11.296	12.907	14.796
482.5	15.568	15.252	14.200	12.293	10.598	10.709	11.924	13.656	15.633
483	16.330	15.998	14.893	12.873	11.131	11.281	12.584	14.442	16.511
483.5	17.123	16.777	15.603	13.479	11.694	11.876	13.266	15.274	17.451
484	17.970	17.577	16.351	14.121	12.278	12.497	13.973	16.139	18.432
484.5	18.852	18.407	17.138	14.800	12.889	13.126	14.710	17.043	19.464
485	19.774	19.284	17.952	15.517	13.531	13.769	15.481	17.989	20.577
485.5	20.739	20.213	18.795	16.268	14.211	14.433	16.293	18.964	21.770
486	21.714	21.177	19.668	17.049	14.911	15.136	17.137	19.986	23.033
486.5	22.714	22.182	20.572	17.853	15.611	15.872	18.008	21.053	24.340
487	23.755	23.220	21.507	18.690	16.325	16.628	18.920	22.153	25.683
487.5	24.827	24.299	22.461	19.525	17.063	17.428	19.876	23.325	27.086
488	25.928	25.395	23.440	20.389	17.815	18.276	20.875	24.547	28.506
488.5	27.036	26.508	24.465	21.269	18.575	19.152	21.908	25.815	29.939
489	28.172	27.644	25.515	22.177	19.362	20.049	22.972	27.125	31.404
489.5	29.343	28.803	26.591	23.114	20.194	20.971	24.079	28.456	32.914
490	30.557	29.991	27.708	24.108	21.070	21.939	25.226	29.841	34.504
490.5	31.813	31.209	28.879	25.143	21.984	22.939	26.397	31.269	36.160
491	33.142	32.461	30.098	26.242	22.946	23.968	27.590	32.728	37.867
491.5	34.549	33.788	31.356	27.347	23.978	25.037	28.828	34.269	39.689

492	36.018	35.176	32.644	28.486	25.071	26.156	30.124	35.867	41.592
492.5	37.534	36.627	33.993	29.650	26.190	27.320	31.464	37.550	43.575
493	39.069	38.116	35.367	30.835	27.331	28.509	32.839	39.296	45.604
493.5	40.604	39.652	36.754	32.024	28.491	29.722	34.275	41.067	47.681
494	42.156	41.215	38.156	33.257	29.656	30.958	35.770	42.884	49.816
494.5	43.730	42.799	39.596	34.512	30.813	32.213	37.320	44.761	52.013
495	45.337	44.367	41.080	35.822	31.952	33.476	38.907	46.660	54.238
495.5	47.022	45.989	42.601	37.175	33.112	34.759	40.533	48.601	56.539
496	48.752	47.623	44.123	38.552	34.310	36.070	42.189	50.556	58.909
496.5	50.572	49.300	45.697	39.987	35.546	37.437	43.877	52.585	61.346
497	52.411	50.995	47.296	41.447	36.819	38.858	45.588	54.684	63.831
497.5	54.250	52.753	48.935	42.909	38.132	40.327	47.341	56.822	66.403
498	56.076	54.556	50.588	44.406	39.487	41.834	49.126	58.978	69.052
498.5	57.926	56.394	52.279	45.910	40.879	43.378	50.957	61.209	71.805
499	59.787	58.238	54.007	47.421	42.289	44.955	52.833	63.528	74.613
499.5	61.698	60.144	55.776	48.989	43.722	46.540	54.763	65.917	77.483
500	63.644	62.047	57.555	50.565	45.190	48.135	56.691	68.327	80.382
500.5	65.701	63.994	59.383	52.186	46.678	49.773	58.638	70.795	83.278
501	67.793	65.971	61.253	53.838	48.168	51.429	60.593	73.307	86.179
501.5	69.954	68.017	63.191	55.528	49.683	53.129	62.614	75.875	89.151
502	72.085	70.116	65.158	57.261	51.243	54.874	64.666	78.429	92.169
502.5	74.257	72.264	67.153	58.985	52.832	56.639	66.732	81.027	95.232
503	76.431	74.456	69.168	60.671	54.436	58.414	68.829	83.697	98.370
503.5	78.661	76.724	71.227	62.385	56.052	60.179	71.013	86.409	101.621
504	80.896	78.971	73.292	64.101	57.713	61.946	73.217	89.110	104.920
504.5	83.229	81.244	75.335	65.820	59.399	63.747	75.459	91.849	108.185
505	85.565	83.536	77.370	67.548	61.051	65.563	77.675	94.576	111.387
505.5	87.960	85.848	79.418	69.333	62.682	67.398	79.928	97.328	114.602
506	90.295	88.180	81.451	71.194	64.326	69.285	82.218	100.074	117.810
506.5	92.633	90.502	83.498	73.070	65.990	71.182	84.484	102.838	120.997
507	94.918	92.793	85.550	74.952	67.636	73.078	86.707	105.642	124.167
507.5	97.218	95.077	87.632	76.854	69.264	74.932	88.941	108.471	127.422
508	99.495	97.304	89.749	78.787	70.922	76.767	91.157	111.283	130.727
508.5	101.828	99.531	91.852	80.690	72.613	78.562	93.382	114.122	134.045
509	104.152	101.755	93.963	82.549	74.286	80.345	95.561	116.916	137.279
509.5	106.524	104.011	96.120	84.426	75.916	82.129	97.725	119.648	140.511
510	108.854	106.308	98.250	86.318	77.556	83.975	99.911	122.266	143.700
510.5	111.202	108.624	100.363	88.140	79.230	85.858	102.079	124.802	146.863
511	113.477	110.866	102.415	89.925	80.878	87.739	104.202	127.271	149.883
511.5	115.745	113.033	104.435	91.649	82.484	89.562	106.268	129.656	152.854
512	117.930	115.082	106.442	93.330	84.021	91.343	108.258	131.999	155.754
512.5	120.131	117.058	108.362	94.942	85.525	92.988	110.246	134.329	158.575
513	122.288	118.953	110.191	96.505	86.991	94.536	112.207	136.625	161.277
513.5	124.418	120.830	112.060	98.066	88.383	95.997	114.112	138.908	163.909

514	126.481	122.737	113.870	99.667	89.771	97.436	115.949	141.149	166.409
514.5	128.524	124.694	115.653	101.246	91.171	98.888	117.761	143.356	168.889
515	130.501	126.654	117.426	102.837	92.585	100.354	119.557	145.496	171.251
515.5	132.450	128.616	119.188	104.387	94.050	101.793	121.283	147.505	173.597
516	134.312	130.509	120.992	105.886	95.489	103.211	122.864	149.404	175.917
516.5	136.147	132.331	122.701	107.335	96.858	104.558	124.338	151.245	178.142
517	137.883	134.045	124.302	108.732	98.144	105.839	125.767	152.981	180.339
517.5	139.565	135.757	125.890	110.077	99.316	107.042	127.148	154.671	182.514
518	141.178	137.412	127.398	111.388	100.367	108.192	128.407	156.341	184.552
518.5	142.751	139.043	128.816	112.643	101.306	109.347	129.603	157.970	186.491
519	144.277	140.635	130.158	113.873	102.140	110.478	130.806	159.509	188.260
519.5	145.816	142.223	131.398	115.051	102.973	111.568	132.015	160.906	189.923
520	147.316	143.738	132.619	116.155	103.806	112.554	133.112	162.138	191.392
520.5	148.801	145.116	133.701	117.185	104.629	113.406	134.079	163.281	192.589
521	150.194	146.333	134.703	118.170	105.439	114.158	135.026	164.268	193.681
521.5	151.493	147.511	135.625	119.084	106.283	114.830	135.945	165.085	194.617
522	152.627	148.534	136.486	119.915	107.103	115.403	136.772	165.826	195.447
522.5	153.637	149.465	137.295	120.675	107.844	115.938	137.494	166.529	196.232
523	154.463	150.323	138.050	121.379	108.444	116.422	138.170	167.134	197.023
523.5	155.131	151.117	138.779	122.005	108.918	116.908	138.808	167.620	197.816
524	155.685	151.883	139.518	122.543	109.315	117.366	139.362	167.995	198.448
524.5	156.154	152.524	140.159	123.003	109.634	117.736	139.738	168.289	198.836
525	156.576	153.019	140.793	123.375	109.856	118.016	139.998	168.529	199.088
525.5	156.975	153.512	141.316	123.671	110.058	118.241	140.146	168.624	199.057
526	157.298	153.865	141.734	123.893	110.235	118.390	140.190	168.635	198.791
526.5	157.656	154.140	142.046	124.014	110.385	118.494	140.102	168.577	198.405
527	157.938	154.330	142.221	124.095	110.504	118.505	139.941	168.412	198.025
527.5	158.120	154.447	142.295	124.121	110.524	118.444	139.734	168.127	197.696
528	158.232	154.528	142.241	124.086	110.444	118.317	139.488	167.804	197.337
528.5	158.163	154.471	142.028	124.021	110.289	118.134	139.155	167.391	196.884
529	157.993	154.300	141.786	123.918	110.071	117.836	138.747	166.934	196.410
529.5	157.727	154.042	141.490	123.723	109.772	117.512	138.283	166.392	195.752
530	157.308	153.678	141.120	123.459	109.426	117.106	137.771	165.748	194.871
530.5	156.863	153.233	140.712	123.070	109.012	116.671	137.196	164.988	193.843
531	156.359	152.709	140.291	122.648	108.599	116.209	136.548	164.043	192.759
531.5	155.826	152.125	139.856	122.188	108.130	115.698	135.837	162.966	191.601
532	155.323	151.527	139.363	121.672	107.614	115.131	135.056	161.862	190.413
532.5	154.745	150.885	138.780	121.130	107.023	114.585	134.234	160.734	189.171
533	154.124	150.176	138.143	120.578	106.411	113.936	133.319	159.648	187.900
533.5	153.452	149.382	137.449	120.011	105.790	113.270	132.374	158.576	186.581
534	152.689	148.516	136.651	119.429	105.118	112.517	131.440	157.496	185.148
534.5	151.833	147.583	135.754	118.715	104.391	111.720	130.516	156.391	183.649
535	150.854	146.572	134.844	117.944	103.663	110.903	129.543	155.163	182.121
535.5	149.817	145.488	133.939	117.142	102.953	110.058	128.566	153.845	180.490

536	148.765	144.379	132.982	116.289	102.264	109.171	127.504	152.458	178.830
536.5	147.669	143.311	132.023	115.384	101.543	108.318	126.425	151.039	177.161
537	146.529	142.235	131.035	114.416	100.778	107.435	125.285	149.627	175.468
537.5	145.322	141.167	130.048	113.457	100.039	106.576	124.138	148.243	173.810
538	144.076	140.093	129.005	112.484	99.268	105.671	123.007	146.835	172.154
538.5	142.747	139.007	127.875	111.434	98.457	104.729	121.934	145.441	170.480
539	141.342	137.913	126.707	110.347	97.609	103.712	120.869	144.027	168.786
539.5	139.948	136.741	125.542	109.281	96.742	102.634	119.865	142.580	167.043
540	138.608	135.482	124.291	108.252	95.829	101.502	118.772	141.090	165.266
540.5	137.337	134.214	123.091	107.299	94.891	100.333	117.589	139.556	163.484
541	136.097	132.824	121.880	106.332	93.876	99.167	116.299	138.050	161.601
541.5	134.831	131.409	120.690	105.423	92.852	98.059	114.970	136.591	159.749
542	133.552	129.941	119.521	104.474	91.787	97.001	113.586	135.133	157.941
542.5	132.189	128.447	118.316	103.452	90.699	96.007	112.237	133.696	156.167
543	130.736	127.003	117.049	102.303	89.655	95.014	110.874	132.259	154.383
543.5	129.184	125.588	115.810	101.083	88.683	94.026	109.588	130.786	152.631
544	127.654	124.194	114.488	99.789	87.728	93.016	108.343	129.303	150.899
544.5	126.164	122.841	113.164	98.531	86.812	91.938	107.100	127.785	149.179
545	124.730	121.463	111.742	97.279	85.890	90.807	105.860	126.262	147.347
545.5	123.320	120.110	110.330	96.117	84.935	89.707	104.678	124.746	145.451
546	121.959	118.692	108.937	94.962	83.925	88.637	103.473	123.231	143.553
546.5	120.598	117.215	107.558	93.871	82.842	87.589	102.317	121.729	141.640
547	119.207	115.742	106.184	92.795	81.758	86.554	101.119	120.241	139.685
547.5	117.717	114.260	104.882	91.694	80.675	85.521	99.896	118.749	137.795
548	116.201	112.793	103.615	90.535	79.614	84.494	98.650	117.295	136.015
548.5	114.678	111.297	102.359	89.382	78.592	83.471	97.343	115.830	134.322
549	113.137	109.808	101.046	88.212	77.608	82.411	96.024	114.366	132.669
549.5	111.569	108.343	99.752	87.061	76.656	81.374	94.699	112.905	131.009
550	110.002	106.887	98.428	85.860	75.691	80.345	93.347	111.435	129.343
550.5	108.450	105.436	97.083	84.684	74.722	79.301	92.077	109.961	127.639
551	106.920	104.034	95.704	83.574	73.782	78.268	90.857	108.474	125.860
551.5	105.405	102.629	94.318	82.477	72.823	77.193	89.666	106.955	124.058
552	103.926	101.262	92.976	81.356	71.870	76.130	88.514	105.475	122.300
552.5	102.482	99.859	91.652	80.250	70.926	75.063	87.324	104.039	120.536
553	101.048	98.429	90.313	79.169	69.997	73.995	86.162	102.586	118.847
553.5	99.642	96.920	89.028	78.091	69.055	72.958	84.966	101.132	117.163
554	98.215	95.392	87.763	76.924	68.072	71.932	83.725	99.702	115.462
554.5	96.771	93.887	86.529	75.694	67.090	70.910	82.506	98.235	113.771
555	95.297	92.410	85.307	74.494	66.131	69.918	81.297	96.741	112.056
555.5	93.804	90.971	84.063	73.317	65.153	68.872	80.087	95.184	110.315
556	92.313	89.592	82.811	72.127	64.152	67.853	78.906	93.649	108.600
556.5	90.827	88.280	81.540	70.980	63.130	66.853	77.728	92.211	106.834
557	89.347	86.996	80.246	69.910	62.136	65.874	76.574	90.776	105.131
557.5	87.932	85.637	78.960	68.928	61.135	64.910	75.400	89.373	103.488

558	86.532	84.263	77.673	67.924	60.139	63.934	74.181	88.034	101.824
558.5	85.142	82.888	76.448	66.868	59.165	62.954	72.970	86.705	100.162
559	83.761	81.466	75.250	65.793	58.264	61.983	71.772	85.344	98.505
559.5	82.395	80.025	74.048	64.700	57.393	60.974	70.574	83.940	96.821
560	81.054	78.594	72.842	63.544	56.530	59.964	69.388	82.511	95.169
560.5	79.686	77.218	71.628	62.383	55.625	58.984	68.227	81.134	93.449
561	78.280	75.879	70.419	61.260	54.717	58.021	67.079	79.749	91.717
561.5	76.891	74.538	69.208	60.250	53.769	57.043	65.928	78.341	90.048
562	75.497	73.210	67.959	59.302	52.793	56.046	64.771	76.967	88.390
562.5	74.142	71.923	66.743	58.353	51.798	55.046	63.620	75.614	86.726
563	72.790	70.603	65.518	57.429	50.853	54.036	62.482	74.201	85.119
563.5	71.469	69.230	64.256	56.503	49.943	53.023	61.339	72.755	83.504
564	70.182	67.840	63.002	55.533	49.086	51.990	60.177	71.276	81.906
564.5	68.866	66.449	61.746	54.498	48.241	51.006	59.017	69.819	80.288
565	67.512	65.054	60.481	53.366	47.381	50.047	57.848	68.389	78.622
565.5	66.125	63.687	59.244	52.239	46.532	49.087	56.687	66.989	76.979
566	64.712	62.364	58.004	51.153	45.665	48.126	55.544	65.619	75.350
566.5	63.366	61.104	56.823	50.053	44.772	47.190	54.427	64.319	73.714
567	62.042	59.913	55.672	49.015	43.880	46.250	53.366	63.024	72.158
567.5	60.763	58.731	54.514	48.034	42.998	45.323	52.317	61.742	70.645
568	59.533	57.585	53.401	47.139	42.138	44.404	51.282	60.446	69.152
568.5	58.347	56.444	52.323	46.284	41.306	43.522	50.246	59.146	67.710
569	57.161	55.256	51.264	45.387	40.452	42.661	49.220	57.879	66.294
569.5	55.944	54.059	50.252	44.493	39.623	41.811	48.197	56.639	64.903
570	54.671	52.868	49.237	43.611	38.803	40.963	47.164	55.397	63.539
570.5	53.434	51.689	48.244	42.699	37.996	40.149	46.139	54.191	62.151
571	52.231	50.532	47.251	41.775	37.192	39.352	45.156	53.052	60.793
571.5	51.071	49.411	46.242	40.845	36.431	38.567	44.191	51.936	59.467
572	49.947	48.325	45.232	39.947	35.680	37.800	43.242	50.838	58.133
572.5	48.865	47.305	44.233	39.099	34.959	37.052	42.299	49.741	56.817
573	47.825	46.297	43.229	38.267	34.225	36.306	41.380	48.678	55.549
573.5	46.800	45.301	42.262	37.472	33.516	35.573	40.500	47.647	54.312
574	45.774	44.333	41.308	36.698	32.828	34.826	39.644	46.605	53.117
574.5	44.766	43.397	40.387	35.949	32.141	34.104	38.794	45.567	51.929
575	43.785	42.455	39.491	35.211	31.469	33.389	37.970	44.577	50.764
575.5	42.835	41.527	38.623	34.476	30.838	32.675	37.182	43.604	49.626
576	41.896	40.593	37.776	33.720	30.234	31.968	36.425	42.650	48.493
576.5	40.944	39.689	36.922	32.964	29.644	31.269	35.675	41.709	47.376
577	39.997	38.785	36.066	32.204	29.038	30.568	34.934	40.815	46.298
577.5	39.061	37.898	35.238	31.454	28.432	29.887	34.200	39.952	45.253
578	38.146	37.028	34.415	30.717	27.845	29.219	33.481	39.085	44.237
578.5	37.261	36.199	33.622	30.023	27.248	28.592	32.745	38.230	43.238
579	36.398	35.382	32.862	29.367	26.654	28.001	31.998	37.405	42.272
579.5	35.574	34.588	32.138	28.766	26.069	27.442	31.258	36.584	41.346

580	34.795	33.796	31.446	28.189	25.513	26.905	30.557	35.760	40.435
580.5	34.023	33.032	30.797	27.631	24.955	26.374	29.895	34.944	39.535
581	33.267	32.276	30.181	27.077	24.417	25.839	29.275	34.169	38.657
581.5	32.510	31.540	29.580	26.516	23.877	25.311	28.692	33.432	37.818
582	31.762	30.835	28.975	25.935	23.373	24.776	28.155	32.711	36.998
582.5	31.050	30.172	28.359	25.370	22.891	24.249	27.626	32.013	36.191
583	30.359	29.539	27.739	24.810	22.454	23.733	27.086	31.340	35.386
583.5	29.677	28.908	27.106	24.281	22.023	23.220	26.531	30.679	34.615
584	29.022	28.271	26.447	23.770	21.627	22.722	25.972	30.004	33.875
584.5	28.378	27.651	25.792	23.277	21.211	22.231	25.398	29.330	33.142
585	27.754	27.020	25.182	22.786	20.804	21.735	24.826	28.671	32.418
585.5	27.112	26.379	24.595	22.292	20.368	21.262	24.264	28.036	31.718
586	26.459	25.744	24.035	21.761	19.914	20.818	23.709	27.420	31.021
586.5	25.834	25.119	23.500	21.244	19.460	20.385	23.177	26.826	30.334
587	25.231	24.515	22.999	20.732	19.028	19.967	22.658	26.258	29.627
587.5	24.627	23.918	22.513	20.250	18.603	19.560	22.153	25.706	28.915
588	24.039	23.325	22.006	19.799	18.209	19.171	21.667	25.150	28.240
588.5	23.456	22.760	21.492	19.375	17.828	18.780	21.190	24.591	27.584
589	22.914	22.214	21.006	18.982	17.480	18.370	20.719	24.033	26.960
589.5	22.372	21.698	20.530	18.609	17.132	17.969	20.277	23.472	26.373
590	21.844	21.211	20.064	18.212	16.790	17.590	19.851	22.937	25.820
590.5	21.321	20.738	19.602	17.814	16.446	17.225	19.431	22.412	25.300
591	20.826	20.284	19.154	17.407	16.115	16.870	19.015	21.913	24.796
591.5	20.341	19.835	18.719	17.008	15.781	16.525	18.614	21.440	24.255
592	19.858	19.381	18.301	16.614	15.446	16.198	18.221	20.972	23.719
592.5	19.378	18.933	17.882	16.220	15.122	15.872	17.825	20.509	23.167
593	18.919	18.473	17.479	15.847	14.810	15.549	17.433	20.067	22.611
593.5	18.450	18.028	17.096	15.495	14.506	15.223	17.070	19.616	22.053
594	18.000	17.619	16.726	15.151	14.211	14.912	16.725	19.193	21.512
594.5	17.567	17.228	16.366	14.831	13.920	14.606	16.381	18.778	20.995
595	17.163	16.856	16.005	14.530	13.642	14.307	16.044	18.386	20.515
595.5	16.799	16.499	15.641	14.253	13.379	14.023	15.727	18.010	20.037
596	16.450	16.142	15.288	13.998	13.116	13.757	15.426	17.637	19.593
596.5	16.114	15.784	14.940	13.735	12.845	13.483	15.113	17.266	19.174
597	15.785	15.415	14.597	13.469	12.572	13.214	14.803	16.899	18.778
597.5	15.430	15.043	14.264	13.195	12.299	12.948	14.493	16.518	18.382
598	15.062	14.675	13.935	12.900	12.021	12.677	14.178	16.159	17.996
598.5	14.692	14.307	13.621	12.592	11.736	12.403	13.847	15.793	17.609
599	14.321	13.955	13.309	12.278	11.452	12.134	13.514	15.451	17.228
599.5	13.976	13.627	12.994	11.975	11.200	11.873	13.189	15.126	16.839
600	13.646	13.315	12.689	11.689	10.977	11.624	12.891	14.804	16.458
600.5	13.343	13.018	12.398	11.406	10.760	11.371	12.599	14.494	16.098
601	13.062	12.735	12.120	11.145	10.561	11.124	12.348	14.187	15.748
601.5	12.796	12.472	11.851	10.902	10.381	10.888	12.114	13.872	15.402

602	12.521	12.209	11.594	10.675	10.204	10.661	11.886	13.571	15.061
602.5	12.249	11.939	11.351	10.459	10.024	10.442	11.657	13.267	14.720
603	11.982	11.666	11.108	10.254	9.829	10.229	11.434	12.979	14.392
603.5	11.716	11.400	10.872	10.065	9.640	10.019	11.198	12.702	14.072
604	11.448	11.137	10.636	9.879	9.448	9.834	10.968	12.427	13.771
604.5	11.173	10.869	10.405	9.675	9.247	9.658	10.731	12.168	13.503
605	10.903	10.602	10.181	9.472	9.043	9.484	10.515	11.935	13.242
605.5	10.646	10.363	9.962	9.268	8.843	9.311	10.305	11.699	12.981
606	10.388	10.129	9.748	9.069	8.642	9.137	10.089	11.464	12.716
606.5	10.127	9.896	9.537	8.873	8.445	8.956	9.880	11.231	12.436
607	9.882	9.674	9.312	8.684	8.251	8.778	9.689	10.996	12.151
607.5	9.647	9.468	9.088	8.514	8.072	8.584	9.498	10.756	11.853
608	9.425	9.274	8.866	8.340	7.895	8.403	9.309	10.513	11.560
608.5	9.203	9.080	8.642	8.155	7.733	8.224	9.118	10.264	11.291
609	8.988	8.876	8.425	7.964	7.586	8.051	8.936	10.036	11.035
609.5	8.790	8.688	8.216	7.774	7.444	7.883	8.758	9.810	10.784
610	8.597	8.494	8.019	7.582	7.304	7.718	8.566	9.587	10.538
610.5	8.402	8.293	7.840	7.389	7.159	7.552	8.380	9.375	10.295
611	8.205	8.086	7.665	7.204	7.013	7.396	8.204	9.160	10.057
611.5	8.015	7.874	7.500	7.037	6.872	7.231	8.029	8.947	9.814
612	7.832	7.677	7.351	6.877	6.721	7.076	7.850	8.740	9.574
612.5	7.645	7.481	7.200	6.727	6.577	6.924	7.669	8.533	9.342
613	7.472	7.288	7.049	6.573	6.450	6.779	7.486	8.344	9.125
613.5	7.307	7.107	6.886	6.433	6.325	6.645	7.314	8.162	8.914
614	7.145	6.934	6.709	6.305	6.207	6.513	7.137	7.989	8.713
614.5	6.987	6.772	6.531	6.168	6.093	6.376	6.966	7.835	8.527
615	6.820	6.617	6.350	6.029	5.975	6.241	6.811	7.676	8.355
615.5	6.648	6.460	6.161	5.897	5.850	6.104	6.665	7.506	8.180
616	6.474	6.318	5.993	5.758	5.718	5.975	6.516	7.331	8.003
616.5	6.297	6.170	5.844	5.620	5.587	5.845	6.364	7.151	7.817
617	6.129	6.027	5.714	5.466	5.467	5.713	6.210	6.967	7.630
617.5	5.964	5.878	5.593	5.318	5.348	5.596	6.064	6.778	7.440
618	5.810	5.720	5.474	5.184	5.236	5.479	5.924	6.598	7.249
618.5	5.665	5.571	5.364	5.048	5.128	5.363	5.789	6.440	7.067
619	5.529	5.427	5.253	4.921	5.015	5.242	5.664	6.292	6.904
619.5	5.394	5.284	5.130	4.808	4.892	5.117	5.548	6.148	6.746
620	5.264	5.151	5.010	4.703	4.767	4.994	5.435	6.014	6.594
620.5	5.136	5.022	4.891	4.606	4.646	4.872	5.318	5.887	6.446
621	5.012	4.912	4.773	4.503	4.528	4.746	5.199	5.757	6.295
621.5	4.890	4.805	4.654	4.399	4.412	4.632	5.086	5.620	6.135
622	4.774	4.696	4.533	4.302	4.295	4.525	4.975	5.480	5.973
622.5	4.654	4.585	4.419	4.205	4.185	4.426	4.859	5.346	5.806
623	4.539	4.466	4.310	4.107	4.082	4.324	4.743	5.219	5.654
623.5	4.425	4.356	4.200	4.012	3.982	4.223	4.628	5.099	5.503

624	4.316	4.243	4.100	3.918	3.886	4.127	4.522	4.980	5.363
624.5	4.212	4.137	4.001	3.828	3.807	4.032	4.412	4.865	5.241
625	4.111	4.040	3.902	3.734	3.735	3.937	4.301	4.755	5.128
625.5	4.018	3.944	3.802	3.637	3.667	3.847	4.203	4.639	5.013
626	3.930	3.851	3.705	3.534	3.590	3.757	4.111	4.521	4.903
626.5	3.837	3.753	3.608	3.440	3.514	3.672	4.025	4.400	4.788
627	3.744	3.645	3.518	3.356	3.431	3.587	3.938	4.281	4.675
627.5	3.649	3.548	3.430	3.273	3.345	3.502	3.843	4.174	4.555
628	3.551	3.445	3.355	3.192	3.255	3.421	3.753	4.070	4.432
628.5	3.453	3.349	3.272	3.118	3.174	3.341	3.660	3.971	4.315
629	3.355	3.262	3.190	3.047	3.097	3.266	3.559	3.879	4.203
629.5	3.264	3.180	3.104	2.974	3.027	3.197	3.463	3.787	4.087
630	3.174	3.110	3.015	2.897	2.952	3.124	3.368	3.695	3.973
630.5	3.085	3.044	2.920	2.822	2.880	3.052	3.275	3.596	3.858
631	3.005	2.973	2.831	2.757	2.801	2.976	3.190	3.494	3.749
631.5	2.924	2.907	2.744	2.691	2.730	2.900	3.102	3.404	3.645
632	2.845	2.836	2.669	2.623	2.661	2.820	3.021	3.317	3.548
632.5	2.766	2.767	2.593	2.562	2.599	2.740	2.945	3.237	3.457
633	2.693	2.691	2.526	2.508	2.541	2.669	2.871	3.163	3.378
633.5	2.630	2.610	2.466	2.454	2.486	2.603	2.803	3.091	3.305
634	2.565	2.533	2.406	2.401	2.429	2.536	2.738	3.019	3.233
634.5	2.504	2.456	2.343	2.345	2.376	2.474	2.673	2.945	3.157
635	2.451	2.382	2.287	2.294	2.319	2.414	2.614	2.864	3.077
635.5	2.396	2.311	2.230	2.235	2.263	2.359	2.551	2.783	2.999
636	2.340	2.248	2.172	2.171	2.208	2.297	2.488	2.705	2.920
636.5	2.279	2.196	2.111	2.105	2.153	2.234	2.419	2.636	2.840
637	2.213	2.144	2.051	2.043	2.095	2.182	2.349	2.573	2.762
637.5	2.150	2.091	1.999	1.983	2.041	2.132	2.282	2.519	2.690
638	2.088	2.043	1.947	1.927	1.982	2.085	2.219	2.466	2.621
638.5	2.027	1.993	1.896	1.875	1.927	2.040	2.160	2.408	2.552
639	1.973	1.942	1.851	1.833	1.877	2.001	2.107	2.347	2.483
639.5	1.920	1.887	1.810	1.792	1.832	1.964	2.061	2.280	2.417
640	1.870	1.833	1.764	1.751	1.788	1.918	2.016	2.208	2.350

4.7. Fl. Intensity data for H₂DTC with variation of surfactant concentrations at 298.15 K

Fl. Intensity of H ₂ DTC with variation of surfactant concentrations in 15% v/v EtOH-water medium									
Fl. Intensity (a.u.)	[SDS]/mM	Fl. Intensity (a.u.)	[DTAB]/mM	Fl. Intensity (a.u.)	[C ₁₆ MImCl]/mM	Fl. Intensity (a.u.)	[16-4 16]/mM	Fl. Intensity (a.u.)	[Tween-60]/mM
0	139.15	0.000	185.74	0.000	221.90	0.0000	158.03	0	169.34
0.0486	140.13	0.120	185.66	0.018	222.47	0.0005	156.77	0.0003	176.63
0.1457	140.02	0.358	185.72	0.055	220.42	0.0014	154.39	0.0010	177.29
0.2906	139.77	0.715	185.09	0.110	218.56	0.0028	147.07	0.0016	177.46
0.4829	140.19	1.306	188.76	0.182	215.49	0.0047	142.25	0.0025	177.75
0.7214	139.70	2.473	186.81	0.271	211.88	0.0070	135.08	0.0038	176.22
1.0757	139.96	4.753	189.19	0.447	206.51	0.0104	124.10	0.0054	175.60
1.5417	140.86	8.044	192.43	0.619	202.83	0.0160	114.87	0.0085	169.85
2.2273	142.70	12.207	209.65	0.951	202.20	0.025	110.51	0.014	165.84
3.1170	144.74	17.078	247.49	1.422	207.23	0.033	111.30	0.023	153.94
4.1919	147.01	21.616	263.86	1.864	218.92	0.045	118.47	0.034	133.84
5.2275	147.71	25.853	274.18	2.412	227.23	0.061	128.97	0.047	126.18
6.4213	148.47	29.819	279.21	3.039	235.20	0.079	139.83	0.065	109.76
7.7509	148.82	33.539	282.94	3.609	242.35	0.104	155.52	0.086	88.00
9.1930	148.59	37.035	284.13	4.130	248.19	0.141	168.26	0.104	74.00
10.7245	148.45	41.901	287.43	4.832	254.48	0.184	185.40	0.129	49.83
12.3231	147.33	49.139	288.15	5.453	259.80	0.228	197.85	0.149	35.44
13.8228	147.55	56.638	292.66	6.007	263.13				
16.5603	145.71	65.053	298.42	6.503	266.26				

4.8. Absorbance data for H₂DTC with variation of its concentrations in 15% EtOH-water medium at 298.15 K

Wavelength/ nm	[H ₂ DTC] / mM								
	0.042	0.045	0.048	0.05	0.056	0.061	0.07	0.082	
200	0.431	0.463	0.493	0.523	0.583	0.641	0.730	0.857	
200.5	0.429	0.462	0.491	0.522	0.582	0.639	0.729	0.854	
201	0.426	0.458	0.486	0.517	0.578	0.634	0.724	0.849	
201.5	0.422	0.454	0.482	0.513	0.573	0.629	0.718	0.844	
202	0.418	0.450	0.478	0.508	0.567	0.623	0.713	0.837	
202.5	0.413	0.444	0.472	0.502	0.561	0.617	0.706	0.830	
203	0.408	0.439	0.466	0.497	0.555	0.611	0.698	0.823	
203.5	0.403	0.434	0.461	0.491	0.549	0.605	0.691	0.814	
204	0.398	0.429	0.456	0.485	0.543	0.598	0.683	0.805	
204.5	0.392	0.423	0.450	0.479	0.537	0.591	0.675	0.797	
205	0.387	0.417	0.444	0.473	0.530	0.584	0.668	0.789	
205.5	0.382	0.411	0.438	0.467	0.523	0.576	0.660	0.780	
206	0.377	0.406	0.432	0.460	0.517	0.569	0.653	0.772	
206.5	0.372	0.401	0.427	0.455	0.511	0.563	0.646	0.764	
207	0.368	0.396	0.422	0.450	0.505	0.558	0.639	0.757	
207.5	0.363	0.392	0.417	0.444	0.500	0.552	0.633	0.750	
208	0.359	0.388	0.412	0.440	0.494	0.547	0.627	0.744	
208.5	0.356	0.384	0.408	0.435	0.490	0.542	0.622	0.738	
209	0.353	0.380	0.405	0.432	0.487	0.538	0.618	0.734	
209.5	0.350	0.378	0.402	0.429	0.483	0.535	0.615	0.730	
210	0.348	0.375	0.399	0.426	0.480	0.531	0.611	0.726	
210.5	0.345	0.372	0.396	0.422	0.477	0.528	0.608	0.724	
211	0.343	0.370	0.394	0.420	0.474	0.526	0.606	0.721	
211.5	0.342	0.368	0.392	0.418	0.472	0.524	0.604	0.720	

212	0.340	0.366	0.390	0.417	0.470	0.522	0.602	0.719
212.5	0.339	0.365	0.389	0.415	0.469	0.521	0.602	0.718
213	0.339	0.364	0.388	0.415	0.469	0.521	0.602	0.719
213.5	0.338	0.364	0.388	0.414	0.469	0.521	0.602	0.720
214	0.338	0.364	0.388	0.414	0.469	0.521	0.603	0.722
214.5	0.339	0.364	0.388	0.415	0.470	0.523	0.604	0.724
215	0.339	0.365	0.389	0.416	0.471	0.524	0.606	0.727
215.5	0.340	0.366	0.390	0.417	0.473	0.526	0.609	0.730
216	0.341	0.367	0.391	0.419	0.474	0.528	0.611	0.734
216.5	0.342	0.368	0.393	0.420	0.476	0.531	0.615	0.738
217	0.343	0.370	0.395	0.422	0.479	0.533	0.618	0.742
217.5	0.345	0.372	0.397	0.424	0.481	0.536	0.621	0.747
218	0.347	0.374	0.399	0.427	0.484	0.540	0.625	0.751
218.5	0.349	0.376	0.401	0.429	0.487	0.543	0.629	0.756
219	0.350	0.378	0.403	0.432	0.490	0.546	0.633	0.762
219.5	0.352	0.380	0.406	0.434	0.493	0.549	0.637	0.767
220	0.354	0.382	0.408	0.437	0.496	0.553	0.641	0.771
220.5	0.357	0.385	0.411	0.440	0.499	0.557	0.645	0.777
221	0.359	0.387	0.414	0.443	0.503	0.560	0.650	0.782
221.5	0.361	0.390	0.417	0.446	0.506	0.564	0.654	0.787
222	0.363	0.392	0.419	0.449	0.510	0.568	0.659	0.793
222.5	0.365	0.395	0.422	0.452	0.513	0.572	0.663	0.798
223	0.368	0.397	0.425	0.455	0.517	0.576	0.667	0.803
223.5	0.370	0.400	0.428	0.458	0.520	0.579	0.672	0.808
224	0.372	0.403	0.431	0.461	0.524	0.583	0.677	0.813
224.5	0.375	0.406	0.434	0.464	0.527	0.587	0.681	0.818
225	0.377	0.408	0.437	0.468	0.531	0.591	0.686	0.823
225.5	0.380	0.411	0.440	0.471	0.535	0.595	0.690	0.829
226	0.382	0.414	0.443	0.475	0.539	0.599	0.695	0.834
226.5	0.385	0.418	0.447	0.479	0.543	0.604	0.700	0.840
227	0.388	0.421	0.450	0.482	0.547	0.608	0.705	0.845
227.5	0.391	0.424	0.454	0.486	0.551	0.613	0.710	0.850
228	0.394	0.428	0.458	0.490	0.556	0.617	0.715	0.856
228.5	0.397	0.431	0.461	0.494	0.560	0.622	0.720	0.862
229	0.400	0.435	0.465	0.498	0.564	0.626	0.726	0.868
229.5	0.403	0.438	0.469	0.502	0.568	0.631	0.731	0.873
230	0.406	0.442	0.473	0.507	0.573	0.636	0.736	0.879
230.5	0.409	0.446	0.477	0.511	0.578	0.641	0.742	0.885
231	0.413	0.449	0.481	0.515	0.582	0.646	0.747	0.891
231.5	0.416	0.453	0.485	0.520	0.587	0.651	0.753	0.897
232	0.420	0.457	0.489	0.524	0.592	0.656	0.759	0.903
232.5	0.423	0.461	0.493	0.528	0.596	0.661	0.764	0.909
233	0.426	0.464	0.497	0.532	0.600	0.665	0.769	0.914
233.5	0.429	0.468	0.500	0.536	0.604	0.669	0.774	0.919
234	0.432	0.471	0.504	0.539	0.608	0.674	0.778	0.924
234.5	0.435	0.474	0.507	0.542	0.612	0.677	0.782	0.929
235	0.438	0.477	0.510	0.546	0.615	0.681	0.786	0.933
235.5	0.440	0.479	0.513	0.549	0.618	0.684	0.790	0.937
236	0.442	0.482	0.515	0.551	0.621	0.687	0.793	0.940
236.5	0.444	0.484	0.518	0.554	0.623	0.690	0.796	0.943
237	0.446	0.486	0.520	0.556	0.626	0.693	0.799	0.946
237.5	0.448	0.488	0.522	0.558	0.628	0.695	0.801	0.948
238	0.449	0.489	0.523	0.559	0.629	0.696	0.802	0.950
238.5	0.450	0.490	0.524	0.560	0.630	0.697	0.803	0.950
239	0.451	0.490	0.524	0.560	0.630	0.697	0.803	0.950
239.5	0.450	0.490	0.524	0.560	0.630	0.696	0.802	0.949
240	0.450	0.489	0.523	0.559	0.628	0.695	0.800	0.946
240.5	0.448	0.488	0.521	0.557	0.626	0.692	0.797	0.942
241	0.446	0.486	0.519	0.554	0.623	0.688	0.792	0.936
241.5	0.444	0.482	0.516	0.551	0.619	0.684	0.786	0.929
242	0.441	0.479	0.511	0.546	0.613	0.678	0.779	0.920
242.5	0.437	0.474	0.506	0.541	0.607	0.671	0.771	0.911
243	0.432	0.469	0.501	0.535	0.601	0.663	0.762	0.900
243.5	0.427	0.464	0.495	0.528	0.593	0.655	0.752	0.888

244	0.422	0.458	0.488	0.522	0.585	0.646	0.741	0.875
244.5	0.416	0.451	0.481	0.514	0.577	0.636	0.730	0.862
245	0.410	0.445	0.474	0.506	0.568	0.626	0.719	0.848
245.5	0.404	0.438	0.467	0.499	0.559	0.616	0.707	0.834
246	0.398	0.431	0.459	0.491	0.550	0.606	0.695	0.819
246.5	0.392	0.424	0.452	0.482	0.540	0.596	0.683	0.805
247	0.385	0.417	0.444	0.474	0.531	0.585	0.670	0.790
247.5	0.379	0.409	0.436	0.466	0.522	0.575	0.658	0.776
248	0.372	0.403	0.429	0.457	0.512	0.565	0.647	0.761
248.5	0.366	0.396	0.421	0.449	0.503	0.555	0.635	0.748
249	0.360	0.389	0.414	0.441	0.494	0.546	0.624	0.735
249.5	0.354	0.382	0.406	0.434	0.486	0.536	0.613	0.722
250	0.347	0.375	0.399	0.426	0.477	0.526	0.603	0.709
250.5	0.341	0.368	0.392	0.418	0.468	0.517	0.592	0.696
251	0.335	0.361	0.385	0.410	0.460	0.508	0.582	0.684
251.5	0.329	0.355	0.378	0.403	0.452	0.499	0.572	0.673
252	0.323	0.349	0.371	0.396	0.444	0.491	0.562	0.661
252.5	0.318	0.343	0.365	0.389	0.436	0.482	0.553	0.651
253	0.313	0.337	0.359	0.383	0.429	0.474	0.544	0.641
253.5	0.307	0.332	0.353	0.376	0.422	0.467	0.536	0.632
254	0.302	0.326	0.347	0.370	0.416	0.460	0.528	0.623
254.5	0.298	0.321	0.342	0.365	0.410	0.453	0.520	0.614
255	0.294	0.317	0.337	0.360	0.404	0.447	0.514	0.607
255.5	0.290	0.313	0.333	0.355	0.398	0.442	0.507	0.599
256	0.286	0.309	0.328	0.351	0.394	0.436	0.501	0.593
256.5	0.283	0.305	0.325	0.347	0.389	0.431	0.496	0.587
257	0.280	0.301	0.321	0.343	0.385	0.427	0.491	0.582
257.5	0.276	0.298	0.318	0.339	0.381	0.423	0.487	0.577
258	0.274	0.295	0.315	0.336	0.378	0.419	0.482	0.572
258.5	0.271	0.293	0.312	0.333	0.374	0.415	0.478	0.568
259	0.269	0.290	0.309	0.330	0.371	0.412	0.475	0.563
259.5	0.267	0.288	0.307	0.327	0.368	0.409	0.471	0.560
260	0.265	0.286	0.305	0.325	0.365	0.406	0.468	0.556
260.5	0.263	0.284	0.302	0.323	0.363	0.403	0.465	0.553
261	0.261	0.282	0.300	0.321	0.361	0.401	0.463	0.550
261.5	0.259	0.280	0.298	0.319	0.359	0.399	0.460	0.548
262	0.258	0.279	0.297	0.317	0.357	0.397	0.458	0.545
262.5	0.256	0.277	0.295	0.315	0.355	0.394	0.455	0.542
263	0.255	0.275	0.293	0.313	0.353	0.392	0.453	0.540
263.5	0.253	0.273	0.292	0.312	0.351	0.390	0.451	0.537
264	0.252	0.272	0.290	0.310	0.349	0.388	0.448	0.535
264.5	0.250	0.270	0.288	0.308	0.346	0.385	0.446	0.532
265	0.248	0.268	0.286	0.306	0.344	0.383	0.443	0.529
265.5	0.247	0.266	0.284	0.304	0.342	0.381	0.440	0.526
266	0.245	0.265	0.282	0.302	0.340	0.378	0.438	0.522
266.5	0.243	0.262	0.280	0.299	0.337	0.375	0.434	0.518
267	0.241	0.260	0.278	0.297	0.334	0.372	0.431	0.514
267.5	0.239	0.258	0.275	0.294	0.331	0.369	0.427	0.510
268	0.237	0.256	0.273	0.291	0.328	0.366	0.423	0.506
268.5	0.234	0.253	0.270	0.288	0.325	0.362	0.419	0.501
269	0.232	0.250	0.267	0.285	0.322	0.358	0.415	0.496
269.5	0.229	0.248	0.264	0.282	0.318	0.354	0.410	0.491
270	0.227	0.245	0.261	0.279	0.315	0.351	0.406	0.486
270.5	0.224	0.242	0.258	0.276	0.311	0.347	0.401	0.480
271	0.222	0.239	0.255	0.273	0.307	0.343	0.397	0.475
271.5	0.219	0.236	0.252	0.269	0.304	0.339	0.392	0.469
272	0.216	0.233	0.249	0.266	0.300	0.334	0.387	0.464
272.5	0.213	0.230	0.246	0.263	0.296	0.330	0.382	0.458
273	0.210	0.227	0.242	0.259	0.292	0.326	0.377	0.452
273.5	0.207	0.224	0.239	0.255	0.288	0.321	0.371	0.446
274	0.204	0.221	0.235	0.252	0.284	0.317	0.366	0.440
274.5	0.202	0.217	0.232	0.248	0.280	0.312	0.361	0.433
275	0.198	0.214	0.228	0.245	0.276	0.308	0.356	0.427
275.5	0.195	0.211	0.225	0.241	0.272	0.303	0.351	0.421

276	0.193	0.207	0.221	0.237	0.268	0.298	0.345	0.414
276.5	0.189	0.204	0.218	0.233	0.263	0.294	0.340	0.407
277	0.186	0.201	0.214	0.229	0.259	0.289	0.335	0.401
277.5	0.183	0.198	0.211	0.226	0.255	0.284	0.329	0.394
278	0.180	0.194	0.207	0.222	0.251	0.280	0.324	0.388
278.5	0.177	0.191	0.204	0.218	0.246	0.275	0.319	0.381
279	0.174	0.188	0.200	0.215	0.242	0.271	0.313	0.375
279.5	0.171	0.184	0.197	0.211	0.238	0.266	0.308	0.368
280	0.168	0.181	0.193	0.207	0.234	0.261	0.303	0.361
280.5	0.165	0.178	0.190	0.203	0.229	0.257	0.297	0.355
281	0.162	0.174	0.186	0.199	0.225	0.252	0.291	0.348
281.5	0.159	0.171	0.182	0.196	0.221	0.247	0.286	0.342
282	0.155	0.168	0.179	0.192	0.217	0.242	0.280	0.335
282.5	0.152	0.165	0.176	0.188	0.213	0.238	0.275	0.329
283	0.150	0.161	0.172	0.185	0.209	0.233	0.270	0.323
283.5	0.147	0.158	0.168	0.181	0.204	0.229	0.265	0.317
284	0.143	0.155	0.165	0.177	0.200	0.224	0.259	0.310
284.5	0.140	0.151	0.161	0.173	0.196	0.219	0.254	0.303
285	0.137	0.148	0.158	0.169	0.191	0.214	0.248	0.297
285.5	0.134	0.144	0.154	0.166	0.187	0.209	0.243	0.290
286	0.131	0.141	0.151	0.162	0.183	0.205	0.238	0.284
286.5	0.128	0.138	0.148	0.158	0.179	0.201	0.233	0.278
287	0.125	0.135	0.145	0.155	0.175	0.196	0.228	0.272
287.5	0.122	0.132	0.141	0.152	0.171	0.192	0.223	0.267
288	0.119	0.129	0.138	0.148	0.168	0.188	0.218	0.261
288.5	0.117	0.126	0.135	0.145	0.164	0.184	0.214	0.256
289	0.114	0.124	0.132	0.142	0.161	0.180	0.209	0.250
289.5	0.112	0.121	0.130	0.139	0.157	0.177	0.205	0.245
290	0.109	0.119	0.127	0.137	0.154	0.173	0.201	0.241
290.5	0.107	0.117	0.125	0.134	0.151	0.170	0.197	0.236
291	0.105	0.114	0.122	0.131	0.149	0.167	0.194	0.232
291.5	0.103	0.112	0.120	0.129	0.146	0.164	0.191	0.228
292	0.101	0.110	0.118	0.127	0.144	0.161	0.187	0.224
292.5	0.099	0.108	0.116	0.125	0.141	0.159	0.184	0.220
293	0.098	0.107	0.114	0.123	0.139	0.156	0.181	0.217
293.5	0.096	0.105	0.112	0.121	0.137	0.154	0.179	0.214
294	0.095	0.103	0.111	0.119	0.135	0.151	0.176	0.211
294.5	0.093	0.102	0.109	0.118	0.133	0.150	0.174	0.208
295	0.092	0.100	0.108	0.116	0.132	0.148	0.172	0.206
295.5	0.091	0.099	0.106	0.115	0.130	0.146	0.170	0.204
296	0.090	0.098	0.105	0.114	0.129	0.145	0.168	0.202
296.5	0.089	0.097	0.104	0.112	0.127	0.143	0.166	0.200
297	0.088	0.096	0.103	0.111	0.126	0.142	0.165	0.198
297.5	0.087	0.095	0.102	0.110	0.125	0.141	0.163	0.196
298	0.086	0.094	0.101	0.109	0.124	0.139	0.162	0.194
298.5	0.085	0.094	0.101	0.108	0.123	0.138	0.161	0.193
299	0.084	0.093	0.100	0.108	0.122	0.137	0.160	0.192
299.5	0.084	0.092	0.099	0.107	0.121	0.136	0.159	0.190
300	0.083	0.091	0.098	0.106	0.120	0.135	0.158	0.189
300.5	0.083	0.091	0.097	0.105	0.120	0.134	0.156	0.188
301	0.082	0.090	0.097	0.105	0.119	0.134	0.156	0.187
301.5	0.082	0.090	0.096	0.104	0.118	0.133	0.155	0.186
302	0.081	0.089	0.096	0.103	0.117	0.132	0.154	0.185
302.5	0.080	0.088	0.095	0.103	0.117	0.131	0.153	0.183
303	0.080	0.088	0.094	0.102	0.116	0.130	0.152	0.182
303.5	0.079	0.087	0.094	0.101	0.115	0.130	0.151	0.181
304	0.079	0.087	0.093	0.101	0.115	0.129	0.150	0.180
304.5	0.078	0.086	0.093	0.100	0.114	0.128	0.150	0.179
305	0.078	0.086	0.092	0.099	0.113	0.127	0.149	0.178
305.5	0.077	0.085	0.091	0.099	0.112	0.127	0.148	0.177
306	0.076	0.083	0.090	0.097	0.110	0.125	0.146	0.175
306.5	0.074	0.082	0.088	0.095	0.109	0.123	0.144	0.173
307	0.074	0.081	0.088	0.095	0.108	0.122	0.143	0.172
307.5	0.073	0.081	0.087	0.094	0.107	0.121	0.142	0.171

308	0.073	0.080	0.086	0.094	0.107	0.120	0.141	0.170
308.5	0.072	0.080	0.086	0.093	0.106	0.120	0.140	0.169
309	0.071	0.079	0.085	0.092	0.105	0.119	0.139	0.168
309.5	0.071	0.078	0.084	0.092	0.104	0.118	0.138	0.166
310	0.070	0.078	0.084	0.091	0.104	0.117	0.137	0.165
310.5	0.070	0.077	0.083	0.090	0.103	0.116	0.137	0.164
311	0.069	0.077	0.083	0.090	0.102	0.116	0.136	0.163
311.5	0.069	0.076	0.082	0.089	0.102	0.115	0.135	0.162
312	0.068	0.076	0.082	0.089	0.101	0.114	0.134	0.161
312.5	0.068	0.075	0.081	0.088	0.100	0.113	0.133	0.160
313	0.067	0.075	0.081	0.087	0.099	0.113	0.132	0.159
313.5	0.067	0.074	0.080	0.087	0.099	0.112	0.131	0.158
314	0.067	0.074	0.079	0.086	0.098	0.111	0.130	0.157
314.5	0.066	0.073	0.079	0.086	0.098	0.110	0.130	0.156
315	0.066	0.073	0.079	0.085	0.097	0.110	0.129	0.155
315.5	0.065	0.072	0.078	0.085	0.097	0.109	0.128	0.154
316	0.065	0.072	0.078	0.084	0.096	0.109	0.127	0.153
316.5	0.065	0.072	0.077	0.084	0.096	0.108	0.127	0.152
317	0.064	0.071	0.077	0.083	0.095	0.108	0.126	0.152
317.5	0.064	0.071	0.077	0.083	0.095	0.107	0.125	0.151
318	0.064	0.071	0.076	0.083	0.094	0.107	0.125	0.150
318.5	0.063	0.070	0.076	0.083	0.094	0.106	0.125	0.150
319	0.063	0.070	0.076	0.082	0.094	0.106	0.124	0.149
319.5	0.063	0.070	0.076	0.082	0.094	0.106	0.124	0.149
320	0.063	0.070	0.075	0.082	0.094	0.106	0.124	0.149
320.5	0.063	0.070	0.075	0.082	0.093	0.105	0.123	0.149
321	0.063	0.070	0.075	0.082	0.093	0.105	0.123	0.148
321.5	0.063	0.070	0.075	0.082	0.093	0.105	0.123	0.148
322	0.063	0.070	0.075	0.082	0.093	0.105	0.123	0.148
322.5	0.063	0.070	0.075	0.082	0.093	0.106	0.123	0.148
323	0.063	0.070	0.076	0.082	0.094	0.106	0.123	0.148
323.5	0.063	0.070	0.076	0.082	0.094	0.106	0.124	0.148
324	0.064	0.070	0.076	0.082	0.094	0.106	0.124	0.148
324.5	0.064	0.071	0.076	0.083	0.094	0.106	0.124	0.149
325	0.064	0.071	0.076	0.083	0.094	0.106	0.124	0.149
325.5	0.064	0.071	0.077	0.083	0.095	0.107	0.125	0.150
326	0.064	0.072	0.077	0.084	0.095	0.107	0.125	0.150
326.5	0.065	0.072	0.078	0.084	0.096	0.108	0.125	0.150
327	0.065	0.072	0.078	0.084	0.096	0.108	0.126	0.151
327.5	0.066	0.073	0.078	0.085	0.096	0.109	0.127	0.151
328	0.066	0.073	0.079	0.085	0.097	0.109	0.127	0.152
328.5	0.066	0.073	0.079	0.086	0.098	0.110	0.128	0.153
329	0.067	0.074	0.080	0.086	0.098	0.110	0.128	0.154
329.5	0.067	0.074	0.080	0.087	0.099	0.111	0.129	0.155
330	0.068	0.075	0.081	0.088	0.099	0.112	0.130	0.155
330.5	0.068	0.076	0.081	0.088	0.100	0.113	0.131	0.156
331	0.069	0.076	0.082	0.089	0.101	0.113	0.132	0.157
331.5	0.069	0.077	0.083	0.089	0.101	0.114	0.133	0.158
332	0.070	0.077	0.083	0.090	0.102	0.115	0.133	0.159
332.5	0.070	0.078	0.084	0.091	0.103	0.116	0.134	0.160
333	0.071	0.079	0.085	0.092	0.104	0.116	0.135	0.161
333.5	0.072	0.079	0.085	0.092	0.104	0.117	0.136	0.162
334	0.072	0.080	0.086	0.093	0.105	0.118	0.137	0.163
334.5	0.073	0.080	0.086	0.094	0.106	0.119	0.138	0.164
335	0.073	0.081	0.087	0.094	0.107	0.120	0.139	0.166
335.5	0.074	0.082	0.088	0.095	0.108	0.121	0.140	0.167
336	0.075	0.082	0.089	0.096	0.109	0.122	0.141	0.168
336.5	0.075	0.083	0.090	0.097	0.109	0.123	0.143	0.169
337	0.076	0.084	0.090	0.098	0.110	0.124	0.144	0.171
337.5	0.077	0.084	0.091	0.099	0.111	0.125	0.145	0.172
338	0.077	0.085	0.092	0.099	0.112	0.126	0.146	0.173
338.5	0.078	0.086	0.093	0.100	0.113	0.127	0.147	0.174
339	0.079	0.087	0.094	0.101	0.114	0.128	0.148	0.176
339.5	0.079	0.088	0.094	0.102	0.115	0.129	0.149	0.177

340	0.080	0.089	0.095	0.103	0.116	0.130	0.150	0.178
340.5	0.081	0.089	0.096	0.104	0.117	0.131	0.151	0.179
341	0.083	0.092	0.099	0.107	0.120	0.134	0.154	0.183
341.5	0.086	0.095	0.102	0.110	0.123	0.137	0.158	0.187
342	0.087	0.096	0.102	0.111	0.124	0.138	0.159	0.188
342.5	0.088	0.096	0.103	0.111	0.125	0.140	0.160	0.190
343	0.089	0.097	0.104	0.112	0.126	0.141	0.161	0.191
343.5	0.089	0.098	0.105	0.113	0.127	0.141	0.162	0.192
344	0.090	0.099	0.106	0.114	0.128	0.142	0.164	0.194
344.5	0.090	0.099	0.107	0.115	0.129	0.143	0.165	0.195
345	0.091	0.100	0.107	0.115	0.130	0.145	0.166	0.196
345.5	0.092	0.101	0.108	0.116	0.130	0.146	0.167	0.197
346	0.092	0.102	0.109	0.117	0.131	0.146	0.168	0.198
346.5	0.093	0.102	0.110	0.118	0.132	0.147	0.169	0.200
347	0.094	0.103	0.110	0.119	0.133	0.148	0.170	0.201
347.5	0.094	0.104	0.111	0.120	0.134	0.149	0.171	0.202
348	0.095	0.104	0.111	0.120	0.134	0.150	0.172	0.203
348.5	0.095	0.105	0.112	0.121	0.135	0.151	0.173	0.204
349	0.096	0.105	0.113	0.121	0.136	0.151	0.174	0.205
349.5	0.096	0.106	0.113	0.122	0.136	0.152	0.174	0.206
350	0.097	0.106	0.114	0.123	0.137	0.153	0.175	0.207
350.5	0.097	0.107	0.114	0.123	0.138	0.153	0.176	0.208
351	0.097	0.107	0.115	0.124	0.138	0.154	0.177	0.208
351.5	0.098	0.107	0.115	0.124	0.139	0.154	0.177	0.209
352	0.098	0.108	0.115	0.124	0.139	0.155	0.177	0.209
352.5	0.098	0.108	0.116	0.125	0.139	0.155	0.178	0.210
353	0.099	0.108	0.116	0.125	0.140	0.155	0.178	0.210
353.5	0.099	0.109	0.116	0.125	0.140	0.156	0.179	0.211
354	0.099	0.109	0.116	0.125	0.140	0.156	0.179	0.211
354.5	0.099	0.109	0.116	0.126	0.140	0.156	0.179	0.211
355	0.099	0.109	0.116	0.126	0.140	0.156	0.179	0.211
355.5	0.099	0.109	0.117	0.126	0.140	0.156	0.179	0.211
356	0.099	0.109	0.117	0.126	0.140	0.156	0.179	0.212
356.5	0.099	0.109	0.116	0.126	0.140	0.156	0.179	0.211
357	0.099	0.109	0.116	0.125	0.140	0.156	0.179	0.211
357.5	0.099	0.109	0.116	0.125	0.140	0.156	0.179	0.211
358	0.099	0.109	0.116	0.125	0.140	0.156	0.179	0.211
358.5	0.099	0.108	0.116	0.125	0.140	0.155	0.178	0.210
359	0.098	0.108	0.116	0.125	0.139	0.155	0.178	0.210
359.5	0.098	0.108	0.115	0.124	0.139	0.155	0.177	0.209
360	0.098	0.107	0.115	0.124	0.138	0.154	0.177	0.209
360.5	0.097	0.107	0.115	0.123	0.138	0.154	0.176	0.208
361	0.097	0.107	0.114	0.123	0.137	0.153	0.176	0.207
361.5	0.096	0.106	0.114	0.122	0.137	0.152	0.175	0.207
362	0.096	0.106	0.113	0.122	0.136	0.152	0.174	0.206
362.5	0.095	0.105	0.112	0.121	0.135	0.151	0.173	0.205
363	0.095	0.104	0.112	0.120	0.134	0.150	0.172	0.203
363.5	0.094	0.104	0.111	0.120	0.134	0.149	0.171	0.203
364	0.094	0.103	0.110	0.119	0.133	0.148	0.170	0.201
364.5	0.093	0.102	0.109	0.118	0.132	0.147	0.169	0.200
365	0.092	0.101	0.109	0.117	0.131	0.146	0.168	0.199
365.5	0.091	0.100	0.108	0.116	0.130	0.145	0.167	0.197
366	0.091	0.099	0.107	0.115	0.129	0.144	0.165	0.196
366.5	0.090	0.099	0.106	0.114	0.128	0.143	0.164	0.194
367	0.089	0.098	0.105	0.113	0.126	0.141	0.162	0.193
367.5	0.088	0.097	0.104	0.112	0.125	0.140	0.161	0.191
368	0.087	0.096	0.103	0.111	0.124	0.139	0.160	0.189
368.5	0.086	0.095	0.102	0.110	0.123	0.138	0.158	0.188
369	0.085	0.094	0.100	0.109	0.122	0.136	0.157	0.186
369.5	0.084	0.093	0.099	0.107	0.120	0.135	0.155	0.184
370	0.083	0.092	0.098	0.106	0.119	0.133	0.153	0.182
370.5	0.083	0.091	0.097	0.105	0.118	0.132	0.152	0.181
371	0.082	0.090	0.096	0.104	0.116	0.130	0.150	0.179
371.5	0.081	0.089	0.095	0.103	0.115	0.129	0.149	0.177

372	0.080	0.088	0.094	0.101	0.114	0.128	0.147	0.175
372.5	0.079	0.086	0.093	0.100	0.112	0.126	0.146	0.173
373	0.078	0.085	0.091	0.099	0.111	0.125	0.144	0.172
373.5	0.077	0.084	0.090	0.098	0.110	0.123	0.142	0.170
374	0.076	0.083	0.089	0.096	0.108	0.122	0.141	0.168
374.5	0.075	0.082	0.088	0.095	0.107	0.120	0.139	0.166
375	0.074	0.081	0.087	0.094	0.106	0.119	0.137	0.164
375.5	0.073	0.080	0.086	0.093	0.104	0.117	0.136	0.163
376	0.072	0.079	0.084	0.091	0.103	0.116	0.134	0.161
376.5	0.071	0.078	0.083	0.090	0.101	0.114	0.133	0.159
377	0.070	0.076	0.082	0.089	0.100	0.113	0.131	0.157
377.5	0.069	0.076	0.081	0.088	0.099	0.112	0.130	0.156
378	0.068	0.075	0.080	0.087	0.098	0.110	0.128	0.154
378.5	0.067	0.074	0.079	0.086	0.097	0.109	0.127	0.152
379	0.066	0.073	0.078	0.085	0.095	0.108	0.125	0.151
379.5	0.065	0.072	0.077	0.084	0.094	0.107	0.124	0.150
380	0.065	0.071	0.076	0.083	0.093	0.106	0.123	0.148
380.5	0.064	0.070	0.075	0.082	0.092	0.105	0.122	0.147
381	0.063	0.070	0.075	0.081	0.092	0.104	0.121	0.146
381.5	0.063	0.069	0.074	0.080	0.091	0.103	0.120	0.145
382	0.062	0.068	0.073	0.079	0.090	0.102	0.119	0.144
382.5	0.061	0.068	0.073	0.079	0.089	0.101	0.118	0.143
383	0.061	0.067	0.072	0.078	0.088	0.100	0.117	0.142
383.5	0.060	0.066	0.071	0.077	0.087	0.099	0.116	0.141
384	0.060	0.066	0.070	0.077	0.087	0.099	0.115	0.140
384.5	0.059	0.065	0.070	0.076	0.086	0.098	0.115	0.139
385	0.059	0.065	0.069	0.076	0.086	0.097	0.114	0.139
385.5	0.058	0.064	0.069	0.075	0.085	0.097	0.113	0.138
386	0.058	0.064	0.068	0.075	0.084	0.096	0.113	0.137
386.5	0.058	0.063	0.068	0.074	0.084	0.096	0.112	0.137
387	0.057	0.063	0.068	0.074	0.083	0.095	0.112	0.136
387.5	0.057	0.063	0.067	0.073	0.083	0.095	0.111	0.136
388	0.057	0.062	0.067	0.073	0.083	0.095	0.111	0.136
388.5	0.056	0.062	0.067	0.073	0.082	0.094	0.111	0.135
389	0.056	0.062	0.066	0.072	0.082	0.094	0.110	0.135
389.5	0.056	0.062	0.066	0.072	0.082	0.094	0.110	0.135
390	0.056	0.061	0.066	0.072	0.082	0.093	0.110	0.135
390.5	0.056	0.061	0.066	0.072	0.081	0.093	0.110	0.135
391	0.056	0.061	0.066	0.072	0.081	0.093	0.110	0.135
391.5	0.056	0.061	0.065	0.072	0.081	0.093	0.110	0.135
392	0.055	0.061	0.065	0.071	0.081	0.093	0.109	0.135
392.5	0.055	0.061	0.065	0.071	0.081	0.093	0.109	0.135
393	0.055	0.061	0.065	0.071	0.081	0.093	0.110	0.135
393.5	0.055	0.061	0.065	0.071	0.081	0.093	0.110	0.135
394	0.055	0.061	0.065	0.071	0.081	0.093	0.110	0.135
394.5	0.055	0.061	0.065	0.071	0.081	0.093	0.110	0.136
395	0.055	0.061	0.065	0.071	0.081	0.093	0.110	0.136
395.5	0.056	0.061	0.065	0.071	0.081	0.093	0.110	0.136
396	0.056	0.061	0.065	0.071	0.081	0.094	0.110	0.137
396.5	0.056	0.061	0.065	0.072	0.082	0.094	0.111	0.137
397	0.056	0.061	0.065	0.072	0.082	0.094	0.111	0.137
397.5	0.056	0.061	0.066	0.072	0.082	0.094	0.111	0.138
398	0.056	0.061	0.066	0.072	0.082	0.094	0.112	0.138
398.5	0.056	0.061	0.066	0.072	0.082	0.095	0.112	0.139
399	0.056	0.061	0.066	0.072	0.082	0.095	0.112	0.139
399.5	0.056	0.062	0.066	0.072	0.083	0.095	0.113	0.140
400	0.057	0.062	0.066	0.073	0.083	0.096	0.113	0.141
400.5	0.057	0.062	0.067	0.073	0.083	0.096	0.114	0.141
401	0.057	0.062	0.067	0.073	0.083	0.096	0.114	0.142
401.5	0.057	0.062	0.067	0.073	0.084	0.097	0.115	0.143
402	0.057	0.063	0.067	0.074	0.084	0.097	0.115	0.143
402.5	0.058	0.063	0.068	0.074	0.084	0.098	0.116	0.144
403	0.058	0.063	0.068	0.074	0.085	0.098	0.116	0.145
403.5	0.058	0.064	0.068	0.075	0.085	0.099	0.117	0.146

404	0.059	0.064	0.069	0.075	0.086	0.099	0.118	0.147
404.5	0.059	0.064	0.069	0.076	0.086	0.100	0.118	0.148
405	0.059	0.065	0.069	0.076	0.087	0.100	0.119	0.148
405.5	0.060	0.065	0.070	0.076	0.087	0.101	0.120	0.150
406	0.060	0.065	0.070	0.077	0.088	0.102	0.121	0.150
406.5	0.060	0.066	0.071	0.077	0.088	0.102	0.122	0.151
407	0.061	0.066	0.071	0.078	0.089	0.103	0.122	0.152
407.5	0.061	0.067	0.072	0.078	0.089	0.104	0.123	0.154
408	0.062	0.067	0.072	0.079	0.090	0.104	0.124	0.155
408.5	0.062	0.067	0.072	0.079	0.091	0.105	0.125	0.156
409	0.063	0.068	0.073	0.080	0.091	0.106	0.126	0.157
409.5	0.063	0.068	0.073	0.080	0.092	0.106	0.127	0.158
410	0.063	0.069	0.074	0.081	0.092	0.107	0.127	0.159
410.5	0.064	0.069	0.074	0.081	0.093	0.108	0.128	0.160
411	0.064	0.070	0.075	0.082	0.094	0.109	0.129	0.161
411.5	0.065	0.070	0.075	0.082	0.094	0.109	0.130	0.162
412	0.065	0.071	0.076	0.083	0.095	0.110	0.131	0.164
412.5	0.066	0.071	0.076	0.083	0.095	0.111	0.132	0.165
413	0.067	0.072	0.077	0.085	0.097	0.112	0.133	0.167
413.5	0.067	0.073	0.078	0.085	0.098	0.113	0.135	0.168
414	0.067	0.073	0.078	0.086	0.098	0.114	0.135	0.169
414.5	0.067	0.073	0.078	0.086	0.098	0.114	0.136	0.170
415	0.068	0.073	0.079	0.086	0.099	0.115	0.137	0.171
415.5	0.068	0.074	0.079	0.087	0.099	0.115	0.138	0.172
416	0.069	0.074	0.080	0.087	0.100	0.116	0.138	0.173
416.5	0.068	0.074	0.080	0.087	0.100	0.116	0.139	0.174
417	0.068	0.074	0.080	0.087	0.100	0.117	0.139	0.174
417.5	0.069	0.075	0.080	0.088	0.101	0.117	0.140	0.176
418	0.069	0.075	0.081	0.089	0.102	0.118	0.141	0.177
418.5	0.070	0.076	0.081	0.089	0.102	0.119	0.142	0.178
419	0.070	0.076	0.082	0.089	0.103	0.120	0.143	0.179
419.5	0.071	0.077	0.082	0.090	0.104	0.120	0.144	0.180
420	0.071	0.077	0.083	0.091	0.104	0.121	0.145	0.181
420.5	0.071	0.077	0.083	0.091	0.104	0.122	0.146	0.182
421	0.072	0.078	0.084	0.092	0.105	0.122	0.146	0.183
421.5	0.072	0.078	0.084	0.092	0.106	0.123	0.147	0.184
422	0.073	0.079	0.084	0.092	0.106	0.123	0.148	0.185
422.5	0.073	0.079	0.085	0.093	0.107	0.124	0.148	0.186
423	0.073	0.079	0.085	0.093	0.107	0.125	0.149	0.187
423.5	0.074	0.080	0.086	0.094	0.108	0.125	0.150	0.188
424	0.074	0.080	0.086	0.094	0.108	0.126	0.150	0.189
424.5	0.074	0.080	0.086	0.095	0.109	0.126	0.151	0.189
425	0.075	0.081	0.087	0.095	0.109	0.127	0.152	0.190
425.5	0.075	0.081	0.087	0.095	0.109	0.127	0.152	0.191
426	0.075	0.081	0.087	0.096	0.110	0.128	0.153	0.192
426.5	0.075	0.082	0.088	0.096	0.110	0.128	0.153	0.192
427	0.076	0.082	0.088	0.096	0.110	0.129	0.154	0.193
427.5	0.076	0.082	0.088	0.097	0.111	0.129	0.154	0.193
428	0.076	0.082	0.088	0.097	0.111	0.129	0.155	0.194
428.5	0.076	0.082	0.089	0.097	0.111	0.129	0.155	0.194
429	0.076	0.083	0.089	0.097	0.111	0.130	0.155	0.195
429.5	0.077	0.083	0.089	0.097	0.112	0.130	0.155	0.195
430	0.077	0.083	0.089	0.098	0.112	0.130	0.156	0.196
430.5	0.077	0.083	0.089	0.098	0.112	0.130	0.156	0.196
431	0.077	0.083	0.089	0.098	0.112	0.131	0.156	0.196
431.5	0.077	0.083	0.089	0.098	0.112	0.131	0.156	0.196
432	0.077	0.083	0.089	0.098	0.112	0.131	0.156	0.196
432.5	0.077	0.083	0.089	0.098	0.112	0.131	0.156	0.197
433	0.077	0.083	0.089	0.098	0.112	0.131	0.157	0.197
433.5	0.077	0.083	0.089	0.098	0.112	0.131	0.156	0.197
434	0.077	0.083	0.089	0.098	0.112	0.131	0.156	0.196
434.5	0.077	0.083	0.089	0.098	0.112	0.131	0.156	0.196
435	0.077	0.083	0.089	0.098	0.112	0.131	0.156	0.196
435.5	0.077	0.083	0.089	0.098	0.112	0.130	0.156	0.196

436	0.077	0.083	0.089	0.097	0.112	0.130	0.156	0.196
436.5	0.076	0.083	0.089	0.097	0.112	0.130	0.156	0.195
437	0.076	0.082	0.089	0.097	0.111	0.130	0.155	0.195
437.5	0.076	0.082	0.088	0.097	0.111	0.129	0.155	0.194
438	0.076	0.082	0.088	0.096	0.111	0.129	0.154	0.194
438.5	0.076	0.082	0.088	0.096	0.110	0.129	0.154	0.193
439	0.075	0.081	0.088	0.096	0.110	0.128	0.153	0.193
439.5	0.075	0.081	0.087	0.095	0.109	0.128	0.153	0.192
440	0.075	0.081	0.087	0.095	0.109	0.127	0.152	0.191
440.5	0.074	0.080	0.086	0.094	0.109	0.126	0.151	0.190
441	0.074	0.080	0.086	0.094	0.108	0.126	0.151	0.190
441.5	0.074	0.080	0.086	0.094	0.108	0.125	0.150	0.189
442	0.073	0.079	0.085	0.093	0.107	0.125	0.149	0.188
442.5	0.073	0.079	0.084	0.093	0.106	0.124	0.149	0.187
443	0.072	0.078	0.084	0.092	0.106	0.123	0.148	0.186
443.5	0.072	0.078	0.083	0.091	0.105	0.122	0.147	0.184
444	0.071	0.077	0.083	0.091	0.104	0.122	0.146	0.183
444.5	0.071	0.077	0.082	0.090	0.104	0.121	0.145	0.182
445	0.070	0.076	0.082	0.090	0.103	0.120	0.144	0.181
445.5	0.070	0.075	0.081	0.089	0.102	0.119	0.143	0.179
446	0.069	0.075	0.080	0.088	0.101	0.118	0.141	0.178
446.5	0.068	0.074	0.080	0.087	0.100	0.117	0.140	0.176
447	0.068	0.073	0.079	0.086	0.099	0.116	0.139	0.175
447.5	0.067	0.073	0.078	0.086	0.098	0.115	0.138	0.173
448	0.066	0.072	0.077	0.085	0.097	0.114	0.136	0.172
448.5	0.066	0.071	0.077	0.084	0.096	0.113	0.135	0.170
449	0.065	0.070	0.076	0.083	0.095	0.112	0.134	0.168
449.5	0.064	0.070	0.075	0.082	0.094	0.110	0.132	0.167
450	0.063	0.069	0.074	0.081	0.094	0.109	0.131	0.165
450.5	0.063	0.068	0.073	0.081	0.092	0.108	0.130	0.163
451	0.062	0.067	0.073	0.080	0.091	0.107	0.128	0.161
451.5	0.061	0.067	0.072	0.079	0.090	0.106	0.127	0.160
452	0.061	0.066	0.071	0.078	0.089	0.104	0.125	0.158
452.5	0.060	0.065	0.070	0.077	0.088	0.103	0.124	0.156
453	0.059	0.064	0.069	0.076	0.087	0.102	0.122	0.154
453.5	0.058	0.063	0.068	0.075	0.086	0.100	0.121	0.152
454	0.057	0.063	0.067	0.074	0.085	0.099	0.119	0.151
454.5	0.057	0.062	0.066	0.073	0.084	0.098	0.118	0.149
455	0.056	0.061	0.066	0.072	0.083	0.097	0.116	0.147
455.5	0.055	0.060	0.065	0.071	0.082	0.096	0.115	0.145
456	0.055	0.059	0.064	0.070	0.081	0.094	0.114	0.143
456.5	0.054	0.058	0.063	0.069	0.080	0.093	0.112	0.141
457	0.053	0.058	0.062	0.068	0.078	0.092	0.110	0.139
457.5	0.052	0.057	0.061	0.067	0.077	0.091	0.109	0.137
458	0.051	0.056	0.060	0.066	0.076	0.089	0.107	0.135
458.5	0.051	0.055	0.059	0.065	0.075	0.088	0.106	0.134
459	0.050	0.054	0.058	0.064	0.074	0.087	0.104	0.132
459.5	0.049	0.053	0.058	0.063	0.073	0.085	0.103	0.130
460	0.048	0.052	0.057	0.063	0.072	0.084	0.101	0.128
460.5	0.047	0.052	0.056	0.062	0.071	0.083	0.100	0.126
461	0.047	0.051	0.055	0.061	0.070	0.082	0.098	0.124
461.5	0.046	0.050	0.054	0.060	0.068	0.080	0.097	0.122
462	0.045	0.049	0.053	0.059	0.067	0.079	0.095	0.120
462.5	0.044	0.048	0.052	0.058	0.066	0.078	0.093	0.118
463	0.043	0.047	0.051	0.057	0.065	0.076	0.092	0.116
463.5	0.043	0.047	0.050	0.056	0.064	0.075	0.090	0.114
464	0.042	0.046	0.050	0.055	0.063	0.074	0.089	0.112
464.5	0.041	0.045	0.049	0.054	0.062	0.073	0.087	0.111
465	0.040	0.044	0.048	0.053	0.061	0.071	0.086	0.109
465.5	0.040	0.043	0.047	0.052	0.060	0.070	0.084	0.107
466	0.039	0.042	0.046	0.051	0.059	0.069	0.083	0.105
466.5	0.038	0.042	0.045	0.050	0.057	0.067	0.081	0.103
467	0.037	0.041	0.044	0.049	0.056	0.066	0.080	0.101
467.5	0.036	0.040	0.043	0.048	0.055	0.065	0.078	0.099

468	0.036	0.039	0.042	0.047	0.054	0.064	0.077	0.097
468.5	0.035	0.038	0.042	0.046	0.053	0.063	0.076	0.096
469	0.034	0.037	0.041	0.045	0.052	0.061	0.074	0.094
469.5	0.033	0.037	0.040	0.044	0.051	0.060	0.072	0.092
470	0.033	0.036	0.039	0.043	0.050	0.059	0.071	0.090
470.5	0.032	0.035	0.038	0.042	0.049	0.058	0.069	0.088
471	0.031	0.034	0.037	0.042	0.048	0.056	0.068	0.086
471.5	0.030	0.034	0.036	0.041	0.047	0.055	0.067	0.085
472	0.030	0.033	0.036	0.040	0.046	0.054	0.065	0.083
472.5	0.029	0.032	0.035	0.039	0.045	0.053	0.064	0.081
473	0.028	0.031	0.034	0.038	0.044	0.052	0.063	0.080
473.5	0.028	0.031	0.033	0.037	0.043	0.051	0.061	0.078
474	0.027	0.030	0.033	0.036	0.042	0.050	0.060	0.076
474.5	0.026	0.029	0.032	0.036	0.041	0.049	0.059	0.075
475	0.026	0.029	0.031	0.035	0.040	0.048	0.057	0.073
475.5	0.025	0.028	0.030	0.034	0.039	0.047	0.056	0.072
476	0.025	0.027	0.030	0.033	0.038	0.046	0.055	0.070
476.5	0.024	0.027	0.029	0.032	0.038	0.045	0.054	0.069
477	0.023	0.026	0.028	0.032	0.037	0.044	0.053	0.067
477.5	0.023	0.025	0.028	0.031	0.036	0.043	0.052	0.066
478	0.022	0.025	0.027	0.030	0.035	0.042	0.050	0.064
478.5	0.022	0.024	0.026	0.030	0.034	0.041	0.049	0.063
479	0.021	0.024	0.026	0.029	0.033	0.040	0.048	0.062
479.5	0.021	0.023	0.025	0.028	0.033	0.039	0.047	0.061
480	0.020	0.022	0.025	0.028	0.032	0.038	0.046	0.059
480.5	0.020	0.022	0.024	0.027	0.031	0.037	0.045	0.058
481	0.019	0.021	0.023	0.026	0.031	0.036	0.044	0.057
481.5	0.018	0.021	0.023	0.026	0.030	0.036	0.043	0.056
482	0.018	0.020	0.022	0.025	0.029	0.035	0.042	0.054
482.5	0.017	0.020	0.022	0.025	0.029	0.034	0.042	0.053
483	0.017	0.019	0.021	0.024	0.028	0.033	0.041	0.052
483.5	0.017	0.019	0.021	0.024	0.027	0.033	0.040	0.051
484	0.016	0.018	0.020	0.023	0.027	0.032	0.039	0.050
484.5	0.016	0.018	0.020	0.023	0.026	0.031	0.038	0.049
485	0.016	0.017	0.019	0.022	0.026	0.031	0.038	0.048
485.5	0.015	0.017	0.019	0.022	0.025	0.030	0.037	0.047
486	0.015	0.017	0.018	0.021	0.025	0.030	0.036	0.046
486.5	0.014	0.016	0.018	0.021	0.024	0.029	0.035	0.046
487	0.014	0.016	0.018	0.020	0.024	0.028	0.035	0.045
487.5	0.014	0.016	0.017	0.020	0.023	0.028	0.034	0.044
488	0.013	0.015	0.017	0.020	0.023	0.027	0.033	0.043
488.5	0.013	0.015	0.017	0.019	0.022	0.027	0.033	0.042
489	0.013	0.015	0.016	0.019	0.022	0.026	0.032	0.042
489.5	0.012	0.014	0.016	0.018	0.021	0.026	0.032	0.041
490	0.012	0.014	0.016	0.018	0.021	0.025	0.031	0.040
490.5	0.012	0.014	0.015	0.018	0.020	0.025	0.030	0.039
491	0.011	0.013	0.015	0.017	0.020	0.024	0.030	0.039
491.5	0.011	0.013	0.014	0.017	0.020	0.024	0.029	0.038
492	0.011	0.013	0.014	0.016	0.019	0.024	0.029	0.037
492.5	0.011	0.012	0.014	0.016	0.019	0.023	0.028	0.037
493	0.010	0.012	0.014	0.016	0.019	0.023	0.028	0.036
493.5	0.010	0.012	0.013	0.016	0.018	0.022	0.027	0.036
494	0.010	0.012	0.013	0.015	0.018	0.022	0.027	0.035
494.5	0.010	0.011	0.013	0.015	0.018	0.021	0.026	0.035
495	0.010	0.011	0.013	0.015	0.017	0.021	0.026	0.034
495.5	0.009	0.011	0.012	0.014	0.017	0.021	0.026	0.033
496	0.009	0.011	0.012	0.014	0.017	0.020	0.025	0.033
496.5	0.009	0.010	0.012	0.014	0.016	0.020	0.025	0.032
497	0.009	0.010	0.012	0.014	0.016	0.020	0.025	0.032
497.5	0.008	0.010	0.011	0.013	0.016	0.019	0.024	0.031
498	0.008	0.010	0.011	0.013	0.016	0.019	0.024	0.031
498.5	0.008	0.010	0.011	0.013	0.015	0.019	0.023	0.030
499	0.008	0.009	0.011	0.013	0.015	0.018	0.023	0.030
499.5	0.008	0.009	0.010	0.012	0.015	0.018	0.023	0.030

500	0.007	0.009	0.010	0.012	0.014	0.018	0.022	0.029
500.5	0.007	0.009	0.010	0.012	0.014	0.018	0.022	0.029
501	0.007	0.009	0.010	0.012	0.014	0.017	0.021	0.028
501.5	0.007	0.008	0.010	0.012	0.014	0.017	0.021	0.028
502	0.007	0.008	0.010	0.011	0.013	0.017	0.021	0.027
502.5	0.007	0.008	0.009	0.011	0.013	0.016	0.021	0.027
503	0.006	0.008	0.009	0.011	0.013	0.016	0.020	0.027
503.5	0.006	0.008	0.009	0.011	0.013	0.016	0.020	0.026
504	0.006	0.008	0.009	0.010	0.013	0.016	0.020	0.026
504.5	0.006	0.007	0.009	0.010	0.012	0.016	0.019	0.026
505	0.006	0.007	0.008	0.010	0.012	0.015	0.019	0.025
505.5	0.006	0.007	0.008	0.010	0.012	0.015	0.019	0.025
506	0.005	0.007	0.008	0.010	0.012	0.015	0.019	0.025
506.5	0.005	0.007	0.008	0.010	0.012	0.015	0.018	0.024
507	0.005	0.007	0.008	0.010	0.011	0.014	0.018	0.024
507.5	0.005	0.007	0.008	0.010	0.011	0.014	0.018	0.024
508	0.005	0.006	0.007	0.009	0.011	0.014	0.018	0.024
508.5	0.005	0.006	0.007	0.009	0.011	0.014	0.018	0.023
509	0.005	0.006	0.007	0.009	0.011	0.014	0.017	0.023
509.5	0.005	0.006	0.007	0.009	0.010	0.013	0.017	0.023
510	0.005	0.006	0.007	0.009	0.010	0.013	0.017	0.022
510.5	0.005	0.006	0.007	0.008	0.010	0.013	0.017	0.022
511	0.004	0.006	0.007	0.008	0.010	0.013	0.016	0.022
511.5	0.004	0.005	0.007	0.008	0.010	0.013	0.016	0.022
512	0.004	0.005	0.006	0.008	0.010	0.013	0.016	0.021
512.5	0.004	0.005	0.006	0.008	0.010	0.012	0.016	0.021
513	0.004	0.005	0.006	0.008	0.010	0.012	0.016	0.021
513.5	0.004	0.005	0.006	0.008	0.010	0.012	0.016	0.021
514	0.004	0.005	0.006	0.008	0.009	0.012	0.015	0.021
514.5	0.004	0.005	0.006	0.008	0.009	0.012	0.015	0.020
515	0.004	0.005	0.006	0.007	0.009	0.012	0.015	0.020
515.5	0.003	0.005	0.006	0.007	0.009	0.012	0.015	0.020
516	0.003	0.005	0.006	0.007	0.009	0.011	0.015	0.020
516.5	0.003	0.005	0.005	0.007	0.009	0.011	0.015	0.020
517	0.003	0.005	0.005	0.007	0.009	0.011	0.015	0.019
517.5	0.003	0.004	0.005	0.007	0.008	0.011	0.014	0.019
518	0.003	0.004	0.005	0.007	0.008	0.011	0.014	0.019
518.5	0.003	0.004	0.005	0.007	0.008	0.011	0.014	0.019
519	0.003	0.004	0.005	0.007	0.008	0.011	0.014	0.019
519.5	0.003	0.004	0.005	0.007	0.008	0.011	0.014	0.018
520	0.003	0.004	0.005	0.006	0.008	0.010	0.014	0.018
520.5	0.003	0.004	0.005	0.006	0.008	0.010	0.013	0.018
521	0.003	0.004	0.005	0.006	0.008	0.010	0.013	0.018
521.5	0.003	0.004	0.005	0.006	0.008	0.010	0.013	0.018
522	0.003	0.004	0.005	0.006	0.008	0.010	0.013	0.018
522.5	0.002	0.004	0.005	0.006	0.008	0.010	0.013	0.018
523	0.002	0.003	0.005	0.006	0.007	0.010	0.013	0.017
523.5	0.002	0.003	0.004	0.006	0.007	0.010	0.013	0.017
524	0.002	0.003	0.004	0.006	0.007	0.010	0.013	0.017
524.5	0.002	0.003	0.004	0.006	0.007	0.010	0.013	0.017
525	0.002	0.003	0.004	0.006	0.007	0.010	0.012	0.017
525.5	0.002	0.003	0.004	0.006	0.007	0.009	0.012	0.017
526	0.002	0.003	0.004	0.005	0.007	0.009	0.012	0.017
526.5	0.002	0.003	0.004	0.005	0.007	0.009	0.012	0.017
527	0.002	0.003	0.004	0.005	0.007	0.009	0.012	0.016
527.5	0.002	0.003	0.004	0.005	0.007	0.009	0.012	0.016
528	0.002	0.003	0.004	0.005	0.007	0.009	0.012	0.016
528.5	0.002	0.003	0.004	0.005	0.007	0.009	0.012	0.016
529	0.002	0.003	0.004	0.005	0.007	0.009	0.012	0.016
529.5	0.002	0.003	0.004	0.005	0.006	0.009	0.012	0.016
530	0.002	0.003	0.004	0.005	0.006	0.009	0.011	0.016
530.5	0.002	0.003	0.004	0.005	0.006	0.009	0.011	0.016
531	0.002	0.003	0.004	0.005	0.006	0.009	0.011	0.016
531.5	0.001	0.003	0.003	0.005	0.006	0.008	0.011	0.015

788	0.003	0.003	0.004	0.005	0.005	0.006	0.007	0.009
788.5	0.003	0.003	0.004	0.005	0.005	0.006	0.007	0.009
789	0.003	0.003	0.004	0.005	0.005	0.006	0.007	0.009
789.5	0.003	0.003	0.004	0.005	0.005	0.006	0.007	0.009
790	0.003	0.003	0.004	0.005	0.005	0.006	0.007	0.009
790.5	0.003	0.003	0.004	0.005	0.005	0.006	0.007	0.009
791	0.003	0.003	0.004	0.005	0.005	0.006	0.007	0.009
791.5	0.003	0.003	0.004	0.005	0.005	0.006	0.007	0.009
792	0.003	0.003	0.004	0.005	0.005	0.006	0.007	0.009
792.5	0.003	0.003	0.004	0.005	0.005	0.006	0.007	0.009
793	0.003	0.003	0.004	0.005	0.005	0.006	0.007	0.009
793.5	0.003	0.003	0.004	0.005	0.005	0.006	0.007	0.009
794	0.003	0.003	0.004	0.005	0.005	0.006	0.007	0.009
794.5	0.003	0.003	0.004	0.005	0.005	0.006	0.007	0.009
795	0.003	0.003	0.004	0.005	0.005	0.006	0.007	0.009
795.5	0.003	0.003	0.004	0.005	0.005	0.006	0.007	0.009
796	0.003	0.003	0.004	0.005	0.005	0.006	0.007	0.009
796.5	0.003	0.003	0.004	0.005	0.005	0.006	0.007	0.009
797	0.003	0.003	0.004	0.005	0.005	0.006	0.007	0.009
797.5	0.003	0.003	0.004	0.005	0.005	0.006	0.007	0.009
798	0.003	0.003	0.004	0.005	0.005	0.006	0.007	0.009
798.5	0.003	0.003	0.004	0.005	0.005	0.006	0.007	0.009
799	0.003	0.003	0.004	0.005	0.005	0.006	0.007	0.009
799.5	0.003	0.003	0.004	0.005	0.005	0.006	0.007	0.008
800	0.003	0.003	0.004	0.005	0.005	0.006	0.006	0.008

4.9. Absorbance intensity data for H₂DTC with different concentrations at three different wavelength at 298.15 K

[H ₂ DTC] / mM	absorbance intensity		
	434 nm	238 nm	356 nm
0.0000	0.000	0.000	0.000
0.0018	0.001	0.013	0.002
0.0062	0.005	0.044	0.007
0.0104	0.010	0.079	0.014
0.0144	0.016	0.120	0.022
0.0183	0.022	0.154	0.030
0.0220	0.027	0.184	0.037
0.0257	0.033	0.221	0.045
0.0291	0.043	0.271	0.057
0.0325	0.052	0.311	0.067
0.0358	0.057	0.345	0.075
0.0389	0.065	0.383	0.084
0.0420	0.077	0.449	0.099
0.0449	0.083	0.489	0.109
0.0478	0.089	0.523	0.117
0.0505	0.098	0.559	0.126
0.0558	0.112	0.629	0.140
0.0608	0.131	0.696	0.156
0.0699	0.156	0.802	0.179
0.0819	0.196	0.950	0.212
0.0921	0.236	1.083	0.234
0.1010	0.277	1.205	0.254
0.1088	0.314	1.310	0.272
0.1157	0.353	1.416	0.291
0.1218	0.389	1.510	0.310
0.1272	0.415	1.595	0.328
0.1322	0.447	1.674	0.346
0.1366	0.465	1.732	0.361

4.10. Data for determination of binding constants of H₂DTC in different micellar medium (in 15% EtOH- water) at 298.15 K

SDS		DTAB		C ₁₆ MImCl		16-4 16		Tween-60	
$1/([D]_{0+} [S]_m) / M^{-1}$	$1/[A-A_0]$	$1/([D]_{0+} [S]_m)$	$1/[A-A_0]$	$1/([D]_{0+} [S]_m)$	$1/[A-A_0]$	$1/([D]_{0+} [S]_m)$	$1/[A-A_0]$	$1/([D]_{0+} [S]_m)$	$1/[A-A_0]$
178.91	233.94	188.41	31.25	1809.43	21.28	2928.86	27.78	3237.40	-12.66
100.13	133.22	93.49	22.22	1112.46	16.95	2732.09	23.81	3120.90	-9.62
67.74	96.40	61.07	19.23	813.84	14.93	2529.72	21.74	3002.10	-8.06
59.56	77.72	43.16	18.52	607.92	14.08	2374.17	20.41	2768.17	-6.17
		31.26	18.87	469.33	12.99				
				357.70	11.90				
				279.26	11.63				
				218.17	11.11				

4.11. Data for determination of partition coefficient of H₂DTC in solvent to the different micellar medium (15% EtOH-water) at 298.15 K

SDS		DTAB		C ₁₆ MImCl		16-4 16		Tween-60	
$(1/[S]_m) / M^{-1}$	$\{[D]_0/([A]_0-[A])\} / M$	$1/[S]_m$	$\{[D]_0/([A]_0-[A])\} / M$	$1/[S]_m$	$\{[D]_0/([A]_0-[A])\} / M$	$1/[S]_m$	$\{[D]_0/([A]_0-[A])\} / M$	$1/[S]_m$	$\{[D]_0/([A]_0-[A])\} / M$
146.20	0.077	96.26	0.0068	1692.31	0.0052	29913.25	0.0086	39840.64	0.0025
103.30	0.034	62.24	0.0059	1086.08	0.0046	17235.44	0.0073	18779.34	0.0019
69.17	0.026	43.74	0.0057	747.97	0.0043	11454.75	0.0067	10220.77	0.0014
60.67	0.021	31.56	0.0058	548.64	0.0040	8833.92	0.0063		
				401.99	0.0037	6005.28	0.0064		
				305.54	0.0036				
				233.88	0.0034				

Chapter-V

5.1. Tensiometry data of surfactants at phosphate buffer (pH 7) [concentration = 20 μ M] at 298.15 K

In PB pH 7.0		BM (20 μ M) in PB pH7.0		In PB pH 7.0		BM (20 μ M) in PB pH7.0		In PB pH 7.0		BM (20 μ M) in PB pH7.0		In PB pH 7.0		BM (20 μ M) in PB pH7.0	
[NaC]/mM	γ /mN.m ⁻¹	[NaC]/mM	γ /mN.m ⁻¹	[NaDC]/mM	γ /mN.m ⁻¹	[NaDC]/mM	γ /mN.m ⁻¹	[SDDS]/mM	γ /mN.m ⁻¹	[SDDS]/mM	γ /mN.m ⁻¹	[SDBS]/mM	γ /mN.m ⁻¹	[SDBS]/mM	γ /mN.m ⁻¹
0.000	64.3	0.000	59.3	0.000	65.0	0.000	56.3	0.000	65.0	0.000	59.1	0.000	65.0	0.000	59.3
0.084	61.3	0.042	57.2	0.019	62.9	0.024	52.8	0.163	56.8	0.071	53.1	0.047	48.6	0.020	49.0
0.252	58.3	0.084	56.4	0.056	58.0	0.072	49.0	0.325	52.2	0.143	51.3	0.093	43.2	0.040	46.7
0.670	55.0	0.168	54.8	0.112	54.3	0.144	47.8	0.487	48.8	0.214	50.0	0.140	37.6	0.060	44.8
1.501	52.0	0.252	54.3	0.187	51.7	0.239	46.0	0.649	46.3	0.321	48.5	0.186	36.0	0.080	43.2
2.736	49.2	0.377	52.7	0.280	49.4	0.382	44.0	0.892	44.2	0.463	46.7	0.279	33.4	0.110	42.4
4.762	46.7	0.503	51.3	0.391	47.6	0.559	43.0	1.377	41.3	0.641	45.7	0.465	30.2	0.159	41.0
7.532	44.3	0.670	51.3	0.530	46.1	0.793	42.0	2.183	37.9	0.854	43.8	0.743	28.9	0.229	38.3
11.362	43.0	0.920	50.0	0.713	43.6	1.107	40.2	3.785	32.2	1.102	41.8	1.205	28.1	0.328	34.7
15.771	43.7	1.169	48.9	0.940	41.5	1.509	39.4	5.374	30.1	1.386	39.8	2.124	27.9	0.475	32.0
21.015	43.8	1.584	47.3	1.209	40.0	2.074	38.3	6.950	30.3	1.739	38.2	3.940	27.9	0.671	30.5
27.582	43.8	2.408	46.5	1.562	38.6	2.846	37.5	9.292	32.2	2.163	36.0	6.170	27.9	0.961	29.7
35.175	43.8	3.632	45.2	2.000	37.7	3.810	38.0	11.607	32.5	2.726	34.6			1.625	29.8
43.492	43.5	5.640	44.2	2.509	36.7	5.045	39.6	14.651	32.9	3.427	33.0			2.544	29.7
53.424	43.5	9.542	43.5	3.091	36.1	6.515	40.6	18.392	33.1	4.473	31.0			4.279	29.9
		16.914	43.9	3.738	36.9	8.178	41.0	25.662	33.4	6.204	29.6			7.396	30.2
		23.764	43.7	4.443	38.4	9.992	41.3			9.276	31.7			12.508	30.2
		36.101	43.7	5.200	38.1	11.915	41.5			12.295	32.2				
		46.906	43.7	6.073	39.5	13.910	41.7			16.565	32.9				
						15.941	41.7			21.676	33.3				
						17.977	41.7			27.853	33.5				
						19.995	41.7			39.549	33.8				
						21.972	41.7			60.610	33.7				

5.2. Calorimetry data of surfactants at phosphate buffer (pH 7) [concentration = 20 μ M] at 298.15 K

In PB pH 7.0		BM (20 μ M) in PB pH7.0		In PB pH 7.0		BM (20 μ M) in PB pH7.0		In PB pH 7.0		BM (20 μ M) in PB pH7.0		In PB pH 7.0		BM (20 μ M) in PB pH7.0	
[NaC]/mM	ΔH_{dil}^0 /kJ.mol ⁻¹	[NaC]/mM	ΔH_{dil}^0 /kJ.mol ⁻¹	[NaDC]/ mM	ΔH_{dil}^0 /kJ.mol ⁻¹	[NaDC]/ mM	ΔH_{dil}^0 /kJ.mol ⁻¹	[SDDS] /mM	ΔH_{dil}^0 /kJ.mol ⁻¹	[SDDS] /mM	ΔH_{dil}^0 /kJ.mol ⁻¹	[SDBS]/mM	ΔH_{dil}^0 /kJ.mol ⁻¹	[SDBS]/mM	ΔH_{dil}^0 /kJ.mol ⁻¹
0		0	--	0		0	--	0		0		0	--	0	-
0.509	-0.160	0.685	-0.031	0.110	0.400	0.763	1.392	0.532	-1.686	0.537	-6.368	0.066	0.149	0.066	-0.505
2.546	-0.155	1.366	0.052	0.763	0.421	1.406	2.256	2.669	-1.545	2.670	-8.378	0.328	0.185	0.328	-0.124
4.566	-0.147	2.044	0.007	1.406	0.437	2.040	3.938	4.787	-1.311	4.783	-10.321	0.587	0.217	0.587	0.527
6.561	-0.127	3.390	-0.045	2.040	0.473	2.664	4.548	6.925	-0.988	6.875	-10.900	0.844	0.267	0.844	-1.190
8.538	-0.081	4.722	-0.008	2.664	0.508	3.278	4.828	8.946	-0.602	8.946	-9.297	1.098	0.331	1.098	-0.783
10.498	-0.034	6.042	0.030	3.278	0.548	3.883	4.860	10.997	-0.335	10.995	-7.817	1.349	0.344	1.349	-0.560
14.348	0.023	7.347	0.047	3.883	0.551	4.478	4.714	13.021	-0.162	13.024	-6.566	1.598	0.319	1.598	-0.416
16.245	0.049	8.639	0.043	4.478	0.527	5.064	4.575	15.035	-0.092	15.032	-5.656	1.845	0.296	1.845	-0.350
18.121	0.066	9.918	-0.018	5.064	0.479	5.639	4.449	17.019	-0.087	17.019	-4.901	2.089	0.274	2.089	-0.321
19.978	0.077	11.184	-0.033	5.639	0.429	6.205	4.417	18.984	-0.094	18.984	-4.944	2.330	0.251	2.330	-0.278
21.814	0.083	13.674	-0.068	6.205	0.376	6.762	4.439	20.929	-0.097	20.929	-4.733	2.569	0.236	2.569	-0.275
23.630	0.081	15.507	-0.060	6.762	0.317	7.309	4.430	22.853	-0.098	22.853	-4.554	2.805	0.214	2.805	-0.271
25.426	0.085	17.310	-0.078					24.755	-0.098	24.755	-4.427	3.038	0.200	3.038	-0.253
27.203	0.073	19.082	-0.084					26.637	-0.097	26.637	-4.408	3.269	0.180	3.269	-0.264
28.959	0.070	20.824	-0.078					28.498	-0.095	28.498	-4.152	3.497	0.170	3.497	-0.247
30.695	0.071	22.537	-0.069					30.338	-0.093	30.338	-4.023	3.723	0.157	3.723	-0.223
32.411	0.076	24.218	-0.063					32.156	-0.092	32.156	-3.905	3.946	0.145	3.946	-0.224
34.107	0.099							33.954	-0.089	33.954	-3.741	4.167	0.135	4.167	-0.213
								35.731	-0.087	35.731	-3.634	4.385	0.117	4.385	-0.206
								37.486		37.486		4.601		4.601	

5.3. Raw calorimetry data (Time vs. Heat flow) of surfactants at phosphate buffer (pH 7) [concentration = 20 μ M] at 298.15 K

In PB pH 7.0		BM (20 μ M) in PB pH7.0		In PB pH 7.0		BM (20 μ M) in PB pH7.0		In PB pH 7.0		BM (20 μ M) in PB pH7.0		In PB pH 7.0		BM (20 μ M) In PB pH7.0	
Time/min	μ cal/sec	Time/min	μ cal/sec	Time/min	μ cal/sec	Time/min	μ cal/sec	Time/min	μ cal/sec	Time/min	μ cal/sec	Time/min	μ cal/sec	Time/min	μ cal/sec
0.08	4.83	0.08	5.02	0.08	4.91	0.08	7.12	0.08	9.90	0.08	7.12	0.08	0.03	0.08	8.29
0.17	4.83	0.17	5.03	0.17	4.91	0.17	7.12	0.17	9.92	0.17	7.12	0.17	0.01	0.17	8.29
0.25	4.84	0.25	5.03	0.25	4.91	0.25	7.13	0.25	9.92	0.25	7.13	0.25	0.00	0.25	8.29
0.33	4.83	0.33	5.03	0.33	4.91	0.33	7.13	0.33	9.93	0.33	7.13	0.33	-0.01	0.33	8.29
0.42	4.83	0.42	5.03	0.42	4.91	0.42	7.13	0.42	9.93	0.42	7.13	0.42	-0.01	0.42	8.29
0.50	4.83	0.50	5.04	0.50	4.91	0.50	7.13	0.50	9.93	0.50	7.13	0.50	-0.03	0.50	8.30
0.58	4.83	0.58	5.04	0.58	4.91	0.58	7.13	0.58	9.93	0.58	7.13	0.58	-0.01	0.58	8.30
0.67	4.83	0.67	5.04	0.67	4.91	0.67	7.13	0.67	9.93	0.67	7.13	0.67	0.02	0.67	8.30
0.75	4.84	0.75	5.05	0.75	4.91	0.75	7.13	0.75	9.93	0.75	7.13	0.75	0.00	0.75	8.30
0.83	4.83	0.83	5.05	0.83	4.91	0.83	7.13	0.83	9.94	0.83	7.13	0.83	-0.01	0.83	8.30
0.92	4.83	0.92	5.05	0.92	4.91	0.92	7.13	0.92	9.94	0.92	7.13	0.92	-0.01	0.92	8.30
1.00	4.83	1.00	5.06	1.00	4.91	1.00	7.13	1.00	9.94	1.00	7.13	1.00	0.02	1.00	8.30
1.08	4.83	1.08	4.58	1.08	4.91	1.08	6.21	1.08	9.94	1.08	6.21	1.08	-0.10	1.08	8.29
1.17	4.73	1.17	3.91	1.17	4.99	1.17	4.34	1.17	9.70	1.17	4.34	1.17	-0.09	1.17	8.27
1.25	4.13	1.25	5.05	1.25	5.01	1.25	7.32	1.25	8.02	1.25	7.32	1.25	0.04	1.25	8.27
1.33	4.31	1.33	5.35	1.33	4.90	1.33	7.37	1.33	7.42	1.33	7.37	1.33	0.02	1.33	8.30
1.42	4.63	1.42	5.15	1.42	4.91	1.42	7.15	1.42	7.18	1.42	7.15	1.42	0.00	1.42	8.30
1.50	4.71	1.50	5.07	1.50	4.92	1.50	7.16	1.50	8.79	1.50	7.16	1.50	-0.01	1.50	8.30
1.58	4.72	1.58	5.08	1.58	4.91	1.58	7.17	1.58	9.63	1.58	7.17	1.58	0.01	1.58	8.29
1.67	4.73	1.67	5.10	1.67	4.90	1.67	7.16	1.67	9.82	1.67	7.16	1.67	0.00	1.67	8.30
1.75	4.74	1.75	5.11	1.75	4.91	1.75	7.16	1.75	9.86	1.75	7.16	1.75	0.00	1.75	8.30
1.83	4.76	1.83	5.10	1.83	4.91	1.83	7.16	1.83	9.90	1.83	7.16	1.83	0.01	1.83	8.30
1.92	4.76	1.92	5.09	1.92	4.90	1.92	7.16	1.92	9.93	1.92	7.16	1.92	0.01	1.92	8.30
2.00	4.77	2.00	5.08	2.00	4.91	2.00	7.16	2.00	9.95	2.00	7.16	2.00	0.01	2.00	8.30
2.08	4.77	2.08	5.10	2.08	4.91	2.08	7.16	2.08	9.97	2.08	7.16	2.08	0.00	2.08	8.31
2.17	4.78	2.17	5.09	2.17	4.91	2.17	7.16	2.17	9.97	2.17	7.16	2.17	0.01	2.17	8.31
2.25	4.78	2.25	5.10	2.25	4.91	2.25	7.17	2.25	9.97	2.25	7.17	2.25	0.00	2.25	8.31
2.33	4.78	2.33	5.10	2.33	4.91	2.33	7.16	2.33	9.97	2.33	7.16	2.33	0.01	2.33	8.31

2.42	4.79	2.42	5.11	2.42	4.91	2.42	7.16	2.42	9.97	2.42	7.16	2.42	0.01	2.42	8.31
2.50	4.79	2.50	5.11	2.50	4.91	2.50	7.16	2.50	9.97	2.50	7.16	2.50	0.00	2.50	8.31
2.58	4.79	2.58	5.11	2.58	4.91	2.58	7.17	2.58	9.96	2.58	7.17	2.58	0.02	2.58	8.31
2.67	4.79	2.67	5.12	2.67	4.91	2.67	7.17	2.67	9.98	2.67	7.17	2.67	0.02	2.67	8.31
2.75	4.79	2.75	5.12	2.75	4.91	2.75	7.17	2.75	9.98	2.75	7.17	2.75	0.00	2.75	8.31
2.83	4.79	2.83	5.13	2.83	4.91	2.83	7.17	2.83	9.98	2.83	7.17	2.83	-0.02	2.83	8.31
2.92	4.79	2.92	5.13	2.92	4.91	2.92	7.16	2.92	9.98	2.92	7.16	2.92	-0.02	2.92	8.32
3.00	4.79	3.00	5.13	3.00	4.91	3.00	7.16	3.00	9.98	3.00	7.16	3.00	-0.01	3.00	8.32
3.08	4.80	3.08	4.07	3.08	4.91	3.08	3.69	3.08	9.98	3.08	3.69	3.08	-0.29	3.08	8.32
3.17	4.71	3.17	3.65	3.17	5.01	3.17	-21.35	3.17	9.54	3.17	-21.35	3.17	0.40	3.17	8.35
3.25	4.18	3.25	3.94	3.25	5.56	3.25	-28.12	3.25	7.75	3.25	-28.12	3.25	0.83	3.25	8.28
3.33	4.40	3.33	4.28	3.33	5.84	3.33	-22.61	3.33	5.80	3.33	-22.61	3.33	0.28	3.33	8.22
3.42	4.74	3.42	5.45	3.42	5.42	3.42	-12.20	3.42	3.83	3.42	-12.20	3.42	0.09	3.42	8.32
3.50	4.79	3.50	5.56	3.50	5.11	3.50	-3.48	3.50	4.33	3.50	-3.48	3.50	0.07	3.50	8.34
3.58	4.78	3.58	5.28	3.58	5.03	3.58	3.52	3.58	5.12	3.58	3.52	3.58	0.05	3.58	8.32
3.67	4.77	3.67	5.20	3.67	5.00	3.67	6.29	3.67	6.35	3.67	6.29	3.67	0.04	3.67	8.31
3.75	4.76	3.75	5.27	3.75	4.96	3.75	6.41	3.75	7.12	3.75	6.41	3.75	0.05	3.75	8.32
3.83	4.76	3.83	5.30	3.83	4.93	3.83	6.59	3.83	7.70	3.83	6.59	3.83	0.04	3.83	8.31
3.92	4.77	3.92	5.28	3.92	4.90	3.92	6.81	3.92	8.13	3.92	6.81	3.92	0.03	3.92	8.31
4.00	4.77	4.00	5.27	4.00	4.90	4.00	6.96	4.00	8.48	4.00	6.96	4.00	0.02	4.00	8.31
4.08	4.77	4.08	5.27	4.08	4.89	4.08	7.05	4.08	8.73	4.08	7.05	4.08	0.01	4.08	8.31
4.17	4.77	4.17	5.24	4.17	4.89	4.17	7.10	4.17	9.05	4.17	7.10	4.17	0.02	4.17	8.31
4.25	4.77	4.25	5.22	4.25	4.89	4.25	7.14	4.25	9.15	4.25	7.14	4.25	0.02	4.25	8.31
4.33	4.77	4.33	5.22	4.33	4.89	4.33	7.16	4.33	9.35	4.33	7.16	4.33	0.02	4.33	8.31
4.42	4.77	4.42	5.22	4.42	4.89	4.42	7.18	4.42	9.51	4.42	7.18	4.42	-0.01	4.42	8.31
4.50	4.77	4.50	5.23	4.50	4.90	4.50	7.19	4.50	9.64	4.50	7.19	4.50	0.01	4.50	8.31
4.58	4.77	4.58	5.23	4.58	4.90	4.58	7.20	4.58	9.72	4.58	7.20	4.58	0.00	4.58	8.31
4.67	4.77	4.67	5.23	4.67	4.90	4.67	7.20	4.67	9.79	4.67	7.20	4.67	-0.02	4.67	8.31
4.75	4.77	4.75	5.22	4.75	4.91	4.75	7.20	4.75	9.82	4.75	7.20	4.75	-0.01	4.75	8.31
4.83	4.77	4.83	5.23	4.83	4.91	4.83	7.19	4.83	9.84	4.83	7.19	4.83	-0.01	4.83	8.32
4.92	4.77	4.92	5.24	4.92	4.91	4.92	7.19	4.92	9.86	4.92	7.19	4.92	-0.02	4.92	8.32
5.00	4.77	5.00	5.24	5.00	4.91	5.00	7.18	5.00	9.87	5.00	7.18	5.00	-0.01	5.00	8.32

5.08	4.77	5.08	4.73	5.08	4.91	5.08	2.56	5.08	9.89	5.08	2.56	5.08	-0.27	5.08	8.31
5.17	4.69	5.17	6.11	5.17	5.00	5.17	-23.18	5.17	9.77	5.17	-23.18	5.17	0.10	5.17	8.09
5.25	4.19	5.25	5.20	5.25	5.54	5.25	-28.29	5.25	9.48	5.25	-28.29	5.25	0.53	5.25	8.53
5.33	4.35	5.33	4.21	5.33	5.86	5.33	-28.16	5.33	8.91	5.33	-28.16	5.33	0.22	5.33	8.46
5.42	4.70	5.42	4.99	5.42	5.49	5.42	-23.33	5.42	8.39	5.42	-23.33	5.42	0.09	5.42	8.12
5.50	4.75	5.50	5.36	5.50	5.18	5.50	-13.27	5.50	8.48	5.50	-13.27	5.50	0.01	5.50	8.20
5.58	4.75	5.58	5.28	5.58	5.03	5.58	-4.34	5.58	8.42	5.58	-4.34	5.58	-0.07	5.58	8.28
5.67	4.75	5.67	5.22	5.67	4.99	5.67	3.05	5.67	8.42	5.67	3.05	5.67	-0.03	5.67	8.30
5.75	4.74	5.75	5.25	5.75	4.96	5.75	6.32	5.75	8.56	5.75	6.32	5.75	-0.01	5.75	8.31
5.83	4.75	5.83	5.27	5.83	4.93	5.83	6.45	5.83	8.74	5.83	6.45	5.83	-0.04	5.83	8.31
5.92	4.75	5.92	5.28	5.92	4.91	5.92	6.54	5.92	8.90	5.92	6.54	5.92	-0.07	5.92	8.30
6.00	4.75	6.00	5.28	6.00	4.90	6.00	6.75	6.00	9.02	6.00	6.75	6.00	-0.03	6.00	8.30
6.08	4.75	6.08	5.27	6.08	4.90	6.08	6.88	6.08	9.13	6.08	6.88	6.08	-0.02	6.08	8.30
6.17	4.75	6.17	5.29	6.17	4.90	6.17	6.97	6.17	9.22	6.17	6.97	6.17	-0.01	6.17	8.31
6.25	4.75	6.25	5.29	6.25	4.90	6.25	7.04	6.25	9.32	6.25	7.04	6.25	0.00	6.25	8.31
6.33	4.76	6.33	5.29	6.33	4.90	6.33	7.09	6.33	9.39	6.33	7.09	6.33	0.03	6.33	8.31
6.42	4.76	6.42	5.28	6.42	4.91	6.42	7.13	6.42	9.45	6.42	7.13	6.42	0.03	6.42	8.31
6.50	4.76	6.50	5.30	6.50	4.91	6.50	7.15	6.50	9.51	6.50	7.15	6.50	0.03	6.50	8.31
6.58	4.76	6.58	5.29	6.58	4.91	6.58	7.17	6.58	9.57	6.58	7.17	6.58	0.02	6.58	8.31
6.67	4.76	6.67	5.28	6.67	4.92	6.67	7.18	6.67	9.61	6.67	7.18	6.67	0.01	6.67	8.31
6.75	4.76	6.75	5.28	6.75	4.92	6.75	7.18	6.75	9.65	6.75	7.18	6.75	0.01	6.75	8.32
6.83	4.76	6.83	5.30	6.83	4.92	6.83	7.19	6.83	9.69	6.83	7.19	6.83	0.01	6.83	8.32
6.92	4.76	6.92	5.32	6.92	4.92	6.92	7.19	6.92	9.71	6.92	7.19	6.92	0.01	6.92	8.32
7.00	4.75	7.00	5.29	7.00	4.92	7.00	7.19	7.00	9.74	7.00	7.19	7.00	0.01	7.00	8.32
7.08	4.76	7.08	4.50	7.08	4.92	7.08	1.24	7.08	9.76	7.08	1.24	7.08	-0.12	7.08	8.27
7.17	4.68	7.17	4.74	7.17	5.01	7.17	-24.93	7.17	9.56	7.17	-24.93	7.17	0.17	7.17	8.38
7.25	4.19	7.25	5.35	7.25	5.54	7.25	-28.29	7.25	9.04	7.25	-28.29	7.25	0.42	7.25	9.13
7.33	4.32	7.33	4.84	7.33	5.87	7.33	-28.28	7.33	10.15	7.33	-28.28	7.33	0.04	7.33	8.74
7.42	4.67	7.42	5.13	7.42	5.54	7.42	-28.06	7.42	10.85	7.42	-28.06	7.42	0.04	7.42	8.40
7.50	4.73	7.50	5.26	7.50	5.24	7.50	-22.82	7.50	10.80	7.50	-22.82	7.50	0.06	7.50	8.32
7.58	4.73	7.58	5.26	7.58	5.06	7.58	-13.29	7.58	10.46	7.58	-13.29	7.58	0.04	7.58	8.32
7.67	4.73	7.67	5.29	7.67	5.01	7.67	-4.84	7.67	10.17	7.67	-4.84	7.67	-0.02	7.67	8.32

7.75	4.73	7.75	5.32	7.75	4.97	7.75	2.33	7.75	10.06	7.75	2.33	7.75	-0.03	7.75	8.32
7.83	4.73	7.83	5.37	7.83	4.94	7.83	5.88	7.83	10.03	7.83	5.88	7.83	-0.01	7.83	8.32
7.92	4.73	7.92	5.38	7.92	4.92	7.92	6.17	7.92	9.98	7.92	6.17	7.92	0.00	7.92	8.32
8.00	4.73	8.00	5.34	8.00	4.91	8.00	6.32	8.00	9.93	8.00	6.32	8.00	-0.01	8.00	8.32
8.08	4.74	8.08	5.33	8.08	4.91	8.08	6.60	8.08	9.91	8.08	6.60	8.08	-0.08	8.08	8.32
8.17	4.74	8.17	5.37	8.17	4.91	8.17	6.78	8.17	9.89	8.17	6.78	8.17	-0.02	8.17	8.32
8.25	4.74	8.25	5.35	8.25	4.91	8.25	6.89	8.25	9.88	8.25	6.89	8.25	-0.02	8.25	8.32
8.33	4.74	8.33	5.35	8.33	4.91	8.33	6.97	8.33	9.89	8.33	6.97	8.33	0.01	8.33	8.32
8.42	4.74	8.42	5.35	8.42	4.91	8.42	7.02	8.42	9.89	8.42	7.02	8.42	0.02	8.42	8.33
8.50	4.74	8.50	5.34	8.50	4.92	8.50	7.05	8.50	9.89	8.50	7.05	8.50	0.01	8.50	8.33
8.58	4.74	8.58	5.35	8.58	4.92	8.58	7.07	8.58	9.90	8.58	7.07	8.58	0.01	8.58	8.32
8.67	4.74	8.67	5.36	8.67	4.92	8.67	7.10	8.67	9.90	8.67	7.10	8.67	-0.01	8.67	8.32
8.75	4.74	8.75	5.36	8.75	4.93	8.75	7.11	8.75	9.91	8.75	7.11	8.75	0.01	8.75	8.32
8.83	4.74	8.83	5.36	8.83	4.93	8.83	7.12	8.83	9.91	8.83	7.12	8.83	0.02	8.83	8.32
8.92	4.74	8.92	5.36	8.92	4.93	8.92	7.13	8.92	9.92	8.92	7.13	8.92	0.02	8.92	8.32
9.00	4.74	9.00	5.36	9.00	4.93	9.00	7.14	9.00	9.92	9.00	7.14	9.00	0.04	9.00	8.32
9.08	4.74	9.08	4.86	9.08	4.93	9.08	0.39	9.08	9.93	9.08	0.39	9.08	0.01	9.08	8.28
9.17	4.70	9.17	4.43	9.17	5.01	9.17	-25.65	9.17	9.61	9.17	-25.65	9.17	0.91	9.17	7.24
9.25	4.27	9.25	5.02	9.25	5.53	9.25	-28.29	9.25	8.42	9.25	-28.29	9.25	0.96	9.25	7.49
9.33	4.28	9.33	5.12	9.33	5.88	9.33	-28.28	9.33	9.98	9.33	-28.28	9.33	0.27	9.33	8.52
9.42	4.62	9.42	5.38	9.42	5.61	9.42	-28.24	9.42	10.80	9.42	-28.24	9.42	0.10	9.42	8.60
9.50	4.70	9.50	5.36	9.50	5.35	9.50	-24.78	9.50	10.81	9.50	-24.78	9.50	0.06	9.50	8.45
9.58	4.71	9.58	5.34	9.58	5.11	9.58	-15.79	9.58	10.54	9.58	-15.79	9.58	0.04	9.58	8.35
9.67	4.71	9.67	5.37	9.67	5.03	9.67	-7.46	9.67	10.31	9.67	-7.46	9.67	0.03	9.67	8.32
9.75	4.71	9.75	5.40	9.75	4.99	9.75	-0.01	9.75	10.22	9.75	-0.01	9.75	0.01	9.75	8.32
9.83	4.71	9.83	5.40	9.83	4.96	9.83	5.17	9.83	10.18	9.83	5.17	9.83	-0.01	9.83	8.32
9.92	4.72	9.92	5.40	9.92	4.94	9.92	6.22	9.92	10.13	9.92	6.22	9.92	-0.01	9.92	8.32
10.00	4.72	10.00	5.40	10.00	4.92	10.00	6.28	10.00	10.10	10.00	6.28	10.00	-0.01	10.00	8.32
10.08	4.72	10.08	5.41	10.08	4.92	10.08	6.54	10.08	10.07	10.08	6.54	10.08	-0.01	10.08	8.32
10.17	4.72	10.17	5.41	10.17	4.92	10.17	6.74	10.17	10.05	10.17	6.74	10.17	-0.01	10.17	8.32
10.25	4.72	10.25	5.41	10.25	4.92	10.25	6.85	10.25	10.04	10.25	6.85	10.25	-0.02	10.25	8.33
10.33	4.73	10.33	5.41	10.33	4.92	10.33	6.93	10.33	10.03	10.33	6.93	10.33	-0.03	10.33	8.33

10.42	4.73	10.42	5.41	10.42	4.92	10.42	6.98	10.42	9.97	10.42	6.98	10.42	0.00	10.42	8.32
10.50	4.73	10.50	5.42	10.50	4.93	10.50	7.02	10.50	9.92	10.50	7.02	10.50	0.00	10.50	8.33
10.58	4.73	10.58	5.42	10.58	4.93	10.58	7.05	10.58	9.99	10.58	7.05	10.58	0.00	10.58	8.32
10.67	4.73	10.67	5.42	10.67	4.93	10.67	7.07	10.67	10.02	10.67	7.07	10.67	-0.01	10.67	8.32
10.75	4.73	10.75	5.42	10.75	4.94	10.75	7.10	10.75	10.02	10.75	7.10	10.75	0.00	10.75	8.32
10.83	4.73	10.83	5.42	10.83	4.94	10.83	7.12	10.83	10.03	10.83	7.12	10.83	-0.01	10.83	8.33
10.92	4.73	10.92	5.42	10.92	4.94	10.92	7.12	10.92	10.04	10.92	7.12	10.92	-0.01	10.92	8.33
11.00	4.73	11.00	5.42	11.00	4.94	11.00	7.13	11.00	10.05	11.00	7.13	11.00	-0.02	11.00	8.33
11.08	4.73	11.08	5.33	11.08	4.94	11.08	0.94	11.08	10.08	11.08	0.94	11.08	-0.15	11.08	8.26
11.17	4.70	11.17	5.02	11.17	5.02	11.17	-25.28	11.17	9.66	11.17	-25.28	11.17	0.02	11.17	7.05
11.25	4.42	11.25	5.37	11.25	5.54	11.25	-28.28	11.25	8.36	11.25	-28.28	11.25	0.70	11.25	7.44
11.33	4.49	11.33	5.39	11.33	5.88	11.33	-28.26	11.33	9.90	11.33	-28.26	11.33	0.20	11.33	8.60
11.42	4.72	11.42	5.47	11.42	5.66	11.42	-25.20	11.42	10.63	11.42	-25.20	11.42	0.07	11.42	8.66
11.50	4.74	11.50	5.44	11.50	5.42	11.50	-16.23	11.50	10.67	11.50	-16.23	11.50	0.04	11.50	8.48
11.58	4.73	11.58	5.46	11.58	5.15	11.58	-7.95	11.58	10.46	11.58	-7.95	11.58	0.03	11.58	8.36
11.67	4.72	11.67	5.51	11.67	5.06	11.67	-0.77	11.67	10.28	11.67	-0.77	11.67	0.02	11.67	8.33
11.75	4.71	11.75	5.52	11.75	5.01	11.75	4.62	11.75	10.22	11.75	4.62	11.75	0.01	11.75	8.33
11.83	4.71	11.83	5.51	11.83	4.98	11.83	6.08	11.83	10.19	11.83	6.08	11.83	0.00	11.83	8.33
11.92	4.71	11.92	5.50	11.92	4.95	11.92	6.22	11.92	10.15	11.92	6.22	11.92	0.00	11.92	8.33
12.00	4.70	12.00	5.51	12.00	4.94	12.00	6.52	12.00	10.13	12.00	6.52	12.00	0.00	12.00	8.32
12.08	4.70	12.08	5.51	12.08	4.93	12.08	6.74	12.08	10.11	12.08	6.74	12.08	0.00	12.08	8.32
12.17	4.71	12.17	5.51	12.17	4.93	12.17	6.87	12.17	10.10	12.17	6.87	12.17	0.00	12.17	8.32
12.25	4.70	12.25	5.50	12.25	4.93	12.25	6.94	12.25	10.08	12.25	6.94	12.25	0.00	12.25	8.33
12.33	4.70	12.33	5.47	12.33	4.93	12.33	6.99	12.33	10.08	12.33	6.99	12.33	0.00	12.33	8.33
12.42	4.71	12.42	5.46	12.42	4.93	12.42	7.03	12.42	10.07	12.42	7.03	12.42	-0.01	12.42	8.33
12.50	4.71	12.50	5.52	12.50	4.94	12.50	7.05	12.50	10.07	12.50	7.05	12.50	-0.01	12.50	8.33
12.58	4.71	12.58	5.53	12.58	4.94	12.58	7.08	12.58	10.06	12.58	7.08	12.58	-0.01	12.58	8.33
12.67	4.71	12.67	5.52	12.67	4.94	12.67	7.10	12.67	10.06	12.67	7.10	12.67	-0.01	12.67	8.33
12.75	4.71	12.75	5.52	12.75	4.95	12.75	7.11	12.75	10.06	12.75	7.11	12.75	0.00	12.75	8.34
12.83	4.71	12.83	5.52	12.83	4.95	12.83	7.12	12.83	10.06	12.83	7.12	12.83	-0.01	12.83	8.34
12.92	4.71	12.92	5.53	12.92	4.95	12.92	7.13	12.92	10.06	12.92	7.13	12.92	0.00	12.92	8.34
13.00	4.71	13.00	5.53	13.00	4.95	13.00	7.15	13.00	10.06	13.00	7.15	13.00	0.00	13.00	8.34

13.08	4.71	13.08	5.08	13.08	4.95	13.08	1.52	13.08	10.06	13.08	1.52	13.08	-0.16	13.08	8.28
13.17	4.68	13.17	4.63	13.17	5.03	13.17	-24.04	13.17	9.75	13.17	-24.04	13.17	-0.17	13.17	7.18
13.25	4.42	13.25	5.69	13.25	5.54	13.25	-25.49	13.25	8.34	13.25	-25.49	13.25	0.79	13.25	7.56
13.33	4.46	13.33	5.62	13.33	5.83	13.33	-26.84	13.33	9.72	13.33	-26.84	13.33	0.22	13.33	8.61
13.42	4.68	13.42	5.52	13.42	5.67	13.42	-18.82	13.42	10.45	13.42	-18.82	13.42	0.07	13.42	8.65
13.50	4.70	13.50	5.52	13.50	5.51	13.50	-9.87	13.50	10.53	13.50	-9.87	13.50	0.05	13.50	8.48
13.58	4.70	13.58	5.58	13.58	5.23	13.58	-2.35	13.58	10.37	13.58	-2.35	13.58	0.04	13.58	8.37
13.67	4.69	13.67	5.59	13.67	5.11	13.67	3.67	13.67	10.23	13.67	3.67	13.67	0.03	13.67	8.34
13.75	4.68	13.75	5.58	13.75	5.05	13.75	5.92	13.75	10.19	13.75	5.92	13.75	0.02	13.75	8.34
13.83	4.68	13.83	5.57	13.83	5.01	13.83	6.13	13.83	10.17	13.83	6.13	13.83	0.01	13.83	8.34
13.92	4.68	13.92	5.56	13.92	4.97	13.92	6.43	13.92	10.15	13.92	6.43	13.92	0.00	13.92	8.33
14.00	4.67	14.00	5.55	14.00	4.96	14.00	6.72	14.00	10.13	14.00	6.72	14.00	0.00	14.00	8.33
14.08	4.68	14.08	5.52	14.08	4.95	14.08	6.88	14.08	10.12	14.08	6.88	14.08	0.00	14.08	8.33
14.17	4.68	14.17	5.52	14.17	4.94	14.17	6.96	14.17	10.11	14.17	6.96	14.17	0.00	14.17	8.34
14.25	4.67	14.25	5.59	14.25	4.94	14.25	7.01	14.25	10.10	14.25	7.01	14.25	0.01	14.25	8.34
14.33	4.68	14.33	5.59	14.33	4.94	14.33	7.04	14.33	10.09	14.33	7.04	14.33	0.00	14.33	8.34
14.42	4.68	14.42	5.59	14.42	4.94	14.42	7.06	14.42	10.09	14.42	7.06	14.42	0.00	14.42	8.34
14.50	4.68	14.50	5.59	14.50	4.94	14.50	7.08	14.50	10.08	14.50	7.08	14.50	-0.01	14.50	8.34
14.58	4.68	14.58	5.60	14.58	4.95	14.58	7.10	14.58	10.08	14.58	7.10	14.58	0.00	14.58	8.34
14.67	4.68	14.67	5.59	14.67	4.95	14.67	7.12	14.67	10.08	14.67	7.12	14.67	0.00	14.67	8.34
14.75	4.68	14.75	5.57	14.75	4.95	14.75	7.13	14.75	10.08	14.75	7.13	14.75	0.00	14.75	8.34
14.83	4.68	14.83	5.59	14.83	4.95	14.83	7.14	14.83	10.08	14.83	7.14	14.83	0.00	14.83	8.34
14.92	4.68	14.92	5.61	14.92	4.95	14.92	7.15	14.92	10.08	14.92	7.15	14.92	0.00	14.92	8.34
15.00	4.68	15.00	5.60	15.00	4.95	15.00	7.15	15.00	10.08	15.00	7.15	15.00	0.00	15.00	8.35
15.08	4.68	15.08	5.79	15.08	4.95	15.08	2.73	15.08	10.08	15.08	2.73	15.08	-0.15	15.08	8.30
15.17	4.66	15.17	8.25	15.17	5.01	15.17	-21.85	15.17	9.77	15.17	-21.85	15.17	-0.25	15.17	7.32
15.25	4.42	15.25	7.37	15.25	5.44	15.25	-20.08	15.25	8.33	15.25	-20.08	15.25	0.78	15.25	7.63
15.33	4.43	15.33	5.31	15.33	5.79	15.33	-22.89	15.33	9.63	15.33	-22.89	15.33	0.23	15.33	8.62
15.42	4.65	15.42	5.04	15.42	5.67	15.42	-14.78	15.42	10.32	15.42	-14.78	15.42	0.08	15.42	8.64
15.50	4.67	15.50	5.44	15.50	5.56	15.50	-6.34	15.50	10.42	15.50	-6.34	15.50	0.06	15.50	8.48
15.58	4.66	15.58	5.54	15.58	5.28	15.58	0.69	15.58	10.30	15.58	0.69	15.58	0.04	15.58	8.38
15.67	4.66	15.67	5.51	15.67	5.14	15.67	5.30	15.67	10.19	15.67	5.30	15.67	0.02	15.67	8.35

15.75	4.65	15.75	5.51	15.75	5.08	15.75	6.20	15.75	10.16	15.75	6.20	15.75	0.02	15.75	8.35
15.83	4.65	15.83	5.51	15.83	5.03	15.83	6.42	15.83	10.15	15.83	6.42	15.83	0.01	15.83	8.35
15.92	4.65	15.92	5.51	15.92	4.99	15.92	6.72	15.92	10.13	15.92	6.72	15.92	0.00	15.92	8.34
16.00	4.65	16.00	5.52	16.00	4.98	16.00	6.89	16.00	10.12	16.00	6.89	16.00	0.00	16.00	8.34
16.08	4.65	16.08	5.53	16.08	4.96	16.08	6.97	16.08	10.11	16.08	6.97	16.08	-0.01	16.08	8.34
16.17	4.65	16.17	5.52	16.17	4.96	16.17	7.02	16.17	10.10	16.17	7.02	16.17	0.00	16.17	8.34
16.25	4.65	16.25	5.52	16.25	4.95	16.25	7.05	16.25	10.10	16.25	7.05	16.25	0.00	16.25	8.34
16.33	4.65	16.33	5.53	16.33	4.95	16.33	7.07	16.33	10.09	16.33	7.07	16.33	0.00	16.33	8.35
16.42	4.65	16.42	5.54	16.42	4.95	16.42	7.09	16.42	10.09	16.42	7.09	16.42	0.00	16.42	8.35
16.50	4.66	16.50	5.54	16.50	4.95	16.50	7.10	16.50	10.09	16.50	7.10	16.50	0.00	16.50	8.35
16.58	4.66	16.58	5.54	16.58	4.95	16.58	7.12	16.58	10.08	16.58	7.12	16.58	0.00	16.58	8.35
16.67	4.66	16.67	5.55	16.67	4.95	16.67	7.13	16.67	10.09	16.67	7.13	16.67	0.00	16.67	8.35
16.75	4.66	16.75	5.55	16.75	4.96	16.75	7.14	16.75	10.09	16.75	7.14	16.75	0.00	16.75	8.35
16.83	4.66	16.83	5.55	16.83	4.95	16.83	7.16	16.83	10.08	16.83	7.16	16.83	0.00	16.83	8.35
16.92	4.66	16.92	5.55	16.92	4.96	16.92	7.17	16.92	10.08	16.92	7.17	16.92	0.01	16.92	8.35
17.00	4.66	17.00	5.55	17.00	4.95	17.00	7.17	17.00	10.08	17.00	7.17	17.00	0.00	17.00	8.35
17.08	4.66	17.08	5.54	17.08	4.95	17.08	2.78	17.08	10.08	17.08	2.78	17.08	-0.13	17.08	8.30
17.17	4.64	17.17	5.89	17.17	5.00	17.17	-20.86	17.17	9.80	17.17	-20.86	17.17	-0.36	17.17	7.41
17.25	4.42	17.25	6.29	17.25	5.39	17.25	-18.90	17.25	8.37	17.25	-18.90	17.25	0.79	17.25	7.73
17.33	4.41	17.33	5.56	17.33	5.73	17.33	-20.00	17.33	9.58	17.33	-20.00	17.33	0.23	17.33	8.62
17.42	4.61	17.42	5.45	17.42	5.62	17.42	-10.05	17.42	10.22	17.42	-10.05	17.42	0.07	17.42	8.64
17.50	4.63	17.50	5.59	17.50	5.54	17.50	-1.75	17.50	10.35	17.50	-1.75	17.50	0.05	17.50	8.47
17.58	4.63	17.58	5.60	17.58	5.29	17.58	4.14	17.58	10.26	17.58	4.14	17.58	0.04	17.58	8.38
17.67	4.63	17.67	5.56	17.67	5.16	17.67	6.05	17.67	10.17	17.67	6.05	17.67	0.03	17.67	8.36
17.75	4.63	17.75	5.55	17.75	5.09	17.75	6.26	17.75	10.15	17.75	6.26	17.75	0.02	17.75	8.35
17.83	4.63	17.83	5.56	17.83	5.04	17.83	6.60	17.83	10.14	17.83	6.60	17.83	0.01	17.83	8.35
17.92	4.63	17.92	5.57	17.92	5.01	17.92	6.85	17.92	10.12	17.92	6.85	17.92	0.01	17.92	8.35
18.00	4.63	18.00	5.57	18.00	4.99	18.00	6.97	18.00	10.11	18.00	6.97	18.00	0.01	18.00	8.35
18.08	4.63	18.08	5.57	18.08	4.98	18.08	7.03	18.08	10.11	18.08	7.03	18.08	0.01	18.08	8.35
18.17	4.63	18.17	5.57	18.17	4.97	18.17	7.06	18.17	10.10	18.17	7.06	18.17	-0.01	18.17	8.35
18.25	4.63	18.25	5.58	18.25	4.96	18.25	7.08	18.25	10.10	18.25	7.08	18.25	-0.01	18.25	8.35
18.33	4.64	18.33	5.58	18.33	4.96	18.33	7.09	18.33	10.10	18.33	7.09	18.33	-0.01	18.33	8.35

18.42	4.64	18.42	5.58	18.42	4.96	18.42	7.10	18.42	10.09	18.42	7.10	18.42	0.00	18.42	8.35
18.50	4.64	18.50	5.58	18.50	4.96	18.50	7.11	18.50	10.09	18.50	7.11	18.50	0.00	18.50	8.36
18.58	4.64	18.58	5.59	18.58	4.96	18.58	7.13	18.58	10.09	18.58	7.13	18.58	0.00	18.58	8.35
18.67	4.64	18.67	5.60	18.67	4.96	18.67	7.14	18.67	10.09	18.67	7.14	18.67	0.01	18.67	8.35
18.75	4.64	18.75	5.59	18.75	4.96	18.75	7.15	18.75	10.09	18.75	7.15	18.75	0.00	18.75	8.36
18.83	4.64	18.83	5.59	18.83	4.96	18.83	7.16	18.83	10.08	18.83	7.16	18.83	0.00	18.83	8.35
18.92	4.65	18.92	5.59	18.92	4.96	18.92	7.17	18.92	10.08	18.92	7.17	18.92	0.00	18.92	8.35
19.00	4.65	19.00	5.60	19.00	4.96	19.00	7.18	19.00	10.08	19.00	7.18	19.00	0.00	19.00	8.36
19.08	4.65	19.08	5.58	19.08	4.95	19.08	2.89	19.08	10.08	19.08	2.89	19.08	-0.14	19.08	8.31
19.17	4.63	19.17	5.94	19.17	5.00	19.17	-17.79	19.17	9.80	19.17	-17.79	19.17	-0.40	19.17	7.46
19.25	4.45	19.25	6.44	19.25	5.37	19.25	-13.72	19.25	8.39	19.25	-13.72	19.25	0.76	19.25	7.77
19.33	4.41	19.33	5.68	19.33	5.66	19.33	-18.02	19.33	9.57	19.33	-18.02	19.33	0.25	19.33	8.62
19.42	4.59	19.42	5.50	19.42	5.52	19.42	-7.93	19.42	10.17	19.42	-7.93	19.42	0.08	19.42	8.63
19.50	4.61	19.50	5.63	19.50	5.47	19.50	0.48	19.50	10.29	19.50	0.48	19.50	0.05	19.50	8.48
19.58	4.62	19.58	5.66	19.58	5.28	19.58	5.28	19.58	10.22	19.58	5.28	19.58	0.04	19.58	8.39
19.67	4.62	19.67	5.63	19.67	5.15	19.67	6.12	19.67	10.15	19.67	6.12	19.67	0.03	19.67	8.37
19.75	4.62	19.75	5.61	19.75	5.08	19.75	6.32	19.75	10.13	19.75	6.32	19.75	0.02	19.75	8.37
19.83	4.61	19.83	5.62	19.83	5.04	19.83	6.67	19.83	10.13	19.83	6.67	19.83	0.01	19.83	8.36
19.92	4.62	19.92	5.62	19.92	5.01	19.92	6.89	19.92	10.12	19.92	6.89	19.92	0.01	19.92	8.36
20.00	4.62	20.00	5.63	20.00	4.99	20.00	6.98	20.00	10.11	20.00	6.98	20.00	0.00	20.00	8.35
20.08	4.62	20.08	5.62	20.08	4.98	20.08	7.04	20.08	10.10	20.08	7.04	20.08	0.00	20.08	8.35
20.17	4.62	20.17	5.62	20.17	4.97	20.17	7.07	20.17	10.10	20.17	7.07	20.17	0.00	20.17	8.36
20.25	4.62	20.25	5.63	20.25	4.96	20.25	7.08	20.25	10.10	20.25	7.08	20.25	0.01	20.25	8.35
20.33	4.63	20.33	5.63	20.33	4.96	20.33	7.09	20.33	10.09	20.33	7.09	20.33	0.00	20.33	8.36
20.42	4.63	20.42	5.62	20.42	4.96	20.42	7.11	20.42	10.09	20.42	7.11	20.42	0.00	20.42	8.36
20.50	4.63	20.50	5.63	20.50	4.96	20.50	7.12	20.50	10.09	20.50	7.12	20.50	0.00	20.50	8.36
20.58	4.63	20.58	5.64	20.58	4.96	20.58	7.13	20.58	10.09	20.58	7.13	20.58	0.00	20.58	8.36
20.67	4.64	20.67	5.64	20.67	4.96	20.67	7.15	20.67	10.09	20.67	7.15	20.67	0.00	20.67	8.36
20.75	4.64	20.75	5.63	20.75	4.96	20.75	7.16	20.75	10.09	20.75	7.16	20.75	0.00	20.75	8.36
20.83	4.64	20.83	5.63	20.83	4.96	20.83	7.17	20.83	10.09	20.83	7.17	20.83	0.00	20.83	8.36
20.92	4.64	20.92	5.63	20.92	4.95	20.92	7.18	20.92	10.09	20.92	7.18	20.92	0.00	20.92	8.36
21.00	4.64	21.00	5.64	21.00	4.96	21.00	7.18	21.00	10.09	21.00	7.18	21.00	0.00	21.00	8.36

21.08	4.64	21.08	5.62	21.08	4.95	21.08	3.89	21.08	10.09	21.08	3.89	21.08	-0.14	21.08	8.33
21.17	4.63	21.17	6.01	21.17	5.00	21.17	-19.62	21.17	9.84	21.17	-19.62	21.17	-0.44	21.17	7.55
21.25	4.45	21.25	6.56	21.25	5.35	21.25	-19.91	21.25	8.43	21.25	-19.91	21.25	0.74	21.25	7.74
21.33	4.41	21.33	5.75	21.33	5.58	21.33	-17.34	21.33	9.53	21.33	-17.34	21.33	0.25	21.33	8.61
21.42	4.57	21.42	5.54	21.42	5.44	21.42	-5.41	21.42	10.11	21.42	-5.41	21.42	0.07	21.42	8.63
21.50	4.60	21.50	5.68	21.50	5.41	21.50	2.71	21.50	10.25	21.50	2.71	21.50	0.04	21.50	8.49
21.58	4.60	21.58	5.72	21.58	5.24	21.58	5.91	21.58	10.20	21.58	5.91	21.58	0.03	21.58	8.40
21.67	4.61	21.67	5.68	21.67	5.13	21.67	6.15	21.67	10.14	21.67	6.15	21.67	0.03	21.67	8.37
21.75	4.61	21.75	5.66	21.75	5.07	21.75	6.42	21.75	10.13	21.75	6.42	21.75	0.02	21.75	8.37
21.83	4.61	21.83	5.66	21.83	5.03	21.83	6.74	21.83	10.12	21.83	6.74	21.83	0.01	21.83	8.36
21.92	4.61	21.92	5.66	21.92	4.99	21.92	6.92	21.92	10.12	21.92	6.92	21.92	0.00	21.92	8.36
22.00	4.61	22.00	5.66	22.00	4.98	22.00	7.01	22.00	10.10	22.00	7.01	22.00	0.00	22.00	8.36
22.08	4.62	22.08	5.66	22.08	4.97	22.08	7.05	22.08	10.10	22.08	7.05	22.08	0.00	22.08	8.36
22.17	4.62	22.17	5.67	22.17	4.97	22.17	7.08	22.17	10.10	22.17	7.08	22.17	0.00	22.17	8.36
22.25	4.62	22.25	5.67	22.25	4.96	22.25	7.10	22.25	10.10	22.25	7.10	22.25	0.00	22.25	8.36
22.33	4.63	22.33	5.67	22.33	4.96	22.33	7.11	22.33	10.10	22.33	7.11	22.33	0.00	22.33	8.36
22.42	4.63	22.42	5.66	22.42	4.95	22.42	7.12	22.42	10.10	22.42	7.12	22.42	0.00	22.42	8.36
22.50	4.63	22.50	5.66	22.50	4.95	22.50	7.14	22.50	10.10	22.50	7.14	22.50	-0.01	22.50	8.36
22.58	4.63	22.58	5.69	22.58	4.95	22.58	7.17	22.58	10.09	22.58	7.17	22.58	0.00	22.58	8.36
22.67	4.64	22.67	5.68	22.67	4.95	22.67	7.18	22.67	10.09	22.67	7.18	22.67	0.00	22.67	8.36
22.75	4.64	22.75	5.68	22.75	4.95	22.75	7.19	22.75	10.09	22.75	7.19	22.75	0.00	22.75	8.36
22.83	4.64	22.83	5.68	22.83	4.95	22.83	7.20	22.83	10.09	22.83	7.20	22.83	0.00	22.83	8.36
22.92	4.64	22.92	5.68	22.92	4.95	22.92	7.21	22.92	10.09	22.92	7.21	22.92	0.00	22.92	8.36
23.00	4.64	23.00	5.68	23.00	4.95	23.00	7.22	23.00	10.09	23.00	7.22	23.00	0.00	23.00	8.36
23.08	4.64	23.08	5.66	23.08	4.95	23.08	3.89	23.08	10.09	23.08	3.89	23.08	-0.12	23.08	8.34
23.17	4.63	23.17	6.03	23.17	4.99	23.17	-20.32	23.17	9.85	23.17	-20.32	23.17	-0.50	23.17	7.62
23.25	4.50	23.25	6.73	23.25	5.33	23.25	-21.87	23.25	8.49	23.25	-21.87	23.25	0.72	23.25	7.76
23.33	4.44	23.33	5.86	23.33	5.52	23.33	-15.56	23.33	9.54	23.33	-15.56	23.33	0.26	23.33	8.61
23.42	4.57	23.42	5.56	23.42	5.34	23.42	-2.75	23.42	10.09	23.42	-2.75	23.42	0.07	23.42	8.63
23.50	4.60	23.50	5.70	23.50	5.32	23.50	4.67	23.50	10.22	23.50	4.67	23.50	0.05	23.50	8.49
23.58	4.60	23.58	5.75	23.58	5.21	23.58	6.27	23.58	10.18	23.58	6.27	23.58	0.04	23.58	8.40
23.67	4.61	23.67	5.71	23.67	5.10	23.67	6.22	23.67	10.12	23.67	6.22	23.67	0.03	23.67	8.37

23.75	4.61	23.75	5.70	23.75	5.05	23.75	6.52	23.75	10.12	23.75	6.52	23.75	0.03	23.75	8.37
23.83	4.61	23.83	5.70	23.83	5.01	23.83	6.81	23.83	10.12	23.83	6.81	23.83	0.01	23.83	8.36
23.92	4.61	23.92	5.71	23.92	4.99	23.92	6.96	23.92	10.11	23.92	6.96	23.92	0.01	23.92	8.36
24.00	4.62	24.00	5.71	24.00	4.97	24.00	7.04	24.00	10.10	24.00	7.04	24.00	0.00	24.00	8.36
24.08	4.62	24.08	5.71	24.08	4.96	24.08	7.09	24.08	10.10	24.08	7.09	24.08	0.00	24.08	8.36
24.17	4.62	24.17	5.70	24.17	4.96	24.17	7.12	24.17	10.10	24.17	7.12	24.17	0.00	24.17	8.36
24.25	4.62	24.25	5.70	24.25	4.95	24.25	7.14	24.25	10.10	24.25	7.14	24.25	0.00	24.25	8.36
24.33	4.63	24.33	5.71	24.33	4.95	24.33	7.15	24.33	10.10	24.33	7.15	24.33	0.00	24.33	8.36
24.42	4.63	24.42	5.72	24.42	4.95	24.42	7.17	24.42	10.10	24.42	7.17	24.42	0.00	24.42	8.37
24.50	4.63	24.50	5.72	24.50	4.95	24.50	7.18	24.50	10.09	24.50	7.18	24.50	0.00	24.50	8.37
24.58	4.64	24.58	5.71	24.58	4.95	24.58	7.20	24.58	10.09	24.58	7.20	24.58	0.00	24.58	8.37
24.67	4.64	24.67	5.71	24.67	4.95	24.67	7.21	24.67	10.09	24.67	7.21	24.67	0.00	24.67	8.37
24.75	4.64	24.75	5.72	24.75	4.95	24.75	7.22	24.75	10.09	24.75	7.22	24.75	0.00	24.75	8.36
24.83	4.64	24.83	5.72	24.83	4.94	24.83	7.23	24.83	10.09	24.83	7.23	24.83	0.00	24.83	8.36
24.92	4.64	24.92	5.72	24.92	4.95	24.92	7.24	24.92	10.10	24.92	7.24	24.92	0.00	24.92	8.37
25.00	4.64	25.00	5.72	25.00	4.95	25.00	7.24	25.00	10.09	25.00	7.24	25.00	0.00	25.00	8.37
25.08	4.64	25.08	5.70	25.08	4.94	25.08	4.28	25.08	10.09	25.08	4.28	25.08	-0.12	25.08	8.34
25.17	4.64	25.17	6.10	25.17	4.96	25.17	-20.14	25.17	9.89	25.17	-20.14	25.17	-0.46	25.17	7.65
25.25	4.54	25.25	6.84	25.25	5.19	25.25	-22.91	25.25	8.56	25.25	-22.91	25.25	0.67	25.25	7.79
25.33	4.48	25.33	5.92	25.33	5.46	25.33	-14.37	25.33	9.51	25.33	-14.37	25.33	0.23	25.33	8.61
25.42	4.57	25.42	5.60	25.42	5.31	25.42	-0.97	25.42	10.06	25.42	-0.97	25.42	0.07	25.42	8.62
25.50	4.60	25.50	5.72	25.50	5.27	25.50	5.66	25.50	10.20	25.50	5.66	25.50	0.04	25.50	8.49
25.58	4.61	25.58	5.79	25.58	5.17	25.58	6.39	25.58	10.17	25.58	6.39	25.58	0.03	25.58	8.40
25.67	4.61	25.67	5.76	25.67	5.09	25.67	6.31	25.67	10.12	25.67	6.31	25.67	0.03	25.67	8.38
25.75	4.62	25.75	5.75	25.75	5.04	25.75	6.61	25.75	10.12	25.75	6.61	25.75	0.02	25.75	8.37
25.83	4.62	25.83	5.76	25.83	5.00	25.83	6.85	25.83	10.12	25.83	6.85	25.83	0.01	25.83	8.37
25.92	4.62	25.92	5.75	25.92	4.97	25.92	6.98	25.92	10.12	25.92	6.98	25.92	0.00	25.92	8.37
26.00	4.62	26.00	5.74	26.00	4.96	26.00	7.05	26.00	10.11	26.00	7.05	26.00	0.00	26.00	8.37
26.08	4.63	26.08	5.74	26.08	4.96	26.08	7.10	26.08	10.10	26.08	7.10	26.08	0.00	26.08	8.37
26.17	4.63	26.17	5.74	26.17	4.95	26.17	7.13	26.17	10.10	26.17	7.13	26.17	0.00	26.17	8.37
26.25	4.63	26.25	5.75	26.25	4.94	26.25	7.16	26.25	10.10	26.25	7.16	26.25	0.00	26.25	8.37
26.33	4.64	26.33	5.74	26.33	4.94	26.33	7.18	26.33	10.10	26.33	7.18	26.33	0.01	26.33	8.37

26.42	4.64	26.42	5.74	26.42	4.94	26.42	7.20	26.42	10.10	26.42	7.20	26.42	0.00	26.42	8.37
26.50	4.64	26.50	5.76	26.50	4.94	26.50	7.21	26.50	10.10	26.50	7.21	26.50	0.00	26.50	8.37
26.58	4.65	26.58	5.78	26.58	4.94	26.58	7.23	26.58	10.10	26.58	7.23	26.58	0.01	26.58	8.37
26.67	4.65	26.67	5.77	26.67	4.94	26.67	7.24	26.67	10.10	26.67	7.24	26.67	0.00	26.67	8.37
26.75	4.65	26.75	5.76	26.75	4.94	26.75	7.25	26.75	10.10	26.75	7.25	26.75	0.00	26.75	8.37
26.83	4.65	26.83	5.76	26.83	4.94	26.83	7.26	26.83	10.10	26.83	7.26	26.83	0.00	26.83	8.38
26.92	4.65	26.92	5.76	26.92	4.94	26.92	7.26	26.92	10.09	26.92	7.26	26.92	0.00	26.92	8.38
27.00	4.65	27.00	5.77	27.00	4.94	27.00	7.26	27.00	10.10	27.00	7.26	27.00	0.00	27.00	8.38
27.08	4.65	27.08	5.73	27.08	4.93	27.08	4.62	27.08	10.09	27.08	4.62	27.08	-0.12	27.08	8.36
27.17	4.64	27.17	6.05	27.17	4.95	27.17	-20.01	27.17	9.89	27.17	-20.01	27.17	-0.48	27.17	7.66
27.25	4.56	27.25	6.91	27.25	5.16	27.25	-23.40	27.25	8.61	27.25	-23.40	27.25	0.66	27.25	7.82
27.33	4.56	27.33	6.00	27.33	5.42	27.33	-13.49	27.33	9.53	27.33	-13.49	27.33	0.25	27.33	8.61
27.42	4.60	27.42	5.63	27.42	5.27	27.42	0.09	27.42	10.04	27.42	0.09	27.42	0.08	27.42	8.62
27.50	4.60	27.50	5.75	27.50	5.21	27.50	6.28	27.50	10.19	27.50	6.28	27.50	0.04	27.50	8.49
27.58	4.60	27.58	5.84	27.58	5.13	27.58	6.54	27.58	10.16	27.58	6.54	27.58	0.03	27.58	8.40
27.67	4.60	27.67	5.80	27.67	5.06	27.67	6.41	27.67	10.11	27.67	6.41	27.67	0.03	27.67	8.38
27.75	4.60	27.75	5.79	27.75	5.02	27.75	6.68	27.75	10.12	27.75	6.68	27.75	0.02	27.75	8.38
27.83	4.61	27.83	5.79	27.83	4.99	27.83	6.87	27.83	10.12	27.83	6.87	27.83	0.01	27.83	8.37
27.92	4.61	27.92	5.79	27.92	4.96	27.92	6.99	27.92	10.11	27.92	6.99	27.92	0.01	27.92	8.37
28.00	4.61	28.00	5.79	28.00	4.95	28.00	7.06	28.00	10.10	28.00	7.06	28.00	0.00	28.00	8.37
28.08	4.62	28.08	5.79	28.08	4.95	28.08	7.11	28.08	10.10	28.08	7.11	28.08	0.00	28.08	8.38
28.17	4.62	28.17	5.79	28.17	4.94	28.17	7.15	28.17	10.10	28.17	7.15	28.17	0.00	28.17	8.37
28.25	4.62	28.25	5.80	28.25	4.94	28.25	7.18	28.25	10.10	28.25	7.18	28.25	0.01	28.25	8.37
28.33	4.63	28.33	5.79	28.33	4.93	28.33	7.20	28.33	10.10	28.33	7.20	28.33	0.00	28.33	8.37
28.42	4.63	28.42	5.80	28.42	4.93	28.42	7.22	28.42	10.10	28.42	7.22	28.42	0.00	28.42	8.38
28.50	4.64	28.50	5.80	28.50	4.94	28.50	7.24	28.50	10.10	28.50	7.24	28.50	0.00	28.50	8.38
28.58	4.64	28.58	5.80	28.58	4.94	28.58	7.25	28.58	10.10	28.58	7.25	28.58	0.00	28.58	8.38
28.67	4.64	28.67	5.81	28.67	4.94	28.67	7.26	28.67	10.10	28.67	7.26	28.67	0.00	28.67	8.38
28.75	4.65	28.75	5.80	28.75	4.94	28.75	7.27	28.75	10.10	28.75	7.27	28.75	0.00	28.75	8.38
28.83	4.65	28.83	5.80	28.83	4.94	28.83	7.27	28.83	10.10	28.83	7.27	28.83	0.00	28.83	8.38
28.92	4.65	28.92	5.80	28.92	4.94	28.92	7.28	28.92	10.10	28.92	7.28	28.92	0.00	28.92	8.38
29.00	4.65	29.00	5.80	29.00	4.94	29.00	7.29	29.00	10.10	29.00	7.29	29.00	0.00	29.00	8.38

29.08	4.66	29.08	5.79			29.08	5.25	29.08	10.10	29.08	5.25	29.08	-0.12	29.08	8.36
29.17	4.65	29.17	6.07			29.17	-20.07	29.17	9.94	29.17	-20.07	29.17	-0.45	29.17	7.74
29.25	4.61	29.25	7.06			29.25	-26.13	29.25	8.71	29.25	-26.13	29.25	0.62	29.25	7.79
29.33	4.60	29.33	6.11			29.33	-12.80	29.33	9.48	29.33	-12.80	29.33	0.21	29.33	8.60
29.42	4.61	29.42	5.65			29.42	1.20	29.42	10.01	29.42	1.20	29.42	0.08	29.42	8.62
29.50	4.61	29.50	5.78			29.50	6.85	29.50	10.18	29.50	6.85	29.50	0.04	29.50	8.49
29.58	4.62	29.58	5.87			29.58	6.66	29.58	10.16	29.58	6.66	29.58	0.03	29.58	8.41
29.67	4.62	29.67	5.85			29.67	6.48	29.67	10.11	29.67	6.48	29.67	0.03	29.67	8.39
29.75	4.62	29.75	5.83			29.75	6.74	29.75	10.11	29.75	6.74	29.75	0.02	29.75	8.38
29.83	4.62	29.83	5.84			29.83	6.92	29.83	10.12	29.83	6.92	29.83	0.02	29.83	8.38
29.92	4.62	29.92	5.83			29.92	7.01	29.92	10.12	29.92	7.01	29.92	0.00	29.92	8.38
30.00	4.62	30.00	5.83			30.00	7.09	30.00	10.10	30.00	7.09	30.00	0.01	30.00	8.37
30.08	4.63	30.08	5.83			30.08	7.14	30.08	10.10	30.08	7.14	30.08	0.00	30.08	8.37
30.17	4.63	30.17	5.83			30.17	7.18	30.17	10.10	30.17	7.18	30.17	0.01	30.17	8.37
30.25	4.64	30.25	5.83			30.25	7.20	30.25	10.10	30.25	7.20	30.25	0.01	30.25	8.37
30.33	4.64	30.33	5.83			30.33	7.22	30.33	10.10	30.33	7.22	30.33	0.00	30.33	8.37
30.42	4.64	30.42	5.83			30.42	7.24	30.42	10.10	30.42	7.24	30.42	0.00	30.42	8.37
30.50	4.65	30.50	5.83			30.50	7.26	30.50	10.10	30.50	7.26	30.50	0.00	30.50	8.38
30.58	4.65	30.58	5.83			30.58	7.27	30.58	10.10	30.58	7.27	30.58	0.00	30.58	8.38
30.67	4.66	30.67	5.84			30.67	7.28	30.67	10.10	30.67	7.28	30.67	0.00	30.67	8.38
30.75	4.66	30.75	5.84			30.75	7.29	30.75	10.10	30.75	7.29	30.75	0.00	30.75	8.38
30.83	4.67	30.83	5.85			30.83	7.29	30.83	10.10	30.83	7.29	30.83	0.00	30.83	8.38
30.92	4.67	30.92	5.84			30.92	7.29	30.92	10.10	30.92	7.29	30.92	0.00	30.92	8.38
31.00	4.67	31.00	5.84			31.00	7.29	31.00	10.10	31.00	7.29	31.00	0.00	31.00	8.37
31.08	4.68	31.08	5.82			31.08	5.33	31.08	10.10	31.08	5.33	31.08	-0.10	31.08	8.36
31.17	4.67	31.17	6.04			31.17	-19.63	31.17	9.94	31.17	-19.63	31.17	-0.42	31.17	7.76
31.25	4.66	31.25	7.01			31.25	-24.43	31.25	8.76	31.25	-24.43	31.25	0.56	31.25	7.80
31.33	4.68	31.33	6.12			31.33	-11.31	31.33	9.52	31.33	-11.31	31.33	0.21	31.33	8.59
31.42	4.68	31.42	5.70			31.42	2.35	31.42	10.01	31.42	2.35	31.42	0.06	31.42	8.61
31.50	4.66	31.50	5.83			31.50	7.32	31.50	10.17	31.50	7.32	31.50	0.04	31.50	8.48
31.58	4.66	31.58	5.92			31.58	6.76	31.58	10.15	31.58	6.76	31.58	0.03	31.58	8.40
31.67	4.66	31.67	5.88			31.67	6.58	31.67	10.11	31.67	6.58	31.67	0.02	31.67	8.38

31.75	4.65	31.75	5.86			31.75	6.79	31.75	10.11	31.75	6.79	31.75	0.02	31.75	8.38
31.83	4.66	31.83	5.86			31.83	6.93	31.83	10.12	31.83	6.93	31.83	0.01	31.83	8.37
31.92	4.66	31.92	5.86			31.92	7.02	31.92	10.12	31.92	7.02	31.92	0.00	31.92	8.37
32.00	4.66	32.00	5.86			32.00	7.08	32.00	10.11	32.00	7.08	32.00	0.00	32.00	8.37
32.08	4.66	32.08	5.85			32.08	7.13	32.08	10.10	32.08	7.13	32.08	0.00	32.08	8.37
32.17	4.67	32.17	5.85			32.17	7.17	32.17	10.10	32.17	7.17	32.17	0.00	32.17	8.37
32.25	4.67	32.25	5.86			32.25	7.20	32.25	10.10	32.25	7.20	32.25	0.00	32.25	8.37
32.33	4.68	32.33	5.86			32.33	7.23	32.33	10.11	32.33	7.23	32.33	0.00	32.33	8.37
32.42	4.68	32.42	5.86			32.42	7.24	32.42	10.10	32.42	7.24	32.42	0.00	32.42	8.37
32.50	4.69	32.50	5.86			32.50	7.26	32.50	10.10	32.50	7.26	32.50	0.00	32.50	8.38
32.58	4.69	32.58	5.86			32.58	7.27	32.58	10.10	32.58	7.27	32.58	0.00	32.58	8.38
32.67	4.70	32.67	5.87			32.67	7.28	32.67	10.10	32.67	7.28	32.67	0.00	32.67	8.37
32.75	4.70	32.75	5.87			32.75	7.29	32.75	10.10	32.75	7.29	32.75	0.00	32.75	8.38
32.83	4.70	32.83	5.87			32.83	7.29	32.83	10.10	32.83	7.29	32.83	0.00	32.83	8.38
32.92	4.70	32.92	5.87			32.92	7.30	32.92	10.10	32.92	7.30	32.92	0.00	32.92	8.38
33.00	4.71	33.00	5.87			33.00	7.30	33.00	10.10	33.00	7.30	33.00	0.00	33.00	8.38
33.08	4.71	33.08	5.85			33.08	5.58	33.08	10.10	33.08	5.58	33.08	-0.10	33.08	8.37
33.17	4.70	33.17	6.07			33.17	-19.27	33.17	9.97	33.17	-19.27	33.17	-0.40	33.17	7.80
33.25	4.72	33.25	7.07			33.25	-24.65	33.25	8.82	33.25	-24.65	33.25	0.52	33.25	7.80
33.33	4.77	33.33	6.16			33.33	-10.39	33.33	9.52	33.33	-10.39	33.33	0.19	33.33	8.58
33.42	4.75	33.42	5.72			33.42	3.19	33.42	9.99	33.42	3.19	33.42	0.06	33.42	8.60
33.50	4.73	33.50	5.85			33.50	7.62	33.50	10.16	33.50	7.62	33.50	0.04	33.50	8.48
33.58	4.72	33.58	5.94			33.58	6.82	33.58	10.16	33.58	6.82	33.58	0.03	33.58	8.41
33.67	4.71	33.67	5.91			33.67	6.62	33.67	10.11	33.67	6.62	33.67	0.02	33.67	8.39
33.75	4.71	33.75	5.89			33.75	6.84	33.75	10.12	33.75	6.84	33.75	0.01	33.75	8.38
33.83	4.71	33.83	5.89			33.83	6.97	33.83	10.12	33.83	6.97	33.83	0.01	33.83	8.38
33.92	4.71	33.92	5.89			33.92	7.05	33.92	10.12	33.92	7.05	33.92	0.00	33.92	8.38
34.00	4.71	34.00	5.89			34.00	7.11	34.00	10.11	34.00	7.11	34.00	0.00	34.00	8.38
34.08	4.72	34.08	5.88			34.08	7.15	34.08	10.10	34.08	7.15	34.08	0.01	34.08	8.38
34.17	4.72	34.17	5.88			34.17	7.19	34.17	10.10	34.17	7.19	34.17	0.00	34.17	8.38
34.25	4.72	34.25	5.89			34.25	7.21	34.25	10.10	34.25	7.21	34.25	0.01	34.25	8.37
34.33	4.73	34.33	5.89			34.33	7.24	34.33	10.11	34.33	7.24	34.33	0.00	34.33	8.37

34.42	4.73	34.42	5.88			34.42	7.25	34.42	10.11	34.42	7.25	34.42	0.00	34.42	8.38
34.50	4.73	34.50	5.89			34.50	7.27	34.50	10.10	34.50	7.27	34.50	0.00	34.50	8.37
34.58	4.74	34.58	5.90			34.58	7.28	34.58	10.11	34.58	7.28	34.58	0.00	34.58	8.37
34.67	4.74	34.67	5.90			34.67	7.29	34.67	10.10	34.67	7.29	34.67	0.00	34.67	8.38
34.75	4.74	34.75	5.89			34.75	7.29	34.75	10.10	34.75	7.29	34.75	0.00	34.75	8.38
34.83	4.74	34.83	5.90			34.83	7.30	34.83	10.10	34.83	7.30	34.83	0.00	34.83	8.38
34.92	4.74	34.92	5.91			34.92	7.30	34.92	10.10	34.92	7.30	34.92	0.00	34.92	8.38
35.00	4.75	35.00	5.90			35.00	7.30	35.00	10.10	35.00	7.30	35.00	0.00	35.00	8.38
35.08	4.75	35.08	5.88			35.08	5.85	35.08	10.10	35.08	5.85	35.08	-0.09	35.08	8.37
35.17	4.75	35.17	6.06			35.17	-18.49	35.17	9.98	35.17	-18.49	35.17	-0.56	35.17	7.81
35.25	4.77	35.25	7.06			35.25	-24.22	35.25	8.85	35.25	-24.22	35.25	0.58	35.25	7.82
35.33	4.85	35.33	6.19			35.33	-10.06	35.33	9.54	35.33	-10.06	35.33	0.25	35.33	8.58
35.42	4.82	35.42	5.75			35.42	3.45	35.42	9.97	35.42	3.45	35.42	0.06	35.42	8.60
35.50	4.79	35.50	5.88			35.50	7.85	35.50	10.15	35.50	7.85	35.50	0.04	35.50	8.48
35.58	4.78	35.58	5.96			35.58	6.94	35.58	10.16	35.58	6.94	35.58	0.03	35.58	8.41
35.67	4.77	35.67	5.95			35.67	6.70	35.67	10.10	35.67	6.70	35.67	0.03	35.67	8.39
35.75	4.77	35.75	5.93			35.75	6.89	35.75	10.12	35.75	6.89	35.75	0.02	35.75	8.38
35.83	4.77	35.83	5.93			35.83	7.00	35.83	10.13	35.83	7.00	35.83	0.01	35.83	8.38
35.92	4.77	35.92	5.93			35.92	7.07	35.92	10.12	35.92	7.07	35.92	0.01	35.92	8.38
36.00	4.77	36.00	5.92			36.00	7.12	36.00	10.11	36.00	7.12	36.00	0.00	36.00	8.37
36.08	4.77	36.08	5.92			36.08	7.16	36.08	10.10	36.08	7.16	36.08	0.00	36.08	8.37
36.17	4.77	36.17	5.92			36.17	7.19	36.17	10.10	36.17	7.19	36.17	0.01	36.17	8.37
36.25	4.77	36.25	5.92			36.25	7.22	36.25	10.10	36.25	7.22	36.25	0.00	36.25	8.38
36.33	4.77	36.33	5.92			36.33	7.24	36.33	10.10	36.33	7.24	36.33	0.00	36.33	8.38
36.42	4.77	36.42	5.92			36.42	7.25	36.42	10.11	36.42	7.25	36.42	0.00	36.42	8.38
36.50	4.77	36.50	5.92			36.50	7.27	36.50	10.11	36.50	7.27	36.50	0.00	36.50	8.38
36.58	4.78	36.58	5.92			36.58	7.28	36.58	10.11	36.58	7.28	36.58	0.01	36.58	8.38
36.67	4.78	36.67	5.92			36.67	7.29	36.67	10.10	36.67	7.29	36.67	0.01	36.67	8.38
36.75	4.78	36.75	5.92			36.75	7.30	36.75	10.10	36.75	7.30	36.75	0.01	36.75	8.38
36.83	4.78	36.83	5.92			36.83	7.30	36.83	10.10	36.83	7.30	36.83	-0.01	36.83	8.38
36.92	4.79	36.92	5.92			36.92	7.31	36.92	10.10	36.92	7.31	36.92	-0.01	36.92	8.38
37.00	4.79	37.00	5.93			37.00	7.31	37.00	10.10	37.00	7.31	37.00	-0.01	37.00	8.38

37.08	4.79	37.08	5.92			37.08	6.65	37.08	10.11	37.08	6.65	37.08	-0.08	37.08	8.37
37.17	4.78	37.17	6.09			37.17	-15.43	37.17	10.01	37.17	-15.43	37.17	-0.52	37.17	7.88
37.25	4.82	37.25	7.11			37.25	-24.69	37.25	8.93	37.25	-24.69	37.25	0.51	37.25	7.79
37.33	4.91	37.33	6.22			37.33	-10.43	37.33	9.51	37.33	-10.43	37.33	0.24	37.33	8.57
37.42	4.88	37.42	5.78			37.42	3.27	37.42	9.95	37.42	3.27	37.42	0.08	37.42	8.60
37.50	4.85	37.50	5.88			37.50	8.15	37.50	10.13	37.50	8.15	37.50	0.07	37.50	8.48
37.58	4.83	37.58	5.97			37.58	7.15	37.58	10.15	37.58	7.15	37.58	0.05	37.58	8.40
37.67	4.82	37.67	5.96			37.67	6.77	37.67	10.11	37.67	6.77	37.67	0.03	37.67	8.39
37.75	4.81	37.75	5.95			37.75	6.92	37.75	10.12	37.75	6.92	37.75	0.02	37.75	8.38
37.83	4.81	37.83	5.93			37.83	7.02	37.83	10.12	37.83	7.02	37.83	0.00	37.83	8.38
37.92	4.81	37.92	5.95			37.92	7.08	37.92	10.12	37.92	7.08	37.92	-0.01	37.92	8.38
38.00	4.81	38.00	5.95			38.00	7.13	38.00	10.10	38.00	7.13	38.00	0.00	38.00	8.37
38.08	4.81	38.08	5.93			38.08	7.17	38.08	10.10	38.08	7.17	38.08	0.00	38.08	8.37
38.17	4.81	38.17	5.92			38.17	7.20	38.17	10.11	38.17	7.20	38.17	0.00	38.17	8.38
38.25	4.81	38.25	5.93			38.25	7.23	38.25	10.11	38.25	7.23	38.25	0.00	38.25	8.38
38.33	4.81	38.33	5.95			38.33	7.25	38.33	10.11	38.33	7.25	38.33	0.00	38.33	8.38
38.42	4.81	38.42	5.94			38.42	7.26	38.42	10.11	38.42	7.26	38.42	-0.01	38.42	8.38
38.50	4.81	38.50	5.93			38.50	7.27	38.50	10.11	38.50	7.27	38.50	-0.01	38.50	8.38
38.58	4.81	38.58	5.95			38.58	7.28	38.58	10.10	38.58	7.28	38.58	0.00	38.58	8.38
38.67	4.81	38.67	5.96			38.67	7.29	38.67	10.10	38.67	7.29	38.67	0.00	38.67	8.37
38.75	4.82	38.75	5.96			38.75	7.30	38.75	10.10	38.75	7.30	38.75	0.00	38.75	8.38
38.83	4.82	38.83	5.96			38.83	7.30	38.83	10.10	38.83	7.30	38.83	0.00	38.83	8.38
38.92	4.82	38.92	5.96			38.92	7.30	38.92	10.10	38.92	7.30	38.92	0.01	38.92	8.38
39.00	4.82	39.00	5.94			39.00	7.30	39.00	10.10	39.00	7.30	39.00	0.01	39.00	8.38
39.08	4.82	39.08	5.93			39.08	6.15	39.08	10.10	39.08	6.15	39.08	-0.06	39.08	8.37
39.08	4.82	39.17	6.13			39.17	-17.38	39.17	10.00	39.17	-17.38	39.17	-0.49	39.17	7.90
39.08	4.82	39.25	7.23			39.25	-23.32	39.25	8.97	39.25	-23.32	39.25	0.50	39.25	7.83
39.08	4.82	39.33	6.26			39.33	-8.40	39.33	9.55	39.33	-8.40	39.33	0.21	39.33	8.55
39.08	4.82	39.42	5.75			39.42	4.61	39.42	9.94	39.42	4.61	39.42	0.05	39.42	8.58
39.08	4.82	39.50	5.89			39.50	8.30	39.50	10.11	39.50	8.30	39.50	0.03	39.50	8.46
39.08	4.82	39.58	6.02			39.58	7.09	39.58	10.14	39.58	7.09	39.58	0.02	39.58	8.40
39.08	4.82	39.67	6.01			39.67	6.80	39.67	10.11	39.67	6.80	39.67	0.02	39.67	8.38

39.08	4.82	39.75	5.95			39.75	6.95	39.75	10.12	39.75	6.95	39.75	0.01	39.75	8.38
39.08	4.82	39.83	5.94			39.83	7.04	39.83	10.13	39.83	7.04	39.83	0.01	39.83	8.38
39.08	4.82	39.92	5.96			39.92	7.07	39.92	10.11	39.92	7.07	39.92	0.01	39.92	8.38
39.08	4.82	40.00	5.99			40.00	7.10	40.00	10.10	40.00	7.10	40.00	0.01	40.00	8.37
39.08	4.82	40.08	5.95			40.08	7.14	40.08	10.10	40.08	7.14	40.08	0.00	40.08	8.37
39.08	4.82	40.17	5.93			40.17	7.19	40.17	10.10	40.17	7.19	40.17	0.00	40.17	8.38
39.08	4.82	40.25	5.95			40.25	7.22	40.25	10.10	40.25	7.22	40.25	0.00	40.25	8.38
39.08	4.82	40.33	5.96			40.33	7.24	40.33	10.11	40.33	7.24	40.33	-0.01	40.33	8.38
39.08	4.82	40.42	5.99			40.42	7.26	40.42	10.10	40.42	7.26	40.42	0.00	40.42	8.38
39.08	4.82	40.50	5.96			40.50	7.28	40.50	10.10	40.50	7.28	40.50	0.00	40.50	8.38
39.08	4.82	40.58	5.95			40.58	7.28	40.58	10.10	40.58	7.28	40.58	0.00	40.58	8.38
39.08	4.82	40.67	5.96			40.67	7.29	40.67	10.10	40.67	7.29	40.67	0.00	40.67	8.38
39.08	4.82	40.75	5.96			40.75	7.29	40.75	10.10	40.75	7.29	40.75	0.00	40.75	8.38
39.08	4.82	40.83	5.96			40.83	7.30	40.83	10.10	40.83	7.30	40.83	0.00	40.83	8.38
39.08	4.82	40.92	5.96			40.92	7.29	40.92	10.10	40.92	7.29	40.92	0.00	40.92	8.37
39.08	4.82	41.00	5.96			41.00	7.30	41.00	10.10	41.00	7.30	41.00	0.00	41.00	8.37
								41.08	10.10						

5.4. Absorbance of BM in presence and absence of different concentration of individual surfactant at 298.15 K [[concentration of BM = 10 μ M]

wavelength/nm	Absorption intensity vs. wavelength (nm) for different concentration of each surfactant. BM concentration is fixed in 10 μ M				
	free BM (0 mM)	NaC (16.27 mM)	NaDC (4.08 mM)	SDDS (6.70 mM)	SDBS (0.39 mM)
500	0.005	0.043	0.024	0.093	0.078
499	0.005	0.043	0.024	0.093	0.078
498	0.005	0.043	0.024	0.093	0.078
497	0.005	0.043	0.024	0.093	0.079
496	0.005	0.043	0.024	0.093	0.079
495	0.005	0.044	0.025	0.093	0.080
494	0.005	0.044	0.025	0.094	0.080
493	0.006	0.044	0.025	0.094	0.080
492	0.006	0.044	0.025	0.094	0.080
491	0.006	0.044	0.025	0.094	0.081
490	0.006	0.044	0.025	0.094	0.081
489	0.006	0.044	0.025	0.094	0.081
488	0.006	0.044	0.025	0.095	0.082
487	0.006	0.044	0.026	0.095	0.082
486	0.006	0.045	0.026	0.095	0.082
485	0.006	0.045	0.026	0.095	0.083
484	0.006	0.045	0.026	0.095	0.083
483	0.006	0.045	0.026	0.096	0.084
482	0.006	0.045	0.026	0.096	0.084
481	0.006	0.045	0.026	0.096	0.084
480	0.006	0.046	0.027	0.096	0.085
479	0.006	0.046	0.027	0.097	0.085
478	0.006	0.046	0.027	0.097	0.085
477	0.006	0.046	0.027	0.097	0.086
476	0.006	0.046	0.027	0.097	0.086
475	0.006	0.046	0.027	0.097	0.086
474	0.006	0.047	0.027	0.097	0.087
473	0.006	0.047	0.028	0.098	0.087
472	0.006	0.047	0.028	0.098	0.088
471	0.006	0.047	0.028	0.098	0.088
470	0.006	0.047	0.028	0.098	0.088
469	0.006	0.047	0.028	0.098	0.089
468	0.006	0.047	0.028	0.099	0.089
467	0.006	0.048	0.029	0.099	0.090
466	0.006	0.048	0.029	0.099	0.090
465	0.006	0.048	0.029	0.099	0.090
464	0.006	0.048	0.029	0.099	0.091
463	0.006	0.048	0.029	0.100	0.091
462	0.006	0.048	0.029	0.100	0.091
461	0.006	0.049	0.029	0.100	0.092
460	0.006	0.049	0.030	0.100	0.092
459	0.006	0.049	0.030	0.101	0.093

458	0.006	0.049	0.030	0.101	0.093
457	0.006	0.049	0.030	0.101	0.094
456	0.006	0.050	0.030	0.101	0.094
455	0.006	0.050	0.031	0.101	0.094
454	0.007	0.050	0.031	0.102	0.095
453	0.007	0.050	0.031	0.102	0.095
452	0.007	0.050	0.031	0.102	0.096
451	0.007	0.051	0.031	0.102	0.096
450	0.007	0.051	0.031	0.102	0.096
449	0.007	0.051	0.032	0.103	0.097
448	0.007	0.051	0.032	0.103	0.097
447	0.007	0.052	0.032	0.103	0.098
446	0.007	0.052	0.032	0.104	0.098
445	0.007	0.052	0.032	0.104	0.099
444	0.007	0.052	0.033	0.104	0.099
443	0.007	0.052	0.033	0.105	0.100
442	0.007	0.053	0.033	0.105	0.100
441	0.007	0.053	0.033	0.105	0.101
440	0.007	0.053	0.034	0.106	0.101
439	0.007	0.053	0.034	0.106	0.102
438	0.007	0.054	0.034	0.106	0.102
437	0.007	0.054	0.034	0.106	0.102
436	0.007	0.054	0.035	0.107	0.103
435	0.007	0.055	0.035	0.107	0.103
434	0.007	0.055	0.035	0.108	0.104
433	0.007	0.055	0.035	0.108	0.105
432	0.007	0.056	0.035	0.108	0.105
431	0.008	0.056	0.036	0.109	0.106
430	0.008	0.056	0.036	0.109	0.106
429	0.008	0.057	0.036	0.109	0.107
428	0.008	0.057	0.037	0.110	0.107
427	0.008	0.057	0.037	0.110	0.108
426	0.008	0.058	0.037	0.110	0.108
425	0.008	0.058	0.038	0.111	0.109
424	0.008	0.058	0.038	0.111	0.109
423	0.008	0.059	0.038	0.112	0.110
422	0.008	0.059	0.038	0.112	0.111
421	0.008	0.059	0.039	0.112	0.111
420	0.008	0.060	0.039	0.113	0.112
419	0.008	0.060	0.039	0.113	0.113
418	0.008	0.061	0.040	0.114	0.113
417	0.009	0.061	0.040	0.114	0.114
416	0.009	0.061	0.040	0.114	0.115
415	0.009	0.062	0.041	0.115	0.115
414	0.009	0.062	0.041	0.115	0.116
413	0.009	0.062	0.041	0.116	0.117
412	0.009	0.063	0.042	0.116	0.117
411	0.009	0.063	0.042	0.117	0.118
410	0.009	0.064	0.042	0.117	0.119

409	0.009	0.064	0.043	0.118	0.119
408	0.009	0.065	0.043	0.118	0.120
407	0.009	0.065	0.043	0.119	0.121
406	0.010	0.066	0.044	0.119	0.122
405	0.010	0.066	0.044	0.120	0.122
404	0.010	0.067	0.045	0.120	0.123
403	0.010	0.067	0.045	0.121	0.124
402	0.010	0.068	0.045	0.121	0.125
401	0.010	0.068	0.046	0.122	0.126
400	0.010	0.069	0.046	0.122	0.126
399	0.010	0.069	0.046	0.123	0.127
398	0.011	0.070	0.047	0.123	0.128
397	0.011	0.070	0.047	0.124	0.129
396	0.011	0.070	0.048	0.124	0.130
395	0.011	0.071	0.048	0.125	0.131
394	0.011	0.072	0.049	0.125	0.131
393	0.011	0.072	0.049	0.126	0.132
392	0.011	0.073	0.049	0.126	0.133
391	0.011	0.073	0.050	0.127	0.134
390	0.012	0.074	0.050	0.128	0.135
389	0.012	0.074	0.051	0.128	0.136
388	0.012	0.075	0.051	0.129	0.137
387	0.012	0.075	0.052	0.129	0.138
386	0.012	0.076	0.052	0.130	0.139
385	0.012	0.077	0.053	0.130	0.140
384	0.013	0.077	0.053	0.131	0.141
383	0.013	0.078	0.054	0.132	0.142
382	0.013	0.078	0.054	0.132	0.143
381	0.013	0.079	0.054	0.133	0.144
380	0.013	0.079	0.055	0.133	0.145
379	0.012	0.077	0.052	0.133	0.143
378	0.011	0.075	0.049	0.131	0.141
377	0.010	0.074	0.048	0.131	0.140
376	0.011	0.075	0.048	0.132	0.142
375	0.011	0.076	0.049	0.133	0.143
374	0.011	0.077	0.049	0.134	0.144
373	0.011	0.077	0.050	0.135	0.145
372	0.012	0.078	0.051	0.136	0.147
371	0.012	0.079	0.052	0.137	0.148
370	0.012	0.080	0.053	0.137	0.149
369	0.013	0.081	0.053	0.138	0.151
368	0.013	0.082	0.054	0.140	0.152
367	0.014	0.083	0.055	0.141	0.154
366	0.014	0.084	0.056	0.142	0.155
365	0.015	0.086	0.057	0.143	0.157
364	0.016	0.087	0.058	0.144	0.159
363	0.016	0.088	0.059	0.146	0.161
362	0.017	0.090	0.060	0.147	0.162
361	0.018	0.091	0.062	0.149	0.164

360	0.019	0.093	0.063	0.150	0.167
359	0.020	0.094	0.064	0.152	0.169
358	0.021	0.096	0.066	0.154	0.171
357	0.021	0.098	0.068	0.156	0.173
356	0.023	0.099	0.069	0.158	0.176
355	0.024	0.102	0.071	0.160	0.179
354	0.025	0.104	0.073	0.162	0.181
353	0.026	0.106	0.075	0.164	0.184
352	0.027	0.108	0.076	0.166	0.186
351	0.029	0.110	0.078	0.168	0.189
350	0.030	0.112	0.080	0.170	0.192
349	0.032	0.115	0.083	0.173	0.195
348	0.033	0.117	0.085	0.175	0.198
347	0.035	0.120	0.087	0.178	0.202
346	0.036	0.122	0.089	0.180	0.205
345	0.038	0.125	0.091	0.183	0.208
344	0.040	0.127	0.093	0.185	0.212
343	0.041	0.130	0.096	0.188	0.215
342	0.043	0.133	0.098	0.191	0.219
341	0.045	0.135	0.100	0.194	0.223
340	0.047	0.139	0.104	0.197	0.228
339	0.050	0.144	0.109	0.201	0.235
338	0.052	0.150	0.116	0.206	0.243
337	0.054	0.154	0.119	0.210	0.249
336	0.056	0.157	0.122	0.213	0.253
335	0.057	0.160	0.124	0.215	0.257
334	0.059	0.162	0.126	0.218	0.260
333	0.060	0.164	0.128	0.220	0.264
332	0.062	0.167	0.130	0.222	0.268
331	0.063	0.169	0.132	0.225	0.272
330	0.064	0.172	0.134	0.227	0.276
329	0.065	0.174	0.136	0.229	0.279
328	0.066	0.176	0.138	0.231	0.282
327	0.067	0.178	0.140	0.232	0.285
326	0.068	0.180	0.141	0.234	0.288
325	0.068	0.182	0.143	0.236	0.291
324	0.069	0.184	0.144	0.238	0.294
323	0.070	0.186	0.146	0.240	0.297
322	0.070	0.188	0.147	0.241	0.301
321	0.070	0.190	0.148	0.242	0.303
320	0.071	0.191	0.150	0.244	0.306
319	0.071	0.193	0.151	0.245	0.310
318	0.071	0.195	0.152	0.246	0.313
317	0.071	0.196	0.153	0.247	0.316
316	0.071	0.198	0.154	0.249	0.318
315	0.071	0.199	0.155	0.250	0.321
314	0.071	0.201	0.157	0.251	0.324
313	0.071	0.202	0.158	0.252	0.327
312	0.071	0.204	0.159	0.253	0.330

311	0.072	0.206	0.160	0.255	0.333
310	0.072	0.208	0.161	0.256	0.337
309	0.072	0.210	0.162	0.258	0.340
308	0.072	0.212	0.164	0.259	0.344
307	0.072	0.214	0.165	0.261	0.348
306	0.073	0.217	0.167	0.263	0.353
305	0.073	0.220	0.170	0.266	0.359
304	0.074	0.223	0.172	0.268	0.364
303	0.075	0.227	0.174	0.271	0.370
302	0.077	0.232	0.178	0.275	0.378
301	0.078	0.237	0.182	0.280	0.385
300	0.080	0.241	0.186	0.284	0.393
299	0.082	0.247	0.190	0.289	0.402
298	0.084	0.253	0.195	0.295	0.412
297	0.087	0.261	0.201	0.301	0.423
296	0.090	0.269	0.207	0.308	0.434
295	0.093	0.277	0.214	0.316	0.445
294	0.097	0.287	0.222	0.325	0.458
293	0.102	0.298	0.231	0.337	0.472
292	0.108	0.312	0.242	0.349	0.486
291	0.113	0.324	0.253	0.361	0.499
290	0.119	0.336	0.263	0.372	0.510
289	0.123	0.346	0.272	0.382	0.520
288	0.126	0.355	0.280	0.390	0.529
287	0.130	0.365	0.287	0.399	0.538
286	0.134	0.375	0.296	0.409	0.548
285	0.138	0.387	0.306	0.420	0.560
284	0.143	0.399	0.316	0.431	0.570
283	0.146	0.408	0.324	0.439	0.577
282	0.149	0.414	0.329	0.445	0.581
281	0.149	0.418	0.331	0.448	0.583
280	0.150	0.420	0.333	0.450	0.584
279	0.149	0.422	0.333	0.451	0.584
278	0.149	0.422	0.334	0.452	0.584
277	0.147	0.422	0.333	0.451	0.586
276	0.146	0.421	0.332	0.450	0.589
275	0.144	0.419	0.330	0.448	0.596
274	0.142	0.416	0.328	0.445	0.604
273	0.139	0.413	0.325	0.442	0.613
272	0.136	0.408	0.321	0.438	0.623
271	0.133	0.403	0.316	0.433	0.630
270	0.130	0.398	0.312	0.428	0.635
269	0.127	0.393	0.307	0.423	0.645
268	0.123	0.388	0.302	0.418	0.665
267	0.120	0.383	0.297	0.413	0.688
266	0.116	0.378	0.293	0.407	0.710
265	0.113	0.373	0.288	0.403	0.735
264	0.110	0.368	0.284	0.398	0.767
263	0.107	0.363	0.280	0.393	0.809

262	0.104	0.358	0.276	0.389	0.859
261	0.101	0.354	0.272	0.385	0.910
260	0.099	0.351	0.269	0.382	0.961
259	0.097	0.348	0.267	0.380	1.012
258	0.095	0.345	0.265	0.377	1.064
257	0.094	0.343	0.263	0.376	1.115
256	0.092	0.341	0.262	0.375	1.169
255	0.092	0.341	0.261	0.375	1.226
254	0.091	0.341	0.261	0.375	1.281
253	0.091	0.342	0.262	0.378	1.326
252	0.091	0.343	0.263	0.381	1.365
251	0.092	0.345	0.265	0.385	1.402
250	0.093	0.349	0.268	0.392	1.438
249	0.094	0.353	0.272	0.401	1.469
248	0.096	0.358	0.276	0.413	1.497
247	0.099	0.365	0.282	0.428	1.524
246	0.102	0.375	0.290	0.451	1.549
245	0.107	0.387	0.300	0.481	1.573
244	0.112	0.401	0.311	0.520	1.598
243	0.119	0.418	0.326	0.568	1.626
242	0.128	0.442	0.345	0.629	1.663
241	0.140	0.470	0.369	0.712	1.708
240	0.153	0.503	0.397	0.817	1.757
239	0.171	0.543	0.431	0.941	1.816
238	0.194	0.594	0.474	1.091	1.898
237	0.222	0.657	0.526	1.286	2.009
236	0.252	0.726	0.584	1.527	2.148
235	0.288	0.805	0.651	1.797	2.323
234	0.332	0.901	0.733	2.092	2.540
233	0.379	1.008	0.826	2.427	2.773
232	0.426	1.115	0.925	2.760	2.947
231	0.475	1.226	1.020	2.986	3.029
230	0.527	1.346	1.112	3.091	3.072
229	0.578	1.468	1.209	3.123	3.108
228	0.624	1.583	1.303	3.129	3.127
227	0.664	1.684	1.386	3.130	3.118
226	0.700	1.778	1.462	3.128	3.109
225	0.736	1.873	1.537	3.130	3.111
224	0.768	1.965	1.609	3.137	3.113
223	0.794	2.045	1.674	3.143	3.114
222	0.818	2.122	1.731	3.144	3.117
221	0.844	2.205	1.787	3.140	3.119
220	0.870	2.290	1.849	3.140	3.110
219	0.895	2.371	1.914	3.144	3.095
218	0.922	2.452	1.978	3.142	3.088
217	0.952	2.540	2.045	3.129	3.080
216	0.987	2.634	2.125	3.118	3.066
215	1.022	2.716	2.214	3.108	3.059
214	1.063	2.784	2.303	3.094	3.051

213	1.113	2.846	2.389	3.089	3.024
212	1.171	2.888	2.478	3.074	3.000
211	1.236	2.896	2.567	3.037	2.977
210	1.307	2.880	2.637	3.001	2.935
209	1.383	2.852	2.668	2.965	2.885
208	1.467	2.806	2.663	2.916	2.826
207	1.566	2.738	2.624	2.837	2.746
206	1.674	2.637	2.555	2.726	2.624
205	1.774	2.515	2.434	2.610	2.482
204	1.847	2.369	2.257	2.475	2.320
203	1.856	2.169	2.044	2.273	2.127
202	1.759	1.924	1.813	2.034	1.912
201	1.554	1.633	1.520	1.757	1.624
200	1.389	1.433	1.306	1.562	1.412

5.5. Fl. Intensity data of BM (10 μ M) in presence and absence of different NaC concentration in phosphate buffer pH 7.0

wave length / nm	Interaction of BM (10 μ M) in presence of different [NaC] in phosphate buffer pH 7.0											
	Free BM	0.15 mM	0.22 mM	0.26 mM	0.29 mM	0.36 mM	0.44 mM	0.73 mM	1.59 mM	5.63 mM	6.97 mM	16.27 mM
300	384	392	383	377	371	356	351	335	325	312	309	309
302	493	498	488	477	468	448	437	411	393	373	369	369
304	621	623	610	594	582	555	539	500	476	449	445	445
306	749	746	730	710	695	660	640	589	560	528	524	523
308	869	865	843	820	802	762	736	675	641	606	600	601
310	983	977	953	925	904	859	828	758	720	681	674	676
312	1108	1099	1070	1039	1014	962	926	845	802	758	751	754
314	1246	1234	1201	1165	1136	1075	1032	939	890	840	831	836
316	1393	1378	1340	1299	1265	1195	1147	1037	982	925	914	918
318	1541	1521	1479	1432	1394	1318	1261	1137	1075	1008	996	999
320	1674	1650	1604	1553	1511	1426	1365	1227	1159	1083	1070	1073
322	1790	1765	1716	1660	1612	1522	1456	1308	1233	1149	1135	1138
324	1894	1867	1815	1755	1703	1609	1538	1379	1299	1206	1191	1194
326	1991	1960	1907	1840	1785	1686	1611	1442	1358	1257	1238	1241
328	2089	2052	1996	1926	1866	1765	1683	1503	1413	1302	1281	1284
330	2187	2146	2085	2010	1948	1840	1753	1563	1466	1344	1321	1320
332	2284	2236	2170	2090	2026	1912	1820	1620	1515	1382	1358	1354
334	2375	2320	2250	2165	2098	1980	1883	1673	1560	1414	1388	1383
336	2454	2393	2319	2231	2160	2038	1936	1716	1597	1439	1412	1403
338	2519	2452	2376	2280	2205	2082	1977	1750	1624	1455	1426	1415
340	2567	2494	2413	2315	2237	2111	2005	1773	1640	1462	1430	1418
342	2603	2522	2437	2337	2258	2127	2020	1784	1646	1459	1426	1411
344	2629	2538	2452	2345	2268	2136	2025	1786	1643	1449	1415	1396
346	2642	2547	2456	2347	2268	2137	2024	1782	1635	1435	1399	1376
348	2650	2544	2451	2342	2262	2129	2016	1772	1621	1415	1377	1352

350	2647	2533	2439	2329	2247	2115	2000	1757	1602	1393	1351	1324
352	2629	2511	2417	2307	2222	2092	1977	1734	1577	1363	1320	1293
354	2601	2480	2384	2274	2189	2058	1946	1703	1545	1329	1287	1257
356	2563	2437	2343	2231	2147	2019	1908	1667	1509	1291	1249	1219
358	2511	2382	2289	2178	2095	1969	1861	1623	1467	1249	1208	1177
360	2449	2319	2226	2119	2036	1914	1806	1575	1422	1205	1163	1133
362	2381	2251	2159	2053	1972	1852	1746	1523	1372	1157	1117	1086
364	2304	2175	2085	1980	1901	1785	1684	1468	1318	1109	1069	1038
366	2221	2092	2006	1905	1827	1715	1618	1409	1263	1059	1020	989
368	2132	2005	1922	1823	1748	1643	1547	1347	1206	1007	970	940
370	2038	1916	1836	1739	1670	1568	1478	1285	1148	957	921	891
372	1942	1824	1747	1655	1588	1493	1405	1220	1091	906	872	843
374	1843	1729	1656	1568	1505	1415	1330	1156	1032	855	823	795
376	1745	1637	1566	1485	1423	1338	1257	1094	975	806	775	749
378	1646	1543	1477	1398	1340	1259	1185	1030	918	757	728	703
380	1548	1452	1388	1313	1260	1184	1113	968	862	710	682	659
382	1451	1361	1301	1231	1181	1110	1043	907	807	664	639	615
384	1358	1273	1217	1151	1103	1038	976	849	756	621	597	574
386	1270	1190	1137	1075	1031	970	913	794	706	579	557	536
388	1184	1109	1059	1002	960	905	851	741	659	541	519	500
390	1102	1033	987	933	894	843	793	690	614	503	483	466
392	1025	960	917	867	830	784	737	642	572	468	450	433
394	950	891	851	805	771	728	685	596	531	435	418	403
396	882	826	789	746	715	675	635	554	494	405	388	375
398	815	765	731	691	662	625	588	514	458	376	361	348
400	755	708	676	639	613	579	545	476	425	349	336	323
402	697	653	624	590	566	535	503	441	393	325	312	301
404	641	602	575	545	522	494	465	408	365	301	290	280
406	591	556	531	503	481	457	430	378	338	280	270	260
408	545	512	489	464	444	422	398	350	314	261	251	243
410	503	473	451	428	410	390	368	324	291	243	235	226
412	462	436	416	395	379	360	340	301	271	226	219	212
414	426	402	384	365	350	333	315	279	251	211	204	198
416	392	371	354	337	323	308	291	258	234	198	191	185
418	361	341	327	311	298	284	270	240	217	185	179	173
420	332	315	302	287	275	263	250	223	202	173	167	162
422	306	290	278	265	255	244	232	207	189	162	156	152
424	282	268	257	245	236	226	215	192	176	151	147	143
426	260	248	238	227	219	210	200	179	164	142	138	135
428	240	229	221	211	203	195	186	167	154	134	130	127
430	222	213	205	196	189	182	173	156	144	127	123	120
432	206	197	191	182	176	170	162	147	136	120	116	114
434	191	183	178	170	164	158	152	137	128	113	110	108
436	177	171	166	159	153	148	142	129	121	108	105	104

438	164	159	154	148	143	139	133	122	114	102	100	99
440	152	148	144	138	134	130	126	114	108	98	95	94
442	141	138	135	130	126	122	118	108	102	93	91	90
444	131	129	126	122	118	115	111	102	96	89	86	86
446	122	120	118	114	111	108	105	96	91	85	83	82
448	113	112	111	107	104	102	99	91	87	81	79	78
450	105	105	104	101	98	97	93	86	82	77	75	75
452	98	99	98	95	93	91	88	82	78	73	72	72
454	91	93	92	89	88	86	84	78	74	70	69	69
456	85	87	87	85	83	82	79	74	71	67	66	66
458	79	82	82	80	79	78	76	70	68	64	63	63
460	74	77	78	76	75	74	72	67	65	62	61	61
462	69	73	74	72	71	71	69	64	62	59	58	59
464	64	69	70	69	68	68	66	61	59	57	56	57
466	60	65	67	66	65	65	63	58	57	55	54	55
468	57	62	64	63	62	62	60	56	55	53	52	53
470	53	58	61	60	59	59	57	53	52	51	50	51
472	50	56	58	57	57	57	55	51	50	49	48	49
474	47	53	55	55	55	54	53	49	48	47	46	47
476	44	51	53	52	52	52	51	47	46	46	45	45
478	42	48	51	50	51	50	49	46	45	44	43	44
480	39	46	49	48	49	49	47	44	43	43	42	43
482	37	44	47	47	47	47	46	42	42	41	40	41
484	36	43	45	45	45	45	44	41	41	40	39	40
486	34	41	44	43	44	44	42	40	39	39	38	39
488	32	39	42	42	42	42	41	38	38	37	37	38
490	30	37	40	40	41	41	40	37	37	36	36	36
492	29	36	39	39	39	39	38	36	35	35	35	35
494	28	34	37	37	38	38	37	34	34	34	33	34
496	26	33	36	36	36	37	36	33	33	33	32	33
498	25	31	34	34	35	35	34	32	32	31	31	32
500	24	30	33	33	33	34	33	30	30	30	30	31

5.6. Fl. Intensity data of BM (10 μ M) in presence and absence of different SDBS concentration in phosphate buffer pH 7.0

wavelength/ nm	Interaction of BM (10 μ M) in presence of different [SDBS] in phosphate buffer pH 7.0										
	[SDBS] = 0 mM	0.02	0.04	0.06	0.09	0.11	0.13	0.17	0.22	0.30	0.39
300	403	396	486	462	378	388	384	383	369	341	319
302	514	499	530	504	453	447	429	416	395	362	343
304	647	619	620	587	547	531	502	480	451	411	390
306	777	738	722	682	643	620	581	552	515	467	444
308	900	852	825	778	737	709	662	625	581	524	499
310	1019	959	927	873	826	795	739	697	646	579	551
312	1146	1075	1036	974	921	884	821	772	713	637	604
314	1289	1203	1156	1084	1024	981	908	852	782	696	659
316	1439	1338	1284	1202	1132	1083	998	934	855	755	715
318	1591	1473	1412	1320	1240	1185	1088	1014	925	814	769
320	1728	1594	1527	1426	1337	1275	1168	1086	988	865	815
322	1850	1699	1627	1519	1422	1355	1238	1148	1042	909	856
324	1956	1793	1717	1602	1496	1425	1300	1204	1089	948	892
326	2055	1878	1800	1677	1565	1489	1359	1255	1134	984	924
328	2158	1965	1884	1756	1636	1554	1416	1308	1178	1023	961
330	2258	2050	1967	1833	1706	1619	1474	1362	1227	1064	1003
332	2358	2137	2050	1911	1777	1686	1533	1419	1279	1113	1053
334	2450	2216	2129	1987	1846	1754	1592	1475	1333	1164	1107
336	2532	2285	2198	2053	1906	1811	1643	1526	1382	1212	1158
338	2598	2341	2254	2106	1956	1858	1684	1566	1420	1252	1203
340	2646	2381	2292	2145	1992	1890	1716	1595	1447	1281	1236
342	2683	2407	2317	2172	2016	1912	1735	1612	1465	1302	1259
344	2707	2423	2333	2188	2030	1924	1746	1624	1476	1316	1276
346	2722	2429	2340	2195	2035	1931	1752	1631	1483	1326	1289
348	2728	2429	2342	2197	2034	1930	1752	1632	1484	1332	1298
350	2722	2418	2334	2188	2027	1923	1745	1626	1481	1334	1305
352	2705	2399	2315	2171	2011	1908	1731	1615	1472	1330	1304
354	2675	2368	2286	2145	1986	1885	1709	1595	1456	1319	1295
356	2634	2326	2246	2110	1952	1854	1679	1566	1435	1301	1280
358	2580	2274	2197	2064	1910	1812	1642	1531	1402	1274	1257
360	2518	2216	2139	2011	1860	1766	1597	1492	1364	1243	1227
362	2447	2147	2076	1953	1804	1711	1549	1447	1322	1207	1192
364	2367	2074	2005	1886	1741	1652	1495	1397	1277	1167	1154
366	2281	1997	1931	1817	1676	1590	1440	1343	1230	1125	1114
368	2190	1912	1851	1742	1607	1525	1380	1288	1180	1080	1070
370	2094	1828	1769	1665	1536	1458	1318	1230	1129	1035	1026
372	1994	1741	1684	1585	1463	1387	1254	1172	1076	987	979
374	1891	1652	1598	1505	1387	1316	1189	1111	1021	938	931
376	1790	1563	1513	1424	1313	1246	1126	1053	967	890	882
378	1688	1472	1426	1342	1239	1175	1062	993	913	841	834
380	1588	1384	1340	1263	1165	1105	999	934	860	794	786
382	1490	1296	1257	1185	1092	1036	938	876	807	745	740
384	1393	1212	1176	1108	1022	971	878	820	757	699	694
386	1303	1133	1099	1037	955	908	822	768	709	655	651
388	1215	1057	1025	967	892	847	767	717	662	613	609
390	1131	984	954	901	831	790	716	669	619	574	569
392	1051	914	887	839	774	736	667	623	577	535	532
394	975	849	824	779	719	684	620	580	537	499	496

396	904	787	765	724	668	636	577	540	500	466	462
398	836	729	708	670	619	590	535	501	465	434	430
400	773	674	656	622	574	547	496	465	432	403	400
402	713	623	606	575	532	507	460	432	401	375	373
404	657	574	559	530	491	468	426	400	372	349	346
406	606	530	516	490	454	433	395	371	346	324	322
408	558	488	476	453	419	401	366	344	321	302	300
410	514	451	439	418	388	371	339	319	298	281	279
412	473	415	405	387	359	344	314	296	277	262	260
414	435	383	374	357	332	318	291	275	258	244	243
416	401	354	345	330	307	295	270	255	240	228	226
418	369	326	319	305	285	274	251	237	224	213	212
420	340	301	295	282	264	254	234	221	208	199	198
422	313	278	273	261	245	236	217	206	195	186	185
424	288	257	252	242	227	219	202	193	182	174	174
426	266	238	233	225	211	204	189	180	170	164	163
428	246	220	217	209	197	191	176	168	159	154	153
430	227	205	201	195	183	178	165	158	150	144	144
432	211	190	188	182	171	167	155	148	141	136	136
434	195	177	175	169	160	156	145	139	133	129	129
436	181	165	163	158	150	146	137	132	126	122	122
438	168	154	153	149	141	138	129	124	119	115	116
440	156	144	143	139	132	130	121	117	112	109	110
442	145	134	134	130	124	122	115	111	106	103	104
444	135	126	125	122	116	115	108	105	101	98	99
446	125	117	117	115	110	109	102	99	95	93	94
448	116	110	110	108	103	103	96	94	90	88	89
450	109	104	103	102	98	97	91	89	86	84	85
452	102	98	98	96	92	92	87	85	82	80	80
454	95	92	92	91	88	87	82	80	78	76	77
456	89	87	87	86	83	83	78	77	74	72	73
458	84	82	83	82	79	79	74	73	70	69	70
460	78	77	78	78	75	75	71	70	67	66	66
462	74	73	74	74	71	71	68	66	64	63	63
464	70	69	70	70	68	68	65	63	61	60	60
466	66	66	67	67	65	65	62	61	58	57	58
468	62	63	64	64	62	62	59	58	56	55	55
470	59	60	61	61	59	60	56	55	53	52	53
472	56	57	59	59	57	57	54	53	51	50	50
474	53	55	56	56	54	55	52	51	49	48	48
476	50	53	54	54	52	53	50	49	47	46	46
478	47	50	52	52	50	51	48	47	45	44	44
480	45	48	50	50	48	49	46	45	43	42	43
482	43	47	48	48	47	47	44	44	42	41	41
484	41	45	46	46	45	46	43	42	40	39	39
486	40	43	45	45	43	44	41	41	39	38	38
488	38	42	43	43	42	43	40	40	38	37	37
490	36	40	41	42	40	41	39	38	36	35	35
492	35	39	40	40	39	40	37	37	35	34	34
494	33	37	38	39	37	38	36	35	34	33	33
496	32	35	37	37	36	37	34	34	32	31	32
498	30	34	35	35	34	35	33	33	31	30	30
500	29	33	34	34	33	34	32	31	30	29	29

5.7. Fluorescence area of BM in presence of different surfactant concentrations at 298.15 K

Fluorescence area of BM in presence different concentration of surfactants ($\lambda_{\text{emission}} = 347 \text{ nm}$)							
[NaC]/ mM	10^{-4}F	[NaDC]/ mM	10^{-4}F	[SDDS]/ mM	10^{-4}F	[SDBS]/ mM	10^{-4}F
0.00	20.2	0.14	17.4	0.00	18.8	0.00	20.4
0.04	19.4	0.20	17.5	0.05	17.9	0.01	19.0
0.07	20.4	0.40	15.9	0.10	17.7	0.02	18.3
0.11	19.9	0.59	16.0	0.15	17.2	0.03	17.0
0.15	19.5	0.78	15.2	0.20	16.9	0.04	17.7
0.18	18.9	0.97	15.0	0.25	16.6	0.05	17.3
0.22	18.8	1.42	13.2	0.30	15.7	0.07	16.7
0.26	18.0	1.85	12.3	0.35	15.0	0.09	15.5
0.29	17.4	2.26	10.8	0.40	14.6	0.11	14.8
0.33	17.0	2.66	10.9	0.45	14.6	0.13	13.5
0.37	16.5	3.40	10.8	0.50	14.1	0.17	12.6
0.44	15.6	4.08	10.5	0.60	14.1	0.22	11.6
0.51	15.1			0.70	14.0	0.26	11.2
0.73	13.9			0.90	13.5	0.30	10.5
0.95	13.5			1.30	13.5	0.39	10.2
1.16	13.1			1.89	12.8	0.69	9.8
1.59	12.8			3.84	12.0	0.90	9.7
2.87	12.5			6.70	11.1	1.10	9.6
4.27	11.7			9.49	11.1	1.51	9.3
5.63	11.3			18.20	10.7	1.92	9.2
6.98	11.0			33.44	10.6		
16.28	10.9						
19.11	10.6						
24.42	10.7						

5.8. Stern Volmer quenching data (F_0/F) of BM in presence of different surfactant concentrations at 298.15 K

Stren-Volmer (SV) F_0/F of BM (10 μ M) at different quencher (Surfactant) concentration							
10 ⁴ [NaC]/mM	F_0/F	10 ⁴ [NaDC] / mM	F_0/F	10 ⁴ [SDDS]/ mM	F_0/F	10 ⁴ [SDBS] /mM	F_0/F
0	1.0	0.00	1.0	0.00	1.0	0.00	1.0
1.46	1.0	4.00	1.1	0.48	1.0	2.18	1.1
2.19	1.1	7.84	1.1	1.00	1.1	4.35	1.2
2.56	1.1	14.20	1.3	2.01	1.1	8.70	1.3
2.92	1.2	18.50	1.4	3.01	1.2	10.90	1.4
3.65	1.2	26.60	1.5	4.01	1.3	13.00	1.5
4.38	1.3	40.80	1.6	5.01	1.3	17.40	1.6
7.29	1.5					21.70	1.8
						30.30	1.9
						38.90	2.0

5.9. log plot data of BM in presence of different surfactant concentrations in log scale at 298.15 K

log plot of BM (10 μ M) in presence of different [surfactant]							
log ([NaC])	log{(F ₀ -F)/F}	log ([NaDC])	log{(F ₀ -F)/F}	log ([SDDS])	log{(F ₀ -F)/F}	log ([SDBS])	log{(F ₀ -F)/F}
-3.835	-1.427	-3.398	-1.077	-4.318	-1.306	-4.662	-0.936
-3.659	-1.123	-3.106	-0.878	-3.998	-1.200	-4.361	-0.817
-3.592	-0.912	-2.847	-0.520	-3.697	-0.957	-4.061	-0.499
-3.534	-0.790	-2.732	-0.391	-3.521	-0.711	-3.964	-0.420
-3.437	-0.639	-2.575	-0.294	-3.396	-0.539	-3.885	-0.290
-3.358	-0.532	-2.390	-0.192	-3.300	-0.479	-3.760	-0.210
-3.137	-0.340					-3.664	-0.119
						-3.519	-0.025
						-3.410	-0.003

5.10. Molar ellipticity data of SB (5 μM) in presence of different NaC concentration 298.15 K

wavelength/nm	Molar Ellipticity ($([\theta] \times 10^{-3} / \text{deg.cm}^2.\text{dmol}^{-1})$) of BM (5 μM) in presence of varying concentration of NaC								
	free BM	[NaC]= 0.18 mM	0.54 mM	1.07 mM	1.76 mM	3.46 mM	6.36 mM	9.35 mM	12.7 mM
350	-0.044	-0.066	0.054	0.035	-0.164	-0.161	-0.153	-0.076	0.059
349	-0.017	-0.074	0.026	0.055	-0.139	-0.148	-0.137	-0.068	0.055
348	0.012	-0.071	0.013	0.078	-0.111	-0.136	-0.122	-0.059	0.052
347	0.040	-0.058	0.015	0.096	-0.083	-0.126	-0.109	-0.046	0.050
346	0.065	-0.037	0.031	0.106	-0.054	-0.121	-0.101	-0.028	0.049
345	0.082	-0.011	0.053	0.104	-0.028	-0.120	-0.098	-0.006	0.047
344	0.086	0.015	0.075	0.088	-0.004	-0.125	-0.102	0.016	0.044
343	0.078	0.036	0.090	0.061	0.015	-0.137	-0.114	0.031	0.040
342	0.058	0.049	0.090	0.027	0.027	-0.155	-0.134	0.036	0.035
341	0.033	0.052	0.073	-0.009	0.028	-0.177	-0.161	0.030	0.031
340	0.009	0.046	0.040	-0.044	0.018	-0.201	-0.192	0.016	0.028
339	-0.010	0.033	-0.004	-0.075	-0.004	-0.223	-0.225	-0.004	0.029
338	-0.019	0.017	-0.052	-0.100	-0.034	-0.241	-0.254	-0.025	0.033
337	-0.019	-0.001	-0.098	-0.119	-0.067	-0.251	-0.275	-0.043	0.042
336	-0.014	-0.021	-0.135	-0.132	-0.096	-0.255	-0.288	-0.059	0.057
335	-0.008	-0.042	-0.159	-0.140	-0.117	-0.252	-0.292	-0.073	0.079
334	-0.004	-0.065	-0.171	-0.142	-0.127	-0.244	-0.289	-0.087	0.107
333	-0.005	-0.089	-0.171	-0.138	-0.125	-0.233	-0.280	-0.100	0.139
332	-0.010	-0.114	-0.161	-0.128	-0.116	-0.220	-0.267	-0.111	0.170
331	-0.016	-0.135	-0.144	-0.115	-0.103	-0.208	-0.251	-0.116	0.196
330	-0.020	-0.152	-0.124	-0.100	-0.093	-0.196	-0.231	-0.113	0.211
329	-0.019	-0.162	-0.102	-0.088	-0.086	-0.186	-0.209	-0.099	0.213
328	-0.011	-0.167	-0.081	-0.082	-0.084	-0.178	-0.186	-0.074	0.202
327	0.002	-0.170	-0.062	-0.083	-0.085	-0.174	-0.164	-0.040	0.184
326	0.019	-0.170	-0.046	-0.091	-0.087	-0.174	-0.148	-0.003	0.165
325	0.035	-0.171	-0.035	-0.103	-0.086	-0.177	-0.137	0.033	0.152
324	0.047	-0.169	-0.027	-0.115	-0.083	-0.182	-0.133	0.064	0.149
323	0.052	-0.165	-0.021	-0.124	-0.078	-0.190	-0.134	0.087	0.153
322	0.050	-0.155	-0.018	-0.125	-0.072	-0.199	-0.136	0.101	0.161
321	0.042	-0.141	-0.015	-0.121	-0.068	-0.208	-0.139	0.105	0.166
320	0.030	-0.124	-0.016	-0.114	-0.069	-0.221	-0.141	0.098	0.164
319	0.017	-0.111	-0.022	-0.110	-0.077	-0.236	-0.146	0.082	0.153
318	0.005	-0.105	-0.036	-0.112	-0.094	-0.257	-0.157	0.059	0.135
317	-0.003	-0.112	-0.060	-0.125	-0.121	-0.281	-0.175	0.033	0.116
316	-0.009	-0.132	-0.095	-0.147	-0.157	-0.309	-0.203	0.008	0.100
315	-0.012	-0.162	-0.136	-0.174	-0.199	-0.336	-0.237	-0.015	0.090
314	-0.015	-0.196	-0.177	-0.200	-0.241	-0.359	-0.274	-0.036	0.085
313	-0.021	-0.228	-0.211	-0.217	-0.276	-0.375	-0.307	-0.055	0.082
312	-0.032	-0.253	-0.232	-0.221	-0.299	-0.383	-0.333	-0.075	0.077
311	-0.047	-0.267	-0.241	-0.213	-0.306	-0.384	-0.352	-0.098	0.068

310	-0.068	-0.270	-0.240	-0.197	-0.299	-0.382	-0.365	-0.126	0.054
309	-0.093	-0.266	-0.236	-0.182	-0.286	-0.380	-0.375	-0.155	0.039
308	-0.122	-0.257	-0.239	-0.177	-0.274	-0.382	-0.387	-0.182	0.023
307	-0.154	-0.247	-0.254	-0.189	-0.274	-0.391	-0.403	-0.201	0.008
306	-0.186	-0.238	-0.285	-0.221	-0.290	-0.406	-0.420	-0.210	-0.007
305	-0.216	-0.233	-0.327	-0.268	-0.321	-0.426	-0.438	-0.207	-0.024
304	-0.241	-0.231	-0.373	-0.323	-0.362	-0.446	-0.451	-0.193	-0.045
303	-0.258	-0.232	-0.412	-0.374	-0.400	-0.464	-0.459	-0.172	-0.068
302	-0.264	-0.237	-0.438	-0.412	-0.426	-0.477	-0.459	-0.149	-0.090
301	-0.258	-0.244	-0.446	-0.430	-0.432	-0.485	-0.452	-0.127	-0.107
300	-0.244	-0.252	-0.438	-0.426	-0.419	-0.487	-0.440	-0.108	-0.113
299	-0.223	-0.259	-0.422	-0.405	-0.390	-0.485	-0.425	-0.094	-0.107
298	-0.201	-0.264	-0.403	-0.374	-0.355	-0.480	-0.408	-0.085	-0.092
297	-0.181	-0.267	-0.388	-0.339	-0.323	-0.473	-0.389	-0.083	-0.070
296	-0.163	-0.268	-0.379	-0.308	-0.299	-0.463	-0.370	-0.086	-0.046
295	-0.147	-0.266	-0.376	-0.284	-0.284	-0.449	-0.350	-0.094	-0.024
294	-0.126	-0.262	-0.373	-0.267	-0.274	-0.429	-0.330	-0.101	-0.002
293	-0.099	-0.253	-0.365	-0.256	-0.265	-0.403	-0.309	-0.101	0.023
292	-0.063	-0.239	-0.348	-0.248	-0.251	-0.369	-0.287	-0.090	0.054
291	-0.022	-0.218	-0.322	-0.239	-0.232	-0.328	-0.264	-0.062	0.092
290	0.018	-0.190	-0.290	-0.227	-0.209	-0.284	-0.240	-0.020	0.134
289	0.050	-0.156	-0.256	-0.211	-0.186	-0.242	-0.213	0.031	0.174
288	0.064	-0.122	-0.226	-0.193	-0.168	-0.205	-0.186	0.080	0.204
287	0.059	-0.091	-0.206	-0.174	-0.159	-0.179	-0.160	0.116	0.218
286	0.036	-0.069	-0.197	-0.157	-0.159	-0.165	-0.138	0.134	0.214
285	0.001	-0.058	-0.199	-0.145	-0.166	-0.164	-0.123	0.132	0.197
284	-0.037	-0.057	-0.207	-0.141	-0.179	-0.171	-0.115	0.114	0.173
283	-0.071	-0.063	-0.217	-0.145	-0.194	-0.181	-0.116	0.090	0.149
282	-0.095	-0.071	-0.224	-0.157	-0.207	-0.190	-0.125	0.069	0.132
281	-0.110	-0.079	-0.223	-0.174	-0.218	-0.194	-0.139	0.056	0.123
280	-0.117	-0.086	-0.213	-0.192	-0.225	-0.195	-0.159	0.052	0.121
279	-0.121	-0.091	-0.196	-0.206	-0.227	-0.196	-0.180	0.054	0.123
278	-0.122	-0.098	-0.176	-0.213	-0.222	-0.202	-0.201	0.058	0.126
277	-0.121	-0.107	-0.158	-0.212	-0.212	-0.216	-0.219	0.061	0.127
276	-0.117	-0.119	-0.147	-0.204	-0.198	-0.239	-0.232	0.062	0.127
275	-0.108	-0.130	-0.146	-0.193	-0.181	-0.268	-0.237	0.063	0.123
274	-0.095	-0.139	-0.156	-0.184	-0.166	-0.297	-0.234	0.067	0.114
273	-0.082	-0.141	-0.173	-0.182	-0.159	-0.321	-0.225	0.072	0.100
272	-0.075	-0.138	-0.193	-0.189	-0.161	-0.333	-0.217	0.073	0.079
271	-0.081	-0.131	-0.213	-0.205	-0.176	-0.335	-0.214	0.066	0.051
270	-0.104	-0.126	-0.229	-0.231	-0.202	-0.327	-0.221	0.045	0.018
269	-0.143	-0.126	-0.240	-0.261	-0.234	-0.316	-0.239	0.009	-0.017
268	-0.195	-0.135	-0.249	-0.292	-0.268	-0.309	-0.265	-0.038	-0.049
267	-0.251	-0.152	-0.259	-0.320	-0.297	-0.308	-0.290	-0.087	-0.076

266	-0.303	-0.174	-0.271	-0.340	-0.317	-0.317	-0.304	-0.128	-0.099
265	-0.343	-0.196	-0.288	-0.350	-0.327	-0.333	-0.302	-0.156	-0.119
264	-0.369	-0.213	-0.306	-0.353	-0.329	-0.353	-0.281	-0.168	-0.137
263	-0.382	-0.224	-0.322	-0.348	-0.327	-0.373	-0.247	-0.169	-0.155
262	-0.385	-0.227	-0.334	-0.341	-0.324	-0.390	-0.209	-0.165	-0.170
261	-0.386	-0.224	-0.337	-0.335	-0.325	-0.403	-0.179	-0.161	-0.180
260	-0.388	-0.216	-0.332	-0.334	-0.332	-0.410	-0.164	-0.160	-0.183
259	-0.394	-0.208	-0.319	-0.336	-0.344	-0.411	-0.167	-0.163	-0.178
258	-0.405	-0.203	-0.303	-0.342	-0.359	-0.408	-0.185	-0.167	-0.168
257	-0.418	-0.203	-0.289	-0.349	-0.375	-0.403	-0.212	-0.172	-0.159
256	-0.430	-0.212	-0.280	-0.353	-0.389	-0.399	-0.239	-0.177	-0.156
255	-0.439	-0.232	-0.281	-0.354	-0.404	-0.402	-0.264	-0.188	-0.163
254	-0.447	-0.262	-0.292	-0.354	-0.422	-0.417	-0.287	-0.207	-0.178
253	-0.457	-0.302	-0.316	-0.359	-0.449	-0.449	-0.311	-0.237	-0.200
252	-0.475	-0.346	-0.352	-0.377	-0.491	-0.499	-0.341	-0.278	-0.227
251	-0.507	-0.391	-0.402	-0.413	-0.549	-0.566	-0.382	-0.327	-0.260
250	-0.558	-0.434	-0.465	-0.470	-0.624	-0.643	-0.436	-0.383	-0.305
249	-0.631	-0.475	-0.540	-0.548	-0.709	-0.722	-0.503	-0.449	-0.369
248	-0.722	-0.522	-0.626	-0.639	-0.798	-0.800	-0.585	-0.528	-0.458
247	-0.827	-0.581	-0.723	-0.735	-0.883	-0.872	-0.681	-0.626	-0.573
246	-0.939	-0.661	-0.828	-0.831	-0.960	-0.942	-0.791	-0.745	-0.708
245	-1.051	-0.767	-0.942	-0.924	-1.031	-1.017	-0.916	-0.886	-0.853
244	-1.161	-0.897	-1.063	-1.017	-1.099	-1.105	-1.052	-1.040	-1.000
243	-1.271	-1.046	-1.194	-1.119	-1.175	-1.210	-1.199	-1.200	-1.145
242	-1.388	-1.207	-1.337	-1.241	-1.267	-1.338	-1.353	-1.364	-1.298
241	-1.523	-1.378	-1.497	-1.395	-1.386	-1.490	-1.521	-1.539	-1.478
240	-1.693	-1.568	-1.685	-1.591	-1.543	-1.674	-1.717	-1.744	-1.708
239	-1.917	-1.795	-1.915	-1.840	-1.752	-1.901	-1.964	-2.009	-2.015
238	-2.217	-2.088	-2.211	-2.159	-2.030	-2.193	-2.294	-2.366	-2.420
237	-2.620	-2.479	-2.599	-2.565	-2.403	-2.580	-2.737	-2.841	-2.939
236	-3.151	-2.998	-3.107	-3.082	-2.898	-3.093	-3.320	-3.453	-3.589
235	-3.832	-3.664	-3.758	-3.732	-3.540	-3.759	-4.054	-4.210	-4.385
234	-4.676	-4.482	-4.558	-4.529	-4.341	-4.591	-4.938	-5.112	-5.343
233	-5.678	-5.438	-5.500	-5.472	-5.298	-5.582	-5.954	-6.153	-6.473
232	-6.810	-6.504	-6.550	-6.535	-6.384	-6.701	-7.078	-7.324	-7.770
231	-8.018	-7.635	-7.661	-7.672	-7.551	-7.901	-8.276	-8.609	-9.207
230	-9.233	-8.779	-8.775	-8.823	-8.740	-9.125	-9.515	-9.976	-10.734
229	-10.379	-9.880	-9.834	-9.923	-9.889	-10.316	-10.757	-11.382	-12.287
228	-11.391	-10.885	-10.793	-10.917	-10.945	-11.425	-11.969	-12.772	-13.808
227	-12.229	-11.753	-11.629	-11.773	-11.875	-12.421	-13.118	-14.098	-15.264
226	-12.890	-12.465	-12.336	-12.485	-12.666	-13.293	-14.185	-15.332	-16.658
225	-13.398	-13.027	-12.930	-13.071	-13.327	-14.049	-15.167	-16.484	-18.028
224	-13.802	-13.466	-13.434	-13.564	-13.881	-14.715	-16.082	-17.599	-19.430
223	-14.153	-13.826	-13.873	-14.003	-14.361	-15.327	-16.971	-18.745	-20.906

222	-14.491	-14.155	-14.273	-14.423	-14.802	-15.924	-17.882	-19.982	-22.472
221	-14.838	-14.490	-14.651	-14.850	-15.240	-16.540	-18.856	-21.333	-24.105
220	-15.202	-14.852	-15.023	-15.303	-15.710	-17.198	-19.913	-22.778	-25.767
219	-15.581	-15.246	-15.410	-15.796	-16.240	-17.911	-21.046	-24.259	-27.432
218	-15.981	-15.668	-15.834	-16.343	-16.856	-18.684	-22.228	-25.720	-29.122
217	-16.421	-16.121	-16.325	-16.959	-17.574	-19.518	-23.435	-27.146	-30.914
216	-16.931	-16.625	-16.914	-17.660	-18.402	-20.425	-24.666	-28.596	-32.910
215	-17.543	-17.216	-17.624	-18.456	-19.336	-21.428	-25.962	-30.190	-35.182
214	-18.275	-17.933	-18.464	-19.350	-20.362	-22.558	-27.392	-32.055	-37.699
213	-19.115	-18.798	-19.423	-20.328	-21.457	-23.841	-29.017	-34.237	-40.263
212	-20.016	-19.790	-20.462	-21.360	-22.584	-25.271	-30.841	-36.617	-42.512
211	-20.900	-20.834	-21.517	-22.391	-23.693	-26.785	-32.755	-38.861	-43.966
210	-21.673	-21.804	-22.498	-23.346	-24.712	-28.246	-34.520	-40.454	-44.147
209	-22.242	-22.551	-23.303	-24.129	-25.539	-29.443	-35.788	-40.809	-42.720
208	-22.529	-22.936	-23.819	-24.626	-26.051	-30.119	-36.176	-39.436	-39.606
207	-22.476	-22.864	-23.933	-24.713	-26.106	-30.020	-35.374	-36.116	-35.042
206	-22.045	-22.305	-23.548	-24.277	-25.575	-28.964	-33.249	-31.014	-29.544
205	-21.206	-21.289	-22.596	-23.232	-24.369	-26.892	-29.914	-24.697	-23.793
204	-19.944	-19.879	-21.046	-21.543	-22.472	-23.911	-25.727	-18.014	-18.466
203	-18.254	-18.142	-18.927	-19.250	-19.962	-20.287	-21.217	-11.898	-14.083
202	-16.162	-16.123	-16.327	-16.474	-17.011	-16.398	-16.959	-7.127	-10.895
201	-13.737	-13.844	-13.396	-13.410	-13.863	-12.661	-13.425	-4.130	-8.869
200	-11.101	-11.321	-10.334	-10.298	-10.786	-9.439	-10.876	-2.896	-7.740
199	-8.420	-8.609	-7.373	-7.386	-8.023	-6.967	-9.312	-3.016	-7.137
198	-5.881	-5.829	-4.741	-4.887	-5.743	-5.310	-8.508	-3.832	-6.706
197	-3.656	-3.180	-2.636	-2.936	-4.015	-4.366	-8.110	-4.647	-6.205
196	-1.859	-0.917	-1.197	-1.578	-2.809	-3.911	-7.760	-4.920	-5.547
195	-0.525	0.709	-0.478	-0.767	-2.021	-3.673	-7.203	-4.389	-4.772
194	0.397	1.517	-0.451	-0.390	-1.514	-3.408	-6.349	-3.092	-3.998
193	1.025	1.462	-1.005	-0.302	-1.163	-2.954	-5.269	-1.293	-3.340
192	1.498	0.654	-1.976	-0.365	-0.882	-2.261	-4.134	0.642	-2.869
191	1.938	-0.661	-3.171	-0.472	-0.634	-1.381	-3.135	2.380	-2.590
190	2.414	-2.163	-4.401	-0.563	-0.424	-0.429	-2.411	3.711	-2.457

Severin Dms 17.06.2022

List of Publications and Reprints

For Thesis:

1. A detailed assessment on the interaction of sodium alginate with a surface-active ionic liquid and a conventional surfactant: a multitechnique approach; **S. Das** and S. Ghosh, *Phys. Chem. Chem. Phys.*, 2022, **24**, 13738-13762.
2. Studies on the self-aggregation, interfacial and thermodynamic properties of a surface active imidazolium based ionic liquid in aqueous solution: Effects of salt and temperature; **S. Das**, N. Patra, A. Banerjee, B. Das, S. Ghosh; *J. Mol. Liq.*, 2020, 320, 114497.
3. Formation of Mixed Micelle in an Aqueous Mixture of a Surface Active Ionic Liquid and a Conventional Surfactant: Experiment and Modeling; **S. Das**, S. Ghosh, B. Das; *Journal of Chemical & Engineering Data*, 2018, **63**, 3784-3800.

Other Publications:

4. Addressing the Exigent Role of a Coumarin Fluorophore toward Finding the Suitable Microenvironment of Biomimicking and Biomolecular Systems: Steering to Project the Drug Designing and Drug Delivery Study; S. Paul, P. Roy, **S. Das**, S. Ghosh, P. Saha Sardar, and A. Majhi; *ACS Omega*, 2021, **6**, 11878–11896.
5. Detailed Physicochemical Interaction of Inulin with Some Conventional Surfactants and Surface Active Ionic Liquid; N. Patra, A. Mal, **S. Das**, S. Ghosh; *J. Mol. Liq.*, 2021, **340**, 116849.
6. Theoretical Approaches on the Synergistic Interaction between Double Headed Anionic Amino Acid-Based Surfactants and Hexadecyltrimethylammonium Bromide; M. Barai, M. K. Mandal, H. Sultana, E. Manna, **S. Das**, K. Nag, S. Ghosh, A. Patra, A. K. Panda; *J Surfactants Deterg*, 2020, **23**, 891-902.
7. Effect of an anionic surfactant (SDS) on the photoluminescence of graphene oxide (GO) in acidic and alkaline medium; P. Saha, D K. Pyne, S Ghosh, S. Banerjee, **S. Das**, S. Ghosh, P. Dutta, A. Halder; *RSC Advances*, 2018, **8**, 584-595.

Conference Publication:

- Interaction of Poly Acrylic Acid with Surfactants and Exploring the Role of β -CD; Conference: *International Conference on Emerging Technologies for Sustainable Development* (ICETSD'19); N. Patra, A. Mal, **S. Das**, S. Ghosh. (*Conference Paper*)

Poster Presentation:

- **Presented a poster** at the 23rd West Bengal State Science and Technology Congress, 2016 on 28-29th February, 2016. (**Topic: Effect of Salts on the Self-Aggregation Behavior of Surface Active Ionic Liquids (SAILs) and the Determination of Aggregation Number**)
- **Presented a poster** at the National Seminar on Chemical Sciences: Today and Tomorrow (CSTT-2019) on March 14, 2019 under CAS II program organized by Department of Chemistry, Jadavpur University. (**Topic: Interaction of Bromelain with Surfactants: A UV-Vis and Fluorescence Study**).
- **Presented poster** at NATCOSEB- 2017 on November 10-12, 2017, jointly organized by ISSST and School of Chemistry, Sambalpur University, Odisha. (**Topic: Mixed Micelle formation in an aqueous mixture of Surfactants: A Thermodynamic and Theoretical Study**)

Oral Presentation:

- **Invited speaker** at TSSRA on September 12, 2019, organized by Department of Chemistry and Chemical Technology, Vidyasagar University and ISSST, Kolkata (**Topic: Aggregation of Surface Active Imidazolium Ionic Liquid in Aqueous Solution: Effect of Temperature and Salts**).
- **Presented oral** in the 25th West Bengal State Science and Technology Congress, 2018 held on 4-5th March, 2018 at the Science City, Kolkata, organized by Department of Higher Education, Science and Technology and Biotechnology, Government of West Bengal. (**Topic: Effect of Salts on the Self-Aggregation Behavior of Surface Active Ionic Liquids (SAILs) and the Determination of Aggregation Number**)



Cite this: *Phys. Chem. Chem. Phys.*,
2022, 24, 13738

A detailed assessment on the interaction of sodium alginate with a surface-active ionic liquid and a conventional surfactant: a multitechnique approach†

Sourav Das and Soumen Ghosh *

An investigation has been made on the interaction of a biodegradable anionic polyelectrolyte, sodium alginate (NaAlg), with two oppositely charged cationic surfactants, 1-hexadecyl-3-methyl imidazolium chloride ($C_{16}MImCl$) and 1-hexadecyl triphenylphosphonium bromide ($C_{16}TPB$), the former is a surface active ionic liquid (SAIL) and the latter a conventional surfactant over a wide concentration regime of the polyelectrolyte. Dual influence of electrostatic and hydrophobic interactions plays in this investigation when mixing surfactants with an oppositely charged polyelectrolyte. A number of different experimental techniques, e.g., conductometry, tensiometry, steady state and time resolved spectrofluorimetry, turbidimetry, isothermal titration calorimetry (ITC), dynamic light scattering (DLS), attenuated total reflection (ATR), high resolution transmission electron microscopy (HR-TEM) and fluorescence microscopy, have been implemented to get comprehensive information about the interaction of the oppositely charged polyelectrolyte and surfactants. Tensiometry study reveals the existence of several conformations of NaAlg influenced by different concentrations of surfactants titrated to it and these are abbreviated as critical aggregation concentration (cac), saturated concentration of polymer-surfactant complex (C_s) and finally extended critical micelle concentration (C_m^*) due to the aggregation of the surfactant itself, appearing in chronological order from low to high concentrations of surfactants. Apart from tensiometry, these above concentrations have been well found and the values are well comparable when investigating polyelectrolyte-surfactant interaction by other physicochemical techniques as well. Irreversible phase separation of the oppositely charged polyelectrolyte-surfactant complex (PS-complex) occurs at higher polyelectrolyte concentration investigated here for both the surfactants in the vicinity of cac for $C_{16}MImCl$ and near C_m^{*1} for $C_{16}TPB$ and finally persists after further addition of surfactants above the formation of free micelles. Several bulk and interfacial parameters, viz., Gibbs free energy of micellization (ΔG_m°), enthalpy of micellization (ΔH_m°), entropy of micellization (ΔS_m°), degree of counterion binding (β), surface excess at cmc (Γ_{max}), area minimum (A_{min}), surface pressure at cmc (π_{cmc}), pC_{20} , packing parameter (P), hydrodynamic radius (r) and aggregation number (N_a) of two surfactants both in the presence and absence of NaAlg, have been calculated for these investigated systems. Characterization of NaAlg, both surfactants and their individual complexes was performed using FTIR-ATR. DLS shows the distribution of size of polymer surfactant complexes over a wide range of surfactant concentrations at a fixed polyelectrolyte concentration, while HR-TEM study reveals not only the size of agglomerated clusters of the PS-complex but also its shapes. Images of NaAlg-surfactant complexes were also captured using fluorescence microscopy in solution phase. A strong PS-complex in the presence of $C_{16}MImCl$ has been reported here over $C_{16}TPB$.

Received 14th January 2022,
Accepted 5th May 2022

DOI: 10.1039/d2cp00221c

rsc.li/pccp

Centre for Surface Science, Physical Chemistry Section, Department of Chemistry,
Jadavpur University, Kolkata 700 032, India. E-mail: gsoumen70@hotmail.com

† Electronic supplementary information (ESI) available. See DOI: <https://doi.org/10.1039/d2cp00221c>

1. Introduction

Surfactants form a specific type of aggregate in both aqueous and non-aqueous solvents at a threshold concentration, called critical micelle concentration (cmc).^{1–3} Significant attention has been paid for decades until now^{4–14} to the oppositely



Studies on the self-aggregation, interfacial and thermodynamic properties of a surface active imidazolium-based ionic liquid in aqueous solution: Effects of salt and temperature

Sourav Das^a, Nitai Patra^a, Arnab Banerjee^b, Bijan Das^{b,*}, Soumen Ghosh^{a,*}

^a Centre for Surface Science, Physical Chemistry Section, Department of Chemistry, Jadavpur University, Kolkata 700 032, India

^b Department of Chemistry, Presidency University, Kolkata 700 073, India

ARTICLE INFO

Article history:

Received 10 June 2020

Received in revised form 14 September 2020

Accepted 1 October 2020

Available online 9 October 2020

Keywords:

Self-aggregation of surface active ionic liquid

Conductometry

Tensiometry

Isothermal titration calorimetry

Dynamic light scattering

Steady-state and time-resolved fluorescence

ABSTRACT

The influence of four sodium salts (NaCl, NaBr, Na₂SO₄, and Na₃PO₄) on the self-aggregation, interfacial, and thermodynamic properties of a surface active ionic liquid (1-hexadecyl-3-methylimidazolium chloride, C₁₆MImCl) has been explored in aqueous solutions by conductometry, tensiometry, spectrofluorimetry, isothermal titration calorimetry and dynamic light scattering (DLS). Analyses of the critical micellar concentration (*cmc*) values indicate that the anions of the added salts promote the self-aggregation of C₁₆MImCl in the order: Cl⁻ < Br⁻ < PO₄³⁻ < SO₄²⁻. Dehydration of imidazolium head groups, in general, governs the process of micellization of aqueous C₁₆MImCl in presence of the investigated salts within the investigated temperature range (298.15–318.15 K), while the melting of iceberg takes the leading role below 303.15 K for the C₁₆MImCl–Na₃PO₄ system. The results indicate that addition of salt leads to a greater spontaneity of micellization, and that exothermicity prevails in these systems. Differential effect of the salts on the interfacial properties of C₁₆MImCl has been interpreted on the basis of the coupled influence of the electrostatic charge neutralization of surfactants at the interface, and the van der Waals repulsion of surfactant tails and electrostatic repulsion of surfactant head groups. C₁₆MImCl has been predicted to form spherical micelles in presence of varying amounts of NaCl, Na₂SO₄ and Na₃PO₄, while there occurs probably a transition in the micellar geometry from spherical to non-spherical shape when added NaBr concentration exceeds 0.01 mol.kg⁻¹. Fluorescence studies demonstrate that a combined quenching mechanism is operative for the quenching of pyrene fluorescence in the investigated C₁₆MImCl–salt systems. Micellar aggregation numbers obtained from Steady State Fluorescence Quenching method have always been found to be somewhat smaller than those estimated from Time Resolved Fluorescence Quenching method. The order of instability of the C₁₆MImCl–micelles ascertained from Zeta potential measurements conform to what has been inferred from the *cmc* values. The hydrodynamic diameters of C₁₆MImCl–micelles, obtained from DLS studies, have been found to increase with increasing salinity of the solutions.

© 2020 Published by Elsevier B.V.

1. Introduction

In recent years, considerable attention is being paid to the studies on ionic liquids with surface activity (commonly referred to as surface active ionic liquids) in colloid and interface science [1–9]. Surface active ionic liquids, like conventional surfactants, form self-aggregates [10–18] owing to the balance of hydrophilic and hydrophobic interactions above a particular concentration known as the critical micellar concentration (*cmc*) [19–22]. Current interest in the area of surface active ionic liquids stems from the ease of fine-tuning of the hydrophobicity of ionic liquid molecules by varying the length of the hydrocarbon

chains, the type of the head-group or the nature and size of the counterions which might permit the modulation of the structure and the delicate dynamics of their self-aggregates for specific purposes. Additives could also result in the modification of the interaction and self-aggregation behavior of surfactants appreciably [23–35]. Studies on surfactant solutions in presence of a salt have been shown to provide important insight into various interactions prevailing in these solutions [32–36]. Surfactant–salt mixtures find widespread use in biological, technological, medical formulations, pharmaceuticals, enhanced oil recovery for the purpose of improved solubilization, suspension and dispersion [2]. Various organic and inorganic salts in combination with various surfactants are also used for this purpose [3–9,14–47]. However, there had been, so far, a very few attempts which explored the effect of salts on the self-aggregation properties of surface active ionic liquid solutions [48–52]. Keeping this in view, we have taken up a

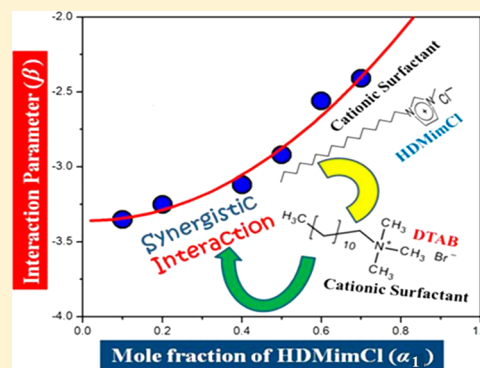
* Corresponding authors.

E-mail addresses: bijan.chem@presiuniv.ac.in (B. Das), gsoumen17@yahoo.co.in (S. Ghosh).

Formation of Mixed Micelle in an Aqueous Mixture of a Surface Active Ionic Liquid and a Conventional Surfactant: Experiment and Modeling

Sourav Das,[†] Soumen Ghosh,[†] and Bijan Das^{*,‡,§}[†]Centre for Surface Science, Physical Chemistry Section, Department of Chemistry, Jadavpur University, Kolkata 700 032, India[‡]Department of Chemistry, Presidency University, Kolkata 700 073, India

ABSTRACT: The aggregation behavior in binary mixtures of two surfactants, 1-hexadecyl-3-methylimidazolium chloride and dodecyltrimethylammonium bromide, has been investigated in aqueous solutions using conductometric, tensiometric, spectrofluorimetric, and zeta potential measurements. The counterion binding, aggregation number, and anisotropy of the micellar environment have been ascertained. The results have been analyzed on the basis of the theories of Clint, Rubingh, and Motomura. The thermodynamic parameters of the micellization process have been evaluated and discussed. The interfacial adsorptions of the mixed surfactants including their surface excesses and headgroup areas have also been evaluated. The existence of an attractive interaction among the constituents of the mixed surfactant systems investigated has been inferred.



1. INTRODUCTION

Surfactants find widespread applications in both industry and everyday life.^{1–3} Because of the amphiphilic chemical structure, surfactant in an aqueous solution has a preference toward interfacial adsorption at low concentration, whereas beyond a critical concentration, it self-aggregates to form an assembled structure whose size, shape, and average number of amphiphile per aggregated structure depend on the amphiphile concentration and other physicochemical parameters like temperature, presence of salt, etc. The critical amphiphile concentration required for the onset of the formation of an aggregated structure, referred to as a micelle, is called the critical micellar concentration (cmc).^{4–6}

Mixed surfactant systems almost invariably manifest enhanced interfacial properties (e.g., decreased critical micellar concentration, higher surface activity, etc.) compared to those of their individual components.^{7–15} This behavior of mixed surfactants allows their use in low concentrations in the cosmetic industry to avoid potential skin irritation.^{16,17} It can also be beneficial for the environment, as the amount of surfactants released and hence their impact could be substantially reduced.¹⁸ In the pharmaceutical field, the absorption of various drugs in the human body is found to be enhanced by mixed micelles.^{19–21} Mixtures of cationic and anionic surfactants find use in cleansing products to facilitate their dissolution and improved tolerance of water hardness.²² In view of the remarkable application potential and economic viability of mixed surfactant systems, a significant amount of research work has been devoted to searching and elucidating the physicochemical properties of these systems.

Recent years have witnessed^{23–31} an upsurge of interest in the self-aggregation aptitude of a new class of ionic liquids, known as the surface active ionic liquids (ILs). This is because of the possibility of fine-tuning of the hydrophobicity of ionic liquid molecules by varying the length of the alkyl chains, the type of the headgroup, or the nature and size of the counterions which might permit the modulation of the structure and the delicate dynamics of their micellar aggregates for specific purposes.

The micellar and thermodynamic properties of the imidazolium-based surface active ionic liquids^{32,33} and their mixtures with anionic, nonionic, zwitterionic, and gemini surfactants have been investigated in detail.^{34,35} However, studies involving ILs and cationic surfactants are scarce with the exception of very few reports.^{36,37} In general, mixtures of cationic surfactants have, so far, been paid relatively less attention.^{11,33,38}

In this work, the micellar and thermodynamic behavior of the mixed micelles formed in the aqueous mixtures of two cationic surfactants—1-hexadecyl-3-methylimidazolium chloride (HDMimCl) and dodecyltrimethylammonium bromide (DTAB)—has been investigated in order to shed light on various interactions prevailing in this system. The two surfactants with different lengths of the alkyl groups have been selected such that they differ in their cmc's by 1 order of magnitude, capable of producing discernible effects in their mixtures.

Received: May 8, 2018

Accepted: August 28, 2018

Published: September 10, 2018

Addressing the Exigent Role of a Coumarin Fluorophore toward Finding the Suitable Microenvironment of Biomimicking and Biomolecular Systems: Steering to Project the Drug Designing and Drug Delivery Study

Sandip Paul, Pritam Roy, Sourav Das, Soumen Ghosh, Pinki Saha Sardar,* and Anjoy Majhi*

Cite This: *ACS Omega* 2021, 6, 11878–11896

Read Online

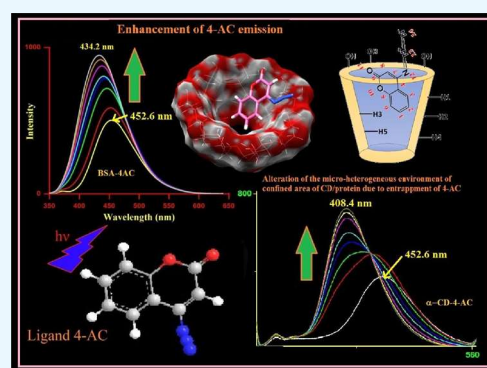
ACCESS |

Metrics & More

Article Recommendations

Supporting Information

ABSTRACT: The photophysics of 4-azidocoumarin (4-AC), a novel fluorescent coumarin derivative, is well established by the investigation of the alteration of the microheterogeneous environment comprising two types of systems: supramolecular systems, cyclodextrins (CDs), and biomolecular systems, serum albumins (SAs). The enhanced emission of the ligand with the organized assemblies like α -CD, β -CD, and γ -CD by steady-state and time-resolved fluorescence and fluorescence anisotropy at 298 K is compared with those of bovine serum albumin (BSA) and human serum albumin (HSA). The remarkable enhancement of the emission of ligand 4-AC along with the blue shift of the emission for both the systems are visualized as the incorporation of 4-AC into the hydrophobic core of the CDs and proteins mainly due to reduction of nonradiative decay process in the hydrophobic interior of CDs and SAs. The binding constants at 298 K and the single binding site are estimated using enhanced emission and anisotropy of the bound ligand in both the systems. The marked enhancement of the fluorescence anisotropy indicates that the ligand molecule experiences a motionally constrained environment within the CDs and SAs. Rotational correlation time (θ_c) of the bound ligand 4-AC is calculated in both the categories of the confined environment using time-resolved anisotropy at 298 K. Molecular docking studies for both the variety of complexes of the ligand throw light to assess the location of the ligand and the microenvironment around the ligand in the ligand–CD and ligand–protein complexes. Solvent variation study of the probe 4-AC molecule in different polar protic and aprotic solvents clearly demonstrates the polarity and hydrogen-bonding ability of the solvents, which supports the alteration of the microenvironments around 4-AC due to binding with the biomimicking as well as biomolecular systems. Dynamic light scattering is employed to determine the hydrodynamic diameter of free BSA/HSA and complexes of BSA/HSA with the ligand 4-AC.



INTRODUCTION

The microenvironment responsive ligands or drugs have been an emergent application in the recent times for investigations on drug designing or drug delivery research. Perturbation or alteration of the microenvironment surrounding a ligand/drug molecule is a prime concern of the current medical science and life science projects.^{1–9} The nature of the microenvironment surrounding a ligand or drug or any other molecule has been explored by a variety of spectroscopic techniques, among which fluorescence spectroscopy seems to be the most widely used technique.^{2,10–12} Fluorescent probes are powerful tools for biosensing and bioimaging because of their high sensitivity, specificity, high fluorescence intensity, excellent solubility, biocompatibility, and simple preparation.¹³ Hence, development of fluorescent probes, specifically for biological settings and clinical settings, has attracted intense interest.^{13–16} Till date, different kinds of fluorescent probes are commercially available and can be used in biological investigations.¹³

Coumarin molecules, as a family of molecules, exhibit a wide range of fluorescence emission properties; hence, they are used as a fluorescent probe, and they also have a wide range of biological importance.^{17–26} For example, azidocoumarins are known to be used in biomolecular photoaffinity labelling.²⁷ It may also be noted that photostability is an important criteria for a molecule to become a good fluorescent probe.²⁸ The use of fluorescent probes in some biomolecular systems and biomimicking systems, in many times, helps to amend some structural change of these systems, advocating the challenging roles of those probes toward the environments.^{3–6,9,29–32}

Received: January 10, 2021

Accepted: April 9, 2021

Published: April 22, 2021





Detailed physicochemical interaction of inulin with some conventional surfactants and surface active ionic liquid



Nitai Patra^{a,b}, Arpan Mal^a, Sourav Das^a, Soumen Ghosh^{a,*}

^a Centre for Surface Science, Physical Chemistry Section, Department of Chemistry, Jadavpur University, Kolkata 700 032, India

^b Central Footwear Training Centre, Phani Bhusan Pathak Road, Pujali, P.S.- Budge Budge, 24 Parganas (S), Kolkata 700 138, India

ARTICLE INFO

Article history:

Received 5 November 2020

Revised 2 June 2021

Accepted 25 June 2021

Available online 12 July 2021

Keywords:

Inulin

Surface active ionic liquid

Cationic conventional and gemini surfactants

Different techniques

ABSTRACT

Inulin, a carbohydrate based polymer has immense applications in industries of human aids. There are very limited interactive studies on this polymer although there are numerous applications. In the present study, interactions of inulin with different amphiphiles lead to interesting characteristics as identified by various physicochemical methods. Tensiometry, conductometry, isothermal titration calorimetry, turbidimetry, etc. have been employed to characterize the phenomenological changes. Cationic type amphiphiles, e.g., surface active ionic liquid, conventional, and gemini surfactants provide very fruitful interactions. These amphiphiles form small aggregates with the polymer at low concentration, coacervates at moderate concentration and free micelles at higher concentrations of the amphiphiles. Inulin-amphiphiles interaction has been supported by different morphological studies also.

© 2021 Elsevier B.V. All rights reserved.

1. Introduction

Polymer-surfactant interactions are common and captivating in various fields, such as medicinal and pharmaceutical industries, cosmetics, detergency, drug encapsulation, enhanced oil recovery, paints, coatings etc [1–8]. Inulin, a non-structural, storage carbohydrate, heterogeneous polysaccharide of fructose units, consists of chain-terminating glucosyl moieties and a repetitive fructosyl moiety, [9,10] which are linked by β (2, 1) bonds. That is why its caloric value is very low. The degree of polymerization (DP) of standard inulin ranges from 2 to 60. After removing the fractions with DP lower than 10 during manufacturing process, the remaining product is high performance inulin [11]. Inulin is found in the leeks, onions, wheat, asparagus (*Asparagus officinalis*) garlic, Jerusalem artichoke (*Helianthus tuberosus*) and chicory (*Cichorium intybus*) root [12,13]. This polymer has some typical contributions towards the health of human body by reducing the risk of diseases [14]. Inulin acts as prebiotics due to its nature of inhibiting the growth of pathogenic microorganism and it is used as a potentially treating colon dysfunction as it stimulates the growth of the beneficial bacteria (e.g., *biofidobacteria*) in the colon [15,16]. Inulin is also effective for its promotion of good digestive health, lipid metabolism, enhancement of mineral bioavailability, reducing growth of cancer and tumor cell growth [17–25]. It has been observed that there are

formations of coacervates in the polymer-surfactant interactions in many cases. The coacervates can be used for solubilization and encapsulation of lipophilic drugs. It is also convenient for the synthesis and delivery of nanoparticles [26]. Researchers have distinguished strongly interacting systems (polymers and surfactants with opposite charges) [27–30] from weakly interacting systems (usually neutral polymer and charged surfactant) [31–34]. There are examples of interactions of conventional surfactants as well as ionic liquids with different types of polymers, such as hydroxymethyl cellulose, carboxymethyl cellulose [29,35–38], carbohydrate polymers, viz., starch [39,40], amylose [41], amylopectin [42,43] etc. Interaction of inulin also has been shown in recent studies in aqueous and different solvent media [44,45]. However, there are infrequent studies on the interaction of inulin with amphiphiles [24]. In the present study, interaction of inulin has been performed with cationic amphiphiles of different types of head and tail groups. Cetyl pyridinium chloride (CPC), tetramethylene-1,4-bis(dimethyltetradecylammonium) bromide (14–4–14), 1-decyl-3-methyl imidazolium chloride [DMIM][Cl], and 3-(N,N-Dimethylmyristylammonio) propanesulfonate (DMAPS) have been used for the interaction with inulin. This study has been explored by the tensiometry, conductometry, isothermal titration calorimetry and turbidimetry measurements. The size and shape of the aggregated inulin-amphiphile were analysed by DLS, FESEM and TEM techniques.

* Corresponding author.

E-mail address: gsoumen70@hotmail.com (S. Ghosh).

Theoretical Approaches on the Synergistic Interaction between Double-Headed Anionic Amino Acid-Based Surfactants and Hexadecyltrimethylammonium Bromide

Manas Barai¹ · Manas Kumar Mandal¹ · Habiba Sultana¹ · Emili Manna² · Sourav Das³ · Kaushik Nag⁴ · Soumen Ghosh³ · Anuttam Patra⁵ · Amiya Kumar Panda¹ 

Received: 1 October 2019 / Revised: 11 March 2020 / Accepted: 15 March 2020
© 2020 AOCS

Abstract Theoretical investigations on the micellization of mixtures of (i) amino acid-based anionic surfactants [AAS: *N*-dodecyl derivatives of aminomalonate, -aspartate, and -glutamate] and (ii) hexadecyltrimethylammonium bromide (HTAB), were carried out at different mole ratios. Variation in the theoretical values of critical micelle concentration (CMC), mole fraction of surfactants in the micellar phase (X), at the interface (X^σ), interaction parameters at the bulk/interface (β^R/β^σ), ideality/nonideality of the mixing processes, and activity coefficients (f) were evaluated using Rubingh, Rosen, Motomora, and Sarmoria-Puvvada-Blankshtein models. CMC values significantly deviate from the theoretically calculated values, indicating associative interaction. With increasing mole fraction of AAS (α_{AAS}), the magnitude of the (β^R/β^σ) values gradually decreased, considered to attributable to hydrophobic interactions. With increasing α_{AAS} , the micellar mole fraction of HTAB (X_2) decreased insignificantly and

X_2 values were higher than those compared to AAS for all combinations, due to the dominance of HTAB in micelles. Micellar mole fraction at the ideal state of AAS (X_1^{ideal}) differed from micellar mole fraction of AAS (X_1), indicating nonideality in the mixed micellization process. Gibbs free energy of micellization (ΔG_m) values are more negative than the free energy of micellization for ideal mixing ($\Delta G_m^{\text{ideal}}$), indicating the micellization process is spontaneous. With increasing α_{AAS} , the enthalpy of micellization (ΔH_m) and entropy of micellization (ΔS_m) values gradually increased, which indicates micellization is exothermic. The different physicochemical parameters of the mixed micelles are correlated with the variation in the spacer length between the two carboxylate groups of AAS.

Keywords Mixed micelle · Synergism · Interaction parameter · Micellar composition · Activity coefficient

Supporting information Additional supporting information may be found online in the Supporting Information section at the end of the article.

✉ Amiya Kumar Panda
akpanda@mail.vidyasagar.ac.in

¹ Department of Chemistry, Vidyasagar University, Midnapore, West Bengal 721102, India

² Centre for Life Sciences, Vidyasagar University, Midnapore, West Bengal 721102, India

³ Centre for Surface Science, Department of Chemistry, Jadavpur University, Kolkata, West Bengal 700032, India

⁴ Department of Biochemistry, Memorial University of Newfoundland, St. John's, Canada

⁵ Chemistry of Interfaces Group, Luleå University of Technology-SE-97187, Luleå, Sweden

J Surfact Deterg (2020).

Abbreviations

α_{AAS}	mole fraction of AAS
α_i	stoichiometric mole fraction
β^R, β^σ	interaction parameters at the bulk and interface
$\Delta H_m, \Delta G_m$ and ΔS_m	changes in enthalpy, free energy and entropy of micellization
$\Delta G_m^{\text{ideal}}$	free energy of micellization for ideal mixing
Γ_{max}	surface excess
A_{min}	minimum molecular area of the surfactant at the air-water interface


 Cite this: *RSC Adv.*, 2018, 8, 584

Effect of an anionic surfactant (SDS) on the photoluminescence of graphene oxide (GO) in acidic and alkaline medium†

 Prosenjit Saha,^a Dinesh Kumar Pyne,^a Srijon Ghosh,^b Soumadip Banerjee,^b Sourav Das,^c Soumen Ghosh,^c Partha Dutta^{*d} and Arnab Halder^{id}^{*a}

An anionic surfactant (SDS) modulates the photoluminescence of graphene oxide (GO) in both acidic and alkaline medium. In the acidic medium (pH \approx 2), formation of hemi spherical surface micelles on the GO sheets creates a non-polar environment around the fluorophoric moiety of GO and hinders the solvent relaxation. This leads to a significant 36 nm blue shift of the photoluminescence band, whereas in alkaline medium (pH \approx 10), SDS interacts with GO sheets in a different way due to the presence of negatively charged carboxylate ions at the GO edges. The repulsion between the negatively charged GO sheets and the intercalation of SDS within the basal planes of GO may weaken π - π stacking interaction which produces largely separate layers of GO. The largely separated GO sheets due to very weak stacking interactions among successive layers may behave almost like isolated functionalized GO, resulting in an enhancement of the photoluminescence intensity at 303 nm.

 Received 1st November 2017
Accepted 16th December 2017

DOI: 10.1039/c7ra12024a

rsc.li/rsc-advances

Introduction

Graphene, a monolayer of sp^2 -hybridised carbon atoms with a two dimensional honey-comb sheet structure, and graphene based nano materials have become a popular research topic in nanomaterials science due to their unique optical and mechanical properties^{1–6} and many technological^{7–9} and biological applications,¹⁰ since its discovery in 2004. Functionalized graphene sheets or graphene oxide (GO) obtained by treating graphite with strong oxidizers, was primarily considered only as a precursor for graphene, but as a result of oxidation, the band gap of graphene is enhanced and graphene oxide has drawn tremendous research interest for its optical properties^{11–18} which are somehow limited for graphene because of its zero band gap. On the other hand due to the availability of several oxygen containing functional groups (epoxy, hydroxyl, carboxyl) on the surface and sheet edges^{19,20} and high surface area, GO interacts with many organic, inorganic, biomolecules, polymers^{21–23} and surfactants^{24–28} to produce several GO based nanomaterials and nanocomposites. Adsorption of surfactants

on the GO surface plays an important role for many practical applications in Li-ion battery electrodes^{29,30} and metal-oxide films.^{31,32} Introduction of electrostatic repulsive or steric factors increases the stability of the aqueous GO system.²⁸ This can be obtained by increasing the pH of the medium above the pK_a of the carboxylic groups through the utilization of electrostatic repulsion between the negative charges of carboxyl groups on the edges of the GO sheet.^{33–35} But when the carbon to oxygen ratio is high, pH adjustment is not practically possible. In this situation, stability of the aqueous GO system may be enhanced by using surfactants. The charged head groups of adsorbed ionic surfactants may provide electrostatic repulsion or steric interaction. Considering this fact in mind, the different research groups investigated the stability of GO in aqueous medium in the presence of sodium dodecyl sulphate (SDS) by various methods and also studied the interaction between GO and SDS. Hsieh *et al.* observed the adsorption behavior of SDS on functionalized graphene sheet (FGS) by conductometric titration.²⁷ According to them, the surface of FGS is completely covered by monolayer adsorption of 12 μ M SDS concentration, when FGS has carbon to oxygen ratio is 18 and they found the critical surface aggregation concentration (CSAC) for surface micelle formation on FGS as 1.5 mM.²⁷ In another work, related to the stability of FGS in the presence of SDS by optical microscopy and UV-vis study, Aksay and coworkers showed that FGS achieved significant stability in aqueous medium above the monolayer adsorption concentration ($\geq 40 \mu$ M) of SDS.²⁸ Glover *et al.* reported the charge driven selective adsorption of SDS on graphene oxide by atomic force microscopy and showed that the amount of selective adsorption of SDS depends on the degree of

^aDepartment of Chemistry, Presidency University, Kolkata – 700073, India. E-mail: arnab.chem@presiuniv.ac.in; Tel: +91 3340529846

^bIndian Association for the Cultivation of Science, Jadavpur, Kolkata – 700 032, India

^cCentre for Surface Science, Physical Chemistry Section, Department of Chemistry, Jadavpur University, Kolkata-700032, India

^dDepartment of Chemistry, Maharaja Manindra Chandra College, Kolkata – 700003, India. E-mail: par_dut@yahoo.com; Tel: +91 9433464396

† Electronic supplementary information (ESI) available. See DOI: 10.1039/c7ra12024a

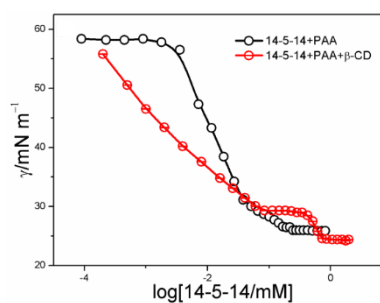


Interaction of Poly Acrylic Acid with Surfactants and Exploring the Role of β -CD

Nitai Patra, Arpan Mal, Sourav Das, and Soumen Ghosh*

Centre for Surface Science, Physical Chemistry Section, Department of Chemistry, Jadavpur University Kolkata-700 032, India, Email:gsoumen70@hotmail.com/ patrasquare@gmail.com

ABSTRACT: Interaction of polymers with surfactant has extensive applications in pharmaceutical industries as well as in cosmetics, detergents, pesticides, and enhanced oil recovery. In this study, poly acrylic acid (PAA) has been used along with surfactants, such as pure Triphenyl tetradecyl phosphonium bromide (TTPB), pentamethylene-1, 4-bis (dimethyltetradecylammonium bromide) (14-5-14) to investigate the polymer-surfactant interaction in both aqueous and aqueous β -CD media.



1. INTRODUCTION

Studies on interaction of polymers with surfactant have extensive applications in industries, pharmaceuticals, cosmetics, detergents, pesticides, and enhanced oil recovery. There are specific interests on the polymer and ionic surfactant systems because of its typical physicochemical properties at different possible combinations. The basic principles of the interactions between polymer and surfactant are explored by Kwak et al.¹, Goddard and Ananthapadmanabhan et al.,² and others.³⁻⁵ There are still controversies and uncertainties on the nature and mode of complex behavior in surfactant-polymer systems. Poly (acrylic acid), known as PAA, is a synthetic cross linked homo polyelectrolyte because it loses its acidic (carboxylic) protons at neutral pH of water. The association processes of linear poly (acrylic acid) polymers with surfactants have been explored by the measurement of adsorption,^{6,7} surface tension,⁷ fluorescence,⁸⁻¹¹ dye solubilization,⁸ and conductivity^{8, 12} methods. The interaction is mainly hydrophobic for anionic surfactant, and is favored for non-ionized polymer¹³. To maintain the electro neutrality conditions, the surfactant is accompanied by its counterions, which increase the osmotic pressure inside the aggregates and cause their swelling¹⁴. In the case of a cationic surfactant, the association process with poly (acrylic acid) may result in a phase separation when the carboxylic groups are neutralized by the cationic groups of the

surfactant.^{15, 16} The interaction with a non-ionic surfactant is usually weak except for the association of poly (acrylic acid) with ethoxylated surfactants.^{8, 17-20} In these systems, hydrogen bonding between the carboxylic groups and the oxygen of the ethylene oxide chain contributes to the aggregation. However, studies on the interaction of PAA and similar polymer poly (methacrylic acid) with cationic surfactants are scarce in the literature.^{16,21} The effect of cyclodextrins on the surfactant-polymer complex is limited in the literature.²² In this study, the effect of β -CD has been observed in the PAA-surfactant complex by the measurement of tensiometry.

2. EXPERIMENTAL SECTION

2.1. Materials. Triphenyl tetradecyl phosphonium bromide (TTPB) and β -cyclodextrin (β -CD) (purity $\geq 97\%$) were purchased from Caledon Laboratories, LTD, Canada. and Sigma Aldrich, respectively. Pentamethylene-1, 4-bis (dimethyltetradecylammonium bromide) (14-5-14) was synthesized using the standard procedure. Double distilled water (κ 2-3 $\mu\text{S cm}^{-1}$ at 25°C) was applied for sample preparation. All the experiments were performed under a fixed temperature.

2.2. Methods.

Tensiometry- Tensiometric measurements were done with a du Noüy tensiometer (Krüss, Germany), using a platinum ring detachment method. 5 mL of PAA/PAA+ β -CD solution was